APPENDIX G

Appendix G - Review of the Hydraulic Conductivity and Geotechnical Characteristics, Longwall 10A Height of Fracture Borehole, Subsidence Impact Assessment for Selected Archaeological Heritage Sites

This page has been left blank intentionally.

Strata Control Technology

REPORT TO:

TAHMOOR MINE

Review of the Hydraulic Conductivity and Geotechnical Characteristics of the Overburden at Tahmoor South

TAH4083 REVISION 1

Mining Research and Consulting Group
SCT Operations Pty Ltd PO Box 824 Wollongong NSW 2520 Australia
sctnsw@sct.gs

REPORT TO

Ron Bush
Approvals Manager
Tahmoor South Project
Tahmoor Coal
PO Box 100
TAHMOOR NSW 2573

SUBJECT

Review of the Hydraulic Conductivity and Geotechnical Characteristics of the Overburden at Tahmoor South

REPORT NO

TAH4083 Revision 1

PREPARED BY

Winton Gale, Yvette Heritage and Mahdi Zourabadi

DATE

4 December 2013

.....
Winton J. Gale
Managing Director

SUMMARY

The Tahmoor South Project, is a proposed extension of Tahmoor Mine to the south of the current workings. The main target seam is the Bulli Seam and in the Tahmoor South area it is at a depth of 375m to 420m.

The purpose of this assessment is to characterise the geotechnical and hydrological properties of the overburden strata in the Tahmoor South Project area to with the primary aim to:

i. Characterise the insitu hydraulic conductivity of the rock mass in the Tahmoor South area.

ii. Characterise the geotechnical characteristics of the strata with primary regard to hydrological impacts.

iii. Review the mining and caving related impacts on groundwater and subsidence anticipated in the area.

The characterisation is also aimed to provide input properties for numerical models to assess the caving related impacts and the ground water response to mining in the Tahmoor South Project area.

The geotechnical rock properties and stress field have been characterised and are consistent with the expectation from Tahmoor North and the Illawarra coal measures.

The hydrological testing program using Lugeon testing has provided an extensive data set to analyse the hydraulic conductivity of the overburden rock mass. The results were consistent with that of Tahmoor North and elsewhere in the Illawarra coal measures.

The hydraulic conductivity of the rock fabric within core sample indicates that some sections of the Hawkesbury Sandstone and Bulgo Sandstone have high inherent conductivity, however the conductivity of the rest of the strata section is typically low.

It is expected that the flow within the rock mass will be primarily via discontinuities in the rock mass. In areas of high conductivity within the Hawkesbury Sandstone and Bulgo Sandstone flow through the fabric is also expected, however the conductivity is similar to that for the discontinuities within those units.

The in situ hydraulic conductivity of the rock mass in Tahmoor South has been estimated by statistical analysis of packer tests, discontinuities in the strata and the in situ stress field.

The summary of the three dimensional hydraulic conductivity over the Tahmoor South Project area is presented in Table A. In this K11, K22 and K33 represent the maximum, intermediate and minimum conductivity respectively. The direction is represented by the plunge and trend.

Table A: Summary of the three dimensional conductivity for each depth

Depth (m)	Average Principal Hydraulic conductivity tensor (m/s)				
	K11 Plunge/Trend	K22 Plunge/Trend	K33 Plunge/Trend	K_H/K_v	K_H/K_h
50 (0-100)	1.1e-6 2/137	9.45e-7 7/228	3.19e-7 82/30	3.45	1.16
150 (100-200)	9.94e-8 2/136	8.6e-8 7/227	2.34e-8 83/29	4.25	1.1
250 (200-300)	3.83e-8 0/136	2.79e-8 16/226	1.57e-8 74/47	2.44	1.37
350 (300-400)	1.23e-8 2/137	9.52e-9 10/227	4.2e-9 80/35	2.87	1.29
450 (>400)	5.54e-9 2/137	4.49e-9 8/227	1.47e-9 82/32	3.77	1.23

In general, the maximum conductivity is horizontal and in a NW-SE direction, and the magnitude decreases with depth.

A review of the piezometer data in the Tahmoor South Project area has defined the pore pressure distribution within the Bulli and Wongawilli Seams.

It was noted that the current Bulli Seam extraction has depressurised the Bulli Seam within a lateral zone of approximately 700-1200m about the panels. Depressurisation of the Wongawilli Seam has also occurred but it does not appear to be as extensive.

The expected height depressurisation above the longwall panels in the Tahmoor South area is presented. The resultant average overburden conductivity within the subsided ground above the panels has been also estimated. It is expected that the height to which the caved strata is totally depressurised will extend approximately 210-216m above the Bulli Seam.

The vertical conductivity of the caved and subsided strata above the panels was assessed by computer analysis, and indicates that the average vertical conductivity of less than 10^{-7} m/s.

It was found that a 50m thick constrained zone formed at approximately 200m above the Bulli Seam roof. This zone would be expected to significantly constrain water migration from the surface. The anticipated height of depressurisation is consistent with the location of the constrained zone.

TABLE OF CONTENTS

PAGE NO

1. INTRODUCTION

The Tahmoor South Project, owned by Tahmoor Coal Pty Ltd (Tahmoor Coal), is a proposed extension of Tahmoor Mine to the south of the current workings. Tahmoor Coal is a wholly owned unit within Glencore's coal division (Glencore Xstrata plc). The main target seam is the Bulli Seam and in the Tahmoor South area it is at a depth of 375m to 420m. Figure 1 shows the location of Tahmoor South proposed longwall panels in relation to the existing Tahmoor Mine. The Tahmoor South proposed mine plan consists of two mine areas, the central Domain consisting of 9 panels and an the Eastern Domain consisting of 5 panels.

The purpose of this assessment is to characterise the geotechnical and hydrological properties of the overburden strata to with the primary aim to:

i. Characterise the insitu hydraulic conductivity of the rock mass in the Tahmoor South area.

ii. Characterise the geotechnical characteristics of the strata with primary regard to hydrological impacts.

iii. Review the mining and caving related impacts on groundwater and subsidence anticipated in the area based on published information

iv. Estimate the vertical and hydrological conductivity of the overburden above longwall panels in the Tahmoor South area on the basis of simulation of the caving characteristics of the site.

The information used in this report has been a combination of reports provided by Tahmoor Coal together with information collated and produced by SCT Operations.

The primary material used is referenced.

2. GEOLOGICAL SUMMARY

The Bulli Seam is the current target seam while the Lower Wongawilli Seam, about 25m below, is the second target seam. The Bulli Seam has 375-420m depth of cover in the Central Domain, while the Eastern Domain has a depth of cover ranging approximately 385-460m. The depth of cover over the site is presented in Figure 2. These two areas are separated by faults, while the western margin of the Central Domain is also bound by a fault. The strata dips to the northeast where the Bulli Seam has a dip of approximately 1.5°.

The stratigraphic sequence consists of the Permian Illawarra Coal Measures containing the target Bulli and Wongawilli Seams, overlain by the Triassic Narrabeen Group consisting of interbedded sandstone and claystone units, and the Hawkesbury Sandstone. Figure 3 shows the general stratigraphic sequence for borehole TBC008. The Bald Hill Claystone is included in the Narrabeen Group and is approximately 200m above the Bulli Seam. The formation thicknesses are relatively consistent across the Tahmoor South mine area and TBC008 is therefore a good representation of the mine area.

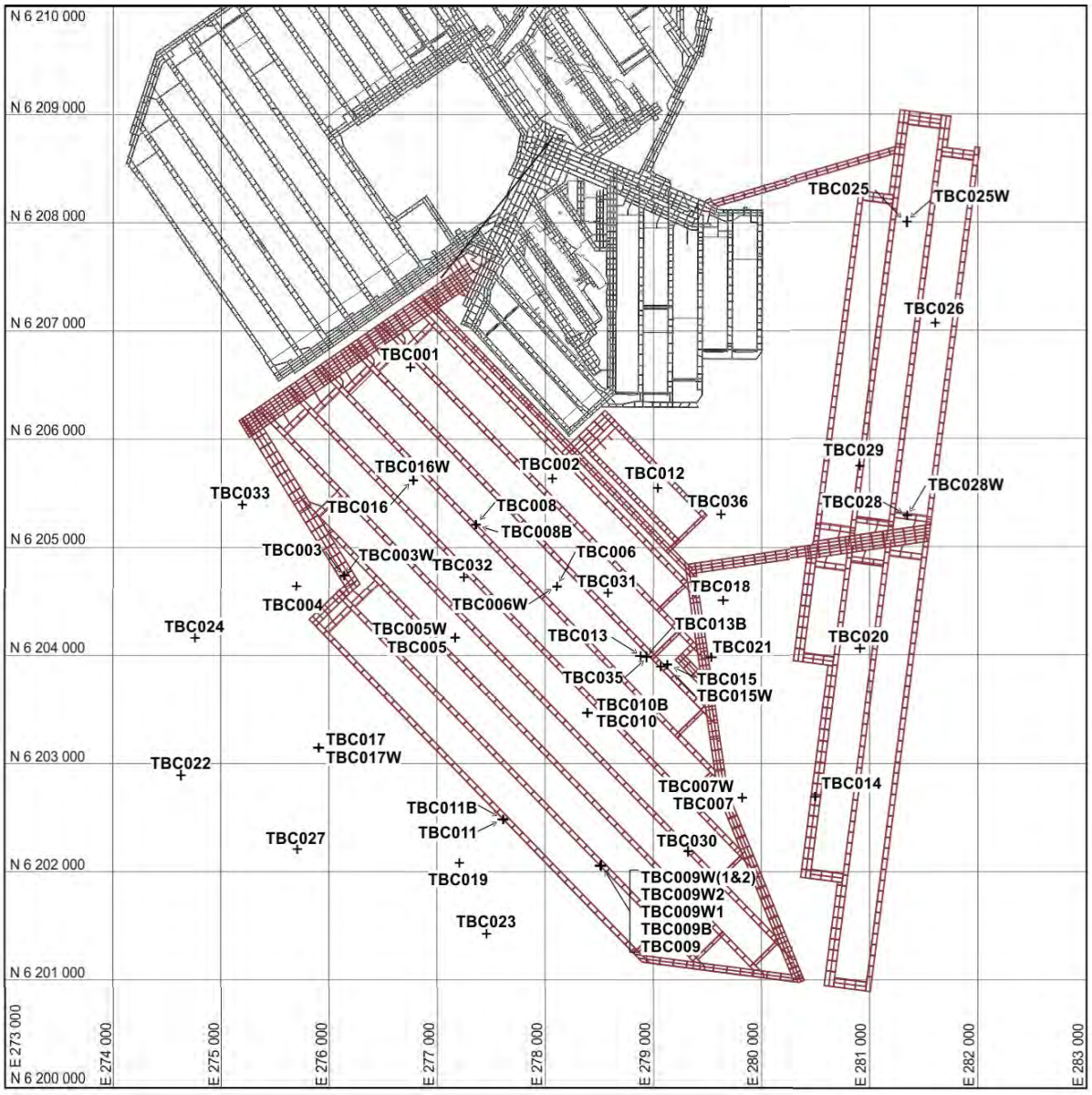

Figure 1: Tahmoor North and South mine plans showing location of boreholes used in the study.

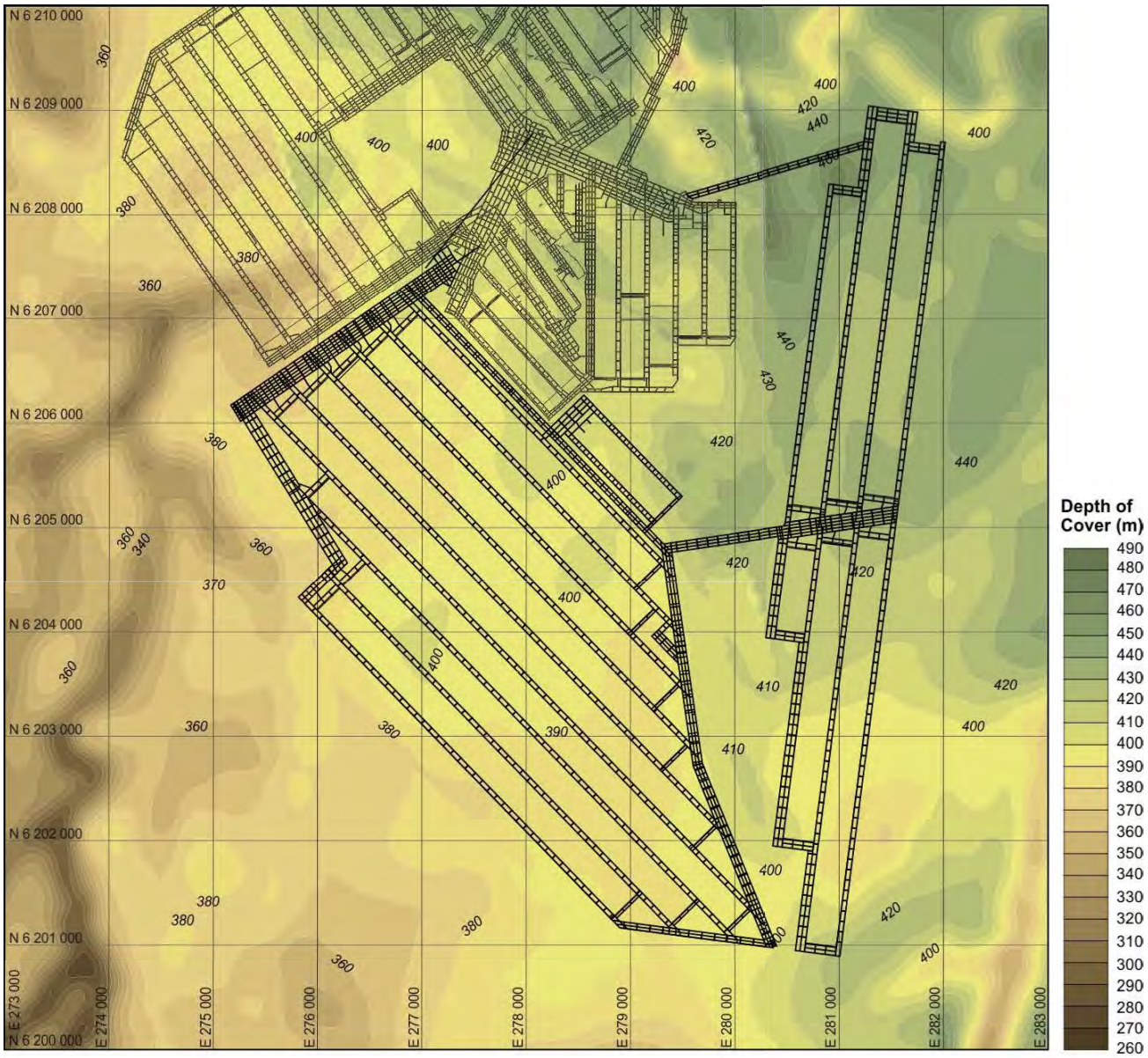

Figure 2: Bulli Seam depth of cover contours.

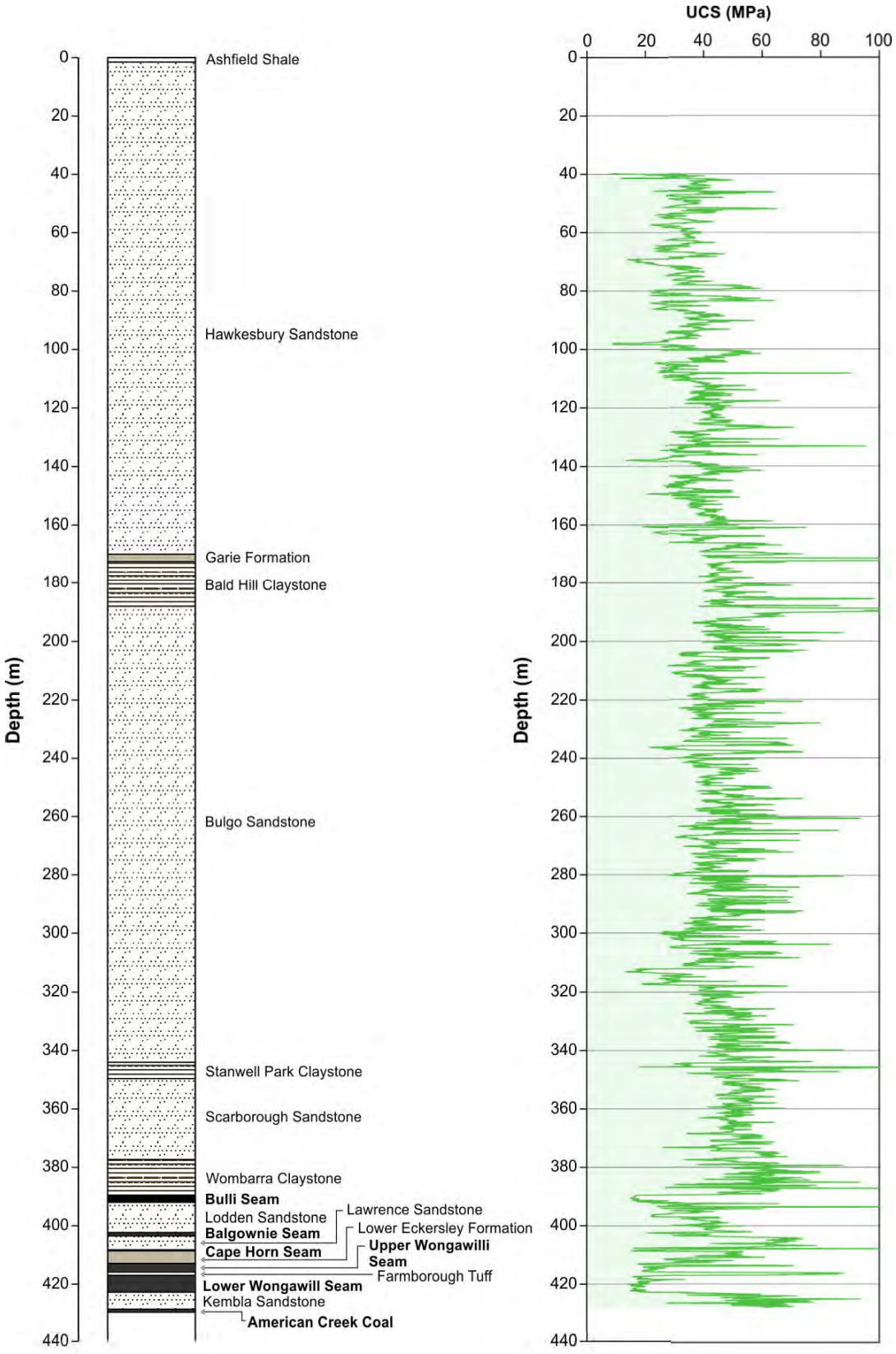

Figure 3: Stratigraphic section for TBC008.

3. LITERATURE REVIEW

The literature review aimed to gather all relevant information in relation to groundwater and overburden response to the longwall mining and caving process. The literature review consisted of reviewing Tahmoor Mine technical reports from third party consultants in addition to technical papers relevant to Tahmoor Mine's experience. The relevant information that was reviewed and collated consisted of:

- Overburden groundwater and pore pressure.
- Subsidence.
- Height of fracturing.
- Overburden conductivity.
- Zone of total depressurisation.

3.1 Overburden Groundwater and Pore Pressure

Groundwater assessments are routinely conducted by third party consultant Geoterra in the form of yearly and end of panel reports. These reports include groundwater levels, overburden pore pressures and stream flow assessments in relation to longwall extraction caving and subsidence.

Piezometers installed throughout the overburden are a key tool in understanding the pore pressure profile above and adjacent to longwall panels. To date, longwall extraction has not occurred beneath multi-piezometer strings and the pore pressure information that has been reported to date are the shallow standpipe piezometers monitoring the groundwater level. Shallow standpipe piezometers are useful for measuring the groundwater level however multi-piezometer boreholes are required to observe the pore pressure profile of the overburden affected by longwall extraction.

The Geoterra yearly Groundwater Report for 2011-2012 (Geoterra Report, 2012) shows a summary of all piezometers to date. Some key notes coming from the Geoterra summary reports are:

- Shallow standpipe piezometers are installed above Longwalls 22-26.
- Groundwater piezometers show no significant permanent drop in groundwater level above longwall panels.
- There are no piezometers covering the depth profile in the extracted longwall panels (5 multi-piezometer holes are located in Longwall panels 29-33).

Key points extracted from the Geoterra end of panel reports include:

- Subsidence has not been observed to effect overall stream flows.
- P1 and P2 holes over and adjacent to previous longwall panels have showed initial pore pressure drops up to 9m but have then recovered.

3.2 Subsidence

Mine Subsidence Engineering Consultants (MSEC) provide end of panel reports to Tahmoor Mine outlining the predicted and observed subsidence above the Tahmoor North longwall panels.

The summary of subsidence as at LW 26 indicated that the maximum subsidence noted was 1382mm, which includes the effect of multiple adjacent panels.

A summary of the factors which can affect the magnitude of subsidence has been reported in a paper by Gale and Sheppard (2011) investigating the increased subsidence about Longwall panels 24A and 25.

Longwall panels 24A and 25 both show increased maximum subsidence to approximately 1.0-1.2m, where predicted subsidence was in the order of 0.5-0.6m. In the study by Gale and Sheppard it became apparent that the increased subsidence is likely to be due to reduction in joint friction and stiffness due to the weathering process in the strata above the water table where the water table is considerably lower due to the Bargo Gorge. The intact rock properties were not changed, only the properties of the joints were altered.

Key characteristics of the strata where increased subsidence occurred were:

- Increased water table depth.
- Higher fracture conductivity.
- Reduced friction and joint stiffness.

It has been noted that subsidence adjacent to the Bargo gorge has remained anomalous relative to that typical of the Tahmoor site.

3.3 Height of Fracture

The height of fracturing above a longwall panel can be described as the zone from which the overburden transitions between bridging characteristics and observed fracture dilation of new fractures or remobilisation of existing fractures. The bridging strata will still show sagging characteristics however shear movement on bedding planes typically occurs with minimal dilation. (Mills, 2011).

This height of fracture zone, as observed from monitoring and modelling of goafs, is typically between 1-1.75 times the panel width and can be approximated to 1.5 times the panel width. The height of fracture zone however, does not necessarily equate to the zone of increased conductivity

as the conductivity is dependent on the networking and connectivity of the fracture system (Gale, 2008). Likewise, the height of fracture may not equate to the height of total depressurisation due to the connectivity of the fracture network. The overburden conductivity and zone of total depressurisation is discussed in the following Sections (3.4 to 3.6).

3.4 Hydrological Concepts Related to Longwall Mining

Extraction of coal via longwall methods is the most common method currently used. Extracted coal thickness typically ranges from 2-4.5m for conventional systems and may be higher for top coal caving systems. Longwall panels are typically 200-400m wide and 1-3km long. They are therefore essentially long rectangular panels. As a result of this simple geometry, the overburden subsidence behaviour is largely controlled by the panel width (shortest dimension). The panel length has no major impact on the overall result, other than at the panel start and finish line area. This simple geometry allows much of the overburden caving characteristics to be analysed as a two dimensional problem, related to panel width.

The extraction of coal causes stresses in the ground to be redistributed around the panel during mining. This stress distribution may result in overstressing of the strata and creation of new fractures. The location and extent of such fractures depends on the strata and depth of mining. Extraction of the coal also causes caving of the immediate roof (5-20m depending on the strata types) behind the supports to form a goaf. Above this goaf zone, the strata tend to part along particular bedding planes and form "beams or plates". These subside onto the goaf as an interlocked but fractured network of bedding planes, pre-existing joints, mining induced fractures and bending related fractures within the beams.

Tensile fracturing and dilation of existing jointing occurs in the upper zones of the overburden as a result of bending strains. The development of these zones is dependent on panel geometry and depth.

Caving and cracked beam subsidence movements tend to occur up to a height of 1-1.7 times the panel width. Examples of this have been monitored by surface to seam extensometers (Mills and O'Grady 1998, Holla and Armstrong 1986, Holla and Buizen 1991, Guo et al. 2005, Hatherley et al. 2003) and predicted to occur from computer models (Gale 2006). This indicates that cracking and deflection related to such caving and cracked beam subsidence could extend to the surface for panel widths greater than 0.75-1 times depth.

Empirical data of mine subsidence indicates that significant subsidence movements tend to initiate at panel width to depth ratios in the range of 0.7-1. The inference on this data is that for panel widths less an approximately 0.7 times depth there is sufficient overburden thickness above the caved and cracked zone to span across the panel.

A study of this effect was presented by Gale (2006) whereby computer modelling of caving and subsidence for various panel widths was compared to

empirical subsidence measurements. The results indicated that the height of major caving and cracking extended approximately 1-1.5 time panel width and the resultant subsidence was a function of goaf stiffness and panel geometry. The results are presented in Figure 4 and are consistent with the empirical subsidence database.

Forster and Enever (1992) developed a conceptual model of overburden caving behaviour based on the concept of zones within the overburden strata. This was developed from studies about the Lake Macquarie area in Newcastle (NSW) area. The conceptual model has four zones:

i. A highly disturbed zone extending for some relatively short distance above the mining section.

ii. A fractured zone which is considered to be totally destressed and shows a large increase in bulk permeability. Material in this zone has subsided, but remains essentially in its original geometry, but with open fractures and bedding planes.

iii. A constrained zone where there is no change in vertical permeability, but a likely increase in horizontal permeability.

iv. A surface zone where there is increased vertical permeability above the flanks of the panel.

These conceptual zones is presented in Figure 5 are generally consistent with zones referred to previously, however the relative heights of the various zones, and their vertical conductivity is difficult to apply to other sites, particularly with variation in depth and subsidence.

It is noted that in situations where there is no connected fracture networks developed from the mine to the surface (in the width to depth range less than approximately 0.7) local surface fracturing may occur about valleys and complex topographic outcrops. In these cases the fracture zones are very localised about the topographic feature and do not connect into the mine. In these cases, water may be redirected laterally in the near surface strata, but does not enter the mine.

Longwall mining creates additional fractures and changes the conductivity of pre-existing fractures. However, the creation of these fractures alone does not necessarily imply that a direct hydraulic connection exists over this zone. In order for mine inflow to occur, the fractures created must form a connected and conductive network to allow significant volumes of inflow.

Work by Gale (2008) concluded that the frequency, networking and aperture of fractures increases with increasing overburden strain and subsidence. Therefore, whilst panel width typically controls the height of fracturing, the network connectivity and conductivity of fractures is controlled by the magnitude of strain and subsidence. Panel width, depth and seam thickness influence strain and subsidence.

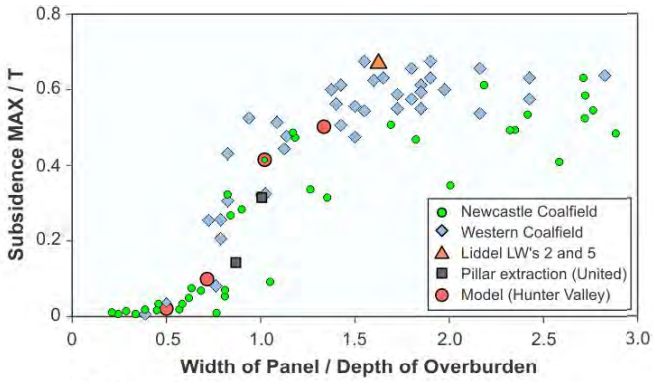

a) General Relationship.

w/d = 0.5

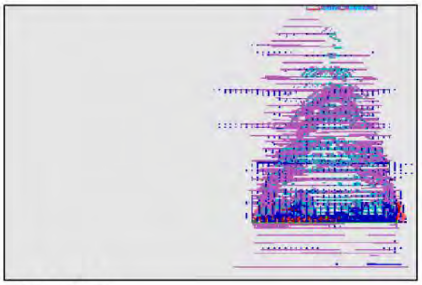

w/d = 0.66

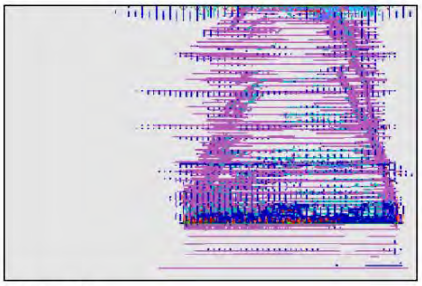

w/d = 1.0

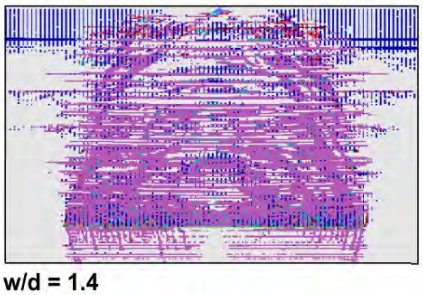

w/d = 1.4

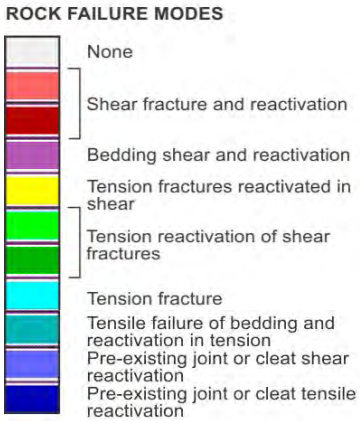

b) Modelled Strata Fracture.

Figure 4: Modelling of strata fracture and subsidence for various panel geometries compared to empirical subsidence data.

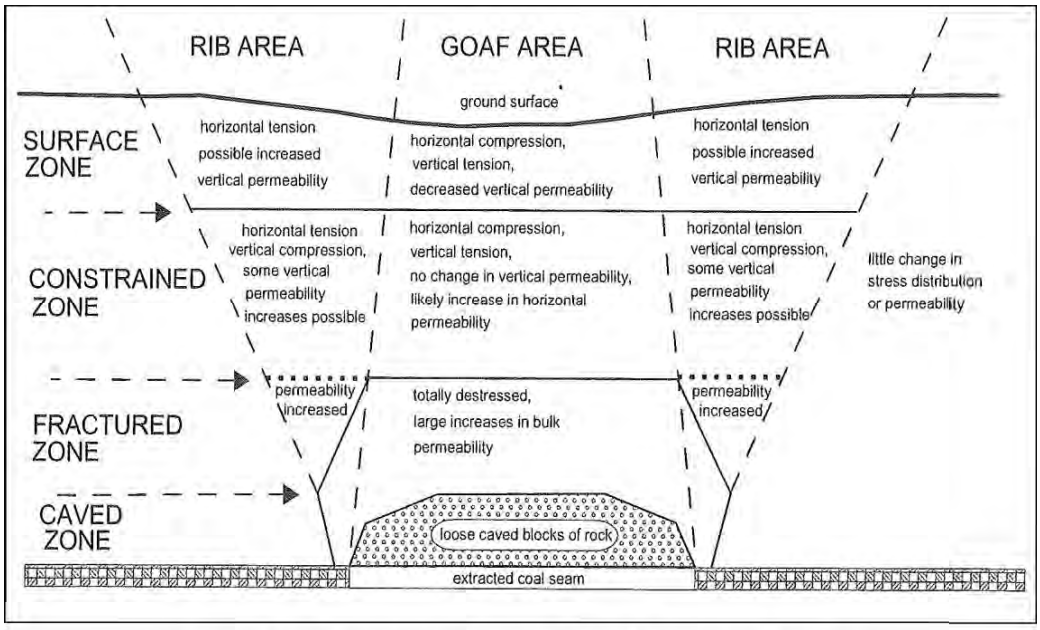

Figure 5: Conceptual zones above a longwall panel.
(From Foster and Enever 1992)

Geological factors also have an impact. It was found that the fracture connectivity was greater in stiff sandstone rich strata relative to strata having many coal and tuffaceous units. This was related to the ability of the overburden to flex and displace onto the goaf rather than fracture and rotate about the ribsides.

Other geological variations have been noted where a significant thickness of clay material occurs. In this case the clay may have the effect of constraining the fracture network either due to the fact that it can strain without fracturing or it is able to heal fractures by expansion of the clay. The nature of this is likely to be site specific and dependent on the clay material.

Gale (2008) found that a constrained zone within the overburden formed where the average conductivity above the extraction panel was less than approximately 10^{-6} m/s. The nature of the overburden under these situations is similar to the concept of a constrained zone forwarded by Forster and Enever. These conditions exist for certain combinations of subsidence and depth as shown in Figure 6. However, as the amount of subsidence increases, or depth decreases the conductivity of the overburden increases to the point whereby a constrained zone cannot form and significant depressurisation of the overburden occurs. Where the overburden conductivity is greater than approximately 10^{-3} m/s significant impact on natural streams and aquifers has been experienced.

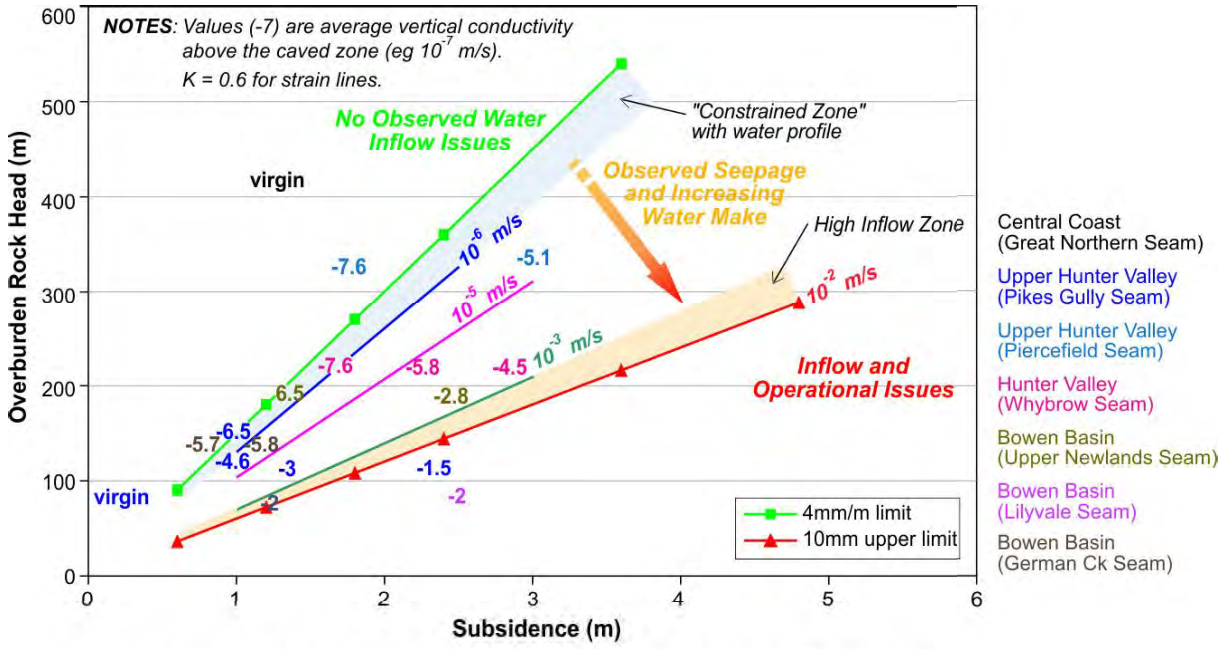

Figure 6: Overburden conductivity above longwall panels.

3.5 General Overburden Conductivity

The conductivity of the overburden has been assessed in detail in Gale (2008) compiling measured and modelled data to produce a trend relating subsidence and overburden depth to conductivity. A summary of the findings are presented In Figure 6. It was found that for a consistent overburden rock head, increased subsidence relates to an increase in average vertical conductivity of the overburden.

For Tahmoor South where the overburden is generally 390m and the maximum subsidence is expected to be approximately 0.9-1.6m then the graph estimates the average vertical conductivity to surface to be at in situ levels, less than $1x10^{-7}$m/s. This estimate relates to a single panel.

3.6 Zone of Total Depressurisation

The zone of total depressurisation has been assessed by Tammetta (2012) where data from numerous mine sites has been compiled producing a trend to determine height of complete groundwater drainage taking into account depth, panel width and extraction height. The relationship is presented in Figure 7 with the height on the y axis and a function of the depth, panel width and extraction height on the x axis.

Using Tammetta's relationship for Tahmoor South with an overburden depth of 390m, an extraction height of 2.5m and panel width of 300m, U = 3568, which equates to a total depressurisation height of 210m. The overburden depth increases to the northeast where depths range up to 460m. Figure 8 shows a contour plot of the height of total depressurisation using Tammetta's relationship. The height of total depressurisation is generally 208-210m, however it increases to approximately 216m in the northeast at the greater depths.

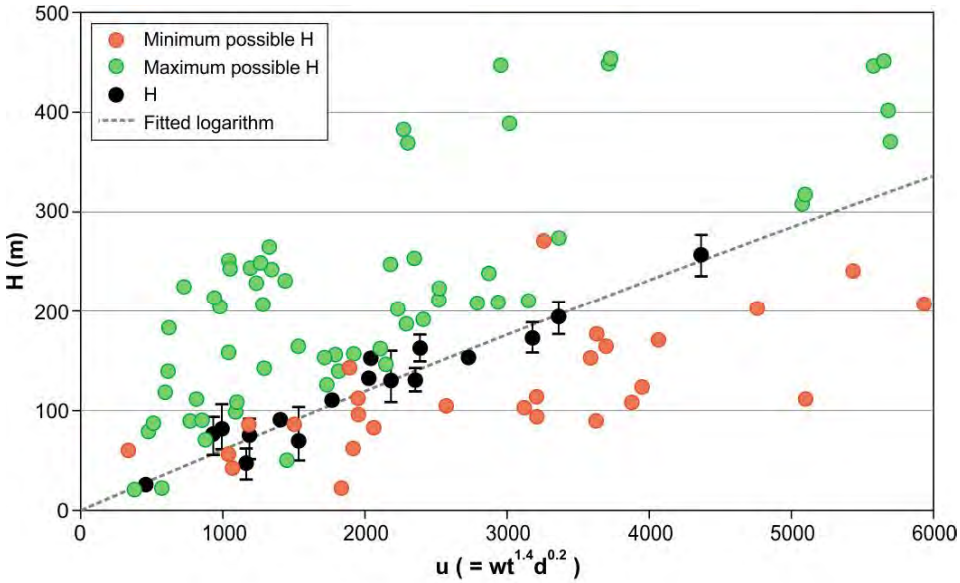

Figure 7: Estimation of the height of total depressurisation above a longwall panel (Ref: Tammetta, 2012).

4. GEOTECHNICAL CHARACTERISATION

Tahmoor Coal provided the lab testing results for 26 HQ cored boreholes from the Tahmoor South area. Rock testing has a number of objectives including, but not limited to, the following:

- To provide characterisation of the range of rock types in the stratigraphic profile.
- To compliment the hydrological packer and perm testing data.
- To enable correlation of rock strength with geophysics (sonic velocity).
- To capture the variability in rock geotechnical properties across the mine lease.
- To provide suitable geotechnical properties for further design analysis.

There were a total of 269 sedimentary rock samples tested at Strata Testing Services. Results collated for the current dataset comprised of data from the following test methods:

- Uniaxial Compressive Strength (UCS) – 177 tests.
- Multi-Stage Triaxial Compression – 92 tests.

Young's Modulus, moisture content, and density were also calculated for each sample.

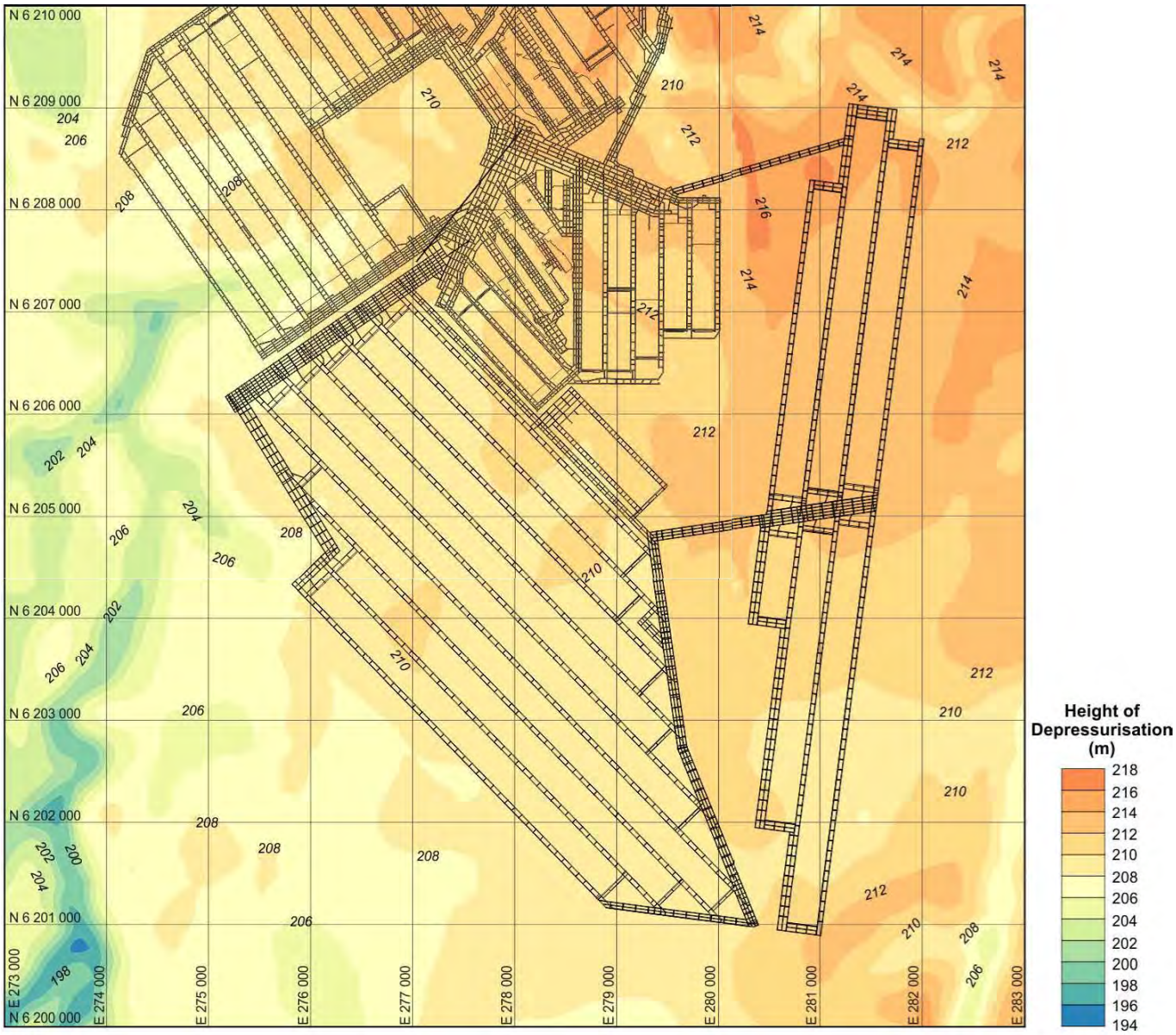

Figure 8: Contours of height of total depressurisation using the Tammetta (2012) relationship.

The samples tested represented the range of rock types present in the Tahmoor sequence. In total 87 sandstone (14 interbedded sandstone samples), 13 siltstone (3 interbedded siltstone samples), 96 mudstone, 23 shale, 13 coal, 14 tuffaceous and 6 claystone samples were tested by the lab.

4.1 Unconfined Compressive Strength

SCT compiled the tri-axial test data with the UCS test data to make a comprehensive dataset of all rock tests. The tri-axial test data was extrapolated to zero confinement to estimate the UCS for the tri-axial samples. The complete dataset consists of 269 samples.

A histogram of the UCS results is presented in Figure 9. The UCS results range from 19.9MPa to 151.6MPa. 80% of the samples range between 35-90MPa while 60% of the samples range between 40-75MPa.

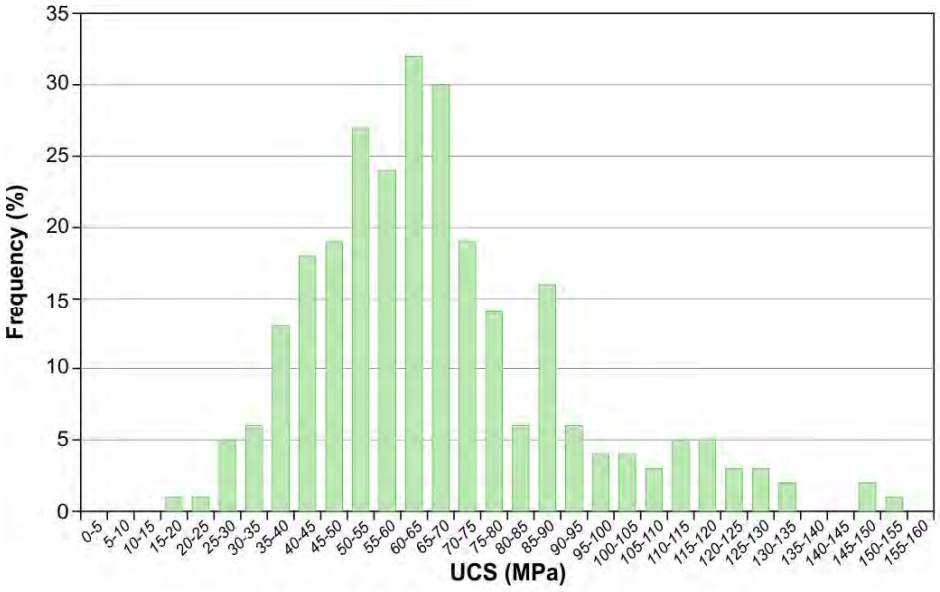

Figure 9: Frequency histogram showing UCS distribution.

The UCS depth profile for the Tahmoor South samples is presented in Figure 10a where a scatter of data exists due to the small depth range of 340m to 470m. Figure 10b shows a cluster of sampling in the immediate roof and floor of the Bulli Seam in addition to a larger number of samples in the 20m Bulli Seam roof than the scatter of samples below the Bulli Seam. There does appear to be a UCS trend with overburden depth or relative stratigraphic location to the Bulli Seam. Figure 10c includes borehole TNC046B from the Tahmoor North area with samples covering the full overburden depth profile. From this one borehole, a reduction in strength is not evident until approximately the top 100m.

Rock strength characterised by lithology is presented in Figure 11. There is no obvious trend where rock strength reduces with a reduction in grain size, however the UCS for sandstone and siltstone is on average higher than the shale, mudstone and claystone UCS averages. Tuff in the Southern Coalfield is generally tuffaceous sandstone whereby the strength is typically similar to that of sandstone as observed here. Mudstone and Sandstone show a large range in UCS corresponding with the largest number of samples for that rock type. Coal shows a strength range of 25-65MPa.

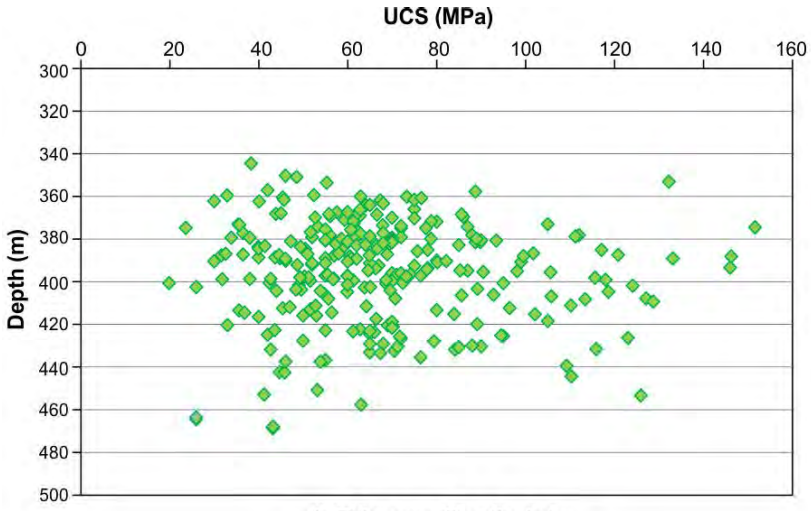

a) Tahmoor South data.

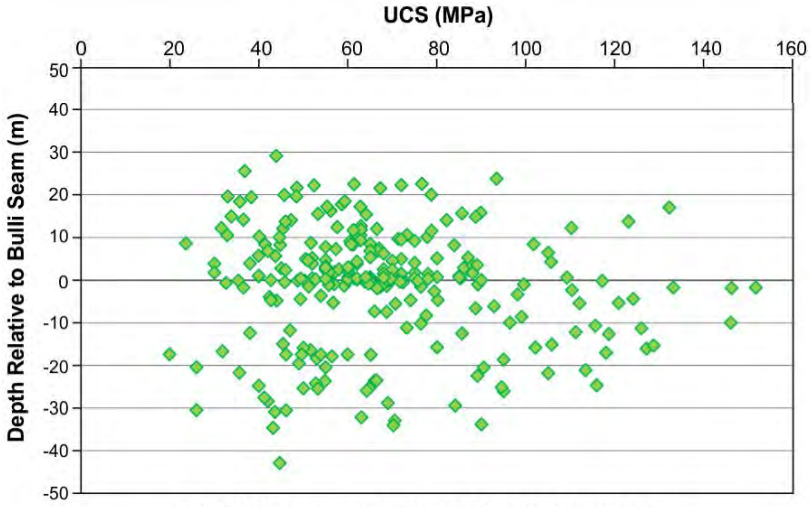

b) UCS versus depth relative to Bulli Seam.

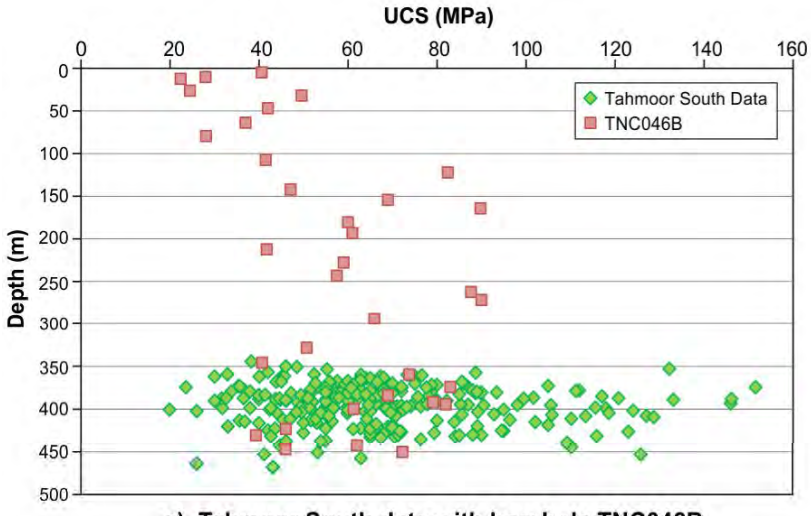

c) Tahmoor South data with borehole TNC046B.

Figure 10: UCS depth profile.

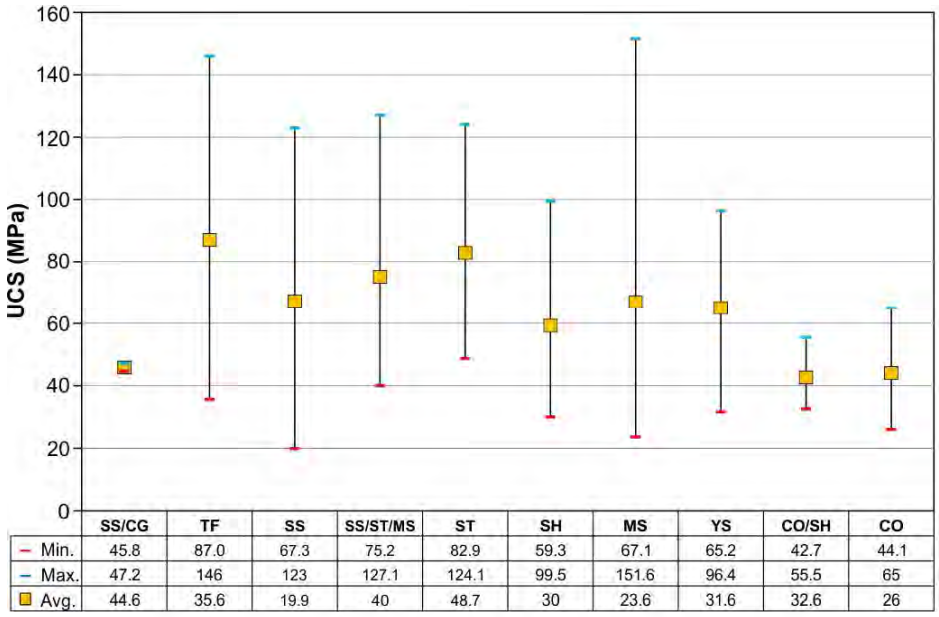

	SS/CG	TF	SS	SS/ST/MS	ST	SH	MS	YS	CO/SH	CO
Min.	45.8	87.0	67.3	75.2	82.9	59.3	67.1	65.2	42.7	44.1
Max.	47.2	146	123	127.1	124.1	99.5	151.6	96.4	55.5	65
Avg.	44.6	35.6	19.9	40	48.7	30	23.6	31.6	32.6	26

Figure 11: Relationship between UCS and lithology.

4.2 Rock Modulus – Youngs Modulus

The elastic modulus of the rock is a measure of its stiffness. The modulus and UCS relationship is presented in Figure 12. There is a general trend of increasing modulus where UCS in MPa is between 4 and 5 times the modulus in GPa. The trend can also be address as modulus as the subject:

$$E\ (GPa) = 0.2359 \times UCS\ (MPa)$$

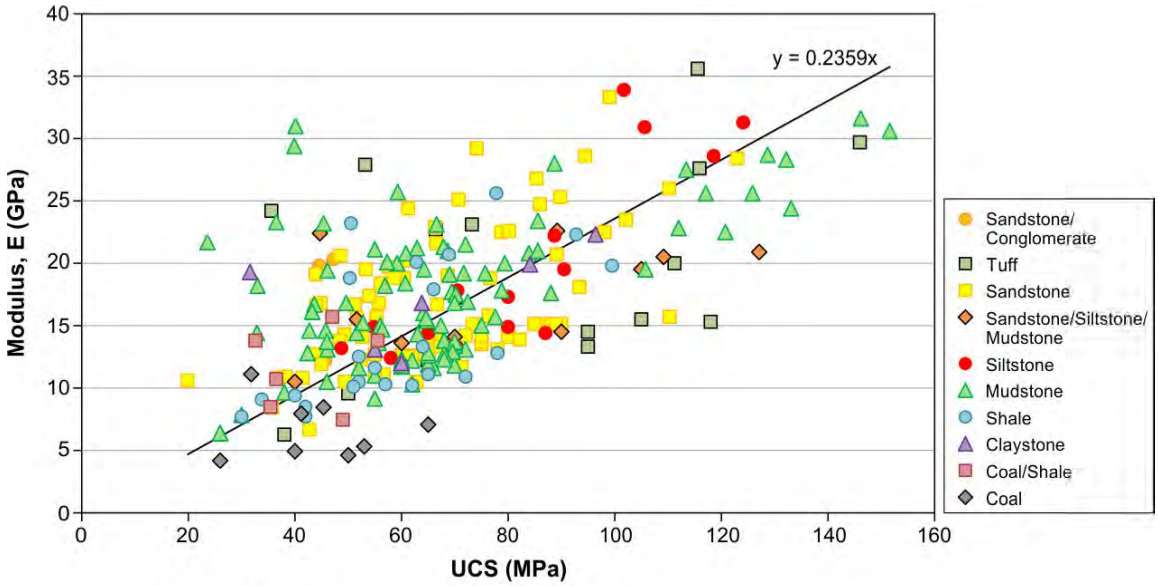

Figure 12: Relationship between UCS and Modulus, E.

Rocks with a higher ratio of modulus to UCS have the potential to fail earlier than other strata, as they will attract more horizontal stress and have a lower UCS. The interbedded sandstone/conglomerate, shaly coal and higher strength siltstones above 100MPa exhibit this higher modulus to UCS ratio. The higher strength sandstones above 100MPa have the opposite characteristics of higher strength with lower modulus and stress.

4.3 Moisture Content

The relationship between the moisture content and UCS is presented in Figure 13. The figure shows and inverse relationship between moisture content and UCS whereby the higher the moisture content the weaker the sample. Generally samples with more than 3% moisture content are less than 50MPa UCS. Inversely, samples greater than 100MPa in UCS have less than 2% moisture content.

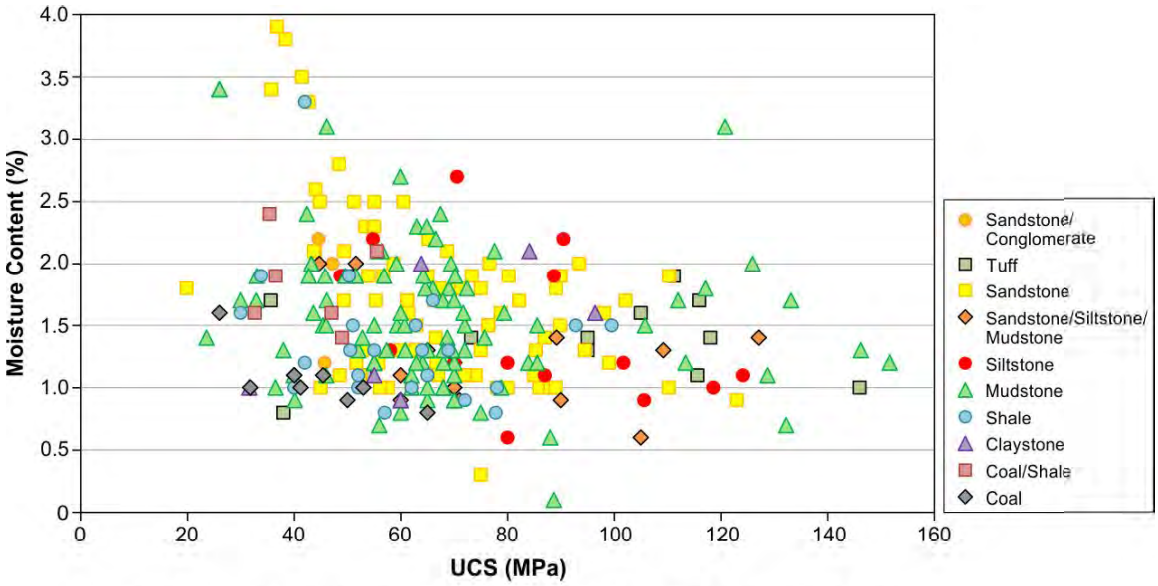

Figure 13: Relationship between UCS and moisture content.

4.4 Sonic Velocity and UCS Correlation

Sonic velocity and UCS have a correlation whereby the UCS generally increases exponentially with sonic velocity. This relationship can be used with the sonic velocity obtained from borehole geophysical logs to create a UCS profile of the borehole.

The field sonic velocity data was translated from geophysical logs of sonic transit time. Sample intervals on lithological boundaries with more than 10% variance were not included in the analysis, nor were tuff unit or coal units and the trend relies on the grain to grain contact in clastic rocks. 152 samples met the conditions for inclusion into the sonic velocity and UCS relationship.

The sonic velocity and UCS relationship is presented in Figure 14, where the coal samples have been plotted, however excluded from the analysis. The Tahmoor South exponential trendline of the current dataset, together with SCTs Southern Coalfield trendline shows that Tahmoor South data is in line with the general trend of the Southern Coalfield. The exponential relationship between laboratory UCS and field sonic is as follows:

Inferred UCS (MPa) = 2.3271 x Exp (0.0008 x sonic velocity (m/s))

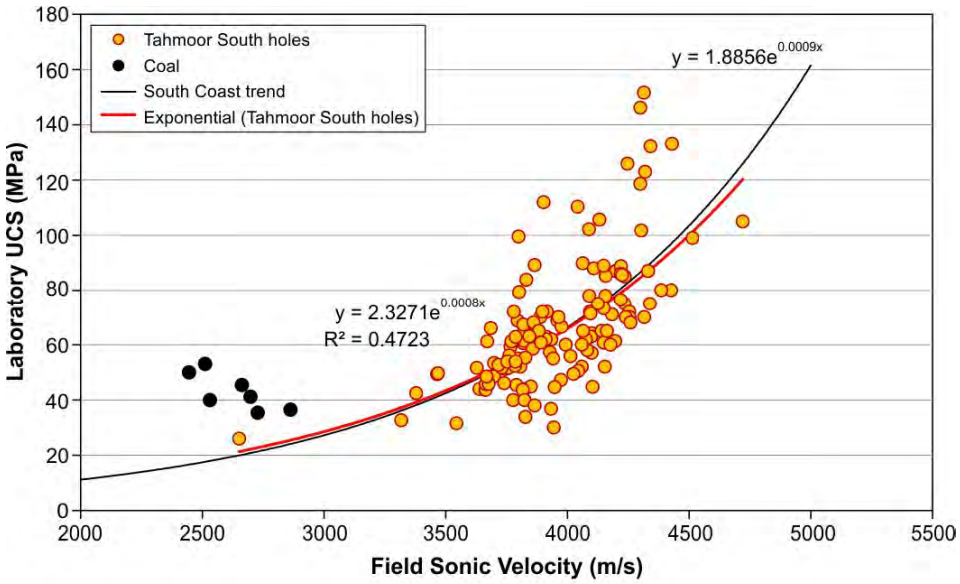

Figure 14: Relationship between UCS and sonic velocity.

The correlation between laboratory UCS and inferred UCS using the exponential relationship is presented in Figure 15. A perfect relationship would be on the 1:1 line. The exponential trend provides a reasonable correlation of the dataset for less than 90MPa laboratory UCS where the data is with 20MPa of the laboratory UCS. Above 90MPa laboratory UCS, the exponential trend can underestimate the inferred UCS, with only 2 of the 13 samples plotting within the 20MPa error band.

4.5 Tri-axial Strength Testing of Intact Material

The tri-axial test method used was a multi-stage tri-axial test whereby a single sample is tested at varied confining pressures to obtain the intact and residual failure envelopes. Confining pressure stages of 2MPa, 5MPa and 10MPa were used on the samples, where at each stage the sample is loaded to near failure and then loaded until failure at the last stage.

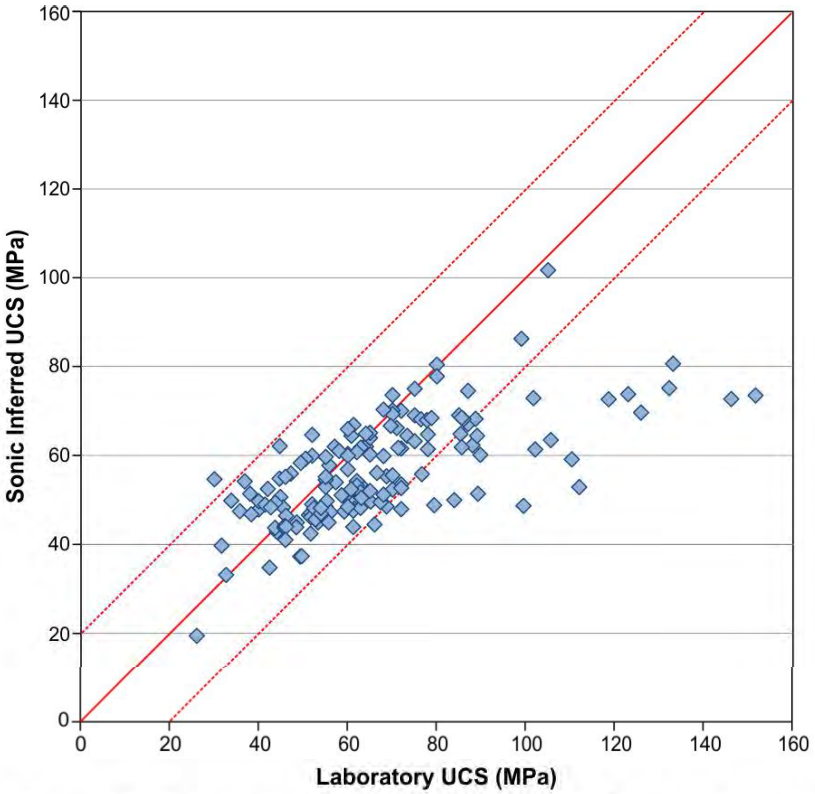

Figure 15: Relationship between laboratory UCS and inferred UCS.

Intact material friction angle and cohesion has been analysed from the tri-axial test results to define the ability of a material to gain strength with confinement. The friction angle and cohesion has been plotted in relation to the rock type in Figure 16 and Figure 17, respectively.

The friction angle dataset for Tahmoor South ranges between 31 and 48°. This friction angle dataset is relatively high and relates to the high strength dataset at Tahmoor.

The greater the friction angle, the greater strength the rock gains with confinement. A friction angle of 20° corresponds with 2 times the strength for every 1MPa confinement, while a friction angle of 30° corresponds with 3 times the strength for every 1MPa confinement. This trend is not linear as a friction angle of 37° corresponds with 4 times the strength for every 1MPa confinement.

The cohesion is a measurement of matrix cementation. There is a general trend of reducing cohesion with grain size where sandstone has on average 17.5MPa cohesion, followed by siltstone with 16.8MPa, mudstone 15.4MPa and claystone 13.2MPa.

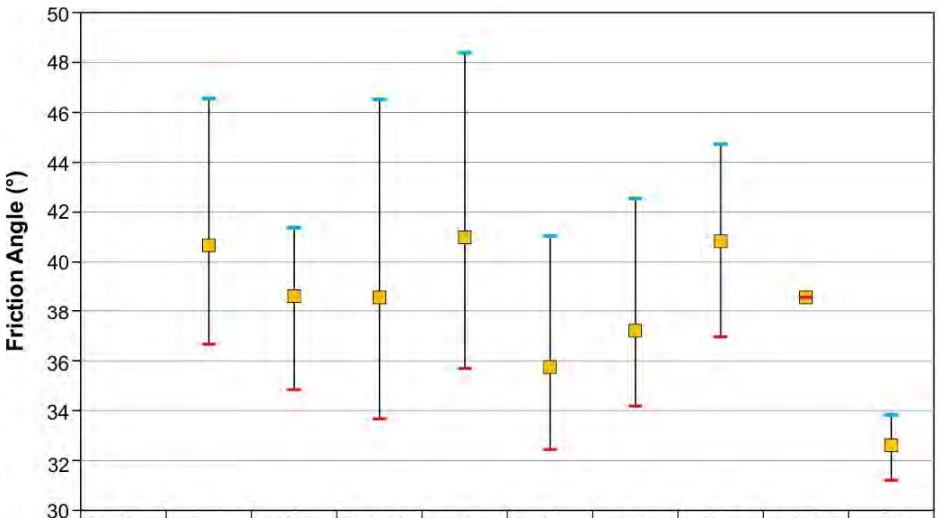

	SS/CG	TF	SS	SS/ST/MS	ST	SH	MS	YS	CO/SH	CO
Min.	0.0	40.7	38.6	38.6	41.0	35.7	37.2	40.8	38.6	32.6
Max.	0.0	46.6	41.4	46.5	48.4	41.0	42.5	44.7	38.6	33.8
Avg.	0.0	36.7	34.8	33.7	35.7	32.4	34.2	36.9	38.6	31.2

Figure 16: Relationship between friction angle and lithology.

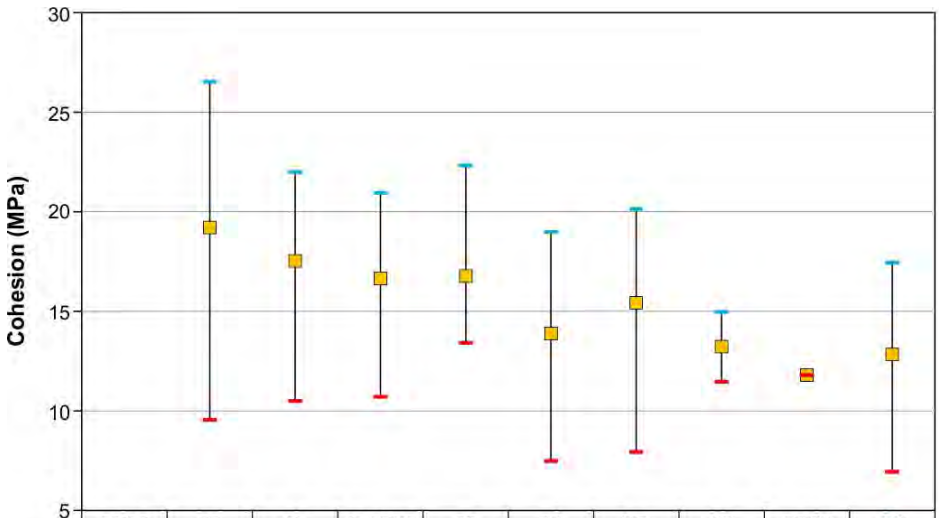

	SS/CG	TF	SS	SS/ST/MS	ST	SH	MS	YS	CO/SH	CO
Min.	0.0	19.2	17.5	16.6	16.8	13.9	15.4	13.2	11.8	12.8
Max.	0.0	26.5	22.0	20.9	22.3	19.0	20.1	15.0	11.8	17.4
Avg.	0.0	9.5	10.5	10.7	13.4	7.5	7.9	11.5	11.8	6.9

Figure 17: Relationship between cohesion and lithology.

4.6 Stress Field

The stress field is typically dominated by the major principal stress being horizontal. Stress measurements within Tahmoor North mine show a variable direction of the major principal stress, however it is typically N-NE to NNW. The variation in direction is related to structural domains. The vertical stress is related to the overburden load and is typically 0.025 *depth (m) in MPa. The intermediate stress is also horizontal and oriented at 90° to the maximum principal stress.

The stress field in Tahmoor South is also somewhat variable but the dominant direction of the major horizontal stress is NW-SE. The direction of the major horizontal stress as determined from acoustic scanner data, compiled by Gordon (2013), is presented in Figure 18. This shows the data for both the northern and southern areas.

The ratio of the maximum horizontal stress to minimum horizontal stress is likely to be variable but in general on the basis of stress measurements in the area, undertaken by Sigra and SCT, would be expected to be approximately 1.5:1.

On the basis of stress measurements by SCT and Sigra (Sigra 2013) the maximum tectonic stress factor for strata about the Bulli Seam would be expected be variable but typically range from 0.8 to 1.

The magnitude of the major horizontal stress throughout the overburden sequence is discussed in Section 8 and the general trend anticipated is presented in Figure 45.

4.7 Rock Mass Discontinuities

The discontinuities within the rock mass are joint and bedding partings.

The jointing within the overburden has been determined from acoustic scanner data (ASIMS 2012). The detailed joint patterns that relate to particular boreholes are contained in Appendix 1. In general the joint pattern is consistent over the area. The joint data is presented in Figure 19 and indicates that the joint sets are typically vertical and strike NW-SE and NE-SE. Joint sets have been defined and presented in Figure 20.

Bedding parting planes were a common discontinuity within the rock mass. In general they are horizontal as depicted in Figure 19.

5. HYDRAULIC CONDUCTIVITY REVIEW

The hydraulic conductivity of the overburden is relevant to mining issues including groundwater and environmental assessments, mine inflow and gas drainage. An understanding of in situ overburden conductivity is necessary to understand the mining impacts from longwall extraction and caving. The hydraulic conductivity data is used as inputs into regional groundwater models and more localised longwall caving models.

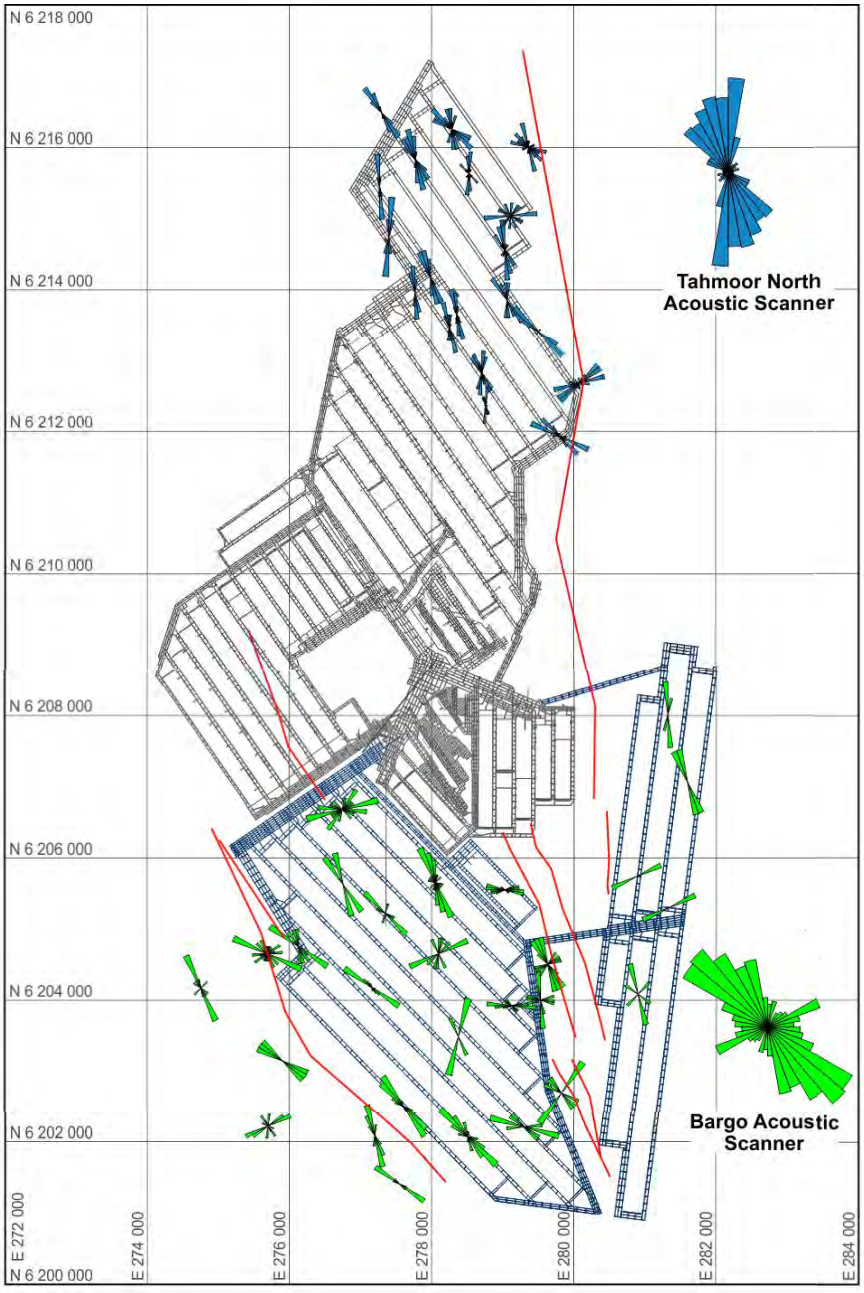

Figure 18: Summary of horizontal stress direction from acoustic scanner. *(Gordon 2013).*

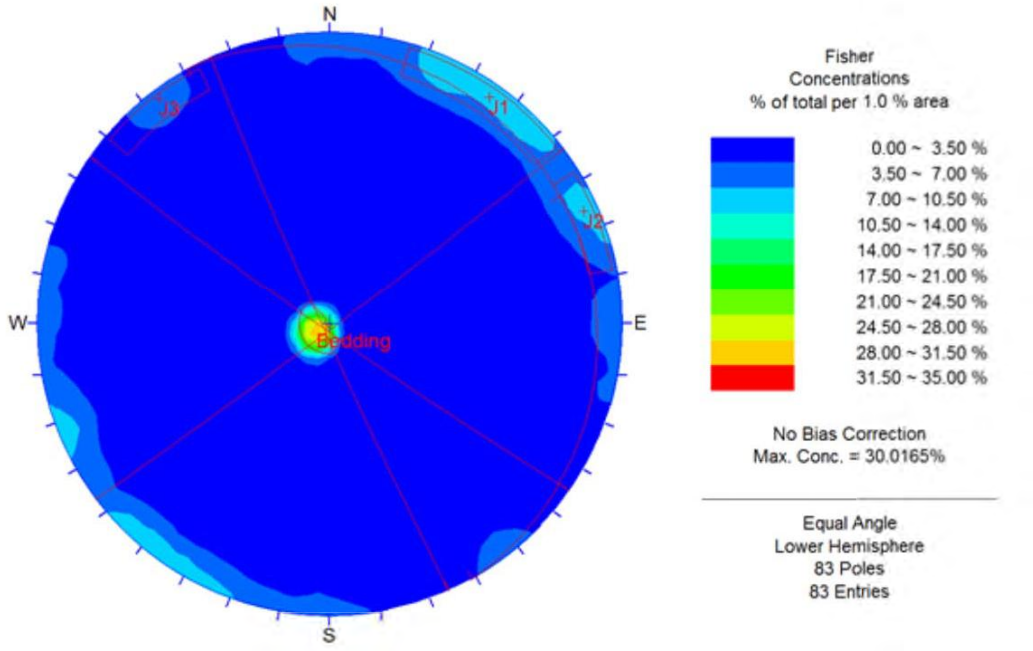

Figure 19: Contour diagram of all discontinuities detected by acoustic scanner.

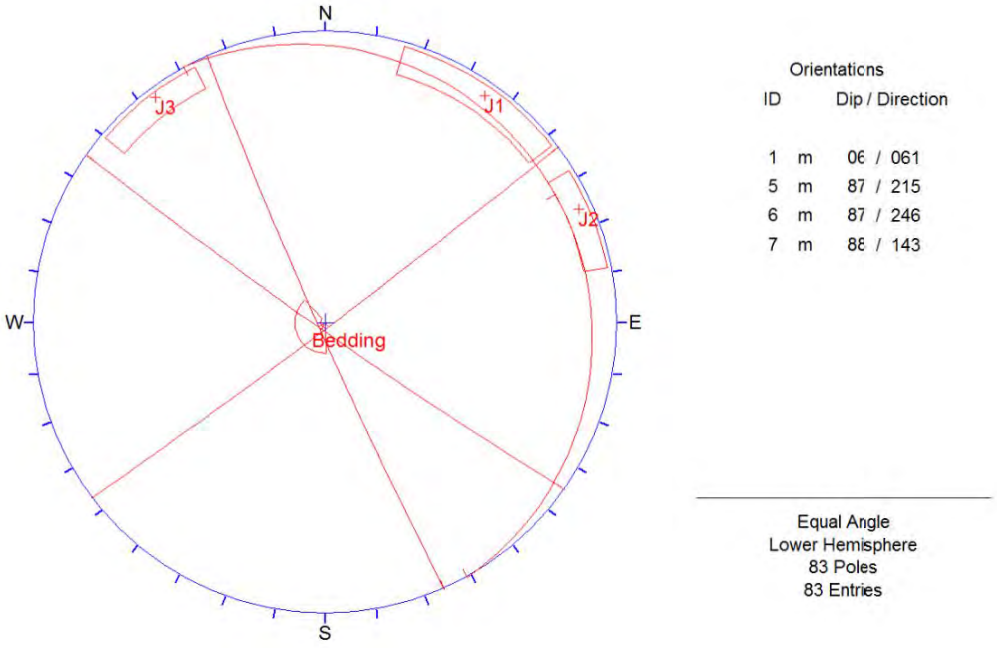

Figure 20: Dominant discontinuity sets detected by acoustic scanner.

The hydraulic conductivity of the overburden has been characterised with core permeability testing and lugeon style borehole packer testing. Core permeability testing measures the primary permeability of the rock, where in this case small (2cm diameter) cores were sub-cored from HQ core, and tested in a laboratory. The core permeability results were provided to SCT by Tahmoor Coal. The lugeon style packer testing is a test of the secondary permeability or the hydraulic conductivity of the rock fabric and the fracture network which intersects the test interval. The borehole packer testing was conducted by SCT under instruction by Tahmoor and third party groundwater consultants.

5.1 Hydraulic Conductivity of Core Samples

The core samples were tested to obtain both horizontal and vertical permeability.

The term conductivity and permeability are used interchangeably in this section.

Samples were selected from non coal stratigraphic units from the Hawkesbury Sandstone through to below the Tongarra Seam. The core permeability results are summarised for each stratigraphic unit in Table 1 and Figure 21. The stratigraphic units are presented where the uppermost unit is on the left of the graph and sequentially to the right the lower stratigraphic units are plotted. There is a general trend where the conductivity reduces with the lower stratigraphic units. The step trend observed also coincides with a change in source material for the rock unit from lithic in the Permian units to quartz in the Triassic units. This change in source material also coincides with a change in the matrix material therefore giving lower primary porosity in the Permian strata.

The range in permeability results for each stratigraphic unit coincides with the number of samples taken in that unit. The Bulgo Sandstone and Scarborough Sandstone consisted of 6 and 5 samples respectively and the results ranges approximately 4 orders of magnitude. The Wombarra Claystone consisted of 3 samples while the remaining units consisted of 1 or 2 samples each. The Bald Hill claystone had 10 samples tested.

Due to the nature of the core permeability testing where a relatively small sample is tested, and due to the nature of lithological variability in a rock unit, the permeability test result is highly dependent on the sedimentary bed that was subcored for testing. Therefore this can produce high variability in the results with the testing of more samples. However, if testing a significant number of samples, the results can give a good indication of the range in permeability for that unit.

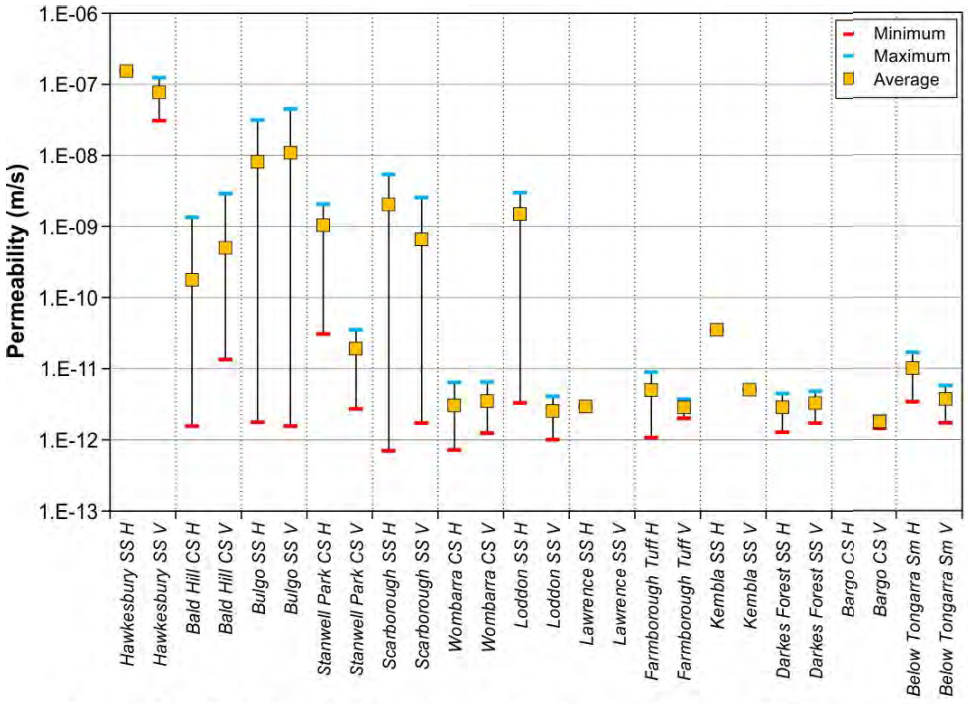

Figure 21: Relationship between core permeability and stratigraphic unit.
Note: horizontal and vertical permeability are not differentiated.

Table 1: Core permeability results summary

Stratigraphic Unit	Permeability (m/s)			No. of Samples
	Maximum	Minimum	Average	
Hawkesbury SS H	1.6E-07	1.5E-07	1.5E-07	2
Hawkesbury SS V	1.2E-07	3.1E-08	7.7E-08	2
Bald Hill CS H	1.6E-09	1.7E-12	2.9E-10	10
Bald Hill CS V	6.6E-09	2.0E-11	8.1E-10	10
Bulgo SS H	3.1E-08	1.8E-12	8.2E-09	6
Bulgo SS V	4.5E-08	1.5E-12	1.1E-08	6
Stanwell Park CS H	2.0E-09	3.1E-11	1.0E-09	2
Stanwell Park CS V	3.5E-11	2.7E-12	1.9E-11	2
Scarborough SS H	5.4E-09	6.9E-13	2.0E-09	5
Scarborough SS V	2.5E-09	1.7E-12	6.6E-10	5
Wombarra CS H	6.4E-12	7.2E-13	3.0E-12	3
Wombarra CS V	6.4E-12	1.2E-12	3.5E-12	3
Loddon SS H	3.0E-09	3.3E-12	1.5E-09	2
Loddon SS V	4.1E-12	1.0E-12	2.5E-12	2
Lawrence SS H	2.9E-12	2.9E-12	2.9E-12	1
Lawrence SS V				
Farmborough Tuff H	8.9E-12	1.1E-12	5.0E-12	2
Farmborough Tuff V	3.7E-12	2.0E-12	2.8E-12	2
Kembla SS H	3.5E-11	3.5E-11	3.5E-11	1
Kembla SS V	5.0E-12	5.0E-12	5.0E-12	1
Darkes Forest SS H	4.4E-12	1.3E-12	2.8E-12	2
Darkes Forest SS V	4.8E-12	1.7E-12	3.2E-12	2
Bargo CS H				
Bargo CS V	2.1E-12	1.4E-12	1.8E-12	2
Below Tongarra Sm H	1.7E-11	3.4E-12	1.0E-11	2
Below Tongarra Sm V	5.7E-12	1.7E-12	3.7E-12	2

H=Horizontal permeability V=vertical permeability

The conductivity of the Bald Hill claystone samples show a large variation but similar to the other Permian rock units. The Hawkesbury Sandstone displays the greatest permeability of approximating $1x10^{-7}$m/s to $1x10^{-8}$m/s. The Bulgo Sandstone shows a large variation in results however the mean is approximately $1x10^{-8}$ m/s. The Stanwell Park Claystone and Scarborough Sandstone shows an upper permeability of about $1x10^{-9}$m/s. The remaining units all show primary permeability in the order of 1x10-11m/s to 1x10-12m/s. The vertical permeability within the Loddon Sandstone is low however one test of the horizontal permeability provided a result of $2X10^{-9}$ m/s which has extended the range.

Overall, the results show that the permeability of the rock fabric is variable but within the range anticipated from regional information.

5.2 Lugeon Style Packer Testing Conductivity

The aim of lugeon style borehole packer testing is to determine the hydraulic conductivity of the strata throughout the stratigraphic sequence. This conductivity characterises the conductivity of the rock fabric and the fracture network within the test horizons throughout the overburden. 449 packer tests were conducted over 29 boreholes in the Tahmoor South area.

The tests conducted covered all stratigraphic horizons from the Hawkesbury Sandstone to the Wilton Formation. The lugeon test results are summarised for each stratigraphic unit in Table 2 and Figure 22. Zero conductivity denotes the lower limit of this style of test which is of the order of $1x10^{-11}$m/s. The units higher in the stratigraphic sequence including the Hawkesbury Sandstone, Bald Hill Claystone and Bulgo Sandstone, have upper conductivity bounds approximately ranging from $1x10^{-7}$m/s to $1x10^{-5}$m/s, while the non coal units below this have upper bounds ranging $1x10^{-9}$m/s to $1x10^{-8}$m/s. The target seams of the Bulli Seam and Lower Wongawilli Seam have test conductivities ranging from zero flow approximately $1x10^{-11}$m/s to $1x10^{-7}$m/s.

The large range in conductivity results for each unit is related to the nature of flow through the rock. The flow is facilitated by the fracture network and as such if a fracture or fracture network is not intersected in the test interval then the flow is likely to be reduced. This is somewhat dependent on the nature of the fabric permeability of the stratigraphic unit tested, whereby if the permeability is high then the lugeon test will determine flow within the fabric and any fractures which intersect the test interval.

5.3 Conductivity Depth Profile

The primary and secondary conductivity data can also presented in relation to overburden depth where every data point is plotted. Figure 23 shows the hydraulic conductivity data for all packer tests and core permeability tests in the Tahmoor South area. The packer test results show a distinct trend whereby the conductivity reduces with increasing overburden depth. Tests above 150-200m overburden depth show conductivity ranging from approximately $1x10^{-8}$m/s to $1x10^{-5}$m/s. Below 150-200m there is a change in

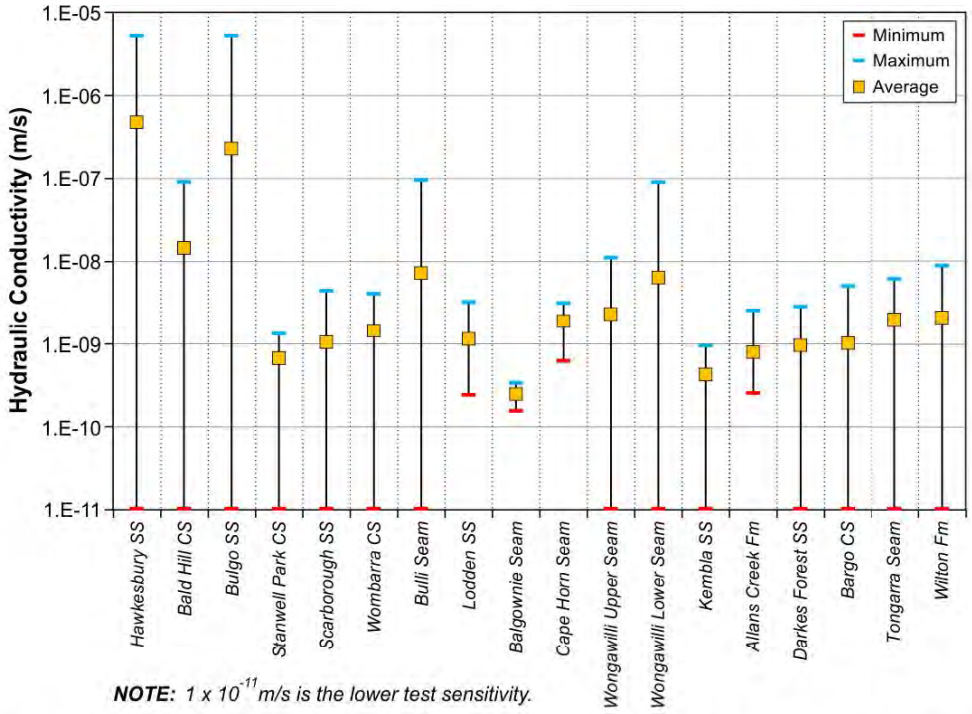

Figure 22: Relationship between packer test conductivity and stratigraphic unit.

Table 2: Summary of hydraulic conductivity from lugeon style packer testing

Stratigraphic Unit	Hydraulic Conductivity (m/s)			No. of Samples
	Maximum	Minimum	Average	
Hawkesbury SS	5.2E-06	1.0E-11	4.8E-07	134
Bald Hill CS	9.0E-08	1.0E-11	1.4E-08	13
Bulgo SS	5.2E-06	1.0E-11	2.3E-07	133
Stanwell Park CS	1.3E-09	1.0E-11	6.6E-10	2
Scarborough SS	4.3E-09	1.0E-11	1.0E-09	28
Wombarra CS	4.0E-09	1.0E-11	1.4E-09	12
Bulli Seam	9.5E-08	1.0E-11	7.2E-09	29
Loddon SS	3.2E-09	2.4E-10	1.1E-09	4
Balgownie Seam	3.3E-10	1.5E-10	2.4E-10	2
Cape Horn Seam	3.1E-09	6.1E-10	1.9E-09	2
Wongawilli Upper Seam	1.1E-08	1.0E-11	2.3E-09	10
Wongawilli Lower Seam	8.9E-08	1.0E-11	6.3E-09	29
Kembla SS	9.3E-10	1.0E-11	4.2E-10	6
Allans Creek Fm	2.5E-09	2.5E-10	7.8E-10	6
Darkes Forest SS	2.8E-09	1.0E-11	9.4E-10	11
Bargo CS	5.0E-09	1.0E-11	9.9E-10	10
Tongarra Seam	6.0E-09	1.0E-11	1.9E-09	11
Wilton Fm	8.7E-09	1.0E-11	2.0E-09	7

conductivity range, where positive flow tests (excluding $1x10^{-11}$m/s) have conductivities ranging from $1x10^{-10}$m/s to $1x10^{-8}$m/s. There is a transition at about 200-300m where the upper bound tests reach up to $1x10^{-7}$m/s.

The reduction in conductivity with depth is related to the increase in confining stress with depth. The step reduction at approximately 200m depth corresponds with 5MPa overburden load, which has been tested with laboratory experiments at the University of Wollongong where 5MPa has shown significant reduction in fracture conductivity.

The core permeability test results have also been plotted on Figure 23 and although some tests have shown higher permeability beds, the majority of core permeability results are less than $1x10^{-11}$m/s which corresponds with the no flow intervals of packer testing. This indicates that the conductivity of the sequence is facilitated by flow through a fracture network and that confining pressure has a large influence on the magnitude of conductivity.

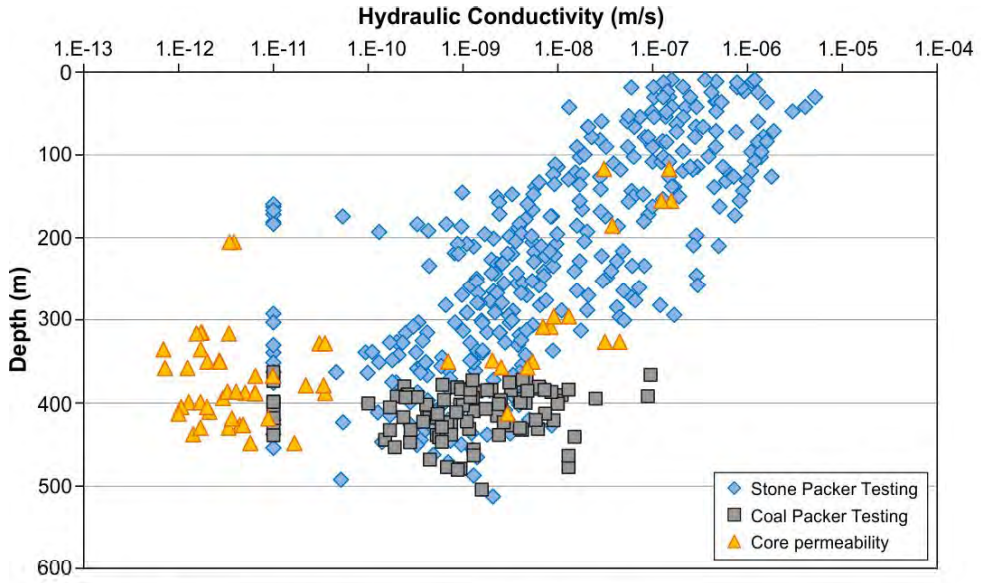

Figure 23: Relationship between overburden depth and hydraulic conductivity.

5.4 Fracture Conductivity

The previous sections detailing primary and secondary permeability have shown that the majority of flow through the rock is fracture facilitated flow. Here the fracture frequency is assessed to determine whether a relationship exists between fracture frequency and conductivity.

Figure 24 shows the packer test conductivity in relation to the number of fractures or defects in the test interval. These defects consist of faults, joints and bedding fractures. Fracture zones have also been logged which consist of a larger number of fractures in that interval or fault/shear zones that are brecciated or gouged. These are plotted as zone data.

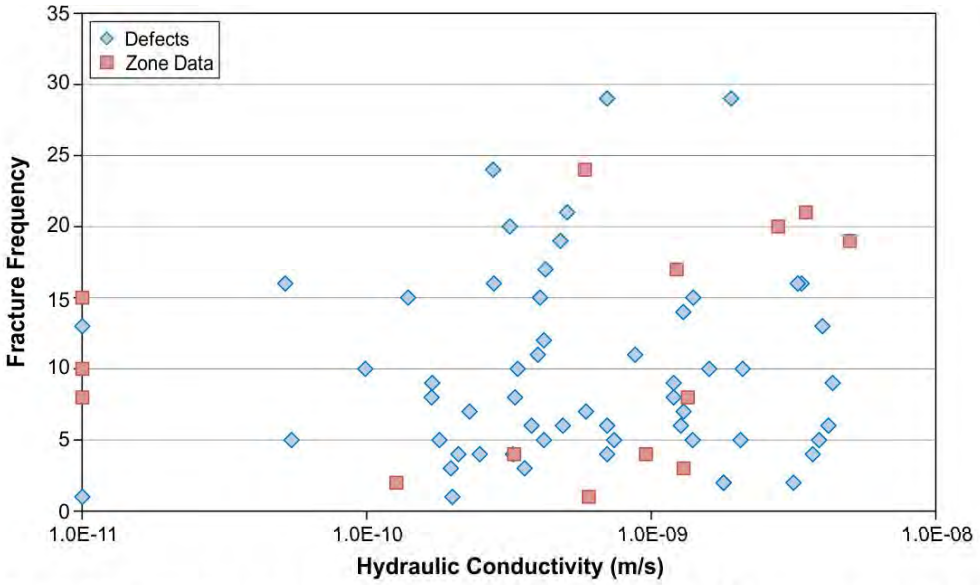

Figure 24: Relationship between fracture frequency and hydraulic conductivity.

There is no obvious relationship with fracture frequency and conductivity due to the variability in fracture characteristics. Fractures can exist and be closed by the confining pressure and therefore do not host any flow.

Therefore it can be summarised that although fractures are required to host flow, the conductivity is more influenced by the confining pressure on the fractures rather than the number of fractures in the interval.

6. PIEZOMETRIC PRESSURE OF TARGET SEAMS

The pore pressure profile is monitored using Vibrating Wire Piezometer (VWP) arrays throughout the stratigraphic profile. Typically an array consists of VWPs in the Wongawilli Seam, Bulli Seam, Scarborough Sandstone, the Bulgo Sandstone, Bald Hill Claystone and the Hawkesbury Sandstone.

The pore pressure in the Bulli Seam shows both in situ pore pressure and a region of reduced pore pressure around existing longwall panels of Tahmoor Mine. The Bulli Seam pore pressure contours for Tahmoor South are presented in Figure 25 and show the phreatic surface for the Bulli Seam pore pressure. Dummy points have been applied to the existing workings equating to zero pore pressure. The Wongawilli Seam phreatic surface is presented in Figure 26 and shows a similar trend to the Bulli Seam dipping to the North East.

The pore pressure contours are presented in relation to the Relative Level (RL) datum. At a distance from the Tahmoor Mine longwalls the pore pressure generally dips to the north east. The depressurised longwall panels impact an area around the longwalls as observed in boreholes located adjacent to the longwall panels. To determine the distance impacted by the reduced pore pressure, cross sections through the Bulli and Wongawilli Seam phreatic surfaces have been produced and are presented in Figure 27.

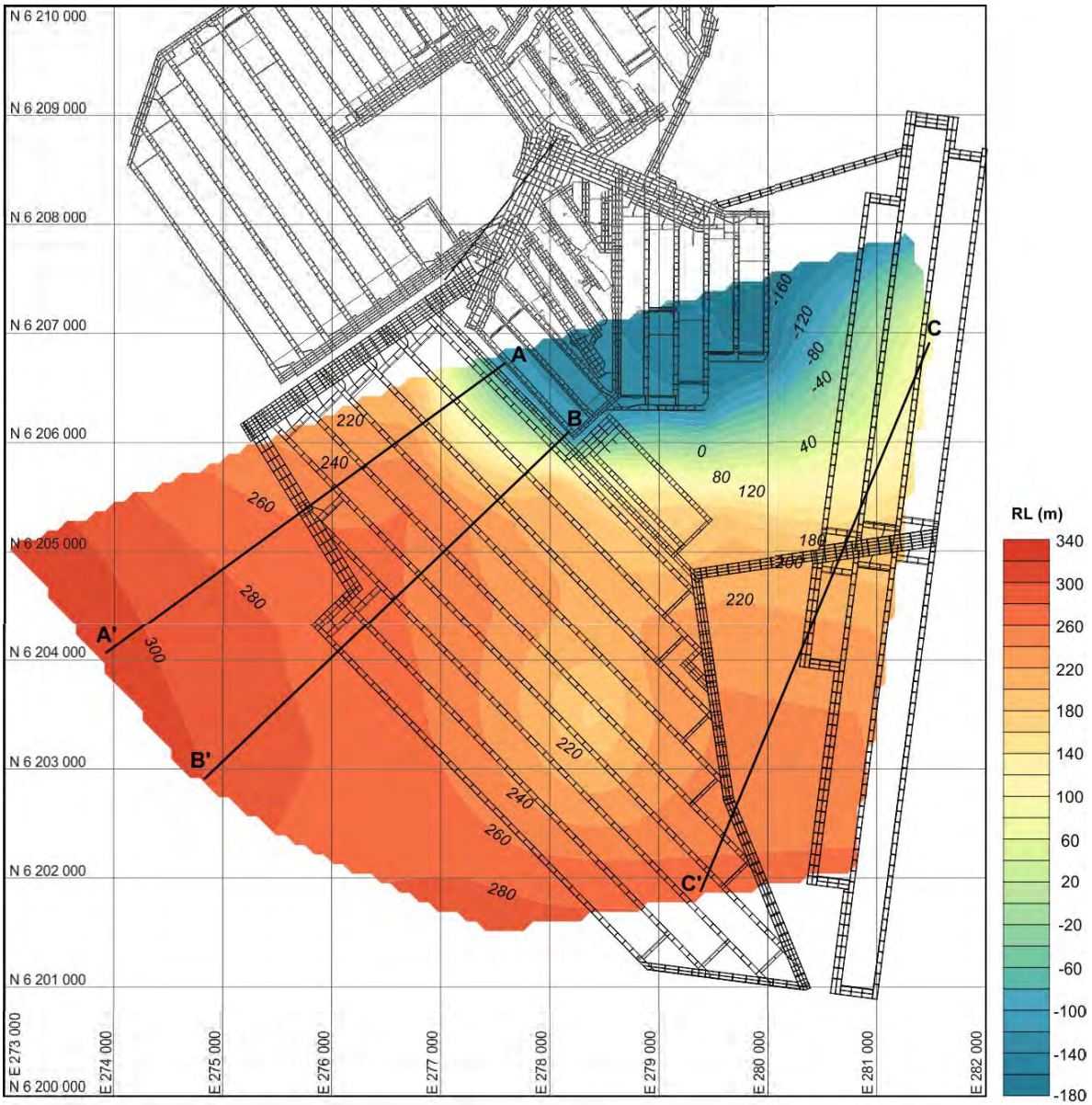

Figure 25: Bulli Seam phreatic surface based on Vibrating Wire Piezometer data.

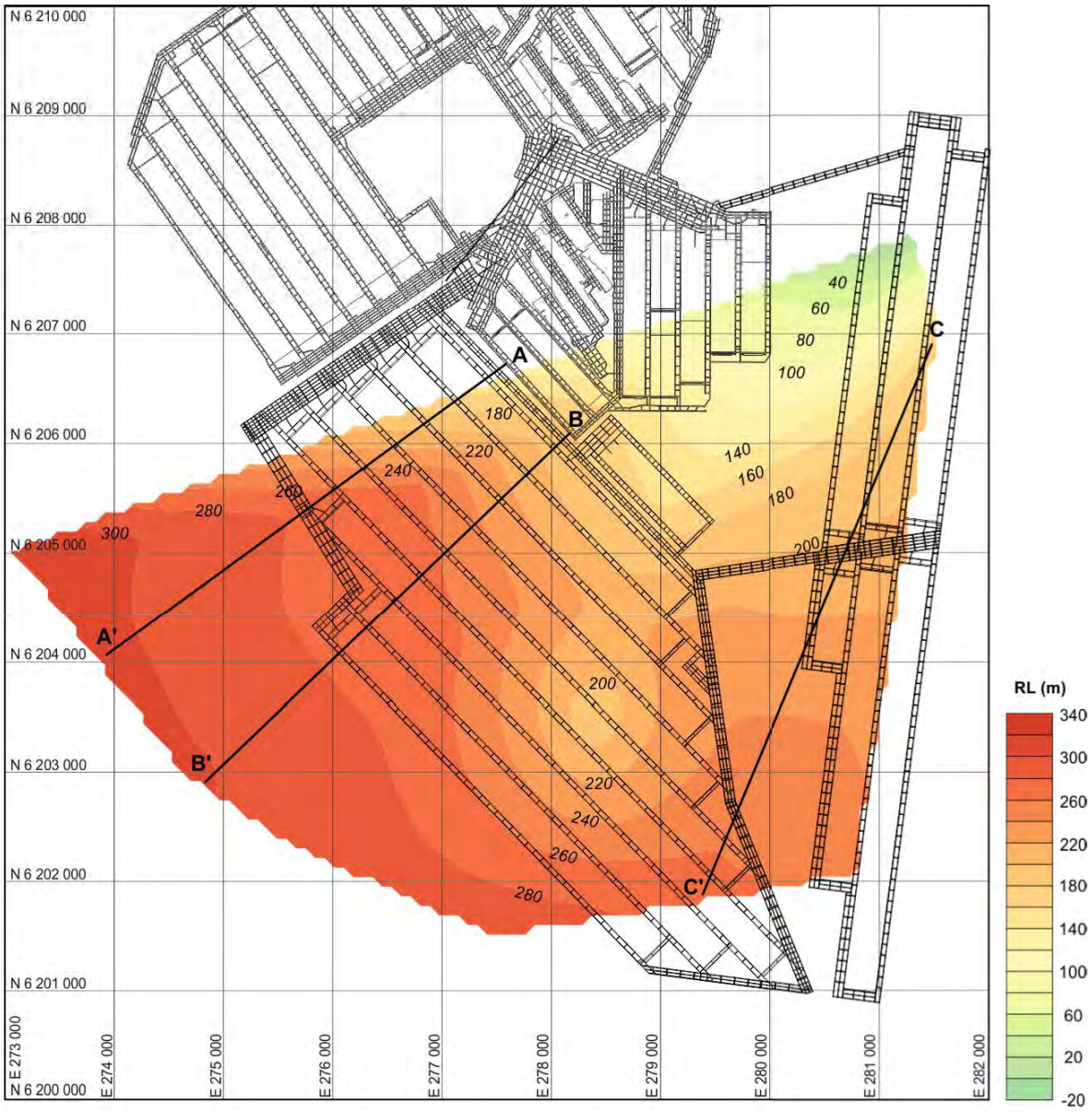

Figure 26: Wongawilli Seam phreatic surface based on Vibrating Wire Piezometer data.

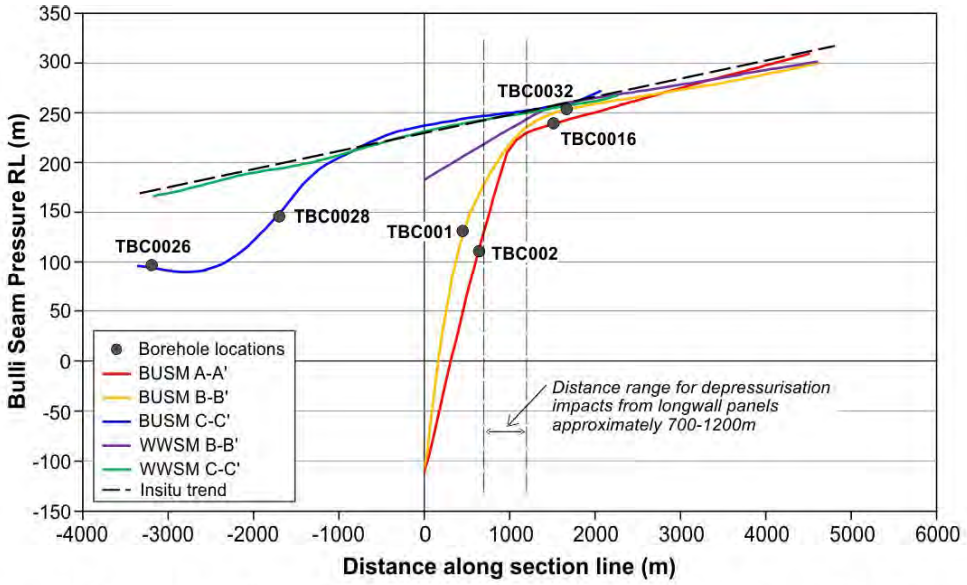

Figure 27: Cross sections through the Bulli and Wongawilli Seam phreatic surfaces.

The cross sections for both the Bulli and Wongawilli Seams show a phreatic surface trend with a consistent in situ dip. The dip in the Bulli Seam and Wongawilli Seam phreatic surfaces is evident where the phreatic surface drop is approximately 22m head over a 1km distance.

Cross sections A-A' and B-B' for the Bulli Seam show the in situ dip and then superimposed onto this dip is the drop in pressure adjacent to the existing Tahmoor Mine longwall panels. The impact of the pressure reduction is observed a distance of approximately 700m-1200m from the longwall. This range is due to the sparse boreholes making it difficult to constrain the data. There are no boreholes close enough to the east of the longwalls to constrain the drop in pore pressure adjacent to the eastern panels. The Wongawilli Seam B-B' cross section shows a drop in pore pressure below the existing longwall panels reacting to the pore pressure reduction in the Bulli Seam.

Cross section C-C' in the Bulli Seam at a distance from the longwall panels shows the general in situ trend of seam pressure with some variation to the north. It is unknown whether the drop in pressure off the in situ trend line is due to the mine depressurisation or due to local effects possibly from fault structures. However the Wongawilli Seam C-C' cross section does not show a deviation from the in situ trend and so it may be suggested that the Bulli Seam drop is more localised than an effect of longwall extraction.

6.1 APPROACH TO DETERMINE THE THREE DIMENSIONAL CONDUCTIVITY OVER THE TAHMOOR SOUTH AREA

The hydraulic conductivity of the rock mass is a key parameter for the estimation of water inflow about underground excavations. The conductivity of the rock mass is a combination of the conductivity of the rock fabric, bedding partings and joint planes (discontinuities) which exist in the overall rock mass.

Pre-existing discontinuities within rock mass can have a large contribution on hydraulic behaviour of the rock mass under moderate to low stress conditions. The magnitude of the stress will modify the aperture of the discontinuities, whereby at high stress the aperture is essentially closed and at low stress the aperture is open and related to the normal stiffness of the discontinuity.

Therefore, the geometrical properties of discontinuities and the stress field together with the conductivity of the rock fabric control the magnitude and orientation of hydraulic conductivity tensor.

Lugeon style packer test is the common field test for estimation of hydraulic conductivity of the rock mass, and a program of field measurement has been undertaken at Tahmoor South. These tests provide valuable information about average hydraulic conductivity (non directional), however the directional and anisotropic nature of hydraulic conductivity cannot be determined by packer test.

This section of the report represents a combination of the packer test results with an analytical investigation of the hydraulic conductivity of jointed rocks in the Tahmoor South area. The analytical approach is based on a method developed by Snow (1969). The analysis of packer tests provides valuable information about average conductivity at various depths and the relationship between conductivity and depth. The packer test results have been used to check the validation of results obtained from analytical method.

Hydraulic conductivity of the overburden investigated in detail on the basis of:

i. Statistical analysis of packer tests.

ii. Definition of the relationship between hydraulic conductivity and depth based on packer tests.

iii. Estimation of the three dimensional hydraulic conductivity tensor based on the geometrical properties of discontinuities using an analytical method.

iv. Comparison of calculated values for hydraulic conductivity with statistical analysis of packer tests.

6.2 Statistical Analysis of Packer Test's Results

The packer test data comprises 631 Lugeon tests conducted in different boreholes throughout Tahmoor South area. These tests provide valuable results about hydraulic conductivity of jointed rocks in different depth throughout the site. Considering spatial nature of hydraulic conductivity of jointed rocks, statistical analysis of packer test's results presents better understanding about their trend, average and standard deviation in different depth. There are 62 tests in reported results for which their value are outside the range of the test equipment (lower than 1×10^{-11} m/s or higher

than 1.6×10^{-6} m/s) and as such they have been filtered out to maintain the integrity of the data set.

The hydraulic conductivity of the rock mass decreases with increasing depth. This behaviour reflects the effect of confining stress on hydraulic aperture of rock joints and porosity of intact rock. Figure 28 presents the hydraulic conductivity measurements at Tahmoor South relative to depth. The conductivity is presented in a log scale.

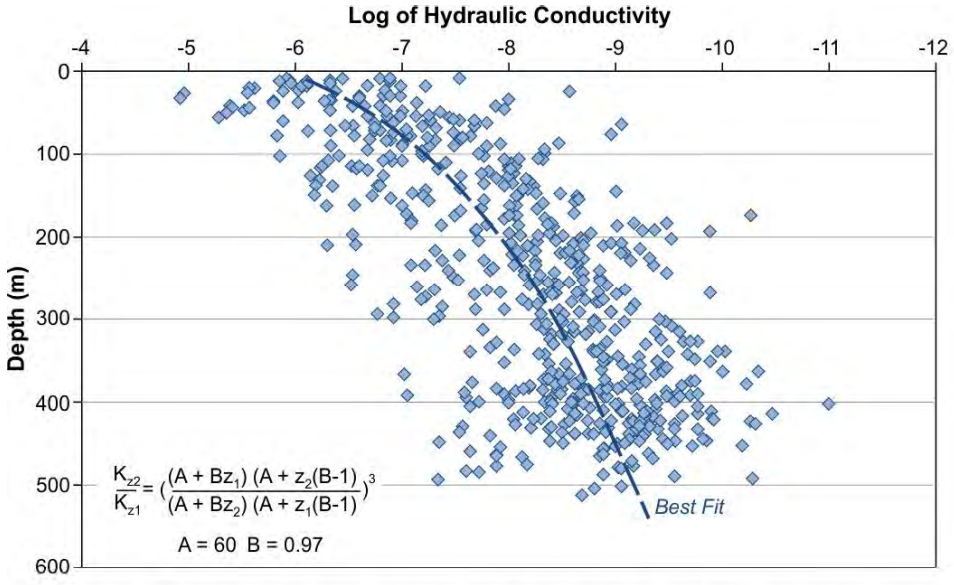

Figure 28: Log of hydraulic conductivity versus depth for Tahmoor Colliery.

There is an obvious trend between hydraulic conductivity and depth despite high scattering in different depth. A curve fitted to this trend (most visible trend) which represents the ratio between hydraulic conductivity in different depth. This empirical equation provides ability to estimate the average hydraulic conductivity in any desired depth (z_2) using available information in a given depth (z_1).

The results demonstrate that the conductivity is a combination of rock fabric, joints and bedding partings. It is noted that bedding partings were the dominant flow pathway in the boreholes where detailed testing and structural logging of the core was conducted.

The statistical analysis of hydraulic conductivity was performed for depth ranges of 0-100, 100-200, 200-300, 300-400 and higher than 400m by an averaging method and method which introduced by Raymer (2001). The procedure is explained in detail for depth 0-100m and repeated for other depths.

6.2.1 Statistical Analysis of Packet Tests for Depth 0-100m

A histogram of 111 Lugeon tests conducted for shallow depth (0-100m) is shown in Figure 29. Most of results in this figure are less than 2×10^{-6} m/s with arithmetic average 7.56×10^{-7} m/s and standard deviation of 1.76×10^{-6} m/s.

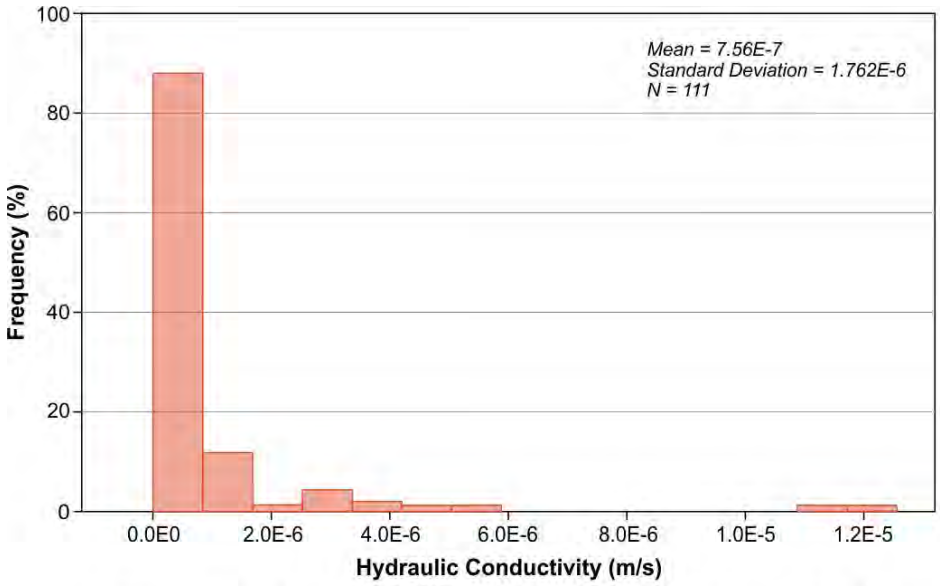

Figure 29: Histogram of packer test results for depth 0-100m.

The cumulative curve of the same data as shown in Figure 30. The hydraulic conductivity values are sorted into order and their logarithm (base 10) is plotted against the inverse cumulative value of the standard normal distribution for the percentile of sorted order. Percentile is a dimensionless value calculated as:

$$P_i = \frac{(i-0.5)}{n} \qquad (1)$$

where i is a value of sorted order ($i=1$ represents the lowest hydraulic conductivity), and n is the total number of tests (111 tests for depth 0-100m).

To explain the procedure, hydraulic conductivity for test number 10 (in order from lowest to highest) is 1.32×10^{-8} m/s. Percentile for this test point calculated equal with 8.56% (Eq.1). Assuming the standard normal distribution, the inverse cumulative value for 0.856 is -1.368, meaning that this percentile is located 1.368 times of standard deviation below the standard normal distribution mean of zero.

High and low end results are more visible by applying this method to packer tests (Figure 30). High end results can be a sign of fractured zone or fault with high hydraulic conductivity. Apart from these two boundaries, it is possible to fit a line to this graph as shown in Figure 31. The equation of

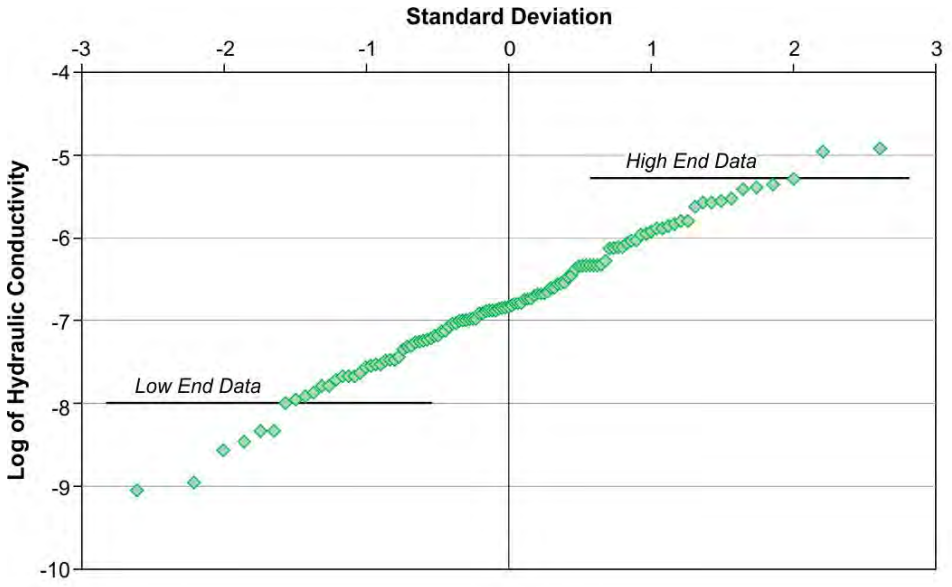

Figure 30: Log normal plot of packer test results for depth 0-100m.

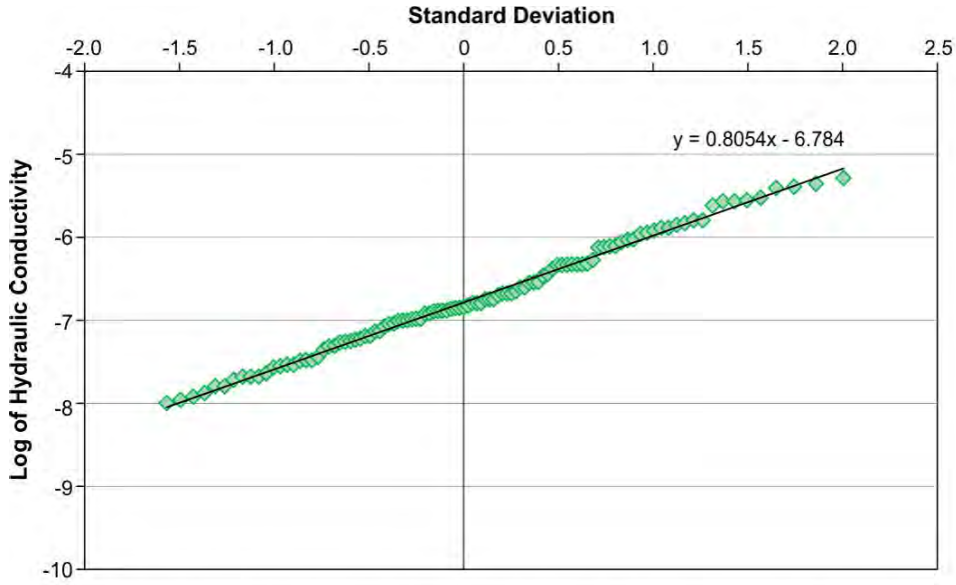

Figure 31: Best fit, upper and lower bound to linear section of Log normal plot of packer test results for depth 0-100m.

fitted line is called Log-Normal Model which its intercept with vertical axis represents the median value of hydraulic conductivity distribution. Most probable average for hydraulic conductivity can be calculated as area under the fitted line. Statistical results of hydraulic conductivity for depth 0-100m are shown in Table 3.

Table 3: Statistical results of packer tests in Tahmoor Mine – Depth 0-100m

	Average hydraulic conductivity (m/s)	Standard Deviation (m/s)
Arithmetic Mean –Packer tests	7.56e-7	1.76e-6
Geometrical Mean	1.59e-7	-
Area under best fit	7.29e-7	-

6.2.2 Statistical Analysis of Packet Tests for Depth 100-200m

The histogram of 106 packer tests conducted in depth 100-200m is presented in Figure 32. This histogram shows that most of results were less than 2.5×10^{-7} m/s with arithmetic average 1.07×10^{-7} m/s and standard deviation of 2.09×10^{-7} m/s.

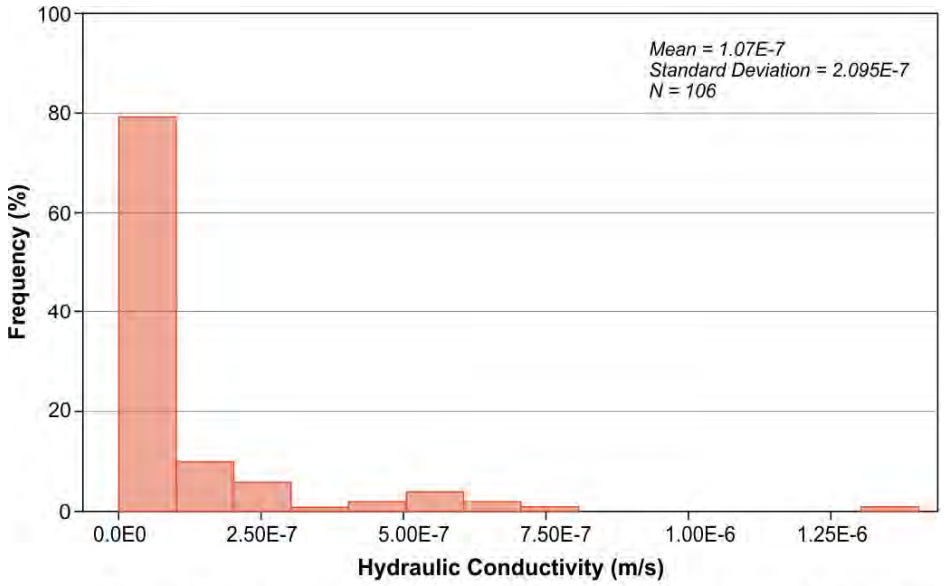

Figure 32: Histogram of packer test results for depth 100-200m.

Cumulative curve of packer test's results are shown in Figure 33. High end results for this depth represent hydraulic conductivity between 2.9×10^{-7} to 1.4×10^{-6} m/s. These values are expected for shear zones and faults. The best fit to middle section of cumulative curve is shown in Figure 34. Using Log-normal Model obtained from best fit, the most probable average hydraulic conductivity for depth 100-200m and other statistical results are summarised in Table 4.

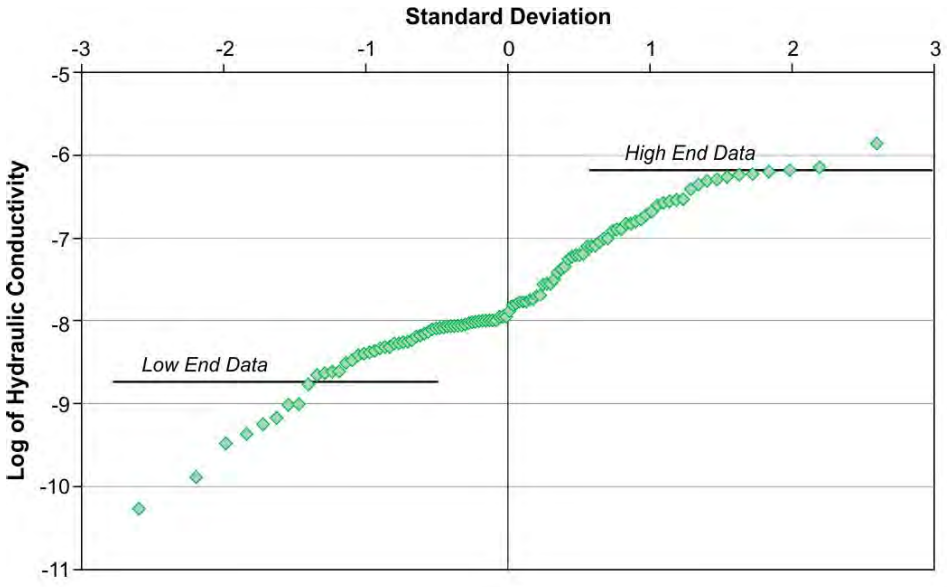

Figure 33: Log normal plot of packer test results for depth 100-200m.

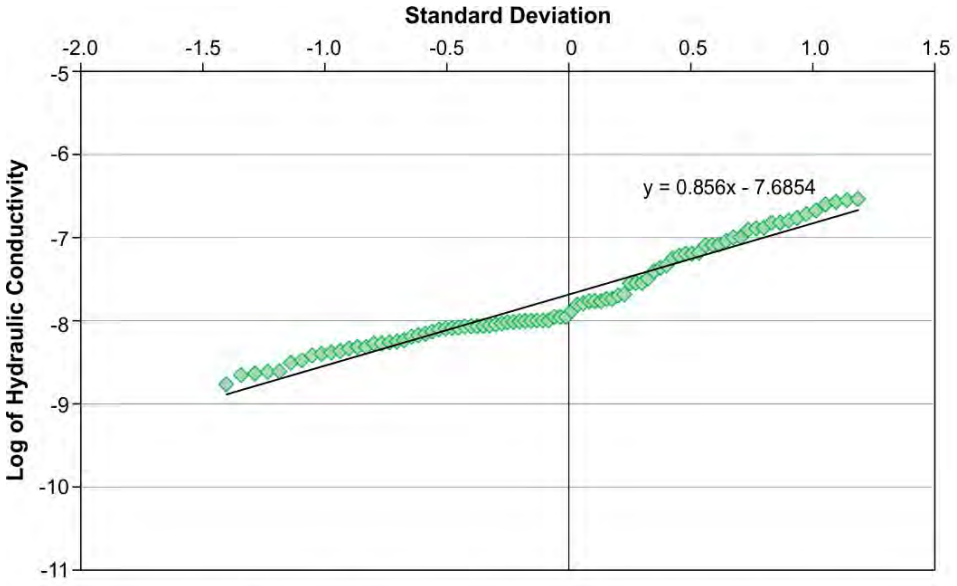

Figure 34: Best fit, upper and lower bound to linear section of Log normal plot of packer test results for depth 100-200m.

Table 4: Statistical Results of Packer tests in Tahmoor Mine – Depth 100-200m

	Average hydraulic conductivity (m/s)	Standard Deviation (m/s)
Arithmetic Mean –Packer tests	1.07e-7	2.1e-7
Geometrical Mean	2e-8	-
Area under best fit	1.09e-7	-

6.2.3 Statistical Analysis of Packet Tests for Depth 200-300m

108 packer tests were conducted in depth between 200 to 300m of different boreholes. The histogram and cumulative curve for these tests are shown in Figures 35 and 36. Most of results in this horizon are less than 1×10^{-7} m/s with arithmetic average 2.65×10^{-8} m/s and standard deviation of 6.98×10^{-8} m/s. The most probable average hydraulic conductivity is 1.55×10^{-8} m/s which obtained by calculating the area under the best fit to middle section of cumulative curve presented within Figure 10. The results for depth 200-300m are summarised in Table 5.

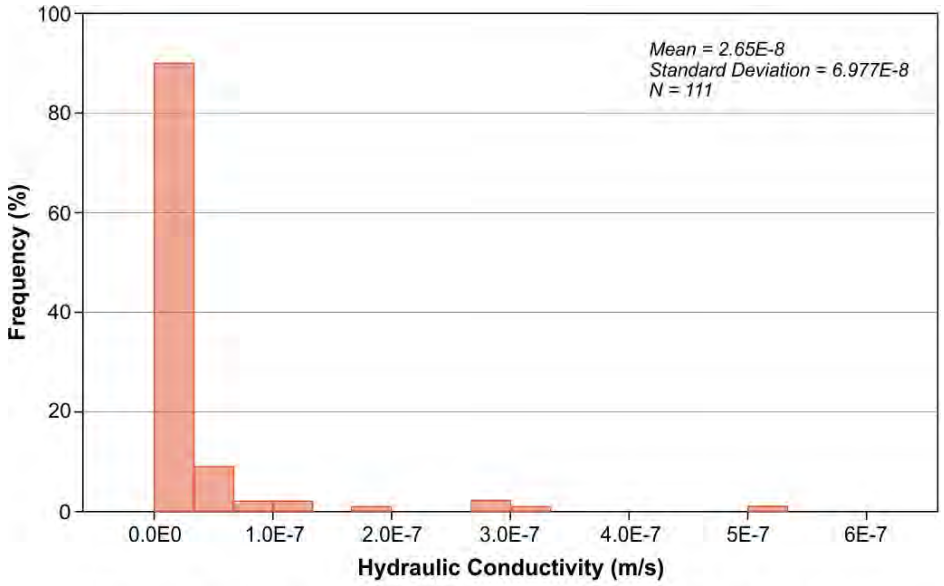

Figure 35: Histogram of packer test results for depth 200-300m.

Table 5: Statistical results of packer tests in Tahmoor Mine – depth 100-200m

	Average hydraulic conductivity (m/s)	Standard Deviation (m/s)
Arithmetic Mean –Packer tests	2.65e-8	6.98e-8
Geometrical Mean	5.32e-9	-
Area under best fit	1.55e-8	-

6.2.4 Statistical Analysis of Packet Tests for Depth 300-400m

The histogram of 130 Lugeon tests conducted for depth 300-400 is shown in Figure 37. This histogram presents that most of results are less than 2×10^{-8} m/s with arithmetic average 5.09×10^{-9} m/s and standard deviation of 1.27×10^{-8} m/s. Figure 38 presents the cumulative curve and the best fit to the overall data set. The most probable average of hydraulic conductivity for this horizon is equal with 4.22×10^{-9} m/s is summarised in Table 6.

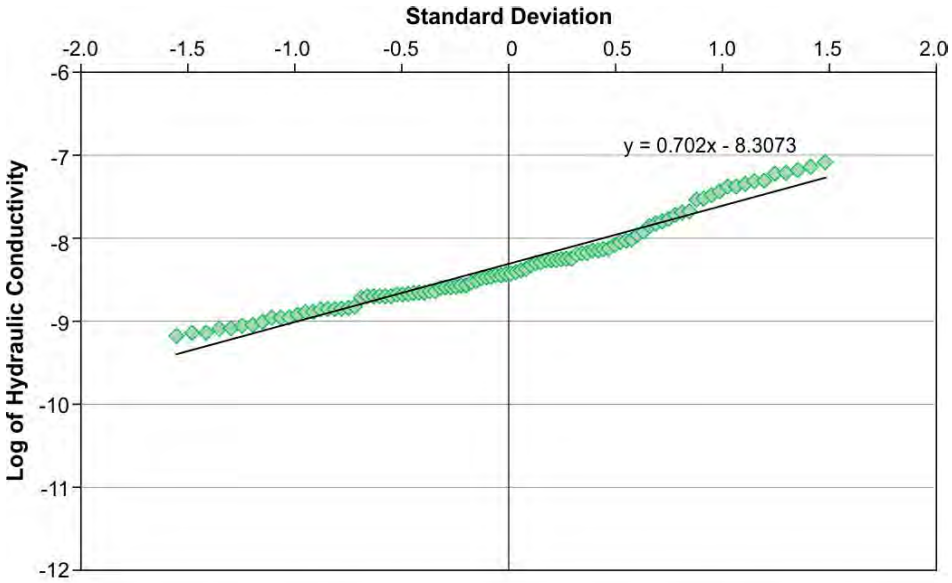

Figure 36: Best fit, upper and lower bound to linear section of Log normal plot of packer test results for depth 200-300m.

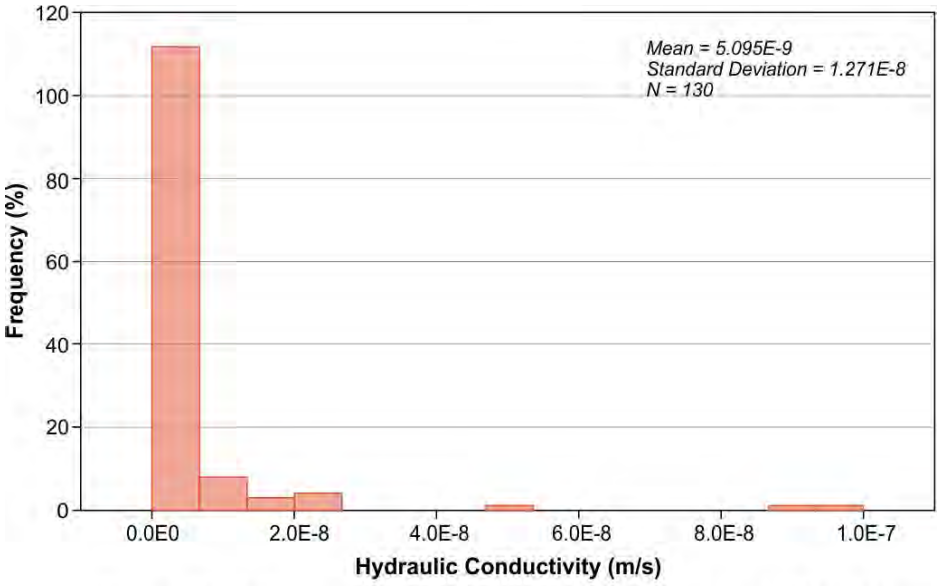

Figure 37: Histogram of packer test results for depth 300-400m.

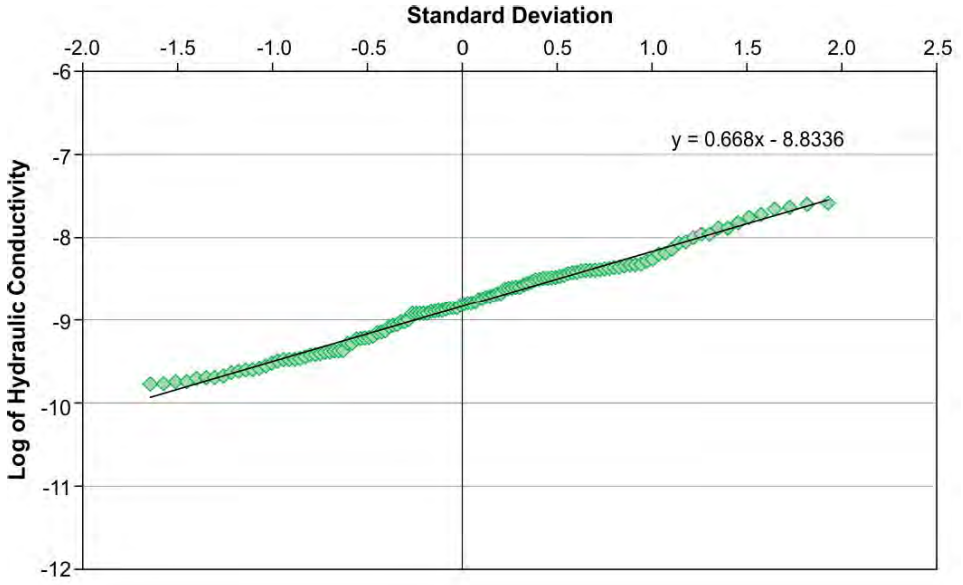

Figure 38: Best fit, upper and lower bound to linear section of Log normal plot of packer test results for depth 300-400m.

Table 6: Statistical results of packer tests in Tahmoor Mine – Depth 100-200m

	Average hydraulic conductivity (m/s)	Standard Deviation (m/s)
Arithmetic Mean –Packer tests	5.09e-9	1.27e-8
Geometrical Mean	1.5e-9	-
Area under best fit	4.22e-9	-

6.2.5 Statistical Analysis of Packet Tests for Depth > 400m

The histogram of 114 packer tests conducted in depth higher than 400m in different boreholes is presented in Figure 39. This figure shows that most of results were less than 1×10^{-8} m/s with arithmetic average 4.2×10^{-9} m/s and standard deviation of 8.08×10^{-9} m/s. Cumulative curve of packer tests have high end values between 1.2×10^{-8} -4.6×10^{-8} m/s for hydraulic conductivity . The most probable average hydraulic conductivity as area under the best fit to middle section of cumulative curve is 3.56×10^{-9} m/s and is presented in Figure 40. The summary data is presented in Table 7.

Table 7: Statistical results of packer tests in Tahmoor Mine – Depth >400m

	Average hydraulic conductivity (m/s)	Standard Deviation (m/s)
Arithmetic Mean –Packer tests	4.2e-9	8.08e-9
Geometrical Mean	1.22e-9	-
Area under best fit	3.56e-9	-

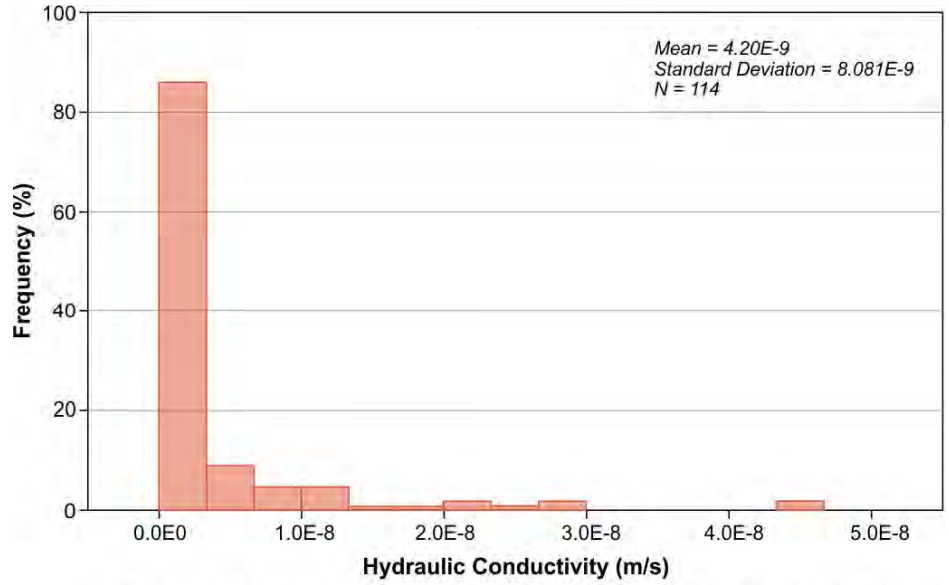

Figure 39: Histogram of packer test results for depth >400m.

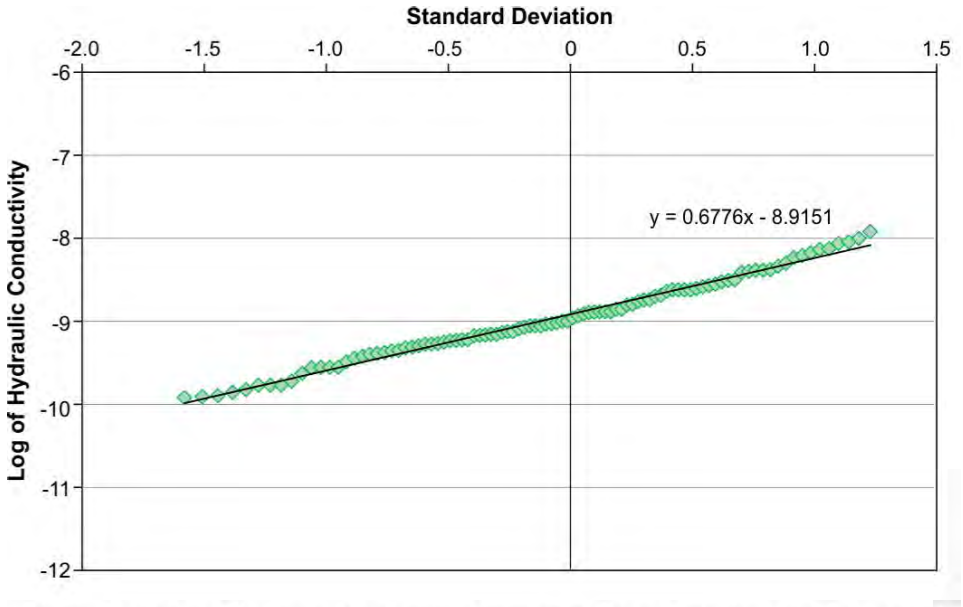

Figure 40: Best fit, upper and lower bound to linear section of Log normal plot of packer test results for depth >400m.

7. ASSESSMENT OF FLOW PATHWAYS WITHIN THE ROCK MASS

The flow within the rock mass is a combination of flow within the pore space fabric of the rock and that through discontinuities which cut through the rock strata. The discontinuities are joints, bedding partings and faults.

An example of the joint network in the Permian strata is presented in Figure 41.

Figure 41: Typical rock joints in sedimentary rocks in a rock platform (plan view), Sydney Basin.

In order to assess the potential for flow within the pore space of the fabric, the hydraulic conductivity of core samples have been analysed and plotted in Figure 42 relative to the average conductivity line defined in Section 6.2.1.

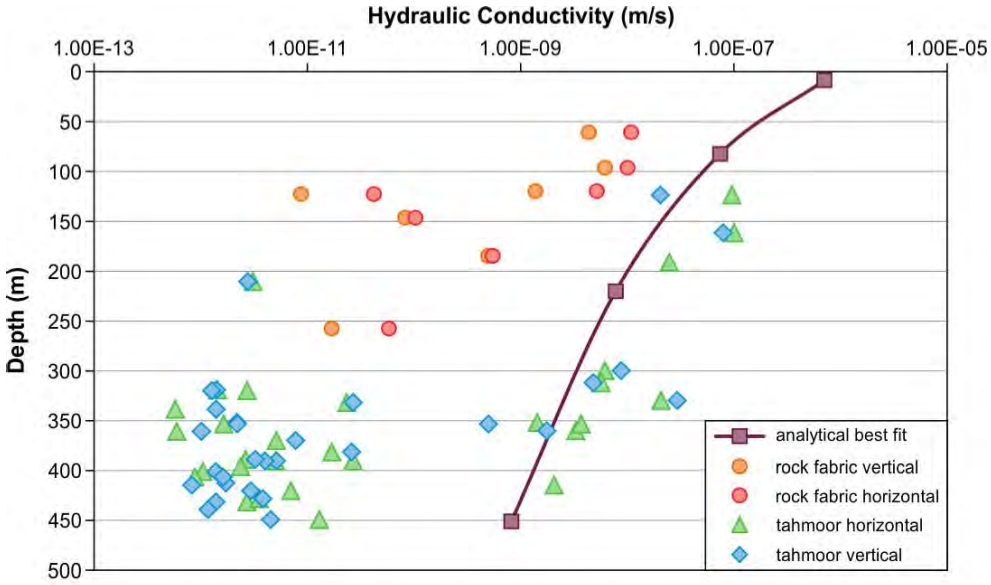

Figure 42: Conductivity of core samples for Tahmoor and other Illawarra coal measure sites.

The core conductivity data is from the Illawarra Coal Measures and the Tahmoor South data set is labelled. The result show that in general the fabric conductivity is significantly less than the best fit for the lugeon test results. The exception is that for certain sections the Hawkesbury sandstone and the Bulgo sandstone which are known to have elevated porosity. The conductivity within these units appears to be quite variable over the coalfield and also within the stratigraphic units themselves.

Therefore, in general, the flow within the rock mass is considered to be primarily via the network of discontinuities, however flow through the rock fabric in certain sections of the Hawkesbury Sandstone and the Bulgo Sandstone would occur with similar conductivity as the average conductivity of the network of discontinuities. Irrespective of the variability of the pore space conductivity for the units, it is considered that the analytical best fit provides a good overall representation of flow within the rock mass within the Illawarra Coal field. This includes flow via discontinuities or pores space fabric.

The core testing of conductivity provides values of conductivity in the vertical and horizontal directions. This provides an indication of the degree of interbedding within the sample, whereby if the sample has a bedded nature with variable grain size and potentially finer grained bands (representing bedding) then the conductivity of a sample parallel to the bands will be greater than across the bands. In the case of a non- banded material the conductivity would be isotropic.

The data from Tahmoor South and other Illawarra Coal Measure tests are presented in Figure 43 in terms of the ratio of horizontal to vertical conductivity for the sample. It is clear that the data sets are consistent and that in general the ratio is typically in the range of 0.5 to 2. There are clear exceptions where the horizontal conductivity is much greater (up to at least 8 times) and these would represent cases where the sample has a bedded or laminated fabric. The variability in the ratio is not a function of the formation but is generally consistent across all stratigraphic formations.

In general, it appears that there is no fundamental fabric anisotropy (horizontal to vertical) other than on the basis of the rock type and the degree of lamination within the unit. In the rock mass, joints would cross cut the bedding or lamination within the rock fabric and allow flow to occur across the laminations which limit the flow within the pore fabric.

On this basis, the analysis has been extended to determine the most likely directional properties of the conductivity within the overburden. This is based on flow within the discontinuity network. The flow within the discontinuities is defined by their orientation and the confining stress normal to the discontinuity.

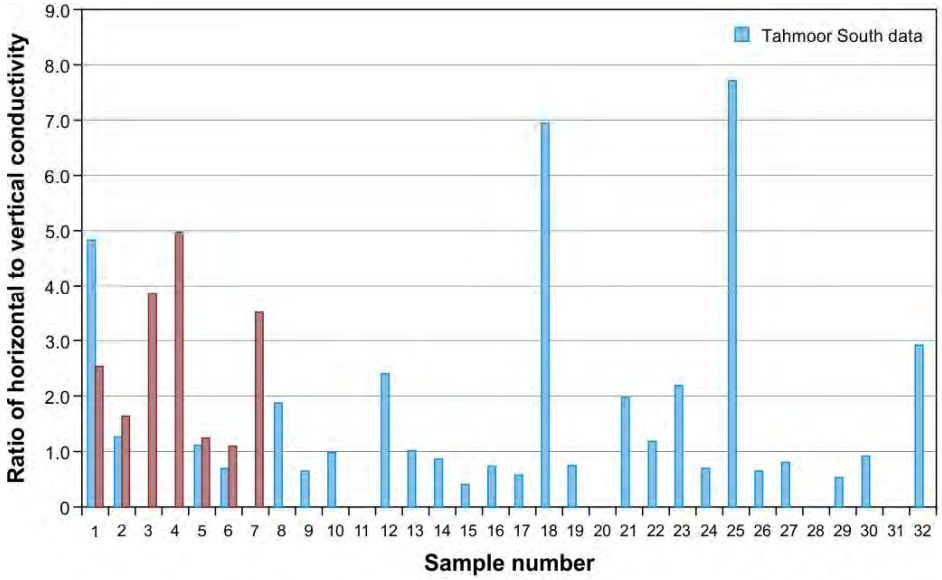

Figure 43: Ratio of horizontal to vertical conductivity for core samples.

8. HYDRAULIC CONDUCTIVITY TENSOR-ANALYTICAL CALCULATION

The hydraulic conductivity of jointed rocks is a tensor for which its magnitude and orientation are controlled by geometrical properties of rock joints, bedding and the stress field.

The effect of discontinuities is greatest in rocks with low porosity. In rocks with a relatively high porosity (such as the Hawkesbury Sandstone) the effect of flow in discontinuities is less as flow within the rock fabric readily occurs within some units (as discussed above).

The Lugeon test provides valuable information about average hydraulic conductivity however, the directional and anisotropic nature of hydraulic conductivity within the overall rock mass cannot be determined within the test itself.

In this section, hydraulic conductivity tensor for Tahmoor South is estimated by Snow's analytical method. Snow (1969) introduced first comprehensive analytical method by considering rock joints as infinite plane inside rock. In this method, combination of joint orientation, spacing and hydraulic aperture gives the hydraulic conductivity tensor as:

$$k_{ij} = \frac{g}{12\vartheta}\sum_{k=1}^{n}\frac{a_k^3}{s_k}\left(\delta_{ij} - n_{ik}n_{jk}\right) \qquad (2)$$

where, n is number of joint sets, a_k and s_k are hydraulic aperture and spacing of k_{th} joint set, δ_{ij} is the Kronecker delta and n_{ik} and n_{jk} are direction cosines of the unit vector normal to each joint set in the x, y and z direction. Rock joints are considered as infinite plane in Snow's method. The assumption of infinite areal extent for rock joints is acceptable when joints are longer than 15 times of their spacing (Wei, 1995). In sedimentary rocks, especially for

Sydney Basin, length of rock joints is sufficient long to accept infinite areal extent for them. An example of jointing within a wave cut platform in the Sydney Basin is presented in Figure 41 which shows the spacing and continuity of the high angle fracture systems within the Permian strata.

According to Eq.2, orientation (dip/dip direction), spacing and hydraulic aperture of rock joints are required to calculate hydraulic conductivity tensor. Borehole Acoustic Scanner reports (conducted by ASIMS 2012) contain valuable information about orientation and spacing of detected rock joints. This information has been combined with defect logs to determine orientation and spacing of rock joints in different boreholes.

The hydraulic aperture of rock joints has the greatest effect on the magnitude of hydraulic conductivity. This parameter depends on the mechanical aperture (visible opening of joints), joint roughness and confining (normal) stress.

There are not any direct measuring methods to determine the hydraulic aperture of discontinuities within the rock mass. Back analysis of the flow rate inside individual joint is the most common procedure to estimate its value indirectly. Hydraulic aperture of rock joints decreases with increasing applied stress. Therefore, several researchers introduced a reducing trend between hydraulic aperture and depth (Wei, 1995; Jiang *et al.*, 2010; Zoorabadi *et al.,* 2013). Zoorabadi *et al.* (2013) introduced three reducing trends as lower bound, most probable and upper bound between hydraulic aperture and depth. This is presented in Figure 44. Data from the USA, Sweden, Iran and Australia (including the Tahmoor South data) have been used. The equations were obtained from back analysing Lugeon style packer tests with assuming hydrostatic stress condition in the tested section. Joint frequency and intersection angle between rock joints in each tested horizon with borehole axis have been considered for back analysing.

In-situ stress condition in the most real cases is not hydrostatic so, it is important to find magnitude of applied stress on each joint set based on orientation of joints and principal stress's orientation. Then, equivalent depth (z_{eq}) for each joint set can be determined by following equation:

$$z_{eq} = \sigma_i / \gamma \qquad (3)$$

where, σi is applied stress on joint set number i and γ is unit weight of rock (0.025 MN/m^3 for sedimentary rocks). Nemcik *et al.* (2005) presented a statistical analysis of measured stress in Australian coal mines. This is presented in Figure 45. Overcore stress measurements for Tahmoor North mine is included in this data set. The most probable trend of this information shows that ratio between horizontal maximum stress and vertical stress in Australian coal mines (in NSW and QLD) is more than 2. In the other hand, based on measured stress in different boreholes in Tahmoor Mine (Sigra, 2010) the average ratio between maximum horizontal stress and minimum horizontal stress is 1.5. Furthermore, these measurements represent a strong NW orientation for maximum horizontal stress in the Tahmoor South area.

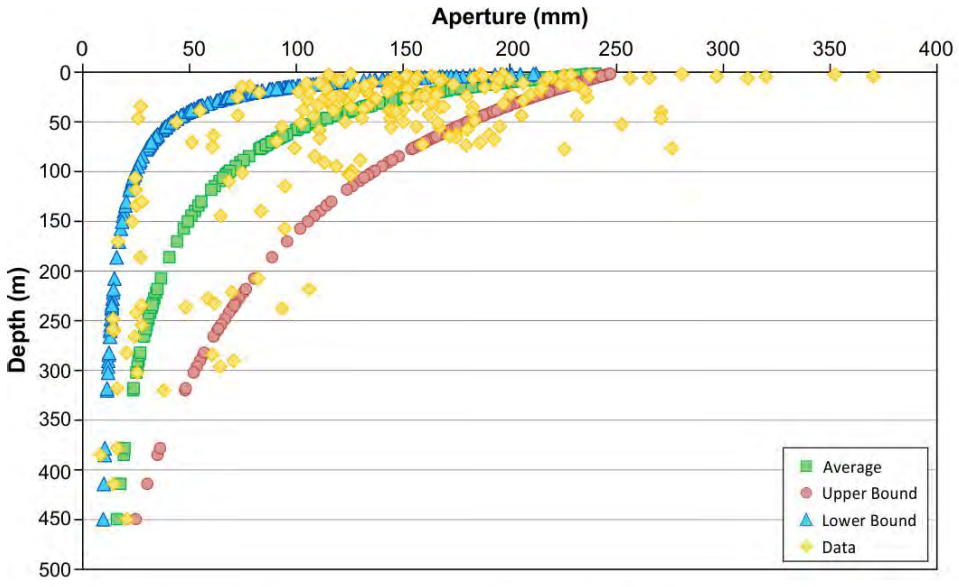

Figure 44: Hydraulic aperture of bedding partings and joints versus depth.

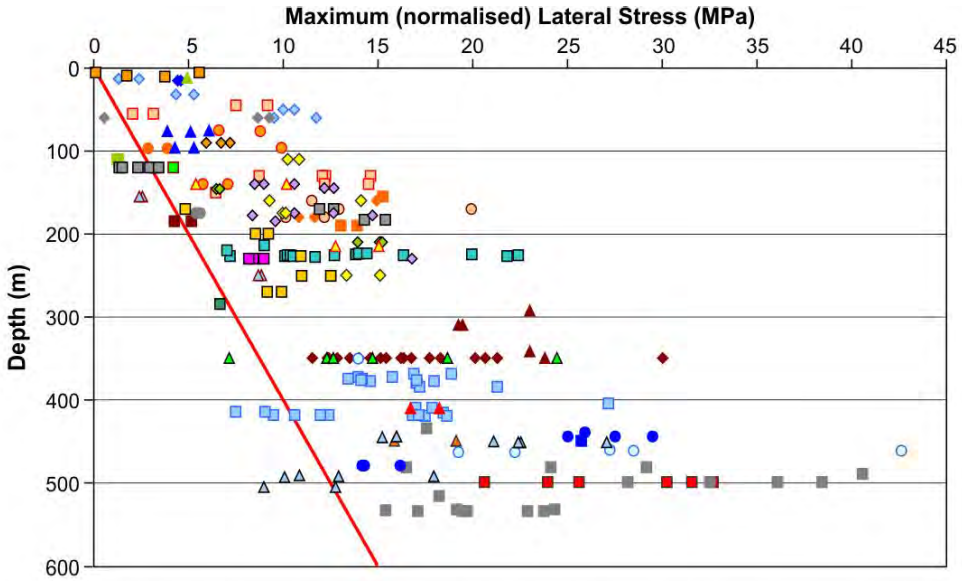

Figure 45: Measured and normalised maximum lateral stress versus overburden depth in Australian coal mines *(Nemcik et al. 2005)*.

The hydraulic conductivity tensor is calculated for different depth (the midpoint of each depth range is selected for calculation. This calculation conducted for each horizon within the various boreholes over the area.

In following sections, summarised results for each horizon presented and results for each borehole listed in the Appendix. Bedding planes are almost horizontal all though the study area (with average dip of 6˚) and their

hydraulic aperture are larger than other joint sets due to the minimum stress being essentially vertical. Therefore, the maximum and intermediate components of calculated hydraulic conductivity (K_{11}, K_{22}) in the most boreholes are essentially horizontal and minimum component (K_{33}) is sub-vertical.

8.1 Hydraulic Conductivity Tensor for Depth 450m (>400m)

Using the most probable trend in Figure 45 (average), the ratio between maximum horizontal stress and vertical for depth 450m would be 2.13. The hydraulic tensor is calculated on the basis of the in-situ stress magnitude and orientation together with the orientation of each joint set in each borehole (from acoustic scanner. The magnitude of the principal hydraulic conductivity tensors in each borehole are shown in Figures 46 to 48. In these figures, the horizontal axis presents each borehole used in the analysis (eg number 13 for borehole TBC014, number 19 for borehole TBC021 and number 27 for borehole TBC029). Figure 49 shows the orientation average hydraulic conductivity tensors calculated for depth 450m.

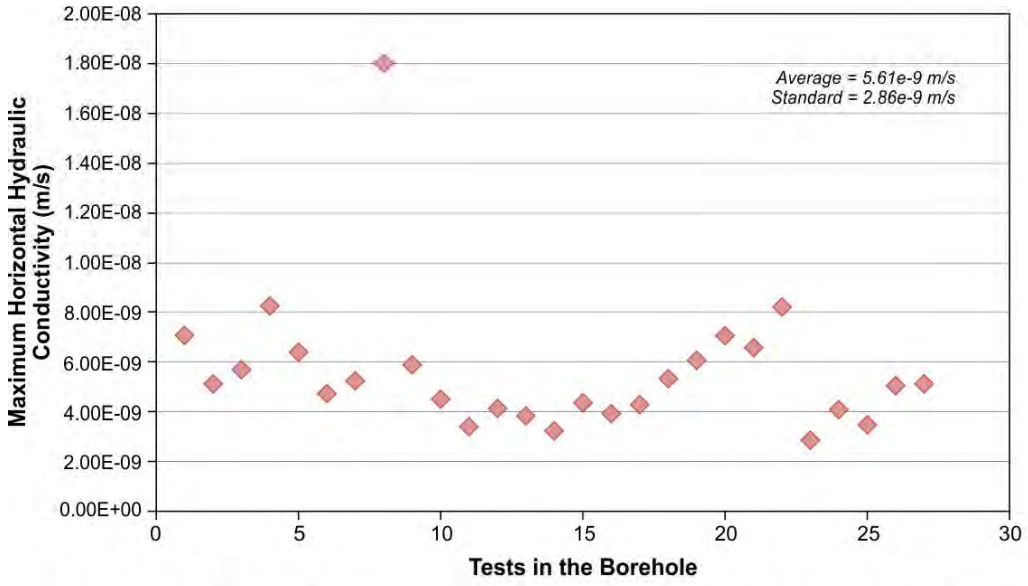

Figure 46: Maximum horizontal conductivity in different borehole for depth 450m.

The average principal component of hydraulic conductivity (tensor averaging, Hudson & Harrison, 1997 p.53) and their orientation are listed in Table 8.

Table 8: Average principal hydraulic conductivity components and their orientation for depth 450m

	K_{11} [m/s]	K_{22} [m/s]	K_{33} [m/s]
Snow Method	5.54e-9	4.49e-9	1.47e-9
Plunge/Trend	2/137	8/227	82/32

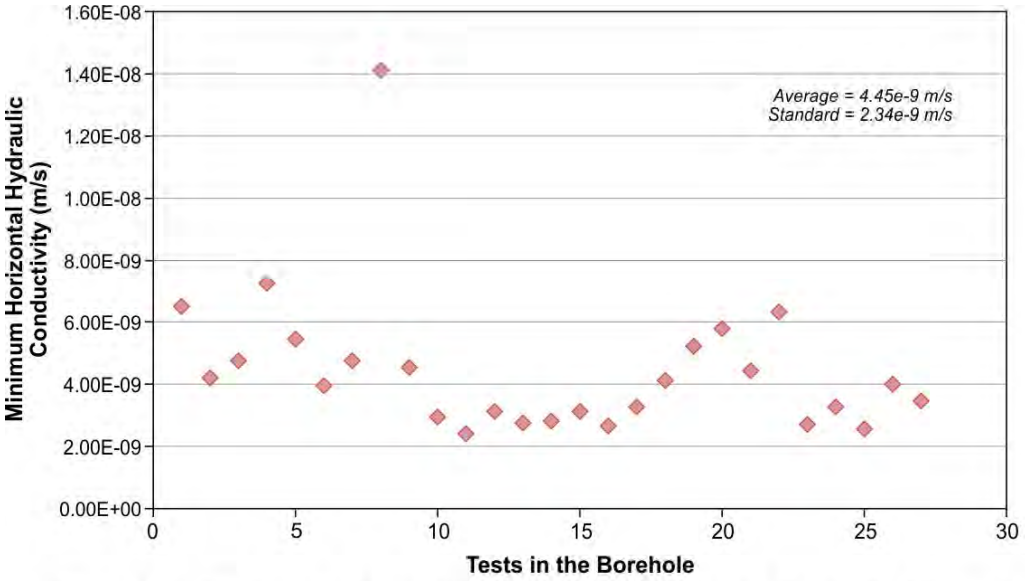

Figure 47: Minimum horizontal conductivity in different borehole for depth 450m.

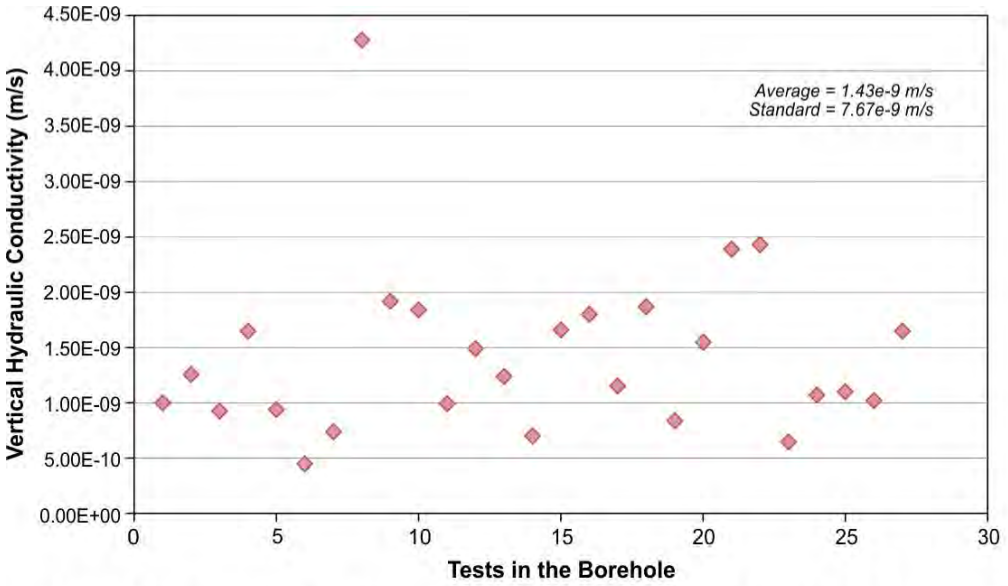

Figure 48: Vertical hydraulic conductivity in different borehole for depth 450m.

In Table 9 statistical results of packer test and calculated average value from hydraulic conductivity are listed. This information demonstrates a good agreement between packer test and calculated results. Based on calculated results, the ratio between maximum horizontal and vertical hydraulic conductivity is 3.77 which shows a significant anisotropy in hydraulic behaviour of jointed rock in this depth.

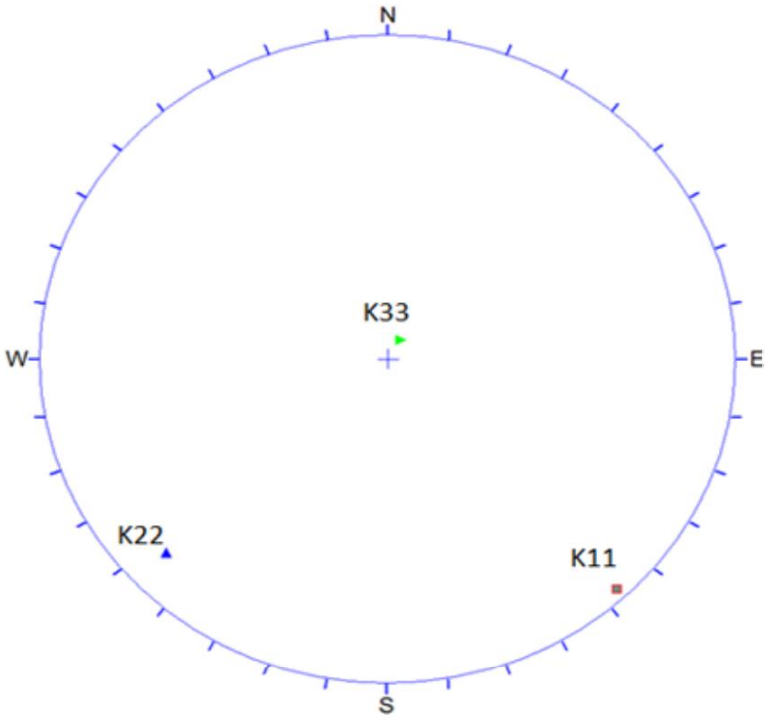

Figure 49: Orientation of principal components of hydraulic conductivity for depth 450m.

Table 9: Packer test's results and computed hydraulic conductivity for depth <400m

	Average hydraulic conductivity for depth <400 (m/s)	Standard Deviation (m/s)
Arithmetic Mean -Packer tests	4.2e-9	8.08e-9
Geometrical Mean	1.22e-9	-
Area under best fit	3.56e-9	-
Analytical model	3.83e-9	1.92e-9
K_H/K_v	3.77	
K_H/K_h	1.23	

8.2 Hydraulic Conductivity Tensor for Depth 350m (300-400m)

Based on the most probable stress trend (Figure 45), the ratio between maximum horizontal stress and overburden stress for depth 350m is about 2.13. Joint set spacing is similar to depth 450 and obtained from acoustic scanner information. Bedding plane spacing estimated using defect logs. Details of geometrical properties of joint sets and calculated hydraulic conductivity tensor for each borehole are presented in Appendix 1. The magnitude of the principal components of hydraulic conductivity tensor are presented in Figures 50 to 53.

The average calculated principal components hydraulic conductivity are presented in Table 10 and show that maximum and intermediate hydraulic conductivity tensors are sub-horizontal and minimum tensor is sub-vertical.

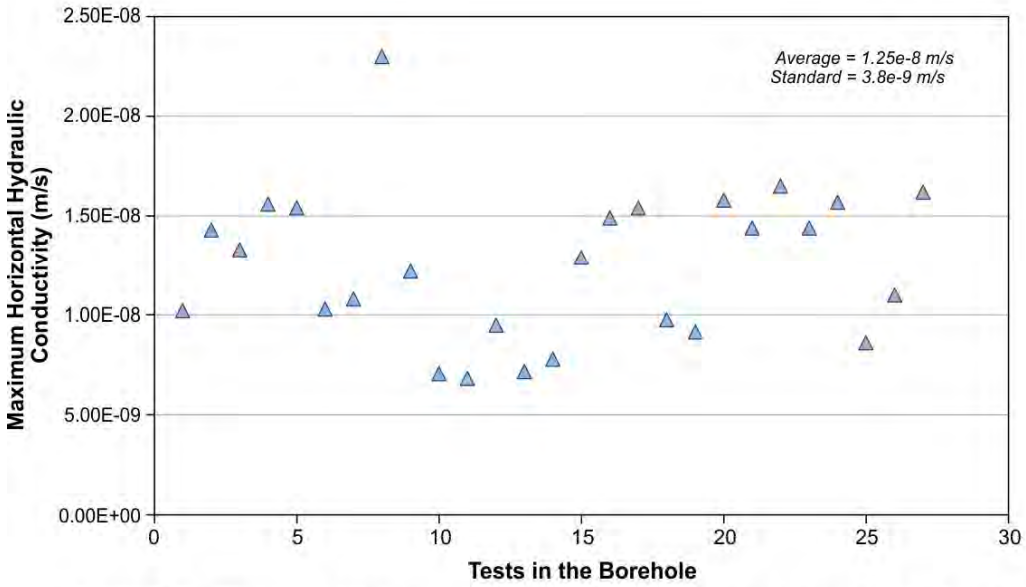

Figure 50: Maximum horizontal conductivity in different borehole for depth 350m.

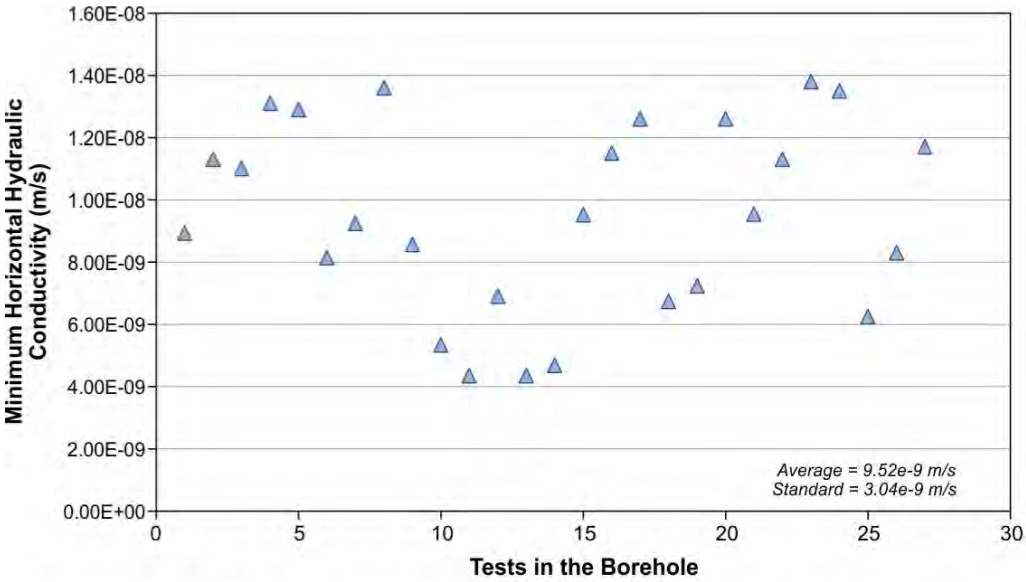

Figure 51: Minimum horizontal conductivity in different borehole for depth 350m.

As it expected, bedding planes are the primary control on hydraulic conductivity of jointed rocks in this horizon and the ratio between maximum horizontal conductivity and vertical conductivity is 2.87. The information presented in Table 11 shows an acceptable agreement between calculated average hydraulic conductivity and results from statistical analysis of packer tests.

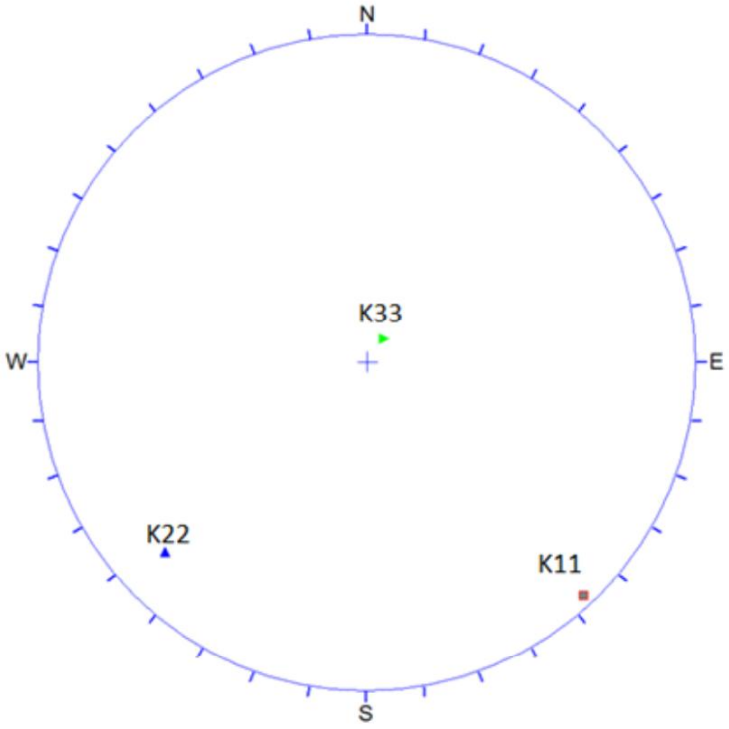

Figure 53: Orientation of principal components of hydraulic conductivity for depth 350m.

Table 10: Average principal hydraulic conductivity components and their orientation for depth 350m

	K_{11} [m/s]	K_{22} [m/s]	K_{33} [m/s]	Mean [m/s]
Snow Method	1.23e-8	9.52e-9	4.2e-9	8.67e-9
Plunge/Trend	2/137	10/227	80/35	

Table11: Packer test's results and computed hydraulic conductivity for depth 300-400m

	Average hydraulic conductivity for depth 300-400 (m/s)	Standard Deviation (m/s)
Arithmetic Mean -Packer tests	5.09e-9	1.27e-8
Geometrical Mean	1.5e-9	-
Area under best fit	4.22e-9	-
Analytical model	8.67e-9	2.56e-9
K_H/K_v	2.87	
K_H/K_h	1.29	

8.3 Hydraulic Conductivity Tensor for Depth 250m (200-300m)

The orientation and spacing of rock joints in this depth are assumed to be same as depth 350m. Based on the most probable stress trend in Figure 45, the ratio between maximum horizontal stress and vertical stress is approximately 2.1. The results of the analytical method for calculation of hydraulic conductivity tensor in depth 250 are presented in Figure 54 to 57.

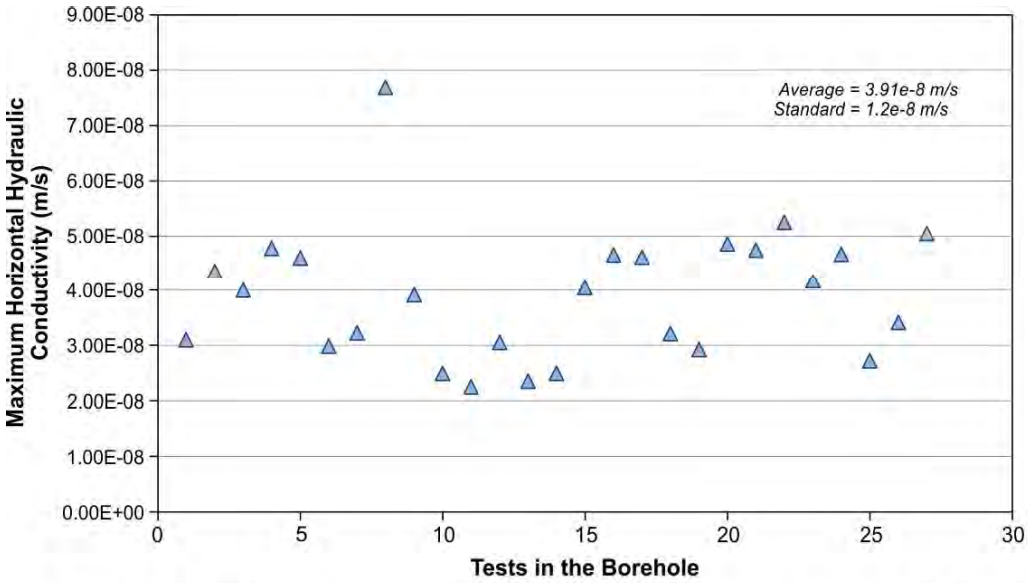

Figure 54: Maximum horizontal conductivity in different borehole for depth 250m.

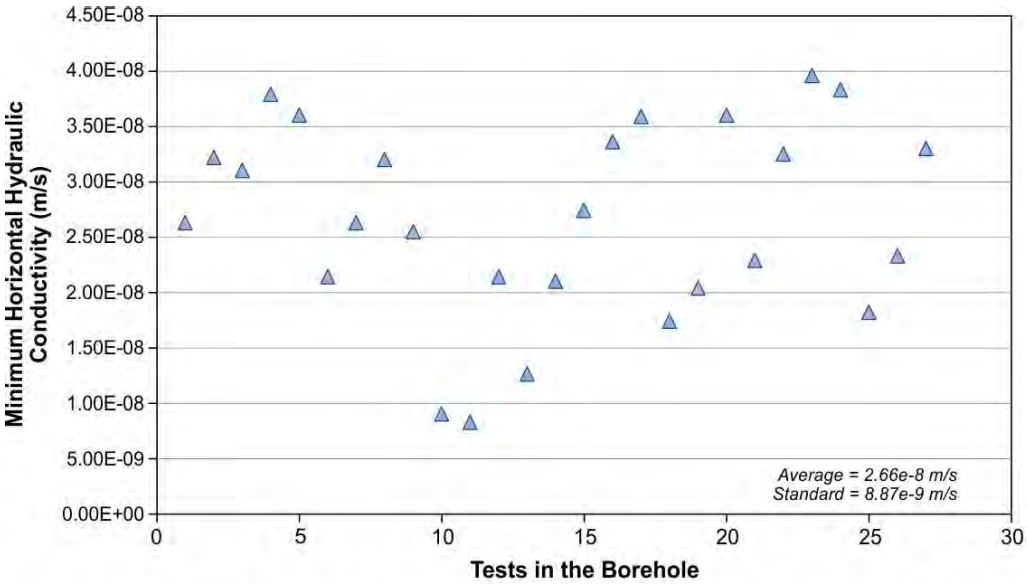

Figure 55: Minimum horizontal conductivity in different borehole for depth 250m.

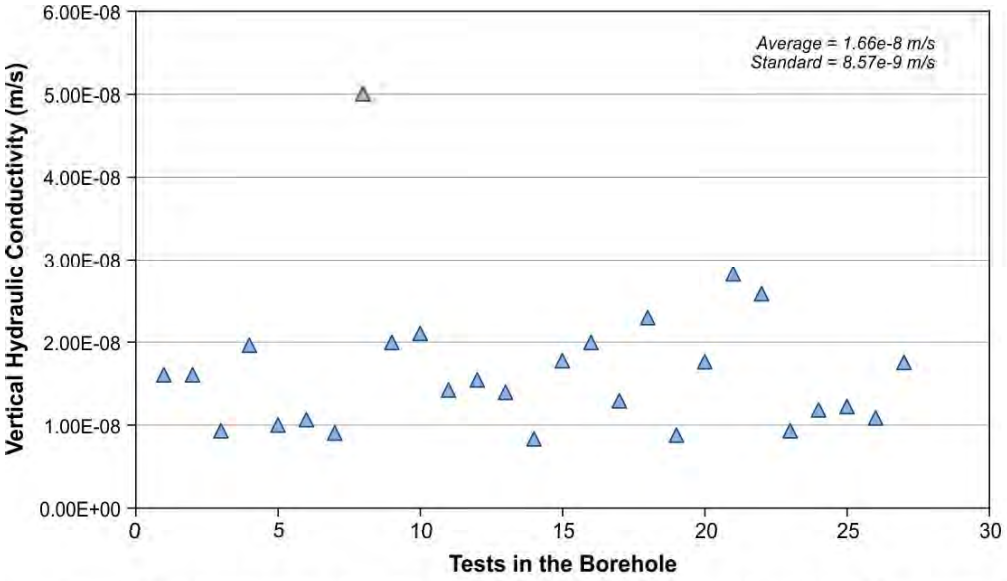

Figure 56: Vertical hydraulic conductivity in different borehole for depth 250m.

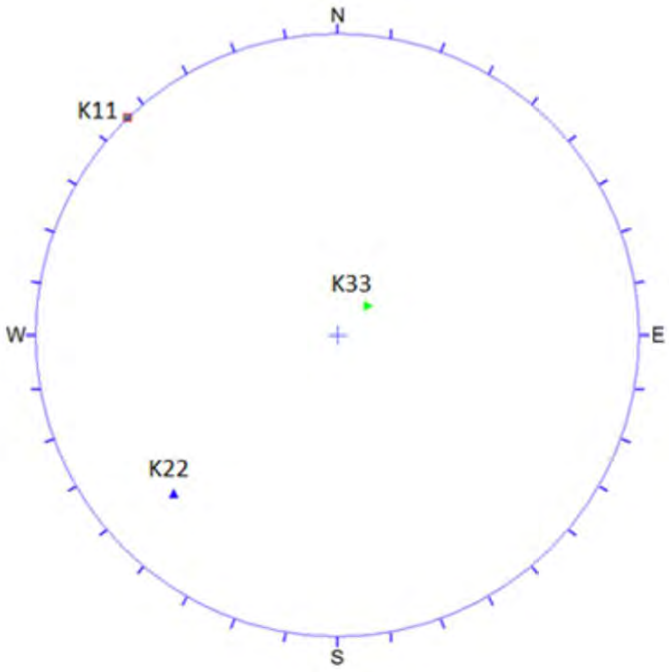

Figure 57: Orientation of principal components of hydraulic conductivity for depth 250m.

Table 12 presents the average calculated principal hydraulic conductivities for depth 250m. The maximum principal hydraulic conductivity is horizontal and the ratio between it and vertical conductivity is 2. The ratios are presented in Table 13. There is a good agreement between statistical results of packer tests and calculated hydraulic conductivity.

Table 12: Average principal hydraulic conductivity components and their orientation for depth 250m

	K_{11} [m/s]	K_{22} [m/s]	K_{33} [m/s]	Mean [m/s]
Snow Method	3.83e-8	2.79e-8	1.57e-8	2.73e-8
Plunge/Trend	0/136	16/226	74/47	

Table 13: Packer test's results and computed hydraulic conductivity for depth 200-300

	Average hydraulic conductivity for depth 200-300 (m/s)	Standard Deviation (m/s)
Arithmetic Mean -Packer tests	2.65e-8	6.98e-8
Geometrical Mean	5.32e-9	-
Area under best fit	1.55e-8	
Analytical model	2.73e-8	8.2e-9
K_H/K_v	2.44	
K_H/K_h	1.37	

8.4 Hydraulic Conductivity Tensor for Depth 150m (100-200m)

Hawkesbury Sandstone is the most dominant lithology between ground surface and depth 200m in Tahmoor Mine. Sub-horizontal bedding planes are the most important type of discontinuity in Sydney Basin as general and in Hawkesbury Sandstone specially and Joint sets are near vertical (Pells Consulting, 1985). Therefore for this analysis, it is assumed that discontinuity sets (bedding plane and joint sets) are same for all boreholes and their orientation was obtained by considering discontinuity sets (from acoustic scanner reports) in all boreholes.

Figures 58 and 59 represent the contour and scatter plots of all discontinuities detected by acoustic scanner method in different boreholes. Based on the concentration of discontinuity's poles, four sets determined. Poles of bedding planes have the highest concentration which shows a relatively uniform bedding plane through the area.

As can be seen in Figures 58 and 59, the poles concentration can be summarised as joint sets. The major joint sets are presented in Figure 60. It is noted that the orientations of dominant discontinuity sets detected by acoustic scanner are similar to results of photogrammetry method conducted by SCT Operation along the Sea Cliff Bridge area (outcrop of Hawkesbury Sandstone). The results are presented in Table 14. Joint sets 1, 2, 3 from acoustic scanner method match with joint sets A, B, C from photogrammetry method.

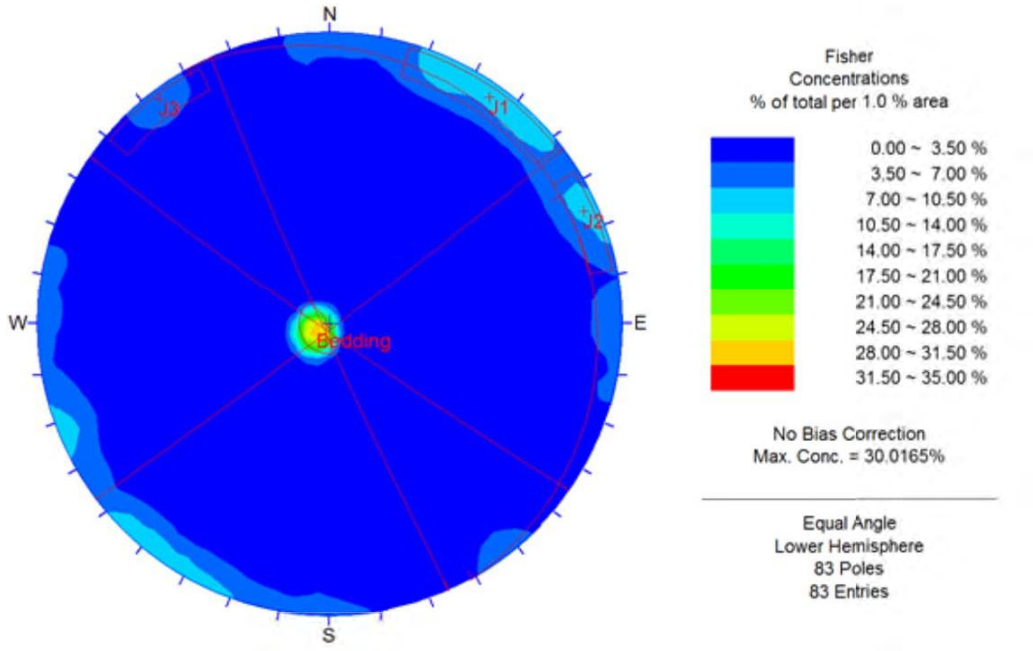

Figure 58: Contour diagram of all discontinuities detected by acoustic scanner.

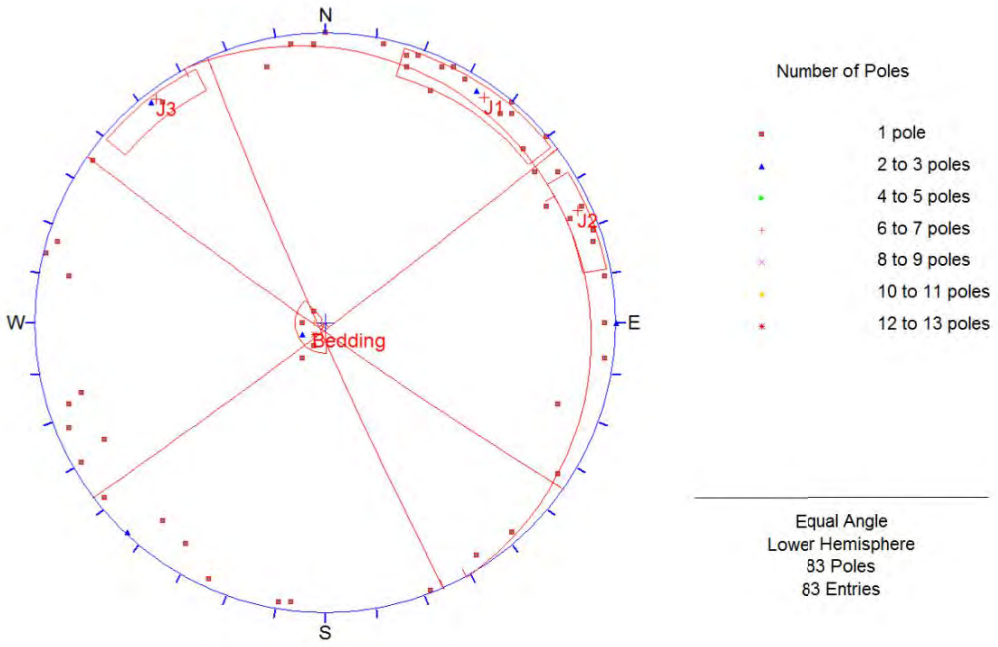

Figure 59: Scatter plot of all discontinuities detected by acoustic scanner.

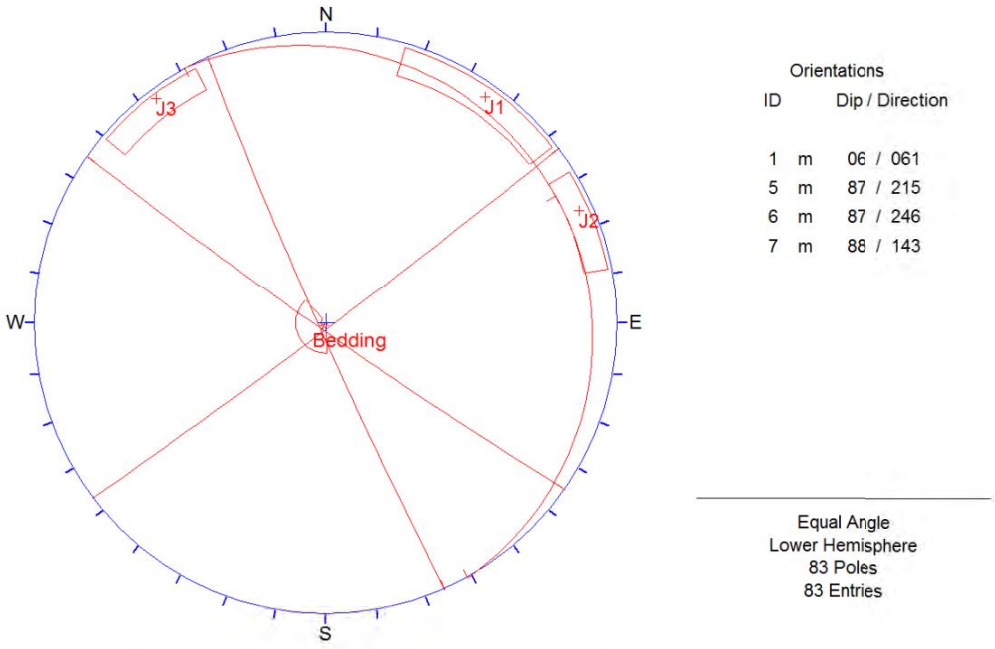

Figure 60: Dominant discontinuity sets detected by acoustic scanner.

Table 14: Results from photogrammetry - Sea Cliff Bridge

Joint Set	Bearing Trend	Spacing [m]	
		Ave	STD
Bedding	NE	2.35	2.1
Set A	NNE	2.8	2.4
Set B	NE	4.8	2.8
Set C	NW-NNW	2.6	1.8

In Table.14, the spacing of bedding plane and joint sets determined from photogrammetry method are listed. However, spacing of bedding planes in depth 150m (100-200m) are estimated from the defect logs of borehole TBC015 (the only existing defect log for this depth).

The most probable ratio between maximum horizontal stress and vertical stress in depth 150m is 2.17. Considering magnitude and orientation of in-situ stress along with orientation of joint sets, geometrical properties of discontinuity sets which used for calculation of hydraulic conductivity are presented in Table15.

Magnitude and orientation of principal hydraulic conductivity tensors are calculated and presented in Table16 and Figure 61.

Table 15: Geometrical properties of discontinuity sets for depth 150m (100-200m)

Joint Set	Dip/Dir	Dip	Equivalent Depth [m] (based on stress orientation)	Spacing	Hydraulic aperture [μm]
Bedding	61	6	150	1.25	50
Set 1	215	87	217	2.8	35
Set 2	246	87	217	4.8	35
Set 3	143	88	326	2.6	23

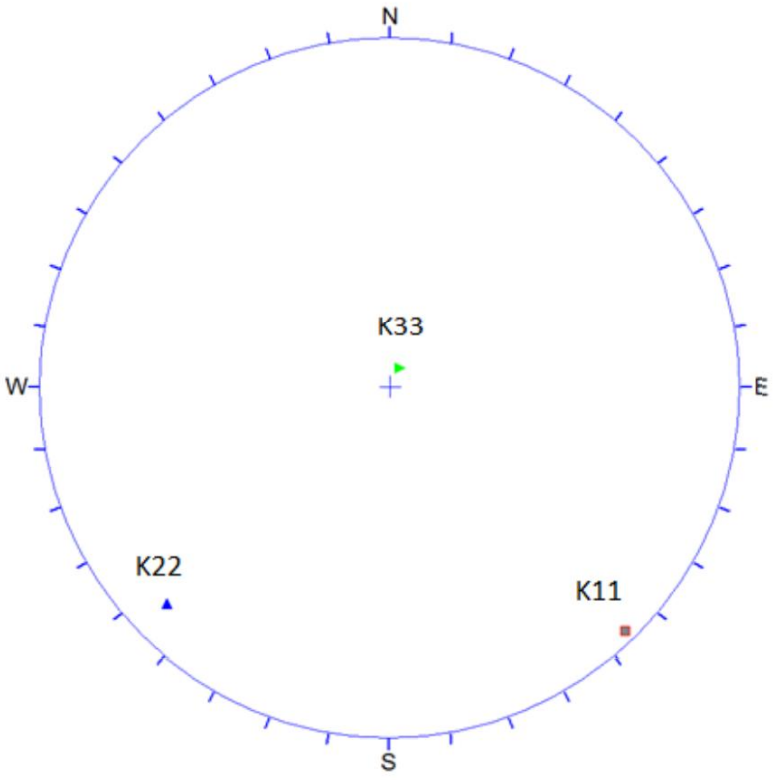

Figure 61: Orientation of principal components of hydraulic conductivity for depth 150m.

Table 16: Principal hydraulic conductivity components and their orientation for depth 150m (100-200m)

	K_{11} [m/s]	K_{22} [m/s]	K_{33} [m/s]	Mean [m/s]
Snow Method	9.94e-8	8.6e-8	2.34e-8	6.95e-8
Plunge/Trend	2/136	7/226	83/29	

As expected, bedding planes have highest contribution on hydraulic conductivity in depth 150m and sub-vertical joint sets act as connecting channel between bedding planes. Based on these results, a transverse isotropic hydraulic conductivity has been obtained for jointed rock in depth 100-200m for Tahmoor South. The ratio between maximum horizontal and vertical hydraulic conductivity is 4.25. Furthermore, there is an acceptable agreement between calculated values and statistical results of packer tests.

Table 17: Packer test's results and computed hydraulic conductivity for depth 100-200m

	Average hydraulic conductivity for depth 100-200 (m/s)	Standard Deviation (m/s)
Arithmetic Mean -Packer tests	1.07e-7	2.1e-7
Geometrical Mean	2e-8	-
Area under best fit	1.09e-7	
Analytical model	6.95e-8	8.2e-9
K_H/K_v	4.25	
K_H/K_h	1.1	

8.5 Hydraulic Conductivity Tensor for Depth 50m (0-100m)

As mentioned in previous section, the Hawkesbury Sandstone is the dominant lithology at shallow depth in the Tahmoor South area. Therefore, discontinuity sets which found in previous section were used for depth 50m as well. Bedding spacing determined from photogrammetry was considered for the calculation of hydraulic conductivity. The conductivity results are presented in Table 18. Analysis of stress and conductivity results in 110 μm as hydraulic aperture of bedding planes in depth 50m. The hydraulic aperture of joint sets was determined according to orientation of maximum horizontal stress and dip direction of joint sets.

Table 18: Geometrical properties of discontinuity sets for depth 50m (0-100m)

Joint Set	Dip/Dir	Dip	Equivalent Depth [m] (based on stress orientation)	Spacing	Length	Hydraulic aperture [μm]
Bedding	61	6	50	2.35	Infinite	110
Set 1	215	87	79	2.8	Infinite	82
Set 2	246	87	79	4.8	Infinite	82
Set 3	143	88	119	2.6	Infinite	60

Considering ratio between maximum horizontal stress and vertical stress equal with 2.37, hydraulic conductivity tensor is calculated as Table 19 and Figure 62. Results show that the magnitudes of maximum and minimum principal components of horizontal hydraulic conductivity are close together (transverse isotropic hydraulic conductivity condition). Furthermore, ratio between maximum horizontal hydraulic conductivity and vertical conductivity is 3.45 (Table 20).

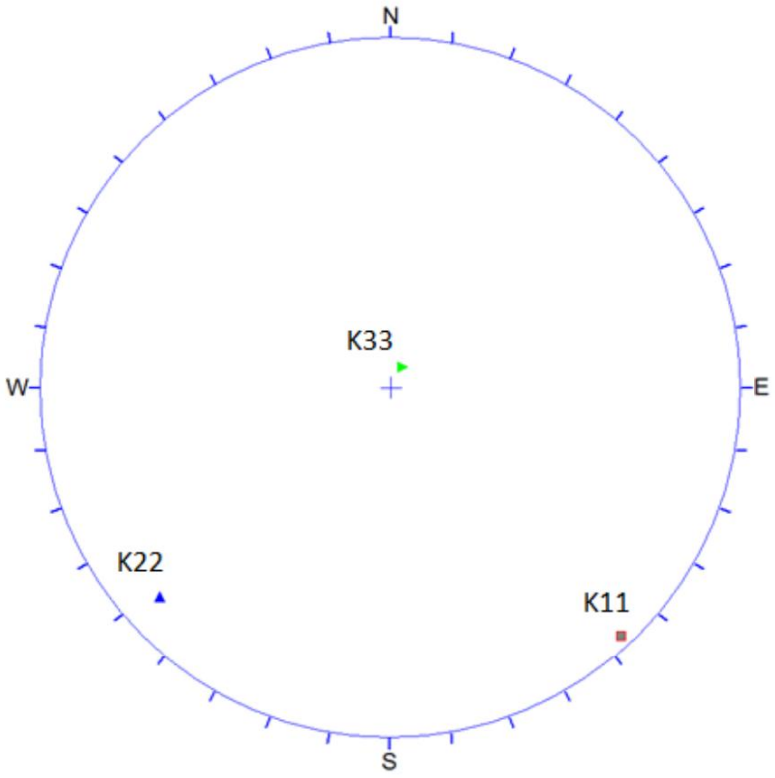

Figure 62: Orientation of principal components of hydraulic conductivity for depth 50m.

Table 19: Principal hydraulic conductivity components and their orientation for depth 50m (0-100m)

	K_{11} [m/s]	K_{22} [m/s]	K_{33} [m/s]	Mean [m/s]
Snow Method	1.1e-6	9.45e-7	3.19e-7	7.87e-7
Plunge/Trend	2/137	7/228	82/30	

Table 20: Packer test's results and computed hydraulic conductivity for depth 0-100m

	Average hydraulic conductivity for depth 0-100 (m/s)	Standard Deviation (m/s)
Arithmetic Mean -Packer tests	7.56e-7	1.76e-6
Geometrical Mean	1.59e-7	-
Area under best fit	7.29e-7	-
Analytical model	7.87e-7	-
K_H/K_v	3.45	
K_H/K_h	1.16	

9. DISCUSSION OF RESULTS FOR THE ESTIMATION OF THE THREE DIMENSIONAL HYDRAULIC CONDUCTIVITY

The hydraulic conductivity of the rock mass in Tahmoor South has been estimated by statistical analysis of packer tests and analytical method in this report.

The analysis is based on the premise that the majority of flow is hosted via discontinuities. It is noted that some sandstone units such as the Hawkesbury Sandstone and the Bulgo Sandstone have relatively high conductivity in certain sections of the sequence, however the results in these sections are consistent with flow within the fabric and within discontinuities. Elsewhere in the sequence the dominant flow appears to be within the discontinuities of the rock mass.

A combination of information gained from acoustic scanner method, in-situ stress measurement and defect logs has been used for the analytical calculation. Hydraulic conductivity tensors calculated by the analytical method offers more information about hydraulic conductivity of jointed rocks. A good agreement between the calculated values and statistical results of packer tests represent a validation for selected input data and applied method. The correlation is presented in Figure 63.

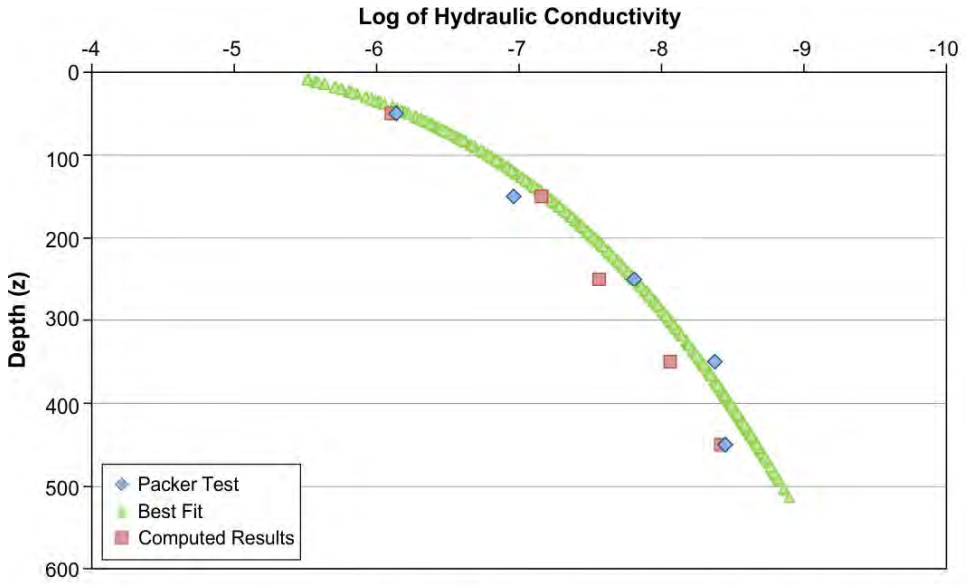

Figure 63: Comparison of results from packer tests and analytical method.

A summary of calculated results and statistical analysis of packer tests are presented in Table 21.

Table 21: Summary of calculated results and statistical analysis of packer tests

Depth (m)	Hydraulic conductivity (m/s)		
	Arithmetic Mean -Packer tests	Raymer Method	Calculated Average
50 (0-100)	7.56e-7	7.29e-7	7.87e-7
150 (100-200)	1.07e-7	1.09e-7	6.65e-8
250 (200-300)	2.65e-8	1.55e-8	2.73e-8
350 (300-400)	5.09e-9	4.22e-9	8.67e-9
450 (>400)	4.2e-9	3.56e-9	3.83e-9

The maximum and intermediate components of calculated hydraulic conductivity (K_{11}, K_{22}) in most boreholes) are essentially horizontal and the minimum component (K_{33}) is sub-vertical. In Table 22, the average principal components of the calculated hydraulic conductivity for each depth along with their orientation are presented. Figure 64 presents the polar plot of trend of the calculated principal hydraulic components for the various depths. They display the same orientation and are primarily controlled by the bedding planes and to a lesser extent the joint planes and stress field.

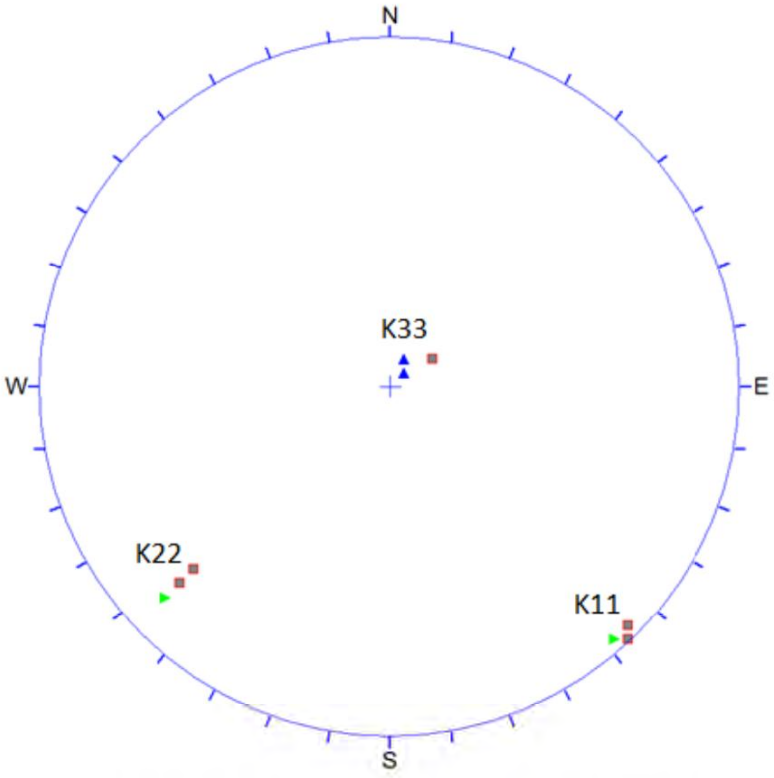

Figure 64: Orientation of principal components of hydraulic conductivity in Tahmoor Colliery.

Table 22: Summary of the conductivity tensors for each depth

Depth (m)	Average Principal Hydraulic conductivity tensor (m/s)				
	K11 Plunge/Trend	K22 Plunge/Trend	K33 Plunge/Trend	K_H/K_v	K_H/K_h
50 (0-100)	1.1e-6 2/137	9.45e-7 7/228	3.19e-7 82/30	3.45	1.16
150 (100-200)	9.94e-8 2/136	8.6e-8 7/227	2.34e-8 83/29	4.25	1.1
250 (200-300)	3.83e-8 0/136	2.79e-8 16/226	1.57e-8 74/47	2.44	1.37
350 (300-400)	1.23e-8 2/137	9.52e-9 10/227	4.2e-9 80/35	2.87	1.29
450 (>400)	5.54e-9 2/137	4.49e-9 8/227	1.47e-9 82/32	3.77	1.23

The results are considered to represent the best estimate of the conductivity tensor within the insitu rock mass. This is based on an analysis of conductivity of the rock fabric (pore space fabric) and the flow within discontinuities within the rock mass. It is recognised that the conductivity of sections of the Hawkesbury Sandstone and the Bulgo Sandstone have a high conductivity, however this is similar to the average fracture based conductivity and well within the scatter of the data used within the analysis.

10. HYDRAULIC CONDUCTIVITY ABOVE LONGWALL PANELS IN THE TAHMOOR SOUTH AREA

The aim of this section is to assess the hydraulic conductivity of the overburden above the longwall panels extracted in the Bulli Seam for the proposed panels in the Tahmoor South area. This is based on the site specific information of the site.

The geotechnical and hydrological characterisation of the area was undertaken and has been presented in Sections 4, 5 and 8.

The approach used was to develop a computer model of the geotechnical characteristics of the strata in the area. The extraction of a longwall panel was then simulated in the model. The results provided information to determine the:

i. Mining induced fracture systems in the roof and floor strata.

ii. Caving characteristics of the overburden strata within the geotechnical environment.

iii. Subsidence estimates.

iv. Hydraulic conductivity of the fracture systems which formed in the overburden and floor strata.

10.1. Background Information

The proposed mine area is presented in Figure 1 together with the location of boreholes used for the development of the computer model.

The depth of the Bulli Seam was presented in Figure 2 ranges from approximately 380m to 440m. A typical geotechnical section of the strata was selected and a depth of 400m was considered to be representative of the area. Boreholes TBC 2,5,32 were used as a cross section line across the panels. The geotechnical properties of the overburden strata were determined on the basis of geophysical relationships of strength and shale fraction. This information was complemented with core testing of the key rock types from the Tahmoor South area and other core tests conducted previously by CSIRO (1986) and SCT Operations (2010).

The unconfined compressive strength properties of the strata were determined on the basis of a relationship of sonic velocity as presented in section 4.4.

*UCS (MPa) =2.3271*10^(0.0008*sonic velocity (m/s))*

The strength profile of the strata used in the model is presented in Figure 65a in terms of UCS for TBC 2,5 and 32. The section used in the model is also presented in Figure 65b. The manifestation of this within the geotechnical model is presented in Figure 66.

11. MODEL AND APPROACH TO ASSESS THE HYDRAULIC CONDUCTIVITY OF THE OVERBURDEN ABOVE THE LONGWALL PANELS

The assessment of overburden caving and hydraulic conductivity of the overburden was undertaken using a computer model of the geological/geotechnical section as characterised in Section 4 and 5.

The Bulli Seam was modelled as 2.4m thick.

The aim of the model was to simulate caving, mining induced fracture formation, stress redistributions, ground displacement and pore pressure changes in the strata about extraction panel as it was formed.

The panel is extracted on sequential basis and the stress and fracture geometry develops progressively as the model extracts the coal. This process is necessary to simulate the actual process

Once this was undertaken, the model was assessed to determine the hydraulic conductivity of the strata sections above the Bulli Seam.

The model was a two dimensional cross section across 3 panels as presented in Figure 66. The two dimensional model is used as it is not feasible to incorporate the required level of detail into a three dimensional model.

This approach gives good detail of the rock deformation geometry and displacements anticipated throughout the overburden

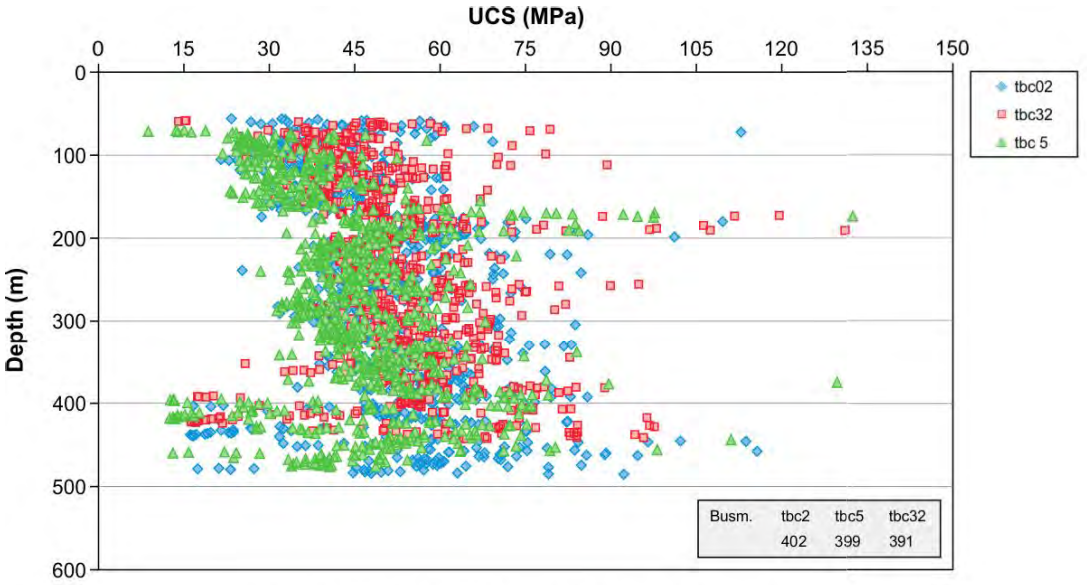

65a: UCS for TBC 2, 5 and 32 relative to depth.

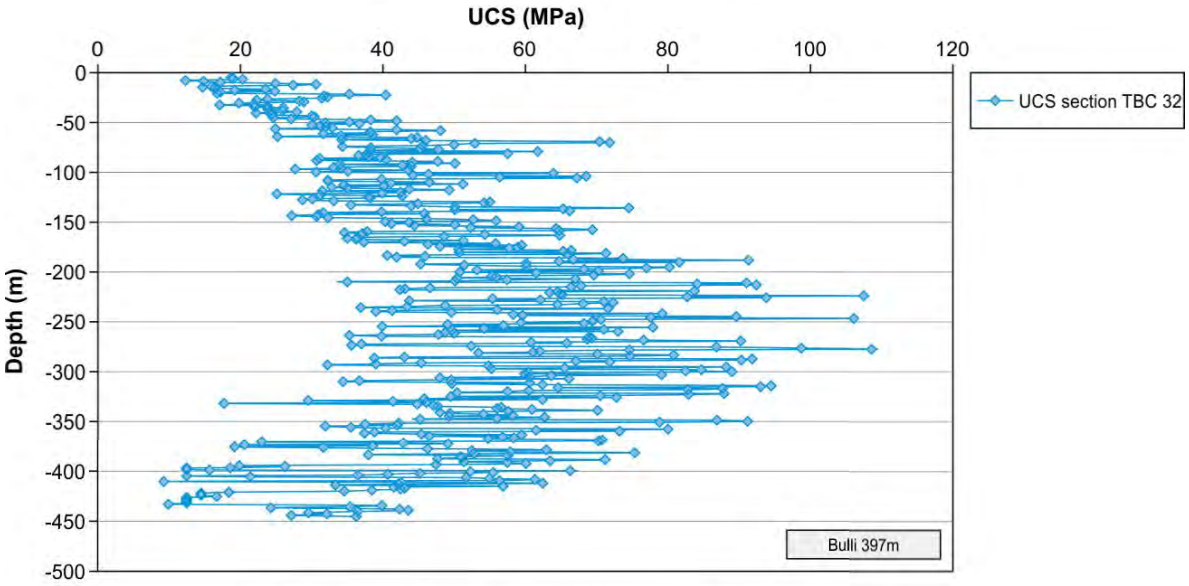

65b: UCS profile in the model based on TBC 32.

Figure 65: UCS Profile of the model and TBC 2, 5 and 32.

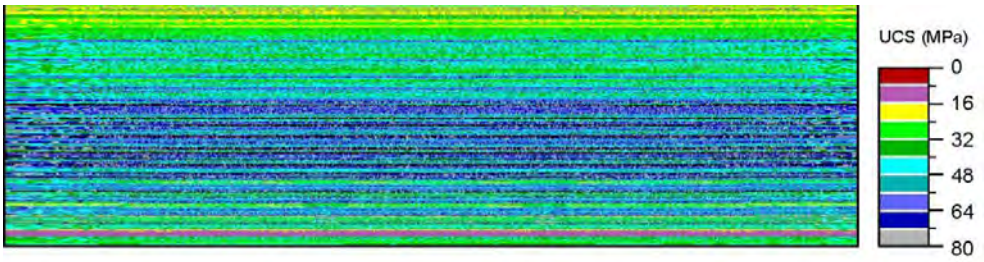

Figure 66: UCS layers within the model.

11.1 Background and Approach to Computer Modelling

Computer modelling of strata caving, overburden fracture and strata strength characteristics has been developing over the last 15 years and applied to coal mining activities. The models are based on geotechnical properties estimated from a combination of bore core testing, geophysical strength relationships and prior experience. Therefore, the computer models are estimates of the geotechnical characteristics of the overburden. Not all properties can be derived from borehole analyses, and estimates need to be made on the basis of either previous work or parametric evaluation of the impact of potential variation in certain properties.

It is very important to undertake verification studies to confirm that the models are simulating the deformation mechanics of the strata in a suitable manner. To that end, validation studies have formed an important part of the modelling process.

The modelling approach and validation data has been reported, the most recent being Gale and Sheppard (2011), which details modelling undertaken at Tahmoor North.

The code used in the model is FLAC and uses a coupled rock failure and fluid flow system to simulate the behaviour of the strata and fluid pressure/flow effects. The rock failure and permeability routines have been developed by SCT Operations and more realistically represent the rock fracture mechanics than is available in the standard codes. Rock failure is based on Mohr-Coulomb criteria relevant to the confining conditions within the ground.

The general strength characteristics of the rock materials in the intact and post failure range are presented in Figure 67. Tensile strength of the rock materials is in the range of 8-10% of the UCS.

The in situ strength of the rock materials is reduced to 0.58 the laboratory UCS. This is consistent with the general Hoek and Brown relationships but also is consistent with scale effects as reported from other methods.

The model simulates rock fracture and stores the orientation of the fractures. Shear fracture, tension fracture of the rock, bedding plane shear and tension fracture of bedding is determined in the simulation. The stability of pre-existing jointing, faults or cleat is also addressed in the simulations where appropriate.

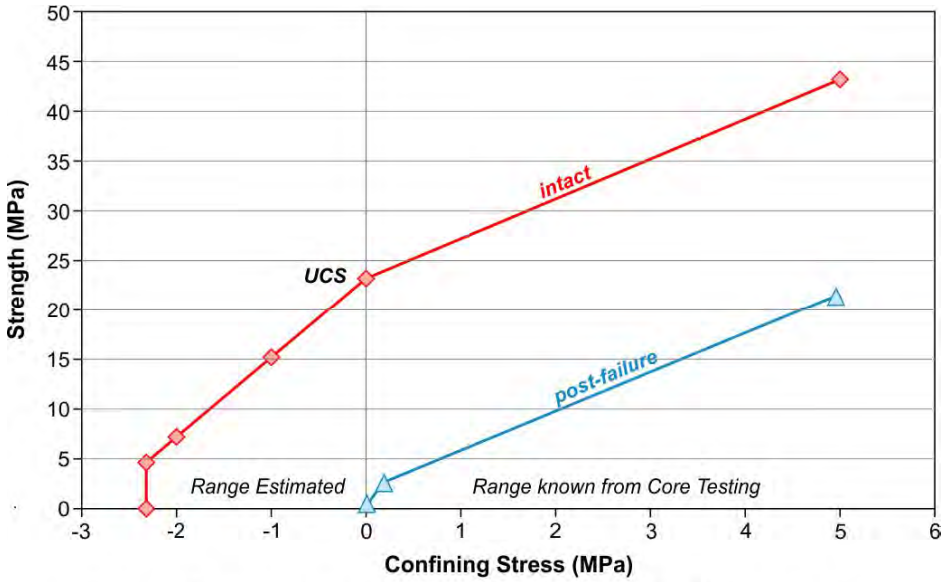

Figure 67: Generalised strength characteristics for rock units.

Consolidation of the goaf occurs as the weight of the caved strata increases in the extracted areas.

Ground displacements, rock fracture and stress redistributions can be assessed within various rock units and geometries about the extraction panel.

In the models the caved material forms the goaf. The goaf develops strength on the basis of:

i. An increasing stiffness with vertical strain

ii. Confinement within the goaf material which has developed as a result of the overburden converging onto the goaf.

The goaf loading characteristics are based on field extensometer data, together with measured vertical abutment load balance and subsidence validation from previous studies. The general goaf loading characteristics are presented in Figure 68.

Each layer in the model is based on the average strength for that unit as per Figure 65. However, the strength is allowed to vary by up to 40% in a random manner within the layer. This variation is input to be consistent with laboratory testing information and to recognise the natural variability of material strength in a sedimentary environment.

Also, jointing is incorporated within the model on a random manner with an average spacing of 4m. Bedding plane partings are similarly included with an average vertical spacing of 3m.

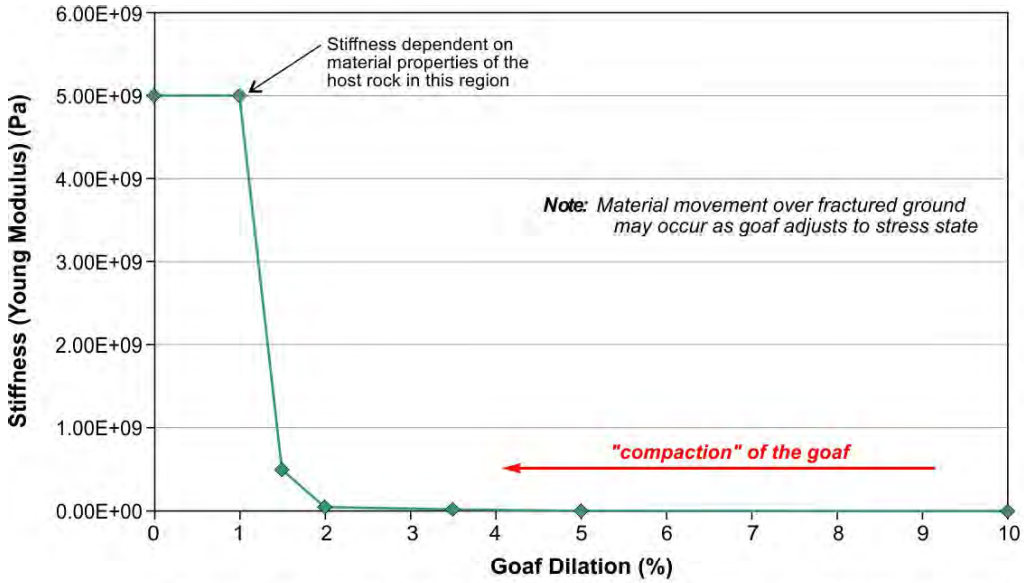

Figure 68: General goaf loading characteristics used in the model.

In the model, the rock properties utilised are:

i. UCS and tensile strength.

ii. Young's Modulus, Poisson's Ratio.

iii. Triaxial strength factor (relates to friction angle).

iv. Bedding plane cohesion, friction and tensile strength.

v. Joint and bedding parting cohesion and friction angle.

A range of these properties for the key rock types is presented in Table 23.

Table 23: Rock strength properties used

Rock Type	UCS (MPa)	Young's Modulus (GPa)	Bedding Cohesion (MPa)	Bedding Friction (deg)	Triaxial Strength Factor
Laminated Sandstone	50	14	4	36	4
Laminated Siltstone	40	11	2	30	4
Laminated Siltstone	20	6	2	30	4
Carbonaceous Mudstone	30	9	2	25	4

Each rock unit defined in the model is characterised by these properties, however, for ease of visualisation, the UCS has been used to present the range in rock properties within the sections.

The coal seam is modelled on the basis of in situ strength rather than strength obtained from core. This is a standard approach due to the

sampling problems with coal and the availability of large scale measurements of coal. Overall, the in situ strength of coal is relatively similar and is typically in the range of 6-8MPa. The strength of the coal has been modelled as 7MPa.

A number of the bedding plane parameters (in particular) have been estimated from experience and previous rock tests from the general area.

Stress measurements have been conducted in the Tahmoor South area by Sigra which determine the stress at a number of locations within the overburden. In other areas of the Tahmoor North Mine stress measurements have been conducted by SCT Operations and CSIRO.

The tectonic stress factor is a means of defining the stress environment irrespective of the rock type in which the measurement was taken. The tectonic stress factor at the Bulli Seam level was modelled as 0.7 for a depth of 400m which is oriented across the longwall panels. Information on the stress direction is available from the acoustic scanner interpretation and indicates that the major horizontal stress is in a N-NE S-SW direction.

The horizontal stress in each rock unit is defined by the following relationship:
Horizontal stress (MPa) = E (GPa)*tsf + (v/(1-v)*vertical stress (MPa)

The horizontal stress is input into the model for each layer or rock unit. The horizontal stress within a rock unit is composed of components relating to vertical stress (Poisson's Ratio effect) and from tectonic strain caused by crustal movements. The stresses relating to crustal movements are typically related to the stiffness of the unit and the higher the Young's Modulus of the unit the higher the stress within it.

However, adjustments are made to be consistent with the depth stress relationship of the area. In general, the horizontal stress is determined by the tectonic strain (formula used above) and stress modifications caused by faulting and slip along structures in the upper crust. These effects are incorporated in the stress field within the model.

The in situ hydraulic conductivity of the strata is input into the model on the basis of packer tests (lugeon) over the site together with a regional data base of the conductivity of joints and bedding planes relative to confining stresses in the strata. In this case, the conductivity was assumed from the SCT database, and is controlled by the confining stress across the structure.

The relationship used in the model is presented in Figure 69 in terms of confining stress across the plane.

The depth of the water table was modelled as 50m below surface and it was assumed that pre existing joints and bedding had a reduced friction and cohesion in this zone, as was noted to occur in the southern zones of LW 24-25 (Gale and Sheppard 2011).

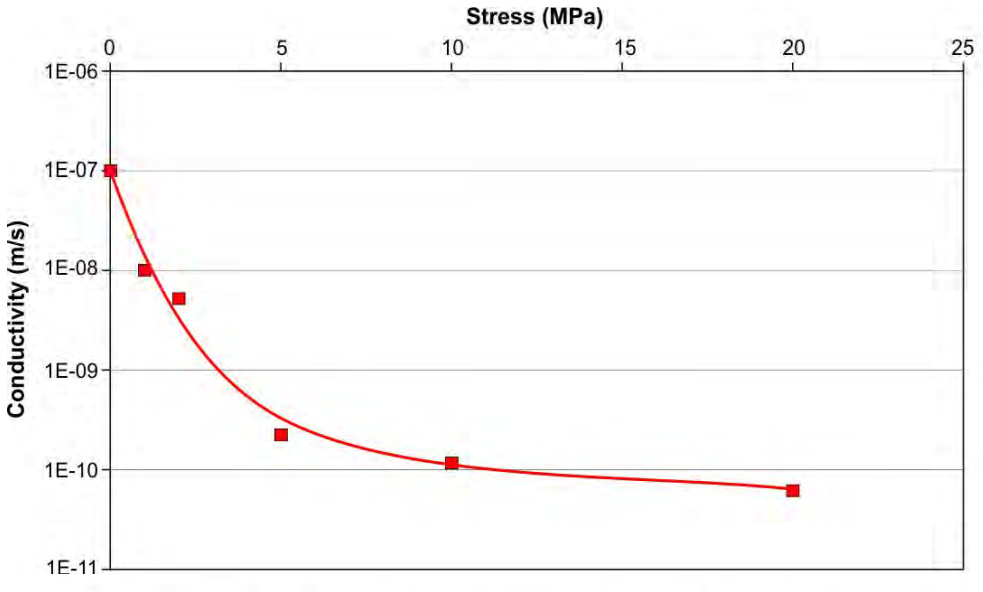

Figure 69: Stress / conductivity relationship used for insitu conductivity.

The nominal panel width was 300m however the effect of a 250m panel width was also assessed regarding the impact of a narrower panel on overburden conductivity. The seam thickness modelled was 2.4m.

11.2 Large Scale Caving

The large scale fracture distribution is presented in Figure 70 and shows that bedding plane shear is common throughout the overburden and extends to the surface. Bedding plane slip is common on the clay / tuffaceous units.

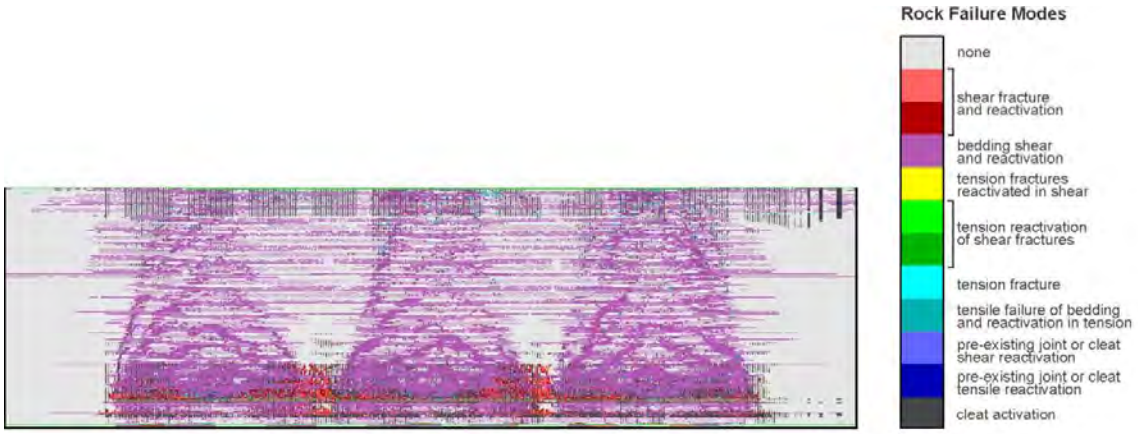

Figure 70: Large scale fracture distribution.

Bedding partings and joints in the weathered section of the overburden surface are also mobilised. Shear fracture through the rock occurs about the seam and in the floor. Tension fractures form as part of the caving process as rock units subside onto the goaf. Jointing is also mobilised about the extraction zone and throughout the overburden.

Fracture zones appear to form in the floor and may provide an enhanced connection to the Wongawilli seam.

The strata fractures above the chain pillars and allows the pillars to yield.

The subsidence which resulted from the coal extraction within the model is presented in Figure 71. The subsidence was approximately 0.9 m for a single panel and increased up to approximately 1.2-1.3m for multiple panels as a function of chain pillar subsidence.

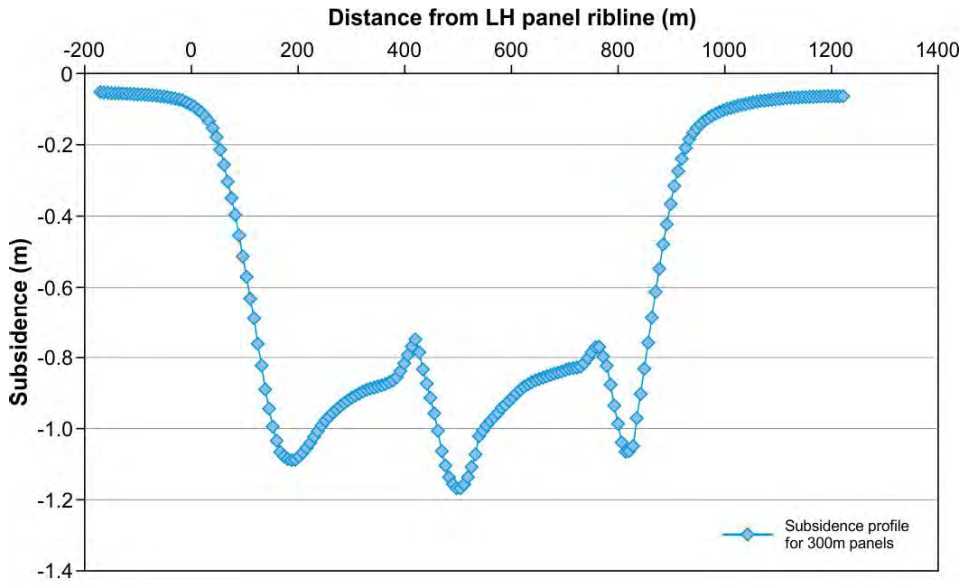

Figure 71: Subsidence characteristics for three panels.

The subsidence with a 250m wide panel is presented in Figure 72 in terms of comparison with a single panel.

The subsurface caving or displacements are presented in Figure 73 as an "extensometer plot" this shows the displacement from the surface to the seam down the centre of LW2. This shows that most of the caving related displacements occur up to approximately 150m above the seam and above this the ground tends to subside.

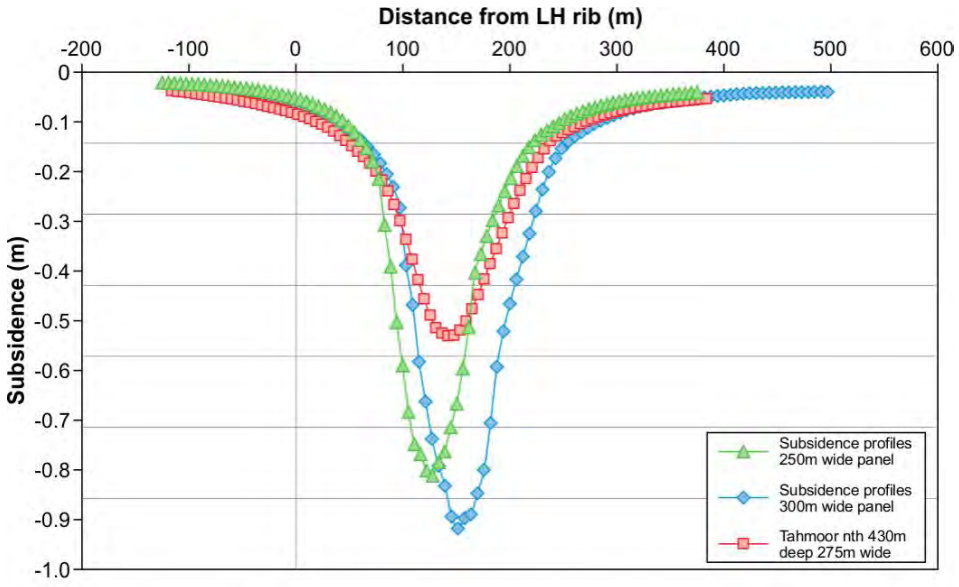

Figure 72: Subsidence for 250m and 300m in single panels.

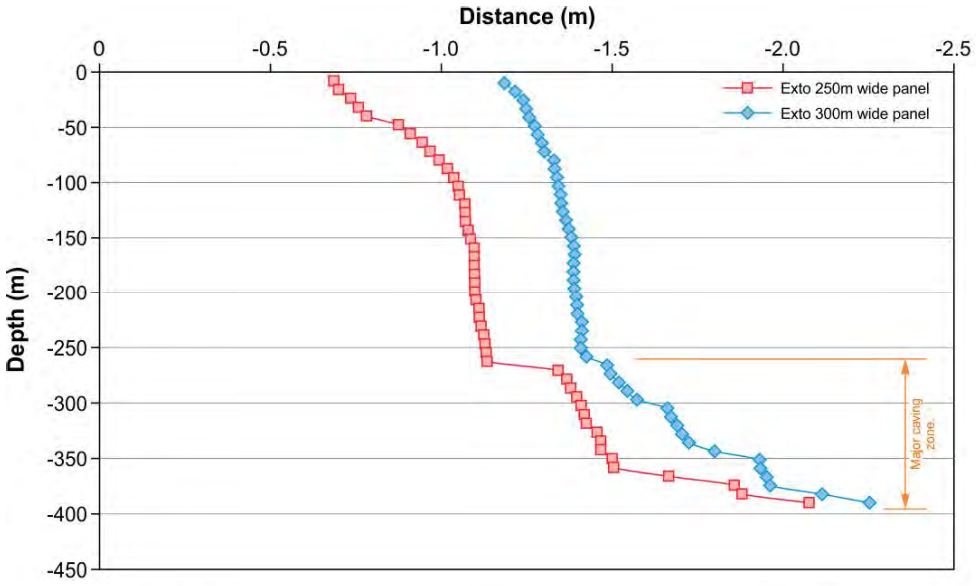

Figure 73: Surface extensometer plots for 250m and 300m wide panels.

11.2 Hydraulic Conductivity of the Strata

The in situ overburden conductivity modelled is modelled on the basis of the vertical and horizontal conductivity within each element.

The conductivity is the greater of that associated with flow through the rock fabric or through a mining induced fracture formed within the element.
The conductivity is enhanced by the creation of mining induced fractures and dilation of pre-existing fractures. Quantification of the fracture induced

conductivity is estimated within the model on the basis of the equivalent material conductivity calculated from aperture flow within a fracture. The conductivity (k) estimated from the flow quantity through a $1m^2$ area with unit pressure gradient. This then simplifies to solve k as approximately equal to:

$$k = e^3 \times 10^{-6} \; m/s$$

where: e is the hydraulic aperture (m).

The aperture of the fractures will vary depending on confining pressure such that conductivity reduces in areas of increased stress normal to the fracture and vice versa.

Once rock fracture occurs due to mining, the dilation of the strata is considered to be related to fracture dilation. This is calculated in each element on the basis of change in length once material stiffness effects have been taken into account. It has been assumed that there is one fracture per element in the model and that the aperture is equal to the average dilation. The effect of surface roughness on the actual hydraulic aperture is difficult to predict. Other workers have assessed these effects and found that flow may vary up to 70% depending on surface effects (Brown 1987, Witherspoon et al. 1980). The approach used for this analysis is to assume a surface undulation of 0.5mm on the fractures which reduces the hydraulic aperture from the physical aperture. This dilation reduction (0.5mm) is used in an attempt to account for surface roughness of the fractures.

The fracture and joint dilation within the model is then analysed on the basis of the aperture formula to obtain an estimate of the conductivity that the fracture would represent.

It is important to establish the effective conductivity of the system which is related the pathway or flow network that fluid may migrate through the fractures and rock fabric.

The flow network is determined by introducing a pore pressure gradient through the model and allowing flow to occur through the fractures and bedding planes which exist. Not all fractures will allow flow and only those which are part of a connected network will allow flow to occur through the model.

The effective conductivity of the model is then determined by assessing the flow and pore pressure gradient within the model on the basis of:

$$K \; (m/s) = Q \; (\text{flow } m^3/s) \; / \; (\text{pore pressure gradient} * \text{Area } (m^2).)$$

Both the vertical and horizontal conductivity can be calculated in this manner, however, the primary aim of this report is to assess the vertical connections between the Bulli seam and the surface.

11.3 Vertical Hydraulic Conductivity about the 300m wide Longwall Panels

The vertical hydraulic conductivity as determined from the fracture networks within the model of the three 300m wide panels is presented in Figure 74. This shows the major zones along which the vertical flow occurs. In general the major zones are contained within the zone up to 200m above the seam.

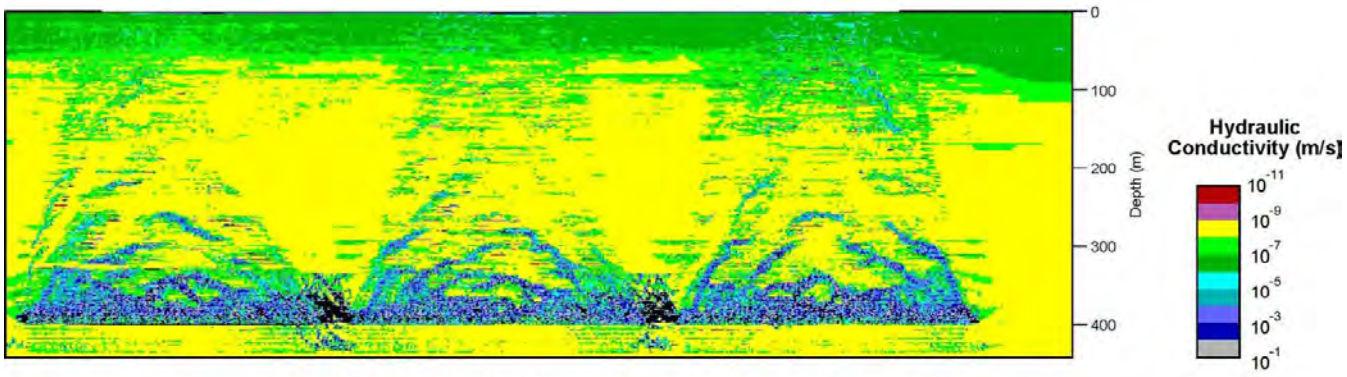

Figure 74: Vertical hydraulic conductivity in the model.

Above this vertical flow is primarily very localised along bedding planes and fracture planes developed during subsidence movements of the strata above the "caving zone".

The horizontal conductivity is presented in Figure 75 and shows that there is significant horizontal conductivity within the caved zone but also within the parted bedding planes adjacent to the panel edges. These areas represent the zones in the overburden which will have the greatest bedding parting as a response to subsidence movement (shear and opening). There is also major horizontal conductivity in the upper strata within 100m of the surface.

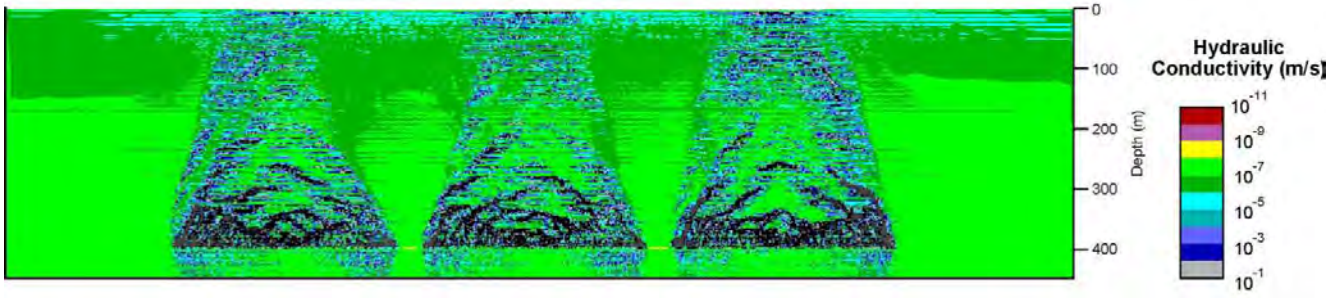

Figure 75: Horizontal hydraulic conductivity in the model.

The vertical conductivity profile from the goaf up to the surface has been plotted in Figure 76 as an average for each 1m layer in the model across the 3 panels. This data has been averaged on the basis of a 5 m running average. The averaging process is presented in Gale 2008 and Scott 1975.

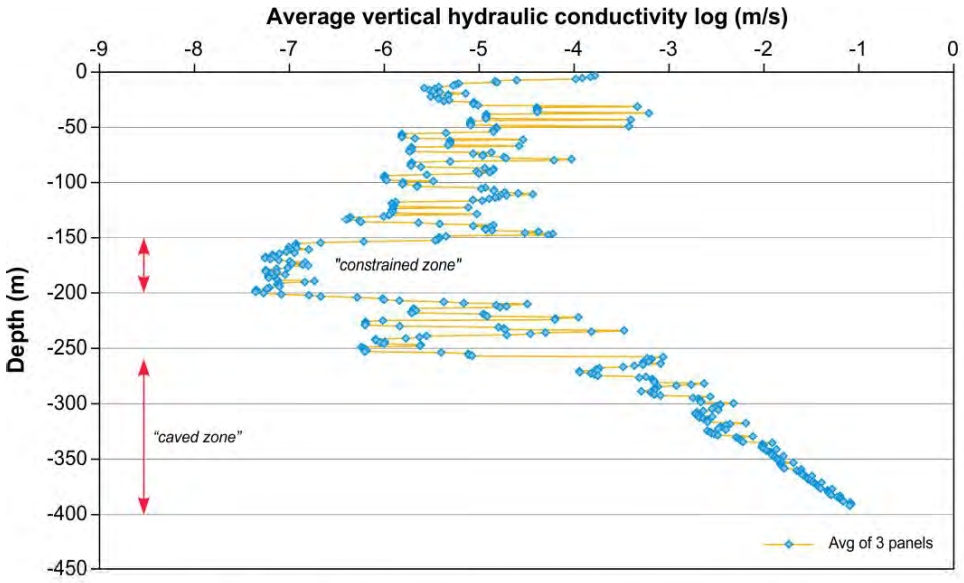

Figure 76: Running 5m average of vertical conductivity in the model.

The plot shows the high conductivity within the caving zone (up to approximately 200m below surface). Above this the conductivity is typically in the range of 10^{-6} to 10^{-7}m/s with the exception of a zone between 150 and 200m below surface which has a conductivity of the order 10^{-8}m/s. This zone forms a "constrained zone" between the goaf and the surface.

The conductivity above the longwall panels presented is that of the bulk rock mass. It consists of the conductivity of the rock units and the rock fracture system. The overall rock mass wall behave as a "dual permeability" and "dual porosity" mass.

The net effect of the fracture and conductivity zones on the cumulative conductivity is presented in Figure 77. This figure displays the 5m running average data together with the cumulative data plotted relative to the a point:

i. At the surface and progressing down toward goaf.

ii. At the top of the extracted seam and progressing up toward the surface.

This presents the average total conductivity of the overburden to be approximately 10^{-7}m/s however this comprises a number of discrete zones which would impact on the pore pressure distribution and flow rates within the strata above the panels.

The cumulative vertical conductivity plot and the running average plot from the seam to surface provides a good indication of the height of depressurisation anticipated in the strata section. It would be anticipated that the strata below the constrained zone (approximately 200-220m above the seam) would drain quicker that above and as such create a depressurised zone. This location is very similar to that obtained from the relationship of Tammetta, 2012 which predicts a height of 200-210m.

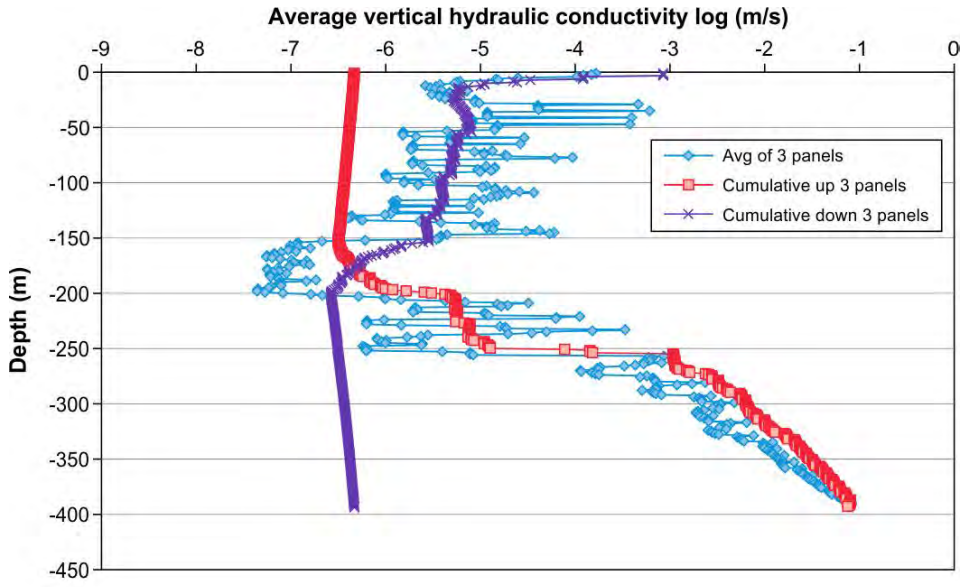

Figure 77: Cumulative vertical conductivity in the overburden.

11.4 Effect of 250m Wide Panels

The effect of the narrower panel was assessed on the basis of a single 250m wide panel compared with the 300m wide panels analysed previously.

The result is presented in Figure 78 and shows that the cumulative conductivity is slightly reduced by essential similar to the 300m wide panels. It was noted that the height of effective caving zone was reduced in the 250m wide case relative to the 300m wide panels.

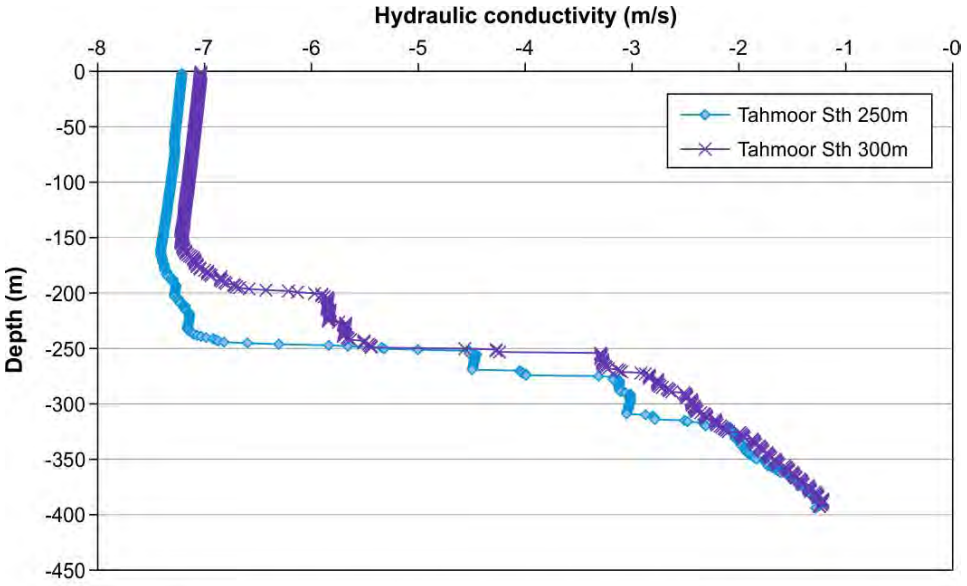

Figure 78: Comparison of the cumulative vertical conductivity for 250m and 300m panels.

12. REFERENCES

ASIMS, 2012, Acoustic Scanner Reports for Boreholes TBC001 to TBC029, Tahmoor Colliery.

Forster, I and Enever, J, 1992, 'Hydrological response of overburden strata to underground mining', Office of Energy Report Vol. 1, pp. 104.

Gale, WJ, 2006, 'Water inflow issues above longwall panels', in proceedings of 7th Underground Coal Operators Conference (Coal 2006), Sustainable Coal Mine Development, 5-7 July 2006, University of Wollongong, NSW, pp. 175-179.

Gale, W, 2008. Aquifer Inflow Prediction above Longwall Panels, ACARP Project C13013, 2008.

Gale, W, and Sheppard, I, 2011. Investigation into Abnormal Increased Subsidence above Longwall Panels at Tahmoor Colliery NSW, Proceedings of the Eighth Triennial Conference on Management of Subsidence; State of the Art, 15-17 May 2011.

Geoterra Report, 2012 Tahmoor Colliery Annual Groundwater Report 2011-2012 Ta17-R1B

Gordon Nick 2013. Additional Notes on Stress Orientation February 2013

Guo, H, Shen, B, Chen, S, Poole, G, 2005, 'Feasibility study on subsidence control using overburden injection technology', ACARP Report C12019.

Hatherley, P, Gale, W, Medhurst, T, King, A, Craig, S, Poulsen, B, Luo, X, 2003, '3D effects of longwall caving as revealed by micro seismic monitoring', ACARP Report C9012.

Holla, L and Armstrong, M, 1986, 'Measurement of sub surface strata movement by multi-wire borehole instrumentation', Bull. Proc. AusIMM, Vol 291, No 7, pp. 65-72.

Holla, L and Buizen, M, 1991, 'The ground movement, strata fracturing and changes in permeability due to deep longwall mining', Int. Rock Mech. & Min, Sci. 28 2/3, pp. 207-217.

Hudson, J.A., Harrison, J.P. 1997. Engineering Rock Mechanics, An introduction to the principals. Elsivier Science Ldt.

Jiang, X.W., Wang, X.Sh., Wan, L., 2010. Semi-empirical equations for the systematic decrease in permeability with depth in porous and fractured media. Hydrogeology Journal. Vol. 18, pp. 839-850.
Lithology and Defect logs for Tahmoor Colliery.

Mills, KW, 2011. Developments in Understanding Subsidence with Improved Monitoring, Proceedings of the Eighth Triennial Conference on Management of Subsidence; State of the Art, 15-17 May 2011.

Nemcik, J., Gale, E., Mills, K., 2005. Statistical analysis of underground stress measurements in Australian coal mines. Bowen Basin Symposium.

Mills, KW & O'Grady, P, 1998, 'Impact of longwall width on overburden behaviour' in proceedings of 1st Australasian Coal Operators Conference (Coal98), 18-20 February 1998, University of Wollongong, pp. 147-155.

Pells Consulting, 1985, A thumbnail engineering geology of the Triassic rocks of the Sydney area.

Raymer, J.H., "Predicting Groundwater Inflow into Hard-Rock Tunnels: Estimating the High-End of the Permeability Distribution," 2001 Proceedings of the Rapid Excavation and Tunneling Conference, Society for Mining, Metallurgy and Exploration, Inc.

SCT Operation, Packer Test Summary Reports.

Sigra PTY LTD, 2010, In Situ Stress Testing, Tahmoor Colliery.

Sigra PTY LTD, 2012, Stress Analysis – Tahmoor North and Bargo Areas.

Snow, D.T. Anisotropic permeability of fractured media. Water Resources research, 1969; 5: 1273-1289.

Tammetta, P, 2012. Estimation of the Height of Complete Groundwater Drainage Above Mined Longwall Panels, Ground Water 2012, National Groundwater Association, 2012

Wei, Z.Q., Egger, P., Descoeudres, F., 1995. Permeability prediction of jointed rock mass. Int. J. Rock Mech. Min. Sci. Vol. 32, No.3, pp. 251-161.

Zoorabadi M, Saydam S, Timms W, Hebblewhite B. 2013. Estimation of hydraulic aperture of rock joints as a function of depth. Submitted on Geotechnical and Geological Engineering, an International Journal.

Zoorabadi M, Indraratna B, Nemcik J. A new equation for the equivalent hydraulic conductivity of the rock mass around a tunnel. International Journal of Rock Mechanics & Mining Sciences. 2012a; 54: 125-125.

Zoorabadi M, Saydam S, Timms W, Hebblewhite B. Sensitivity analysis of effective parameters on the permeability of rock mass around a tunnel. 7th Asian Rock Mechanics Symposium, Seoul, South Korea. 2012b; 944-949.

APPENDIX 1 - DETAIL OF CALCULATED RESULTS FOR DEPTH 450M (<400M)

In situ stress

$\frac{\sigma_H}{\sigma_v} = 2.13$

$\frac{\sigma_H}{\sigma_h} = 1.5$

Orientation of Principal Stress= NW

TBC001

Joint Set	Dip/Dir	Dip	Equivalent Depth [m] (based on stress orientation)	Spacing	Hydraulic aperture [μm]
Bedding	46	7	450	0.53	16
Set 1	318	89	960	0.68	5
Set 2	67	90	639	1.21	10
Set 3	200	88	798	2.48	7

Hydraulic conductivity of rock mass

	K_{11} [m/s]	K_{22} [m/s]	K_{33} [m/s]	Mean [m/s]
Snow Method	7.04e-9	6.49e-9	1e-9	4.85e-9
Plunge/Trend	3/294	8/203	82/43	

TBC002

Joint Set	Dip/Dir	Dip	Equivalent Depth [m] (based on stress orientation)	Spacing	Hydraulic aperture [μm]
Bedding	39	7	450	0.83	16
Set 1	260	88	798	0.38	7
Set 2	213	87	639	1.52	10

Hydraulic conductivity of rock mass

	K_{11} [m/s]	K_{22} [m/s]	K_{33} [m/s]	Mean [m/s]
Snow Method	5.1e-9	4.19e-9	1.26e-9	3.5e-9
Plunge/Trend	3/299	8/209	81/46	

TBC003

Joint Set	Dip/Dir	Dip	Equivalent Depth [m] (based on stress orientation)	Spacing	Hydraulic aperture [μm]
Bedding	46	8	450	0.7	16
Set 1	214	87	639	0.92	10

Hydraulic conductivity of rock mass

	K_{11} [m/s]	K_{22} [m/s]	K_{33} [m/s]	Mean [m/s]
Snow Method	5.67e-9	4.74e-9	9.26e-10	3.78e-9
Plunge/Trend	2/146	9/236	81/46	

TBC004

Joint Set	Dip/Dir	Dip	Equivalent Depth [m] (based on stress orientation)	Spacing	Hydraulic aperture [μm]
Bedding	55	8	450	0.48	16
Set 1	241	81	639	0.66	10
Set 2	288	81	960	0.86	5
Set 3	173	89	798	0.89	7

Hydraulic conductivity of rock mass

	K_{11} [m/s]	K_{22} [m/s]	K_{33} [m/s]	Mean [m/s]
Snow Method	8.23e-9	7.23e-9	1.65e-9	5.71e-9
Plunge/Trend	1/302	8/212	82/36	

TBC005

Joint Set	Dip/Dir	Dip	Equivalent Depth [m] (based on stress orientation)	Spacing	Hydraulic aperture [μm]
Bedding	52	4	450	0.61	16
Set 1	222	89	639	0.86	10

Hydraulic conductivity of rock mass

	K_{11} [m/s]	K_{22} [m/s]	K_{33} [m/s]	Mean [m/s]
Snow Method	6.38e-9	5.44e-9	9.38e-10	4.25e-9
Plunge/Trend	1/138	5/228	86/41	

TBC006

Joint Set	Dip/Dir	Dip	Equivalent Depth [m] (based on stress orientation)	Spacing	Hydraulic aperture [μm]
Bedding	89	5	450	0.86	16
Set 1	219	86	639	1.01	10
Set 2	270	88	798	1.88	7

Hydraulic conductivity of rock mass

	K_{11} [m/s]	K_{22} [m/s]	K_{33} [m/s]	Mean [m/s]
Snow Method	4.72e-9	3.94e-9	9.48e-10	3.2e-9
Plunge/Trend	4/136	3/226	85/359	

TBC007

Joint Set	Dip/Dir	Dip	Equivalent Depth [m] (based on stress orientation)	Spacing	Hydraulic aperture [μm]
Bedding	64	9	450	0.72	16
Set 1	9	89	798	0.84	7
Set 2	238	87	639	1.95	10

Hydraulic conductivity of rock mass

	K_{11} [m/s]	K_{22} [m/s]	K_{33} [m/s]	Mean [m/s]
Snow Method	5.22e-9	4.74e-9	7.36e-10	3.57e-9
Plunge/Trend	4/143	9/233	80/29	

TBC008

Joint Set	Dip/Dir	Dip	Equivalent Depth [m] (based on stress orientation)	Spacing	Hydraulic aperture [μm]
Bedding	125	4	450	0.24	16
Set 1	39	84	639	0.22	10
Set 2	73	86	798	0.41	7

Hydraulic conductivity of rock mass

	K_{11} [m/s]	K_{22} [m/s]	K_{33} [m/s]	Mean [m/s]
Snow Method	1.8e-8	1.41e-8	4.28e-9	1.21e-8
Plunge/Trend	4/137	3/227	85/357	

TBC009

Joint Set	Dip/Dir	Dip	Equivalent Depth [m] (based on stress orientation)	Spacing	Hydraulic aperture [μm]
Bedding	62	6	450	0.79	16
Set 1	25	87	639	0.83	10
Set 2	251	88	636	0.82	10

Hydraulic conductivity of rock mass

	K_{11} [m/s]	K_{22} [m/s]	K_{33} [m/s]	Mean [m/s]
Snow Method	5.86e-9	4.53e-9	1.92e-9	4.1e-9
Plunge/Trend	1/132	10/222	80/36	

TBC010

Joint Set	Dip/Dir	Dip	Equivalent Depth [m] (based on stress orientation)	Spacing	Hydraulic aperture [μm]
Bedding	73	7	450	1.2	16
Set 1	108	90	960	0.69	5
Set 2	199	90	639	0.47	10

Hydraulic conductivity of rock mass

	K_{11} [m/s]	K_{22} [m/s]	K_{33} [m/s]	Mean [m/s]
Snow Method	4.49e-9	2.93e-9	1.84e-9	3.1e-9
Plunge/Trend	6/161	11/252	78/42	

TBC011

Joint Set	Dip/Dir	Dip	Equivalent Depth [m] (based on stress orientation)	Spacing	Hydraulic aperture [μm]
Bedding	29	17	450	1.47	16
Set 1	230	89	639	0.72	10

Hydraulic conductivity of rock mass

	K_{11} [m/s]	K_{22} [m/s]	K_{33} [m/s]	Mean [m/s]
Snow Method	3.38e-9	2.39e-9	9.93e-10	2.25e-9
Plunge/Trend	6/310	27/217	62/52	

TBC012

Joint Set	Dip/Dir	Dip	Equivalent Depth [m] (based on stress orientation)	Spacing	Hydraulic aperture [μm]
Bedding	66	5	450	1.19	16
Set 1	33	85	639	0.84	10
Set 2	75	83	639	1.5	10
Set 3	144	87	960	1.34	5

Hydraulic conductivity of rock mass

	K_{11} [m/s]	K_{22} [m/s]	K_{33} [m/s]	Mean [m/s]
Snow Method	4.11e-9	3.11e-9	1.49e-9	2.91e-9
Plunge/Trend	2/134	13/225	76/35	

TBC014

Joint Set	Dip/Dir	Dip	Equivalent Depth [m] (based on stress orientation)	Spacing	Hydraulic aperture [μm]
Bedding	39	7	450	1.25	16
Set 1	199	85	639	0.7	10
Set 2	105	89	960	1.18	5

Hydraulic conductivity of rock mass

	K_{11} [m/s]	K_{22} [m/s]	K_{33} [m/s]	Mean [m/s]
Snow Method	3.81e-9	2.74e-9	1.24e-9	2.6e-9
Plunge/Trend	3/161	8/251	82/53	

TBC015

Joint Set	Dip/Dir	Dip	Equivalent Depth [m] (based on stress orientation)	Spacing	Hydraulic aperture [μm]
Bedding	29	8	450	1.27	16
Set 1	62	82	639	1.61	10
Set 2	6	90	798	1.26	7
Set 3	101	84	960	4.33	5

Hydraulic conductivity of rock mass

	K_{11} [m/s]	K_{22} [m/s]	K_{33} [m/s]	Mean [m/s]
Snow Method	3.21e-9	2.8e-9	7e-10	2.24e-9
Plunge/Trend	3/310	11/219	78/52	

TBC016

Joint Set	Dip/Dir	Dip	Equivalent Depth [m] (based on stress orientation)	Spacing	Hydraulic aperture [μm]
Bedding	49	5	450	1.15	16
Set 1	252	90	639	0.85	10
Set 2	209	87	639	1.12	10

Hydraulic conductivity of rock mass

	K_{11} [m/s]	K_{22} [m/s]	K_{33} [m/s]	Mean [m/s]
Snow Method	4.34e-9	3.11e-9	1.66e-9	3.04e-9
Plunge/Trend	0/306	9/216	82/36	

TBC017

Joint Set	Dip/Dir	Dip	Equivalent Depth [m] (based on stress orientation)	Spacing	Hydraulic aperture [μm]
Bedding	59	8	450	1.46	16
Set 1	44	90	639	0.61	10
Set 2	142	88	960	1.31	5
Set 3	269	89	639	1.67	10

Hydraulic conductivity of rock mass

	K_{11} [m/s]	K_{22} [m/s]	K_{33} [m/s]	Mean [m/s]
Snow Method	3.9e-9	2.64e-9	1.8e-9	2.77e-9
Plunge/Trend	1/127	24/216	67/34	

TBC018

Joint Set	Dip/Dir	Dip	Equivalent Depth [m] (based on stress orientation)	Spacing	Hydraulic aperture [μm]
Bedding	54	4	450	1.05	16
Set 1	52	88	639	0.74	10
Set 2	340	90	960	1.26	5

Hydraulic conductivity of rock mass

	K_{11} [m/s]	K_{22} [m/s]	K_{33} [m/s]	Mean [m/s]
Snow Method	4.26e-9	3.25e-9	1.15e-9	2.9e-9
Plunge/Trend	0/129	7/219	83/38	

TBC019

Joint Set	Dip/Dir	Dip	Equivalent Depth [m] (based on stress orientation)	Spacing	Hydraulic aperture [μm]
Bedding	47	9	450	0.9	16
Set 1	150	88	960	0.89	5
Set 2	68	89	639	0.91	10
Set 3	209	89	639	0.87	10

Hydraulic conductivity of rock mass

	K_{11} [m/s]	K_{22} [m/s]	K_{33} [m/s]	Mean [m/s]
Snow Method	5.31e-9	4.1e-9	1.87e-9	3.74e-9
Plunge/Trend	0/133	16/223	74/42	

TBC021

Joint Set	Dip/Dir	Dip	Equivalent Depth [m] (based on stress orientation)	Spacing	Hydraulic aperture [μm]
Bedding	57	9	450	0.64	16
Set 1	61	89	639	0.93	10

Hydraulic conductivity of rock mass

	K_{11} [m/s]	K_{22} [m/s]	K_{33} [m/s]	Mean [m/s]
Snow Method	6.05e-9	5.21e-9	8.39e-10	4.03e-9
Plunge/Trend	1/299	11/209	79/32	

TBC022

Joint Set	Dip/Dir	Dip	Equivalent Depth [m] (based on stress orientation)	Spacing	Hydraulic aperture [μm]
Bedding	83	6	450	0.59	16
Set 1	228	85	639	0.58	10
Set 2	303	88	960	0.64	5

Hydraulic conductivity of rock mass

	K_{11} [m/s]	K_{22} [m/s]	K_{33} [m/s]	Mean [m/s]
Snow Method	7.03e-9	5.77e-9	1.55e-9	4.78e-9
Plunge/Trend	3/130	5/220	84/18	

TBC023

Joint Set	Dip/Dir	Dip	Equivalent Depth [m] (based on stress orientation)	Spacing	Hydraulic aperture [μm]
Bedding	58	7	450	0.78	16
Set 1	220	89	639	0.38	10
Set 2	178	89	798	0.91	7

Hydraulic conductivity of rock mass

	K_{11} [m/s]	K_{22} [m/s]	K_{33} [m/s]	Mean [m/s]
Snow Method	6.56e-9	4.42e-9	2.39e-9	4.46e-9
Plunge/Trend	3/144	13/235	77/42	

TBC024

Joint Set	Dip/Dir	Dip	Equivalent Depth [m] (based on stress orientation)	Spacing	Hydraulic aperture [μm]
Bedding	85	8	450	0.55	16
Set 1	207	88	639	0.52	10
Set 2	248	85	639	0.92	10

.

Hydraulic conductivity of rock mass

	K_{11} [m/s]	K_{22} [m/s]	K_{33} [m/s]	Mean [m/s]
Snow Method	8.19e-9	6.31e-9	2.43e-9	5.64e-9
Plunge/Trend	6/139	7/230	81/0	

TBC025

Joint Set	Dip/Dir	Dip	Equivalent Depth [m] (based on stress orientation)	Spacing	Hydraulic aperture [μm]
Bedding	78	5	450	1.36	16
Set 1	276	90	798	0.71	7
Set 2	179	89	798	1.07	7

Hydraulic conductivity of rock mass

	K_{11} [m/s]	K_{22} [m/s]	K_{33} [m/s]	Mean [m/s]
Snow Method	2.84e-9	2.69e-9	6.47e-10	2.06e-9
Plunge/Trend	3/252	5/162	84/9	

TBC026

Joint Set	Dip/Dir	Dip	Equivalent Depth [m] (based on stress orientation)	Spacing	Hydraulic aperture [μm]
Bedding	84	5	450	1.06	16
Set 1	245	88	639	0.95	10
Set 2	168	84	798	4.15	7
Set 3	124	89	960	4.15	5
Set 4	204	82	639	6.05	10

Hydraulic conductivity of rock mass

	K_{11} [m/s]	K_{22} [m/s]	K_{33} [m/s]	Mean [m/s]
Snow Method	4.07e-9	3.26e-9	1.07e-9	2.8e-9
Plunge/Trend	2/120	5/210	84/0	

TBC027

Joint Set	Dip/Dir	Dip	Equivalent Depth [m] (based on stress orientation)	Spacing	Hydraulic aperture [μm]
Bedding	87	5	450	1.35	16
Set 1	235	83	639	0.81	10
Set 2	328	88	960	1.1	5

Hydraulic conductivity of rock mass

	K_{11} [m/s]	K_{22} [m/s]	K_{33} [m/s]	Mean [m/s]
Snow Method	3.46e-9	2.55e-9	1.1e-9	2.36e-9
Plunge/Trend	3/125	2/215	86/346	

TBC028

Joint Set	Dip/Dir	Dip	Equivalent Depth [m] (based on stress orientation)	Spacing	Hydraulic aperture [μm]
Bedding	61	8	450	0.83	16
Set 1	192	88	639	0.79	10

Hydraulic conductivity of rock mass

	K_{11} [m/s]	K_{22} [m/s]	K_{33} [m/s]	Mean [m/s]
Snow Method	5.02e-9	3.99e-9	1.02e-9	3.34e-9
Plunge/Trend	6/168	6/259	81/35	

TBC029

Joint Set	Dip/Dir	Dip	Equivalent Depth [m] (based on stress orientation)	Spacing	Hydraulic aperture [μm]
Bedding	43	9	450	0.98	16
Set 1	205	90	639	0.47	10

Hydraulic conductivity of rock mass

	K_{11} [m/s]	K_{22} [m/s]	K_{33} [m/s]	Mean [m/s]
Snow Method	5.1e-9	3.45e-9	1.65e-9	3.4e-9
Plunge/Trend	3/155	17/246	73/56	

APPENDIX-2 - DETAIL OF CALCULATED RESULTS FOR DEPTH 350M (300-400M)

In situ stress

$\frac{\sigma_H}{\sigma_v} = 2.13$

$\frac{\sigma_H}{\sigma_h} = 1.5$

Orientation of Principal Stress= NW

TBC001

Joint Set	Dip/Dir	Dip	Equivalent Depth [m] (based on stress orientation)	Spacing	Hydraulic aperture [μm]
Bedding	46	7	350	1.06	22
Set 1	318	89	764	0.68	8
Set 2	67	90	497	1.21	14
Set 3	200	88	621	2.48	11

Hydraulic conductivity of rock mass

	K_{11} [m/s]	K_{22} [m/s]	K_{33} [m/s]	Mean [m/s]
Snow Method	1.02e-8	8.93e-9	2.84e-9	7.34e-9
Plunge/Trend	3/294	9/204	81/42	

TBC002

Joint Set	Dip/Dir	Dip	Equivalent Depth [m] (based on stress orientation)	Spacing	Hydraulic aperture [μm]
Bedding	39	7	350	0.81	22
Set 1	260	88	621	0.38	11
Set 2	213	87	497	1.52	14

Hydraulic conductivity of rock mass

	K_{11} [m/s]	K_{22} [m/s]	K_{33} [m/s]	Mean [m/s]
Snow Method	1.43e-8	1.13e-8	4.28e-9	9.95e-9
Plunge/Trend	3/294	8/204	81/46	

TBC003

Joint Set	Dip/Dir	Dip	Equivalent Depth [m] (based on stress orientation)	Spacing	Hydraulic aperture [μm]
Bedding	46	8	350	0.79	22
Set 1	214	87	497	0.92	14

Hydraulic conductivity of rock mass

	K_{11} [m/s]	K_{22} [m/s]	K_{33} [m/s]	Mean [m/s]
Snow Method	1.33e-8	1.1e-8	2.4e-9	8.88e-9
Plunge/Trend	2/146	9/236	81/46	

TBC004

Joint Set	Dip/Dir	Dip	Equivalent Depth [m] (based on stress orientation)	Spacing	Hydraulic aperture [μm]
Bedding	55	8	350	0.73	22
Set 1	241	81	497	0.66	14
Set 2	288	81	764	0.86	8
Set 3	173	89	621	0.89	11

Hydraulic conductivity of rock mass

	K_{11} [m/s]	K_{22} [m/s]	K_{33} [m/s]	Mean [m/s]
Snow Method	1.56e-8	1.31e-8	5.1e-9	1.12e-8
Plunge/Trend	1/303	8/213	82/38	

TBC005

Joint Set	Dip/Dir	Dip	Equivalent Depth [m] (based on stress orientation)	Spacing	Hydraulic aperture [μm]
Bedding	52	4	350	0.67	22
Set 1	222	89	497	0.86	14

Hydraulic conductivity of rock mass

	K_{11} [m/s]	K_{22} [m/s]	K_{33} [m/s]	Mean [m/s]
Snow Method	1.54e-8	1.29e-8	2.57e-9	1.03e-8
Plunge/Trend	1/138	5/228	86/42	

TBC006

Joint Set	Dip/Dir	Dip	Equivalent Depth [m] (based on stress orientation)	Spacing	Hydraulic aperture [µm]
Bedding	89	5	350	1.19	22
Set 1	219	86	497	1.01	14
Set 2	270	88	621	1.88	11

Hydraulic conductivity of rock mass

	K_{11} [m/s]	K_{22} [m/s]	K_{33} [m/s]	Mean [m/s]
Snow Method	1.03e-8	8.14e-9	2.8e-9	7.1e-9
Plunge/Trend	4/133	4/234	85/359	

TBC007

Joint Set	Dip/Dir	Dip	Equivalent Depth [m] (based on stress orientation)	Spacing	Hydraulic aperture [μm]
Bedding	64	9	350	0.98	22
Set 1	9	89	621	0.84	11
Set 2	238	87	497	1.95	14

Hydraulic conductivity of rock mass

	K_{11} [m/s]	K_{22} [m/s]	K_{33} [m/s]	Mean [m/s]
Snow Method	1.08e-8	9.24e-9	2.38e-9	7.48e-9
Plunge/Trend	5/148	10/239	79/32	

TBC008

Joint Set	Dip/Dir	Dip	Equivalent Depth [m] (based on stress orientation)	Spacing	Hydraulic aperture [μm]
Bedding	125	4	350	0.79	22
Set 1	39	84	497	0.22	14
Set 2	73	86	621	0.41	11

Hydraulic conductivity of rock mass

	K_{11} [m/s]	K_{22} [m/s]	K_{33} [m/s]	Mean [m/s]
Snow Method	2.3e-8	1.36e-8	1.07e-8	1.58e-8
Plunge/Trend	4/135	54/231	36/42	

TBC009

Joint Set	Dip/Dir	Dip	Equivalent Depth [m] (based on stress orientation)	Spacing	Hydraulic aperture [μm]
Bedding	62	6	350	1.13	22
Set 1	25	87	497	0.83	14
Set 2	251	88	497	0.82	14

Hydraulic conductivity of rock mass

	K_{11} [m/s]	K_{22} [m/s]	K_{33} [m/s]	Mean [m/s]
Snow Method	1.22e-8	8.56e-9	5.25e-9	8.67e-9
Plunge/Trend	1/131	15/222	75/38	

TBC010

Joint Set	Dip/Dir	Dip	Equivalent Depth [m] (based on stress orientation)	Spacing	Hydraulic aperture [μm]
Bedding	73	7	350	3.71	22
Set 1	108	90	764	0.69	8
Set 2	199	90	497	0.47	14

Hydraulic conductivity of rock mass

	K_{11} [m/s]	K_{22} [m/s]	K_{33} [m/s]	Mean [m/s]
Snow Method	7.06e-9	5.34e-9	2.9e-9	5.1e-9
Plunge/Trend	8/161	82/314	4/71	

TBC011

Joint Set	Dip/Dir	Dip	Equivalent Depth [m] (based on stress orientation)	Spacing	Hydraulic aperture [μm]
Bedding	29	17	350	2.3	22
Set 1	230	89	497	0.72	14

Hydraulic conductivity of rock mass

	K_{11} [m/s]	K_{22} [m/s]	K_{33} [m/s]	Mean [m/s]
Snow Method	6.83e-9	4.35e-9	2.49e-9	4.55e-9
Plunge/Trend	6/310	43/214	46/47	

TBC012

Joint Set	Dip/Dir	Dip	Equivalent Depth [m] (based on stress orientation)	Spacing	Hydraulic aperture [μm]
Bedding	66	5	350	1.48	22
Set 1	33	85	497	0.84	14
Set 2	75	83	497	1.5	14
Set 3	144	87	764	1.34	8

Hydraulic conductivity of rock mass

	K_{11} [m/s]	K_{22} [m/s]	K_{33} [m/s]	Mean [m/s]
Snow Method	9.48e-9	6.9e-9	4.13e-9	6.84e-9
Plunge/Trend	3/135	19/225	71/37	

TBC014

Joint Set	Dip/Dir	Dip	Equivalent Depth [m] (based on stress orientation)	Spacing	Hydraulic aperture [μm]
Bedding	39	7	350	2.16	22
Set 1	199	85	497	0.7	14
Set 2	105	89	764	1.18	8

Hydraulic conductivity of rock mass

	K_{11} [m/s]	K_{22} [m/s]	K_{33} [m/s]	Mean [m/s]
Snow Method	7.17e-9	4.35e-9	3.51e-9	5e-9
Plunge/Trend	3/160	13/251	77/57	

TBC015

Joint Set	Dip/Dir	Dip	Equivalent Depth [m] (based on stress orientation)	Spacing	Hydraulic aperture [μm]
Bedding	29	8	350	1.34	22
Set 1	62	82	497	1.61	14
Set 2	6	90	621	1.26	11
Set 3	101	84	764	4.33	8

Hydraulic conductivity of rock mass

	K_{11} [m/s]	K_{22} [m/s]	K_{33} [m/s]	Mean [m/s]
Snow Method	7.77e-9	4.68e-9	2.1e-9	5.84e-9
Plunge/Trend	8/281	18/188	70/33	

TBC016

Joint Set	Dip/Dir	Dip	Equivalent Depth [m] (based on stress orientation)	Spacing	Hydraulic aperture [μm]
Bedding	49	5	350	0.97	22
Set 1	252	90	497	0.85	14
Set 2	209	87	497	1.12	14

Hydraulic conductivity of rock mass

	K_{11} [m/s]	K_{22} [m/s]	K_{33} [m/s]	Mean [m/s]
Snow Method	1.29e-8	9.51e-9	4.57e-9	8.98e-9
Plunge/Trend	0/306	8/216	82/38	

TBC017

Joint Set	Dip/Dir	Dip	Equivalent Depth [m] (based on stress orientation)	Spacing	Hydraulic aperture [μm]
Bedding	59	8	350	0.82	22
Set 1	44	90	497	0.61	14
Set 2	142	88	764	1.31	8
Set 3	269	89	497	1.67	14

Hydraulic conductivity of rock mass

	K_{11} [m/s]	K_{22} [m/s]	K_{33} [m/s]	Mean [m/s]
Snow Method	1.49e-8	1.15e-8	5.15e-9	1.05e-8
Plunge/Trend	1/306	13/216	77/33	

TBC018

Joint Set	Dip/Dir	Dip	Equivalent Depth [m] (based on stress orientation)	Spacing	Hydraulic aperture [μm]
Bedding	54	4	350	0.7	22
Set 1	52	88	497	0.74	14
Set 2	340	90	764	1.26	8

Hydraulic conductivity of rock mass

	K_{11} [m/s]	K_{22} [m/s]	K_{33} [m/s]	Mean [m/s]
Snow Method	1.54e-8	1.26e-8	3.29e-9	1.04e-8
Plunge/Trend	0/130	6/220	84/38	

TBC019

Joint Set	Dip/Dir	Dip	Equivalent Depth [m] (based on stress orientation)	Spacing	Hydraulic aperture [μm]
Bedding	47	9	350	1.63	22
Set 1	150	88	764	0.89	8
Set 2	68	89	497	0.91	14
Set 3	209	89	497	0.87	14

Hydraulic conductivity of rock mass

	K_{11} [m/s]	K_{22} [m/s]	K_{33} [m/s]	Mean [m/s]
Snow Method	9.75e-9	6.73e-9	5.01e-9	7.16e-9
Plunge/Trend	1/134	35/224	55/43	

TBC021

Joint Set	Dip/Dir	Dip	Equivalent Depth [m] (based on stress orientation)	Spacing	Hydraulic aperture [μm]
Bedding	57	9	350	1.21	22
Set 1	61	89	497	0.93	14

Hydraulic conductivity of rock mass

	K_{11} [m/s]	K_{22} [m/s]	K_{33} [m/s]	Mean [m/s]
Snow Method	9.51e-9	7.23e-9	2.28e-9	6.34e-9
Plunge/Trend	1/299	14/209	76/32	

TBC022

Joint Set	Dip/Dir	Dip	Equivalent Depth [m] (based on stress orientation)	Spacing	Hydraulic aperture [μm]
Bedding	83	6	350	0.72	22
Set 1	228	85	497	0.58	14
Set 2	303	88	764	0.64	8

Hydraulic conductivity of rock mass

	K_{11} [m/s]	K_{22} [m/s]	K_{33} [m/s]	Mean [m/s]
Snow Method	1.58e-8	1.26e-8	4.47e-9	1.1e-8
Plunge/Trend	3/129	6/219	84/12	

TBC023

Joint Set	Dip/Dir	Dip	Equivalent Depth [m] (based on stress orientation)	Spacing	Hydraulic aperture [μm]
Bedding	58	7	350	1.09	22
Set 1	220	89	497	0.38	14
Set 2	178	89	621	0.91	11

Hydraulic conductivity of rock mass

	K_{11} [m/s]	K_{22} [m/s]	K_{33} [m/s]	Mean [m/s]
Snow Method	1.44e-8	9.54e-9	5.99e-9	9.96e-9
Plunge/Trend	14/323	59/243	72/47	

TBC024

Joint Set	Dip/Dir	Dip	Equivalent Depth [m] (based on stress orientation)	Spacing	Hydraulic aperture [μm]
Bedding	85	8	350	0.82	22
Set 1	207	88	497	0.52	14
Set 2	248	85	497	0.92	14

Hydraulic conductivity of rock mass

	K_{11} [m/s]	K_{22} [m/s]	K_{33} [m/s]	Mean [m/s]
Snow Method	1.65e-8	1.13e-8	6.65e-9	1.15e-8
Plunge/Trend	6/139	9/230	79/17	

TBC025

Joint Set	Dip/Dir	Dip	Equivalent Depth [m] (based on stress orientation)	Spacing	Hydraulic aperture [μm]
Bedding	78	5	350	0.67	22
Set 1	276	90	621	0.71	11
Set 2	179	89	621	1.07	11

Hydraulic conductivity of rock mass

	K_{11} [m/s]	K_{22} [m/s]	K_{33} [m/s]	Mean [m/s]
Snow Method	1.44e-8	1.38e-8	2.51e-9	1.03e-8
Plunge/Trend	3/252	5/162	84/10	

TBC026

Joint Set	Dip/Dir	Dip	Equivalent Depth [m] (based on stress orientation)	Spacing	Hydraulic aperture [μm]
Bedding	84	5	350	0.66	22
Set 1	245	88	497	0.95	14
Set 2	168	84	621	4.15	11
Set 3	124	89	764	4.15	8
Set 4	204	82	497	6.05	14

Hydraulic conductivity of rock mass

	K_{11} [m/s]	K_{22} [m/s]	K_{33} [m/s]	Mean [m/s]
Snow Method	1.57e-8	1.35e-8	3e-9	1.07e-8
Plunge/Trend	2/120	5/211	84/5	

TBC027

Joint Set	Dip/Dir	Dip	Equivalent Depth [m] (based on stress orientation)	Spacing	Hydraulic aperture [μm]
Bedding	87	5	350	1.47	22
Set 1	235	83	497	0.81	14
Set 2	328	88	764	1.1	8

Hydraulic conductivity of rock mass

	K_{11} [m/s]	K_{22} [m/s]	K_{33} [m/s]	Mean [m/s]
Snow Method	8.61e-9	6.25e-9	3.11e-9	6e-9
Plunge/Trend	3/125	2/215	86/325	

TBC028

Joint Set	Dip/Dir	Dip	Equivalent Depth [m] (based on stress orientation)	Spacing	Hydraulic aperture [μm]
Bedding	61	8	350	1.04	22
Set 1	192	88	497	0.79	14

Hydraulic conductivity of rock mass

	K_{11} [m/s]	K_{22} [m/s]	K_{33} [m/s]	Mean [m/s]
Snow Method	1.1e-8	8.3e-9	2.8e-9	7.4e-9
Plunge/Trend	6/168	7/256	81/36	

TBC029

Joint Set	Dip/Dir	Dip	Equivalent Depth [m] (based on stress orientation)	Spacing	Hydraulic aperture [μm]
Bedding	43	9	350	0.75	22
Set 1	205	90	497	0.47	14

Hydraulic conductivity of rock mass

	K_{11} [m/s]	K_{22} [m/s]	K_{33} [m/s]	Mean [m/s]
Snow Method	1.62e-8	1.17e-8	4.56e-9	1.08e-8
Plunge/Trend	3/155	14/246	76/54	

APPENDIX-3 - DETAIL OF CALCULATED RESULTS FOR DEPTH 250M (200-300M)

In situ stress

$\frac{\sigma_H}{\sigma_v} = 2.1$

$\frac{\sigma_H}{\sigma_h} = 1.5$

Orientation of Principal Stress= NW

TBC001

Joint Set	Dip/Dir	Dip	Equivalent Depth [m] (based on stress orientation)	Spacing	Hydraulic aperture [□□]
Bedding	46	7	250	1.06	31
Set 1	318	89	525	0.68	13
Set 2	67	90	350	1.21	22
Set 3	200	88	438	2.48	17

Hydraulic conductivity of rock mass

	K_{11} [m/s]	K_{22} [m/s]	K_{33} [m/s]	Mean [m/s]
Snow Method	3.1e-8	2.63e-8	1.6e-8	2.27e-8
Plunge/Trend	4/292	15/201	75/38	

TBC002

Joint Set	Dip/Dir	Dip	Equivalent Depth [m] (based on stress orientation)	Spacing	Hydraulic aperture [□□]
Bedding	39	7	250	0.81	31
Set 1	260	88	438	0.38	17
Set 2	213	87	350	1.52	22

Hydraulic conductivity of rock mass

	K_{11} [m/s]	K_{22} [m/s]	K_{33} [m/s]	Mean [m/s]
Snow Method	4.36e-8	3.22e-8	1.6e-8	3.06e-8
Plunge/Trend	3/295	9/204	80/44	

TBC003

Joint Set	Dip/Dir	Dip	Equivalent Depth [m] (based on stress orientation)	Spacing	Hydraulic aperture [□□]
Bedding	46	8	250	0.79	31
Set 1	214	87	350	0.92	22

Hydraulic conductivity of rock mass

	K_{11} [m/s]	K_{22} [m/s]	K_{33} [m/s]	Mean [m/s]
Snow Method	4e-8	3.1e-8	9.27e-9	2.66e-8
Plunge/Trend	2/146	10/236	80/47	

TBC004

Joint Set	Dip/Dir	Dip	Equivalent Depth [m] (based on stress orientation)	Spacing	Hydraulic aperture [□□]
Bedding	55	8	250	0.73	31
Set 1	241	81	350	0.66	22
Set 2	288	81	525	0.86	13
Set 3	173	89	438	0.89	17

Hydraulic conductivity of rock mass

	K_{11} [m/s]	K_{22} [m/s]	K_{33} [m/s]	Mean [m/s]
Snow Method	4.78e-8	3.79e-8	1.96e-8	3.51e-8
Plunge/Trend	1/302	7/212	83/41	

TBC005

Joint Set	Dip/Dir	Dip	Equivalent Depth [m] (based on stress orientation)	Spacing	Hydraulic aperture []
Bedding	52	4	250	0.67	31
Set 1	222	89	350	0.86	22

Hydraulic conductivity of rock mass

	K_{11} [m/s]	K_{22} [m/s]	K_{33} [m/s]	Mean [m/s]
Snow Method	4.6e-8	3.6e-8	9.98e-9	3.07e-8
Plunge/Trend	1/138	5/228	85/40	

TBC006

Joint Set	Dip/Dir	Dip	Equivalent Depth [m] (based on stress orientation)	Spacing	Hydraulic aperture []
Bedding	89	5	250	1.19	31
Set 1	219	86	350	1.01	22
Set 2	270	88	438	1.88	17

Hydraulic conductivity of rock mass

	K_{11} [m/s]	K_{22} [m/s]	K_{33} [m/s]	Mean [m/s]
Snow Method	2.98e-8	2.14e-8	1.06e-8	2.06e-8
Plunge/Trend	4/134	3/224	85/357	

TBC007

Joint Set	Dip/Dir	Dip	Equivalent Depth [m] (based on stress orientation)	Spacing	Hydraulic aperture [□□]
Bedding	64	9	250	0.98	31
Set 1	9	89	438	0.84	17
Set 2	238	87	350	1.95	22

Hydraulic conductivity of rock mass

	K_{11} [m/s]	K_{22} [m/s]	K_{33} [m/s]	Mean [m/s]
Snow Method	3.22e-8	2.63e-8	9.01e-9	2.25e-8
Plunge/Trend	5/148	11/239	79/34	

TBC008

Joint Set	Dip/Dir	Dip	Equivalent Depth [m] (based on stress orientation)	Spacing	Hydraulic aperture []
Bedding	125	4	250	0.79	31
Set 1	39	84	350	0.22	22
Set 2	73	86	438	0.41	17

Hydraulic conductivity of rock mass

	K_{11} [m/s]	K_{22} [m/s]	K_{33} [m/s]	Mean [m/s]
Snow Method	7.69e-8	5e-8	3.2e-8	5.29e-8
Plunge/Trend	4/136	72/238	17/44	

TBC009

Joint Set	Dip/Dir	Dip	Equivalent Depth [m] (based on stress orientation)	Spacing	Hydraulic aperture []
Bedding	62	6	250	1.13	31
Set 1	25	87	350	0.83	22
Set 2	251	88	350	0.82	22

Hydraulic conductivity of rock mass

	K_{11} [m/s]	K_{22} [m/s]	K_{33} [m/s]	Mean [m/s]
Snow Method	3.91e-8	2.55e-8	1.99e-8	2.82e-8
Plunge/Trend	1/132	28/222	63/41	

TBC010

Joint Set	Dip/Dir	Dip	Equivalent Depth [m] (based on stress orientation)	Spacing	Hydraulic aperture []
Bedding	73	7	250	3.71	31
Set 1	108	90	525	0.69	13
Set 2	199	90	350	0.47	22

Hydraulic conductivity of rock mass

	K_{11} [m/s]	K_{22} [m/s]	K_{33} [m/s]	Mean [m/s]
Snow Method	2.49e-8	2.1e-8	9.03e-9	1.83e-8
Plunge/Trend	9/161	80/324	2/71	

TBC011

Joint Set	Dip/Dir	Dip	Equivalent Depth [m] (based on stress orientation)	Spacing	Hydraulic aperture []
Bedding	29	17	250	2.3	31
Set 1	230	89	350	0.72	22

Hydraulic conductivity of rock mass

	K_{11} [m/s]	K_{22} [m/s]	K_{33} [m/s]	Mean [m/s]
Snow Method	2.25e-8	1.42e-8	8.27e-9	1.5e-8
Plunge/Trend	6/310	60/201	29/44	

TBC012

Joint Set	Dip/Dir	Dip	Equivalent Depth [m] (based on stress orientation)	Spacing	Hydraulic aperture []
Bedding	66	5	250	1.48	31
Set 1	33	85	350	0.84	22
Set 2	75	83	350	1.5	22
Set 3	144	87	525	1.34	13

Hydraulic conductivity of rock mass

	K_{11} [m/s]	K_{22} [m/s]	K_{33} [m/s]	Mean [m/s]
Snow Method	3.05e-8	2.14e-8	1.54e-8	2.24e-8
Plunge/Trend	3/135	34/227	56/40	

TBC014

Joint Set	Dip/Dir	Dip	Equivalent Depth [m] (based on stress orientation)	Spacing	Hydraulic aperture []
Bedding	39	7	250	2.16	31
Set 1	199	85	350	0.7	22
Set 2	105	89	525	1.18	13

Hydraulic conductivity of rock mass

	K_{11} [m/s]	K_{22} [m/s]	K_{33} [m/s]	Mean [m/s]
Snow Method	2.35e-8	1.39e-8	1.26e-8	1.67e-8
Plunge/Trend	3/160	81/267	9/70	

TBC015

Joint Set	Dip/Dir	Dip	Equivalent Depth [m] (based on stress orientation)	Spacing	Hydraulic aperture []
Bedding	29	8	250	1.34	31
Set 1	62	82	350	1.61	22
Set 2	6	90	438	1.26	17
Set 3	101	84	525	4.33	13

Hydraulic conductivity of rock mass

	K_{11} [m/s]	K_{22} [m/s]	K_{33} [m/s]	Mean [m/s]
Snow Method	2.49e-8	2.1e-8	8.3e-9	1.79e-8
Plunge/Trend	2/314	15/223	75/51	

TBC016

Joint Set	Dip/Dir	Dip	Equivalent Depth [m] (based on stress orientation)	Spacing	Hydraulic aperture []
Bedding	49	5	250	0.97	31
Set 1	252	90	350	0.85	22
Set 2	209	87	350	1.12	22

Hydraulic conductivity of rock mass

	K_{11} [m/s]	K_{22} [m/s]	K_{33} [m/s]	Mean [m/s]
Snow Method	4.04e-8	2.74e-8	1.77e-8	2.85e-8
Plunge/Trend	0/306	11/216	79/37	

TBC017

Joint Set	Dip/Dir	Dip	Equivalent Depth [m] (based on stress orientation)	Spacing	Hydraulic aperture []
Bedding	59	8	250	0.82	31
Set 1	44	90	350	0.61	22
Set 2	142	88	525	1.31	13
Set 3	269	89	350	1.67	22

Hydraulic conductivity of rock mass

	K_{11} [m/s]	K_{22} [m/s]	K_{33} [m/s]	Mean [m/s]
Snow Method	4.66e-8	3.36e-8	1.99e-8	3.34e-8
Plunge/Trend	1/126	18/216	72/34	

TBC018

Joint Set	Dip/Dir	Dip	Equivalent Depth [m] (based on stress orientation)	Spacing	Hydraulic aperture [μm]
Bedding	54	4	250	0.7	31
Set 1	52	88	350	0.74	22
Set 2	340	90	525	1.26	13

Hydraulic conductivity of rock mass

	K_{11} [m/s]	K_{22} [m/s]	K_{33} [m/s]	Mean [m/s]
Snow Method	4.62e-8	3.59e-8	1.29e-8	3.17e-8
Plunge/Trend	0/130	7/220	83/36	

TBC019

Joint Set	Dip/Dir	Dip	Equivalent Depth [m] (based on stress orientation)	Spacing	Hydraulic aperture [μm]
Bedding	47	9	250	1.63	31
Set 1	150	88	525	0.89	13
Set 2	68	89	350	0.91	22
Set 3	209	89	350	0.87	22

Hydraulic conductivity of rock mass

	K_{11} [m/s]	K_{22} [m/s]	K_{33} [m/s]	Mean [m/s]
Snow Method	3.21e-8	2.29e-8	1.74e-8	2.41e-8
Plunge/Trend	1/134	63/227	27/43	

TBC021

Joint Set	Dip/Dir	Dip	Equivalent Depth [m] (based on stress orientation)	Spacing	Hydraulic aperture [μm]
Bedding	57	9	250	1.21	31
Set 1	61	89	350	0.93	22

Hydraulic conductivity of rock mass

	K_{11} [m/s]	K_{22} [m/s]	K_{33} [m/s]	Mean [m/s]
Snow Method	2.92e-8	2.04e-8	8.76e-9	1.95e-8
Plunge/Trend	1/299	17/209	73/31	

TBC022

Joint Set	Dip/Dir	Dip	Equivalent Depth [m] (based on stress orientation)	Spacing	Hydraulic aperture [μm]
Bedding	83	6	250	0.72	31
Set 1	228	85	350	0.58	22
Set 2	303	88	525	0.64	13

Hydraulic conductivity of rock mass

	K_{11} [m/s]	K_{22} [m/s]	K_{33} [m/s]	Mean [m/s]
Snow Method	4.86e-8	3.6e-8	1.76e-8	3.41e-8
Plunge/Trend	3/129	5/219	84/5	

TBC023

Joint Set	Dip/Dir	Dip	Equivalent Depth [m] (based on stress orientation)	Spacing	Hydraulic aperture [μm]
Bedding	58	7	250	1.09	31
Set 1	220	89	350	0.38	22
Set 2	178	89	438	0.91	17

Hydraulic conductivity of rock mass

	K_{11} [m/s]	K_{22} [m/s]	K_{33} [m/s]	Mean [m/s]
Snow Method	4.75e-8	2.82e-8	2.29e-8	3.28e-8
Plunge/Trend	3/145	65/241	24/54	

TBC024

Joint Set	Dip/Dir	Dip	Equivalent Depth [m] (based on stress orientation)	Spacing	Hydraulic aperture [μm]
Bedding	85	8	250	0.82	31
Set 1	207	88	350	0.52	22
Set 2	248	85	350	0.92	22

Hydraulic conductivity of rock mass

	K_{11} [m/s]	K_{22} [m/s]	K_{33} [m/s]	Mean [m/s]
Snow Method	5.25e-8	3.25e-8	2.58e-8	3.7e-8
Plunge/Trend	6/139	14/231	75/28	

TBC025

Joint Set	Dip/Dir	Dip	Equivalent Depth [m] (based on stress orientation)	Spacing	Hydraulic aperture [μm]
Bedding	78	5	250	0.67	31
Set 1	276	90	438	0.71	17
Set 2	179	89	438	1.07	17

Hydraulic conductivity of rock mass

	K_{11} [m/s]	K_{22} [m/s]	K_{33} [m/s]	Mean [m/s]
Snow Method	4.17e-8	3.96e-8	9.27e-9	3.02e-8
Plunge/Trend	3/252	5/162	84/9	

TBC026

Joint Set	Dip/Dir	Dip	Equivalent Depth [m] (based on stress orientation)	Spacing	Hydraulic aperture [μm]
Bedding	84	5	250	0.66	31
Set 1	245	88	350	0.95	22
Set 2	168	84	438	4.15	17
Set 3	124	89	525	4.15	13
Set 4	204	82	350	6.05	22

Hydraulic conductivity of rock mass

	K_{11} [m/s]	K_{22} [m/s]	K_{33} [m/s]	Mean [m/s]
Snow Method	4.67e-8	3.83e-8	1.18e-8	3.23e-8
Plunge/Trend	3/120	5/210	84/4	

TBC027

Joint Set	Dip/Dir	Dip	Equivalent Depth [m] (based on stress orientation)	Spacing	Hydraulic aperture [μm]
Bedding	87	5	250	1.47	31
Set 1	235	83	350	0.81	22
Set 2	328	88	525	1.1	13

Hydraulic conductivity of rock mass

	K_{11} [m/s]	K_{22} [m/s]	K_{33} [m/s]	Mean [m/s]
Snow Method	2.72e-8	1.82e-8	1.22e-8	1.91e-8
Plunge/Trend	3/125	1/35	87/299	

TBC028

Joint Set	Dip/Dir	Dip	Equivalent Depth [m] (based on stress orientation)	Spacing	Hydraulic aperture [μm]
Bedding	61	8	250	1.04	31
Set 1	192	88	350	0.79	22

Hydraulic conductivity of rock mass

	K_{11} [m/s]	K_{22} [m/s]	K_{33} [m/s]	Mean [m/s]
Snow Method	3.41e-8	2.33e-8	1.08e-8	2.27e-8
Plunge/Trend	6/168	8/259	80/42	

TBC029

Joint Set	Dip/Dir	Dip	Equivalent Depth [m] (based on stress orientation)	Spacing	Hydraulic aperture [μm]
Bedding	43	9	250	0.75	31
Set 1	205	90	350	0.47	22

Hydraulic conductivity of rock mass

	K_{11} [m/s]	K_{22} [m/s]	K_{33} [m/s]	Mean [m/s]
Snow Method	5.05e-8	3.3e-8	1.75e-8	3.37e-8
Plunge/Trend	3/155	19/246	71/57	

Strata Control Technology

REPORT TO:

TAHMOOR MINE

Longwall 10A Height of Fracture Borehole for Tahmoor South Project – Observations, Measurements, and Interpretation

TAH4125

Mining Research and Consulting Group
SCT Operations Pty Ltd PO Box 824 Wollongong NSW 2520 Australia
sctnsw@sct.gs

REPORT TO

Ben Streckeisen
Project Manager
Tahmoor South Project
PO Box100
TAHMOOR NSW 2573

SUBJECT

Longwall 10A Height of Fracture Borehole for Tahmoor South Project – Observations, Measurements, and Interpretation

REPORT NO

TAH4125

PREPARED BY

Ken Mills and Ben Blacka

DATE

7 March 2014

Ben Blacka
Geologist

Ken Mills
Principal Geotechnical Engineer

SUMMARY

The Tahmoor South Project (TSP) is a proposed extension of current longwall mining operations at Tahmoor Mine located approximately 75km southwest of Sydney in NSW, Australia. As part of the investigations of potential interactions between the mine and the groundwater, TSP drilled three boreholes above the centre of an existing longwall panel to measure the height of fracturing and the degree of disturbance to the overburden strata caused mining this panel. The TSP commissioned SCT Operations Pty Ltd (SCT) to provide geotechnical logging, hydraulic conductivity testing, borehole camera logging, and other characterisation measurements in borehole TBF040, and two adjacent redrills, to investigate if there was significant connection between the fracture network in the overburden strata and the underlying goaf. This report presents the results of the measurements and observations made during drilling of these boreholes and an interpretation of the results in the context of potential for mining to interact with the groundwater system.

Borehole TBF040 was cored down to a total depth of 243.9m in three holes directly above the centre of Longwall 10A.

Significant water loss was observed throughout the drilling process, primarily through several joint / fracture zones, mainly in the Hawkesbury Sandstone. Defect logging, rock quality designation (RQD), packer testing, daily water usage, borehole camera surveys, and acoustic scanner logging identified fracture zones associated with water loss horizons.

Although it is not possible to unequivocally determine which fractures are mining induced and which are natural, there are several observations that help distinguish the height above which mining induced fracturing is unlikely and the level of disturbance associated with mining induced fractures.

The water loss zones observed at a depth less than 75m are considered likely to be mainly associated with natural joints in the Hawkesbury Sandstone. Drilling water loss zones and open fractures observed below 75m are considered likely to include mining induced fractures. The mining induced fractures are observed to increase in frequency with depth.

Hydraulic conductivity measured using terminal packer testing equipment ranged from a minimum of 3.3×10^{-9}m/s to a maximum of 5.4×10^{-5}m/s but these hydraulic conductivity do not differentiate between horizontal and vertical conductivity. Although there is a general trend of decreasing water loss with depth into the borehole, the water losses are significantly higher than usual for this area.

When left to settle overnight, the water level in the borehole remained in a state of equilibrium at approximately 41m depth below the surface. The water level in the Hawkesbury Sandstone indicated by the piezometers was slightly higher at 38.8m (RL245.6m). This level is consistent with the general trends in groundwater level observed more widely across the

Tahmoor area (Geoterra 2013) which indicate a groundwater level at this location of RL244m.

Borehole breakout observed in TBF040C in the interval 75-79m below surface is inferred as a horizon at which horizontal stresses are elevated at the top of the zone of mining induced fractures. This horizon is approximately 340m (1.45 time panel width) above the mining horizon, an elevation that is consistent with the top of the zone where mining induced fractures are expected based on sag subsidence observations throughout NSW.

These observations indicate that horizontal fractures dominate the failure process above the top of the shear fracture zone, to a height of approximately 1.4-1.7 times panel width. Within the zone of predominantly horizontal fracturing there appears to be only limited pathways for vertical flow.

The borehole camera survey showed water and the fine particulate material carried within TBF040C flowing out of the borehole into an open fracture at a depth of 195.8m below the surface. This 195.8m horizon correlates with the point at which the piezometric pressure gradient first begins to be drawn down below hydrostatic. In the absence of any credible horizontal flow path, the flow pathway from the borehole at 195.8m must be downward into the mine via a tortuous mining induced fracture network.

The point of first evidence of downward flow at 195.8m is approximately 222m above the mining horizon. This distance is 0.94 times the 235m panel width of Longwall 10A and consistent with the inference based on surface subsidence monitoring (Mills 2012) and extensometer monitoring (Mills and O'Grady 1998) that the height of angled shear fracturing extends vertically to a distance above the mining horizon equal to about one times panel width. The significance of the angled shear fracturing is that the vertical pathway for flow downward into the mine through natural joints and matrix permeability is enhanced by the vertical component of this fracturing.

At the TBF040 site, the base of the Bald Hill Claystone is approximately coincident with the point at which the first perceptible flow connection with the mine is observed. The inference that the Bald Hill Claystone has acted as an aquitard to support the groundwater system in the Hawkesbury Sandstone is broadly consistent with the observation of outflow from the borehole at 195.8m below the surface. However, there may be an element of coincidence about the outflow horizon being near the base of the Bald Hill Claystone because the fracture network through the next 20m of Bulgo Sandstone remains sufficiently tortuous to maintain the groundwater so that it is only slightly drawn down below hydrostatic. This state has been maintained for over a month since the piezometers were installed and appears to be in long term equilibrium.

The borehole camera survey and acoustic scanner log indicate that there are a higher number of fractures below the 195.8m horizon than higher up in the sequence consistent with the complete depressurisation inferred just below

the end of the borehole. The piezometric pressure profile indicates that these fractures are vertically connected to the mine at a rate that increases with depth.

The drawdown to full depressurisation indicated by the piezometers is consistent with the height of depressurisation indicated by the approach forwarded by Tammetta (2012), especially if there is a vertical pathway for flow alongside the core barrel lodged in the bottom of the hole so that the lowest piezometer is actually representing the pressure at the bottom of the hole at 243.9m.

TABLE OF CONTENTS

1. INTRODUCTION

The Tahmoor South Project (TSP) is a proposed extension of current longwall mining operations at Tahmoor Mine located approximately 75km southwest of Sydney in NSW, Australia. As part of the investigations of potential interactions between the mine and the groundwater, TSP drilled a borehole, TBF040, above the centre of an existing longwall panel to measure the height of fracturing and the degree of disturbance to the overburden strata caused by this earlier mining. The TSP commissioned SCT Operations Pty Ltd (SCT) to provide geotechnical logging, hydraulic conductivity testing, borehole camera logging, and other characterisation measurements in borehole TBF040 in order to determine the connection between the fracture network in the overburden strata and the underlying goaf. This report presents the results of the measurements and observations made during drilling of TBF040.

The report is structured to provide a review of the factual information followed by an interpretation of these results in the context of other work and the implications for groundwater modelling. Details of the site and the three boreholes that were drilled are described in Section 2, a summary of the lithology in Section 3, details of defect spacing and frequency in Section 4, the results of various hydraulic characterisation testing conducted in Section 5, and the borehole camera survey and acoustic scanner logging in Sections 6 and 7 respectively. Section 8 presents the results of the piezometer monitoring. Section 9 presents an interpretation of the results. Details of logs, borehole camera screenshots and packer testing are presented in the appendices.

2. SITE DESCRIPTION

Three boreholes were drilled on the Tahmoor site TBF040 at the location shown in Figure 1. TBF040 was located on a bush track as close as possible above the centre of Longwall 10A.

Longwall 10A has created a void that is 235m wide. The Bulli Coal Seam was mined at a depth of 417m below the surface at this location. The seam section mined was approximately 2.25m thick and caused surface subsidence in the centre of Longwall 10A of approximately 440mm and above the chain pillars between adjacent panels of 300mm - 400mm.

Three boreholes drilled (TBF040A, TBF040B and TBF040C) are within four metres of each other allowing the data collected to be compiled to represent one composite borehole log. Drilling commenced on 28 October 2013 and was completed on 17 January 2014.

The three boreholes were core drilled, but water loss and drilling issues caused HQ core barrels to become permanently lodged in each of the holes preventing further drilling. Due to poor ground conditions 143.4m to 165m was not cored. The details of each hole are summarised in Table 1.

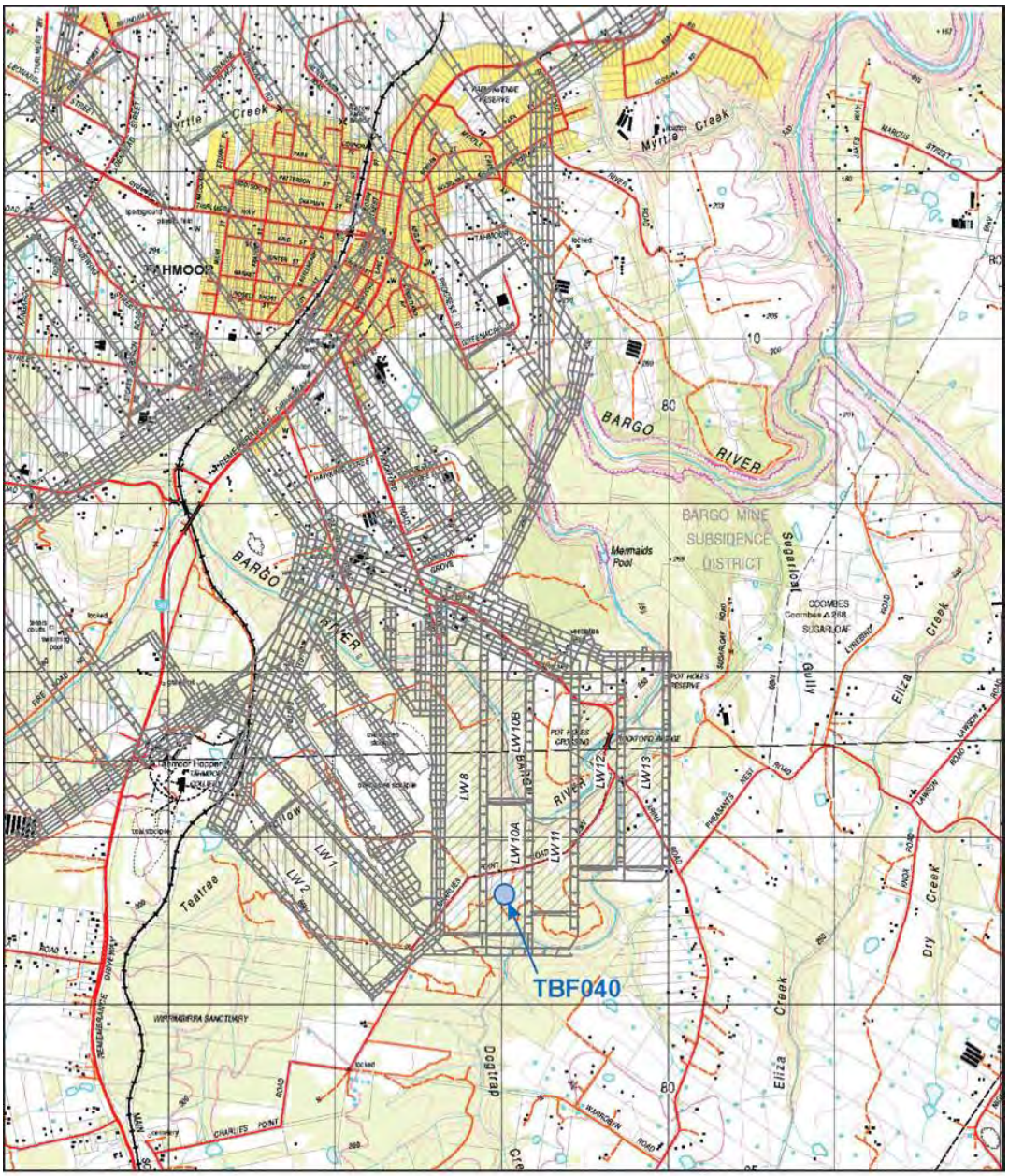

Figure 1: Site plan showing mine plan and location of the borehole TBF040 superimposed onto 1:25,000 topographic series map.

Table 1: Borehole details

Borehole ID	TBF040A	TBF040B	TBF040C
Total Depth (m)	53.3	143.4	243.9
Cored From (m)	0	47.4	165
Cored To (m)	53.3	143.4	243.9
PCD – Open Hole From (m)	N/A	0	0
PCD – Open Hole To (m)	N/A	47.4	165
E	279006.237	279005.649	279007.33
N	6206655.344	6206653.832	6206658.68
RL	284.486	284.411	284.440
HWT Casing Depth	31	45	165 (removed after drilling)
PW Casing Depth	N/A	N/A	74

3. LITHOLOGY

Core recovered from each of the three boreholes from 0m to 143.4m and 165m to 243.9m was logged and photographed to determine the key lithological units. Figure 2 displays a diagram of the stratigraphy and the three boreholes with casing depths plotted relative to Longwall 10A and the surface at natural scale. Appendix 1 shows a graphical representation of the lithology displayed as a composite log, including all logs and testing conducted in each of the boreholes. A complete English lithology log is presented in Appendix 2.

It should be recognised that, while the composite log shown in Appendix 1 is helpful to provide an overview of the stratigraphy, the camera survey, geophysics, and the acoustic scanner log were only run in TBC040C and so are not able to be directly correlated with core and other logs from TBC040A and TBC040B. The background of each of the different logs is coloured to provide an indication of the hole they relate to.

Hawkesbury Sandstone is located from 0m to 174.68m and consists predominantly of medium to coarse sandstone, with some granular sized conglomerate units in places. Weathering of the Hawkesbury Sandstone was present down to 35.4m, this weathered zone displayed significantly weaker core than the rest of the borehole.

The Newport Formation ranges from 174.68m to 179m and consists of interbedded fine to medium sandstone over the top section, with interbedded siltstone and mudstone over the base of the unit.

The Garie Formation is a thin unit overlying the Bald Hill Claystone, located from 179m to 180.22m and is a hard oolitic (small circular grains) claystone.

The Bald Hill Claystone ranges from 180.22m to 196.6m, consisting of a rich red claystone, soft and semi consolidated over the top half becoming harder and consolidated over the bottom half.

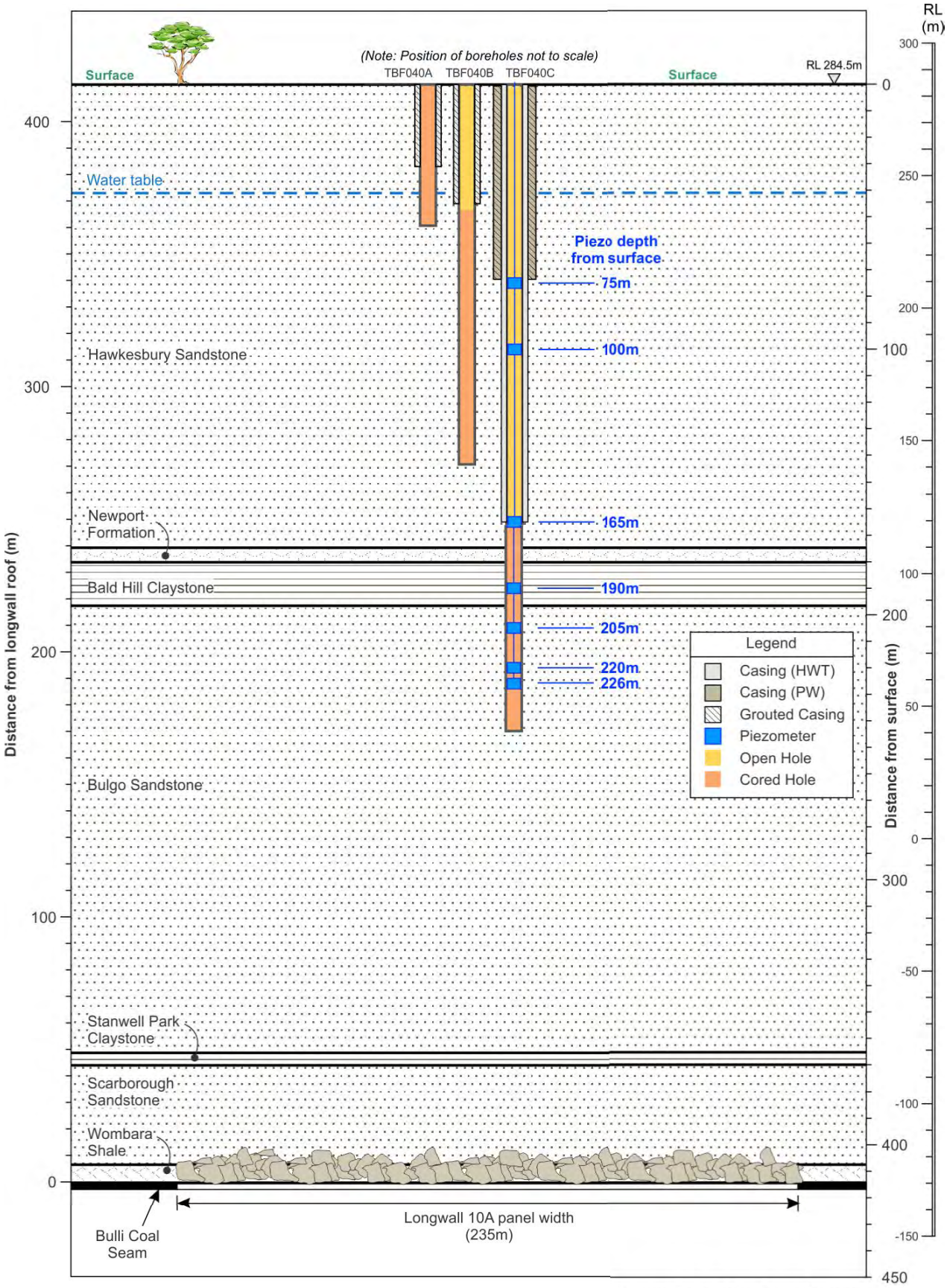

Figure 2: Stratigraphy and overview of borehole TBF040 drawn to natural scale except for borehole locations.

The Bulgo Sandstone is the final unit intersected by the borehole ranging from 196.6m to 243.9m. The Bulgo Sandstone consists of fine to medium sandstone, with some smaller siltstone units throughout.

4. DEFECTS IDENTIFIED FROM CORE LOGGING

In this section, the defects observed in the core logging are described. A defect in this report is defined as any feature which cuts the core. In general, the terms "joint" and "bedding plane" are intended to describe those defects that are natural. The term "fracture" is intended to describe defects that are either drilling induced or mining induced. There is an element of interpretation required to determine whether a defect is drilling induced, natural, or mining induced. Mining induced fractures in the core are limited to those that clearly show evidence of recent shear movement that could reasonably be attributed to mining. It is difficult to differentiate bedding planes from horizontal fractures that have separated vertically based on defect logging of core samples, so some of the bedding planes are likely to be mining induced fractures.

A total of 589 defects were logged over the entire cored section of TBF040. Figure 3 summarises the defect types and number of defects logged. Table 2 presents the defect type and the major geological unit in which it is located. A complete detailed log of all individual defects is presented in Appendix 3.

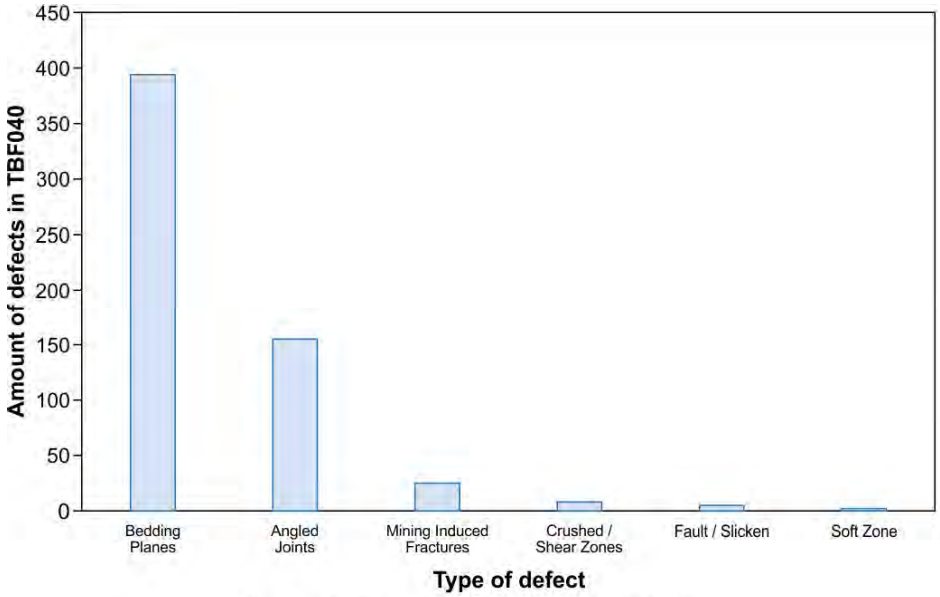

Figure 3: Types of defects identified in core.

Defects identified within the Hawkesbury Sandstone consist predominately of natural bedding planes, with bed angles generally ranging 0-10° dip. These bedding plane orientations are consistent with the orientations of bedding planes observed in other boreholes in the area.

Table 2: Summary of defects, broken into major units identified in core

	Hawkesbury Sandstone	Newport Formation	Garie Formation	Bald Hill Claystone	Bulgo Sandstone	Total
Total defects	426	15	8	26	114	589
Bedding planes	299	9	1	5	80	394
Crushed/shear zones	6	0	0	1	1	8
Mining induced fractures	7	0	0	12	6	25
Joints	111	3	7	8	26	155
Fault/slicken	1	3	0	0	1	5
Sot Zone	2	0	0	0	0	2

Joints within the Hawkesbury Sandstone are also abundant within the core from TBF040, particularly clustered in large zones covering several metres. These jointed zones range from 0-90° and many of the higher angled joints are over a metre in length. These jointed zones apparent in the core may be associated with localised geological structure within close proximity to the borehole or may be drilling induced and a consequence of water loss zones. There were six water loss zones that can be identified as crushed/shear zones in the core.

Seven potential mining induced fractures were logged within the Hawkesbury Sandstone. These fractures are characterized by medium to low angled, unweathered breaks, generally planar in shape, with some signs of movement evident on the face.

The Newport / Garie Formation directly overlying the Bald Hill Claystone wer observed to be highly fractured, consisting of several high angled joints and multiple faults, displaying movement via slickens on the face.

The Bald Hill Claystone core was soft in places, particularly in the top half and sections broke apart quite easily when handled. However, the borehole camera survey indicates that the borehole has remained stable through this section so the soft core appears likely to be drilling induced. The main defects throughout the Bald Hill Claystone were medium angled planar faced joints (possibly mining induced) as well as some higher angled irregular joints towards the base. Packer testing results show these higher angled joints towards the base generally had greater hydraulic conductivity.

The Bulgo Sandstone core showed mainly bedding plane defects with some low angle joints. Other than one low angled jointed zone indicated in the core near the bottom of the borehole, the core did not show any major jointed zones. Six mining induced fractures were identified in the Bulgo Sandstone at medium to low angles.

Analysis of fracturing was done by examination of the core at the drill site. The first determination of the rock character is made by observation of the number of natural breaks in the core. Rock quality designation (RQD) is

determined by dividing the total length of recovered core greater than 10 centimetres per each metre drilled, represented as a percent.

$$RQD\% = \frac{\text{Total length of core} > 10cm}{\text{Metre}} \quad X\ 100$$

The RQD for TBF040 is presented as a graphical representation in Appendix 1 as part of the composite log. Figure 4 shows five categories based on RQD value with rating values ranging from very poor to excellent. The average RQD for this composite hole is 87.3%. All zones consisting of low RQD are located in the Hawkesbury Sandstone and Newport / Garie Formation, with all other major units displaying RQD ratings of greater than 50%. Some major zones of low RQD include:

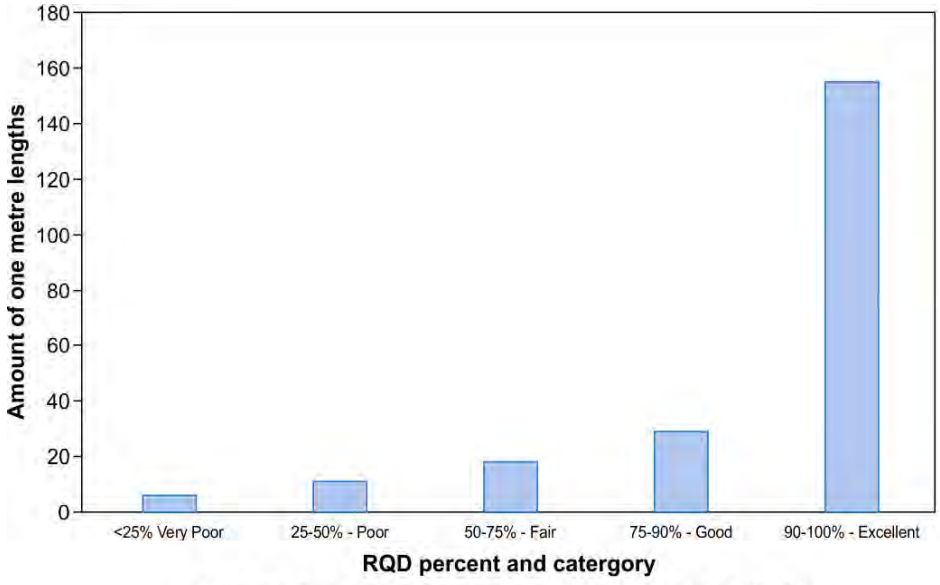

Figure 4: Summary of RQD for borehole TBF040.

- The weathered zone (0m – 35m) of the Hawkesbury Sandstone, in general indicated a lower than average RQD in comparison to the rest of the hole. This lower RQD value is considered normal for cored boreholes and is considered to be associated with surface weathering.

- 51m – 54m: Large vertical fractures were observed in the core of TBF040A within this interval in the Hawkesbury Sandstone. This zone was responsible for large amounts of water loss and resulted in the core barrel remaining permanently lodged in the borehole and the termination of the TBF040A. It is considered likely that the vertical fractures in the core were drilling induced but this zone was not able to be inspected in either the borehole camera survey or acoustic scanner log of TBF040C because casing was present.

- 70m – 74m: Vertical fractures and smaller near horizontal joint zones were observed in the core of TBF040B. There were no vertical defects

observed in TBF040C at the equivalent horizon, but there was a blow out zone observed at this depth at a change of lithology.

- 122m – 126m: A water loss zone where large vertical and medium angled joints were observed in the core from TBF040B. The acoustic scanner log and borehole camera survey in TBF040C showed minor horizontal fractures at 123.7m and 125.5m and a larger fracture at 127.4m, but there were not any vertical defects observed.

- 132m – 141m: Nine meters of highly jointed core were recovered from TBC040B in this interval with fractures ranging from horizontal to vertical. Large amounts of water loss, resulting in the core barrel remaining permanently lodged in the borehole and the termination of the TBF040B occurred at this horizon.

- 179m – 180m: High angled joints were observed throughout the Garie Formation. There joints were evident in the acoustic scanner log.

5. HYDRAULIC CONDUCTIVITY

The hydraulic conductivity of all three TBF040 boreholes was measured in a variety of ways:

- Packer testing.
- Falling head testing.
- Daily water use calculations.
- Daily dip readings of water level.
- Moisture content from core samples.
- Piezometer pressure readings.

5.1 Packer Testing/Falling Head Testing

A total of 25 lugeon style terminal packer tests were conducted. Seven falling head tests were conducted where packer testing was not possible due to high hydraulic conductivity. Packer testing/falling head testing were typically conducted over 6m intervals, with three tests conducted on 9m test intervals. Packer testing was conducted in five pressure stages. Pressure was increased in each of three stages and then subsequently decreased. Flow was recorded every minute for ten minutes at each pressure stage.

Hydraulic conductivity has been calculated using the average of the CANMET, Hoek and Bray, and Houlsby methods. The formulae are outlined in the water pressure test results sheets (Appendix 5). The flow/head gradient determined from an average of the plotted test data of flow versus pressure is used to calculate hydraulic conductivity.

The hydraulic conductivity measured ranges from a minimum of $3.3x10^{-9}$m/s to a maximum of $5.4x10^{-5}$m/s, with an average of $5.1x10^{-6}$m/s. These results indicate a higher hydraulic conductivity than is typical for this area. There is a general trend of decreasing flow with depth into the borehole. Packer testing and falling head testing results are plotted in Figure 5.

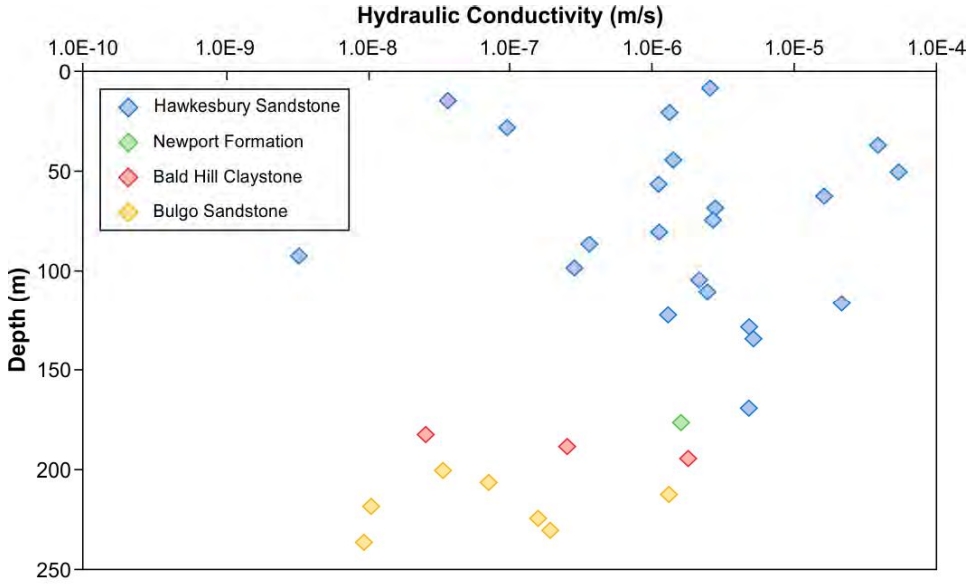

Figure 5: Hydraulic Conductivity results based on packer testing and falling head data.

Many of the test intervals demonstrating high conductivity coincided with fractured zones observed in the core and in the borehole wall, particularly the fractured zones where there had been high water loss during drilling.

5.2 Daily Water Usage

Daily water use into the holes was estimated each day with an accuracy of about +/- 1000 litres. Water left in the drilling tanks at the end of each day and the total amount of five thousand litre water tanks used throughout the day to refill the main drilling tanks were measured. The total water usage for the day was then converted to litres/hour/metres drilled, depending on the total drilling time and metres drilled per day.

The composite log found in Appendix 1 displays the water usage, showing some similar trends to the packer testing results, however variations to the packer testing results are due to water being lost throughout the entire strata (except grouted sections) rather than just that particular drilling interval, whereas packer tests are able to target a particular zone for testing, so that no water is lost elsewhere in the hole. Other factors resulting in large water usage include drilling issues and slow drilling. Both tend to use greater amounts of water.

High water loss zones correlated with poor drilling conditions and/or highly hydraulically conductive strata. Some of the major high water loss areas identified from daily water usage were located in the Hawkesbury Sandstone:

The average water loss for TBF040 was 1445 litres per metre drilled, which is significantly higher than the average water usage observed during drilling of other holes in the TSP area.

5.3 Water Level

Standing water level was measured throughout the drilling process. Daily dip meter reading were taken to determine changes in the water level throughout the drilling. The overnight standing water level remained at 41m +/- 1m in each of the three boreholes.

5.4 Moisture Content

Over the length of the fully cored borehole, a total of 11 moisture samples were taken on site from the drilling splits to determine if there was any evidence of a change in moisture content with depth. The samples were labelled then wrapped in several layers of plastic wrap to maintain moisture content. The samples were then relabelled and stored in a core tray under cover. A range of rock types were selected so as to provide a representative selection of rock types present in the sequence.

Table 3 and Figure 6 show the variation of moisture content with depth. Moisture content ranges from a minimum of 0.2% to a maximum of 8.7%. The weathered zone, above the water table, shows the lowest moisture content consistent with the samples coming from above the water table. There is a general trend of increasing moisture with depth, with the exception of the Bald Hill Claystone, which showed a lower moisture percentage for that depth. There is no obvious relationship between grain size and moisture content.

Table 3: Moisture sample results

Sample Name	From Depth	To Depth	Lithology	Moisture Content %
GT001	15.41	15.64	Weathered Medium Sandstone	0.6
GT002	32.14	32.42	Weathered Medium/Coarse Sandstone	0.2
GT003	56.81	57.14	Weathered Fine/Medium Sandstone	1.3
GT004	67.19	67.49	Medium Sandstone	3.2
GT005	97.74	94.95	Medium/Fine Sandstone	4.4
GT006	113.49	113.76	Conglomerate	2.5
GT007	132.29	132.53	Coarse Sandstone	6.3
GT008	174.37	174.68	Medium Sandstone	8.7
GT009	180.86	181.20	Claystone	2.4
GT0010	203.43	203.71	Conglomerate	6.4
GT0011	234.66	234.97	Medium Sandstone	7.4

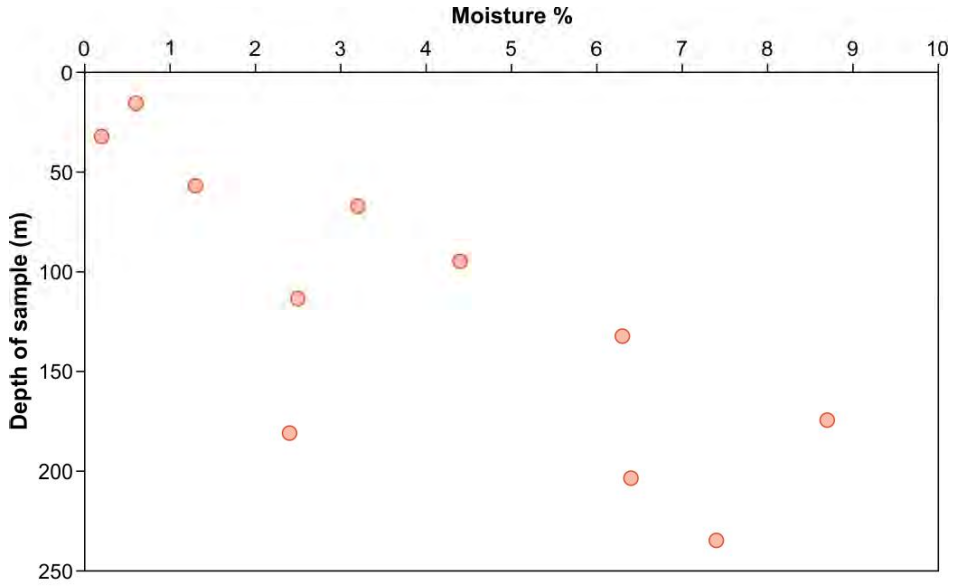

Figure 6: Moisture sample results – displaying a trend of increasing moisture with depth.

6. BOREHOLE CAMERA OBSERVATIONS

At the completion of drilling, a borehole camera was lowered into TBF040C on an electric winch with real time video of the borehole displayed at the surface. The camera has the ability to be remotely controlled and rotated about a horizontal and vertical axis to allow inspection of open fractures and other features in the borehole.

Snapshots from the borehole camera survey are shown in Appendix 6. All photos are taken looking down the borehole.

The depths embedded in the video images and snapshots are only approximate. In the discussion below, the depths have been corrected using the acoustic scanner log and core logging. The embedded depths are less than the actual depth indicated by the core and the acoustic scanner log by approximately 0.9m (0.4-1.2m) over the top 195m of the borehole. The bottom part of the hole was surveyed at a different time and the camera depth in this section is approximately the same as the depth indicated by the acoustic scanner log.

TBF040C was water filled to 41m below surface and cased to 74m below surface. There was also a core barrel lodged in the hole between 236.5m and 243.9m so the borehole was only able to be inspected between 74m and 236.5m. Over this interval, the fractures observed are classified as sub-horizontal, angled, or vertical. In some cases, multiple fractures at the one location are grouped together as a set and counted only as a single fracture zone. Fine particles obscured some sections of the borehole, particularly in the bottom section, but it is considered that most of the fractures that exist there were able to be identified and classified.

Figure 7 shows a histogram of the number of fractures observed using the borehole camera in each 5m interval and a key showing the type of each fracture.

In addition to the open fractures observed in the borehole and classified in Figure 7, a short section of borehole breakout was observed from 75.2 to 75.7 and again at 79.8m. Figure 8 shows a photograph from this section of the borehole. The presence of borehole breakout indicates the horizontal stresses are locally elevated at about 80m below the surface because borehole breakout is not typically observed at this relatively shallow depth.

Blowouts in the borehole thought to be associated with drilling and transitions from one lithology to another were observed at camera indicated depths of 75m, 97m, and 99m.

Fgure 7 shows that the frequency of open fractures increases with depth. There is a section from 100m to 110m where there are no open fractures observed and zones approximately 20m apart where there is only one open fracture apparent in a 5m interval of the borehole. Outside these zones, the frequency of fractures increases with depth. Below 185m, there are at least two fractures apparent in every 5m interval.

Approximately 80% of the open fractures observed by the borehole camera are horizontal or sub-horizontal and 20% are angled from horizontal, most only slightly, but several at 179.2m, 185.1m, 189.2m and 189.8m in the vicinity of the Garie Formation showing a high angle to horizontal. There are no fully vertical fractures evident in the borehole camera logs.

Suspended particles present in the water filled borehole during the camera survey provide a real time indication of the direction of flow within the borehole. Although some of the heavier particles also move downward slightly faster under the action of gravity, the finer particles move primarily with the flow. These particles were observed to be mainly moving downward toward the bottom of the hole at a rate consistent with downward flow from the Hawkesbury Sandstone into the more fractured strata deeper in the hole.

At a depth below surface of 195.8m (194.9 in the camera log), suspended particles were observed moving into a set of horizontal fractures consistent with flow out of the borehole and into the strata at this location. Figure 9 shows a photograph with the direction of flow observed through the movement of suspended particles.

At several other horizons the build-up of particles and colour change on exposed sections of the fracture are indicative of possible flow out of the borehole although definite flow of fine particles was not able to be observed in the video of the camera log reviewed after the survey was completed. Some hints of outflow flow at the time of the camera run are apparent at 209.7m, 209.9m, and 213.1m on open or partly open fracture planes.

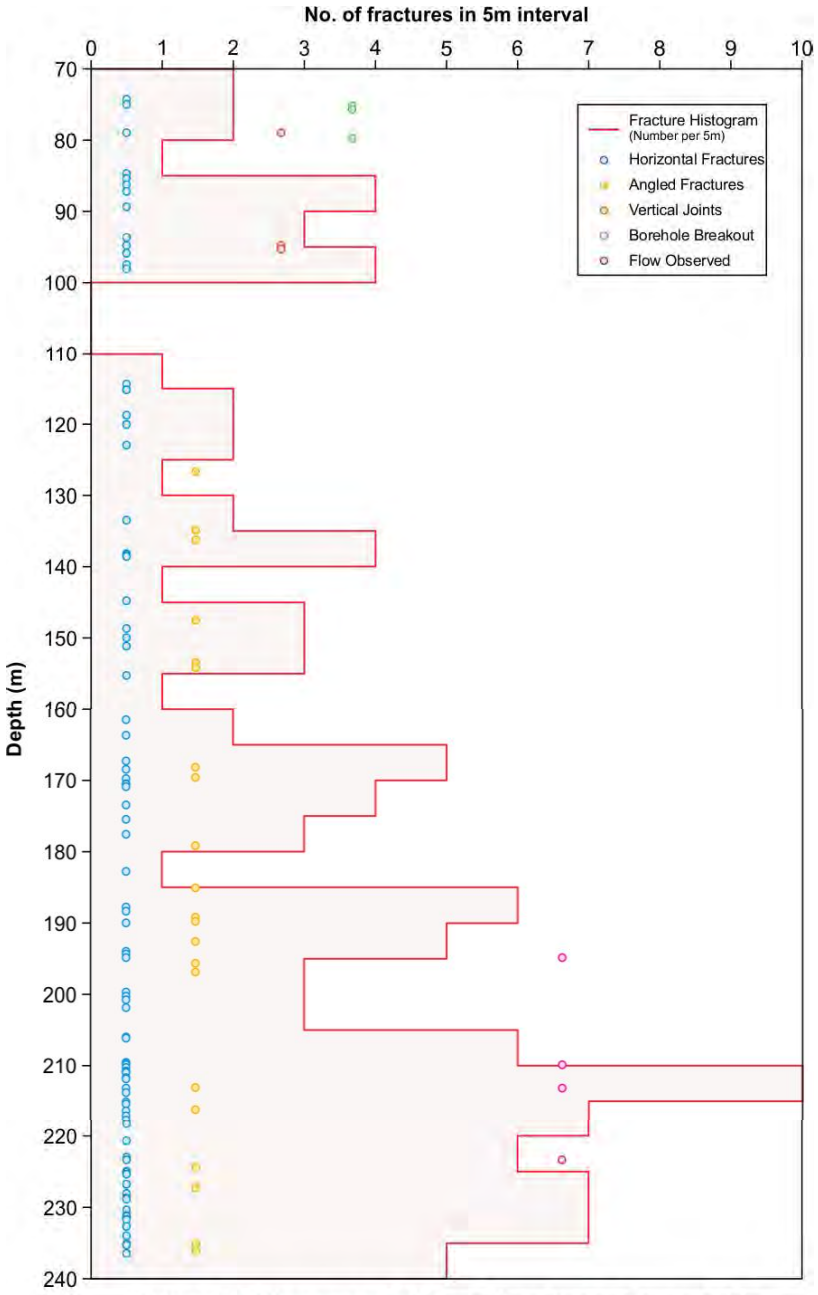

Figure 7: Histogram of open fractures observed in borehole camera survey.

Figure 8: Borehole breakout observed at 79.1m.

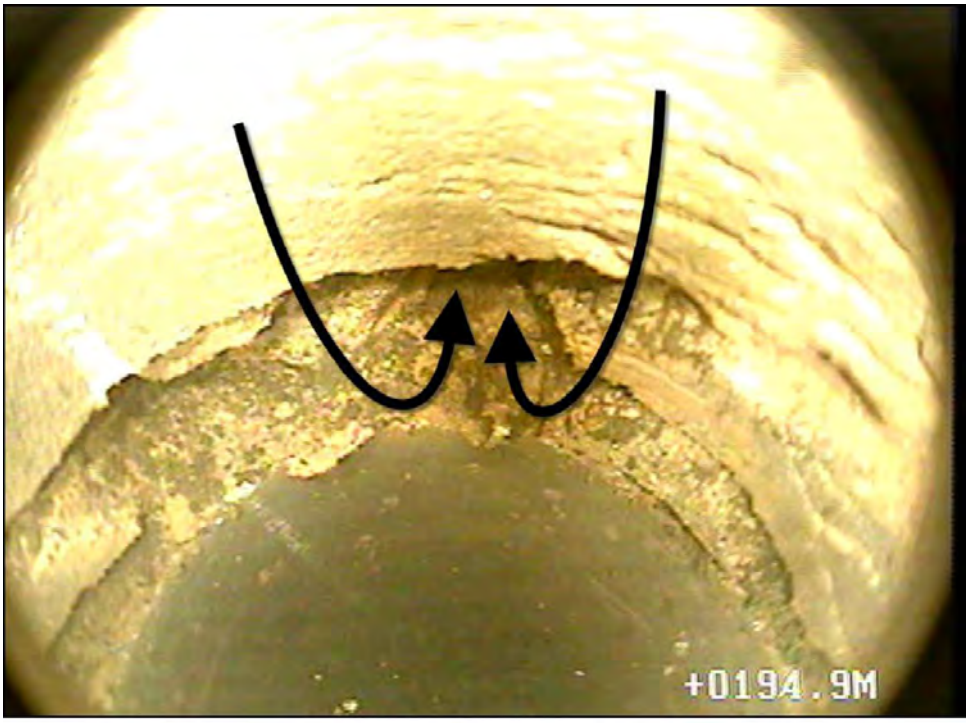

Figure 9: Photograph of fracture at 195.8m (depth adjusted based on acoustic scanner log) showing flow from borehole into fracture.

In the upper part of the borehole in the Hawkesbury Sandstone, there was no sign of flow out of the borehole occurring during the camera survey, but the build-up of fine material in some of the fractures may be evidence of outflow during the period of drilling.

7. ACOUSTIC SCANNER LOG

The acoustic scanner log was run in TBF040C and the results are shown in Appendix 1 alongside the core recovered from TBF040B and TBF040C for the same depth interval and in Appendix 7 in more detail.

Figure 10 shows a histogram of the fracture / joint frequency and dip based on the acoustic scanner logs. A trend of increasing fracture frequency with depth is evident, similar to the trend observed in the borehole camera survey.

The location and dip of the fractures is able to be determined more accurately in the acoustic scanner log. The fracture dips are generally less than 20° except in the Newport / Garie Formation, Bald Hill Claystone, and upper part of the Bulgo Sandstone.

The borehole breakout observed in the borehole camera survey between 74m and 79m depth is apparent in the acoustic scanner log oriented at 150° and 330°magN. Two other short sections of borehole breakout are clearly apparent in the acoustic scanner log at depths of 196.7m and 226.9m with an orientation of approximately 0° and 180°magN.

The orientation of this breakout at 74-79m indicates that the major horizontal stress at this location is oriented at approximately 70°GN. The breakout observed over short intervals in the Bulgo Sandstone indicates the horizontal stresses are very local and oriented at approximately 100°GN.

Figure 11 shows the horizontal stress directions measured previously at Tahmoor Mine. The direction of the elevated horizontal stress observed in the Hawkesbury Sandstone in TBF040C is broadly consistent with the horizontal stress direction measured underground and as breakout in nearby holes. However, the in situ stress direction in the vicinity of TBF040 appears from these other measurements to be somewhat variable in orientation.

8. VIBRATING WIRE PIEZOMETER MONITORING

Seven fully grouted vibrating wire piezometers were installed on 31 January 2014 into TBF040C at the depths shown in Figures 2 and 12. The HWT casing below 74m was withdrawn prior to installation of these piezometers, but a 7m long HQ core barrel lodged at the bottom of the hole remains in place.

Figure 12 shows the hydraulic pressure profile observed on the piezometers observed a week after installation on 6 February 2014 and again a month later on 3 March 2014. No significant change is evident between these two profiles indicating that the pressure profile measured is steady and representative of the groundwater system.

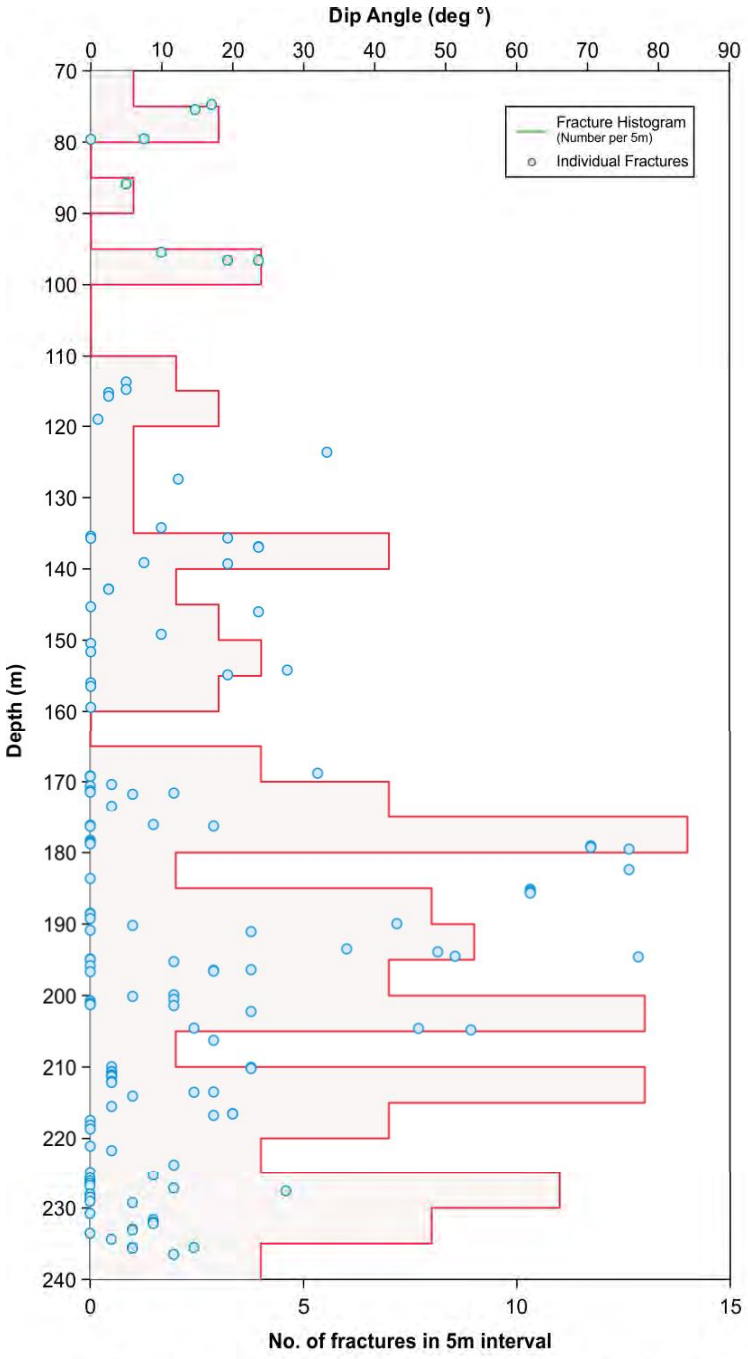

Figure 10: Histogram of fractures / joints observed in acoustic scanner log.

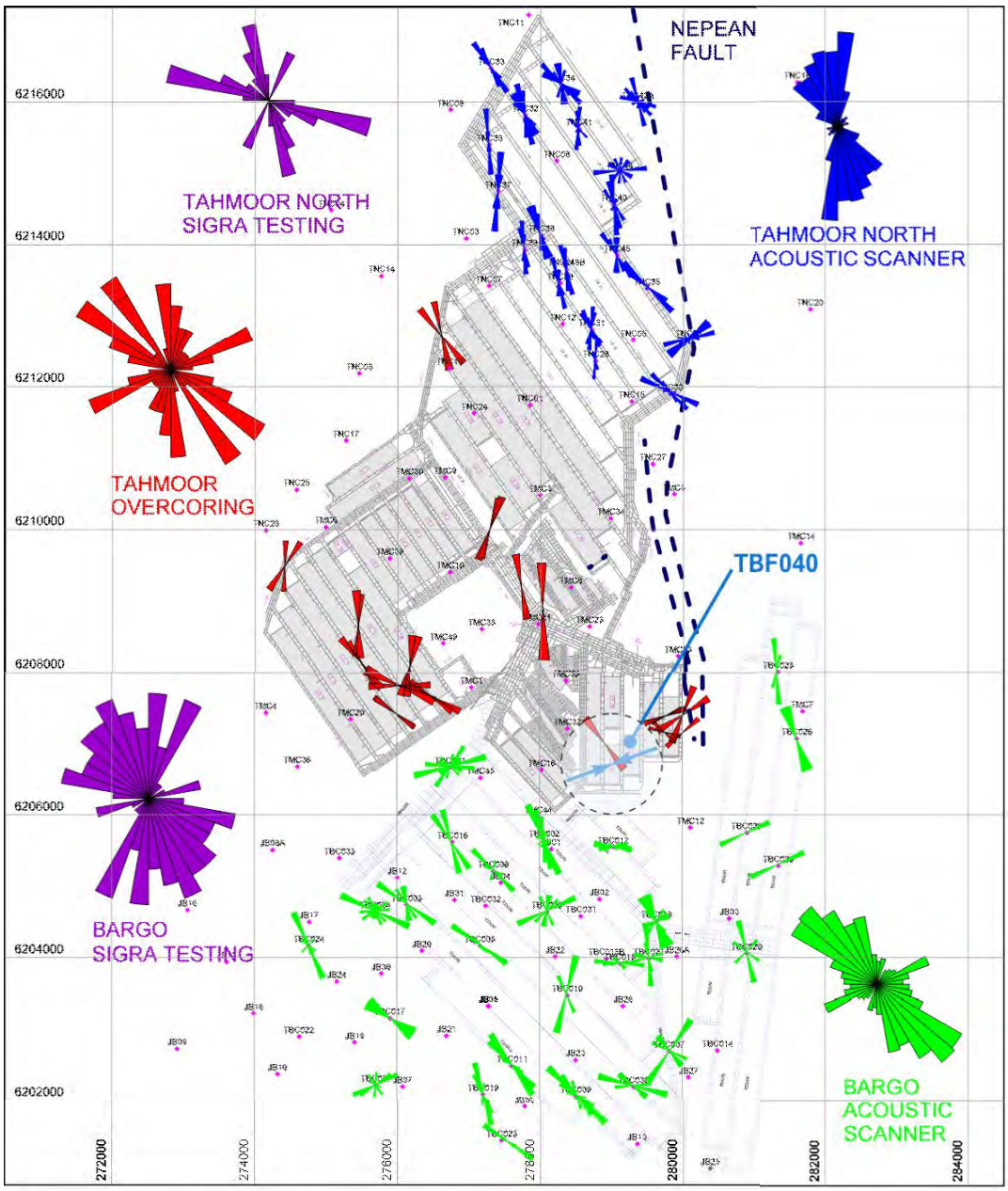

Figure 11: In situ stress orientation observed at Tahmoor mine. (From Figure 1, Gordon 2013)

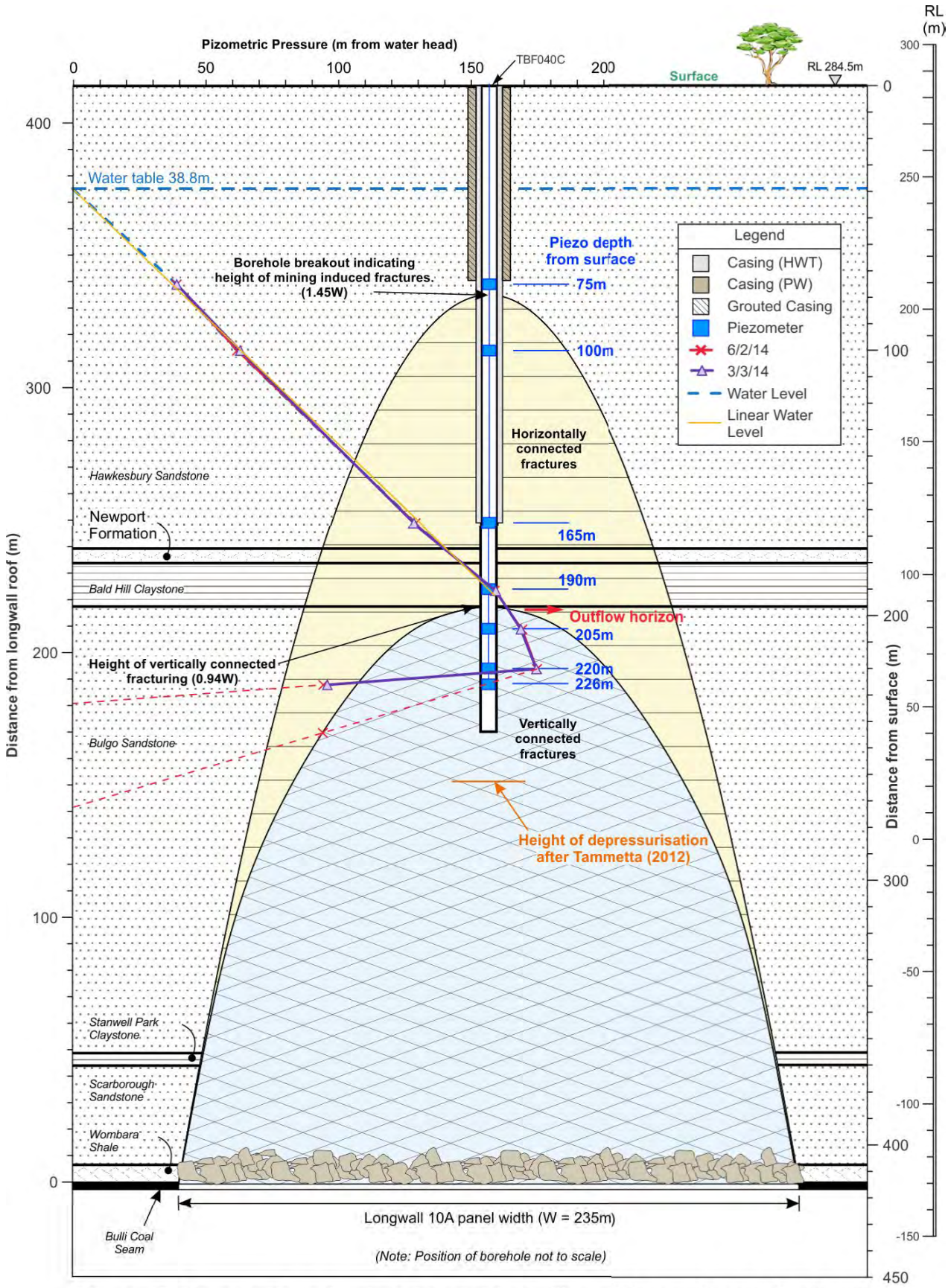

Figure 12: Cross section showing piezometric profile and observations of fracturing and outflow above Longwall 10A.

The top four piezometers indicate a hydrostatic pressure profile consistent with a groundwater level at 38.8m below surface (RL245.6m). The groundwater within the Hawkesbury Sandstone is essentially hydrostatic at this location. The 0.9993 correlation coefficient (R^2) value for a linear interpolation through the pressures indicated by these top four piezometers confirms that there is a high level of correlation between the instruments showing a hydrostatic profile. The gradient of piezometric pressure with depth indicated by the top four piezometers is 1.04MPa/100m and therefore slightly greater than the 0.98MPa/100m expected from density considerations alone. This difference is considered likely to be a result of minor calibration differences between piezometers.

The hydrostatic pressure gradient evident in the Hawkesbury Sandstone and midway through the Bald Hill Claystone at 190m depth begins to be drawn down below hydrostatic at a depth of 205m, some 10m below the base of the Bald Hill Claystone.

A sharp drop in piezometric pressure is evident between the bottom two piezometers at 220m and 226m located about 20m below the base of the Bald Hill Claystone. It is considered possible that because grout tubes were not able to be inserted into the core barrel lodged in the hole during piezometer installation, the bottom piezometer is hydraulically connected to an open section of borehole at the bottom of the hole. This open section extends from the bottom of the hole at 243.9m to at least the top of the core barrel at about 236.5m below surface. There may also be hydraulic connection through open fractures in the strata around the borehole over this lower part of the borehole consistent with the zone in which the core barrel became lodged.

9. INTERPRETATION OF RESULTS

In this section, the results presented in this report are interpreted in the context of the local site. The interpretation presented is based on the observations at this site and elsewhere. The interpretation is isolated in this section from the factual data presented above because it is recognised that other interpretations of the data may be possible.

9.1 Groundwater

The results of the investigation drilling above the centre of Longwall 10A at Tahmoor Mine indicate that the Hawkesbury Sandstone is hydraulically connected through its full section and the groundwater profile within the Hawkesbury Sandstone at this location is hydrostatic.

The groundwater level at RL245.6m is consistent with the water level observed in the Hawkesbury Sandstone across the broad area of Tahmoor Mine and the TSP where water level information is available for approximately 5km in each direction from TBF040. Geoterra (2013, Drawings 3 and 4) shows contours of the water level in the Hawkesbury Sandstone in this area as being approximately 244m based on measurements in other boreholes 0.5-1km away in each direction. This result indicates that the groundwater

in the vicinity of TBF040 is not being locally drawn down below the regional groundwater level as a result of the mining Longwall 10A and adjacent panels.

The 2m difference between the water level measured in the open boreholes at RL243.5m (41m below the surface) during drilling and the water level indicated by the piezometers at RL245.6m when vertical flow in the borehole is precluded is consistent with there being some local drawdown around the borehole while the borehole was open and downward flow occurred.

The rate of recharge from the Hawkesbury Sandstone must have been much greater than any outflows that may have occurred deeper in the overburden strata during the later stages of drilling because the water level remained at about 41m below the surface despite evidence of significance drilling water loss into the formation during drilling.

9.2 Fractures

Natural joints and mining induced fractures are difficult to distinguish with confidence, particularly in core logging. During logging, those fractures that were evident in the core as being unweathered with a texture consistent with recent shear movement were identified as mining induced in the composite log shown in Appendix 1 and the defect log shown in Appendix 3. The borehole camera survey and acoustic scanner log indicate numerous open fractures suggesting that mining induced fractures are more prevalent than indicated from core logging.

The composite logs in Appendix 1 shows vertical fractures are evident in the core in the high water loss zones within the Hawkesbury Sandstone. Vertical fracturing is not typically associated with mining related subsidence movements and so these vertical fractures are considered to be natural in origin. The vertical fractures evident in the core are not apparent in the borehole camera surveys. The vertical fractures observed in the core may be a result of damage to the core recovered from sections of the hole where there is high water loss rather than themselves being the cause of the drilling water loss.

The borehole camera survey and acoustic scanner show that the frequency of open fractures generally increases with depth. A greater number of fractures are observed from the bottom of the Hawkesbury Sandstone downward. The acoustic scanner log indicates that there are high angle joints / fractures in the Newport / Garie Formation, the Bald Hill Claystone, and the upper part of the Bulgo Sandstone that are not evident elsewhere in the hole.

The high angle fractures observed in the Bald Hill Claystone are commonly observed in this stratigraphy unit and are considered to be natural, possibly with some opening caused by ground movements associated with mining.

Many of the horizontal fractures are considered likely to be associated with mining since they appear to be open to varying degrees and increasing in

frequency with depth. The presence of casing in the upper 74m of the borehole precludes determining the frequency of open fractures above this level. However it is apparent from the borehole camera survey and acoustic scanner log that the frequency of open fractures decreases with distance above the coal seam and is at a low level by 100-110m depth below surface. There are some open fractures from 74m to 100m and one of these at about 96m was identified during drilling as a zone of high drilling water loss. These fractures are considered likely to be mining induced because of their high water take during drilling compared to other nearby sites but there may still be some influence of natural jointing within the Hawkesbury Sandstone.

An interesting result of the various methods of fracture measurement used in TBF040 is that there isn't a very strong correlation between any of the various methods and the number of open fractures observed in the borehole camera survey and the acoustic scanner log. The frequency of fractures observed in the core does not correlate closely with the frequency of open fractures observed using the acoustic scanner, the zones of water loss (except in regard to the vertical core fractures which may be an artefact of drilling in a high water loss area), or the variation in packer testing results.

Of all the various methods, the borehole camera survey and acoustic scanner log together with the piezometers are considered to provide the best indication of the presence of mining induced fractures and the characteristics of these fractures. The borehole camera survey shows a broad range of characteristics that help define the nature and openness of fractures, particularly when the borehole is full of water and fine particles able to show flow direction. The acoustic scanner provides accurate depth, orientation, and aperture data that is not available from the borehole camera survey. The piezometers provide a strong indication of vertical conductivity.

9.3 Implications of Borehole Breakout

The presence of borehole breakout in the interval 76-79m indicates that the horizontal stresses are being concentrated at this horizon. The increase in horizontal stress at this horizon is interpreted as providing an indication of the height of mining induced fractures above the goaf.

Observations of surface subsidence profiles clearly show the influence of horizontal stress on the magnitude of subsidence and by implication the processes that cause subsidence (Mills 2012). The processes that cause subsidence show many similarities to the processes that cause roof failure in underground roadways. There is evidence of biased behaviour (Tobin 1998, Mills 2011) and elevated subsidence at longwall start up when the horizontal stresses within the overburden strata are undisturbed and at their greatest magnitude.

Once the overburden strata has failed in horizontal compression, it moves down under the action of gravity to leave open fractures. A consequence of this failure process is that the horizontal stress levels within the failed rock are reduced in magnitude. At the top of the zone of fracture formation, the horizontal stresses are likely to be elevated in the zone where the rock is yet

to fail in horizontal compression. The presence of this zone indicated by borehole breakout can therefore be interpreted to be the height to which rock has failed in horizontal compression as a result of mining Longwall 10A. Above this level, the rock sags elastically without failure and the deformations are able to be accounted for through elastic relaxation (Mills 2012).

The zone of borehole breakout was evident in the interval between 76-79m below surface or approximately 340m above the mining horizon. This height is equivalent to a distance above the mining horizon of 1.45 times the longwall panel width. This observation indicates that the zone of bedding plane separation referred to in Mills (2012) as extending from 1.4 to 1.7 times panel width is also be associated with rock failure as indicated by a reduction in horizontal stress magnitude.

Rock failure has been recognised as being associated with the zone of large downward movement that extends up from the mining horizon to about one times the panel width but this observation of borehole breakout indicates that the zone of bedding plane separation that extends from about one times the panel width to 1.4-1.7 times panel width also involves rock failure rather than elastic sagging down of the intact strata with separation on bedding. Axial splitting of the rock fabric is recognised as a failure mode at low confining pressures during the transition from elastic behaviour to conventional shear failure (Diederichs et al 2004) and the bedding plane separation observed would be consistent with this failure mode.

An attempt was made to measure the in situ stress profile as part of the monitoring program at this site, but unfortunately drilling issues with the development of the specialist techniques used prevented this measurement from being successfully undertaken. A profile of such measurements would be helpful to characterise the horizontal stress transfer within these different zones.

Two other zones of borehole breakout at 196.7m and 226.9m are very short in vertical extent. These zones are interpreted to have occurred where blocks of intact strata are in point contact and the contact stresses are elevated as a result.

9.4 Surface Subsidence

Figure 13 shows the surface subsidence profile that was measured over Longwall 10A and the adjacent panels (MSEC 2014). This profile indicates that elastic strata compression above the chain pillars was 300mm on one side of the panel and 400mm on the other side of the panel. If there was no sag subsidence over the panel, subsidence in the centre of Longwall 10A would have been 350mm. The approximately 440mm of maximum subsidence observed in the centre of the panel implies sag subsidence of approximately 90mm.

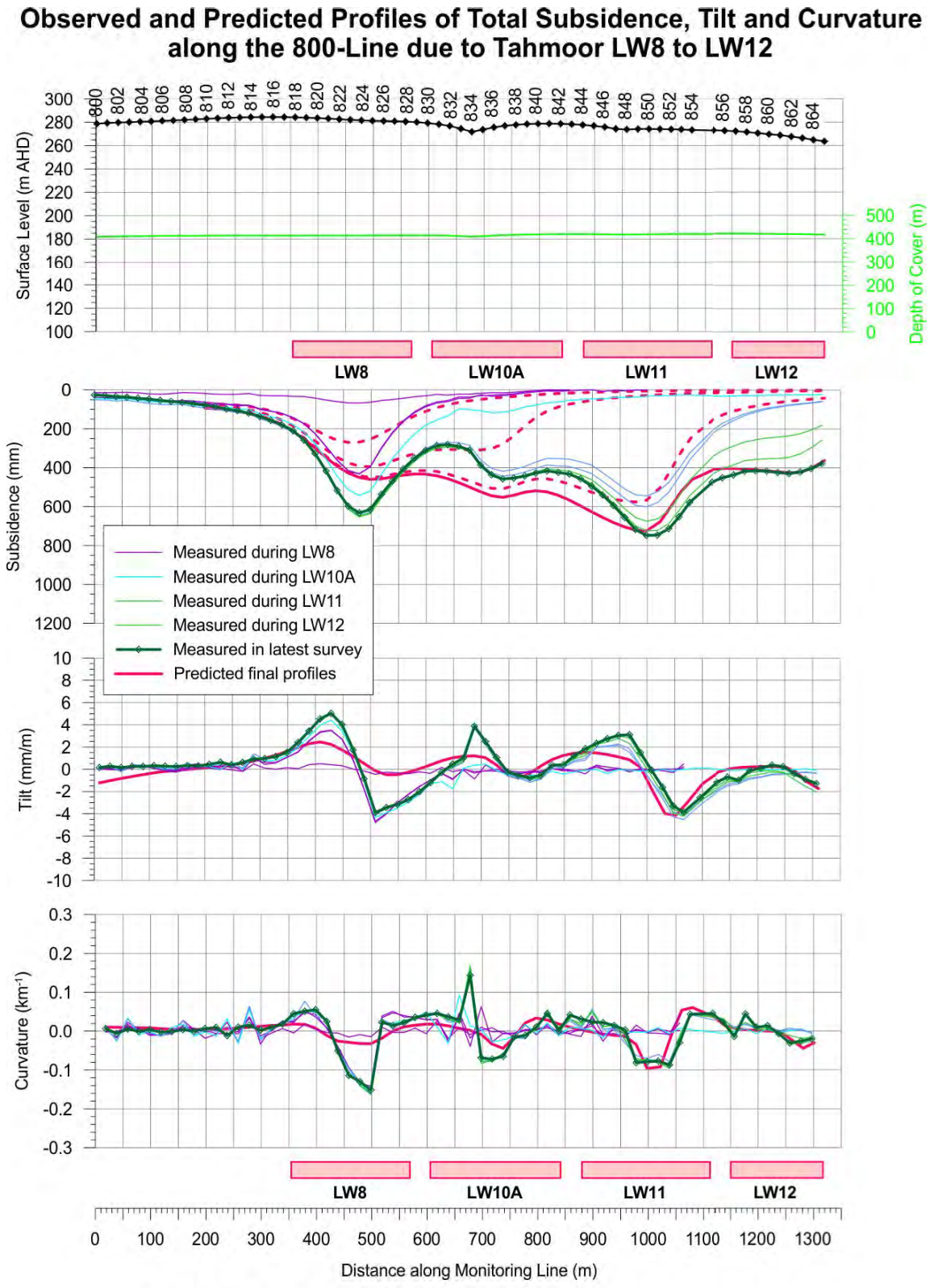

Figure 13: Subsidence above Longwall 10A (MSEC 2014).

For a nominal extraction height of 2.25m, 90mm of sag subsidence is equivalent to approximately 0.04 times extracted seam thickness. The upper part of the overburden strata is inferred from subsidence observations to be able to accommodate up to 0.10 times the extracted mining height within the elastic range i.e. without strata failure. The subsidence data indicates that the surface strata is still within the elastic range.

The observations of borehole breakout and the inference that this breakout indicates the top of the mining induced fracture zone are consistent with the level of surface subsidence observed.

9.5 Fracture Flow

There are a number of observations of fluid flow within the fracture network that provide insight into the nature of groundwater disturbance caused by mining induced ground movements.

The average rate of drilling water loss in TBF040 was observed to be 1445 litres per metre drilled. This rate of drilling water loss is significantly higher than the rate observed during drilling of other holes in the TSP area that are remote from mining activity. The composite log in Appendix 1 shows that the loss zones were predominantly in heavily jointed areas within the Hawkesbury Sandstone at 53-59m, 96m, 123-125m, 134-136m, (165-173m inferred from drilling water loss records alone), and 195m (below the Bald Hill Claystone).

This experience indicates that the rock strata intercepted by TBF040 is more disturbed and has higher hydraulic conductivity than other areas of the TSP remote from mining activity. This increased disturbance may be the result of a local geological structure or the result of mining induced changes to the overburden strata.

Figure 14 shows a summary of the geological structures observed at seam level. There is no geological structure in the immediate vicinity of TBF040, at least at the mining horizon. It is possible that there may be some geological structure present in the upper strata, particularly within the Hawkesbury Sandstone that is not evident at seam level. Although the borehole camera survey was not able to be run in the upper 74m of the Hawkesbury Sandstone and so it is difficult to be conclusive, there does not appear to be any major geological structure evident within the lower 110m of this unit. The fractures are predominantly (approximately 80%) horizontal and the water loss zones and cavities do not appear to be controlled by geological structure.

The variability in horizontal stress direction apparent in Figure 11 in the vicinity of Longwall 10A may be a result of this geological structure.

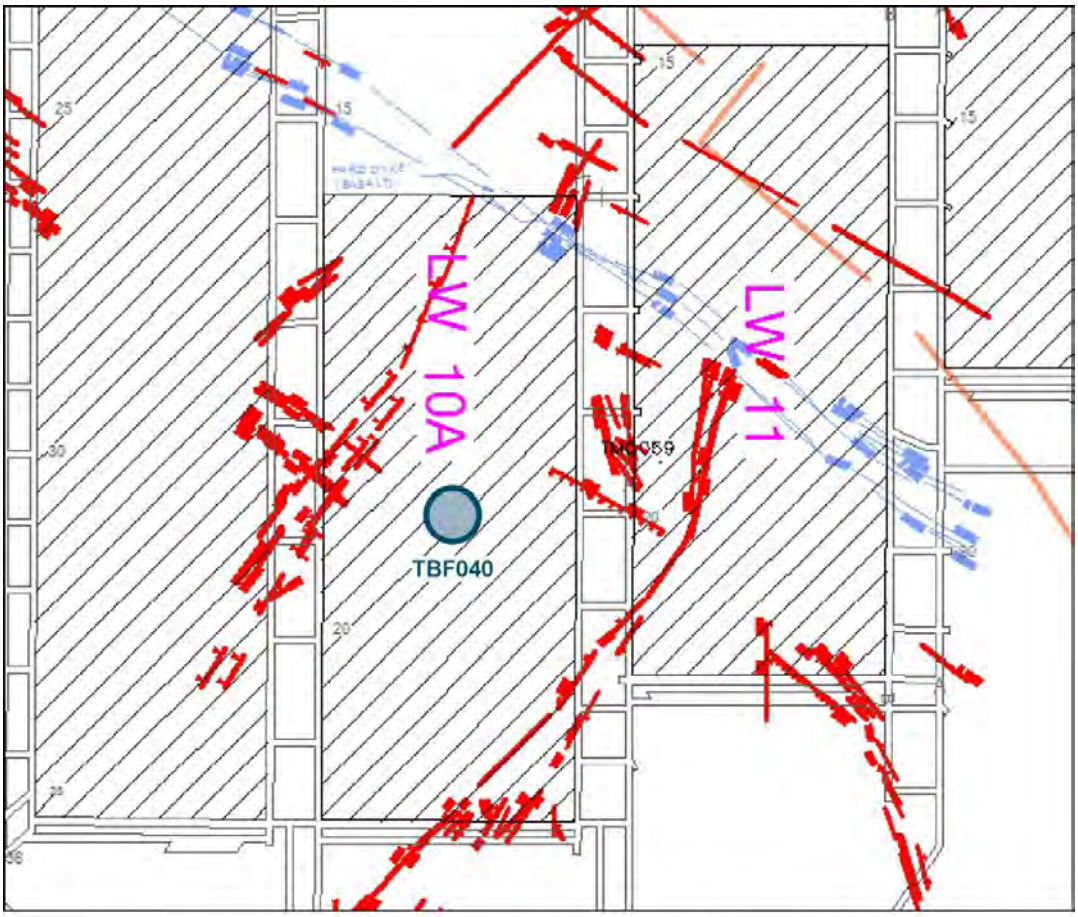

Figure 14: Geological structure observed at seam level.

9.6 Downward Fracture Flow

The camera surveys in TBF040 provide an observation that is very significant in terms of confirming a number of hypotheses.

Water, and the fine particulate material carried within it, was observed during the borehole camera survey in TBC040C to be flowing out of the borehole into an open fracture at a depth of 195.8m. This horizon is below the Bald Hill Claystone in the top of the Bulgo Sandstone.

This observation begs the question of where this water could be flowing to. It is possible that there may be a flow pathway laterally from the hole to some outcrop of the Bulgo Sandstone but the horizontal distance to nearest outcrop of the Bulgo Sandstone is some 30-40km and much further than the vertical proximity to the depressurised fracture network indicated by the piezometer measurements some 30m directly below. The only credible pathway for this flow to be occurring is downward into the mine via the tortuous mining induced fracture network.

The 195.8m horizon into which flow has been observed is consistent with the point at which the piezometric pressure gradient begins to be drawn down below hydrostatic indicated by the piezometers. The implication of this coincidence is that this horizon is the first location vertically down from the surface where there is clearly a pathway downward through the fracture network into the mine.

The point of first evidence of downward flow (at 196.8m) is approximately 222m above the mining horizon. This point is 0.94 times the 235m panel width of Longwall 10A above the mining horizon. This observation is consistent with the inference based on surface subsidence monitoring (Mills 2012) and extensometer monitoring (Mills and O'Grady 1998) that the height of angled shear fracturing extends vertically to a distance above the mining horizon equal to about one panel width and that the angled shear fracturing provides a vertical pathway for flow downward into the mine from this point. Above this horizon, the implication of subsidence and other types of monitoring is that horizontal fractures are more prevalent. Within this zone of predominantly horizontal fracturing there appear to be limited pathways for vertical flow.

The observation of water flowing out of the borehole at a height above the mining horizon of almost one times the panel width is significant because it confirms the height above the mining horizon at this site where fracturing that is vertically connected to the mine first allows perceptible downward flow.

Above this horizon, there are numerous fractures evident and many of these are likely to be mining induced, but these fractures are either not connected vertically, consistent with the inference that fracture formation occurs in a predominantly horizontal direction above this level, or there is no hydraulic gradient to drive flow out of the borehole because there is at least one horizon near the base where vertical flow is restricted sufficiently to be inconsequential.

At the TBF040 site, the base of the Bald Hill Claystone is approximately coincident with the point at which first connection with the mine is observed. The base of the Bald Hill Claystone is located at 193m, but there is typically a transition zone of several metres where interfingering occurs with the Bulgo Sandstone. The core indicates that this transition finishes at about 196.7m as shown in Figure 10. The inference that the Bald Hill Claystone has acted as an aquitard to support the groundwater system in the Hawkesbury Sandstone is consistent with the observed outflow.

However, there may be an element of coincidence about this observation because the fracture network through the next 20m of Bulgo Sandstone remains sufficiently tortuous to prop up the groundwater so that it is only slightly drawn down below hydrostatic. If the Bald Hill Claystone alone was the aquitard, the piezometric pressure in the piezometers at 205m, 220m and 226m should be close to zero. While it is possible that over time, these piezometers may transition back to low pressures following the disturbance caused by drilling, the available piezometer monitoring indicates that

equilibrium groundwater pressures have been maintained for over a month without change suggesting that the Bald Hill Claystone itself is not necessarily the reason that vertical flow is limited. The main restriction to downward flow appears to be the tortuous nature of the fracture network within the top of the Bulgo Sandstone although the Bald Hill Claystone may also be contributing.

Below the 195.8m horizon, the borehole camera survey indicates that there are an increasingly high number of fractures and the piezometric pressure profile indicates that these fractures are vertically connected to the mine at a rate that increases with depth.

At the 195.8 horizon, the vertical connectivity of the fracture network is sufficiently low that flow down the borehole supplied by recharge from the Hawkesbury Sandstone higher up can easily keep up. The borehole remains substantially full of water because the inflow is large and the outflow small, much the same as a leaky bucket stays full when filled sufficiently quickly.

When the recharge flow is restricted by grouting up the hole, the piezometers detect the downward flow as drawdown of the piezometric profile below hydrostatic. There is still sufficient vertical flow at 190m below surface to maintain hydrostatic pressure within the groundwater, but further down, the increasing frequency of fractures and the likelihood that these are more open and more vertically connected nearer to the mining horizon means that downward flow eventually exceeds the rate at which recharge flow can keep up and the piezometric pressure drops to zero.

9.7 Height of Depressurisation

The height of full depressurisation is a convenient concept for groundwater modelling purposes because it provides a bridge between the geomechanical disturbance caused by mining and a characteristic of the groundwater that can be incorporated into hydrogeological models.

Tammetta (2012) presents an empirical method for determining the height of complete depressurisation above a longwall panels based on observations from a comprehensive set of known worldwide experience in the public domain. This method indicates that for the geometry of 235m wide panel at 417m deep, extraction of a 2.25m seam would cause complete depressurisation to 146m above the mining horizon (271m below surface). The actual mining height is difficult to determine with confidence because it may not equal the seam thickness if roof or floor strata is cut out during mining to create additional working height on the longwall face.

Figure 12 shows the height of depressurisation indicated by the Tammetta approach. This height correlates well with the height of drawdown indicated by the piezometric profile, particularly given the ±25m tolerance on the height of depressurisation indicated by the data presented in Tammetta (2012). especially if there is a vertical pathway for flow alongside the core barrel lodged in the bottom of the hole so that the lowest piezometer is actually representing the pressure at the bottom of the hole at 243.9m.

10. CONCLUSIONS

Borehole TBF040 was cored down to a total depth of 243.9m in three holes directly above the centre of Longwall 10A.

Significant water loss was observed throughout the drilling process, primarily through several joint / fracture zones, mainly in the Hawkesbury Sandstone. Defect logging, rock quality designation (RQD), packer testing, daily water usage, borehole camera surveys, and acoustic scanner logging identified fracture zones associated with water loss horizons.

Although it is not possible to unequivocally determine which fractures are mining induced and which are natural, there are several observations that help distinguish the height above which mining induced fracturing is unlikely and the level of disturbance associated with mining induced fractures.

The water loss zones observed at a depth less than 75m are considered likely to be mainly associated with natural joints in the Hawkesbury Sandstone. Drilling water loss zones and open fractures observed below 75m are considered likely to include mining induced fractures. The mining induced fractures are observed to increase in frequency with depth.

Hydraulic conductivity measured using terminal packer testing equipment ranged from a minimum of $3.3x10^{-9}$m/s to a maximum of $5.4x10^{-5}$m/s but these hydraulic conductivity do not differentiate between horizontal and vertical conductivity. Although there is a general trend of decreasing water loss with depth into the borehole, the water losses are significantly higher than usual for this area.

When left to settle overnight, the water level in the borehole remained in a state of equilibrium at approximately 41m depth below the surface. The water level in the Hawkesbury Sandstone indicated by the piezometers was slightly higher at 38.8m (RL245.6m). This level is consistent with the general trends in groundwater level observed more widely across the Tahmoor area (Geoterra 2013) which indicate a groundwater level at this location of RL244m.

Borehole breakout observed in TBF040C in the interval 75-79m below surface is inferred as a horizon at which horizontal stresses are elevated at the top of the zone of mining induced fractures. This horizon is approximately 340m (1.45 time panel width) above the mining horizon, an elevation that is consistent with the top of the zone where mining induced fractures are expected based on sag subsidence observations throughout NSW.

These observations indicate that horizontal fractures dominate the failure process above the top of the shear fracture zone, to a height of approximately 1.4-1.7 times panel width. Within the zone of predominantly horizontal fracturing there appears to be only limited pathways for vertical flow.

The borehole camera survey showed water and the fine particulate material carried within TBF040C flowing out of the borehole into an open fracture at a depth of 195.8m below the surface. This 195.8m horizon correlates with the point at which the piezometric pressure gradient first begins to be drawn down below hydrostatic. In the absence of any credible horizontal flow path, the flow pathway from the borehole at 195.8m must be downward into the mine via a tortuous mining induced fracture network.

The point of first evidence of downward flow at 195.8m is approximately 222m above the mining horizon. This distance is 0.94 times the 235m panel width of Longwall 10A and consistent with the inference based on surface subsidence monitoring (Mills 2012) and extensometer monitoring (Mills and O'Grady 1998) that the height of angled shear fracturing extends vertically to a distance above the mining horizon equal to about one times panel width. The significance of the angled shear fracturing is that the vertical pathway for flow downward into the mine through natural joints and matrix permeability is enhanced by the vertical component of this fracturing.

At the TBF040 site, the base of the Bald Hill Claystone is approximately coincident with the point at which the first perceptible flow connection with the mine is observed. The inference that the Bald Hill Claystone has acted as an aquitard to support the groundwater system in the Hawkesbury Sandstone is broadly consistent with the observation of outflow from the borehole at 195.8m below the surface. However, there may be an element of coincidence about the outflow horizon being near the base of the Bald Hill Claystone because the fracture network through the next 20m of Bulgo Sandstone remains sufficiently tortuous to maintain the groundwater so that it is only slightly drawn down below hydrostatic. This state has been maintained for over a month since the piezometers were installed and appears to be in long term equilibrium.

The borehole camera survey and acoustic scanner log indicate that there are a higher number of fractures below the 195.8m horizon than higher up in the sequence consistent with the complete depressurisation inferred just below the end of the borehole. The piezometric pressure profile indicates that these fractures are vertically connected to the mine at a rate that increases with depth.

The drawdown to full depressurisation indicated by the piezometers is consistent with the height of depressurisation indicated by the approach forwarded by Tammetta (2012), especially if there is a vertical pathway for flow alongside the core barrel lodged in the bottom of the hole so that the lowest piezometer is actually representing the pressure at the bottom of the hole at 243.9m.

11. REFERENCES

Diederichs M.S., P.K Kaiser, and E. Eberhardt 2004 "Damage Initiation and propagation in hard rock during tunnelling and the inflow of near-face stress rotation" International Journal of Rock Mechanics & Mining Sciences 41 (2004) pp785-812.

Geoterra 2013 "Tahmoor South Project Shallow Groundwater Baseline Monitoring" Report to Tahmoor Coal Pty Ltd BAR3-R1A 10 December 2013.

Gordon N. 2013 "Discussion on Stress Orientation and Magnitude" Unpublished Report to Tahmoor Coal dated February 2013.

Mills K.W. 2011 "Developments in Understanding Subsidence with Improved Monitoring" Proceedings of the 8th Triennial Conference on Mine Subsidence , Pokolbin, NSW

Mills K.W. 2012 "Observations of Ground Movement Within the Overburden Strata above Longwall Panels and Implications for Groundwater Impacts" Proceedings of 38th Symposium on the Advances in the Study of the Sydney Basin, Hunter Valley, NSW, May 10-11 2012, pp1-14

Mills K.W. and P. O'Grady 1998 "Impact of Longwall Width on Overburden Strata" Coal 98 Conference Wollongong 18-20 February 1998 pp147-155.

MSEC 2014 "Tahmoor South Project – Longwalls 101 to 206 – Subsidence ground movement predictions and subsidence impact assessments for all natural features and surface infrastructure in support of the Environmental Impact Statement" Report MSEC606 Revision A to TSP dated February 2014.

Tammetta, P, 2012 "Estimation of the Height of Complete Groundwater Drainage Above Mined Longwall Panels" Ground Water 2012, National Groundwater Association, pp1-12.

Tobin, C. 1998 "A Review of the Newcastle Subsidence Prediction Curve" Proceedings of AusIMM No 1 1998 p59-63.

APPENDIX 1 – COMPOSITE LOG
(PDF Only)

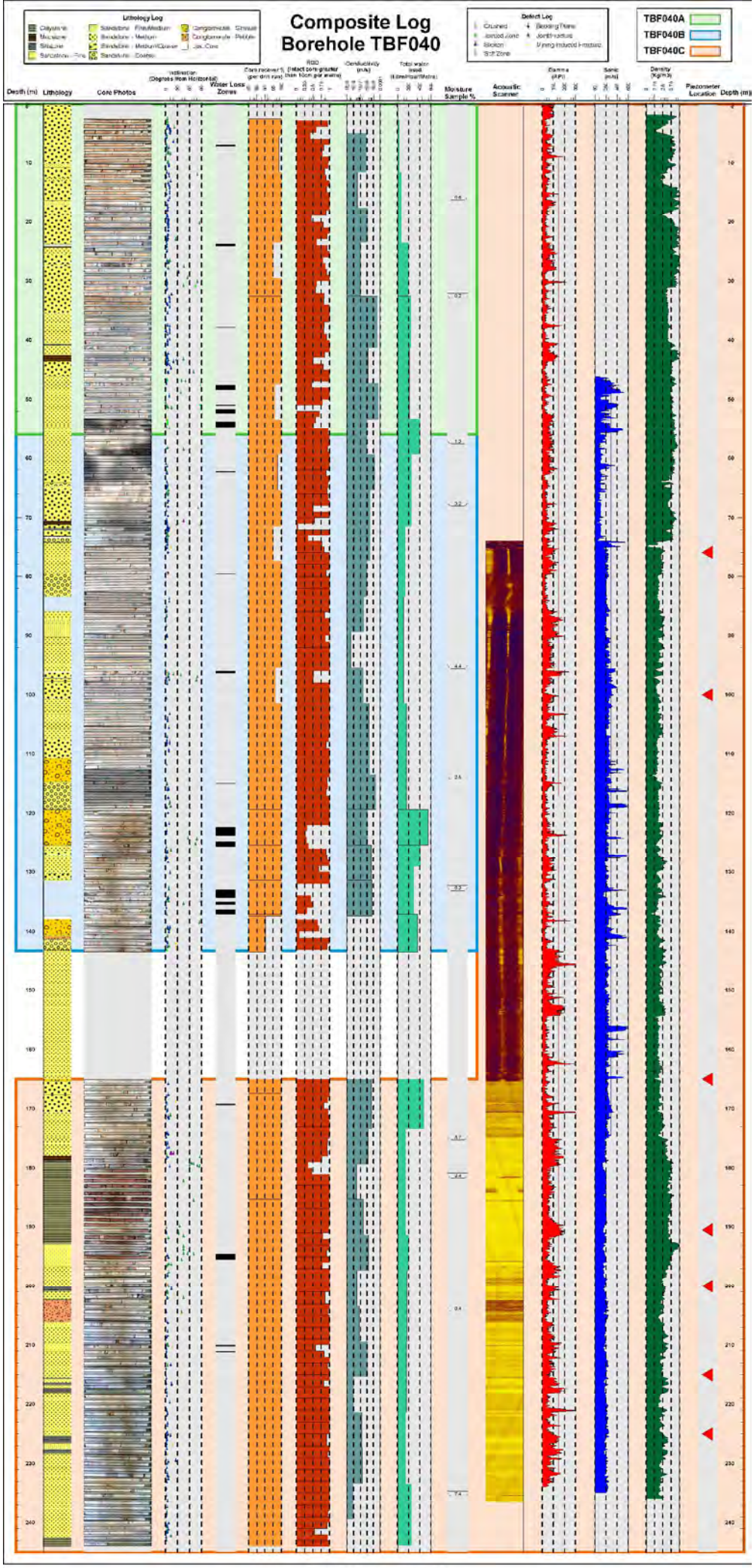

Appendix 1: Composite Log.

APPENDIX 2 – LITHOLOGY LOG
(PDF Only)

Project	Lithology Log	Drill Hole
TBF040		TBF040

Top Depth	Base Depth	Recovered Thickness	Seam	Lithology %	Lithology	Shade	Hue	Colour	Grain Size	Adjective 1	Adjective 2	Adjective 3	Adjective 4	Adjective 5	Adjective 6	Adjective 7	Interrelationship	Weathering	Estimated Strength	Bed Spacing	Comments
2	9.99		Hawkesbury Sandstone		Medium/Coarse Sandstone	Light/Medium	Greyish	Red	Coarse	silty	wisps	in places	quarts	bands	in places			Y	Low	2-5cm	
9.99	10.75	0.76	Hawkesbury Sandstone		Fine/Medium Sandstone	Light/Medium	Greyish	Red	Fine/Medium	silty	wisps	in places						Y	Low	2-5cm	
10.75	12.49	1.74	Hawkesbury Sandstone		Medium/Coarse Sandstone	Light/Medium	Greyish	Red	Coarse	silty	wisps	in places	quarts	bands	in places			Y	Low	2-5cm	
12.49	13.01	0.52	Hawkesbury Sandstone		Medium Sandstone	Light	Greyish		Medium/Coarse	silty	wisps	in places						Y	Low	2-5cm	
13.01	16.32	3.31	Hawkesbury Sandstone		Medium/Coarse Sandstone	Light/Medium	Greyish	Red	Coarse	silty	wisps	in places	quarts	bands	in places			Y	Low	2-5cm	
16.32	17.10	0.78	Hawkesbury Sandstone		Fine/Medium Sandstone	Light	Greyish	Red	Fine/Medium	silty	wisps	in places						Y	Low	5-10cm	
17.10	23.86	6.76	Hawkesbury Sandstone		Medium/Coarse Sandstone	Light/Medium	Greyish	Red	Coarse	silty	wisps	in places	quarts	bands	in places			Y	Low	2-5cm	
23.86	24.16	0.30	Hawkesbury Sandstone		Lost Core																
24.16	24.31	0.15	Hawkesbury Sandstone		Mudstone	Dark		Grey	Very Fine									Y	Low	2-5cm	
24.31	25.46	1.15	Hawkesbury Sandstone		Medium Sandstone	Light		Grey	Medium/Coarse	siltstone	bands	in places						Y	Low	2-5cm	
25.46	27.10	1.64	Hawkesbury Sandstone		Medium/Coarse Sandstone	Light/Medium	Greyish	Red	Coarse	siltstone	bands	over top	pebble	in places				Y	Low	2-5cm	
27.10	27.46	0.36	Hawkesbury Sandstone	75	Medium/Coarse Sandstone	Light/Medium	Greyish	Red	Medium/Coarse									Y	Low	2-5cm	
27.10	27.46	0.36	Hawkesbury Sandstone	25	Claystone	Dark		Grey	Very Fine									Y	Low	2-5cm	
27.46	35.40	7.94	Hawkesbury Sandstone		Medium/Coarse Sandstone	Light/Medium	Greyish	Red	Medium/Coarse									Y	Low	10-30cm	Base of Weathering
35.40	40.63	5.23	Hawkesbury Sandstone		Medium Sandstone	Light/Medium	Greyish		Medium/Coarse									N	Medium	2-5cm	
40.63	40.89	0.26	Hawkesbury Sandstone	50	Siltstone	Medium/Dark	Brownish	Grey	Very Fine/Fine	sandstone	wisps	laminea	siltstone	clasts				N	Medium	5-10cm	
40.63	40.89	0.26	Hawkesbury Sandstone	50	Fine/Medium Sandstone	Medium			Fine/Medium									N	Medium	5-10cm	
40.89	42.51	1.62	Hawkesbury Sandstone		Medium Sandstone	Light/Medium		Grey	Medium/Coarse	pebble	clasts	and	silty	laminea				N	Medium	2-5cm	
42.51	43.49	0.98	Hawkesbury Sandstone		Mudstone	Medium/Dark		Grey	Very Fine	sandstone	bands	throughout	and	siltstone	laminea	throughout		N	Low	1-2cm	
43.49	46.03	2.54	Hawkesbury Sandstone		Medium/Coarse Sandstone	Light/Medium		Grey	Coarse	siltstone	laminea	in places						N	Medium	2-5cm	
46.03	47.48	1.45	Hawkesbury Sandstone		Medium Sandstone	Light/Medium		Grey	Medium/Coarse	silty	wisps	in places						N	Medium	30-100cm	
47.48	47.64	0.16	Hawkesbury Sandstone		Lost Core																
47.64	54.19	6.55	Hawkesbury Sandstone		Medium Sandstone	Light		Grey	Medium/Coarse	Large	siltstone	clasts	in places					N	High	10-30cm	
54.19	54.65	0.46	Hawkesbury Sandstone	70	Medium Sandstone	Medium		Grey	Medium/Coarse	Large	claystone	clasts	throughout	crushed	zone			N	Medium	5-10cm	
54.19	54.65	0.46	Hawkesbury Sandstone	30	Claystone				Very Fine									N	Medium	5-10cm	
54.65	55.28	0.63	Hawkesbury Sandstone		Medium Sandstone	Light		Grey	Medium	abundant	siltstone	clasts	throughout					N	High	5-10cm	
55.28	57.45	2.17	Hawkesbury Sandstone		Medium Sandstone	Light		Grey	Medium									N	Very high	>100cm	
57.45	62.66	5.21	Hawkesbury Sandstone		Medium Sandstone	Light		Grey	Medium	silty	wisps	in places						N	High	10-30cm	
62.66	64.15	1.49	Hawkesbury Sandstone		Medium/Coarse Sandstone	Light		Grey	Coarse	silty	wisps	in places						N	High	10-30cm	
64.15	64.63	0.48	Hawkesbury Sandstone		Coarse Sandstone	Light/Medium		Grey	Very Coarse	pebble	in places	and	mudstone	band	over base			N	High	10-30cm	
64.63	64.98	0.35	Hawkesbury Sandstone		Fine/Medium Sandstone	Light/Medium		Grey	Fine/Medium	abundant	silty	laminea	throughout					N	High	2-5cm	
64.98	70.49	5.51	Hawkesbury Sandstone		Medium/Coarse Sandstone	Light		Grey	Coarse	silty	wisps	in places						N	High	10-30cm	
70.49	71.11	0.62	Hawkesbury Sandstone		Mudstone	Dark	Brownish	Grey	Very Fine									N	Medium	<1cm	
71.11	71.70	0.59	Hawkesbury Sandstone		Medium/Coarse Sandstone	Light		Grey	Coarse	silty	wisps	in places						N	High	10-30cm	
71.70	72.09	0.39	Hawkesbury Sandstone		Siltstone	Dark		Grey	Very Fine/Fine	abundant	mudstone	and	sandstone	laminea	throughout			N	Medium	1-2cm	
72.09	73.14	1.05	Hawkesbury Sandstone		Medium/Coarse Sandstone	Light		Grey	Coarse	silty	wisps	in places						N	High	5-10cm	
73.14	73.31	0.17	Hawkesbury Sandstone		Coarse Sandstone	Light/Medium		Grey	Very Coarse	coarse	quartz	throughout						N	Medium	5-10cm	
73.31	73.61	0.30	Hawkesbury Sandstone		Lost Core																
73.61	74.26	0.65	Hawkesbury Sandstone		Coarse Sandstone	Light/Medium		Grey	Very Coarse	coarse	quartz	throughout						N	Medium	5-10cm	
74.26	79.52	5.26	Hawkesbury Sandstone		Medium Sandstone	Light/Medium		Grey	Medium	abuundant	silty	laminea	throughout					N	High	2-5cm	
79.52	85.9	6.38	Hawkesbury Sandstone		Coarse Sandstone	Light/Medium		Grey	Very Coarse	coarse	sandstone	wisps	coarse	bands	throughout			N	Very high	5-10cm	
79.52	85.9	6.38	Hawkesbury Sandstone		Conglomerate - Granule				Conglomerate - Granule									N	Very high		
85.90	86.87	0.97	Hawkesbury Sandstone		Medium Sandstone	Light/Medium		Grey	Medium	silty	lenses	and	Carbonaceous	wisps	in places			N	Very high	2-5cm	
86.87	90.25	3.38	Hawkesbury Sandstone		Fine/Medium Sandstone	Light		Grey	Fine/Medium	siltstone	quartz	over middle	Carbonaceous	wisps	throughout			N	Very high	>100cm	
90.25	96	5.75	Hawkesbury Sandstone		Medium Sandstone	Light/Medium		Grey	Medium	carbonaceous	wisps	over middle						N	Very high	>100cm	
96.00	96.23	0.23	Hawkesbury Sandstone		Lost Core																
96.23	97	0.77	Hawkesbury Sandstone		Medium/Coarse Sandstone	Light/Medium		Grey	Medium/Coarse	siltstone	pebble	over middle						N	Medium	5-10cm	
97.00	97.18	0.18	Hawkesbury Sandstone		Siltstone	Medium/Dark		Grey	Very Fine/Fine									N	High	5-10cm	
97.18	97.73	0.55	Hawkesbury Sandstone		Medium/Coarse Sandstone	Light/Medium		Grey	Medium/Coarse	Siltstone	clasts	throughout	fine grained	over base				N	High	5-10cm	

Project	Lithology Log	Drill Hole
TBF040		TBF040

Top Depth	Base Depth	Recovered Thickness	Seam	Lithology %	Lithology	Shade	Hue	Colour	Grain Size	Adjective 1	Adjective 2	Adjective 3	Adjective 4	Adjective 5	Adjective 6	Adjective 7	Interrelationship	Weathering	Estimated Strength	Bed Spacing	Comments
97.73	100.62	2.89	Hawkesbury Sandstone		Medium/Coarse Sandstone	Light/Medium		Grey	Medium/Coarse	coarse	bands	throughout						N	High	2-5cm	
100.62	103.21	2.59	Hawkesbury Sandstone		Medium Sandstone	Light/Medium		Grey	Medium									N	Very high	>100cm	
103.21	105.69	2.48	Hawkesbury Sandstone		Medium Sandstone	Light/Medium		Grey	Medium	silty	laminea	throughout						N	High	2-5cm	
105.69	107.4	1.71	Hawkesbury Sandstone		Medium Sandstone	Light/Medium		Grey	Medium									N	Very high	>100cm	
107.40	110.6	3.20	Hawkesbury Sandstone		Medium/Coarse Sandstone	Light/Medium		Grey	Medium/Coarse	silty	lenses	throughout						N	Very high	10-30cm	
110.60	114.75	4.15	Hawkesbury Sandstone		Conglomerate - Granule	Light/Medium		Grey	Conglomerate - Granule	coarse	lenses	in places						N	Very high	10-30cm	
114.75	125.4	10.65	Hawkesbury Sandstone	70	Coarse Sandstone	Light/Medium		Grey	Coarse	conglomerate	bands	in places						N	Very high	5-10cm	
114.75	125.4	10.65	Hawkesbury Sandstone	30	Conglomerate - Granule	Light/Medium		Grey	Conglomerate - Granule								Interbedded	N	Very high	5-10cm	
125.40	126.48	1.08	Hawkesbury Sandstone		Medium Sandstone	Light/Medium		Grey	Medium	pebble	quartz	throughout						N	Very high	2-5cm	
126.48	126.91	0.43	Hawkesbury Sandstone		Medium/Coarse Sandstone	Light		Grey	Medium/Coarse	pebble	bands	in places						N	Very high	10-30cm	
126.91	130.27	3.36	Hawkesbury Sandstone		Medium Sandstone	Light/Medium		Grey	Medium	siltstone	laminea	throughout						N	Very high	2-5cm	
130.27	130.97	0.70	Hawkesbury Sandstone	50	Medium/Coarse Sandstone	Light/Medium		Grey	Medium/Coarse								Interbedded	N	Very high	2-5cm	
130.27	130.97	0.70	Hawkesbury Sandstone	50	Conglomerate - Granule	Light		Grey	Conglomerate - Granule									N	Very high	2-5cm	
130.97	131.4	0.43	Hawkesbury Sandstone		Medium Sandstone	Light/Medium		Grey	Medium	siltstone	laminea	throughout						N	Very high	2-5cm	
131.40	137.4	6.00	Hawkesbury Sandstone	50	Coarse Sandstone	Light/Medium		Grey	Coarse	pebble	clasts	bands	over middle				Interbedded	N	Medium	5-10cm	
131.40	137.4	6.00	Hawkesbury Sandstone	50	Conglomerate - Granule	Light		Grey	Conglomerate - Granule									N	Medium	5-10cm	Hydrocarbons present
137.40	137.99	0.59	Hawkesbury Sandstone		Lost Core																
137.99	140.76	2.77	Hawkesbury Sandstone	50	Coarse Sandstone	Light/Medium		Grey	Very Coarse	pebble	clasts	bands	over middle				Interbedded	N	Medium	5-10cm	
137.99	140.76	2.77	Hawkesbury Sandstone	50	Conglomerate - Granule				Conglomerate - Granule									N	Medium	5-10cm	Hydrocarbons present
140.76	141.26	0.50	Hawkesbury Sandstone		Conglomerate - Pebble	Medium		Grey	Conglomerate - Pebble	coarse	quartz	throughout						N	Medium	10-30cm	
141.26	143.13	1.87	Hawkesbury Sandstone		Coarse Sandstone	Light/Medium		Grey	Very Coarse	Conglomerate	quartz	throughout						N	High	5-10cm	
143.13	143.4	0.27	Hawkesbury Sandstone		Fine Sandstone	Medium		Grey	Fine									N	Medium	5-10cm	
143.40	165	21.60	Hawkesbury Sandstone		Sandstone - No Coring													N			
165	165.38	0.38	Hawkesbury Sandstone		Conglomerate - Granule	Medium		Grey	Conglomerate - Granule	sandstone	bands	over top						N	High	5-10cm	
165.38	167.66	2.28	Hawkesbury Sandstone	75	Medium/Coarse Sandstone	Medium		Grey	Medium/Coarse								Interbedded	N	High	2-5cm	
165.38	167.66	2.28	Hawkesbury Sandstone	25	Conglomerate - Granule	Medium		Grey										N	High	2-5cm	
167.66	170.5	2.84	Hawkesbury Sandstone		Medium/Coarse Sandstone	Medium		Grey	Medium/Coarse	silty	wisps	throughout						N	High	5-10cm	
170.5	174.68	4.18	Hawkesbury Sandstone		Medium Sandstone	Light/Medium		Grey	Medium	silty	lenses	throughout						N	High	2-5cm	
174.68	177.91	3.23	Newport Formation	70	Medium Sandstone	Light/Medium		Grey	Medium	coarse	bands	over middle	and	mudstone	bands	over middle	Interbedded	N	High	10-30cm	
174.68	177.91	3.23	Newport Formation	30	Fine Sandstone				Fine									N	High	10-30cm	
177.91	178.56	0.65	Newport Formation	50	Mudstone	Medium				abuundant	mudstone	clasts	throughout				Clasts of	N	High	2-5cm	
178.56	178.56	0.00	Newport Formation	50	Fine/Medium Sandstone													N	High	2-5cm	
178.56	179	0.44	Newport Formation		Siltstone	Medium		Grey	Very Fine/Fine	claystone	matrix	throughout						N	Medium	5-10cm	
179	180.22	1.22	Garie Formation		Claystone	Light/Medium		Grey	Very Fine	oolitic								N	High	10-30cm	Oolitic
180.22	182.8	2.58	Bald Hill Claystone		Claystone	Medium		Red	Very Fine	soft	bands	in places						N	Low	10-30cm	
182.8	185.5	2.70	Bald Hill Claystone		Claystone	Medium		Red	Very Fine									N	Extreamely low	10-30cm	Semi Consolidated
185.5	189.95	4.45	Bald Hill Claystone		Claystone	Medium		Red	Very Fine	soft	bands	in places						N	Low	10-30cm	
189.95	190.89	0.94	Bald Hill Claystone		Claystone	Light		Grey	Very Fine									N	Low	10-30cm	
190.89	192.8	1.91	Bald Hill Claystone		Claystone	Medium		Red	Very Fine									N	Low	10-30cm	
192.8	196.6	3.80	Bald Hill Claystone	50	Fine Sandstone	Medium		Grey	Very Fine								Intermixed	N	High	10-30cm	
192.8	196.6	3.80	Bald Hill Claystone	50	Claystone	Medium		Red	Fine									N	High	10-30cm	
196.6	200.08	3.48	Bulgo Sandstone		Medium Sandstone	Light/Medium		Grey	Medium	coarse	bands	in places						N	High	10-30cm	
200.08	200.86	0.78	Bulgo Sandstone	60	Siltstone	Medium/Dark		Grey	Very Fine/Fine	carbonaceous	wisps	over middle					Interbedded	N	High	5-10cm	
200.08	200.86	0.78	Bulgo Sandstone	40	Fine/Medium Sandstone				Fine/Medium									N	High	5-10cm	
200.86	202.14	1.28	Bulgo Sandstone		Medium Sandstone	Light		Grey	Medium	mudstone	clasts	in places						N	Very high	10-30cm	
202.14	202.32	0.18	Bulgo Sandstone		Siltstone	Medium/Dark		Grey	Very Fine/Fine	sandstone	bands	over middle						N	High	5-10cm	
202.32	206.06	3.74	Bulgo Sandstone		Conglomerate - Pebble	Medium		Grey	Conglomerate - Pebble									N	Very high	>100cm	
206.06	206.93	0.87	Bulgo Sandstone		Fine Sandstone	Light		Grey	Fine	claystone	bands	over middle						N	Very high	30-100cm	
206.93	209.55	2.62	Bulgo Sandstone		Medium Sandstone	Light/Medium		Grey	Medium	fine grained	sandstone	bands	in places	claystone	bands	over middle		N	Very high	5-10cm	

Project	Lithology Log	Drill Hole
TBF040		TBF040

Top Depth	Base Depth	Recovered Thickness	Seam	Lithology %	Lithology	Shade	Hue	Colour	Grain Size	Adjective 1	Adjective 2	Adjective 3	Adjective 4	Adjective 5	Adjective 6	Adjective 7	Interrelationship	Weathering	Estimated Strength	Bed Spacing	Comments
209.55	211.08	1.53	Bulgo Sandstone	60	Fine Sandstone	Light/Medium		Grey	Fine	siltstone	bands	over top					Interbedded	N	Very high	10-30cm	
209.55	211.08	1.53	Bulgo Sandstone	40	Medium Sandstone	Medium		Grey	Medium									N	Very high	10-30cm	
211.08	215.45	4.37	Bulgo Sandstone		Medium Sandstone	Light/Medium		Grey	Medium	siltstone	bands	in places						N	Very high	30-100cm	
215.45	215.67	0.22	Bulgo Sandstone		Siltstone	Medium/Dark		Grey	Very Fine/Fine	sandstone	laminea	throughout						N	High	<1cm	
215.67	216.27	0.60	Bulgo Sandstone		Fine Sandstone	Light/Medium		Grey	Fine									N	Very high	2-5cm	
216.27	216.71	0.44	Bulgo Sandstone		Siltstone	Medium/Dark		Grey	Fine	sandstone	clasts	throughout						N	High	1-2cm	
216.71	217.25	0.54	Bulgo Sandstone		Fine/Medium Sandstone	Light/Medium		Grey	Fine/Medium	coarse	over base	and	mudstone	clasts	over base			N	Very high	10-30cm	
217.25	218.03	0.78	Bulgo Sandstone		Siltstone	Medium/Dark		Grey	Very Fine/Fine	mudstone	laminea	throughout	sandstone	clasts	over base			N	High	1-2cm	
218.03	225.31	7.28	Bulgo Sandstone		Medium Sandstone	Light/Medium		Grey	Medium	siltstone	bands	over middle						N	Very high	5-10cm	
225.31	226.52	1.21	Bulgo Sandstone		Siltstone	Medium/Dark		Grey	Very Fine/Fine	sandstone	bands	over middle						N	High	1-2cm	
226.52	227.59	1.07	Bulgo Sandstone		Fine/Medium Sandstone	Light/Medium		Grey	Fine/Medium									N	Very high	10-30cm	
227.59	228.23	0.64	Bulgo Sandstone		Siltstone	Medium/Dark		Grey	Very Fine/Fine	sandstone	bands	over middle						N	High	1-2cm	
228.23	242.48	14.25	Bulgo Sandstone		Medium Sandstone	Light/Medium		Grey	Medium	siltstone	bands	in places	soft	clay	bands	over middle		N	High	10-30cm	
242.48	243.9	1.42	Bulgo Sandstone	70	Claystone	Dark		Grey		sandstone	bands	over middle					Interlaminated	N	High	1-2cm	
242.48	243.9	1.42	Bulgo Sandstone	30	Siltstone													N	High	1-2cm	

APPENDIX 3 – DEFECT LOG
(PDF Only)

Defect Log

Drill Hole: TBF040

Defect Depth (Top)	Length (mm)	Broken Zone Top	Broken Zone Base	Defect Type	Defect Cause	Intact	Angle or Min Angle for Broken Zone	Surface Shape	Surface Roughness	Infill		Comments
										Perpendicular Width (mm)	Primary Type	
2.81				Joint	Natural		5	Iregular	Rough			
2.94				Joint	Natural		1	Curvy Planar	Rough			
3.20				Joint	Natural		5	Iregular	Rough			
3.26				Joint	Natural		3	Iregular	Rough			
3.59				Joint	Natural		3	Iregular	Rough			
3.78				Joint	Natural		7	Iregular	Rough			
3.96				Bedding Plane	Natural		5	Iregular	Rough			
4.05				Bedding Plane	Natural		8	Planar	Rough			
4.07				Bedding Plane	Natural		8	Planar	Rough			
4.12				Bedding Plane	Natural		8	Planar	Rough			
4.21				Bedding Plane	Natural		8	Planar	Rough			
4.27				Bedding Plane	Natural		9	Planar	Rough			
4.36				Bedding Plane	Natural		9	Planar	Rough			
4.54				Bedding Plane	Natural		10	Curvy Planar	Rough			
4.68				Bedding Plane	Natural		12	Planar	Medium		ROOT	
4.91				Bedding Plane	Natural		12	Planar	Rough			
5.00				Bedding Plane	Natural		11	Planar	Medium			
5.10				Bedding Plane	Natural		11	Iregular	Rough			
5.24				Bedding Plane	Natural		1	Iregular	Rough			
5.35				Bedding Plane	Natural		1	Iregular	Rough			
5.42				Bedding Plane	Natural		2	Iregular	Rough			
		5.58	5.64	Joint	Natural		4	Iregular	Rough			
5.81				Bedding Plane	Natural		3	Curvy Planar	Medium/Rough			
5.87				Bedding Plane	Natural		3	Planar	Medium/Rough			
5.96				Bedding Plane	Natural		0	Planar	Medium/Rough			
6.54				Bedding Plane	Natural		20	Planar	Medium/Rough			
6.94				Bedding Plane	Natural		0	Planar	Medium/Rough			
		7.07	7.24	Joint	Natural		3	Iregular	Rough			Water Loss Zone
7.37				Bedding Plane	Natural		3	Curvy Planar	Rough			
7.54				Bedding Plane	Natural		8	Curvy Planar	Rough			
7.67				Joint	Natural		6	Iregular	Rough			
7.93				Bedding Plane	Natural		2	Iregular	Polished			
8				Bedding Plane	Natural		0	Planar	Medium/Rough			
8.21				Joint	Natural		7	Iregular	Rough			
8.37				Bedding Plane	Natural		6	Planar	Rough			
8.49				Joint	Natural		7	Iregular	Rough			
8.6				Joint	Natural		12	Iregular	Rough			
8.7				Joint	Natural		1	Iregular	Rough			
4.16				Joint	Natural		22	Iregular	Rough			
4.34				Bedding Plane	Natural		3	Planar	Rough			
		9.78	9.8	Joint	Natural		6	Iregular	Rough			
10.06				Joint	Natural		5	Iregular	Rough			
10.25				Bedding Plane	Natural		8	Planar	Medium/Rough			
10.38				Bedding Plane	Natural		8	Planar	Medium/Rough			
10.41				Bedding Plane	Natural		8	Planar	Medium/Rough			
10.59				Bedding Plane	Natural		8	Planar	Medium/Rough			
10.78				Joint	Natural		1	Iregular	Rough			
11.24				Joint	Natural		1	Iregular	Rough			
11,28				Joint	Natural		1	Iregular	Rough			
11.62				Bedding Plane	Natural		3	Planar	Rough			
11.63				Bedding Plane	Natural		3	Planar	Rough			
11.64				Bedding Plane	Natural		3	Planar	Rough			
11.73				Bedding Plane	Natural		3	Planar	Rough			
11.9				Bedding Plane	Natural		8	Iregular	Rough			
12.04				Joint	Natural	Y	80			2		
12.37				Bedding Plane	Natural		9	Iregular	Rough			
12.47				Bedding Plane	Natural		2	Planar	Rough			
13.16				Bedding Plane	Natural		13	Planar	Rough			
13.48				Bedding Plane	Natural		7	Curvy Planar	Rough			
13.79				Bedding Plane	Natural		8	Planar	Rough			
14.05				Bedding Plane	Natural		10	Iregular	Rough			
14.2				Bedding Plane	Natural		10	Iregular	Rough			
14.29				Bedding Plane	Natural		10	Planar	Rough			
14.6				Joint	Natural		2	Iregular	Rough			
14.89				Bedding Plane	Natural		10	Planar	Rough			
15.19				Bedding Plane	Natural		10	Planar	Rough			
15.32				Bedding Plane	Natural		3	Planar	Rough			
15.69				Joint	Natural		60	Iregular	Rough			
15.94				Bedding Plane	Natural		10	Planar	Medium			
16.36				Bedding Plane	Natural		7	Iregular	Rough			
17.09				Bedding Plane	Natural		4	Iregular	Medium			
17.21				Bedding Plane	Natural		4	Iregular	Rough			
17.51				Bedding Plane	Natural		6	Planar	Medium/Rough			
17.97				Bedding Plane	Natural		5	Planar	Medium/Rough			
18.07				Bedding Plane	Natural		5	Curvy Planar	Medium/Rough			
18.2				Bedding Plane	Natural		2	Curvy Planar	Rough			
18.45				Crushed			2	Crushed	Rough			Possible core loss
18.62				Bedding Plane	Natural		1	Planar	Medium/Rough			
18.83				Bedding Plane	Natural		4	Iregular	Rough			

Defect Log

Drill Hole: TBF040

Defect Depth (Top)	Length (mm)	Broken Zone Top	Broken Zone Base	Defect Type	Defect Cause	Intact	Angle or Min Angle for Broken Zone	Surface Shape	Surface Roughness	Infill		Comments
										Perpendicular Width (mm)	Primary Type	
19.06				Bedding Plane	Natural		4	Iregular	Rough			
19.2				Bedding Plane	Natural		4	Iregular	Rough			
		19.21	19.34	Joint	Natural			Iregular	Rough			
19.41				Bedding Plane	Natural		2	Planar	Rough			
19.46				Bedding Plane	Natural		2	Planar	Rough			
19.59				Bedding Plane	Natural		7	Planar	Rough			
19.62				Bedding Plane	Natural		7	Planar	Rough			
19.69				Bedding Plane	Natural		7	Planar	Rough			
19.79				Bedding Plane	Natural		7	Planar	Rough			
19.86				Bedding Plane	Natural		7	Planar	Rough			
19.95				Bedding Plane	Natural		7	Planar	Rough			
20.16				Bedding Plane	Natural		6	Planar	Rough			
20.34				Bedding Plane	Natural		5	Iregular	Rough			
20.35	110			Joint	Natural		85	Iregular	Rough			
20.42				Bedding Plane	Natural		7	Planar	Rough			
20.7				Bedding Plane	Natural		7	Iregular	Rough			
21.03				Bedding Plane	Natural		7	Planar	Rough			
21.56				Bedding Plane	Natural		7	Planar	Rough			
22.28				Bedding Plane	Natural		6	Planar	Rough			
22.49				Bedding Plane	Natural		5	Planar	Smooth/Medium			
22.86				Bedding Plane	Natural	Y	5					
22.93				Bedding Plane	Natural		6	Planar	Medium/Rough			
23.05				Bedding Plane	Natural		4	Planar	Rough			
23.1				Joint	Natural		25	Iregular	Rough			
23.11				Bedding Plane	Natural		2	Planar	Medium/Rough			
23.24				Bedding Plane	Natural		5	Planar	Rough			
23.44				Bedding Plane	Natural		2	Iregular	Rough			
23.84				Bedding Plane	Natural		3	Iregular	Rough			
		23.86	24.16	Lost Core								Core loss
24.24				Bedding Plane	Natural		3	Planar	Smooth/Medium			
24.31				Bedding Plane	Natural		1	Planar	Medium/Rough			
25.06				Bedding Plane	Natural		4	Iregular	Medium/Rough			
25.21				Bedding Plane	Natural		2	Planar	Smooth/Medium			
26.67				Bedding Plane	Natural		3	Iregular	Smooth/Medium			
26.76				Bedding Plane	Natural		3	Planar	Medium/Rough			
26.64				Joint	Natural		6	Iregular	Rough			
26.72				Joint	Natural		11	Planar	Rough			
26.76				Joint	Natural		11	Planar	Rough			
26.83				Joint	Natural		7	Iregular	Rough			
26.87				Joint	Natural		9	Planar	Rough			
27.04				Bedding Plane			7	Planar	Medium/Rough			
27.1				Bedding Plane	Natural		3	Iregular	Rough			
27.67				Joint	Natural		60	Iregular	Rough			
27.71				Joint	Natural	Y	46					
27.73				Joint	Natural	Y	60					
27.96				Joint	Natural		7	Iregular	Rough			
28.4				Joint	Natural	Y	30					
28.42				Joint	Natural	Y	30					
28.65				Bedding Plane	Natural		33	Iregular	Rough			
28.72				Bedding Plane	Natural		1	Planar	Rough			
29.59				Joint	Natural		55	Iregular	Rough			
29.78				Bedding Plane	Natural		2	Planar	Rough			
29.96				Bedding Plane	Natural		2	Planar	Rough			
30.23				Bedding Plane	Natural		4	Planar	Rough			
30.23	300			Joint	Natural		80	Iregular	Rough			
30.54				Bedding Plane	Natural		4	Planar	Rough			
30.69				Bedding Plane	Natural		2	Curvy Planar	Rough			
30.88				Bedding Plane	Natural		2	Planar	Rough			
30.96				Joint	Natural		45	Iregular	Rough			
		31.01	31.39	Joint	Natural		75	Iregular	Rough			
31.39				Bedding Plane	Natural		4	Iregular	Rough			
31.61				Bedding Plane	Natural	Y	2					
32.12				Joint	Natural		30	Iregular	Rough			
32.39				Bedding Plane	Natural		15	Planar	Rough			
32.79				Bedding Plane	Natural		8	Iregular	Rough			
32.88				Bedding Plane	Natural		10	Iregular	Rough			
32.95				Bedding Plane	Natural		10	Iregular	Rough			
33.06				Bedding Plane	Natural		10	Iregular	Rough			
33.12				Bedding Plane	Natural		10	Iregular	Rough			
33.49				Bedding Plane	Natural		10	Iregular	Rough			
33.64				Bedding Plane	Natural		10	Iregular	Rough			
33.83				Bedding Plane	Natural		2	Iregular	Rough			
34.05				Bedding Plane	Natural		5	Iregular	Rough			
34.34				Joint	Natural		10	Iregular	Rough			
34.49				Bedding Plane	Natural		10	Iregular	Rough			
35.5				Bedding Plane	Natural		5	Iregular	Rough			
36.55				Bedding Plane	Natural		0	Iregular	Rough			
		37.47	37.49	Bedding Plane	Natural			Iregular	Rough			
37.63				Bedding Plane	Natural		5	Iregular	Rough			

Defect Log

Drill Hole: TBF040

Defect Depth (Top)	Length (mm)	Broken Zone Top	Broken Zone Base	Defect Type	Defect Cause	Intact	Angle or Min Angle for Broken Zone	Surface Shape	Surface Roughness	Infill		Comments
										Perpendicular Width (mm)	Primary Type	
37.7				Bedding Plane	Natural		10	Iregular	Rough			
37.71				Bedding Plane	Natural		0	Iregular	Rough			
		37.87	37.93	Joint	Natural							Water Loss
38.13				Bedding Plane	Natural		10	Iregular	Rough			
38.32				Bedding Plane	Natural		10	Iregular	Rough			
38.42				Bedding Plane	Natural		10	Iregular	Rough			
38.54				Bedding Plane	Natural		0	Iregular	Rough			
38.61				Bedding Plane	Natural		2	Iregular	Rough			
38.75				Bedding Plane	Natural		10	Iregular	Rough			
38.92				Bedding Plane	Natural		10	Iregular	Rough			
39.14				Bedding Plane	Natural		5	Iregular	Rough			
39.18				Bedding Plane	Natural		5	Iregular	Rough			
39.92				Bedding Plane	Natural	Y	10					
39.97				Bedding Plane	Natural	Y	10					
40.26				Bedding Plane	Natural		5	Iregular	Rough			
40.63				Bedding Plane	Natural		5	Iregular	Rough			
40.9				Bedding Plane	Natural		5	Iregular	Rough			
42.39				Bedding Plane	Natural		7	Curvy Planar	Medium			
42.54				Bedding Plane	Natural		2	Iregular	Smooth/Medium			
42.6				Bedding Plane	Natural		2	Planar	Smooth/Medium			
42.68				Bedding Plane	Natural		4	Planar	Smooth/Medium			
43.03				Bedding Plane	Natural		1	Planar	Smooth/Medium			
43.04				Bedding Plane	Natural		3	Iregular	Smooth/Medium			
43.07				Bedding Plane	Natural		3	Iregular	Smooth/Medium			
43.12				Bedding Plane	Natural		5	Planar	Smooth/Medium			
	0.02	43.26	43.28	Crushed	Natural		0	Crushed	Smooth/Medium			
43.31				Bedding Plane	Natural		1	Planar	Smooth/Medium			
43.34				Joint	Natural		45	Planar	Smooth/Medium			
43.4				Joint	Natural		27	Iregular	Smooth/Medium			
43.49				Bedding Plane	Natural		7	Iregular	Smooth/Medium			
43.64				Bedding Plane	Natural		20	Planar	Rough			
43.75				Bedding Plane	Natural		20	Planar	Rough			
43.92				Bedding Plane	Natural		5	Iregular	Rough			
43.97				Bedding Plane	Natural		2	Planar	Rough			
44				Bedding Plane	Natural		3	Iregular	Rough			
44.03				Bedding Plane	Natural		3	Iregular	Rough			
44.09				Bedding Plane	Natural		6	Iregular	Rough			
44.26				Bedding Plane	Natural		3	Planar	Rough			
44.29				Joint	Natural		10	Iregular	Rough			
44.33				Bedding Plane	Natural		10	Iregular	Medium/Rough			
44.52				Bedding Plane	Natural		8	Iregular	Rough			
44.75				Bedding Plane	Natural		8	Planar	Rough			
44.88				Bedding Plane	Natural		4	Planar	Medium/Rough			
45.78				Bedding Plane	Natural		8	Planar	Medium/Rough			
47.2				Bedding Plane	Natural		2	Iregular	Rough			
47.23				Bedding Plane	Natural		2	Iregular	Rough			
47.42				Bedding Plane	Natural		2	Planar	Rough			
47.45				Joint	Natural		30	Iregular	Rough			
47.54				Bedding Plane	Natural		7	Planar	Rough			
47.63				Bedding Plane	Natural		8	Iregular	Rough			
47.7				Crushed	Natural		3	Iregular	Rough			
47.71	210			Joint	Natural		80	Iregular	Rough			
49.06				Bedding Plane	Natural		10	Planar	Rough			
50.19				Bedding Plane	Natural		8	Curvy Planar	Medium/Rough			
50.22				Bedding Plane	Natural		8	Curvy Planar	Rough			
50.35				Bedding Plane	Natural		6	Planar	Rough			
50.4				Bedding Plane	Natural		6	Planar	Rough			
50.77				Bedding Plane	Natural		8	Planar	Rough			
50.86			52.05	Joint	Natural		10	Iregular	Rough			Joint zone
52.05			52.3	Lost Core								Lost core
53.48			53.51	Crushed	Natural		2	Iregular	Rough			Cursed zone
53.8			54.19	Joint	Natural		5	Iregular	Rough			Moderately jointed zone
54.19			54.65	Joint	Natural		5	Iregular	Rough			Highly jointed/crushed zone
54.98				Joint	Natural		3	Iregular	Rough			
55.02				Joint	Natural		9	Iregular	Rough			
58.37				Joint	Natural	Y	6					
58.43				Joint	Natural		4	Iregular	Rough			
58.67				Joint	Natural		45	Planar	Rough			
61.03				Bedding Plane	Natural		1	Iregular	Rough			Drill Spin
61.46				Bedding Plane	Natural		4	Planar	Smooth/Medium			
62.19				Joint	Natural		2	Iregular	Rough			
62.26				Lost Core								15cm
62.63				Bedding Plane	Natural		4	Iregular	Rough			
62.66				Bedding Plane	Natural		2	Iregular	Rough			
64.03				Bedding Plane	Natural		3	Iregular	Rough			
64.63				Bedding Plane	Natural		5	Iregular	Rough			
64.65				Bedding Plane	Natural		4	Planar	Rough			
64.66				Bedding Plane	Natural		4	Planar	Rough			
64.96				Bedding Plane	Natural		4	Planar	Medium			

Defect Log

Drill Hole: TBF040

Defect Depth (Top)	Length (mm)	Broken Zone Top	Broken Zone Base	Defect Type	Defect Cause	Intact	Angle or Min Angle for Broken Zone	Surface Shape	Surface Roughness	Infill		Comments
										Perpendicular Width (mm)	Primary Type	
65.18				Bedding Plane	Natural		2	Planar	Rough			
65.47				Joint	Natural		7	Iregular	Rough			
65.88				Joint	Natural		7	Planar	Rough			
65.96				Bedding Plane	Natural		2	Planar	Rough			
66				Joint	Natural		3	Iregular	Rough			
66.19				Joint	Natural		6	Iregular	Rough			
67.19				Bedding Plane	Natural		7	Planar	Rough			
67.49				Bedding Plane	Natural		5	Planar	Medium/Rough			
68.13				Bedding Plane	Natural		6	Curvy Planar	Rough			
68.43	500			Joint	Natural		82	Iregular	Rough			
68.89				Bedding Plane	Natural		2	Planar	Rough			
69.7				Bedding Plane	Natural		6	Curvy Planar	Rough			
70.49				Bedding Plane	Natural		3	Curvy Planar	Rough			
70.53				Bedding Plane	Natural		2	Planar	Smooth			
70.58				Bedding Plane	Natural		2	Iregular	Smooth			
70.62				Bedding Plane	Natural		2	Planar	Smooth			
70.63	60			Slicken	Natural		45	Iregular	PO			
70.68	200			Joint	Natural		90	Iregular	Smooth			
70.87				Bedding Plane	Natural		4	Iregular	Smooth			
71.11				Bedding Plane	Natural		2	Planar	Smooth			
71.15				Joint	Natural		28	Iregular	Smooth/Medium			
71.2	860			Joint	Natural		88	Iregular	Rough			
71.53				Bedding Plane	Natural		5	Iregular	Rough			
71.7				Bedding Plane	Natural		5	Iregular	Medium/Rough			
71.79				Bedding Plane	Natural		9	Iregular	Smooth/Medium			
71.91				Bedding Plane	Natural		4	Planar	Smooth/Medium			
72.06				Bedding Plane	Natural		4	Iregular	Smooth/Medium			
72.18				Bedding Plane	Natural		7	Iregular	Smooth/Medium			
72.53				Bedding Plane	Natural		3	Iregular	Medium/Rough			
72.95				Joint	Natural		5	Iregular	Rough			
73.22				Joint	Natural		7	Iregular	Rough			
73.26				Bedding Plane	Natural		2	Planar	Rough			
73.31			73.61	Lost Core								
73.71				Joint	Natural		5	Planar	Rough			
73.73				Joint	Natural		5	Planar	Rough			
73.84				Joint	Natural		5	Planar	Rough			
73.91				Joint	Natural		5	Planar	Rough			
73.97				Bedding Plane	Natural		2	Planar	Rough			
74.06				Bedding Plane	Natural		3	Iregular	Rough			
74.24				Bedding Plane	Natural		4	Iregular	Rough			
74.32				Bedding Plane	Natural		1	Planar	Medium/Rough			
74.71				Bedding Plane	Natural		4	Iregular	Rough			
74.77				Bedding Plane	Natural		5	Planar	Rough			
75.12				Bedding Plane	Natural		1	Planar	Rough			
75.22				Mining Induced Joint	Mining Induced		13	Iregular	Rough			
75.28				Bedding Plane	Natural		4	Stepped	Medium/Rough			
75.43				Bedding Plane	Natural		1	Planar	Medium/Rough			
76.03				Bedding Plane	Natural		6	Planar	Medium/Rough			
79.42				Bedding Plane	Natural		6	Planar	Medium/Rough			
79.5				Bedding Plane	Natural		6	Planar	Medium/Rough			
79.52				Bedding Plane	Natural		6	Planar	Medium/Rough			
83.88				Bedding Plane	Natural		9	Iregular	Rough			
84.31				Bedding Plane	Natural		9	Planar	Rough			
85.17				Bedding Plane	Natural		2	Planar	Rough			
85.92				Bedding Plane	Natural		3	Iregular	Rough			
85.93				Bedding Plane	Natural		3	Iregular	Rough			
86.73				Joint	Natural		2	Iregular	Rough			
86.77				Bedding Plane	Natural		3	Planar	Rough			
86.79				Joint	Natural		3	Iregular	Rough			
86.87				Joint	Natural		3	Iregular	Rough			
88.49				Bedding Plane	Natural		2	Planar	Medium/Rough			
90.12				Bedding Plane	Natural		4	Iregular	Smooth			
90.16				Bedding Plane	Natural		2	Iregular	Medium/Rough			
90.2				Bedding Plane	Natural		3	Stepped	Medium/Rough			
90.24				Bedding Plane	Natural		1	Planar	Medium/Rough			
91.84				Bedding Plane	Natural		2	Planar	Medium/Rough			
92.01				Bedding Plane	Natural		2	Curvy Planar	Medium/Rough			
95.97				Bedding Plane	Natural		0	Planar	Medium/Rough			
96			96.23	Lost Core								
96.3			96.35	Crushed	Natural		4	Iregular	Smooth/Medium			
96.56				Bedding Plane	Natural		8	Planar	Rough			
96.6				Joint	Natural		20	Planar	Rough			
96.65			96.72	Joint	Natural		6	Iregular	Rough			
96.78				Joint	Natural		38	Iregular	Rough			
96.96				Joint	Natural		7	Iregular	Rough			
97.04				Bedding Plane	Natural		6	Iregular	Smooth/Medium			
97.04		130		Joint	Natural		80	Iregular	Medium			
97.15				Bedding Plane	Natural		1	Iregular	Medium			
97.49				Bedding Plane	Natural		9	Iregular	Medium			

Defect Log

Drill Hole: TBF040

Defect Depth (Top)	Length (mm)	Broken Zone Top	Broken Zone Base	Defect Type	Defect Cause	Intact	Angle or Min Angle for Broken Zone	Surface Shape	Surface Roughness	Infill		Comments
										Perpendicular Width (mm)	Primary Type	
97.63				Bedding Plane	Natural		2	Iregular	Medium			
97.63		70		Joint	Natural		77	Iregular	Medium			
97.7				Bedding Plane	Natural		3	Stepped	Medium			
97.73				Soft Zone	Natural		2	SO				Soft clay zone
98.24				Bedding Plane	Natural		4	Planar	Medium/Rough			
100.61				Bedding Plane	Natural		2	Planar	Medium/Rough			
103.25				Bedding Plane	Natural		10	Iregular	Medium/Rough			
104.12				Bedding Plane	Natural		5	Planar	Medium/Rough			
104.49				Bedding Plane	Natural		5	Planar	Medium/Rough			
105.6				Bedding Plane	Natural		8	Planar	Medium/Rough			
107.16				Bedding Plane	Natural		4	Planar	Medium/Rough			
107.71				Bedding Plane	Natural		3	Planar	Rough			
107.73				Bedding Plane	Natural		3	Planar	Rough			
108.01				Bedding Plane	Natural		10	Planar	Rough			
108.07				Bedding Plane	Natural		10	Iregular	Rough			
108.12				Bedding Plane	Natural		4	Stepped	Rough			
108.41				Bedding Plane	Natural		1	Curvy Planar	Rough			
108.05				Bedding Plane	Natural		2	Planar	Rough			
108.3				Bedding Plane	Natural		10	Planar	Rough			
108.5				Bedding Plane	Natural		3	Iregular	Rough			
109.29				Bedding Plane	Natural		8	Planar	Rough			
109.6				Bedding Plane	Natural		8	Planar	Rough			
111.9				Joint	Natural		3	Iregular	Rough		Coal	
114.95			115.03	Crushed	Natural		3	Iregular	Smooth/Medium			Large conglomerate loose pebbles
115.16				Bedding Plane	Natural	Y	4					
115.21				Joint	Natural		2	Iregular	Rough			
115.97				Bedding Plane	Natural		8	Stepped	Rough			
116.02				Bedding Plane	Natural		8	Planar	Rough			
116.07				Bedding Plane	Natural		5	Iregular	Rough			
117.44				Bedding Plane	Natural		7	Planar	Rough			
118.14				Bedding Plane	Natural		10	Planar	Rough			
trf5g				Joint	Natural		9	Iregular	Rough			
118.88				Joint	Natural		13	Iregular	Rough			
119.11				Bedding Plane	Natural		3	Iregular	Rough			
119.95				Bedding Plane	Natural		6	Iregular	Rough			
121.85				Bedding Plane	Natural		9	Planar	Rough			
122.03				Bedding Plane	Natural		2	Planar	Rough			
122.32	1400			Joint	Natural		90	Iregular	Rough			Major fracture loose pebbles throughout
123.03				Bedding Plane	Natural		3	Iregular	Rough			
123.31				Bedding Plane	Natural		2	Iregular	Rough			
123.46				Bedding Plane	Natural		2	Iregular	Rough			
124.3				Joint	Natural		56	Iregular	Rough			
124.42				Joint	Natural	Y	78					
124.46				Joint	Natural	Y	78					
124.73			900	Joint	Natural		90	Iregular	Rough			Major fracture
125.22				Joint	Natural		75	Iregular	Rough			
125.82				Bedding Plane	Natural		2	Planar	Medium/Rough			
126.26				Mining Induced Joint	Mining Induced		12	Iregular	Rough			
126.36				Joint	Natural		14	Iregular	Polished			
126.65				Bedding Plane	Natural		3	Stepped	Medium/Rough			
126.66				Bedding Plane	Natural		5	Stepped	Medium/Rough		Pyrite	Pyrite infill
126.9				Mining Induced Joint	Mining Induced		10	Iregular	Medium/Rough			Stepped possibly mining induced
127.3				Bedding Plane	Natural		1	Stepped	Medium/Rough			
127.63				Bedding Plane	Natural		4	Iregular	Rough			
127.82				Bedding Plane	Natural		3	Stepped	Rough			
127.9				Bedding Plane	Natural		1	Planar	Rough			
128.38				Bedding Plane	Natural		6	Curvy Planar	Medium/Rough			
129.43	150			Joint	Natural	Y	89					
129.56	160			Joint	Natural	Y						
130.27				Bedding Plane	Natural		11	Planar	Rough			
132.67				Joint	Natural		8	Iregular	Rough			
132.97				Bedding Plane	Natural		8	Planar	Rough			
132.97		132.97	134.34	Joint	Natural		90	Iregular	Rough			Extreamly fractures zone, predominately vrticle
132.97	1370			Joint	Natural		90	Iregular	Rough			
134.46				Bedding Plane	Natural		7	Planar	Rough			
134.53				Bedding Plane	Natural		5	Planar	Rough			
134.55				Bedding Plane	Natural		5	Planar	Rough			
134.6				Bedding Plane	Natural		5	Planar	Rough			
134.65				Bedding Plane	Natural		5	Planar	Rough			
134.84				Joint	Natural		6	Iregular	Rough			
134.96				Joint	Natural		8	Planar	Rough			
134.99				Joint	Natural		8	Planar	Rough			
134.99	500			Joint	Natural		88	Iregular	Rough			
135.02				Joint	Natural		2	Iregular	Rough			
135.4				Joint	Natural		45	Iregular	Rough			
136.05				Bedding Plane	Natural		2	Iregular	Rough			
136.32			137.1	Lost Core								
137.1	1100			Joint	Natural		88	Iregular	Rough			
137.15				Joint	Natural		3	Iregular	Rough			

Defect Log

Drill Hole
TBF040

Defect Depth (Top)	Length (mm)	Broken Zone Top	Broken Zone Base	Defect Type	Defect Cause	Intact	Angle or Min Angle for Broken Zone	Surface Shape	Surface Roughness	Infill		Comments
										Perpendicular Width (mm)	Primary Type	
137.2				Joint	Natural		3	Iregular	Rough			
138.56	150			Joint	Natural		85	Iregular	Rough			
139.37				Bedding Plane	Natural		11	Planar	Rough			
139.41				Bedding Plane	Natural		5	Planar	Rough			
139.55				Bedding Plane	Natural		7	Planar	Rough			
139.71				Bedding Plane	Natural		9	Planar	Rough			
139.73	1180			Joint	Natural		179	Iregular	Rough		Calcite	
140.12				Bedding Plane	Natural		8	Planar	Rough			
140.89				Joint	Natural		5	Iregular	Rough			
141.73				Bedding Plane	Natural		2	Iregular	Rough			
141.96				Bedding Plane	Natural		5	Planar	Rough			
142.04				Mining Induced Joint	Mining Induced		25	Planar	Rough			
142.27				Mining Induced Joint	Mining Induced		30	Planar	Rough			
142.49				Joint	Natural		9	Iregular	Rough			
142.62				Bedding Plane	Natural		5	Planar	Rough			
142.85				Mining Induced Joint	Mining Induced		25	Planar	Rough			
143.13	143.13		143.23	Joint	Natural		4	Iregular	Medium			Shattered zone
165.89				Bedding Plane	Natural		7	Iregular	Rough			
167.7				Bedding Plane	Natural		7	Planar	Medium/Rough			
168.02				Bedding Plane	Natural		2	Planar	Medium/Rough			
168.89				Mining Induced Joint	Mining Induced		25	Iregular	Rough			
168.94				Bedding Plane	Natural		1	Stepped	Rough			
169.01				Bedding Plane	Natural		1	Iregular	Rough			
169.2				Bedding Plane	Natural		3	Curvy Planar	Rough			
169.23				Bedding Plane	Natural		3	Iregular	Rough			
169.31				Soft Zone	Natural		4	Iregular	Medium			Water loss
170.31				Bedding Plane	Natural		5	Iregular	Rough			
170.34				Bedding Plane	Natural		5	Planar	Rough			
170.5				Bedding Plane	Natural		3	Iregular	Rough			Water loss
171.2				Joint	Natural		12	Iregular	Rough			
171.21				Bedding Plane	Natural		1	Planar	Rough			
171.38				Bedding Plane	Natural		7	Stepped	Medium/Rough			
171.49				Bedding Plane	Natural		6	Planar	Medium/Rough			
171.67				Bedding Plane	Natural		8	Planar	Medium/Rough			
174.14				Bedding Plane	Natural		4	Iregular	Rough			
174.26				Bedding Plane	Natural		2	Iregular	Rough			
174.37				Bedding Plane	Natural		7	Planar	Rough			
174.86				Bedding Plane	Natural		1	Planar	Medium/Rough			
175.9				Bedding Plane	Natural		5	Planar	Smooth/Medium			
175.92				Bedding Plane	Natural		1	Planar	Smooth/Medium			
175.96				Bedding Plane	Natural		2	Curvy Planar	Smooth/Medium			
176.09				Joint	Natural		2	Iregular	Rough			
176.17				Bedding Plane	Natural		2	Iregular	Rough			
176.54				Bedding Plane	Natural		8	Iregular	Rough			
176.66				Bedding Plane	Natural		3	Planar	Smooth/Medium			
177.57				Slicken	Natural		15	Iregular	Polished			
177.59				Slicken	Natural		20	Iregular	Polished			
177.63				Slicken	Natural		12	Iregular	Polished			
177.94				Joint	Natural		3	Iregular	Rough			
178.16				Bedding Plane	Natural		6	Planar	Medium/Rough			
178.16	230			Joint	Natural		86	Iregular	Medium/Rough			
178.42				Bedding Plane	Natural		2	Planar	Medium/Rough			
179.2				Joint	Natural		65	Planar	Medium			
179.22				Joint	Natural		65	Planar	Medium			
179.28				Joint	Natural	Y	65					
179.4				Joint	Natural	Y	70					
179.53				Joint	Natural		60	Iregular	Smooth/Medium			
179.6	240			Joint	Natural		80	Iregular	Smooth/Medium			
179.8	260			Joint	Natural	Y	85					
179.79				Bedding Plane	Natural		10	Planar	Smooth/Medium			
182.42				Joint	Natural		45	Planar	Smooth/Medium			
185.68				Joint	Natural		70	Planar	Smooth			Crushed
185.69				Joint	Natural		70	Planar	Smooth			
189.96				Mining Induced Joint	Mining Induced		35	Curvy Planar	Smooth			
190.18				Joint	Natural		2	Iregular	Smooth/Medium			
190.54				Mining Induced Joint	Mining Induced		30	Planar	Smooth/Medium			
190.93				Bedding Plane	Natural		2	Planar	Smooth			
190.95				Mining Induced Joint	Mining Induced		30	Planar	Smooth/Medium			
191.01				Mining Induced Joint	Mining Induced		33	Planar	Smooth/Medium			
191.07				Bedding Plane	Natural		2	Planar	Smooth			
191.15				Mining Induced Joint	Mining Induced		33	Planar	Smooth/Medium			
191.65				Mining Induced Joint	Mining Induced		45	Planar	Smooth			
191.95				Mining Induced Joint	Mining Induced		7	Planar	Smooth			
192.65				Bedding Plane	Natural		1	Iregular	Smooth/Medium			
193.4				Joint	Natural		45	Iregular	Smooth/Medium			
193.87				Mining Induced Joint	Mining Induced		45	Iregular	Medium/Rough			
194.52				Mining Induced Joint	Mining Induced		45	Iregular	Medium/Rough			
194.58				Mining Induced Joint	Mining Induced		55	Iregular	Medium/Rough			
194.61				Mining Induced Joint	Mining Induced		70	Iregular	Medium/Rough			

Defect Log

Drill Hole: TBF040

Defect Depth (Top)	Length (mm)	Broken Zone Top	Broken Zone Base	Defect Type	Defect Cause	Intact	Angle or Min Angle for Broken Zone	Surface Shape	Surface Roughness	Infill		Comments
										Perpendicular Width (mm)	Primary Type	
194.88				Bedding Plane	Natural		4	Planar	Medium			
195.21				Bedding Plane	Natural		7	Planar	Medium			
195.65				Mining Induced Joint	Mining Induced		40	Planar	Medium/Rough			
195.65				Crushed	Natural		1	Crushed	Medium			
196.24				Joint	Natural		8	Iregular	Medium			
196.35				Joint	Natural		14	Planar	Smooth/Medium			
196.5				Joint	Natural		5	Iregular	Smooth/Medium			
196.63				Joint	Natural		2	Iregular	Smooth/Medium			
196.73				Joint	Natural		2	Iregular	Smooth			
197.67				Joint	Natural		8	Iregular	Smooth/Medium			
198.17				Bedding Plane	Natural		5	Planar	Smooth/Medium			
198.29				Bedding Plane	Natural		5	Planar	Smooth/Medium			
199.94				Crushed	Natural		5	Crushed	Medium			
200.09				Joint	Natural		8	Iregular	Medium/Rough			
200.56				Bedding Plane	Natural		15	Planar	Smooth/Medium			
201.1				Bedding Plane	Natural		3	Iregular	Medium			
201.17				Joint	Natural		5	Iregular	Medium/Rough			Fresh
201.19				Joint	Natural		5	Iregular	Medium/Rough			Fresh
201.21				Joint	Natural		5	Iregular	Medium/Rough			Fresh
201.33				Joint	Natural		5	Iregular	Medium/Rough			Fresh
201.36				Mining Induced Joint	Mining Induced		20	Curvy Planar	Medium/Rough			
201.53				Mining Induced Joint	Mining Induced		28	Planar	Rough			
202.07				Joint	Natural		6	Iregular	Rough			
202.11				Bedding Plane	Natural		3	Iregular	Smooth			
202.13				Joint	Natural		45	Iregular	Smooth			
202.2				Bedding Plane	Natural		4	Iregular	Medium			
204.5				Bedding Plane	Natural		2	Planar	Rough			
204.53				Joint	Natural		40	Planar	Rough			
204.84				Mining Induced Joint	Mining Induced		37	Iregular	Rough			
206.21				Bedding Plane	Natural		4	Planar	Medium			
206.34				Bedding Plane	Natural		6	Iregular	Smooth			
207.8				Bedding Plane	Natural		5	Iregular	Medium/Rough			
208.46				Bedding Plane	Natural		6	Stepped	Medium			
208.74				Bedding Plane	Natural		3	Planar	Smooth			
209.92				Bedding Plane	Natural		0	Planar	Smooth			
210.02				Joint	Natural		5	Iregular	Rough			
210.09				Joint	Natural		3	Iregular	Rough			
210.18				Joint	Natural		7	Iregular	Rough			
210.52				Mining Induced Joint	Mining Induced		17	Iregular	Medium/Rough			
210.57				Bedding Plane	Natural		2	Curvy Planar	Medium			
210.58				Bedding Plane	Natural		2	Curvy Planar	Medium			
210.68				Bedding Plane	Natural		2	Curvy Planar	Medium			
211.12				Bedding Plane	Natural		2	Curvy Planar	Medium			
211.21				Bedding Plane	Natural		2	Curvy Planar	Smooth			
211.28				Bedding Plane	Natural		2	Curvy Planar	Smooth/Medium			
211.92				Bedding Plane	Natural		2	Iregular	Medium/Rough			
212.14				Bedding Plane	Natural		3	Planar	Smooth/Medium			
213.42				Bedding Plane	Natural		13	Planar	Medium/Rough			
213.49				Joint	Natural		5	Iregular	Medium/Rough			
214.03				Bedding Plane	Natural		1	Planar	Medium			
215.67				Bedding Plane	Natural		2	Iregular	Smooth/Medium			
216.52				Bedding Plane	Natural		2	Iregular	Smooth/Medium			
216.63				Slicken	Natural		15	Iregular	Polished			
216.7				Bedding Plane	Natural		15	Iregular	Smooth/Medium			
217.41				Bedding Plane	Natural		2	Iregular	Smooth			
218.04				Bedding Plane	Natural		3	Iregular	Smooth			
218.64				Bedding Plane	Natural		3	Curvy Planar	Smooth/Medium			
219.76				Bedding Plane	Natural		10	Planar	Medium/Rough			Fresh
221.06				Bedding Plane	Natural		2	Iregular	Smooth			
221.19				Bedding Plane	Natural		3	Iregular	Medium/Rough			
221.7				Bedding Plane	Natural		5	Planar	Smooth/Medium			
221.95				Bedding Plane	Natural		3	Planar	Medium/Rough			
223.34				Bedding Plane	Natural		5	Planar	Medium/Rough			
223.67				Bedding Plane	Natural		4	Curvy Planar	Medium/Rough			
224.75				Bedding Plane	Natural		4	Iregular	Rough			
225.12				Bedding Plane	Natural		6	Planar	Medium/Rough			
225.31				Bedding Plane	Natural		2	Iregular	Medium/Rough			
225.4				Bedding Plane	Natural		12	Planar	Smooth/Medium			
225.6				Bedding Plane	Natural		3	Curvy Planar	Smooth/Medium			
225.79				Bedding Plane	Natural		2	Planar	Smooth/Medium			
226.08				Bedding Plane	Natural		4	Curvy Planar	Medium			
226.17				Bedding Plane	Natural		2	Planar	Medium			
226.52				Bedding Plane	Natural		2	Stepped	Smooth/Medium			
226.81				Bedding Plane	Natural		3	Planar	Medium/Rough			
226.96				Mining Induced Joint	Mining Induced		17	Iregular	Medium/Rough			
227.14				Bedding Plane	Natural		2	Iregular	Medium/Rough			
227.56				Bedding Plane	Natural		3	Iregular	Medium			
228.01				Bedding Plane	Natural		0	Planar	Smooth/Medium			
228.38				Mining Induced Joint	Mining Induced		5	Iregular	Medium/Rough			Unsure if mining induced

Defect Log

Drill Hole
TBF040

Defect Depth (Top)	Length (mm)	Broken Zone Top	Broken Zone Base	Defect Type	Defect Cause	Intact	Angle or Min Angle for Broken Zone	Surface Shape	Surface Roughness	Infill		Comments
										Perpendicular Width (mm)	Primary Type	
228.44				Bedding Plane	Natural		2	Planar	Smooth/Medium			
229.38				Bedding Plane	Natural		1	Planar	Medium/Rough			
229.54				Bedding Plane	Natural		25	Planar	Medium/Rough			
229.75				Bedding Plane	Natural		7	Planar	Medium/Rough			
230.04				Bedding Plane	Natural		4	Planar	Medium/Rough			
230.77				Bedding Plane	Natural		3	Planar	Smooth/Medium			
231.66				Bedding Plane	Natural		4	Curvy Planar	Smooth/Medium			
232.06				Bedding Plane	Natural		4	Iregular	Smooth/Medium			
232.22				Bedding Plane	Natural		7	Iregular	Medium			
232.64				Bedding Plane	Natural		7	Iregular	Medium			
233				Joint	Natural		2	Iregular	Medium/Rough			
233.12				Bedding Plane	Natural		3	Iregular	Medium/Rough			
234.33				Bedding Plane	Natural		2	Planar	Medium/Rough			
235.48				Bedding Plane	Natural		2	Planar	Smooth/Medium			
236.4				Bedding Plane	Natural		5	Iregular	Medium			
237.44				Bedding Plane	Natural		4	Planar	Medium			
238.16				Joint	Natural		3	Iregular	Medium/Rough			Possibly minning induced
238.27				Joint	Natural		3	Iregular	Medium/Rough			Possibly minning induced
238.55				Bedding Plane	Natural		3	Iregular	Medium/Rough			
238.87				Bedding Plane	Natural		2	Planar	Medium			
238.9				Bedding Plane	Natural		2	Planar	Medium			
240.13				Bedding Plane	Natural		8	Planar	Medium/Rough			
240.45				Bedding Plane	Natural		1	Planar	Medium/Rough			
240.46				Bedding Plane	Natural		1	Planar	Medium/Rough			
240.51				Bedding Plane	Natural		4	Stepped	Medium/Rough			
240.76				Bedding Plane	Natural		4	Iregular	Medium/Rough			
240.78				Bedding Plane	Natural		2	Iregular	Medium/Rough			
241.24				Bedding Plane	Natural		7	Planar	Rough			
241.35				Joint	Natural		4	Planar	Rough			
241.36				Joint	Natural		4	Planar	Rough			
241.4				Joint	Natural		2	Iregular	Rough			
241.43				Joint	Natural		2	Iregular	Rough			
241.51				Joint	Natural		5	Iregular	Rough			
241.62				Joint	Natural		5	Planar	Rough			
241.64				Joint	Natural		5	Planar	Rough			
241.72				Bedding Plane	Natural		5	Planar	Medium			
241.8				Bedding Plane	Natural		2	Iregular	Medium			
242.34				Joint	Natural		13	Planar	Rough			
242.49				Bedding Plane	Natural		2	Planar	Smooth			
242.52				Bedding Plane	Natural		2	Planar	Smooth			
242.54				Bedding Plane	Natural		1	Stepped	Smooth			
243				Bedding Plane	Natural		2	Planar	Smooth			

APPENDIX 4 – DRILLING LOG

Project				Drilling Sheet					Drill Hole	
TBF040									TBF040	
				Drill Run						
Geologists Depth From	Geologists Depth To	Driller Depth From	Driller Depth To	Run No.	Cored Length	Recovered length	Core Loss	Date	Comments	Litres per day
		TBC040A								
2.67	5.55	2.67	5.55	1	2.88	2.88	0	31/10/2013		
5.55	11.55	5.55	11.55	2	6	5.91	0.09	31/10/2013		3000
11.55	17.55	11.55	17.55	3	6	6	0	31/10/2013		
17.55	23.52	17.55	23.55	4	6	5.97	0	31/10/2013		8000
23.52	29.52	23.55	29.55	5	6	5.7	0.3	4/11/2013	Water Loss	
29.52	32.53	29.55	32.55	6	3	3.01	0	4/11/2013		10000
32.53	35.26	32.55	35.3	7	2.75	2.73	0	5/11/2013		
35.26	41.24	35.3	41.3	8	6	5.98	0	5/11/2013	Water Loss	15000
41.24	47.24	41.3	47.3	9	6	6	0	6/11/2013		
47.24	53.3	47.3	53.3	10	6	5.9	0.16	6/11/2013	Water Loss	15000
		TBC040B								
44.35	47.4	44.35	47.4	1	3.05	3.05	0	13/11/13		
47.4	53.4	47.4	53.4	2	6	5.75	0.25	13/11/13	Water Loss	15000
53.4	59.37	53.4	59.4	3	6	5.97	0	14/11/13	Water Loss	15000
59.37	65.4	59.4	65.4	4	6	5.88	0.15	15/11/13	Water Loss	
65.4	71.4	65.4	71.4	5	6	6	0	15/11/13	Water Loss	18000
71.4	77.4	71.4	77.4	6	6	5.7	0.3	18/11/13		
77.4	83.38	77.4	83.4	7	6	5.98	0	18/11/13	Water Loss	13000
83.38	89.44	83.4	89.4	8	6	6.06	0	19/11/13		
89.44	95.41	89.4	95.4	9	6	5.97	0	19/11/13		
95.41	101.41	95.4	101.4	10	6	5.77	0.23	19/11/13	Water Loss	17000
101.41	107.4	101.4	107.4	11	6	5.99	0	20/11/2013		
107.4	113.36	107.4	113.4	12	6	5.96	0	20/11/13		
113.36	119.42	113.4	119.4	13	6	6.08	0	20/11/13	Water Loss	22000
119.42	125.4	119.4	125.4	14	6	5.98	0	21/11/13	Water Loss	15000
125.4	129.07	125.4	129.07	15	3.67	3.67	0	25/11/13		13000
129.07	131.4	129.07	131.4	16	2.33	2.33	0	26/11/13		
131.4	137.1	131.4	137.1	17	5.7	5.7	0	26/11/13		20000
137.1	137.4	137.1	137.4	18	0.3	0.3	0	28/11/13		
137.4	143.4	137.4	143.4	19	6	6	0	28/11/13		17000
		TBC040C								
165	167.4	165	167.4	1	2.4	2.4	0	18/12/2013	Water Loss	
167.4	173.4	167.4	173.4	2	6	6	0	18/12/2013		20000
173.4	179.4	173.4	179.4	3	6	6	0	19/12/2013		
179.4	185.4	179.4	185.4	4	6	6	0	19/12/2013		
185.4	191.47	185.4	191.4	5	6	6.07	0	19/12/2013		25000
191.47	197.47	191.4	197.4	6	6	6	0	20/12/2013		6000
197.47	203.43	197.4	203.4	7	6	5.96	0	7/01/2014		
203.43	209.43	203.4	209.4	8	6	6	0	7/01/2014		17000
209.43	215.45	209.4	215.4	9	6	6.02	0	8/01/2014		
215.45	221.44	215.4	221.40	10	6	5.99	0	8/01/2014		17000
221.44	227.49	221.4	227.4	11	6	6.05	0	9/01/2014		
227.49	233.54	227.4	233.4	12	6	6.05	0	9/01/2014		15000
233.54	239.54	233.4	239.4	13	6	6	0	10/01/2014		
239.54	243.98	239.4	243.9	14	4.5	4.44	0	10/01/2014		16000

Appendix 4: Drilling log.

APPENDIX 5 – PACKER TESTING RESULTS (PDF Only)

Job No: TAH4125

Location: Tahmoor Site No: TBF040 Borehole: TBF040 Depth Range: 5.1 -11.6 m

PACKER TEST RESULTS: K = 2.6E-06 m/s

PROJECT: TAH4125 **Site No:** TBF040 **BORE NAME:** TBF040 **HOLE DIP:** 90 **DIP Direction:** **DATE:** 01-Nov-13

Depth To Bottm Packer Test interval:	11.55	m	HEIGHT OF PRESSURE GAUGE:	1	m (above ground level)
Depth To Top Packer Test interval:	5.05	m	STATIC GROUNDWATER LEVEL:	40.7	m (below ground level)
LENGTH OF STAGE TEST:	6.50	m	SURFACE R.L.		m
BORE DIAMETER:	96	mm			

Recorded flow readings at indicated applied pressure heads.

Stage 1

Gauge Pressure	20	(kPa)
Gauge Pressure	2.04	(m)
Static Pressure	42.2	(m)
Head without loss correction	44.20	(m)
Head loss	1.34	(m)
High flow pressure calibration	0.00	(m)
Total Head	42.86	(m)

Minutes of test	Flowmet read (L)	Flow (L/min)
0	4450	
1	4490	40
2	4528	38
3	4565	37
4	4605	40
5	4644	39
6	4682	38
7	4721	39
8	4761	40
9	4800	39
10	4840	40

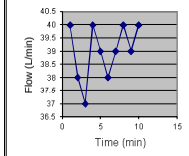

Arithmatic average = 39 (L/min)
Adopted average = 39 (L/min)

Stage 2

Gauge Pressure	40	(kPa)
Gauge Pressure	4.08	(m)
Static Pressure	42.2	(m)
Head without loss correction	46.24	(m)
Head loss	2.60	(m)
High flow pressure calibration	0.00	(m)
Total Head	43.65	(m)

Minutes of test	Flowmet read (L)	Flow (L/min)
0	4986	
1	5040	54
2	5094	54
3	5148	54
4	5202	54
5	5256	54
6	5311	55
7	5365	54
8	5419	54
9	5473	54
10	5528	55

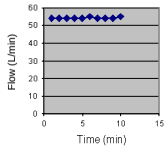

Arithmatic average = 54.2 (L/min)
Adopted average = 54.2 (L/min)

Stage 3

Gauge Pressure	60	(kPa)
Gauge Pressure	6.12	(m)
Static Pressure	42.2	(m)
Head without loss correction	48.28	(m)
Head loss	3.35	(m)
High flow pressure calibratior	0.00	(m)
Total Head	44.93	(m)

Minutes of test	Flowmet read (L)	Flow (L/min)
0	5610	
1	5672	62
2	5734	62
3	5795	61
4	5857	62
5	5919	62
6	5980	61
7	6042	62
8	6103	61
9	6166	63
10	6226	60

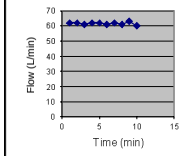

Arithmatic average = 61.6 (L/min)
Adopted average = 61.6 (L/min)

Stage 4

Gauge Pressure	40	(kPa)
Gauge Pressure	4.08	(m)
Static Pressure	42.2	(m)
Head without loss correction	46.24	(m)
Head loss	2.46	(m)
High flow pressure calibration	0.00	(m)
Total Head	43.78	(m)

Minutes of test	Flowmet read (L)	Flow (L/min)
0	6280	
1	6333	53
2	6386	53
3	6439	53
4	6493	54
5	6545	52
6	6597	52
7	6650	53
8	6703	53
9	6755	52
10	6808	53

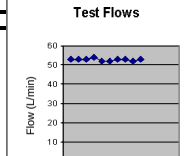

Arithmatic average = 52.8 (L/min)
Adopted average = 52.8 (L/min)

Stage 5

Gauge Pressure	20	(kPa)
Gauge Pressure	2.04	(m)
Static Pressure	42.2	(m)
Head without loss correction	44.20	(m)
Head loss	1.22	(m)
High flow pressure calibration	0.00	(m)
Total Head	42.98	(m)

Minutes of test	Flowmet read (L)	Flow (L/min)
0	6870	
1	6907	37
2	6944	37
3	6980	36
4	7017	37
5	7053	36
6	7090	37
7	7127	37
8	7163	36
9	7200	37
10	7237	37

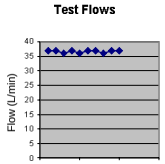

Arithmatic average = 36.7 (L/min)
Adopted average = 37.2 (L/min)

Stage 6

Gauge Pressure	0	(kPa)
Gauge Pressure	0.00	(m)
Static Pressure	42.2	(m)
Head without loss correction	42.17	(m)
Head loss	0.00	(m)
High flow pressure calibratior	0.00	(m)
Total Head	42.17	(m)

Minutes of test	Flowmet read (L)	Flow (L/min)
0	0	
1	0	0
2	0	0
3	0	0
4	0	0
5	0	0
6	0	0
7	0	0
8	0	0
9	0	0
10	0	0

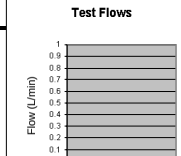

Arithmatic average = 0 (L/min)
Adopted average = 0 (L/min)

Comments:

Calculations used:

$$k = \frac{5.833}{\pi L \sin\alpha}\left(\frac{Q}{H_T}\right)\cdot 10^{-5} \quad \text{m/s} \qquad \text{(CANMET)}$$

$$k = \frac{8.333}{\pi L \sin\alpha}\left(\frac{Q}{H_T}\right)\cdot \ln\left(\frac{L}{r}\right)\cdot 10^{-4} \quad \text{m/s} \qquad \text{(HOEK \& BRAY)}$$

$$lugeon = \frac{Q}{L\sin\alpha}\cdot\frac{100}{H_T} \quad \text{l/m/min} \qquad \text{(HOULSBY)}$$

Stage	Total Head (m)	Flow (l/min)	Calculated Lugeon values: Test Pressure	Q (L/m/min)	Lugeons (L/m/min)	Chosen Lugeon (L/m/min)
1	42.86	39.00	420.46	6.00	14.00	
2	43.65	54.20	428.18	8.34	19.10	
3	44.93	61.60	440.75	9.48	21.09	17.213
4	43.78	52.80	429.48	8.12	18.55	
5	42.98	37.2	421.65	5.72	13.32	

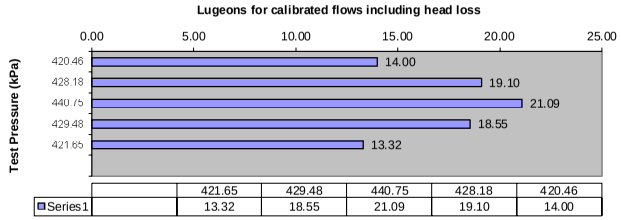

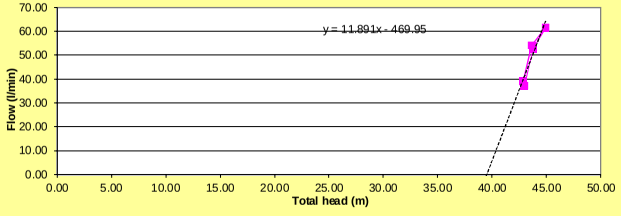

Conductivity Calculations:

MEAN Q/H$_T$	CANMET	HOEK & BRAY	MEAN LUGEONS 17.21	
1.125	3.2E-06	2.3E-06	2.2E-06	m/s
Mean Conductivity		K =	2.6E-06	m/s

Job No: TAH4125

Location: Tahmoor Site No: TBF040 Borehole: TBF040 Depth Range: 11.1 -17.6 m

PACKER TEST RESULTS: K = 3.7E-08 m/s

PROJECT: TAH4125 **Site No:** TBF040 **BORE NAME:** TBF040 **HOLE DIP:** 90 **DIP Direction:** **DATE:** 01-Nov-13

Depth To Bottm Packer Test interval:	17.55	m	HEIGHT OF PRESSURE GAUGE:	1	m (above ground level)
Depth To Top Packer Test interval:	11.05	m	STATIC GROUNDWATER LEVEL:	40.7	m (below ground level)
LENGTH OF STAGE TEST:	6.50	m	SURFACE R.L.		m
BORE DIAMETER:	96	mm			

Recorded flow readings at indicated applied pressure heads.

Stage 1

Gauge Pressure	80	(kPa)
Gauge Pressure	8.15	(m)
Static Pressure	42.5	(m)
Head without loss correction	50.62	(m)
Head loss	0.00	(m)
High flow pressure calibration	0.00	(m)
Total Head	50.62	(m)

Minutes of test	Flowmet read (L)	Flow (L/min)
0	120	
1	121.1	1.1
2	122.2	1.1
3	123.2	1
4	124.1	0.9
5	125	0.9
6	125.9	0.9
7	126.8	0.9
8	127.7	0.9
9	128.5	0.8
10	129.3	0.8

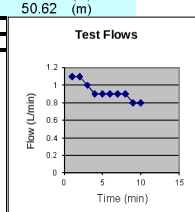

Arithmatic average = 0.93 (L/min)
Adopted average = 0.93 (L/min)

Stage 2

Gauge Pressure	160	(kPa)
Gauge Pressure	16.31	(m)
Static Pressure	42.5	(m)
Head without loss correction	58.77	(m)
Head loss	0.00	(m)
High flow pressure calibration	0.00	(m)
Total Head	58.77	(m)

Minutes of test	Flowmet read (L)	Flow (L/min)
0	131.4	
1	132.6	1.2
2	133.7	1.1
3	134.8	1.1
4	135.8	1
5	136.8	1
6	137.8	1
7	138.8	1
8	139.8	1
9	140.8	1
10	141.8	1

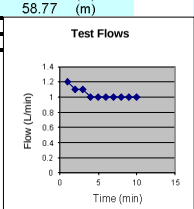

Arithmatic average = 1.04 (L/min)
Adopted average = 1.04 (L/min)

Stage 3

Gauge Pressure	240	(kPa)
Gauge Pressure	24.46	(m)
Static Pressure	42.5	(m)
Head without loss correction	66.93	(m)
Head loss	0.00	(m)
High flow pressure calibration	0.00	(m)
Total Head	66.93	(m)

Minutes of test	Flowmet read (L)	Flow (L/min)
0	143	
1	144.4	1.4
2	145.7	1.3
3	147	1.3
4	148.2	1.2
5	149.4	1.2
6	150.7	1.3
7	151.9	1.2
8	153.2	1.3
9	154.3	1.1
10	155.4	1.1

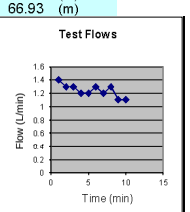

Arithmatic average = 1.24 (L/min)
Adopted average = 1.24 (L/min)

Stage 4

Gauge Pressure	160	(kPa)
Gauge Pressure	16.31	(m)
Static Pressure	42.5	(m)
Head without loss correction	58.77	(m)
Head loss	0.00	(m)
High flow pressure calibration	0.00	(m)
Total Head	58.77	(m)

Minutes of test	Flowmet read (L)	Flow (L/min)
0	155.9	
1	156.6	0.7
2	157.4	0.8
3	158.3	0.9
4	159.2	0.9
5	160.1	0.9
6	161	0.9
7	161.9	0.9
8	162.9	1
9	163.9	1
10	164.8	0.9

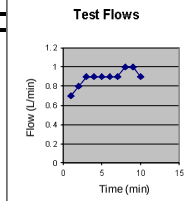

Arithmatic average = 0.89 (L/min)
Adopted average = 0.89 (L/min)

Stage 5

Gauge Pressure	80	(kPa)
Gauge Pressure	8.15	(m)
Static Pressure	42.5	(m)
Head without loss correction	50.62	(m)
Head loss	0.00	(m)
High flow pressure calibration	0.00	(m)
Total Head	50.62	(m)

Minutes of test	Flowmet read (L)	Flow (L/min)
0	164.7	
1	165.1	0.4
2	165.5	0.4
3	166	0.5
4	166.5	0.5
5	167	0.5
6	167.5	0.5
7	168	0.5
8	168.5	0.5
9	169	0.5
10	169.5	0.5

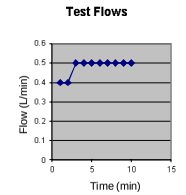

Arithmatic average = 0.48 (L/min)
Adopted average = 0.48 (L/min)

Stage 6

Gauge Pressure	0	(kPa)
Gauge Pressure	0.00	(m)
Static Pressure	42.5	(m)
Head without loss correction	42.47	(m)
Head loss	0.00	(m)
High flow pressure calibration	0.00	(m)
Total Head	42.47	(m)

Minutes of test	Flowmet read (L)	Flow (L/min)
0	0	
1	0	0
2	0	0
3	0	0
4	0	0
5	0	0
6	0	0
7	0	0
8	0	0
9	0	0
10	0	0

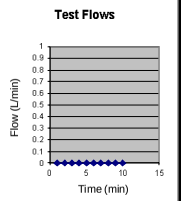

Arithmatic average = 0 (L/min)
Adopted average = 0 (L/min)

Comments:

Calculations used:

$$k = \frac{5.833}{\pi L \sin\alpha}\left(\frac{Q}{H_T}\right)\cdot 10^{-5} \quad \text{m/s} \qquad \text{(CANMET)}$$

$$k = \frac{8.333}{\pi L \sin\alpha}\left(\frac{Q}{H_T}\right)\cdot \ln\left(\frac{L}{r}\right)\cdot 10^{-4} \quad \text{m/s} \qquad \text{(HOEK \& BRAY)}$$

$$lugeon = \frac{Q}{L\sin\alpha}\cdot\frac{100}{H_T} \quad \text{l/m/min} \qquad \text{(HOULSBY)}$$

Stage	Total Head (m)	Flow (l/min)	Calculated Lugeon values: Test Pressure	Q (L/m/min)	Lugeons (L/m/min)	Chosen Lugeon (L/m/min)
1	50.62	0.93	496.57	0.14	0.28	
2	58.77	1.04	576.57	0.16	0.27	
3	66.93	1.24	656.57	0.19	0.29	0.244
4	58.77	0.89	576.57	0.14	0.23	
5	50.62	0.48	496.58	0.07	0.15	

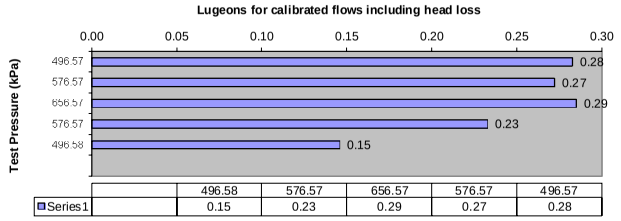

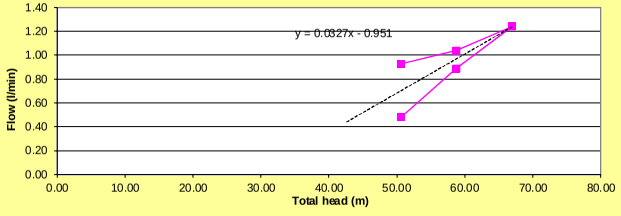

Conductivity Calculations:

MEAN Q/H$_T$	CANMET	HOEK & BRAY	MEAN LUGEONS 0.24	
0.016	4.6E-08	3.2E-08	3.2E-08	m/s
Mean Conductivity		K =	3.7E-08	m/s

Job No: TAH4125

Location: Tahmoor Site No: TBF040 Borehole: TBF040 Depth Range: 17.1 -23.6 m

PACKER TEST RESULTS: K = 1.3E-06 m/s

PROJECT: TAH4125 **Site No:** TBF040 **BORE NAME:** TBF040 **HOLE DIP:** 90 **DIP Direction:** **DATE:** 01-Nov-13

Depth To Bottm Packer Test interval:	23.55	m	HEIGHT OF PRESSURE GAUGE:	1	m (above ground level)
Depth To Top Packer Test interval:	17.05	m	STATIC GROUNDWATER LEVEL:	40.7	m (below ground level)
LENGTH OF STAGE TEST:	6.50	m	SURFACE R.L.		m
BORE DIAMETER:	96	mm			

Recorded flow readings at indicated applied pressure heads.

Stage 1

Gauge Pressure	80	(kPa)
Gauge Pressure	8.15	(m)
Static Pressure	42.8	(m)
Head without loss correction	50.92	(m)
Head loss	0.53	(m)
High flow pressure calibration	0.00	(m)
Total Head	50.39	(m)

Minutes of test	Flowmet read (L)	Flow (L/min)
0	6370	
1	6396	26
2	6420	24
3	6445	25
4	6470	25
5	6495	25
6	6519	24
7	6543	24
8	6566	23
9	6592	26
10	6616	24

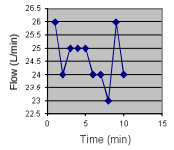

Arithmatic average = 24.6 (L/min)
Adopted average = 24.6 (L/min)

Stage 2

Gauge Pressure	160	(kPa)
Gauge Pressure	16.31	(m)
Static Pressure	42.8	(m)
Head without loss correction	59.07	(m)
Head loss	0.76	(m)
High flow pressure calibration	0.00	(m)
Total Head	58.32	(m)

Minutes of test	Flowmet read (L)	Flow (L/min)
0	6645	
1	6674	29
2	6704	30
3	6732	28
4	6762	30
5	6791	29
6	6820	29
7	6850	30
8	6879	29
9	6908	29
10	6938	30

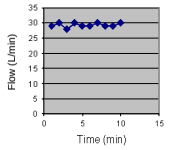

Arithmatic average = 29.3 (L/min)
Adopted average = 29.3 (L/min)

Stage 3

Gauge Pressure	240	(kPa)
Gauge Pressure	24.46	(m)
Static Pressure	42.8	(m)
Head without loss correction	67.23	(m)
Head loss	1.10	(m)
High flow pressure calibratior	0.00	(m)
Total Head	66.13	(m)

Minutes of test	Flowmet read (L)	Flow (L/min)
0	6974	
1	7008	34
2	7044	36
3	7080	36
4	7114	34
5	7149	35
6	7185	36
7	7220	35
8	7255	35
9	7291	36
10	7327	36

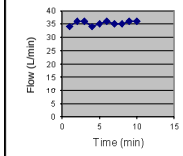

Arithmatic average = 35.3 (L/min)
Adopted average = 35.3 (L/min)

Stage 4

Gauge Pressure	160	(kPa)
Gauge Pressure	16.31	(m)
Static Pressure	42.8	(m)
Head without loss correction	59.07	(m)
Head loss	1.43	(m)
High flow pressure calibration	0.00	(m)
Total Head	57.64	(m)

Minutes of test	Flowmet read (L)	Flow (L/min)
0	7368	
1	7409	41
2	7449	40
3	7489	40
4	7529	40
5	7570	41
6	7610	40
7	7650	40
8	7691	41
9	7731	40
10	7771	40

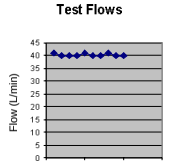

Arithmatic average = 40.3 (L/min)
Adopted average = 40.3 (L/min)

Stage 5

Gauge Pressure	80	(kPa)
Gauge Pressure	8.15	(m)
Static Pressure	42.8	(m)
Head without loss correction	50.92	(m)
Head loss	1.09	(m)
High flow pressure calibration	0.00	(m)
Total Head	49.83	(m)

Minutes of test	Flowmet read (L)	Flow (L/min)
0	7808	
1	7843	35
2	7878	35
3	7913	35
4	7949	36
5	7983	34
6	8019	36
7	8054	35
8	8090	36
9	8124	34
10	8160	36

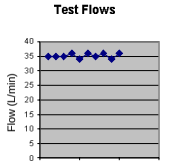

Arithmatic average = 35.2 (L/min)
Adopted average = 35.2 (L/min)

Stage 6

Gauge Pressure	0	(kPa)
Gauge Pressure	0.00	(m)
Static Pressure	42.8	(m)
Head without loss correction	42.77	(m)
Head loss	0.00	(m)
High flow pressure calibratior	0.00	(m)
Total Head	42.77	(m)

Minutes of test	Flowmet read (L)	Flow (L/min)
0	0	
1	0	0
2	0	0
3	0	0
4	0	0
5	0	0
6	0	0
7	0	0
8	0	0
9	0	0
10	0	0

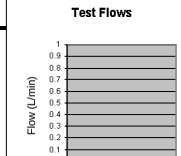

Arithmatic average = 0 (L/min)
Adopted average = 0 (L/min)

Comments:

Calculations used:

$$k = \frac{5.833}{\pi L \sin\alpha}\left(\frac{Q}{H_T}\right)\cdot 10^{-5} \quad \text{m/s} \qquad \text{(CANMET)}$$

$$k = \frac{8.333}{\pi L \sin\alpha}\left(\frac{Q}{H_T}\right)\cdot \ln\left(\frac{L}{r}\right)\cdot 10^{-4} \quad \text{m/s} \qquad \text{(HOEK \& BRAY)}$$

$$lugeon = \frac{Q}{L \sin\alpha}\cdot\frac{100}{H_T} \quad \text{l/m/min} \qquad \text{(HOULSBY)}$$

Stage	Total Head (m)	Flow (l/min)	Calculated Lugeon values: Test Pressure	Q (L/m/min)	Lugeons (L/m/min)	Chosen Lugeon (L/m/min)
1	50.39	24.60	494.28	3.78	7.51	
2	58.32	29.30	572.08	4.51	7.73	
3	66.13	35.30	648.73	5.43	8.21	9.016
4	57.64	40.30	565.45	6.20	10.76	
5	49.83	35.2	488.79	5.42	10.87	

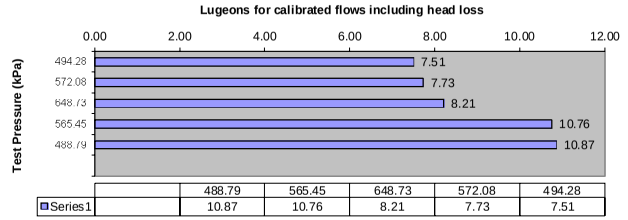

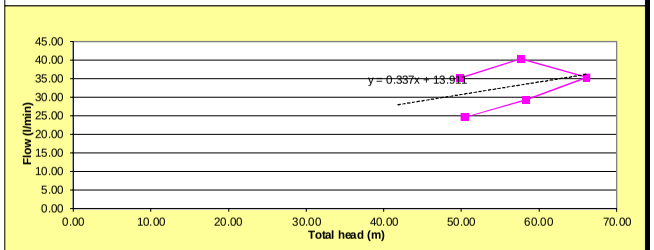

Conductivity Calculations:

MEAN Q/H$_T$	CANMET	HOEK & BRAY	MEAN LUGEONS	
0.581	1.7E-06	1.2E-06	1.2E-06	m/s
Mean Conductivity	K =	1.3E-06	m/s	

Job No: TAH4125

Location: Tahmoor Site No: TBF040 Borehole: TBF040 Depth Range: 23.1 -32.6 m

PACKER TEST RESULTS: K = 9.6E-08 m/s

PROJECT: TAH4125 **Site No:** TBF040 **BORE NAME:** TBF040 **HOLE DIP:** 90 **DIP Direction:** **DATE:** 04-Nov-13

Depth To Bottm Packer Test interval:	32.55	m	HEIGHT OF PRESSURE GAUGE:	1	m (above ground level)
Depth To Top Packer Test interval:	23.05	m	STATIC GROUNDWATER LEVEL:	40.7	m (below ground level)
LENGTH OF STAGE TEST:	9.50	m	SURFACE R.L.		m
BORE DIAMETER:	96	mm			

Recorded flow readings at indicated applied pressure heads.

Stage 1

Gauge Pressure	80	(kPa)
Gauge Pressure	8.15	(m)
Static Pressure	43.1	(m)
Head without loss correction	51.29	(m)
Head loss	0.01	(m)
High flow pressure calibration	0.00	(m)
Total Head	51.28	(m)

Minutes of test	Flowmet read (L)	Flow (L/min)
0	326.7	
1	331	4.3
2	335.3	4.3
3	339.5	4.2
4	343.5	4
5	347.7	4.2
6	352.2	4.5
7	355.7	3.5
8	359.5	3.8
9	363.4	3.9
10	367.5	4.1

Test Flows

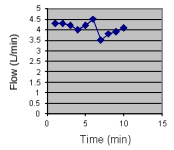

Arithmatic average = 4.08 (L/min)
Adopted average = 4.08 (L/min)

Stage 2

Gauge Pressure	160	(kPa)
Gauge Pressure	16.31	(m)
Static Pressure	43.1	(m)
Head without loss correction	59.45	(m)
Head loss	0.01	(m)
High flow pressure calibration	0.00	(m)
Total Head	59.44	(m)

Minutes of test	Flowmet read (L)	Flow (L/min)
0	380	
1	385	5
2	389.3	4.3
3	393.4	4.1
4	397.3	3.9
5	401.1	3.8
6	404.8	3.7
7	408.5	3.7
8	412.1	3.6
9	415.8	3.7
10	419.4	3.6

Test Flows

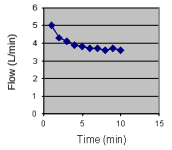

Arithmatic average = 3.94 (L/min)
Adopted average = 3.94 (L/min)

Stage 3

Gauge Pressure	240	(kPa)
Gauge Pressure	24.46	(m)
Static Pressure	43.1	(m)
Head without loss correction	67.60	(m)
Head loss	0.02	(m)
High flow pressure calibration	0.00	(m)
Total Head	67.59	(m)

Minutes of test	Flowmet read (L)	Flow (L/min)
0	423.5	
1	428	4.5
2	432.1	4.1
3	436.3	4.2
4	440	3.7
5	443.9	3.9
6	448	4.1
7	452.4	4.4
8	456.7	4.3
9	461	4.3
10	465.3	4.3

Test Flows

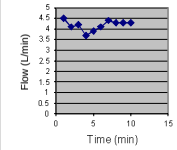

Arithmatic average = 4.18 (L/min)
Adopted average = 4.18 (L/min)

Stage 4

Gauge Pressure	160	(kPa)
Gauge Pressure	16.31	(m)
Static Pressure	43.1	(m)
Head without loss correction	59.45	(m)
Head loss	0.01	(m)
High flow pressure calibration	0.00	(m)
Total Head	59.44	(m)

Minutes of test	Flowmet read (L)	Flow (L/min)
0	464.4	
1	467.6	3.2
2	470.6	3
3	473.6	3
4	476.7	3.1
5	479.7	3
6	482.7	3
7	485.7	3
8	488.6	2.9
9	491.5	2.9
10	494.4	2.9

Test Flows

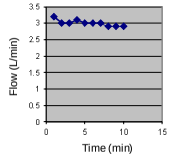

Arithmatic average = 3 (L/min)
Adopted average = 3 (L/min)

Stage 5

Gauge Pressure	80	(kPa)
Gauge Pressure	8.15	(m)
Static Pressure	43.1	(m)
Head without loss correction	51.29	(m)
Head loss	0.00	(m)
High flow pressure calibration	0.00	(m)
Total Head	51.29	(m)

Minutes of test	Flowmet read (L)	Flow (L/min)
0	496.2	
1	498.4	2.2
2	500.8	2.4
3	503.2	2.4
4	505.5	2.3
5	507.6	2.1
6	509.6	2
7	511.6	2
8	513.7	2.1
9	515.7	2
10	517.8	2.1

Test Flows

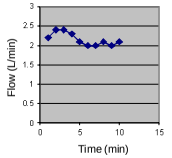

Arithmatic average = 2.16 (L/min)
Adopted average = 2.16 (L/min)

Stage 6

Gauge Pressure	0	(kPa)
Gauge Pressure	0.00	(m)
Static Pressure	43.1	(m)
Head without loss correction	43.14	(m)
Head loss	0.00	(m)
High flow pressure calibration	0.00	(m)
Total Head	43.14	(m)

Minutes of test	Flowmet read (L)	Flow (L/min)
0	0	
1	0	0
2	0	0
3	0	0
4	0	0
5	0	0
6	0	0
7	0	0
8	0	0
9	0	0
10	0	0

Test Flows

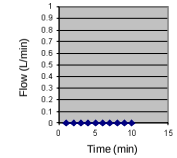

Arithmatic average = 0 (L/min)
Adopted average = 0 (L/min)

Comments:

Calculations used:

$$k = \frac{5.833}{\pi L \sin\alpha}\left(\frac{Q}{H_T}\right)\cdot 10^{-5} \quad \text{m/s} \qquad \text{(CANMET)}$$

$$k = \frac{8.333}{\pi L \sin\alpha}\left(\frac{Q}{H_T}\right)\cdot \ln\left(\frac{L}{r}\right)\cdot 10^{-4} \quad \text{m/s} \qquad \text{(HOEK \& BRAY)}$$

$$lugeon = \frac{Q}{L\sin\alpha}\cdot\frac{100}{H_T} \quad \text{l/m/min} \qquad \text{(HOULSBY)}$$

Stage	Total Head (m)	Flow (l/min)	Calculated Lugeon values: Test Pressure	Q (L/m/min)	Lugeons (L/m/min)	Chosen Lugeon (L/m/min)
1	51.28	4.08	503.06	0.43	0.84	
2	59.44	3.94	583.07	0.41	0.70	
3	67.59	4.18	663.05	0.44	0.65	0.632
4	59.44	3.00	583.13	0.32	0.53	
5	51.29	2.16	503.16	0.23	0.44	

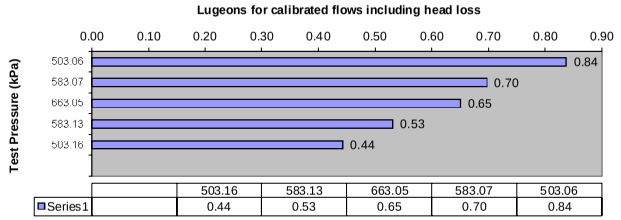

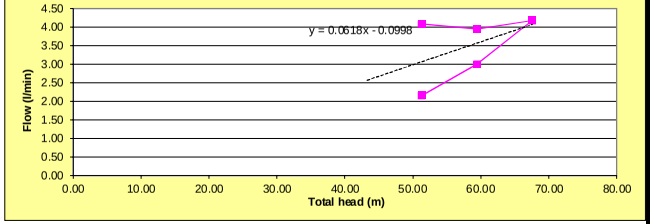

Conductivity Calculations:

MEAN Q/H$_T$	CANMET	HOEK & BRAY	MEAN LUGEONS 0.63	
0.060	1.2E-07	8.9E-08	8.2E-08	m/s
Mean Conductivity		K =	9.6E-08	m/s

Job No: TAH4125

Location: Tahmoor Site No: TBF040 Borehole: TBF040 Depth Range: 32.1 -41.3 m

PACKER TEST RESULTS: K = 3.9E-05 m/s

PROJECT: TAH4125 Site No: TBF040 BORE NAME: TBF040 HOLE DIP: 90 DIP Direction: DATE: 05-Nov-13

Depth To Bottm Packer Test interval:	41.30	m	HEIGHT OF PRESSURE GAUGE:	1	m (above ground level)
Depth To Top Packer Test interval:	32.05	m	STATIC GROUNDWATER LEVEL:	40.7	m (below ground level)
LENGTH OF STAGE TEST:	9.25	m	SURFACE R.L.		m
BORE DIAMETER:	96	mm			

Recorded flow readings at indicated applied pressure heads.

Stage 1

Gauge Pressure	80	(kPa)
Gauge Pressure	8.15	(m)
Static Pressure	43.6	(m)
Head without loss correction	51.74	(m)
Head loss	0.00	(m)
High flow pressure calibration	0.00	(m)
Total Head	51.74	(m)

Minutes of test	Flowmet read (L)	Flow (L/min)
0	0	
1	0	0
2	0	0
3	0	0
4	0	0
5	0	0
6	0	0
7	0	0
8	0	0
9	0	0
10	0	0

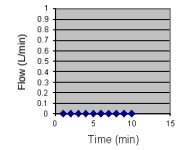

Arithmatic average = 0 (L/min)
Adopted average = 0 (L/min)

Stage 2

Gauge Pressure	160	(kPa)
Gauge Pressure	16.31	(m)
Static Pressure	43.6	(m)
Head without loss correction	59.89	(m)
Head loss	0.00	(m)
High flow pressure calibration	0.00	(m)
Total Head	59.89	(m)

Minutes of test	Flowmet read (L)	Flow (L/min)
0	0	
1	0	0
2	0	0
3	0	0
4	0	0
5	0	0
6	0	0
7	0	0
8	0	0
9	0	0
10	0	0

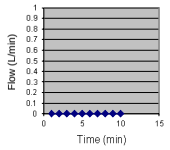

Arithmatic average = 0 (L/min)
Adopted average = 0 (L/min)

Stage 3

Gauge Pressure	240	(kPa)
Gauge Pressure	24.46	(m)
Static Pressure	43.6	(m)
Head without loss correction	68.05	(m)
Head loss	0.00	(m)
High flow pressure calibration	0.00	(m)
Total Head	68.05	(m)

Minutes of test	Flowmet read (L)	Flow (L/min)
0	0	
1	0	0
2	0	0
3	0	0
4	0	0
5	0	0
6	0	0
7	0	0
8	0	0
9	0	0
10	0	0

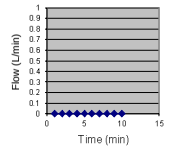

Arithmatic average = 0 (L/min)
Adopted average = 0 (L/min)

Stage 4

Gauge Pressure	160	(kPa)
Gauge Pressure	16.31	(m)
Static Pressure	43.6	(m)
Head without loss correction	59.89	(m)
Head loss	0.00	(m)
High flow pressure calibration	0.00	(m)
Total Head	59.89	(m)

Minutes of test	Flowmet read (L)	Flow (L/min)
0	0	
1	0	0
2	0	0
3	0	0
4	0	0
5	0	0
6	0	0
7	0	0
8	0	0
9	0	0
10	0	0

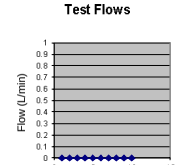

Arithmatic average = 0 (L/min)
Adopted average = 0 (L/min)

Stage 5

Gauge Pressure	80	(kPa)
Gauge Pressure	8.15	(m)
Static Pressure	43.6	(m)
Head without loss correction	51.74	(m)
Head loss	0.00	(m)
High flow pressure calibration	0.00	(m)
Total Head	51.74	(m)

Minutes of test	Flowmet read (L)	Flow (L/min)
0	0	
1	0	0
2	0	0
3	0	0
4	0	0
5	0	0
6	0	0
7	0	0
8	0	0
9	0	0
10	0	0

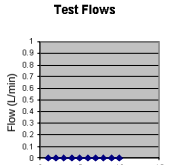

Arithmatic average = 0 (L/min)
Adopted average = 0 (L/min)

Stage 6

Gauge Pressure	0	(kPa)
Gauge Pressure	0.00	(m)
Static Pressure	43.6	(m)
Head without loss correction	43.58	(m)
Head loss	0.00	(m)
High flow pressure calibration	0.00	(m)
Total Head	43.58	(m)

Minutes of test	Flowmet read (L)	Flow (L/min)
0	0	
1	0	0
2	0	0
3	0	0
4	0	0
5	0	0
6	0	0
7	0	0
8	0	0
9	0	0
10	0	0

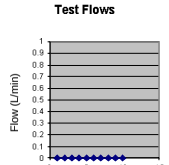

Arithmatic average = 0 (L/min)
Adopted average = 0 (L/min)

Comments:

Calculations used:

$$k = \frac{5.833}{\pi L \sin\alpha}\left(\frac{Q}{H_T}\right)\cdot 10^{-5} \quad \text{m/s} \qquad \text{(CANMET)}$$

$$k = \frac{8.333}{\pi L \sin\alpha}\left(\frac{Q}{H_T}\right)\cdot \ln\left(\frac{L}{r}\right)\cdot 10^{-4} \quad \text{m/s} \qquad \text{(HOEK \& BRAY)}$$

$$lugeon = \frac{Q}{L \sin\alpha}\cdot\frac{100}{H_T} \quad \text{l/m/min} \qquad \text{(HOULSBY)}$$

Stage	Total Head (m)	Flow (l/min)	Calculated Lugeon values: Test Pressure	Q (L/m/min)	Lugeons (L/m/min)	Chosen Lugeon (L/m/min)
1	51.74	0.00	507.56	0.00	0.00	
2	59.89	0.00	587.56	0.00	0.00	
3	68.05	0.00	667.56	0.00	0.00	0.000
4	59.89	0.00	587.56	0.00	0.00	
5	51.74	0	507.56	0.00	0.00	

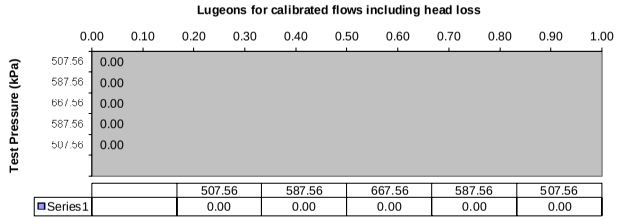

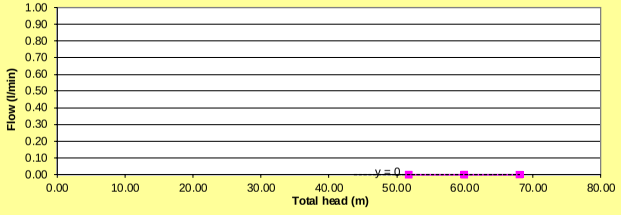

Conductivity Calculations:

MEAN Q/H$_T$	CANMET	HOEK & BRAY	MEAN LUGEONS 0.00	
0.000	0.0E+00	0.0E+00	0.0E+00	m/s

Mean Conductivity K = 3.89E-05 m/s

Job No: TAH4125

Location: Tahmoor Site No: TBF040 Borehole: TBF040 Depth Range: 40.8 -47.3 m

PACKER TEST RESULTS: K = 1.4E-06 m/s

PROJECT: TAH4125 **Site No:** TBF040 **BORE NAME:** TBF040 **HOLE DIP:** 90 **DIP Direction:** **DATE:** 06-Nov-13

Depth To Bottm Packer Test interval:	47.30	m	HEIGHT OF PRESSURE GAUGE:	1	m (above ground level)
Depth To Top Packer Test interval:	40.80	m	STATIC GROUNDWATER LEVEL:	40.7	m (below ground level)
LENGTH OF STAGE TEST:	6.50	m	SURFACE R.L.		m
BORE DIAMETER:	96	mm			

Recorded flow readings at indicated applied pressure heads.

Stage 1

Gauge Pressure	60	(kPa)
Gauge Pressure	6.12	(m)
Static Pressure	44.0	(m)
Head without loss correction	50.07	(m)
Head loss	0.81	(m)
High flow pressure calibration	0.00	(m)
Total Head	49.26	(m)

Minutes of test	Flowmet read (L)	Flow (L/min)
0	510	
1	540	30
2	570	30
3	601	31
4	631	30
5	661	30
6	691	30
7	722	31
8	752	30
9	782	30
10	813	31

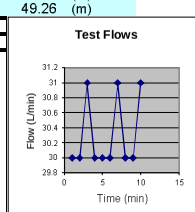

Arithmatic average = 30.3 (L/min)
Adopted average = 30.3 (L/min)

Stage 2

Gauge Pressure	120	(kPa)
Gauge Pressure	12.23	(m)
Static Pressure	44.0	(m)
Head without loss correction	56.18	(m)
Head loss	1.08	(m)
High flow pressure calibration	0.00	(m)
Total Head	55.10	(m)

Minutes of test	Flowmet read (L)	Flow (L/min)
0	885	
1	920	35
2	955	35
3	990	35
4	1025	35
5	1060	35
6	1095	35
7	1130	35
8	1165	35
9	1200	35
10	1235	35

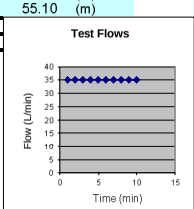

Arithmatic average = 35 (L/min)
Adopted average = 35 (L/min)

Stage 3

Gauge Pressure	180	(kPa)
Gauge Pressure	18.35	(m)
Static Pressure	44.0	(m)
Head without loss correction	62.30	(m)
Head loss	1.39	(m)
High flow pressure calibratior	0.00	(m)
Total Head	60.92	(m)

Minutes of test	Flowmet read (L)	Flow (L/min)
0	1276	
1	1315	39
2	1355	40
3	1395	40
4	1435	40
5	1475	40
6	1514	39
7	1554	40
8	1593	39
9	1633	40
10	1672	39

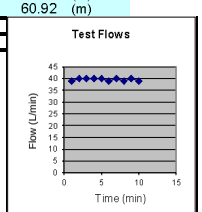

Arithmatic average = 39.6 (L/min)
Adopted average = 39.6 (L/min)

Stage 4

Gauge Pressure	120	(kPa)
Gauge Pressure	12.23	(m)
Static Pressure	44.0	(m)
Head without loss correction	56.18	(m)
Head loss	1.00	(m)
High flow pressure calibration	0.00	(m)
Total Head	55.19	(m)

Minutes of test	Flowmet read (L)	Flow (L/min)
0	1705	
1	1739	34
2	1773	34
3	1807	34
4	1840	33
5	1874	34
6	1908	34
7	1941	33
8	1974	33
9	2008	34
10	2041	33

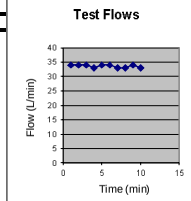

Arithmatic average = 33.6 (L/min)
Adopted average = 33.6 (L/min)

Stage 5

Gauge Pressure	60	(kPa)
Gauge Pressure	6.12	(m)
Static Pressure	44.0	(m)
Head without loss correction	50.07	(m)
Head loss	0.73	(m)
High flow pressure calibration	0.00	(m)
Total Head	49.34	(m)

Minutes of test	Flowmet read (L)	Flow (L/min)
0	2068	
1	2097	29
2	2126	29
3	2155	29
4	2183	28
5	2212	29
6	2240	28
7	2269	29
8	2298	29
9	2327	29
10	2355	28

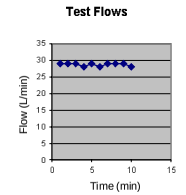

Arithmatic average = 28.7 (L/min)
Adopted average = 28.7 (L/min)

Stage 6

Gauge Pressure	0	(kPa)
Gauge Pressure	0.00	(m)
Static Pressure	44.0	(m)
Head without loss correction	43.95	(m)
Head loss	0.00	(m)
High flow pressure calibratior	0.00	(m)
Total Head	43.95	(m)

Minutes of test	Flowmet read (L)	Flow (L/min)
0	0	
1	0	0
2	0	0
3	0	0
4	0	0
5	0	0
6	0	0
7	0	0
8	0	0
9	0	0
10	0	0

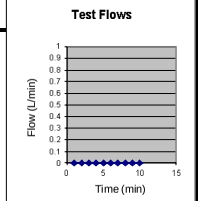

Arithmatic average = 0 (L/min)
Adopted average = 0 (L/min)

Comments:

Calculations used:

$$k = \frac{5.833}{\pi L \sin\alpha}\left(\frac{Q}{H_T}\right)\cdot 10^{-5} \quad \text{m/s} \qquad \text{(CANMET)}$$

$$k = \frac{8.333}{\pi L \sin\alpha}\left(\frac{Q}{H_T}\right)\cdot \ln\left(\frac{L}{r}\right)\cdot 10^{-4} \quad \text{m/s} \qquad \text{(HOEK \& BRAY)}$$

$$lugeon = \frac{Q}{L \sin\alpha}\cdot\frac{100}{H_T} \quad \text{l/m/min} \qquad \text{(HOULSBY)}$$

Stage	Total Head (m)	Flow (l/min)	Calculated Lugeon values: Test Pressure	Q (L/m/min)	Lugeons (L/m/min)	Chosen Lugeon (L/m/min)
1	49.26	30.30	483.22	4.66	9.46	
2	55.10	35.00	540.56	5.38	9.77	
3	60.92	39.60	597.58	6.09	10.00	9.510
4	55.19	33.60	541.39	5.17	9.37	
5	49.34	28.7	484.04	4.42	8.95	

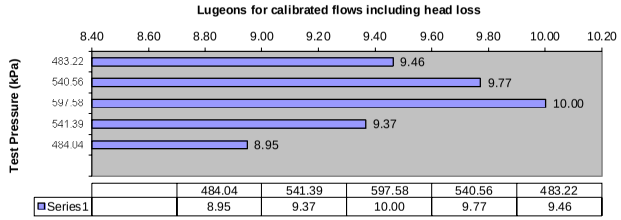

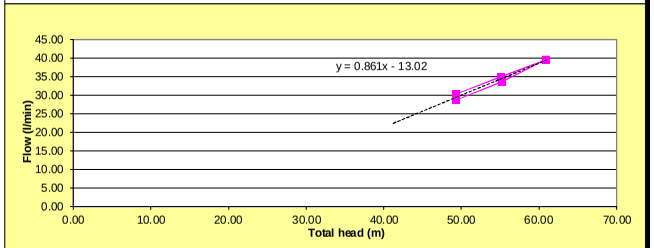

Conductivity Calculations:

MEAN Q/H$_T$	CANMET	HOEK & BRAY	MEAN LUGEONS	
0.621	1.8E-06	1.2E-06	1.2E-06	m/s
Mean Conductivity		K =	1.4E-06	m/s

Job No: TAH4125

Location: Tahmoor Site No: TBF040 Borehole: TBF040 Depth Range: 46.8 -53.3 m

PACKER TEST RESULTS: K = 0.0E+00 m/s

PROJECT: TAH4125 **Site No:** TBF040 **BORE NAME:** TBF040 **HOLE DIP:** 90 **DIP Direction:** **DATE:** 06-Nov-13

Depth To Bottm Packer Test interval:	53.30	m	HEIGHT OF PRESSURE GAUGE:	1	m (above ground level)
Depth To Top Packer Test interval:	46.80	m	STATIC GROUNDWATER LEVEL:	40.7	m (below ground level)
LENGTH OF STAGE TEST:	6.50	m	SURFACE R.L.		m
BORE DIAMETER:	96	mm			

Recorded flow readings at indicated applied pressure heads.

Stage 1

Gauge Pressure	80	(kPa)
Gauge Pressure	8.15	(m)
Static Pressure	44.3	(m)
Head without loss correction	52.41	(m)
Head loss	0.00	(m)
High flow pressure calibration	0.00	(m)
Total Head	52.41	(m)

Minutes of test	Flowmet read (L)	Flow (L/min)
0	0	
1	0	0
2	0	0
3	0	0
4	0	0
5	0	0
6	0	0
7	0	0
8	0	0
9	0	0
10	0	0

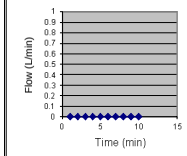

Arithmatic average = 0 (L/min)
Adopted average = 0 (L/min)

Stage 2

Gauge Pressure	160	(kPa)
Gauge Pressure	16.31	(m)
Static Pressure	44.3	(m)
Head without loss correction	60.56	(m)
Head loss	0.00	(m)
High flow pressure calibration	0.00	(m)
Total Head	60.56	(m)

Minutes of test	Flowmet read (L)	Flow (L/min)
0	0	
1	0	0
2	0	0
3	0	0
4	0	0
5	0	0
6	0	0
7	0	0
8	0	0
9	0	0
10	0	0

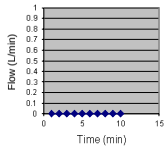

Arithmatic average = 0 (L/min)
Adopted average = 0 (L/min)

Stage 3

Gauge Pressure	240	(kPa)
Gauge Pressure	24.46	(m)
Static Pressure	44.3	(m)
Head without loss correction	68.72	(m)
Head loss	0.00	(m)
High flow pressure calibration	0.00	(m)
Total Head	68.72	(m)

Minutes of test	Flowmet read (L)	Flow (L/min)
0	0	
1	0	0
2	0	0
3	0	0
4	0	0
5	0	0
6	0	0
7	0	0
8	0	0
9	0	0
10	0	0

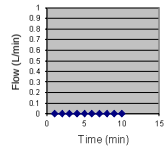

Arithmatic average = 0 (L/min)
Adopted average = 0 (L/min)

Stage 4

Gauge Pressure	160	(kPa)
Gauge Pressure	16.31	(m)
Static Pressure	44.3	(m)
Head without loss correction	60.56	(m)
Head loss	0.00	(m)
High flow pressure calibration	0.00	(m)
Total Head	60.56	(m)

Minutes of test	Flowmet read (L)	Flow (L/min)
0	0	
1	0	0
2	0	0
3	0	0
4	0	0
5	0	0
6	0	0
7	0	0
8	0	0
9	0	0
10	0	0

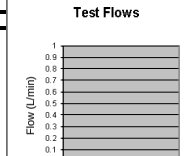

Arithmatic average = 0 (L/min)
Adopted average = 0 (L/min)

Stage 5

Gauge Pressure	80	(kPa)
Gauge Pressure	8.15	(m)
Static Pressure	44.3	(m)
Head without loss correction	52.41	(m)
Head loss	0.00	(m)
High flow pressure calibration	0.00	(m)
Total Head	52.41	(m)

Minutes of test	Flowmet read (L)	Flow (L/min)
0	0	
1	0	0
2	0	0
3	0	0
4	0	0
5	0	0
6	0	0
7	0	0
8	0	0
9	0	0
10	0	0

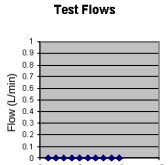

Arithmatic average = 0 (L/min)
Adopted average = 0 (L/min)

Stage 6

Gauge Pressure	0	(kPa)
Gauge Pressure	0.00	(m)
Static Pressure	44.3	(m)
Head without loss correction	44.25	(m)
Head loss	0.00	(m)
High flow pressure calibration	0.00	(m)
Total Head	44.25	(m)

Minutes of test	Flowmet read (L)	Flow (L/min)
0	0	
1	0	0
2	0	0
3	0	0
4	0	0
5	0	0
6	0	0
7	0	0
8	0	0
9	0	0
10	0	0

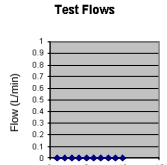

Arithmatic average = 0 (L/min)
Adopted average = 0 (L/min)

Comments: Test failed due to core barrel stuck in hole - Test interval redone in new hole TBF040B

Calculations used:

$$k = \frac{5.833}{\pi L \sin\alpha}\left(\frac{Q}{H_T}\right)\cdot 10^{-5} \quad \text{m/s} \qquad \text{(CANMET)}$$

$$k = \frac{8.333}{\pi L \sin\alpha}\left(\frac{Q}{H_T}\right)\cdot \ln\left(\frac{L}{r}\right)\cdot 10^{-4} \quad \text{m/s} \qquad \text{(HOEK \& BRAY)}$$

$$lugeon = \frac{Q}{L \sin\alpha}\cdot\frac{100}{H_T} \quad \text{l/m/min} \qquad \text{(HOULSBY)}$$

Stage	Total Head (m)	Flow (l/min)	Calculated Lugeon values: Test Pressure	Q (L/m/min)	Lugeons (L/m/min)	Chosen Lugeon (L/m/min)
1	52.41	0.00	514.12	0.00	0.00	
2	60.56	0.00	594.12	0.00	0.00	
3	68.72	0.00	674.12	0.00	0.00	0.000
4	60.56	0.00	594.12	0.00	0.00	
5	52.41	0	514.12	0.00	0.00	

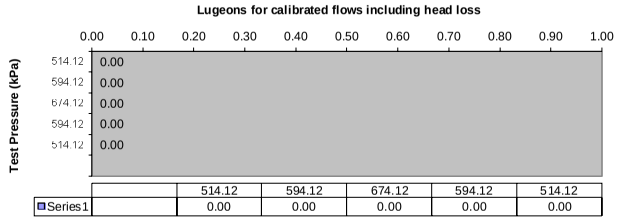

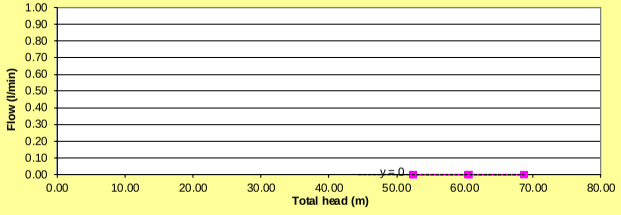

Conductivity Calculations:

MEAN Q/H$_T$	CANMET	HOEK & BRAY	MEAN LUGEONS 0.00	
0.000	0.0E+00	0.0E+00	0.0E+00	m/s

Mean Conductivity K = 0.0E+00 m/s

Job No: TAH4125

Location: Tahmoor Site No: TBF040 Borehole: TBF040 Depth Range: 46.9 -53.4 m

PACKER TEST RESULTS: K = 5.4E-05 m/s

PROJECT: TAH4125B Site No: TBF040 BORE NAME: TBF040 HOLE DIP: 90 DIP Direction: DATE: 13/1/2013

Depth To Bottm Packer Test interval:	53.40	m	HEIGHT OF PRESSURE GAUGE:	1	m (above ground level)
Depth To Top Packer Test interval:	46.90	m	STATIC GROUNDWATER LEVEL:	40.7	m (below ground level)
LENGTH OF STAGE TEST:	6.50	m	SURFACE R.L.		m
BORE DIAMETER:	96	mm			

Recorded flow readings at indicated applied pressure heads.

Stage 1

Gauge Pressure	80	(kPa)
Gauge Pressure	8.15	(m)
Static Pressure	44.3	(m)
Head without loss correction	52.41	(m)
Head loss	0.00	(m)
High flow pressure calibration	0.00	(m)
Total Head	52.41	(m)

Minutes of test	Flowmet read (L)	Flow (L/min)
0	0	
1	0	0
2	0	0
3	0	0
4	0	0
5	0	0
6	0	0
7	0	0
8	0	0
9	0	0
10	0	0

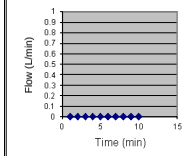

Arithmatic average = 0 (L/min)
Adopted average = 0 (L/min)

Stage 2

Gauge Pressure	160	(kPa)
Gauge Pressure	16.31	(m)
Static Pressure	44.3	(m)
Head without loss correction	60.57	(m)
Head loss	0.00	(m)
High flow pressure calibration	0.00	(m)
Total Head	60.57	(m)

Minutes of test	Flowmet read (L)	Flow (L/min)
0	0	
1	0	0
2	0	0
3	0	0
4	0	0
5	0	0
6	0	0
7	0	0
8	0	0
9	0	0
10	0	0

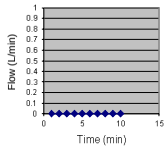

Arithmatic average = 0 (L/min)
Adopted average = 0 (L/min)

Stage 3

Gauge Pressure	240	(kPa)
Gauge Pressure	24.46	(m)
Static Pressure	44.3	(m)
Head without loss correction	68.72	(m)
Head loss	0.00	(m)
High flow pressure calibration	0.00	(m)
Total Head	68.72	(m)

Minutes of test	Flowmet read (L)	Flow (L/min)
0	0	
1	0	0
2	0	0
3	0	0
4	0	0
5	0	0
6	0	0
7	0	0
8	0	0
9	0	0
10	0	0

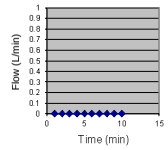

Arithmatic average = 0 (L/min)
Adopted average = 0 (L/min)

Stage 4

Gauge Pressure	160	(kPa)
Gauge Pressure	16.31	(m)
Static Pressure	44.3	(m)
Head without loss correction	60.57	(m)
Head loss	0.00	(m)
High flow pressure calibration	0.00	(m)
Total Head	60.57	(m)

Minutes of test	Flowmet read (L)	Flow (L/min)
0	0	
1	0	0
2	0	0
3	0	0
4	0	0
5	0	0
6	0	0
7	0	0
8	0	0
9	0	0
10	0	0

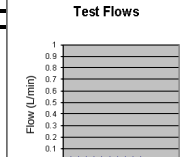

Arithmatic average = 0 (L/min)
Adopted average = 0 (L/min)

Stage 5

Gauge Pressure	80	(kPa)
Gauge Pressure	8.15	(m)
Static Pressure	44.3	(m)
Head without loss correction	52.41	(m)
Head loss	0.00	(m)
High flow pressure calibration	0.00	(m)
Total Head	52.41	(m)

Minutes of test	Flowmet read (L)	Flow (L/min)
0	0	
1	0	0
2	0	0
3	0	0
4	0	0
5	0	0
6	0	0
7	0	0
8	0	0
9	0	0
10	0	0

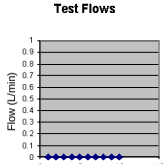

Arithmatic average = 0 (L/min)
Adopted average = 0 (L/min)

Stage 6

Gauge Pressure	0	(kPa)
Gauge Pressure	0.00	(m)
Static Pressure	44.3	(m)
Head without loss correction	44.26	(m)
Head loss	0.00	(m)
High flow pressure calibration	0.00	(m)
Total Head	44.26	(m)

Minutes of test	Flowmet read (L)	Flow (L/min)
0	0	
1	0	0
2	0	0
3	0	0
4	0	0
5	0	0
6	0	0
7	0	0
8	0	0
9	0	0
10	0	0

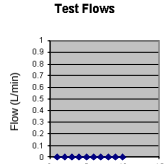

Arithmatic average = 0 (L/min)
Adopted average = 0 (L/min)

Comments:

Calculations used:

$$k = \frac{5.833}{\pi L \sin\alpha}\left(\frac{Q}{H_T}\right)\cdot 10^{-5} \quad \text{m/s} \qquad \text{(CANMET)}$$

$$k = \frac{8.333}{\pi L \sin\alpha}\left(\frac{Q}{H_T}\right)\cdot \ln\left(\frac{L}{r}\right)\cdot 10^{-4} \quad \text{m/s} \qquad \text{(HOEK \& BRAY)}$$

$$lugeon = \frac{Q}{L \sin\alpha}\cdot\frac{100}{H_T} \quad \text{l/m/min} \qquad \text{(HOULSBY)}$$

Stage	Total Head (m)	Flow (l/min)	Calculated Lugeon values: Test Pressure	Q (L/m/min)	Lugeons (L/m/min)	Chosen Lugeon (L/m/min)
1	52.41	0.00	514.17	0.00	0.00	
2	60.57	0.00	594.17	0.00	0.00	
3	68.72	0.00	674.17	0.00	0.00	0.000
4	60.57	0.00	594.17	0.00	0.00	
5	52.41	0	514.17	0.00	0.00	

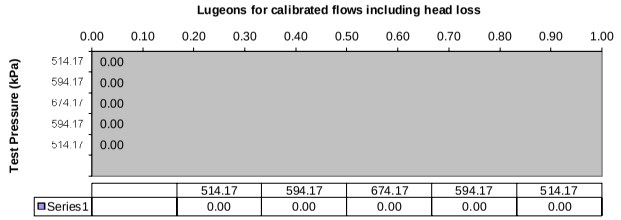

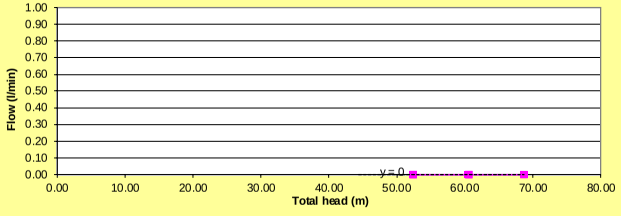

Conductivity Calculations:

MEAN Q/H$_T$	CANMET	HOEK & BRAY	MEAN LUGEONS	
0.000	0.0E+00	0.0E+00	0.0E+00	m/s

Mean Conductivity K = 5.427E-05 m/s

Job No: TAH4125

Location: Tahmoor Site No: TBF040 Borehole: TBF040 Depth Range: 52.9 -59.4 m

PACKER TEST RESULTS: K = 1.1E-06 m/s

PROJECT: TAH4125B **Site No:** TBF040 **BORE NAME:** TBF040 **HOLE DIP:** 90 **DIP Direction:** **DATE:** 14/1/2013

Depth To Bottm Packer Test interval:	59.40	m	HEIGHT OF PRESSURE GAUGE:	1	m (above ground level)
Depth To Top Packer Test interval:	52.90	m	STATIC GROUNDWATER LEVEL:	40.7	m (below ground level)
LENGTH OF STAGE TEST:	6.50	m	SURFACE R.L.		m
BORE DIAMETER:	96	mm			

Recorded flow readings at indicated applied pressure heads.

Stage 1

Gauge Pressure	100	(kPa)
Gauge Pressure	10.19	(m)
Static Pressure	44.6	(m)
Head without loss correction	54.75	(m)
Head loss	0.55	(m)
High flow pressure calibration	0.00	(m)
Total Head	54.20	(m)

Minutes of test	Flowmet read (L)	Flow (L/min)
0	5955	
1	5981	26
2	6006	25
3	6031	25
4	6056	25
5	6080	24
6	6105	25
7	6130	25
8	6155	25
9	6179	24
10	6204	25

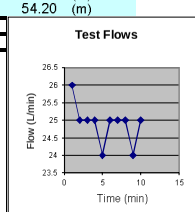

Arithmatic average = 24.9 (L/min)
Adopted average = 24.9 (L/min)

Stage 2

Gauge Pressure	160	(kPa)
Gauge Pressure	16.31	(m)
Static Pressure	44.6	(m)
Head without loss correction	60.87	(m)
Head loss	0.78	(m)
High flow pressure calibration	0.00	(m)
Total Head	60.08	(m)

Minutes of test	Flowmet read (L)	Flow (L/min)
0	6235	
1	6264	29
2	6294	30
3	6323	29
4	6353	30
5	6382	29
6	6412	30
7	6442	30
8	6473	31
9	6503	30
10	6533	30

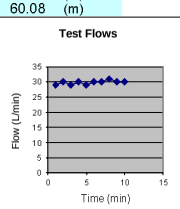

Arithmatic average = 29.8 (L/min)
Adopted average = 29.8 (L/min)

Stage 3

Gauge Pressure	240	(kPa)
Gauge Pressure	24.46	(m)
Static Pressure	44.6	(m)
Head without loss correction	69.02	(m)
Head loss	1.07	(m)
High flow pressure calibratior	0.00	(m)
Total Head	67.95	(m)

Minutes of test	Flowmet read (L)	Flow (L/min)
0	6568	
1	6603	35
2	6638	35
3	6673	35
4	6708	35
5	6743	35
6	6777	34
7	6812	35
8	6846	34
9	6881	35
10	6916	35

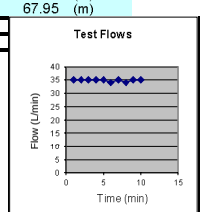

Arithmatic average = 34.8 (L/min)
Adopted average = 34.8 (L/min)

Stage 4

Gauge Pressure	160	(kPa)
Gauge Pressure	16.31	(m)
Static Pressure	44.6	(m)
Head without loss correction	60.87	(m)
Head loss	0.76	(m)
High flow pressure calibration	0.00	(m)
Total Head	60.11	(m)

Minutes of test	Flowmet read (L)	Flow (L/min)
0	6945	
1	6974	29
2	7003	29
3	7033	30
4	7062	29
5	7091	29
6	7121	30
7	7151	30
8	7179	28
9	7209	30
10	7238	29

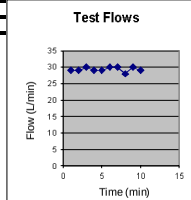

Arithmatic average = 29.3 (L/min)
Adopted average = 29.3 (L/min)

Stage 5

Gauge Pressure	100	(kPa)
Gauge Pressure	10.19	(m)
Static Pressure	44.6	(m)
Head without loss correction	54.75	(m)
Head loss	0.58	(m)
High flow pressure calibration	0.00	(m)
Total Head	54.17	(m)

Minutes of test	Flowmet read (L)	Flow (L/min)
0	7283	
1	7288	25
2	7314	26
3	7340	26
4	7365	25
5	7391	26
6	7416	25
7	7442	26
8	7467	25
9	7493	26
10	7519	26

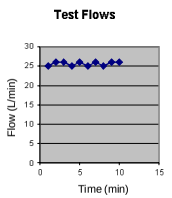

Arithmatic average = 25.6 (L/min)
Adopted average = 25.6 (L/min)

Stage 6

Gauge Pressure	0	(kPa)
Gauge Pressure	0.00	(m)
Static Pressure	44.6	(m)
Head without loss correction	44.56	(m)
Head loss	0.00	(m)
High flow pressure calibratior	0.00	(m)
Total Head	44.56	(m)

Minutes of test	Flowmet read (L)	Flow (L/min)
0	0	
1	0	0
2	0	0
3	0	0
4	0	0
5	0	0
6	0	0
7	0	0
8	0	0
9	0	0
10	0	0

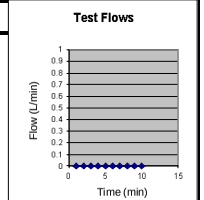

Arithmatic average = 0 (L/min)
Adopted average = 0 (L/min)

Comments:

Calculations used:

$$k = \frac{5.833}{\pi L \sin\alpha}\left(\frac{Q}{H_T}\right)\cdot 10^{-5} \text{ m/s} \quad \text{(CANMET)}$$

$$k = \frac{8.333}{\pi L \sin\alpha}\left(\frac{Q}{H_T}\right)\cdot \ln\left(\frac{L}{r}\right)\cdot 10^{-4} \text{ m/s} \quad \text{(HOEK \& BRAY)}$$

$$lugeon = \frac{Q}{L\sin\alpha}\cdot\frac{100}{H_T} \text{ l/m/min} \quad \text{(HOULSBY)}$$

Stage	Total Head (m)	Flow (l/min)	Calculated Lugeon values: Test Pressure	Q (L/m/min)	Lugeons (L/m/min)	Chosen Lugeon (L/m/min)
1	54.20	24.90	531.74	3.83	7.07	
2	60.08	29.80	589.41	4.58	7.63	
3	67.95	34.80	666.61	5.35	7.88	7.469
4	60.11	29.30	589.67	4.51	7.50	
5	54.17	25.6	531.43	3.94	7.27	

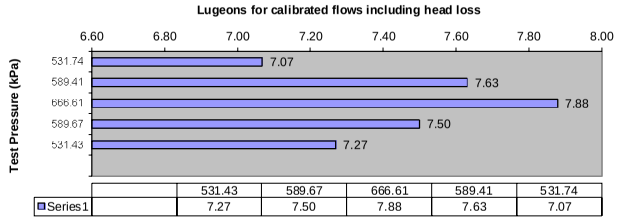

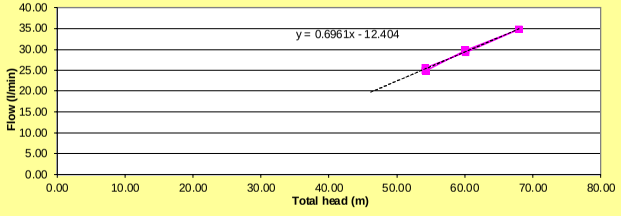

Conductivity Calculations:

MEAN Q/H$_T$	CANMET	HOEK & BRAY	MEAN LUGEONS 7.47	
0.488	1.4E-06	9.8E-07	9.7E-07	m/s
Mean Conductivity	K =	1.1E-06	m/s	

Job No: TAH4125

Location: Tahmoor Site No: TBF040 Borehole: TBF040 Depth Range: 58.9 -65.4 m

PACKER TEST RESULTS: K = 1.6E-05 m/s

PROJECT: TAH4125 **Site No:** TBF040 **BORE NAME:** TBF040 **HOLE DIP:** 90 **DIP Direction:** **DATE:** 15/1/2013

Depth To Bottm Packer Test interval:	65.40	m	HEIGHT OF PRESSURE GAUGE:	1	m (above ground level)
Depth To Top Packer Test interval:	58.90	m	STATIC GROUNDWATER LEVEL:	40.7	m (below ground level)
LENGTH OF STAGE TEST:	6.50	m	SURFACE R.L.		m
BORE DIAMETER:	96	mm			

Recorded flow readings at indicated applied pressure heads.

Stage 1

Gauge Pressure	80	(kPa)
Gauge Pressure	8.15	(m)
Static Pressure	44.9	(m)
Head without loss correction	53.01	(m)
Head loss	0.00	(m)
High flow pressure calibration	0.00	(m)
Total Head	53.01	(m)

Minutes of test	Flowmet read (L)	Flow (L/min)
0	0	
1	0	0
2	0	0
3	0	0
4	0	0
5	0	0
6	0	0
7	0	0
8	0	0
9	0	0
10	0	0

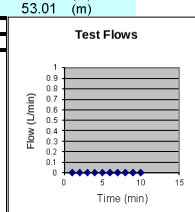

Arithmatic average = 0 (L/min)
Adopted average = 0 (L/min)

Stage 2

Gauge Pressure	160	(kPa)
Gauge Pressure	16.31	(m)
Static Pressure	44.9	(m)
Head without loss correction	61.17	(m)
Head loss	0.00	(m)
High flow pressure calibration	0.00	(m)
Total Head	61.17	(m)

Minutes of test	Flowmet read (L)	Flow (L/min)
0	0	
1	0	0
2	0	0
3	0	0
4	0	0
5	0	0
6	0	0
7	0	0
8	0	0
9	0	0
10	0	0

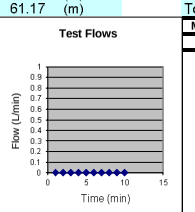

Arithmatic average = 0 (L/min)
Adopted average = 0 (L/min)

Stage 3

Gauge Pressure	240	(kPa)
Gauge Pressure	24.46	(m)
Static Pressure	44.9	(m)
Head without loss correction	69.32	(m)
Head loss	0.00	(m)
High flow pressure calibration	0.00	(m)
Total Head	69.32	(m)

Minutes of test	Flowmet read (L)	Flow (L/min)
0	0	
1	0	0
2	0	0
3	0	0
4	0	0
5	0	0
6	0	0
7	0	0
8	0	0
9	0	0
10	0	0

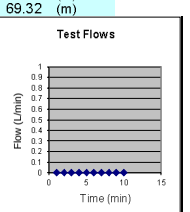

Arithmatic average = 0 (L/min)
Adopted average = 0 (L/min)

Stage 4

Gauge Pressure	160	(kPa)
Gauge Pressure	16.31	(m)
Static Pressure	44.9	(m)
Head without loss correction	61.17	(m)
Head loss	0.00	(m)
High flow pressure calibration	0.00	(m)
Total Head	61.17	(m)

Minutes of test	Flowmet read (L)	Flow (L/min)
0	0	
1	0	0
2	0	0
3	0	0
4	0	0
5	0	0
6	0	0
7	0	0
8	0	0
9	0	0
10	0	0

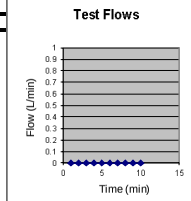

Arithmatic average = 0 (L/min)
Adopted average = 0 (L/min)

Stage 5

Gauge Pressure	80	(kPa)
Gauge Pressure	8.15	(m)
Static Pressure	44.9	(m)
Head without loss correction	53.01	(m)
Head loss	0.00	(m)
High flow pressure calibration	0.00	(m)
Total Head	53.01	(m)

Minutes of test	Flowmet read (L)	Flow (L/min)
0	0	
1	0	0
2	0	0
3	0	0
4	0	0
5	0	0
6	0	0
7	0	0
8	0	0
9	0	0
10	0	0

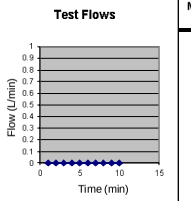

Arithmatic average = 0 (L/min)
Adopted average = 0 (L/min)

Stage 6

Gauge Pressure	0	(kPa)
Gauge Pressure	0.00	(m)
Static Pressure	44.9	(m)
Head without loss correction	44.86	(m)
Head loss	0.00	(m)
High flow pressure calibration	0.00	(m)
Total Head	44.86	(m)

Minutes of test	Flowmet read (L)	Flow (L/min)
0	0	
1	0	0
2	0	0
3	0	0
4	0	0
5	0	0
6	0	0
7	0	0
8	0	0
9	0	0
10	0	0

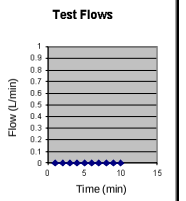

Arithmatic average = 0 (L/min)
Adopted average = 0 (L/min)

Comments:

Calculations used:

$$k = \frac{5.833}{\pi L \sin\alpha}\left(\frac{Q}{H_T}\right)\cdot 10^{-5} \quad \text{m/s} \qquad \text{(CANMET)}$$

$$k = \frac{8.333}{\pi L \sin\alpha}\left(\frac{Q}{H_T}\right)\cdot \ln\left(\frac{L}{r}\right)\cdot 10^{-4} \quad \text{m/s} \qquad \text{(HOEK \& BRAY)}$$

$$lugeon = \frac{Q}{L \sin\alpha}\cdot\frac{100}{H_T} \quad \text{l/m/min} \qquad \text{(HOULSBY)}$$

Stage	Total Head (m)	Flow (l/min)	Calculated Lugeon values: Test Pressure	Q (L/m/min)	Lugeons (L/m/min)	Chosen Lugeon (L/m/min)
1	53.01	0.00	520.05	0.00	0.00	
2	61.17	0.00	600.05	0.00	0.00	
3	69.32	0.00	680.05	0.00	0.00	0.000
4	61.17	0.00	600.05	0.00	0.00	
5	53.01	0	520.05	0.00	0.00	

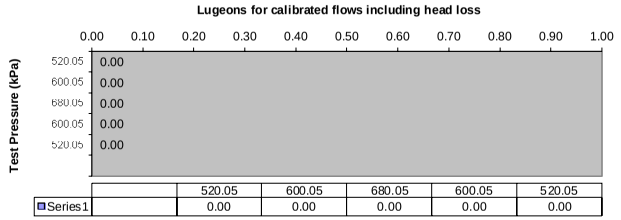

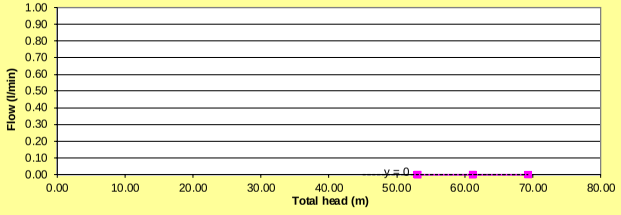

Conductivity Calculations:

MEAN Q/H$_T$	CANMET	HOEK & BRAY	MEAN LUGEONS 0.00	
0.000	0.0E+00	0.0E+00	0.0E+00	m/s

Mean Conductivity K = 1.631E-05 m/s

Job No: TAH4125

Location: Tahmoor Site No: TBF040 Borehole: TBF040 Depth Range: 64.9 -71.4 m

PACKER TEST RESULTS: K = 2.8E-06 m/s

PROJECT: TAH4125 **Site No:** TBF040 **BORE NAME:** TBF040 **HOLE DIP:** 90 **DIP Direction:** **DATE:** 15-Nov-13

Depth To Bottm Packer Test interval:	71.40	m	HEIGHT OF PRESSURE GAUGE:	1	m (above ground level)
Depth To Top Packer Test interval:	64.90	m	STATIC GROUNDWATER LEVEL:	40.7	m (below ground level)
LENGTH OF STAGE TEST:	6.50	m	SURFACE R.L.		m
BORE DIAMETER:	96	mm			

Recorded flow readings at indicated applied pressure heads.

Stage 1

Gauge Pressure	100	(kPa)
Gauge Pressure	10.19	(m)
Static Pressure	45.2	(m)
Head without loss correction	55.35	(m)
Head loss	3.60	(m)
High flow pressure calibration	0.00	(m)
Total Head	51.76	(m)

Minutes of test	Flowmet read (L)	Flow (L/min)
0	530	
1	596	66
2	661	65
3	724	63
4	788	64
5	851	63
6	914	63
7	977	63
8	1041	64
9	1105	64
10	1168	63

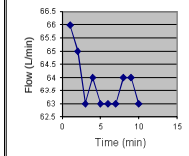

Arithmatic average = 63.8 (L/min)
Adopted average = 63.8 (L/min)

Stage 2

Gauge Pressure	200	(kPa)
Gauge Pressure	20.39	(m)
Static Pressure	45.2	(m)
Head without loss correction	65.54	(m)
Head loss	5.18	(m)
High flow pressure calibration	0.00	(m)
Total Head	60.36	(m)

Minutes of test	Flowmet read (L)	Flow (L/min)
0	1244	
1	1320	76
2	1397	77
3	1473	76
4	1550	77
5	1627	77
6	1703	76
7	1781	78
8	1858	77
9	1933	75
10	2010	77

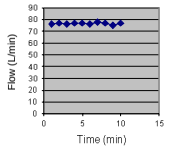

Arithmatic average = 76.6 (L/min)
Adopted average = 76.6 (L/min)

Stage 3

Gauge Pressure	300	(kPa)
Gauge Pressure	30.58	(m)
Static Pressure	45.2	(m)
Head without loss correction	75.74	(m)
Head loss	6.50	(m)
High flow pressure calibratior	0.00	(m)
Total Head	69.24	(m)

Minutes of test	Flowmet read (L)	Flow (L/min)
0	2092	
1	2179	87
2	2264	85
3	2348	84
4	2435	87
5	2520	85
6	2606	86
7	2692	86
8	2779	87
9	2864	85
10	2950	86

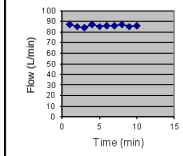

Arithmatic average = 85.8 (L/min)
Adopted average = 85.8 (L/min)

Stage 4

Gauge Pressure	200	(kPa)
Gauge Pressure	20.39	(m)
Static Pressure	45.2	(m)
Head without loss correction	65.54	(m)
Head loss	4.54	(m)
High flow pressure calibration	0.00	(m)
Total Head	61.00	(m)

Minutes of test	Flowmet read (L)	Flow (L/min)
0	3022	
1	3093	71
2	3165	72
3	3236	71
4	3308	72
5	3380	72
6	3451	71
7	3523	72
8	3595	72
9	3668	73
10	3739	71

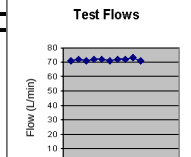

Arithmatic average = 71.7 (L/min)
Adopted average = 71.7 (L/min)

Stage 5

Gauge Pressure	100	(kPa)
Gauge Pressure	10.19	(m)
Static Pressure	45.2	(m)
Head without loss correction	55.35	(m)
Head loss	3.33	(m)
High flow pressure calibration	0.00	(m)
Total Head	52.02	(m)

Minutes of test	Flowmet read (L)	Flow (L/min)
0	3802	
1	3864	62
2	3924	60
3	3986	62
4	4048	62
5	4109	61
6	4170	61
7	4232	62
8	4293	61
9	4355	62
10	4416	61

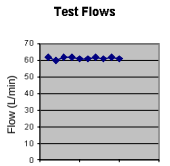

Arithmatic average = 61.4 (L/min)
Adopted average = 61.4 (L/min)

Stage 6

Gauge Pressure	0	(kPa)
Gauge Pressure	0.00	(m)
Static Pressure	45.2	(m)
Head without loss correction	45.16	(m)
Head loss	0.00	(m)
High flow pressure calibratior	0.00	(m)
Total Head	45.16	(m)

Minutes of test	Flowmet read (L)	Flow (L/min)
0	0	
1	0	0
2	0	0
3	0	0
4	0	0
5	0	0
6	0	0
7	0	0
8	0	0
9	0	0
10	0	0

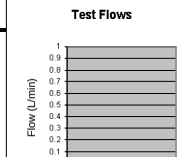

Arithmatic average = 0 (L/min)
Adopted average = 0 (L/min)

Comments:

Calculations used:

$$k = \frac{5.833}{\pi L \sin\alpha}\left(\frac{Q}{H_T}\right)\cdot 10^{-5} \text{ m/s} \quad \text{(CANMET)}$$

$$k = \frac{8.333}{\pi L \sin\alpha}\left(\frac{Q}{H_T}\right)\cdot \ln\left(\frac{L}{r}\right)\cdot 10^{-4} \text{ m/s} \quad \text{(HOEK \& BRAY)}$$

$$lugeon = \frac{Q}{L \sin\alpha}\cdot\frac{100}{H_T} \text{ l/m/min} \quad \text{(HOULSBY)}$$

Stage	Total Head (m)	Flow (l/min)	Calculated Lugeon values: Test Pressure	Q (L/m/min)	Lugeons (L/m/min)	Chosen Lugeon (L/m/min)
1	51.76	63.80	507.72	9.82	18.97	
2	60.36	76.60	592.14	11.78	19.52	
3	69.24	85.80	679.20	13.20	19.07	18.759
4	61.00	71.70	598.44	11.03	18.08	
5	52.02	61.4	510.32	9.45	18.16	

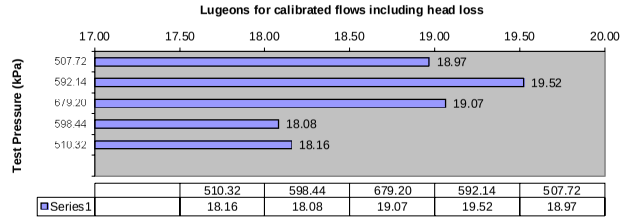

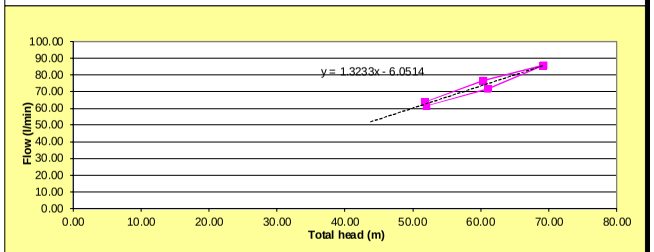

Conductivity Calculations:

MEAN Q/H$_T$	CANMET	HOEK & BRAY	MEAN LUGEONS 18.76	
1.222	3.5E-06	2.4E-06	2.4E-06	m/s
Mean Conductivity		K =	2.8E-06	m/s

Job No: TAH4125

Location: Tahmoor Site No: TBF040 Borehole: TBF040 Depth Range: 70.9 -77.4 m

PACKER TEST RESULTS: K = 2.7E-06 m/s

PROJECT: TAH4125 **Site No:** TBF040 **BORE NAME:** TBF040 **HOLE DIP:** 90 **DIP Direction:** **DATE:** 18-Nov-13

Depth To Bottm Packer Test interval:	77.40	m	HEIGHT OF PRESSURE GAUGE:	1	m (above ground level)
Depth To Top Packer Test interval:	70.90	m	STATIC GROUNDWATER LEVEL:	40.7	m (below ground level)
LENGTH OF STAGE TEST:	6.50	m	SURFACE R.L.		m
BORE DIAMETER:	96	mm			

Recorded flow readings at indicated applied pressure heads.

Stage 1

Gauge Pressure	100	(kPa)
Gauge Pressure	10.19	(m)
Static Pressure	45.5	(m)
Head without loss correction	55.65	(m)
Head loss	4.06	(m)
High flow pressure calibration	0.00	(m)
Total Head	51.59	(m)

Minutes of test	Flowmet read (L)	Flow (L/min)
0	6015	
1	6084	69
2	6153	69
3	6222	69
4	6289	67
5	6357	68
6	6424	67
7	6491	67
8	6559	68
9	6626	67
10	6693	67

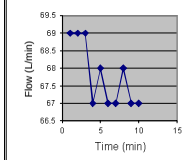

Arithmatic average = 67.8 (L/min)
Adopted average = 67.8 (L/min)

Stage 2

Gauge Pressure	240	(kPa)
Gauge Pressure	24.46	(m)
Static Pressure	45.5	(m)
Head without loss correction	69.92	(m)
Head loss	5.50	(m)
High flow pressure calibration	0.00	(m)
Total Head	64.42	(m)

Minutes of test	Flowmet read (L)	Flow (L/min)
0	6770	
1	6850	80
2	6929	79
3	7007	78
4	7086	79
5	7166	80
6	7244	78
7	7323	79
8	7402	79
9	7482	80
10	7559	77

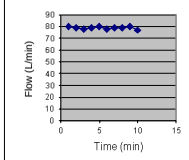

Arithmatic average = 78.9 (L/min)
Adopted average = 78.9 (L/min)

Stage 3

Gauge Pressure	300	(kPa)
Gauge Pressure	30.58	(m)
Static Pressure	45.5	(m)
Head without loss correction	76.04	(m)
Head loss	5.97	(m)
High flow pressure calibratior	0.00	(m)
Total Head	70.07	(m)

Minutes of test	Flowmet read (L)	Flow (L/min)
0	7641	
1	7723	82
2	7806	83
3	7888	82
4	7970	82
5	8051	81
6	8135	84
7	8216	81
8	8299	83
9	8381	82
10	8463	82

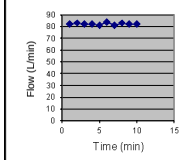

Arithmatic average = 82.2 (L/min)
Adopted average = 82.2 (L/min)

Stage 4

Gauge Pressure	240	(kPa)
Gauge Pressure	24.46	(m)
Static Pressure	45.5	(m)
Head without loss correction	69.92	(m)
Head loss	4.61	(m)
High flow pressure calibration	0.00	(m)
Total Head	65.32	(m)

Minutes of test	Flowmet read (L)	Flow (L/min)
0	8534	
1	8606	72
2	8677	71
3	8750	73
4	8823	73
5	8895	72
6	8967	72
7	9040	73
8	9112	72
9	9184	72
10	9256	72

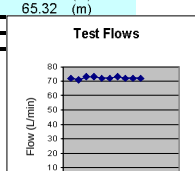

Arithmatic average = 72.2 (L/min)
Adopted average = 72.2 (L/min)

Stage 5

Gauge Pressure	100	(kPa)
Gauge Pressure	10.19	(m)
Static Pressure	45.5	(m)
Head without loss correction	55.65	(m)
Head loss	2.88	(m)
High flow pressure calibration	0.00	(m)
Total Head	52.77	(m)

Minutes of test	Flowmet read (L)	Flow (L/min)
0	9317	
1	9375	58
2	9432	57
3	9489	57
4	9546	57
5	9603	57
6	9661	58
7	9719	58
8	9775	56
9	9832	57
10	9888	56

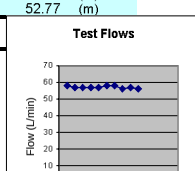

Arithmatic average = 57.1 (L/min)
Adopted average = 57.1 (L/min)

Stage 6

Gauge Pressure	0	(kPa)
Gauge Pressure	0.00	(m)
Static Pressure	45.5	(m)
Head without loss correction	45.46	(m)
Head loss	0.00	(m)
High flow pressure calibratior	0.00	(m)
Total Head	45.46	(m)

Minutes of test	Flowmet read (L)	Flow (L/min)
0	0	
1	0	0
2	0	0
3	0	0
4	0	0
5	0	0
6	0	0
7	0	0
8	0	0
9	0	0
10	0	0

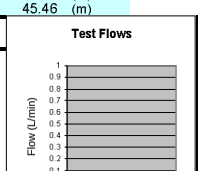

Arithmatic average = 0 (L/min)
Adopted average = 0 (L/min)

Comments:

Calculations used:

$$k = \frac{5.833}{\pi L \sin\alpha}\left(\frac{Q}{H_T}\right)\cdot 10^{-5} \quad \text{m/s} \qquad \text{(CANMET)}$$

$$k = \frac{8.333}{\pi L \sin\alpha}\left(\frac{Q}{H_T}\right)\cdot \ln\left(\frac{L}{r}\right)\cdot 10^{-4} \quad \text{m/s} \qquad \text{(HOEK \& BRAY)}$$

$$lugeon = \frac{Q}{L \sin\alpha}\cdot\frac{100}{H_T} \quad \text{l/m/min} \qquad \text{(HOULSBY)}$$

Stage	Total Head (m)	Flow (l/min)	Calculated Lugeon values: Test Pressure	Q (L/m/min)	Lugeons (L/m/min)	Chosen Lugeon (L/m/min)
1	51.59	67.80	506.10	10.43	20.22	
2	64.42	78.90	631.99	12.14	18.84	
3	70.07	82.20	687.38	12.65	18.05	18.152
4	65.32	72.20	640.76	11.11	17.01	
5	52.77	57.1	517.68	8.78	16.65	

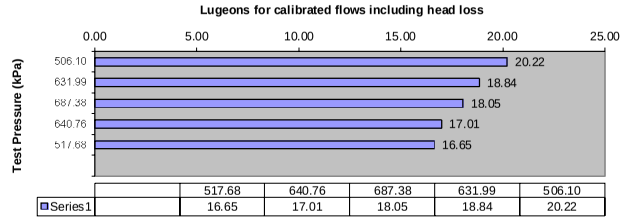

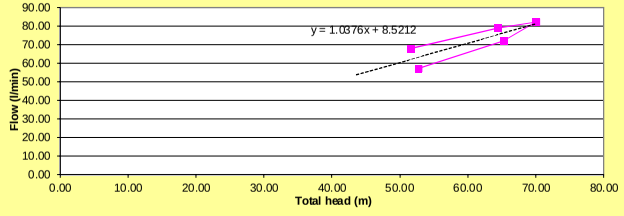

Conductivity Calculations:

MEAN Q/H$_T$	CANMET	HOEK & BRAY	MEAN LUGEONS 18.15	
1.176	3.4E-06	2.4E-06	2.4E-06	m/s
Mean Conductivity		K =	2.7E-06	m/s

Job No: TAH4125

Location: Tahmoor Site No: TBF040 Borehole: TBF040 Depth Range: 76.9 -83.4 m

PACKER TEST RESULTS: K = 1.1E-06 m/s

PROJECT: TAH4125 **Site No:** TBF040 **BORE NAME:** TBF040 **HOLE DIP:** 90 **DIP Direction:** **DATE:** 18-Nov-13

Depth To Bottm Packer Test interval:	83.40	m	HEIGHT OF PRESSURE GAUGE:	1	m (above ground level)
Depth To Top Packer Test interval:	76.90	m	STATIC GROUNDWATER LEVEL:	40.7	m (below ground level)
LENGTH OF STAGE TEST:	6.50	m	SURFACE R.L.		m
BORE DIAMETER:	96	mm			

Recorded flow readings at indicated applied pressure heads.

Stage 1

Gauge Pressure	120	(kPa)
Gauge Pressure	12.23	(m)
Static Pressure	45.8	(m)
Head without loss correction	57.99	(m)
Head loss	0.68	(m)
High flow pressure calibration	0.00	(m)
Total Head	57.31	(m)

Minutes of test	Flowmet read (L)	Flow (L/min)
0	385	
1	414	29
2	442	28
3	470	28
4	498	28
5	526	28
6	553	27
7	580	27
8	608	28
9	636	28
10	663	27

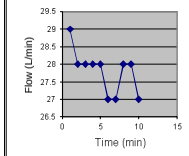

Arithmatic average = 27.8 (L/min)
Adopted average = 27.8 (L/min)

Stage 2

Gauge Pressure	240	(kPa)
Gauge Pressure	24.46	(m)
Static Pressure	45.8	(m)
Head without loss correction	70.22	(m)
Head loss	1.04	(m)
High flow pressure calibration	0.00	(m)
Total Head	69.18	(m)

Minutes of test	Flowmet read (L)	Flow (L/min)
0	695	
1	732	37
2	766	34
3	801	35
4	834	33
5	868	34
6	902	34
7	936	34
8	970	34
9	1004	34
10	1038	34

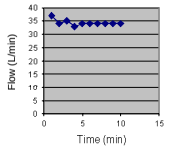

Arithmatic average = 34.3 (L/min)
Adopted average = 34.3 (L/min)

Stage 3

Gauge Pressure	360	(kPa)
Gauge Pressure	36.70	(m)
Static Pressure	45.8	(m)
Head without loss correction	82.45	(m)
Head loss	1.46	(m)
High flow pressure calibratior	0.00	(m)
Total Head	81.00	(m)

Minutes of test	Flowmet read (L)	Flow (L/min)
0	1078	
1	1119	41
2	1160	41
3	1200	40
4	1241	41
5	1281	40
6	1323	42
7	1363	40
8	1403	40
9	1444	41
10	1484	40

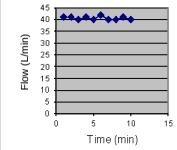

Arithmatic average = 40.6 (L/min)
Adopted average = 40.6 (L/min)

Stage 4

Gauge Pressure	240	(kPa)
Gauge Pressure	24.46	(m)
Static Pressure	45.8	(m)
Head without loss correction	70.22	(m)
Head loss	1.04	(m)
High flow pressure calibration	0.00	(m)
Total Head	69.18	(m)

Minutes of test	Flowmet read (L)	Flow (L/min)
0	1520	
1	1554	34
2	1589	35
3	1623	34
4	1657	34
5	1691	34
6	1726	35
7	1760	34
8	1794	34
9	1829	35
10	1863	34

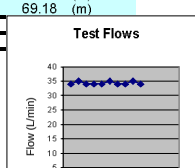

Arithmatic average = 34.3 (L/min)
Adopted average = 34.3 (L/min)

Stage 5

Gauge Pressure	120	(kPa)
Gauge Pressure	12.23	(m)
Static Pressure	45.8	(m)
Head without loss correction	57.99	(m)
Head loss	0.66	(m)
High flow pressure calibration	0.00	(m)
Total Head	57.33	(m)

Minutes of test	Flowmet read (L)	Flow (L/min)
0	1891	
1	1919	28
2	1946	27
3	1973	27
4	2001	28
5	2028	27
6	2056	28
7	2083	27
8	2110	27
9	2138	28
10	2165	27

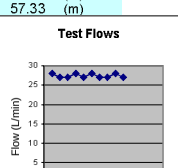

Arithmatic average = 27.4 (L/min)
Adopted average = 27.4 (L/min)

Stage 6

Gauge Pressure	0	(kPa)
Gauge Pressure	0.00	(m)
Static Pressure	45.8	(m)
Head without loss correction	45.76	(m)
Head loss	0.00	(m)
High flow pressure calibratior	0.00	(m)
Total Head	45.76	(m)

Minutes of test	Flowmet read (L)	Flow (L/min)
0	0	
1	0	0
2	0	0
3	0	0
4	0	0
5	0	0
6	0	0
7	0	0
8	0	0
9	0	0
10	0	0

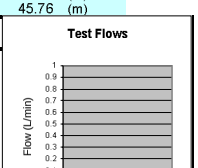

Arithmatic average = 0 (L/min)
Adopted average = 0 (L/min)

Comments:

Calculations used:

$$k = \frac{5.833}{\pi L \sin\alpha}\left(\frac{Q}{H_T}\right)\cdot 10^{-5} \text{ m/s} \quad \text{(CANMET)}$$

$$k = \frac{8.333}{\pi L \sin\alpha}\left(\frac{Q}{H_T}\right)\cdot \ln\left(\frac{L}{r}\right)\cdot 10^{-4} \text{ m/s} \quad \text{(HOEK \& BRAY)}$$

$$lugeon = \frac{Q}{L\sin\alpha}\cdot\frac{100}{H_T} \text{ l/m/min} \quad \text{(HOULSBY)}$$

Stage	Total Head (m)	Flow (l/min)	Calculated Lugeon values: Test Pressure	Q (L/m/min)	Lugeons (L/m/min)	Chosen Lugeon (L/m/min)
1	57.31	27.80	562.18	4.28	7.46	
2	69.18	34.30	678.69	5.28	7.63	
3	81.00	40.60	794.60	6.25	7.71	7.557
4	69.18	34.30	678.69	5.28	7.63	
5	57.33	27.4	562.37	4.22	7.35	

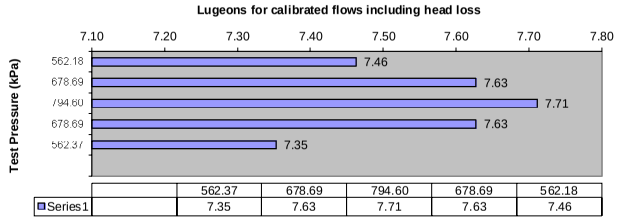

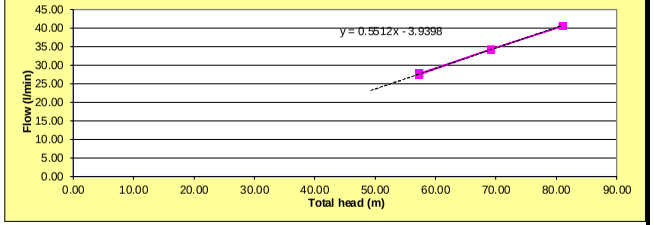

Conductivity Calculations:

MEAN Q/H$_T$	CANMET	HOEK & BRAY	MEAN LUGEONS 7.56	
0.493	1.4E-06	9.9E-07	9.8E-07	m/s
Mean Conductivity		K =	1.1E-06	m/s

Job No: TAH4125

Location: Tahmoor Site No: TBF040 Borehole: TBF040 Depth Range: 82.9 -89.4 m

PACKER TEST RESULTS: K = 3.6E-07 m/s

PROJECT: TAH4125 **Site No:** TBF040 **BORE NAME:** TBF040 **HOLE DIP:** 90 **DIP Direction:** **DATE:** 19-Nov-13

Depth To Bottm Packer Test interval:	89.40	m	HEIGHT OF PRESSURE GAUGE:	1	m (above ground level)
Depth To Top Packer Test interval:	82.90	m	STATIC GROUNDWATER LEVEL:	40.7	m (below ground level)
LENGTH OF STAGE TEST:	6.50	m	SURFACE R.L.		m
BORE DIAMETER:	96	mm			

Recorded flow readings at indicated applied pressure heads.

Stage 1

Gauge Pressure	150	(kPa)
Gauge Pressure	15.29	(m)
Static Pressure	46.1	(m)
Head without loss correction	61.35	(m)
Head loss	0.10	(m)
High flow pressure calibration	0.00	(m)
Total Head	61.25	(m)

Minutes of test	Flowmet read (L)	Flow (L/min)
0	415	
1	425.5	10.5
2	435.5	10
3	445.5	10
4	455.5	10
5	465.5	10
6	475.5	10
7	486	10.5
8	496	10
9	506.5	10.5
10	516.5	10

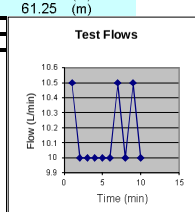

Arithmatic average = 10.15 (L/min)
Adopted average = 10.5 (L/min)

Stage 2

Gauge Pressure	300	(kPa)
Gauge Pressure	30.58	(m)
Static Pressure	46.1	(m)
Head without loss correction	76.64	(m)
Head loss	0.13	(m)
High flow pressure calibration	0.00	(m)
Total Head	76.51	(m)

Minutes of test	Flowmet read (L)	Flow (L/min)
0	531	
1	543	12
2	555.5	12.5
3	568	12.5
4	580	12
5	592.5	12.5
6	604.5	12
7	616.5	12
8	628.5	12
9	640.5	12
10	653	12.5

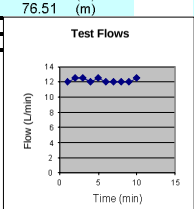

Arithmatic average = 12.2 (L/min)
Adopted average = 12.2 (L/min)

Stage 3

Gauge Pressure	450	(kPa)
Gauge Pressure	45.87	(m)
Static Pressure	46.1	(m)
Head without loss correction	91.93	(m)
Head loss	0.19	(m)
High flow pressure calibration	0.00	(m)
Total Head	91.74	(m)

Minutes of test	Flowmet read (L)	Flow (L/min)
0	669	
1	683.5	14.5
2	698	14.5
3	713	15
4	728	15
5	742.5	14.5
6	757.5	15
7	771.5	14
8	786.5	15
9	800.5	14
10	815.5	15

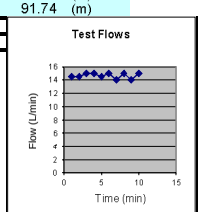

Arithmatic average = 14.65 (L/min)
Adopted average = 14.65 (L/min)

Stage 4

Gauge Pressure	300	(kPa)
Gauge Pressure	30.58	(m)
Static Pressure	46.1	(m)
Head without loss correction	76.64	(m)
Head loss	0.12	(m)
High flow pressure calibration	0.00	(m)
Total Head	76.52	(m)

Minutes of test	Flowmet read (L)	Flow (L/min)
0	826.5	
1	838	11.5
2	849.5	11.5
3	861	11.5
4	873	12
5	884.5	11.5
6	896	11.5
7	907	11
8	919	12
9	930	11
10	941.5	11.5

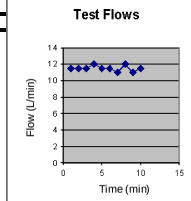

Arithmatic average = 11.5 (L/min)
Adopted average = 11.5 (L/min)

Stage 5

Gauge Pressure	150	(kPa)
Gauge Pressure	15.29	(m)
Static Pressure	46.1	(m)
Head without loss correction	61.35	(m)
Head loss	0.08	(m)
High flow pressure calibration	0.00	(m)
Total Head	61.27	(m)

Minutes of test	Flowmet read (L)	Flow (L/min)
0	950.5	
1	960	9.5
2	970	10
3	980	10
4	989.5	9.5
5	999	9.5
6	1008.5	9.5
7	1018	9.5
8	1028	10
9	1037.5	9.5
10	1047	9.5

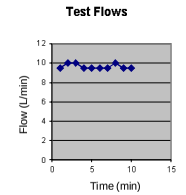

Arithmatic average = 9.65 (L/min)
Adopted average = 9.65 (L/min)

Stage 6

Gauge Pressure	0	(kPa)
Gauge Pressure	0.00	(m)
Static Pressure	46.1	(m)
Head without loss correction	46.06	(m)
Head loss	0.00	(m)
High flow pressure calibration	0.00	(m)
Total Head	46.06	(m)

Minutes of test	Flowmet read (L)	Flow (L/min)
0	0	
1	0	0
2	0	0
3	0	0
4	0	0
5	0	0
6	0	0
7	0	0
8	0	0
9	0	0
10	0	0

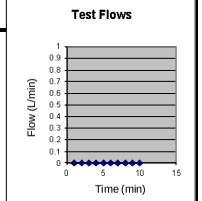

Arithmatic average = 0 (L/min)
Adopted average = 0 (L/min)

Comments:

Calculations used:

$$k = \frac{5.833}{\pi L \sin\alpha}\left(\frac{Q}{H_T}\right)\cdot 10^{-5} \quad \text{m/s} \qquad \text{(CANMET)}$$

$$k = \frac{8.333}{\pi L \sin\alpha}\left(\frac{Q}{H_T}\right)\cdot \ln\left(\frac{L}{r}\right)\cdot 10^{-4} \quad \text{m/s} \qquad \text{(HOEK \& BRAY)}$$

$$lugeon = \frac{Q}{L\sin\alpha}\cdot\frac{100}{H_T} \quad \text{l/m/min} \qquad \text{(HOULSBY)}$$

Stage	Total Head (m)	Flow (l/min)	Calculated Lugeon values: Test Pressure	Q (L/m/min)	Lugeons (L/m/min)	Chosen Lugeon (L/m/min)
1	61.25	10.50	600.87	1.62	2.64	
2	76.51	12.20	750.53	1.88	2.45	
3	91.74	14.65	899.96	2.25	2.46	2.457
4	76.52	11.50	750.68	1.77	2.31	
5	61.27	9.65	601.02	1.48	2.42	

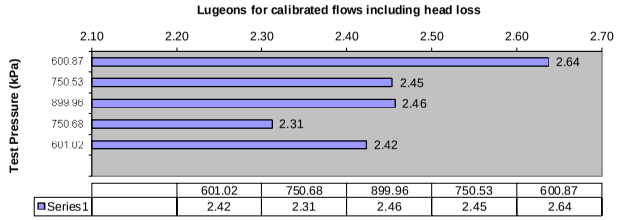

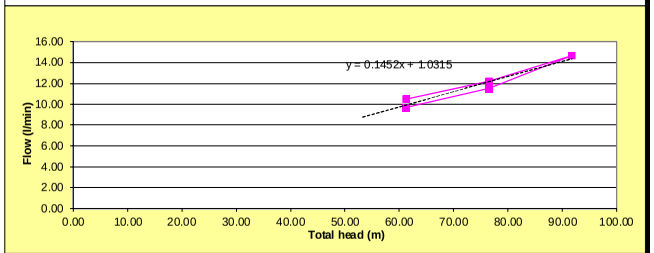

Conductivity Calculations:

MEAN Q/H$_T$	CANMET	HOEK & BRAY	MEAN LUGEONS 2.46	
0.159	4.5E-07	3.2E-07	3.2E-07	m/s
Mean Conductivity		K =	3.6E-07	m/s

Job No: TAH4125

Location: Tahmoor Site No: TBF040 Borehole: TBF040 Depth Range: 88.9 -95.4 m

PACKER TEST RESULTS: K = 3.3E-09 m/s

PROJECT: TAH4125 **Site No:** TBF040 **BORE NAME:** TBF040 **HOLE DIP:** 90 **DIP Direction:** **DATE:** 19-Nov-13

Depth To Bottm Packer Test interval:	95.40	m	HEIGHT OF PRESSURE GAUGE:	1	m (above ground level)
Depth To Top Packer Test interval:	88.90	m	STATIC GROUNDWATER LEVEL:	40.7	m (below ground level)
LENGTH OF STAGE TEST:	6.50	m	SURFACE R.L.		m
BORE DIAMETER:	96	mm			

Recorded flow readings at indicated applied pressure heads.

Stage 1

Gauge Pressure	150	(kPa)
Gauge Pressure	15.29	(m)
Static Pressure	46.4	(m)
Head without loss correction	61.65	(m)
Head loss	0.00	(m)
High flow pressure calibration	0.00	(m)
Total Head	61.65	(m)

Minutes of test	Flowmet read (L)	Flow (L/min)
0	70.3	
1	70.4	0.1
2	70.5	0.1
3	70.6	0.1
4	70.6	0
5	70.7	0.1
6	70.8	0.1
7	70.8	0
8	70.9	0.1
9	70.9	0
10	71	0.1

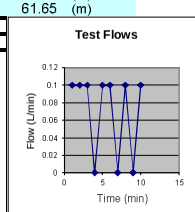

Arithmatic average = 0.07 (L/min)
Adopted average = 0.07 (L/min)

Stage 2

Gauge Pressure	300	(kPa)
Gauge Pressure	30.58	(m)
Static Pressure	46.4	(m)
Head without loss correction	76.94	(m)
Head loss	0.00	(m)
High flow pressure calibration	0.00	(m)
Total Head	76.94	(m)

Minutes of test	Flowmet read (L)	Flow (L/min)
0	71.1	
1	71.2	0.1
2	71.4	0.2
3	71.5	0.1
4	71.6	0.1
5	71.7	0.1
6	71.8	0.1
7	72	0.2
8	72.1	0.1
9	72.2	0.1
10	72.3	0.1

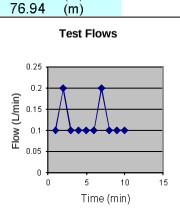

Arithmatic average = 0.12 (L/min)
Adopted average = 0.12 (L/min)

Stage 3

Gauge Pressure	450	(kPa)
Gauge Pressure	45.87	(m)
Static Pressure	46.4	(m)
Head without loss correction	92.23	(m)
Head loss	0.00	(m)
High flow pressure calibratior	0.00	(m)
Total Head	92.23	(m)

Minutes of test	Flowmet read (L)	Flow (L/min)
0	72.5	
1	72.7	0.2
2	72.9	0.2
3	73.2	0.3
4	73.4	0.2
5	73.6	0.2
6	73.8	0.2
7	74	0.2
8	74.2	0.2
9	74.5	0.3
10	74.7	0.2

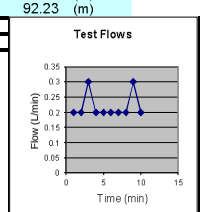

Arithmatic average = 0.22 (L/min)
Adopted average = 0.22 (L/min)

Stage 4

Gauge Pressure	300	(kPa)
Gauge Pressure	30.58	(m)
Static Pressure	46.4	(m)
Head without loss correction	76.94	(m)
Head loss	0.00	(m)
High flow pressure calibration	0.00	(m)
Total Head	76.94	(m)

Minutes of test	Flowmet read (L)	Flow (L/min)
0	74.9	
1	75	0.1
2	75.1	0.1
3	75.2	0.1
4	75.3	0.1
5	75.4	0.1
6	75.5	0.1
7	75.6	0.1
8	75.7	0.1
9	75.8	0.1
10	75.9	0.1

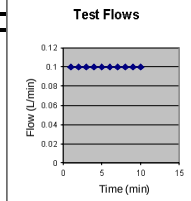

Arithmatic average = 0.1 (L/min)
Adopted average = 0.1 (L/min)

Stage 5

Gauge Pressure	150	(kPa)
Gauge Pressure	15.29	(m)
Static Pressure	46.4	(m)
Head without loss correction	61.65	(m)
Head loss	0.00	(m)
High flow pressure calibration	0.00	(m)
Total Head	61.65	(m)

Minutes of test	Flowmet read (L)	Flow (L/min)
0	75.9	
1	75.9	0
2	75.9	0
3	75.9	0
4	75.9	0
5	75.9	0
6	76	0.1
7	76	0
8	76	0
9	76	0
10	76	0

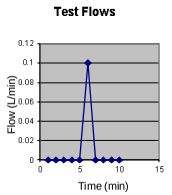

Arithmatic average = 0.01 (L/min)
Adopted average = 0.01 (L/min)

Stage 6

Gauge Pressure	0	(kPa)
Gauge Pressure	0.00	(m)
Static Pressure	46.4	(m)
Head without loss correction	46.36	(m)
Head loss	0.00	(m)
High flow pressure calibratior	0.00	(m)
Total Head	46.36	(m)

Minutes of test	Flowmet read (L)	Flow (L/min)
0	0	
1	0	0
2	0	0
3	0	0
4	0	0
5	0	0
6	0	0
7	0	0
8	0	0
9	0	0
10	0	0

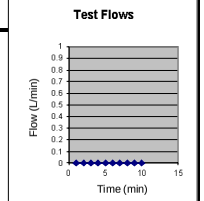

Arithmatic average = 0 (L/min)
Adopted average = 0 (L/min)

Comments:

Calculations used:

$$k = \frac{5.833}{\pi L \sin\alpha}\left(\frac{Q}{H_T}\right)\cdot 10^{-5} \text{ m/s} \quad \text{(CANMET)}$$

$$k = \frac{8.333}{\pi L \sin\alpha}\left(\frac{Q}{H_T}\right)\cdot \ln\left(\frac{L}{r}\right)\cdot 10^{-4} \text{ m/s} \quad \text{(HOEK \& BRAY)}$$

$$lugeon = \frac{Q}{L \sin\alpha}\cdot\frac{100}{H_T} \text{ l/m/min} \quad \text{(HOULSBY)}$$

Stage	Total Head (m)	Flow (l/min)	Calculated Lugeon values: Test Pressure	Q (L/m/min)	Lugeons (L/m/min)	Chosen Lugeon (L/m/min)
1	61.65	0.07	604.77	0.01	0.02	
2	76.94	0.12	754.77	0.02	0.02	
3	92.23	0.22	904.77	0.03	0.04	0.020
4	76.94	0.10	754.77	0.02	0.02	
5	61.65	0.01	604.77	0.00	0.00	

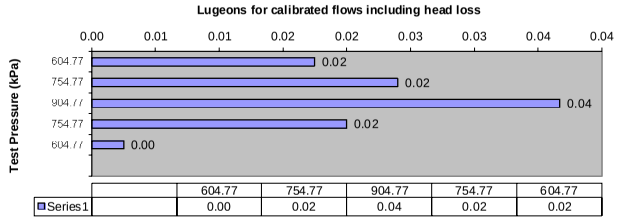

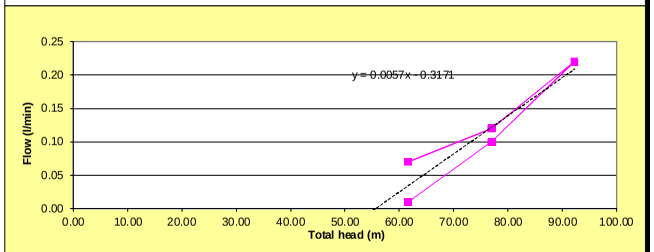

Conductivity Calculations:

MEAN Q/H$_T$	CANMET	HOEK & BRAY	MEAN LUGEONS 0.02	
0.002	4.3E-09	3.0E-09	2.6E-09	m/s
Mean Conductivity		K =	3.3E-09	m/s

Job No: TAH4125

Location: Tahmoor Site No: TBF040 Borehole: TBF040 Depth Range: 94.9 -101.4 m

PACKER TEST RESULTS: K = 2.9E-07 m/s

PROJECT: TAH4125 **Site No:** TBF040 **BORE NAME:** TBF040 **HOLE DIP:** 90 **DIP Direction:** **DATE:** 19-Nov-13

Depth To Bottm Packer Test interval:	101.40	m	HEIGHT OF PRESSURE GAUGE:	1	m (above ground level)
Depth To Top Packer Test interval:	94.90	m	STATIC GROUNDWATER LEVEL:	40.7	m (below ground level)
LENGTH OF STAGE TEST:	6.50	m	SURFACE R.L.		m
BORE DIAMETER:	96	mm			

Recorded flow readings at indicated applied pressure heads.

Stage 1

Gauge Pressure	150	(kPa)
Gauge Pressure	15.29	(m)
Static Pressure	46.7	(m)
Head without loss correction	61.95	(m)
Head loss	0.06	(m)
High flow pressure calibration	0.00	(m)
Total Head	61.89	(m)

Minutes of test	Flowmet read (L)	Flow (L/min)
0	604	
1	612	8
2	620.5	8.5
3	629	8.5
4	637.1	8.1
5	645.2	8.1
6	653	7.8
7	661	8
8	669	8
9	677.1	8.1
10	685	7.9

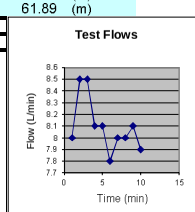

Arithmatic average = 8.1 (L/min)
Adopted average = 8.1 (L/min)

Stage 2

Gauge Pressure	300	(kPa)
Gauge Pressure	30.58	(m)
Static Pressure	46.7	(m)
Head without loss correction	77.24	(m)
Head loss	0.09	(m)
High flow pressure calibration	0.00	(m)
Total Head	77.15	(m)

Minutes of test	Flowmet read (L)	Flow (L/min)
0	696	
1	706.5	10.5
2	717	10.5
3	727.5	10.5
4	738	10.5
5	748.5	10.5
6	758.5	10
7	768.5	10
8	778	9.5
9	788	10
10	797.5	9.5

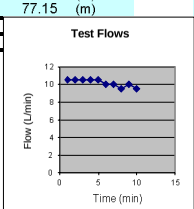

Arithmatic average = 10.15 (L/min)
Adopted average = 10.15 (L/min)

Stage 3

Gauge Pressure	450	(kPa)
Gauge Pressure	45.87	(m)
Static Pressure	46.7	(m)
Head without loss correction	92.53	(m)
Head loss	0.12	(m)
High flow pressure calibratior	0.00	(m)
Total Head	92.41	(m)

Minutes of test	Flowmet read (L)	Flow (L/min)
0	823	
1	835	12
2	847	12
3	858.5	11.5
4	870	11.5
5	882	12
6	893.5	11.5
7	905.5	12
8	917	11.5
9	929	12
10	940.5	11.5

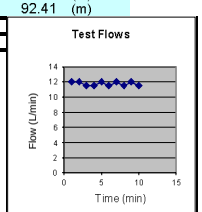

Arithmatic average = 11.75 (L/min)
Adopted average = 11.75 (L/min)

Stage 4

Gauge Pressure	300	(kPa)
Gauge Pressure	30.58	(m)
Static Pressure	46.7	(m)
Head without loss correction	77.24	(m)
Head loss	0.07	(m)
High flow pressure calibration	0.00	(m)
Total Head	77.16	(m)

Minutes of test	Flowmet read (L)	Flow (L/min)
0	946	
1	955.5	9.5
2	964.5	9
3	974	9.5
4	983	9
5	992	9
6	1001	9
7	1010.5	9.5
8	1019.5	9
9	1028.5	9
10	1038	9.5

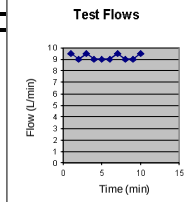

Arithmatic average = 9.2 (L/min)
Adopted average = 9.2 (L/min)

Stage 5

Gauge Pressure	150	(kPa)
Gauge Pressure	15.29	(m)
Static Pressure	46.7	(m)
Head without loss correction	61.95	(m)
Head loss	0.04	(m)
High flow pressure calibration	0.00	(m)
Total Head	61.90	(m)

Minutes of test	Flowmet read (L)	Flow (L/min)
0	41	
1	48.5	7.5
2	55.5	7
3	62.5	7
4	69.5	7
5	76.5	7
6	83.5	7
7	90.5	7
8	98	7.5
9	105	7
10	112	7

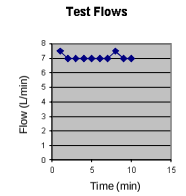

Arithmatic average = 7.1 (L/min)
Adopted average = 7.1 (L/min)

Stage 6

Gauge Pressure	0	(kPa)
Gauge Pressure	0.00	(m)
Static Pressure	46.7	(m)
Head without loss correction	46.66	(m)
Head loss	0.00	(m)
High flow pressure calibratior	0.00	(m)
Total Head	46.66	(m)

Minutes of test	Flowmet read (L)	Flow (L/min)
0	0	
1	0	0
2	0	0
3	0	0
4	0	0
5	0	0
6	0	0
7	0	0
8	0	0
9	0	0
10	0	0

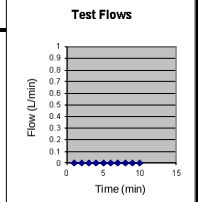

Arithmatic average = 0 (L/min)
Adopted average = 0 (L/min)

Comments:

Calculations used:

$$k = \frac{5.833}{\pi L \sin\alpha}\left(\frac{Q}{H_T}\right)\cdot 10^{-5} \quad \text{m/s} \qquad \text{(CANMET)}$$

$$k = \frac{8.333}{\pi L \sin\alpha}\left(\frac{Q}{H_T}\right)\cdot \ln\left(\frac{L}{r}\right)\cdot 10^{-4} \quad \text{m/s} \qquad \text{(HOEK \& BRAY)}$$

$$lugeon = \frac{Q}{L \sin\alpha}\cdot\frac{100}{H_T} \quad \text{l/m/min} \qquad \text{(HOULSBY)}$$

Stage	Total Head (m)	Flow (l/min)	Calculated Lugeon values: Test Pressure	Q (L/m/min)	Lugeons (L/m/min)	Chosen Lugeon (L/m/min)
1	61.89	8.10	607.14	1.25	2.01	
2	77.15	10.15	756.82	1.56	2.02	
3	92.41	11.75	906.51	1.81	1.96	1.919
4	77.16	9.20	756.98	1.42	1.83	
5	61.90	7.1	607.27	1.09	1.76	

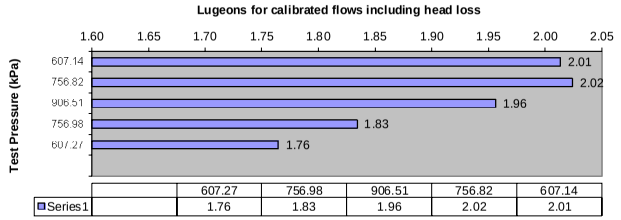

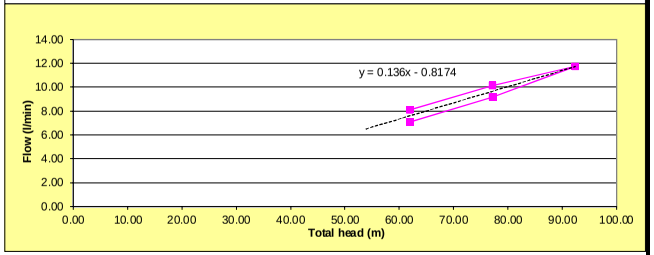

Conductivity Calculations:

MEAN Q/H$_T$	CANMET	HOEK & BRAY	MEAN LUGEONS	
			1.92	
0.125	3.6E-07	2.5E-07	2.5E-07	m/s
Mean Conductivity		K =	2.9E-07	m/s

Job No: TAH4125

Location: Tahmoor Site No: TBF040 Borehole: TBF040 Depth Range: 100.9 -107.4 m

PACKER TEST RESULTS: K = 2.2E-06 m/s

PROJECT: TAH4125 **Site No:** TBF040 **BORE NAME:** TBF040 **HOLE DIP:** 90 **DIP Direction:** **DATE:** 20-Nov-13

Depth To Bottm Packer Test interval:	107.40	m	HEIGHT OF PRESSURE GAUGE:	1	m (above ground level)
Depth To Top Packer Test interval:	100.90	m	STATIC GROUNDWATER LEVEL:	40.7	m (below ground level)
LENGTH OF STAGE TEST:	6.50	m	SURFACE R.L.		m
BORE DIAMETER:	96	mm			

Recorded flow readings at indicated applied pressure heads.

Stage 1

Gauge Pressure	100	(kPa)
Gauge Pressure	10.19	(m)
Static Pressure	47.0	(m)
Head without loss correction	57.15	(m)
Head loss	1.97	(m)
High flow pressure calibration	0.00	(m)
Total Head	55.18	(m)

Minutes of test	Flowmet read (L)	Flow (L/min)
0	4475	
1	4522	47
2	4569	47
3	4616	47
4	4663	47
5	4710	47
6	4757	47
7	4804	47
8	4852	48
9	4900	48
10	4947	47

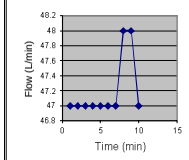

Arithmatic average = 47.2 (L/min)
Adopted average = 47.2 (L/min)

Stage 2

Gauge Pressure	200	(kPa)
Gauge Pressure	20.39	(m)
Static Pressure	47.0	(m)
Head without loss correction	67.34	(m)
Head loss	3.01	(m)
High flow pressure calibration	0.00	(m)
Total Head	64.33	(m)

Minutes of test	Flowmet read (L)	Flow (L/min)
0	5052	
1	5110	58
2	5167	57
3	5226	59
4	5284	58
5	5345	61
6	5402	57
7	5461	59
8	5519	58
9	5578	59
10	5636	58

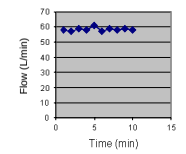

Arithmatic average = 58.4 (L/min)
Adopted average = 58.4 (L/min)

Stage 3

Gauge Pressure	300	(kPa)
Gauge Pressure	30.58	(m)
Static Pressure	47.0	(m)
Head without loss correction	77.54	(m)
Head loss	4.01	(m)
High flow pressure calibratior	0.00	(m)
Total Head	73.53	(m)

Minutes of test	Flowmet read (L)	Flow (L/min)
0	5704	
1	5769	65
2	5836	67
3	5903	67
4	5970	67
5	6038	68
6	6106	68
7	6175	69
8	6242	67
9	6311	69
10	6378	67

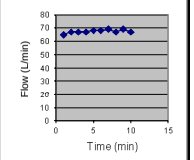

Arithmatic average = 67.4 (L/min)
Adopted average = 67.4 (L/min)

Stage 4

Gauge Pressure	200	(kPa)
Gauge Pressure	20.39	(m)
Static Pressure	47.0	(m)
Head without loss correction	67.34	(m)
Head loss	3.54	(m)
High flow pressure calibration	0.00	(m)
Total Head	63.81	(m)

Minutes of test	Flowmet read (L)	Flow (L/min)
0	6442	
1	6506	64
2	6570	64
3	6633	63
4	6697	64
5	6759	62
6	6822	63
7	6885	63
8	6948	63
9	7012	64
10	7075	63

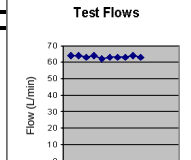

Arithmatic average = 63.3 (L/min)
Adopted average = 63.3 (L/min)

Stage 5

Gauge Pressure	100	(kPa)
Gauge Pressure	10.19	(m)
Static Pressure	47.0	(m)
Head without loss correction	57.15	(m)
Head loss	2.90	(m)
High flow pressure calibration	0.00	(m)
Total Head	54.25	(m)

Minutes of test	Flowmet read (L)	Flow (L/min)
0	7197	
1	7253	56
2	7311	58
3	7368	57
4	7425	57
5	7483	58
6	7540	57
7	7599	59
8	7656	57
9	7712	56
10	7770	58

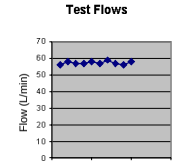

Arithmatic average = 57.3 (L/min)
Adopted average = 57.3 (L/min)

Stage 6

Gauge Pressure	0	(kPa)
Gauge Pressure	0.00	(m)
Static Pressure	47.0	(m)
Head without loss correction	46.96	(m)
Head loss	0.00	(m)
High flow pressure calibratior	0.00	(m)
Total Head	46.96	(m)

Minutes of test	Flowmet read (L)	Flow (L/min)
0	0	
1	0	0
2	0	0
3	0	0
4	0	0
5	0	0
6	0	0
7	0	0
8	0	0
9	0	0
10	0	0

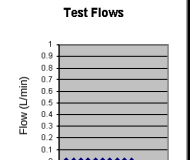

Arithmatic average = 0 (L/min)
Adopted average = 0 (L/min)

Comments:

Calculations used:

$$k = \frac{5.833}{\pi L \sin\alpha}\left(\frac{Q}{H_T}\right)\cdot 10^{-5} \quad \text{m/s} \qquad \text{(CANMET)}$$

$$k = \frac{8.333}{\pi L \sin\alpha}\left(\frac{Q}{H_T}\right)\cdot \ln\left(\frac{L}{r}\right)\cdot 10^{-4} \quad \text{m/s} \qquad \text{(HOEK \& BRAY)}$$

$$lugeon = \frac{Q}{L\sin\alpha}\cdot\frac{100}{H_T} \quad \text{l/m/min} \qquad \text{(HOULSBY)}$$

Stage	Total Head (m)	Flow (l/min)	Calculated Lugeon values: Test Pressure	Q (L/m/min)	Lugeons (L/m/min)	Chosen Lugeon (L/m/min)
1	55.18	47.20	541.35	7.26	13.16	
2	64.33	58.40	631.10	8.98	13.97	
3	73.53	67.40	721.28	10.37	14.10	14.548
4	63.81	63.30	625.93	9.74	15.26	
5	54.25	57.3	532.20	8.82	16.25	

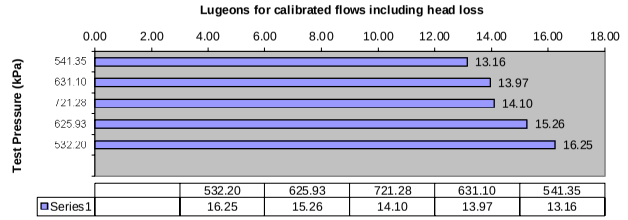

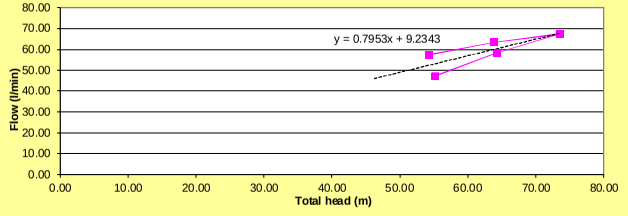

Conductivity Calculations:

MEAN Q/H$_T$	CANMET	HOEK & BRAY	MEAN LUGEONS 14.55	
0.942	2.7E-06	1.9E-06	1.9E-06	m/s
Mean Conductivity		K =	2.2E-06	m/s

Job No: TAH4125

Location: Tahmoor Site No: TBF040 Borehole: TBF040 Depth Range: 106.9 -113.4 m

PACKER TEST RESULTS: K = 2.4E-06 m/s

PROJECT: TAH4125 **Site No:** TBF040 **BORE NAME:** TBF040 **HOLE DIP:** 90 **DIP Direction:** **DATE:** 20-Nov-13

Depth To Bottm Packer Test interval:	113.40	m	HEIGHT OF PRESSURE GAUGE:	1	m (above ground level)
Depth To Top Packer Test interval:	106.90	m	STATIC GROUNDWATER LEVEL:	40.7	m (below ground level)
LENGTH OF STAGE TEST:	6.50	m	SURFACE R.L.		m
BORE DIAMETER:	96	mm			

Recorded flow readings at indicated applied pressure heads.

Stage 1

Gauge Pressure	180	(kPa)
Gauge Pressure	18.35	(m)
Static Pressure	47.3	(m)
Head without loss correction	65.61	(m)
Head loss	5.60	(m)
High flow pressure calibration	0.00	(m)
Total Head	60.01	(m)

Minutes of test	Flowmet read (L)	Flow (L/min)
0	8755	
1	8830	75
2	8901	71
3	8980	79
4	9058	78
5	9140	82
6	9219	79
7	9301	82
8	9385	84
9	9468	83
10	9551	83

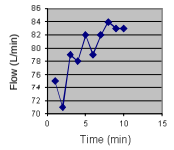

Arithmatic average = 79.6 (L/min)
Adopted average = 79.6 (L/min)

Stage 2

Gauge Pressure	360	(kPa)
Gauge Pressure	36.70	(m)
Static Pressure	47.3	(m)
Head without loss correction	83.95	(m)
Head loss	6.38	(m)
High flow pressure calibration	0.00	(m)
Total Head	77.57	(m)

Minutes of test	Flowmet read (L)	Flow (L/min)
0	9645	
1	9730	85
2	9815	85
3	9901	86
4	9986	85
5	10072	86
6	10156	84
7	10240	84
8	10325	85
9	10410	85
10	10495	85

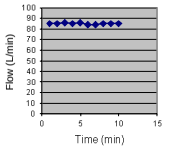

Arithmatic average = 85 (L/min)
Adopted average = 85 (L/min)

Stage 3

Gauge Pressure	540	(kPa)
Gauge Pressure	55.05	(m)
Static Pressure	47.3	(m)
Head without loss correction	102.30	(m)
Head loss	7.22	(m)
High flow pressure calibratio	0.00	(m)
Total Head	95.08	(m)

Minutes of test	Flowmet read (L)	Flow (L/min)
0	718	
1	808	90
2	898	90
3	989	91
4	1079	90
5	1170	91
6	1260	90
7	1351	91
8	1441	90
9	1531	90
10	1622	91

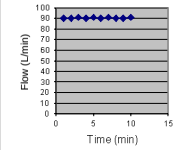

Arithmatic average = 90.4 (L/min)
Adopted average = 90.4 (L/min)

Stage 4

Gauge Pressure	360	(kPa)
Gauge Pressure	36.70	(m)
Static Pressure	47.3	(m)
Head without loss correction	83.95	(m)
Head loss	4.89	(m)
High flow pressure calibration	0.00	(m)
Total Head	79.06	(m)

Minutes of test	Flowmet read (L)	Flow (L/min)
0	1651	
1	1725	74
2	1799	74
3	1874	75
4	1948	74
5	2022	74
6	2096	74
7	2171	75
8	2246	75
9	2320	74
10	2395	75

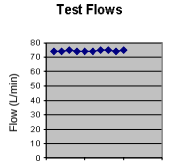

Arithmatic average = 74.4 (L/min)
Adopted average = 74.4 (L/min)

Stage 5

Gauge Pressure	180	(kPa)
Gauge Pressure	18.35	(m)
Static Pressure	47.3	(m)
Head without loss correction	65.61	(m)
Head loss	4.34	(m)
High flow pressure calibration	0.00	(m)
Total Head	61.26	(m)

Minutes of test	Flowmet read (L)	Flow (L/min)
0	2470	
1	2540	70
2	2610	70
3	2680	70
4	2751	71
5	2820	69
6	2890	70
7	2961	71
8	3030	69
9	3100	70
10	3171	71

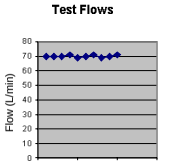

Arithmatic average = 70.1 (L/min)
Adopted average = 70.1 (L/min)

Stage 6

Gauge Pressure	0	(kPa)
Gauge Pressure	0.00	(m)
Static Pressure	47.3	(m)
Head without loss correction	47.26	(m)
Head loss	0.00	(m)
High flow pressure calibratio	0.00	(m)
Total Head	47.26	(m)

Minutes of test	Flowmet read (L)	Flow (L/min)
0	0	
1	0	0
2	0	0
3	0	0
4	0	0
5	0	0
6	0	0
7	0	0
8	0	0
9	0	0
10	0	0

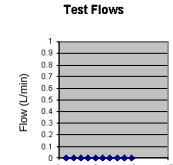

Arithmatic average = 0 (L/min)
Adopted average = 0 (L/min)

Comments:

Calculations used:

$$k = \frac{5.833}{\pi L \sin\alpha}\left(\frac{Q}{H_T}\right)\cdot 10^{-5} \quad \text{m/s} \qquad \text{(CANMET)}$$

$$k = \frac{8.333}{\pi L \sin\alpha}\left(\frac{Q}{H_T}\right)\cdot \ln\left(\frac{L}{r}\right)\cdot 10^{-4} \quad \text{m/s} \qquad \text{(HOEK \& BRAY)}$$

$$lugeon = \frac{Q}{L \sin\alpha}\cdot\frac{100}{H_T} \quad \text{l/m/min} \qquad \text{(HOULSBY)}$$

Stage	Total Head (m)	Flow (l/min)	Calculated Lugeon values: Test Pressure	Q (L/m/min)	Lugeons (L/m/min)	Chosen Lugeon (L/m/min)
1	60.01	79.60	588.68	12.25	20.41	
2	77.57	85.00	760.98	13.08	16.86	
3	95.08	90.40	932.77	13.91	14.63	16.794
4	79.06	74.40	775.62	11.45	14.48	
5	61.26	70.1	601.01	10.78	17.60	

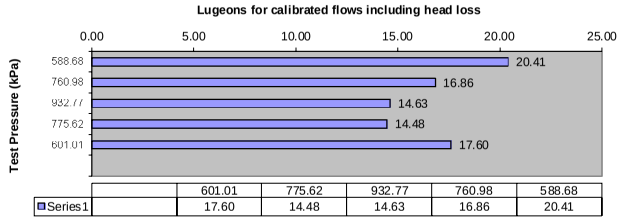

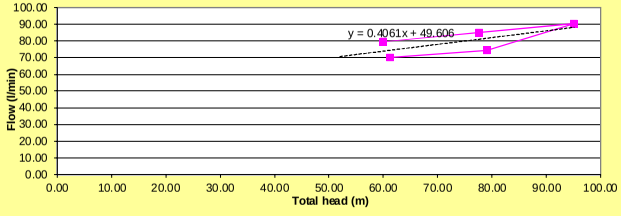

Conductivity Calculations:

MEAN Q/H$_T$	CANMET	HOEK & BRAY	MEAN LUGEONS	
1.052	3.0E-06	2.1E-06	2.2E-06	m/s
	Mean Conductivity	K =	2.4E-06	m/s

Job No: TAH4125

Location: Carborough Downs Site No: N/A Borehole: CD512C Depth Range: 112.9 -119.4 m

PACKER TEST RESULTS: K = 2.2E-05 m/s

PROJECT: TAH4125 **Site No:** N/A **BORE NAME:** CD512C **HOLE DIP:** 90 **DIP Direction:** **DATE:** 20-Nov-13

Depth To Bottm Packer Test interval:	119.40	m	HEIGHT OF PRESSURE GAUGE:	1	m (above ground level)
Depth To Top Packer Test interval:	112.90	m	STATIC GROUNDWATER LEVEL:	40.7	m (below ground level)
LENGTH OF STAGE TEST:	6.50	m	SURFACE R.L.		m
BORE DIAMETER:	96	mm			

Recorded flow readings at indicated applied pressure heads.

Stage 1

Gauge Pressure	100	(kPa)
Gauge Pressure	10.19	(m)
Static Pressure	47.6	(m)
Head without loss correction	57.75	(m)
Head loss	0.00	(m)
High flow pressure calibration	0.00	(m)
Total Head	57.75	(m)

Minutes of test	Flowmet read (L)	Flow (L/min)
0	6010	
1	0	-6010
2	0	0
3	0	0
4	0	0
5	0	0
6	0	0
7	0	0
8	0	0
9	0	0
10	0	0

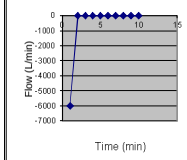

Arithmatic average = -601 (L/min)
Adopted average = 0 (L/min)

Stage 2

Gauge Pressure	200	(kPa)
Gauge Pressure	20.39	(m)
Static Pressure	47.6	(m)
Head without loss correction	67.94	(m)
Head loss	0.00	(m)
High flow pressure calibration	0.00	(m)
Total Head	67.94	(m)

Minutes of test	Flowmet read (L)	Flow (L/min)
0	0	
1	0	0
2	0	0
3	0	0
4	0	0
5	0	0
6	0	0
7	0	0
8	0	0
9	0	0
10	0	0

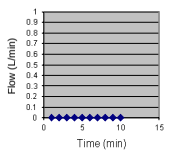

Arithmatic average = 0 (L/min)
Adopted average = 0 (L/min)

Stage 3

Gauge Pressure	300	(kPa)
Gauge Pressure	30.58	(m)
Static Pressure	47.6	(m)
Head without loss correction	78.14	(m)
Head loss	0.00	(m)
High flow pressure calibration	0.00	(m)
Total Head	78.14	(m)

Minutes of test	Flowmet read (L)	Flow (L/min)
0	0	
1	0	0
2	0	0
3	0	0
4	0	0
5	0	0
6	0	0
7	0	0
8	0	0
9	0	0
10	0	0

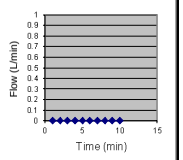

Arithmatic average = 0 (L/min)
Adopted average = 0 (L/min)

Stage 4

Gauge Pressure	200	(kPa)
Gauge Pressure	20.39	(m)
Static Pressure	47.6	(m)
Head without loss correction	67.94	(m)
Head loss	0.00	(m)
High flow pressure calibration	0.00	(m)
Total Head	67.94	(m)

Minutes of test	Flowmet read (L)	Flow (L/min)
0	0	
1	0	0
2	0	0
3	0	0
4	0	0
5	0	0
6	0	0
7	0	0
8	0	0
9	0	0
10	0	0

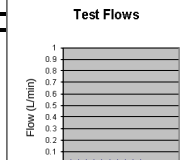

Arithmatic average = 0 (L/min)
Adopted average = 0 (L/min)

Stage 5

Gauge Pressure	100	(kPa)
Gauge Pressure	10.19	(m)
Static Pressure	47.6	(m)
Head without loss correction	57.75	(m)
Head loss	0.00	(m)
High flow pressure calibration	0.00	(m)
Total Head	57.75	(m)

Minutes of test	Flowmet read (L)	Flow (L/min)
0	0	
1	0	0
2	0	0
3	0	0
4	0	0
5	0	0
6	0	0
7	0	0
8	0	0
9	0	0
10	0	0

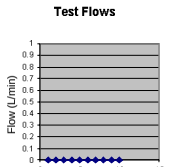

Arithmatic average = 0 (L/min)
Adopted average = 0 (L/min)

Stage 6

Gauge Pressure	0	(kPa)
Gauge Pressure	0.00	(m)
Static Pressure	47.6	(m)
Head without loss correction	47.56	(m)
Head loss	0.00	(m)
High flow pressure calibration	0.00	(m)
Total Head	47.56	(m)

Minutes of test	Flowmet read (L)	Flow (L/min)
0	0	
1	0	0
2	0	0
3	0	0
4	0	0
5	0	0
6	0	0
7	0	0
8	0	0
9	0	0
10	0	0

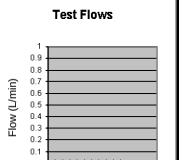

Arithmatic average = 0 (L/min)
Adopted average = 0 (L/min)

Comments:

Calculations used:

$$k = \frac{5.833}{\pi L \sin\alpha}\left(\frac{Q}{H_T}\right)\cdot 10^{-5} \quad \text{m/s} \qquad \text{(CANMET)}$$

$$k = \frac{8.333}{\pi L \sin\alpha}\left(\frac{Q}{H_T}\right)\cdot \ln\left(\frac{L}{r}\right)\cdot 10^{-4} \quad \text{m/s} \qquad \text{(HOEK \& BRAY)}$$

$$lugeon = \frac{Q}{L \sin\alpha}\cdot\frac{100}{H_T} \quad \text{l/m/min} \qquad \text{(HOULSBY)}$$

Stage	Total Head (m)	Flow (l/min)	Calculated Lugeon values: Test Pressure	Q (L/m/min)	Lugeons (L/m/min)	Chosen Lugeon (L/m/min)
1	57.75	0.00	566.54	0.00	0.00	
2	67.94	0.00	666.54	0.00	0.00	
3	78.14	0.00	766.54	0.00	0.00	0.000
4	67.94	0.00	666.54	0.00	0.00	
5	57.75	0	566.54	0.00	0.00	

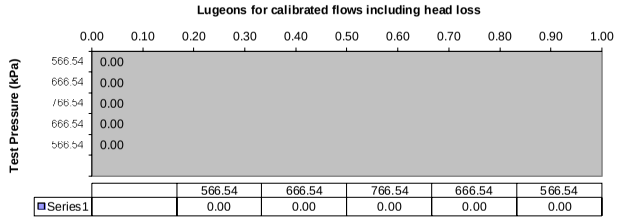

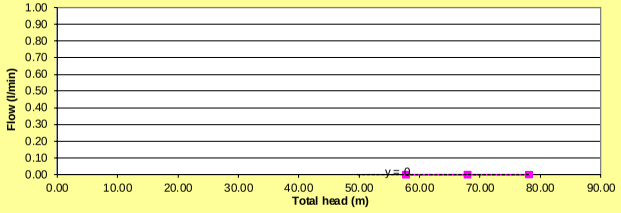

Conductivity Calculations:

MEAN Q/H$_T$	CANMET	HOEK & BRAY	MEAN LUGEONS 0.00	
0.000	0.0E+00	0.0E+00	0.0E+00	m/s
Mean Conductivity		K =	2.2E-05	m/s

Job No: TAH4125

Location: Carborough Downs Site No: N/A Borehole: CD512C Depth Range: 118.9 -125.4 m

PACKER TEST RESULTS: K = 1.3E-06 m/s

PROJECT: TAH4125 **Site No:** N/A **BORE NAME:** CD512C **HOLE DIP:** 90 **DIP Direction:** **DATE:** 21-Nov-13

Depth To Bottm Packer Test interval:	125.40	m	HEIGHT OF PRESSURE GAUGE:	1	m (above ground level)
Depth To Top Packer Test interval:	118.90	m	STATIC GROUNDWATER LEVEL:	40.7	m (below ground level)
LENGTH OF STAGE TEST:	6.50	m	SURFACE R.L.		m
BORE DIAMETER:	96	mm			

Recorded flow readings at indicated applied pressure heads.

Stage 1

Gauge Pressure	180	(kPa)
Gauge Pressure	18.35	(m)
Static Pressure	47.9	(m)
Head without loss correction	66.21	(m)
Head loss	1.09	(m)
High flow pressure calibration	0.00	(m)
Total Head	65.12	(m)

Minutes of test	Flowmet read (L)	Flow (L/min)
0	4141	
1	4180	39
2	4216	36
3	4251	35
4	4286	35
5	4320	34
6	4356	36
7	4390	34
8	4424	34
9	4458	34
10	4492	34

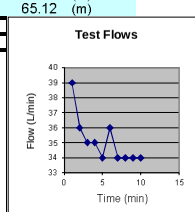

Arithmatic average = 35.1 (L/min)
Adopted average = 35.1 (L/min)

Stage 2

Gauge Pressure	360	(kPa)
Gauge Pressure	36.70	(m)
Static Pressure	47.9	(m)
Head without loss correction	84.55	(m)
Head loss	2.23	(m)
High flow pressure calibration	0.00	(m)
Total Head	82.33	(m)

Minutes of test	Flowmet read (L)	Flow (L/min)
0	4539	
1	4590	51
2	4642	52
3	4691	49
4	4742	51
5	4793	51
6	4842	49
7	4892	50
8	4942	50
9	4991	49
10	5041	50

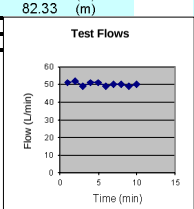

Arithmatic average = 50.2 (L/min)
Adopted average = 50.2 (L/min)

Stage 3

Gauge Pressure	540	(kPa)
Gauge Pressure	55.05	(m)
Static Pressure	47.9	(m)
Head without loss correction	102.90	(m)
Head loss	3.53	(m)
High flow pressure calibratior	0.00	(m)
Total Head	99.37	(m)

Minutes of test	Flowmet read (L)	Flow (L/min)
0	5104	
1	5168	64
2	5231	63
3	5295	64
4	5359	64
5	5424	65
6	5485	61
7	5549	64
8	5612	63
9	5673	61
10	5736	63

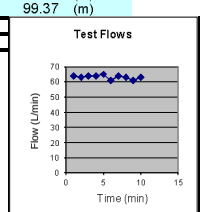

Arithmatic average = 63.2 (L/min)
Adopted average = 63.2 (L/min)

Stage 4

Gauge Pressure	360	(kPa)
Gauge Pressure	36.70	(m)
Static Pressure	47.9	(m)
Head without loss correction	84.55	(m)
Head loss	1.57	(m)
High flow pressure calibration	0.00	(m)
Total Head	82.99	(m)

Minutes of test	Flowmet read (L)	Flow (L/min)
0	5780	
1	5820	40
2	5862	42
3	5904	42
4	5946	42
5	5988	42
6	6031	43
7	6073	42
8	6116	43
9	6158	42
10	6201	43

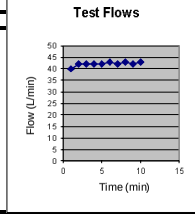

Arithmatic average = 42.1 (L/min)
Adopted average = 42.1 (L/min)

Stage 5

Gauge Pressure	180	(kPa)
Gauge Pressure	18.35	(m)
Static Pressure	47.9	(m)
Head without loss correction	66.21	(m)
Head loss	1.00	(m)
High flow pressure calibration	0.00	(m)
Total Head	65.21	(m)

Minutes of test	Flowmet read (L)	Flow (L/min)
0	6233	
1	6265	32
2	6298	33
3	6331	33
4	6365	34
5	6399	34
6	6433	34
7	6468	35
8	6502	34
9	6535	33
10	6569	34

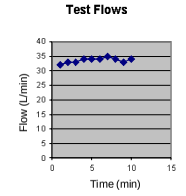

Arithmatic average = 33.6 (L/min)
Adopted average = 33.6 (L/min)

Stage 6

Gauge Pressure	0	(kPa)
Gauge Pressure	0.00	(m)
Static Pressure	47.9	(m)
Head without loss correction	47.86	(m)
Head loss	0.00	(m)
High flow pressure calibratior	0.00	(m)
Total Head	47.86	(m)

Minutes of test	Flowmet read (L)	Flow (L/min)
0	0	
1	0	0
2	0	0
3	0	0
4	0	0
5	0	0
6	0	0
7	0	0
8	0	0
9	0	0
10	0	0

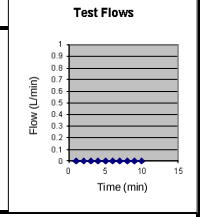

Arithmatic average = 0 (L/min)
Adopted average = 0 (L/min)

Comments:

Calculations used:

$$k = \frac{5.833}{\pi L \sin\alpha}\left(\frac{Q}{H_T}\right)\cdot 10^{-5} \text{ m/s} \quad \text{(CANMET)}$$

$$k = \frac{8.333}{\pi L \sin\alpha}\left(\frac{Q}{H_T}\right)\cdot \ln\left(\frac{L}{r}\right)\cdot 10^{-4} \text{ m/s} \quad \text{(HOEK \& BRAY)}$$

$$lugeon = \frac{Q}{L\sin\alpha}\cdot\frac{100}{H_T} \text{ l/m/min} \quad \text{(HOULSBY)}$$

Stage	Total Head (m)	Flow (l/min)	Calculated Lugeon values: Test Pressure	Q (L/m/min)	Lugeons (L/m/min)	Chosen Lugeon (L/m/min)
1	65.12	35.10	638.80	5.40	8.29	
2	82.33	50.20	807.64	7.72	9.38	
3	99.37	63.20	974.87	9.72	9.78	8.638
4	82.99	42.10	814.12	6.48	7.80	
5	65.21	33.6	639.70	5.17	7.93	

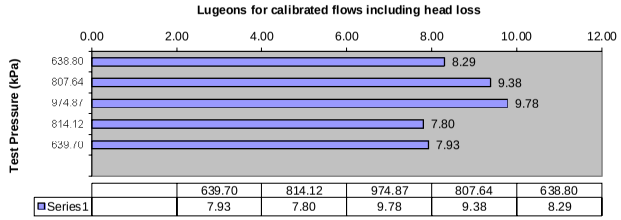

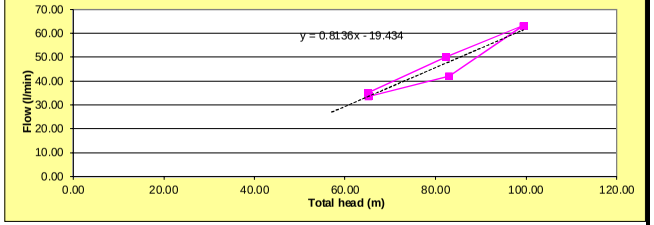

Conductivity Calculations:

MEAN Q/H$_T$	CANMET	HOEK & BRAY	MEAN LUGEONS 8.64	
0.574	1.6E-06	1.1E-06	1.1E-06	m/s
Mean Conductivity	K =	1.3E-06	m/s	

Job No: TAH4125

Location: Tahmoor Site No: TBF040 Borehole: TBF040 Depth Range: 124.9 -131.4 m

PACKER TEST RESULTS: K = 4.8E-06 m/s

PROJECT: TAH4125 **Site No:** TBF040 **BORE NAME:** TBF040 **HOLE DIP:** 90 **DIP Direction:** **DATE:** 25-Nov-13

Depth To Bottm Packer Test interval:	131.40	m	HEIGHT OF PRESSURE GAUGE:	1	m (above ground level)
Depth To Top Packer Test interval:	124.90	m	STATIC GROUNDWATER LEVEL:	40.7	m (below ground level)
LENGTH OF STAGE TEST:	6.50	m	SURFACE R.L.		m
BORE DIAMETER:	96	mm			

Recorded flow readings at indicated applied pressure heads.

Stage 1

Gauge Pressure	100	(kPa)
Gauge Pressure	10.19	(m)
Static Pressure	48.2	(m)
Head without loss correction	58.35	(m)
Head loss	0.00	(m)
High flow pressure calibration	0.00	(m)
Total Head	58.35	(m)

Minutes of test	Flowmet read (L)	Flow (L/min)
0	0	
1	0	0
2	0	0
3	0	0
4	0	0
5	0	0
6	0	0
7	0	0
8	0	0
9	0	0
10	0	0

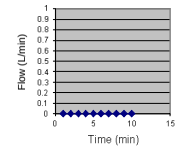

Arithmatic average = 0 (L/min)
Adopted average = 0 (L/min)

Stage 2

Gauge Pressure	200	(kPa)
Gauge Pressure	20.39	(m)
Static Pressure	48.2	(m)
Head without loss correction	68.54	(m)
Head loss	0.00	(m)
High flow pressure calibration	0.00	(m)
Total Head	68.54	(m)

Minutes of test	Flowmet read (L)	Flow (L/min)
0	0	
1	0	0
2	0	0
3	0	0
4	0	0
5	0	0
6	0	0
7	0	0
8	0	0
9	0	0
10	0	0

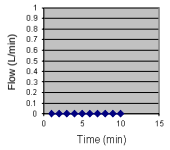

Arithmatic average = 0 (L/min)
Adopted average = 0 (L/min)

Stage 3

Gauge Pressure	300	(kPa)
Gauge Pressure	30.58	(m)
Static Pressure	48.2	(m)
Head without loss correction	78.74	(m)
Head loss	0.00	(m)
High flow pressure calibration	0.00	(m)
Total Head	78.74	(m)

Minutes of test	Flowmet read (L)	Flow (L/min)
0	0	
1	0	0
2	0	0
3	0	0
4	0	0
5	0	0
6	0	0
7	0	0
8	0	0
9	0	0
10	0	0

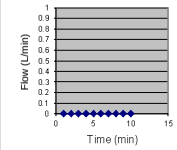

Arithmatic average = 0 (L/min)
Adopted average = 0 (L/min)

Stage 4

Gauge Pressure	200	(kPa)
Gauge Pressure	20.39	(m)
Static Pressure	48.2	(m)
Head without loss correction	68.54	(m)
Head loss	0.00	(m)
High flow pressure calibration	0.00	(m)
Total Head	68.54	(m)

Minutes of test	Flowmet read (L)	Flow (L/min)
0	0	
1	0	0
2	0	0
3	0	0
4	0	0
5	0	0
6	0	0
7	0	0
8	0	0
9	0	0
10	0	0

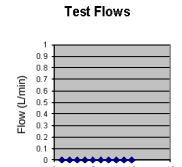

Arithmatic average = 0 (L/min)
Adopted average = 0 (L/min)

Stage 5

Gauge Pressure	100	(kPa)
Gauge Pressure	10.19	(m)
Static Pressure	48.2	(m)
Head without loss correction	58.35	(m)
Head loss	0.00	(m)
High flow pressure calibration	0.00	(m)
Total Head	58.35	(m)

Minutes of test	Flowmet read (L)	Flow (L/min)
0	0	
1	0	0
2	0	0
3	0	0
4	0	0
5	0	0
6	0	0
7	0	0
8	0	0
9	0	0
10	0	0

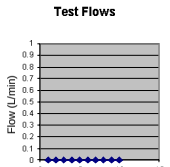

Arithmatic average = 0 (L/min)
Adopted average = 0 (L/min)

Stage 6

Gauge Pressure	0	(kPa)
Gauge Pressure	0.00	(m)
Static Pressure	48.2	(m)
Head without loss correction	48.16	(m)
Head loss	0.00	(m)
High flow pressure calibration	0.00	(m)
Total Head	48.16	(m)

Minutes of test	Flowmet read (L)	Flow (L/min)
0	0	
1	0	0
2	0	0
3	0	0
4	0	0
5	0	0
6	0	0
7	0	0
8	0	0
9	0	0
10	0	0

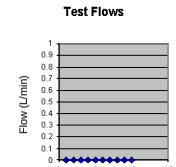

Arithmatic average = 0 (L/min)
Adopted average = 0 (L/min)

Comments:

Calculations used:

$$k = \frac{5.833}{\pi L \sin\alpha}\left(\frac{Q}{H_T}\right)\cdot 10^{-5} \quad \text{m/s} \qquad \text{(CANMET)}$$

$$k = \frac{8.333}{\pi L \sin\alpha}\left(\frac{Q}{H_T}\right)\cdot \ln\left(\frac{L}{r}\right)\cdot 10^{-4} \quad \text{m/s} \qquad \text{(HOEK \& BRAY)}$$

$$lugeon = \frac{Q}{L \sin\alpha}\cdot\frac{100}{H_T} \quad \text{l/m/min} \qquad \text{(HOULSBY)}$$

Stage	Total Head (m)	Flow (l/min)	Calculated Lugeon values: Test Pressure	Q (L/m/min)	Lugeons (L/m/min)	Chosen Lugeon (L/m/min)
1	58.35	0.00	572.43	0.00	0.00	
2	68.54	0.00	672.43	0.00	0.00	
3	78.74	0.00	772.43	0.00	0.00	0.000
4	68.54	0.00	672.43	0.00	0.00	
5	58.35	0	572.43	0.00	0.00	

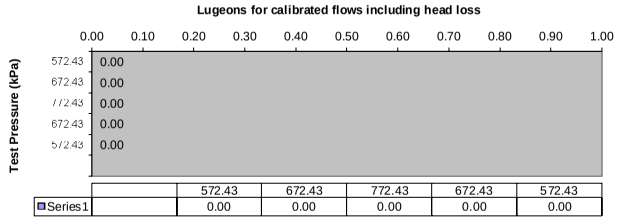

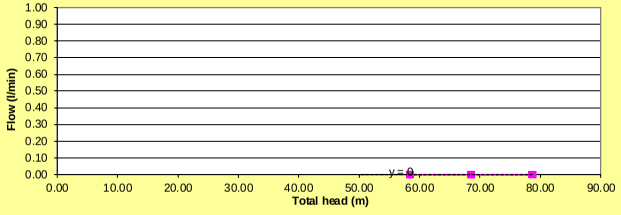

Conductivity Calculations:

MEAN Q/H$_T$	CANMET	HOEK & BRAY	MEAN LUGEONS 0.00	
0.000	0.0E+00	0.0E+00	0.0E+00	m/s

Mean Conductivity K = 4.8E-06 m/s

Job No: TAH4125

Location: Tahmoor **Site No:** TBF040 **Borehole:** TBF040 **Depth Range:** 130.9 -137.4 m

PACKER TEST RESULTS: **K =** 5.2E-06 m/s

PROJECT: TAH4125 **Site No:** TBF040 **BORE NAME:** TBF040 **HOLE DIP:** 90 **DIP Direction:** **DATE:** 26-Nov-13

Depth To Bottm Packer Test interval:	137.40	m	HEIGHT OF PRESSURE GAUGE:	1	m (above ground level)
Depth To Top Packer Test interval:	130.90	m	STATIC GROUNDWATER LEVEL:	40.7	m (below ground level)
LENGTH OF STAGE TEST:	6.50	m	SURFACE R.L.		m
BORE DIAMETER:	96	mm			

Recorded flow readings at indicated applied pressure heads.

Stage 1

Gauge Pressure	100	(kPa)
Gauge Pressure	10.19	(m)
Static Pressure	48.5	(m)
Head without loss correction	58.65	(m)
Head loss	0.00	(m)
High flow pressure calibration	0.00	(m)
Total Head	58.65	(m)

Minutes of test	Flowmet read (L)	Flow (L/min)
0	0	
1	0	0
2	0	0
3	0	0
4	0	0
5	0	0
6	0	0
7	0	0
8	0	0
9	0	0
10	0	0

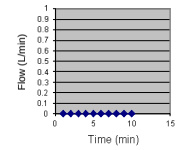

Arithmatic average = 0 (L/min)
Adopted average = 0 (L/min)

Stage 2

Gauge Pressure	200	(kPa)
Gauge Pressure	20.39	(m)
Static Pressure	48.5	(m)
Head without loss correction	68.84	(m)
Head loss	0.00	(m)
High flow pressure calibration	0.00	(m)
Total Head	68.84	(m)

Minutes of test	Flowmet read (L)	Flow (L/min)
0	0	
1	0	0
2	0	0
3	0	0
4	0	0
5	0	0
6	0	0
7	0	0
8	0	0
9	0	0
10	0	0

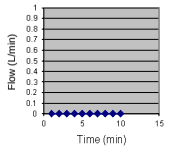

Arithmatic average = 0 (L/min)
Adopted average = 0 (L/min)

Stage 3

Gauge Pressure	300	(kPa)
Gauge Pressure	30.58	(m)
Static Pressure	48.5	(m)
Head without loss correction	79.04	(m)
Head loss	0.00	(m)
High flow pressure calibratior	0.00	(m)
Total Head	79.04	(m)

Minutes of test	Flowmet read (L)	Flow (L/min)
0	0	
1	0	0
2	0	0
3	0	0
4	0	0
5	0	0
6	0	0
7	0	0
8	0	0
9	0	0
10	0	0

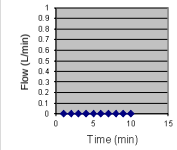

Arithmatic average = 0 (L/min)
Adopted average = 0 (L/min)

Stage 4

Gauge Pressure	200	(kPa)
Gauge Pressure	20.39	(m)
Static Pressure	48.5	(m)
Head without loss correction	68.84	(m)
Head loss	0.00	(m)
High flow pressure calibration	0.00	(m)
Total Head	68.84	(m)

Minutes of test	Flowmet read (L)	Flow (L/min)
0	0	
1	0	0
2	0	0
3	0	0
4	0	0
5	0	0
6	0	0
7	0	0
8	0	0
9	0	0
10	0	0

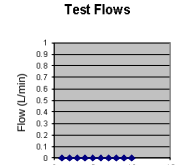

Arithmatic average = 0 (L/min)
Adopted average = 0 (L/min)

Stage 5

Gauge Pressure	100	(kPa)
Gauge Pressure	10.19	(m)
Static Pressure	48.5	(m)
Head without loss correction	58.65	(m)
Head loss	0.00	(m)
High flow pressure calibration	0.00	(m)
Total Head	58.65	(m)

Minutes of test	Flowmet read (L)	Flow (L/min)
0	0	
1	0	0
2	0	0
3	0	0
4	0	0
5	0	0
6	0	0
7	0	0
8	0	0
9	0	0
10	0	0

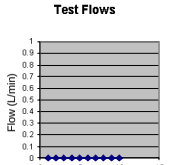

Arithmatic average = 0 (L/min)
Adopted average = 0 (L/min)

Stage 6

Gauge Pressure	0	(kPa)
Gauge Pressure	0.00	(m)
Static Pressure	48.5	(m)
Head without loss correction	48.46	(m)
Head loss	0.00	(m)
High flow pressure calibratior	0.00	(m)
Total Head	48.46	(m)

Minutes of test	Flowmet read (L)	Flow (L/min)
0	0	
1	0	0
2	0	0
3	0	0
4	0	0
5	0	0
6	0	0
7	0	0
8	0	0
9	0	0
10	0	0

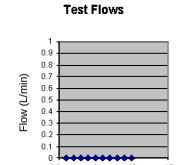

Arithmatic average = 0 (L/min)
Adopted average = 0 (L/min)

Comments:

Calculations used:

$$k = \frac{5.833}{\pi L \sin\alpha}\left(\frac{Q}{H_T}\right)\cdot 10^{-5} \quad \text{m/s} \qquad \text{(CANMET)}$$

$$k = \frac{8.333}{\pi L \sin\alpha}\left(\frac{Q}{H_T}\right)\cdot \ln\left(\frac{L}{r}\right)\cdot 10^{-4} \quad \text{m/s} \qquad \text{(HOEK \& BRAY)}$$

$$lugeon = \frac{Q}{L \sin\alpha}\cdot\frac{100}{H_T} \quad \text{l/m/min} \qquad \text{(HOULSBY)}$$

Stage	Total Head (m)	Flow (l/min)	Calculated Lugeon values: Test Pressure	Q (L/m/min)	Lugeons (L/m/min)	Chosen Lugeon (L/m/min)
1	58.65	0.00	575.37	0.00	0.00	
2	68.84	0.00	675.37	0.00	0.00	
3	79.04	0.00	775.37	0.00	0.00	0.000
4	68.84	0.00	675.37	0.00	0.00	
5	58.65	0	575.37	0.00	0.00	

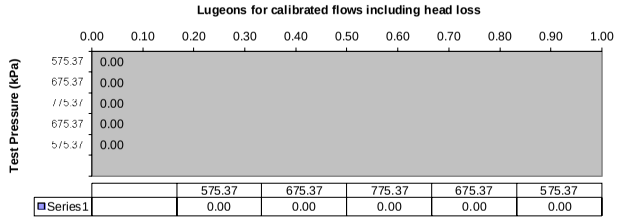

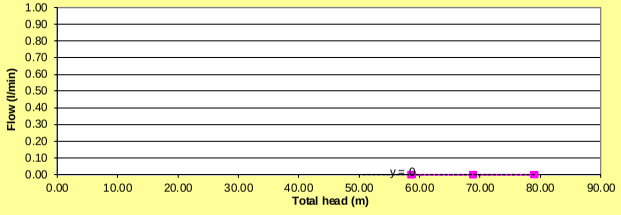

Conductivity Calculations:

MEAN Q/H$_T$	CANMET	HOEK & BRAY	MEAN LUGEONS	
0.000	0.0E+00	0.0E+00	0.0E+00	m/s
Mean Conductivity		K =	5.2E-06	m/s

Job No: TAH4125

Loca Location: Tahmoor Site No: TBF040 Borehole: TBF040 Depth Range: 165.0 -173.4 m

PACI PACKER TEST RESULTS: K = 4.8E-06 m/s

PROJECT: TAH4125 Site No: TBF040 BORE NAME: TBF040 HOLE DIP: 90 DIP Direction: DATE: 18-Dec-13

Depth To Bottm Packer Test interval:	173.40	m	HEIGHT OF PRESSURE GAUGE:	1	m (above ground level)
Depth To Top Packer Test interval:	165.00	m	STATIC GROUNDWATER LEVEL:	40.7	m (below ground level)
LENGTH OF STAGE TEST:	8.40	m	SURFACE R.L.		m
BORE DIAMETER:	96	mm			

Recorded flow readings at indicated applied pressure heads.

Stage 1

Gauge Pressure	100	(kPa)
Gauge Pressure	10.19	(m)
Static Pressure	50.2	(m)
Head without loss correction	60.40	(m)
Head loss	0.00	(m)
High flow pressure calibration	0.00	(m)
Total Head	60.40	(m)

Minutes of test	Flowmet read (L)	Flow (L/min)
0	0	
1	0	0
2	0	0
3	0	0
4	0	0
5	0	0
6	0	0
7	0	0
8	0	0
9	0	0
10	0	0

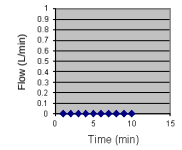

Arithmatic average = 0 (L/min)
Adopted average = 0 (L/min)

Stage 2

Gauge Pressure	200	(kPa)
Gauge Pressure	20.39	(m)
Static Pressure	50.2	(m)
Head without loss correction	70.60	(m)
Head loss	0.00	(m)
High flow pressure calibration	0.00	(m)
Total Head	70.60	(m)

Minutes of test	Flowmet read (L)	Flow (L/min)
0	0	
1	0	0
2	0	0
3	0	0
4	0	0
5	0	0
6	0	0
7	0	0
8	0	0
9	0	0
10	0	0

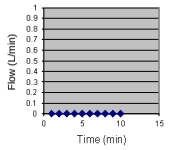

Arithmatic average = 0 (L/min)
Adopted average = 0 (L/min)

Stage 3

Gauge Pressure	300	(kPa)
Gauge Pressure	30.58	(m)
Static Pressure	50.2	(m)
Head without loss correction	80.79	(m)
Head loss	0.00	(m)
High flow pressure calibratior	0.00	(m)
Total Head	80.79	(m)

Minutes of test	Flowmet read (L)	Flow (L/min)
0	0	
1	0	0
2	0	0
3	0	0
4	0	0
5	0	0
6	0	0
7	0	0
8	0	0
9	0	0
10	0	0

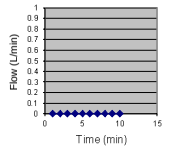

Arithmatic average = 0 (L/min)
Adopted average = 0 (L/min)

Stage 4

Gauge Pressure	200	(kPa)
Gauge Pressure	20.39	(m)
Static Pressure	50.2	(m)
Head without loss correction	70.60	(m)
Head loss	0.00	(m)
High flow pressure calibration	0.00	(m)
Total Head	70.60	(m)

Minutes of test	Flowmet read (L)	Flow (L/min)
0	0	
1	0	0
2	0	0
3	0	0
4	0	0
5	0	0
6	0	0
7	0	0
8	0	0
9	0	0
10	0	0

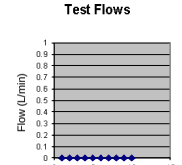

Arithmatic average = 0 (L/min)
Adopted average = 0 (L/min)

Stage 5

Gauge Pressure	100	(kPa)
Gauge Pressure	10.19	(m)
Static Pressure	50.2	(m)
Head without loss correction	60.40	(m)
Head loss	0.00	(m)
High flow pressure calibration	0.00	(m)
Total Head	60.40	(m)

Minutes of test	Flowmet read (L)	Flow (L/min)
0	0	
1	0	0
2	0	0
3	0	0
4	0	0
5	0	0
6	0	0
7	0	0
8	0	0
9	0	0
10	0	0

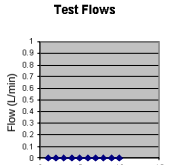

Arithmatic average = 0 (L/min)
Adopted average = 0 (L/min)

Stage 6

Gauge Pressure	0	(kPa)
Gauge Pressure	0.00	(m)
Static Pressure	50.2	(m)
Head without loss correction	50.21	(m)
Head loss	0.00	(m)
High flow pressure calibratior	0.00	(m)
Total Head	50.21	(m)

Minutes of test	Flowmet read (L)	Flow (L/min)
0	0	
1	0	0
2	0	0
3	0	0
4	0	0
5	0	0
6	0	0
7	0	0
8	0	0
9	0	0
10	0	0

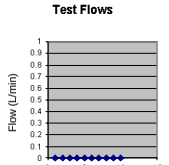

Arithmatic average = 0 (L/min)
Adopted average = 0 (L/min)

Comments:

Calculations used:

$$k = \frac{5.833}{\pi L \sin\alpha}\left(\frac{Q}{H_T}\right)\cdot 10^{-5} \quad \text{m/s} \qquad \text{(CANMET)}$$

$$k = \frac{8.333}{\pi L \sin\alpha}\left(\frac{Q}{H_T}\right)\cdot \ln\left(\frac{L}{r}\right)\cdot 10^{-4} \quad \text{m/s} \qquad \text{(HOEK \& BRAY)}$$

$$lugeon = \frac{Q}{L \sin\alpha}\cdot\frac{100}{H_T} \quad \text{l/m/min} \qquad \text{(HOULSBY)}$$

Stage	Total Head (m)	Flow (l/min)	Calculated Lugeon values: Test Pressure	Q (L/m/min)	Lugeons (L/m/min)	Chosen Lugeon (L/m/min)
1	60.40	0.00	592.56	#DIV/0!	#DIV/0!	
2	70.60	0.00	692.56	#DIV/0!	#DIV/0!	
3	80.79	0.00	792.56	#DIV/0!	#DIV/0!	#DIV/0!
4	70.60	0.00	692.56	#DIV/0!	#DIV/0!	
5	60.40	0	592.56	#DIV/0!	#DIV/0!	

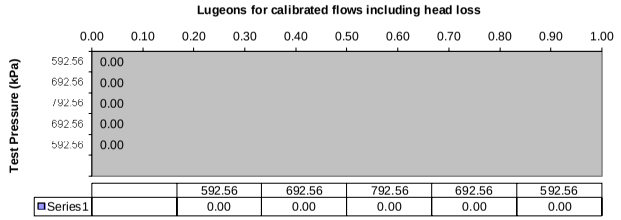

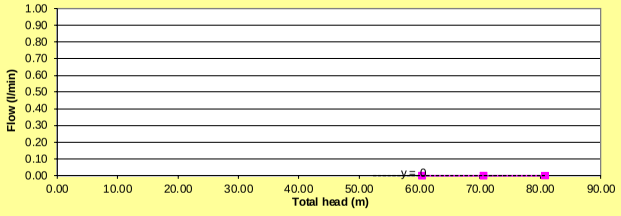

Conductivity Calculations:			MEAN	
MEAN Q/H$_T$	CANMET	HOEK & BRAY	LUGEONS #DIV/0!	
0.000	#DIV/0!	#DIV/0!	#DIV/0!	m/s
Mean Conductivity		K =	4.8E-06	m/s

Job No: TAH4125

Location: Tahmoor Site No: TBF040 Borehole: TBF040 Depth Range: 172.9 -179.4 m

PACKER TEST RESULTS: K = 1.6E-06 m/s

PROJECT: TAH4125 **Site No:** TBF040 **BORE NAME:** TBF040 **HOLE DIP:** 90 **DIP Direction:** **DATE:** 19-Dec-13

Depth To Bottm Packer Test interval:	179.40	m	HEIGHT OF PRESSURE GAUGE:	1	m (above ground level)
Depth To Top Packer Test interval:	172.90	m	STATIC GROUNDWATER LEVEL:	40.7	m (below ground level)
LENGTH OF STAGE TEST:	6.50	m	SURFACE R.L.		m
BORE DIAMETER:	96	mm			

Recorded flow readings at indicated applied pressure heads.

Stage 1

Gauge Pressure	200	(kPa)
Gauge Pressure	20.39	(m)
Static Pressure	50.6	(m)
Head without loss correction	70.94	(m)
Head loss	2.12	(m)
High flow pressure calibration	0.00	(m)
Total Head	68.82	(m)

Minutes of test	Flowmet read (L)	Flow (L/min)
0	720	
1	771	51
2	822	51
3	870	48
4	918	48
5	966	48
6	1015	49
7	1064	49
8	1113	49
9	1162	49
10	1210	48

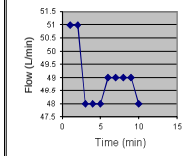

Arithmatic average = 49 (L/min)
Adopted average = 49 (L/min)

Stage 2

Gauge Pressure	400	(kPa)
Gauge Pressure	40.77	(m)
Static Pressure	50.6	(m)
Head without loss correction	91.33	(m)
Head loss	2.90	(m)
High flow pressure calibration	0.00	(m)
Total Head	88.43	(m)

Minutes of test	Flowmet read (L)	Flow (L/min)
0	1265	
1	1321	56
2	1379	58
3	1435	56
4	1493	58
5	1550	57
6	1608	58
7	1665	57
8	1722	57
9	1780	58
10	1838	58

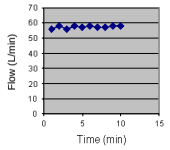

Arithmatic average = 57.3 (L/min)
Adopted average = 57.3 (L/min)

Stage 3

Gauge Pressure	600	(kPa)
Gauge Pressure	61.16	(m)
Static Pressure	50.6	(m)
Head without loss correction	111.72	(m)
Head loss	4.43	(m)
High flow pressure calibratior	0.00	(m)
Total Head	107.29	(m)

Minutes of test	Flowmet read (L)	Flow (L/min)
0	1906	
1	1976	70
2	2047	71
3	2117	70
4	2189	72
5	2259	70
6	2329	70
7	2401	72
8	2472	71
9	2544	72
10	2614	70

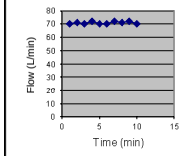

Arithmatic average = 70.8 (L/min)
Adopted average = 70.8 (L/min)

Stage 4

Gauge Pressure	400	(kPa)
Gauge Pressure	40.77	(m)
Static Pressure	50.6	(m)
Head without loss correction	91.33	(m)
Head loss	3.70	(m)
High flow pressure calibration	0.00	(m)
Total Head	87.63	(m)

Minutes of test	Flowmet read (L)	Flow (L/min)
0	2680	
1	2745	65
2	2810	65
3	2876	66
4	2940	64
5	3004	64
6	3069	65
7	3134	65
8	3198	64
9	3262	64
10	3327	65

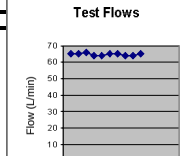

Arithmatic average = 64.7 (L/min)
Adopted average = 64.7 (L/min)

Stage 5

Gauge Pressure	200	(kPa)
Gauge Pressure	20.39	(m)
Static Pressure	50.6	(m)
Head without loss correction	70.94	(m)
Head loss	2.64	(m)
High flow pressure calibration	0.00	(m)
Total Head	68.30	(m)

Minutes of test	Flowmet read (L)	Flow (L/min)
0	3449	
1	3503	54
2	3558	55
3	3613	55
4	3669	56
5	3723	54
6	3778	55
7	3833	55
8	3889	56
9	3945	56
10	3996	51

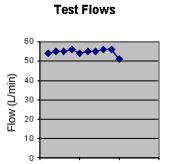

Arithmatic average = 54.7 (L/min)
Adopted average = 54.7 (L/min)

Stage 6

Gauge Pressure	0	(kPa)
Gauge Pressure	0.00	(m)
Static Pressure	50.6	(m)
Head without loss correction	50.56	(m)
Head loss	0.00	(m)
High flow pressure calibratior	0.00	(m)
Total Head	50.56	(m)

Minutes of test	Flowmet read (L)	Flow (L/min)
0	0	
1	0	0
2	0	0
3	0	0
4	0	0
5	0	0
6	0	0
7	0	0
8	0	0
9	0	0
10	0	0

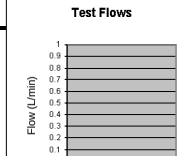

Arithmatic average = 0 (L/min)
Adopted average = 0 (L/min)

Comments:

Calculations used:

$$k = \frac{5.833}{\pi L \sin\alpha}\left(\frac{Q}{H_T}\right)\cdot 10^{-5} \text{ m/s} \quad \text{(CANMET)}$$

$$k = \frac{8.333}{\pi L \sin\alpha}\left(\frac{Q}{H_T}\right)\cdot \ln\left(\frac{L}{r}\right)\cdot 10^{-4} \text{ m/s} \quad \text{(HOEK \& BRAY)}$$

$$lugeon = \frac{Q}{L\sin\alpha}\cdot\frac{100}{H_T} \text{ l/m/min} \quad \text{(HOULSBY)}$$

Stage	Total Head (m)	Flow (l/min)	Calculated Lugeon values: Test Pressure	Q (L/m/min)	Lugeons (L/m/min)	Chosen Lugeon (L/m/min)
1	68.82	49.00	675.16	7.54	10.95	
2	88.43	57.30	867.51	8.82	9.97	
3	107.29	70.80	1052.53	10.89	10.15	10.951
4	87.63	64.70	859.69	9.95	11.36	
5	68.30	54.7	670.04	8.42	12.32	

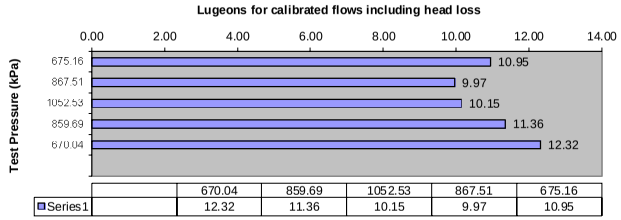

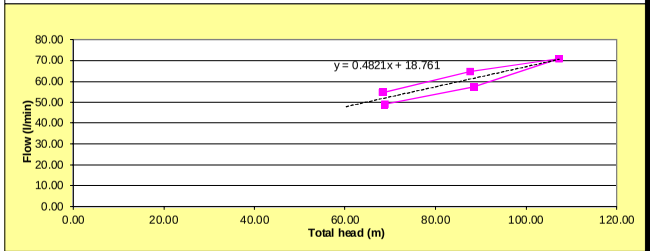

Conductivity Calculations:

MEAN Q/H$_T$	CANMET	HOEK & BRAY	MEAN LUGEONS 10.95	
0.699	2.0E-06	1.4E-06	1.4E-06	m/s
Mean Conductivity	K =	1.6E-06	m/s	

Job No: TAH4125

Location: Tahmoor Site No: TBF040 Borehole: TBF040 Depth Range: 178.9 -185.4 m

PACKER TEST RESULTS: K = 2.6E-08 m/s

PROJECT: TAH4125 **Site No:** TBF040 **BORE NAME:** TBF040 **HOLE DIP:** 90 **DIP Direction:** **DATE:** 19-Dec-13

Depth To Bottm Packer Test interval:	185.40	m	HEIGHT OF PRESSURE GAUGE:	1	m (above ground level)
Depth To Top Packer Test interval:	178.90	m	STATIC GROUNDWATER LEVEL:	40.7	m (below ground level)
LENGTH OF STAGE TEST:	6.50	m	SURFACE R.L.		m
BORE DIAMETER:	96	mm			

Recorded flow readings at indicated applied pressure heads.

Stage 1

Gauge Pressure	100	(kPa)
Gauge Pressure	10.19	(m)
Static Pressure	50.9	(m)
Head without loss correction	61.05	(m)
Head loss	0.00	(m)
High flow pressure calibration	0.00	(m)
Total Head	61.05	(m)

Minutes of test	Flowmet read (L)	Flow (L/min)
0	271.3	
1	271.9	0.6
2	272.4	0.5
3	272.9	0.5
4	273.4	0.5
5	273.9	0.5
6	274.4	0.5
7	274.9	0.5
8	275.4	0.5
9	275.9	0.5
10	276.4	0.5

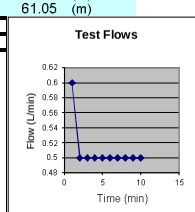

Arithmatic average = 0.51 (L/min)
Adopted average = 0.51 (L/min)

Stage 2

Gauge Pressure	200	(kPa)
Gauge Pressure	20.39	(m)
Static Pressure	50.9	(m)
Head without loss correction	71.24	(m)
Head loss	0.00	(m)
High flow pressure calibration	0.00	(m)
Total Head	71.24	(m)

Minutes of test	Flowmet read (L)	Flow (L/min)
0	278.2	
1	278.8	0.6
2	279.4	0.6
3	280	0.6
4	280.6	0.6
5	281.2	0.6
6	281.9	0.7
7	282.6	0.7
8	283.3	0.7
9	284	0.7
10	284.7	0.7

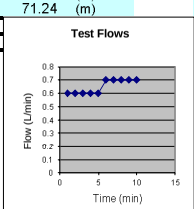

Arithmatic average = 0.65 (L/min)
Adopted average = 0.65 (L/min)

Stage 3

Gauge Pressure	300	(kPa)
Gauge Pressure	30.58	(m)
Static Pressure	50.9	(m)
Head without loss correction	81.44	(m)
Head loss	0.00	(m)
High flow pressure calibration	0.00	(m)
Total Head	81.44	(m)

Minutes of test	Flowmet read (L)	Flow (L/min)
0	286.7	
1	288	1.3
2	289.2	1.2
3	290.4	1.2
4	291.6	1.2
5	293	1.4
6	294.2	1.2
7	295.5	1.3
8	296.9	1.4
9	298.2	1.3
10	299.4	1.2

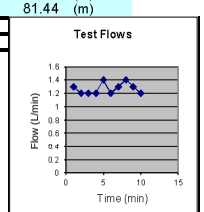

Arithmatic average = 1.27 (L/min)
Adopted average = 1.27 (L/min)

Stage 4

Gauge Pressure	200	(kPa)
Gauge Pressure	20.39	(m)
Static Pressure	50.9	(m)
Head without loss correction	71.24	(m)
Head loss	0.00	(m)
High flow pressure calibration	0.00	(m)
Total Head	71.24	(m)

Minutes of test	Flowmet read (L)	Flow (L/min)
0	300.2	
1	301	0.8
2	301.9	0.9
3	302.8	0.9
4	303.7	0.9
5	304.7	1
6	305.5	0.8
7	306.5	1
8	307.5	1
9	308.4	0.9
10	309.2	0.8

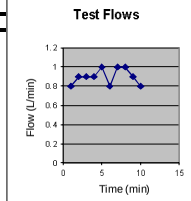

Arithmatic average = 0.9 (L/min)
Adopted average = 0.9 (L/min)

Stage 5

Gauge Pressure	100	(kPa)
Gauge Pressure	10.19	(m)
Static Pressure	50.9	(m)
Head without loss correction	61.05	(m)
Head loss	0.00	(m)
High flow pressure calibration	0.00	(m)
Total Head	61.05	(m)

Minutes of test	Flowmet read (L)	Flow (L/min)
0	309.5	
1	310.1	0.6
2	310.6	0.5
3	311.1	0.5
4	311.6	0.5
5	312.2	0.6
6	312.6	0.4
7	313.2	0.6
8	313.7	0.5
9	314.2	0.5
10	314.7	0.5

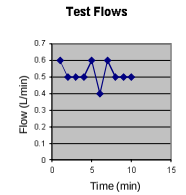

Arithmatic average = 0.52 (L/min)
Adopted average = 0.52 (L/min)

Stage 6

Gauge Pressure	0	(kPa)
Gauge Pressure	0.00	(m)
Static Pressure	50.9	(m)
Head without loss correction	50.86	(m)
Head loss	0.00	(m)
High flow pressure calibration	0.00	(m)
Total Head	50.86	(m)

Minutes of test	Flowmet read (L)	Flow (L/min)
0	0	
1	0	0
2	0	0
3	0	0
4	0	0
5	0	0
6	0	0
7	0	0
8	0	0
9	0	0
10	0	0

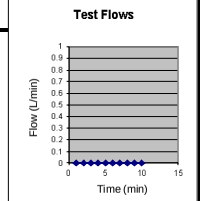

Arithmatic average = 0 (L/min)
Adopted average = 0 (L/min)

Comments:

Calculations used:

$$k = \frac{5.833}{\pi L \sin\alpha}\left(\frac{Q}{H_T}\right)\cdot 10^{-5} \text{ m/s} \quad \text{(CANMET)}$$

$$k = \frac{8.333}{\pi L \sin\alpha}\left(\frac{Q}{H_T}\right)\cdot \ln\left(\frac{L}{r}\right)\cdot 10^{-4} \text{ m/s} \quad \text{(HOEK \& BRAY)}$$

$$lugeon = \frac{Q}{L\sin\alpha}\cdot\frac{100}{H_T} \text{ l/m/min} \quad \text{(HOULSBY)}$$

Stage	Total Head (m)	Flow (l/min)	Calculated Lugeon values: Test Pressure	Q (L/m/min)	Lugeons (L/m/min)	Chosen Lugeon (L/m/min)
1	61.05	0.51	598.91	0.08	0.13	
2	71.24	0.65	698.91	0.10	0.14	
3	81.44	1.27	798.90	0.20	0.24	0.167
4	71.24	0.90	698.91	0.14	0.19	
5	61.05	0.52	598.91	0.08	0.13	

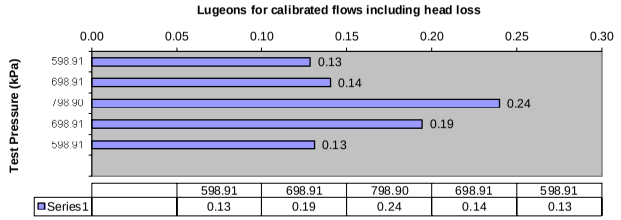

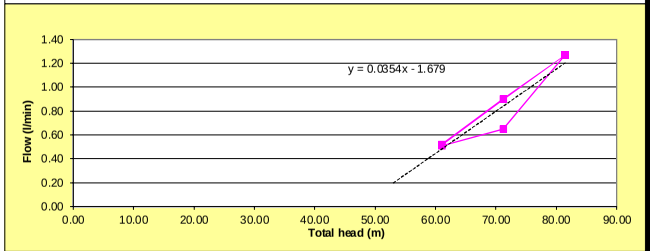

Conductivity Calculations:

MEAN Q/H$_T$	CANMET	HOEK & BRAY	MEAN LUGEONS 0.17	
0.011	3.3E-08	2.3E-08	2.2E-08	m/s
Mean Conductivity		K =	2.6E-08	m/s

Job No: TAH4125

Location: Tahmoor Site No: TBF040 Borehole: TBF040 Depth Range: 184.9 -191.4 m

PACKER TEST RESULTS: K = 2.5E-07 m/s

PROJECT: TAH4125 **Site No:** TBF040 **BORE NAME:** TBF040 **HOLE DIP:** 90 **DIP Direction:** **DATE:** 19-Dec-13

Depth To Bottm Packer Test interval:	191.40	m	HEIGHT OF PRESSURE GAUGE:	1	m (above ground level)
Depth To Top Packer Test interval:	184.90	m	STATIC GROUNDWATER LEVEL:	40.7	m (below ground level)
LENGTH OF STAGE TEST:	6.50	m	SURFACE R.L.		m
BORE DIAMETER:	96	mm			

Recorded flow readings at indicated applied pressure heads.

Stage 1

Gauge Pressure	200	(kPa)
Gauge Pressure	20.39	(m)
Static Pressure	51.2	(m)
Head without loss correction	71.54	(m)
Head loss	0.06	(m)
High flow pressure calibration	0.00	(m)
Total Head	71.49	(m)

Minutes of test	Flowmet read (L)	Flow (L/min)
0	637	
1	646	9
2	654	8
3	662	8
4	670	8
5	678	8
6	686	8
7	695	9
8	703	8
9	710	7
10	718	8

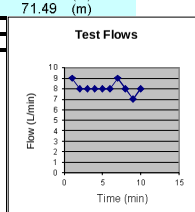

Arithmatic average = 8.1 (L/min)
Adopted average = 8.1 (L/min)

Stage 2

Gauge Pressure	400	(kPa)
Gauge Pressure	40.77	(m)
Static Pressure	51.2	(m)
Head without loss correction	91.93	(m)
Head loss	0.10	(m)
High flow pressure calibration	0.00	(m)
Total Head	91.83	(m)

Minutes of test	Flowmet read (L)	Flow (L/min)
0	730	
1	741	11
2	752	11
3	763	11
4	774	11
5	784	10
6	794	10
7	805	11
8	815	10
9	826	11
10	837	11

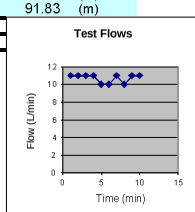

Arithmatic average = 10.7 (L/min)
Adopted average = 10.7 (L/min)

Stage 3

Gauge Pressure	600	(kPa)
Gauge Pressure	61.16	(m)
Static Pressure	51.2	(m)
Head without loss correction	112.32	(m)
Head loss	0.15	(m)
High flow pressure calibratior	0.00	(m)
Total Head	112.17	(m)

Minutes of test	Flowmet read (L)	Flow (L/min)
0	851	
1	864	13
2	877	13
3	890	13
4	903	13
5	916	13
6	929	13
7	942	13
8	955	13
9	968	13
10	981	13

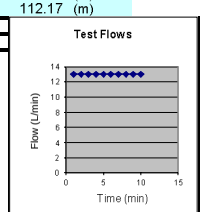

Arithmatic average = 13 (L/min)
Adopted average = 13 (L/min)

Stage 4

Gauge Pressure	400	(kPa)
Gauge Pressure	40.77	(m)
Static Pressure	51.2	(m)
Head without loss correction	91.93	(m)
Head loss	0.09	(m)
High flow pressure calibration	0.00	(m)
Total Head	91.84	(m)

Minutes of test	Flowmet read (L)	Flow (L/min)
0	965	
1	975	10
2	985	10
3	996	11
4	1006	10
5	1016	10
6	1025	9
7	1035	10
8	1045	10
9	1055	10
10	1065	10

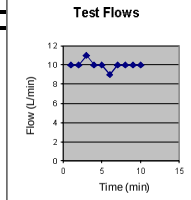

Arithmatic average = 10 (L/min)
Adopted average = 10 (L/min)

Stage 5

Gauge Pressure	200	(kPa)
Gauge Pressure	20.39	(m)
Static Pressure	51.2	(m)
Head without loss correction	71.54	(m)
Head loss	0.04	(m)
High flow pressure calibration	0.00	(m)
Total Head	71.50	(m)

Minutes of test	Flowmet read (L)	Flow (L/min)
0	51	
1	59	8
2	66	7
3	73	7
4	80	7
5	87	7
6	93	6
7	100	7
8	107	7
9	114	7
10	121	7

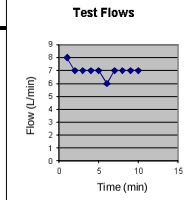

Arithmatic average = 7 (L/min)
Adopted average = 7 (L/min)

Stage 6

Gauge Pressure	0	(kPa)
Gauge Pressure	0.00	(m)
Static Pressure	51.2	(m)
Head without loss correction	51.16	(m)
Head loss	0.00	(m)
High flow pressure calibratior	0.00	(m)
Total Head	51.16	(m)

Minutes of test	Flowmet read (L)	Flow (L/min)
0	0	
1	0	0
2	0	0
3	0	0
4	0	0
5	0	0
6	0	0
7	0	0
8	0	0
9	0	0
10	0	0

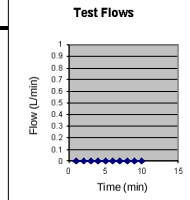

Arithmatic average = 0 (L/min)
Adopted average = 0 (L/min)

Comments:

Calculations used:

$$k = \frac{5.833}{\pi L \sin\alpha}\left(\frac{Q}{H_T}\right)\cdot 10^{-5} \quad \text{m/s} \qquad \text{(CANMET)}$$

$$k = \frac{8.333}{\pi L \sin\alpha}\left(\frac{Q}{H_T}\right)\cdot \ln\left(\frac{L}{r}\right)\cdot 10^{-4} \quad \text{m/s} \qquad \text{(HOEK \& BRAY)}$$

$$lugeon = \frac{Q}{L \sin\alpha}\cdot\frac{100}{H_T} \quad \text{l/m/min} \qquad \text{(HOULSBY)}$$

Stage	Total Head (m)	Flow (l/min)	Calculated Lugeon values: Test Pressure	Q (L/m/min)	Lugeons (L/m/min)	Chosen Lugeon (L/m/min)
1	71.49	8.10	701.29	1.25	1.74	
2	91.83	10.70	900.86	1.65	1.79	
3	112.17	13.00	1100.39	2.00	1.78	1.700
4	91.84	10.00	900.99	1.54	1.68	
5	71.50	7	701.43	1.08	1.51	

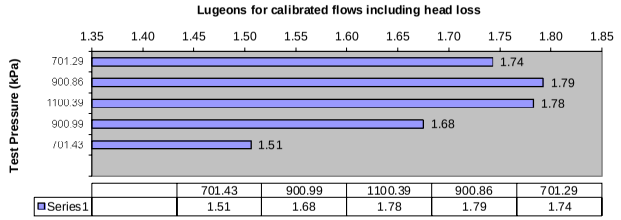

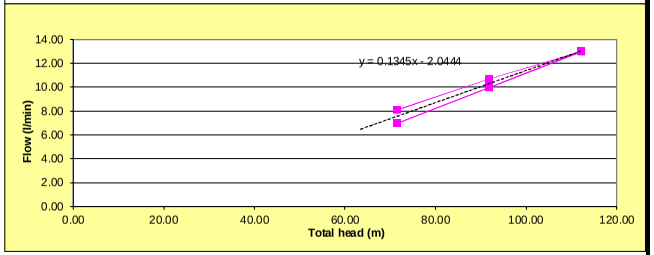

Conductivity Calculations:

MEAN Q/H$_T$	CANMET	HOEK & BRAY	MEAN LUGEONS 1.70	
0.112	3.2E-07	2.2E-07	2.2E-07	m/s
Mean Conductivity	K =	2.5E-07	m/s	

Job No: TAH4125

Location: Tahmoor Site No: TBF040 Borehole: TBF040 Depth Range: 190.9 -197.4 m

PACKER TEST RESULTS: K = 1.8E-06 m/s

PROJECT: TAH4125 **Site No:** TBF040 **BORE NAME:** TBF040 **HOLE DIP:** 90 **DIP Direction:** **DATE:** 19-Dec-13

Depth To Bottm Packer Test interval:	197.40	m	HEIGHT OF PRESSURE GAUGE:	1	m (above ground level)
Depth To Top Packer Test interval:	190.90	m	STATIC GROUNDWATER LEVEL:	40.7	m (below ground level)
LENGTH OF STAGE TEST:	6.50	m	SURFACE R.L.		m
BORE DIAMETER:	96	mm			

Recorded flow readings at indicated applied pressure heads.

Stage 1

Gauge Pressure	200	(kPa)
Gauge Pressure	20.39	(m)
Static Pressure	51.5	(m)
Head without loss correction	71.84	(m)
Head loss	0.00	(m)
High flow pressure calibration	0.00	(m)
Total Head	71.84	(m)

Minutes of test	Flowmet read (L)	Flow (L/min)
0	0	
1	0	0
2	0	0
3	0	0
4	0	0
5	0	0
6	0	0
7	0	0
8	0	0
9	0	0
10	0	0

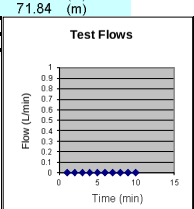

Arithmatic average = 0 (L/min)
Adopted average = 0 (L/min)

Stage 2

Gauge Pressure	400	(kPa)
Gauge Pressure	40.77	(m)
Static Pressure	51.5	(m)
Head without loss correction	92.23	(m)
Head loss	0.00	(m)
High flow pressure calibration	0.00	(m)
Total Head	92.23	(m)

Minutes of test	Flowmet read (L)	Flow (L/min)
0	730	
1	0	-730
2	0	0
3	0	0
4	0	0
5	0	0
6	0	0
7	0	0
8	0	0
9	0	0
10	0	0

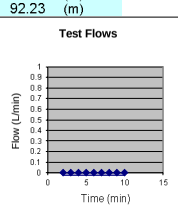

Arithmatic average = -73 (L/min)
Adopted average = 0 (L/min)

Stage 3

Gauge Pressure	600	(kPa)
Gauge Pressure	61.16	(m)
Static Pressure	51.5	(m)
Head without loss correction	112.62	(m)
Head loss	0.00	(m)
High flow pressure calibration	0.00	(m)
Total Head	112.62	(m)

Minutes of test	Flowmet read (L)	Flow (L/min)
0	0	
1	0	0
2	0	0
3	0	0
4	0	0
5	0	0
6	0	0
7	0	0
8	0	0
9	0	0
10	0	0

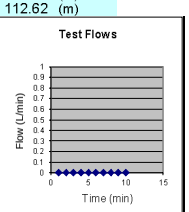

Arithmatic average = 0 (L/min)
Adopted average = 0 (L/min)

Stage 4

Gauge Pressure	400	(kPa)
Gauge Pressure	40.77	(m)
Static Pressure	51.5	(m)
Head without loss correction	92.23	(m)
Head loss	0.00	(m)
High flow pressure calibration	0.00	(m)
Total Head	92.23	(m)

Minutes of test	Flowmet read (L)	Flow (L/min)
0	0	
1	0	0
2	0	0
3	0	0
4	0	0
5	0	0
6	0	0
7	0	0
8	0	0
9	0	0
10	0	0

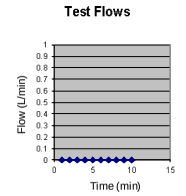

Arithmatic average = 0 (L/min)
Adopted average = 0 (L/min)

Stage 5

Gauge Pressure	200	(kPa)
Gauge Pressure	20.39	(m)
Static Pressure	51.5	(m)
Head without loss correction	71.84	(m)
Head loss	0.00	(m)
High flow pressure calibration	0.00	(m)
Total Head	71.84	(m)

Minutes of test	Flowmet read (L)	Flow (L/min)
0	0	
1	0	0
2	0	0
3	0	0
4	0	0
5	0	0
6	0	0
7	0	0
8	0	0
9	0	0
10	0	0

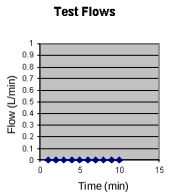

Arithmatic average = 0 (L/min)
Adopted average = 0 (L/min)

Stage 6

Gauge Pressure	0	(kPa)
Gauge Pressure	0.00	(m)
Static Pressure	51.5	(m)
Head without loss correction	51.46	(m)
Head loss	0.00	(m)
High flow pressure calibration	0.00	(m)
Total Head	51.46	(m)

Minutes of test	Flowmet read (L)	Flow (L/min)
0	0	
1	0	0
2	0	0
3	0	0
4	0	0
5	0	0
6	0	0
7	0	0
8	0	0
9	0	0
10	0	0

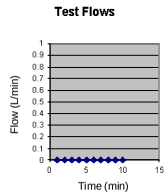

Arithmatic average = 0 (L/min)
Adopted average = 0 (L/min)

Comments:

Calculations used:

$$k = \frac{5.833}{\pi L \sin\alpha}\left(\frac{Q}{H_T}\right)\cdot 10^{-5} \quad \text{m/s} \qquad \text{(CANMET)}$$

$$k = \frac{8.333}{\pi L \sin\alpha}\left(\frac{Q}{H_T}\right)\cdot \ln\left(\frac{L}{r}\right)\cdot 10^{-4} \quad \text{m/s} \qquad \text{(HOEK \& BRAY)}$$

$$lugeon = \frac{Q}{L \sin\alpha}\cdot\frac{100}{H_T} \quad \text{l/m/min} \qquad \text{(HOULSBY)}$$

Stage	Total Head (m)	Flow (l/min)	Calculated Lugeon values: Test Pressure	Q (L/m/min)	Lugeons (L/m/min)	Chosen Lugeon (L/m/min)
1	71.84	0.00	704.80	0.00	0.00	
2	92.23	0.00	904.80	0.00	0.00	
3	112.62	0.00	1104.80	0.00	0.00	0.000
4	92.23	0.00	904.80	0.00	0.00	
5	71.84	0	704.80	0.00	0.00	

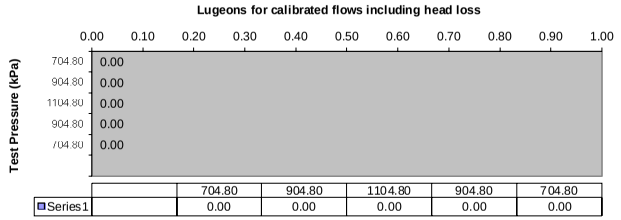

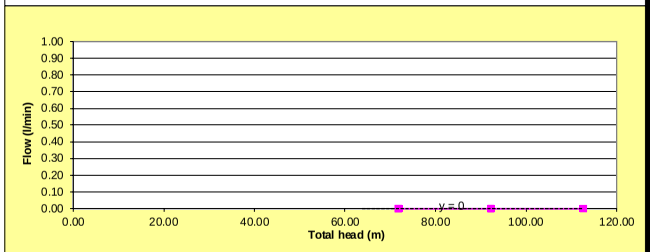

Conductivity Calculations:

MEAN Q/H$_T$	CANMET	HOEK & BRAY	MEAN LUGEONS 0.00	
0.000	0.0E+00	0.0E+00	0.0E+00	m/s

Mean Conductivity K = 1.8E-06 m/s

Job No: TAH4125

Location: Tahmoor **Site No: TBF040** **Borehole: TBF040** **Depth Range: 196.9 -203.4 m**

PACKER TEST RESULTS: **K = 3.4E-08 m/s**

PROJECT: TAH4125 **Site No: TBF040** **BORE NAME: TBF040** **HOLE DIP: 90** **DIP Direction:** **DATE: 07-Jan-14**

Depth To Bottm Packer Test interval:	203.40	m	HEIGHT OF PRESSURE GAUGE:	1	m (above ground level)
Depth To Top Packer Test interval:	196.90	m	STATIC GROUNDWATER LEVEL:	40.7	m (below ground level)
LENGTH OF STAGE TEST:	6.50	m	SURFACE R.L.		m
BORE DIAMETER:	96	mm			

Recorded flow readings at indicated applied pressure heads.

Stage 1

Gauge Pressure	200	(kPa)
Gauge Pressure	20.39	(m)
Static Pressure	51.8	(m)
Head without loss correction	72.14	(m)
Head loss	0.00	(m)
High flow pressure calibration	0.00	(m)
Total Head	72.14	(m)

Minutes of test	Flowmet read (L)	Flow (L/min)
0	698.5	
1	700	1.5
2	701.6	1.6
3	703	1.4
4	704.4	1.4
5	705.8	1.4
6	707.2	1.4
7	708.5	1.3
8	709.8	1.3
9	711	1.2
10	712.4	1.4

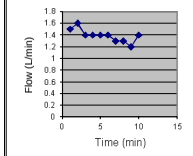

Arithmatic average = 1.39 (L/min)
Adopted average = 1.39 (L/min)

Stage 2

Gauge Pressure	400	(kPa)
Gauge Pressure	40.77	(m)
Static Pressure	51.8	(m)
Head without loss correction	92.53	(m)
Head loss	0.00	(m)
High flow pressure calibration	0.00	(m)
Total Head	92.53	(m)

Minutes of test	Flowmet read (L)	Flow (L/min)
0	715.3	
1	717	1.7
2	718.4	1.4
3	720	1.6
4	721.6	1.6
5	723.1	1.5
6	724.4	1.3
7	725.4	1
8	726.4	1
9	727.4	1
10	728.4	1

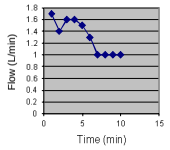

Arithmatic average = 1.31 (L/min)
Adopted average = 1.51667 (L/min)

Stage 3

Gauge Pressure	600	(kPa)
Gauge Pressure	61.16	(m)
Static Pressure	51.8	(m)
Head without loss correction	112.92	(m)
Head loss	0.00	(m)
High flow pressure calibratior	0.00	(m)
Total Head	112.92	(m)

Minutes of test	Flowmet read (L)	Flow (L/min)
0	30.4	
1	32	1.6
2	33.5	1.5
3	35.2	1.7
4	37	1.8
5	38.4	1.4
6	39.9	1.5
7	41.4	1.5
8	42.7	1.3
9	44.3	1.6
10	45.8	1.5

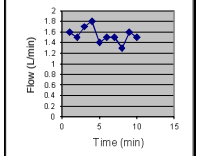

Arithmatic average = 1.54 (L/min)
Adopted average = 1.54 (L/min)

Stage 4

Gauge Pressure	400	(kPa)
Gauge Pressure	40.77	(m)
Static Pressure	51.8	(m)
Head without loss correction	92.53	(m)
Head loss	0.00	(m)
High flow pressure calibration	0.00	(m)
Total Head	92.53	(m)

Minutes of test	Flowmet read (L)	Flow (L/min)
0	46.6	
1	47.9	1.3
2	49	1.1
3	50.3	1.3
4	51.5	1.2
5	52.7	1.2
6	53.9	1.2
7	55	1.1
8	56.3	1.3
9	57.4	1.1
10	58.7	1.3

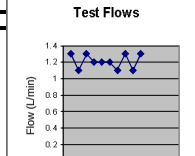

Arithmatic average = 1.21 (L/min)
Adopted average = 1.21 (L/min)

Stage 5

Gauge Pressure	200	(kPa)
Gauge Pressure	20.39	(m)
Static Pressure	51.8	(m)
Head without loss correction	72.14	(m)
Head loss	0.00	(m)
High flow pressure calibration	0.00	(m)
Total Head	72.14	(m)

Minutes of test	Flowmet read (L)	Flow (L/min)
0	58.7	
1	59.8	1.1
2	60.9	1.1
3	61.8	0.9
4	63	1.2
5	63.9	0.9
6	64.8	0.9
7	65.8	1
8	66.7	0.9
9	67.6	0.9
10	68.5	0.9

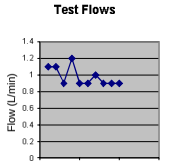

Arithmatic average = 0.98 (L/min)
Adopted average = 0.98 (L/min)

Stage 6

Gauge Pressure	0	(kPa)
Gauge Pressure	0.00	(m)
Static Pressure	51.8	(m)
Head without loss correction	51.76	(m)
Head loss	0.00	(m)
High flow pressure calibratior	0.00	(m)
Total Head	51.76	(m)

Minutes of test	Flowmet read (L)	Flow (L/min)
0	0	
1	0	0
2	0	0
3	0	0
4	0	0
5	0	0
6	0	0
7	0	0
8	0	0
9	0	0
10	0	0

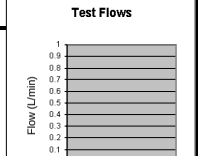

Arithmatic average = 0 (L/min)
Adopted average = 0 (L/min)

Comments:

Calculations used:

$$k = \frac{5.833}{\pi L \sin\alpha}\left(\frac{Q}{H_T}\right)\cdot 10^{-5} \quad \text{m/s} \qquad \text{(CANMET)}$$

$$k = \frac{8.333}{\pi L \sin\alpha}\left(\frac{Q}{H_T}\right)\cdot \ln\left(\frac{L}{r}\right)\cdot 10^{-4} \quad \text{m/s} \qquad \text{(HOEK \& BRAY)}$$

$$lugeon = \frac{Q}{L \sin\alpha}\cdot\frac{100}{H_T} \quad \text{l/m/min} \qquad \text{(HOULSBY)}$$

Stage	Total Head (m)	Flow (l/min)	Calculated Lugeon values: Test Pressure	Q (L/m/min)	Lugeons (L/m/min)	Chosen Lugeon (L/m/min)
1	72.14	1.39	707.72	0.21	0.30	
2	92.53	1.52	907.72	0.23	0.25	
3	112.92	1.54	1107.72	0.24	0.21	0.234
4	92.53	1.21	907.73	0.19	0.20	
5	72.14	0.98	707.73	0.15	0.21	

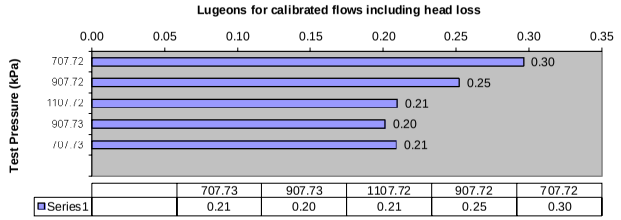

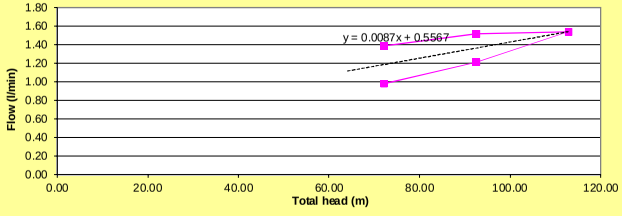

Conductivity Calculations:

MEAN Q/H$_T$	CANMET	HOEK & BRAY	MEAN LUGEONS	
0.015	4.2E-08	3.0E-08	3.0E-08	m/s
	Mean Conductivity	K =	3.4E-08	m/s

Job No: TAH4125

Location: Tahmoor Site No: TBF040 Borehole: TBF040 Depth Range: 202.9 -209.4 m

PACKER TEST RESULTS: K = 7.1E-08 m/s

PROJECT: TAH4125 **Site No:** TBF040 **BORE NAME:** TBF040 **HOLE DIP:** 90 **DIP Direction:** **DATE:** 07-Jan-14

Depth To Bottm Packer Test interval:	209.40	m	HEIGHT OF PRESSURE GAUGE:	1	m (above ground level)
Depth To Top Packer Test interval:	202.90	m	STATIC GROUNDWATER LEVEL:	40.7	m (below ground level)
LENGTH OF STAGE TEST:	6.50	m	SURFACE R.L.		m
BORE DIAMETER:	96	mm			

Recorded flow readings at indicated applied pressure heads.

Stage 1

Gauge Pressure	200	(kPa)
Gauge Pressure	20.39	(m)
Static Pressure	52.1	(m)
Head without loss correction	72.44	(m)
Head loss	0.00	(m)
High flow pressure calibration	0.00	(m)
Total Head	72.44	(m)

Minutes of test	Flowmet read (L)	Flow (L/min)
0	192.5	
1	195	2.5
2	197.2	2.2
3	199.5	2.3
4	201.8	2.3
5	203.9	2.1
6	206	2.1
7	208.1	2.1
8	210.2	2.1
9	212.2	2
10	214.4	2.2

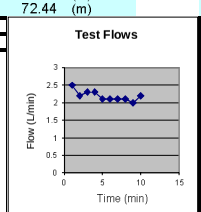

Arithmatic average = 2.19 (L/min)
Adopted average = 2.19 (L/min)

Stage 2

Gauge Pressure	400	(kPa)
Gauge Pressure	40.77	(m)
Static Pressure	52.1	(m)
Head without loss correction	92.83	(m)
Head loss	0.01	(m)
High flow pressure calibration	0.00	(m)
Total Head	92.82	(m)

Minutes of test	Flowmet read (L)	Flow (L/min)
0	17	
1	20.2	3.2
2	23	2.8
3	26	3
4	29	3
5	32	3
6	34.8	2.8
7	37.5	2.7
8	40.4	2.9
9	43	2.6
10	45.8	2.8

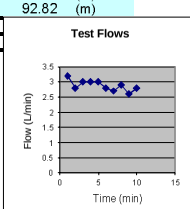

Arithmatic average = 2.88 (L/min)
Adopted average = 2.88 (L/min)

Stage 3

Gauge Pressure	600	(kPa)
Gauge Pressure	61.16	(m)
Static Pressure	52.1	(m)
Head without loss correction	113.22	(m)
Head loss	0.01	(m)
High flow pressure calibratio	0.00	(m)
Total Head	113.21	(m)

Minutes of test	Flowmet read (L)	Flow (L/min)
0	50	
1	54.4	4.4
2	58.4	4
3	62.2	3.8
4	66.1	3.9
5	69.9	3.8
6	73.7	3.8
7	77.3	3.6
8	81.2	3.9
9	85	3.8
10	89	4

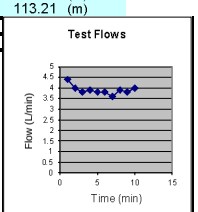

Arithmatic average = 3.9 (L/min)
Adopted average = 3.9 (L/min)

Stage 4

Gauge Pressure	400	(kPa)
Gauge Pressure	40.77	(m)
Static Pressure	52.1	(m)
Head without loss correction	92.83	(m)
Head loss	0.01	(m)
High flow pressure calibration	0.00	(m)
Total Head	92.83	(m)

Minutes of test	Flowmet read (L)	Flow (L/min)
0	92	
1	95	3
2	98	3
3	100.8	2.8
4	103.5	2.7
5	106.4	2.9
6	109.2	2.8
7	112	2.8
8	114.8	2.8
9	117.5	2.7
10	120.2	2.7

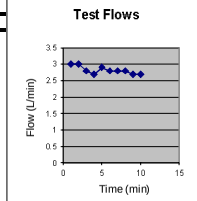

Arithmatic average = 2.82 (L/min)
Adopted average = 2.82 (L/min)

Stage 5

Gauge Pressure	200	(kPa)
Gauge Pressure	20.39	(m)
Static Pressure	52.1	(m)
Head without loss correction	72.44	(m)
Head loss	0.00	(m)
High flow pressure calibration	0.00	(m)
Total Head	72.44	(m)

Minutes of test	Flowmet read (L)	Flow (L/min)
0	22	
1	24	2
2	26.2	2.2
3	28.2	2
4	30.2	2
5	32.2	2
6	34.1	1.9
7	36	1.9
8	38	2
9	40	2
10	42	2

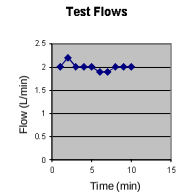

Arithmatic average = 2 (L/min)
Adopted average = 2 (L/min)

Stage 6

Gauge Pressure	0	(kPa)
Gauge Pressure	0.00	(m)
Static Pressure	52.1	(m)
Head without loss correction	52.06	(m)
Head loss	0.00	(m)
High flow pressure calibratio	0.00	(m)
Total Head	52.06	(m)

Minutes of test	Flowmet read (L)	Flow (L/min)
0	0	
1	0	0
2	0	0
3	0	0
4	0	0
5	0	0
6	0	0
7	0	0
8	0	0
9	0	0
10	0	0

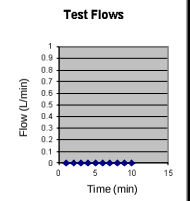

Arithmatic average = 0 (L/min)
Adopted average = 0 (L/min)

Comments:

Calculations used:

$$k = \frac{5.833}{\pi L \sin\alpha}\left(\frac{Q}{H_T}\right)\cdot 10^{-5} \quad \text{m/s} \qquad \text{(CANMET)}$$

$$k = \frac{8.333}{\pi L \sin\alpha}\left(\frac{Q}{H_T}\right)\cdot \ln\left(\frac{L}{r}\right)\cdot 10^{-4} \quad \text{m/s} \qquad \text{(HOEK \& BRAY)}$$

$$lugeon = \frac{Q}{L \sin\alpha}\cdot\frac{100}{H_T} \quad \text{l/m/min} \qquad \text{(HOULSBY)}$$

Stage	Total Head (m)	Flow (l/min)	Calculated Lugeon values: Test Pressure	Q (L/m/min)	Lugeons (L/m/min)	Chosen Lugeon (L/m/min)
1	72.44	2.19	710.64	0.34	0.47	
2	92.82	2.88	910.61	0.44	0.48	
3	113.21	3.90	1110.55	0.60	0.53	0.473
4	92.83	2.82	910.62	0.43	0.47	
5	72.44	2	710.65	0.31	0.42	

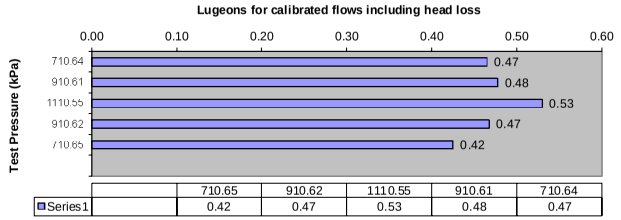

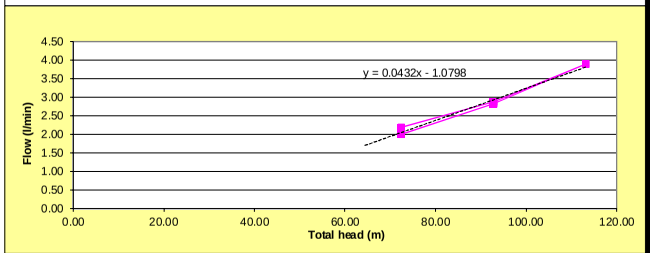

Conductivity Calculations:

MEAN Q/H$_T$	CANMET	HOEK & BRAY	MEAN LUGEONS 0.47	
0.031	9.0E-08	6.3E-08	6.1E-08	m/s
Mean Conductivity		K =	7.1E-08	m/s

Job No: TAH4125

Location: Tahmoor Site No: TBF040 Borehole: TBF040 Depth Range: 208.9 -215.4 m

PACKER TEST RESULTS: K = 1.3E-06 m/s

PROJECT: TAH4125 Site No: TBF040 BORE NAME: TBF040 HOLE DIP: 90 DIP Direction: DATE: 08-Jan-14

Depth To Bottm Packer Test interval:	215.40	m	HEIGHT OF PRESSURE GAUGE:	1	m (above ground level)
Depth To Top Packer Test interval:	208.90	m	STATIC GROUNDWATER LEVEL:	40.7	m (below ground level)
LENGTH OF STAGE TEST:	6.50	m	SURFACE R.L.		m
BORE DIAMETER:	96	mm			

Recorded flow readings at indicated applied pressure heads.

Stage 1

Gauge Pressure	120	(kPa)
Gauge Pressure	12.23	(m)
Static Pressure	52.4	(m)
Head without loss correction	64.59	(m)
Head loss	1.54	(m)
High flow pressure calibration	0.00	(m)
Total Head	63.05	(m)

Minutes of test	Flowmet read (L)	Flow (L/min)
0	200	
1	246	46
2	289	43
3	333	44
4	374	41
5	416	42
6	457	41
7	498	41
8	538	40
9	578	40
10	618	40

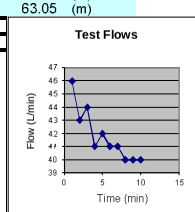

Arithmatic average = 41.8 (L/min)
Adopted average = 41.8 (L/min)

Stage 2

Gauge Pressure	240	(kPa)
Gauge Pressure	24.46	(m)
Static Pressure	52.4	(m)
Head without loss correction	76.82	(m)
Head loss	2.16	(m)
High flow pressure calibration	0.00	(m)
Total Head	74.66	(m)

Minutes of test	Flowmet read (L)	Flow (L/min)
0	8709	
1	8760	51
2	8811	51
3	8861	50
4	8912	51
5	8961	49
6	9010	49
7	9059	49
8	9108	49
9	9155	47
10	9204	49

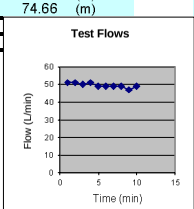

Arithmatic average = 49.5 (L/min)
Adopted average = 49.5 (L/min)

Stage 3

Gauge Pressure	360	(kPa)
Gauge Pressure	36.70	(m)
Static Pressure	52.4	(m)
Head without loss correction	89.05	(m)
Head loss	2.44	(m)
High flow pressure calibration	0.00	(m)
Total Head	86.61	(m)

Minutes of test	Flowmet read (L)	Flow (L/min)
0	9257	
1	9310	53
2	9363	53
3	9416	53
4	9470	54
5	9521	51
6	9574	53
7	9627	53
8	9679	52
9	9731	52
10	9783	52

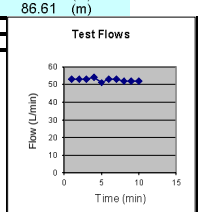

Arithmatic average = 52.6 (L/min)
Adopted average = 52.6 (L/min)

Stage 4

Gauge Pressure	240	(kPa)
Gauge Pressure	24.46	(m)
Static Pressure	52.4	(m)
Head without loss correction	76.82	(m)
Head loss	1.20	(m)
High flow pressure calibration	0.00	(m)
Total Head	75.63	(m)

Minutes of test	Flowmet read (L)	Flow (L/min)
0	9800	
1	9838	38
2	9872	34
3	9908	36
4	9945	37
5	9983	38
6	10019	36
7	10058	39
8	10093	35
9	10132	39
10	10168	36

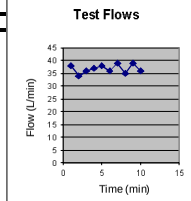

Arithmatic average = 36.8 (L/min)
Adopted average = 36.8 (L/min)

Stage 5

Gauge Pressure	120	(kPa)
Gauge Pressure	12.23	(m)
Static Pressure	52.4	(m)
Head without loss correction	64.59	(m)
Head loss	0.75	(m)
High flow pressure calibration	0.00	(m)
Total Head	63.84	(m)

Minutes of test	Flowmet read (L)	Flow (L/min)
0	10193	
1	10220	27
2	10249	29
3	10277	28
4	10306	29
5	10335	29
6	10364	29
7	10394	30
8	10425	31
9	10455	30
10	10485	30

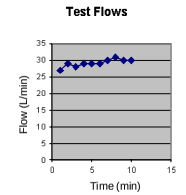

Arithmatic average = 29.2 (L/min)
Adopted average = 29.2 (L/min)

Stage 6

Gauge Pressure	0	(kPa)
Gauge Pressure	0.00	(m)
Static Pressure	52.4	(m)
Head without loss correction	52.36	(m)
Head loss	0.00	(m)
High flow pressure calibration	0.00	(m)
Total Head	52.36	(m)

Minutes of test	Flowmet read (L)	Flow (L/min)
0	0	
1	0	0
2	0	0
3	0	0
4	0	0
5	0	0
6	0	0
7	0	0
8	0	0
9	0	0
10	0	0

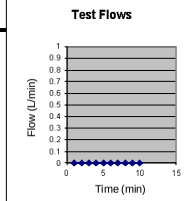

Arithmatic average = 0 (L/min)
Adopted average = 0 (L/min)

Comments:

Calculations used:

$$k = \frac{5.833}{\pi L \sin\alpha}\left(\frac{Q}{H_T}\right)\cdot 10^{-5} \quad \text{m/s} \qquad \text{(CANMET)}$$

$$k = \frac{8.333}{\pi L \sin\alpha}\left(\frac{Q}{H_T}\right)\cdot \ln\left(\frac{L}{r}\right)\cdot 10^{-4} \quad \text{m/s} \qquad \text{(HOEK \& BRAY)}$$

$$lugeon = \frac{Q}{L\sin\alpha}\cdot\frac{100}{H_T} \quad \text{l/m/min} \qquad \text{(HOULSBY)}$$

Stage	Total Head (m)	Flow (l/min)	Calculated Lugeon values: Test Pressure	Q (L/m/min)	Lugeons (L/m/min)	Chosen Lugeon (L/m/min)
1	63.05	41.80	618.48	6.43	10.20	
2	74.66	49.50	732.39	7.62	10.20	
3	86.61	52.60	849.65	8.09	9.34	8.853
4	75.63	36.80	741.89	5.66	7.49	
5	63.84	29.2	626.24	4.49	7.04	

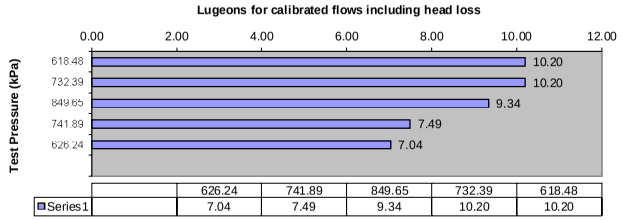

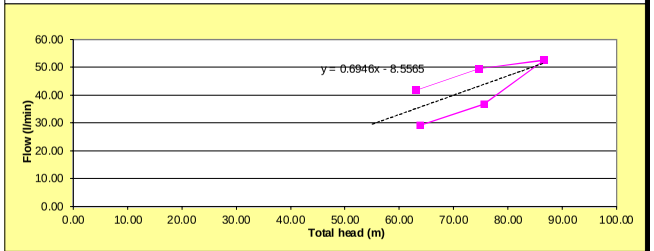

Conductivity Calculations:

MEAN Q/H$_T$	CANMET	HOEK & BRAY	MEAN LUGEONS	
0.579	1.7E-06	1.2E-06	1.2E-06	m/s
	Mean Conductivity	K =	1.3E-06	m/s

Job No: TAH4125

Location: Tahmoor Site No: TBF040 Borehole: TBF040 Depth Range: 214.9 -221.4 m

PACKER TEST RESULTS: K = 1.1E-08 m/s

PROJECT: TAH4125 **Site No:** TBF040 **BORE NAME:** TBF040 **HOLE DIP:** 90 **DIP Direction:** **DATE:** 08-Jan-14

Depth To Bottm Packer Test interval:	221.40	m	HEIGHT OF PRESSURE GAUGE:	1	m (above ground level)
Depth To Top Packer Test interval:	214.90	m	STATIC GROUNDWATER LEVEL:	40.7	m (below ground level)
LENGTH OF STAGE TEST:	6.50	m	SURFACE R.L.		m
BORE DIAMETER:	96	mm			

Recorded flow readings at indicated applied pressure heads.

Stage 1

Gauge Pressure	230	(kPa)
Gauge Pressure	23.45	(m)
Static Pressure	52.7	(m)
Head without loss correction	76.10	(m)
Head loss	0.00	(m)
High flow pressure calibration	0.00	(m)
Total Head	76.10	(m)

Minutes of test	Flowmet read (L)	Flow (L/min)
0	77.2	
1	77.8	0.6
2	78.3	0.5
3	78.7	0.4
4	79.1	0.4
5	79.5	0.4
6	79.9	0.4
7	80.3	0.4
8	80.7	0.4
9	81.1	0.4
10	81.4	0.3

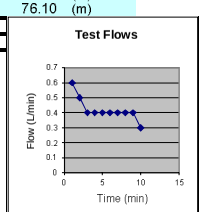

Arithmatic average = 0.42 (L/min)
Adopted average = 0.42 (L/min)

Stage 2

Gauge Pressure	450	(kPa)
Gauge Pressure	45.87	(m)
Static Pressure	52.7	(m)
Head without loss correction	98.53	(m)
Head loss	0.00	(m)
High flow pressure calibration	0.00	(m)
Total Head	98.53	(m)

Minutes of test	Flowmet read (L)	Flow (L/min)
0	82.1	
1	82.7	0.6
2	83.2	0.5
3	83.8	0.6
4	84.3	0.5
5	84.7	0.4
6	85.2	0.5
7	85.6	0.4
8	86.1	0.5
9	86.5	0.4
10	87	0.5

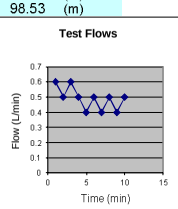

Arithmatic average = 0.49 (L/min)
Adopted average = 0.49 (L/min)

Stage 3

Gauge Pressure	700	(kPa)
Gauge Pressure	71.36	(m)
Static Pressure	52.7	(m)
Head without loss correction	124.01	(m)
Head loss	0.00	(m)
High flow pressure calibratior	0.00	(m)
Total Head	124.01	(m)

Minutes of test	Flowmet read (L)	Flow (L/min)
0	88.1	
1	88.7	0.6
2	89.4	0.7
3	90	0.6
4	90.5	0.5
5	91.1	0.6
6	91.7	0.6
7	92.3	0.6
8	92.9	0.6
9	93.4	0.5
10	94	0.6

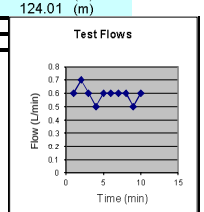

Arithmatic average = 0.59 (L/min)
Adopted average = 0.59 (L/min)

Stage 4

Gauge Pressure	450	(kPa)
Gauge Pressure	45.87	(m)
Static Pressure	52.7	(m)
Head without loss correction	98.53	(m)
Head loss	0.00	(m)
High flow pressure calibration	0.00	(m)
Total Head	98.53	(m)

Minutes of test	Flowmet read (L)	Flow (L/min)
0	94.3	
1	94.7	0.4
2	95.2	0.5
3	95.6	0.4
4	96	0.4
5	96.5	0.5
6	97	0.5
7	97.4	0.4
8	97.9	0.5
9	98.3	0.4
10	98.7	0.4

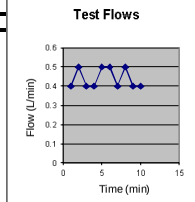

Arithmatic average = 0.44 (L/min)
Adopted average = 0.44 (L/min)

Stage 5

Gauge Pressure	230	(kPa)
Gauge Pressure	23.45	(m)
Static Pressure	52.7	(m)
Head without loss correction	76.10	(m)
Head loss	0.00	(m)
High flow pressure calibration	0.00	(m)
Total Head	76.10	(m)

Minutes of test	Flowmet read (L)	Flow (L/min)
0	98.9	
1	99.2	0.3
2	99.5	0.3
3	99.7	0.2
4	100	0.3
5	100.3	0.3
6	100.5	0.2
7	100.8	0.3
8	101.1	0.3
9	101.3	0.2
10	101.5	0.2

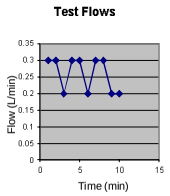

Arithmatic average = 0.26 (L/min)
Adopted average = 0.26 (L/min)

Stage 6

Gauge Pressure	0	(kPa)
Gauge Pressure	0.00	(m)
Static Pressure	52.7	(m)
Head without loss correction	52.66	(m)
Head loss	0.00	(m)
High flow pressure calibratior	0.00	(m)
Total Head	52.66	(m)

Minutes of test	Flowmet read (L)	Flow (L/min)
0	0	
1	0	0
2	0	0
3	0	0
4	0	0
5	0	0
6	0	0
7	0	0
8	0	0
9	0	0
10	0	0

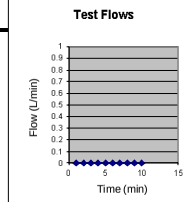

Arithmatic average = 0 (L/min)
Adopted average = 0 (L/min)

Comments:

Calculations used:

$$k = \frac{5.833}{\pi L \sin\alpha}\left(\frac{Q}{H_T}\right)\cdot 10^{-5} \quad \text{m/s} \qquad \text{(CANMET)}$$

$$k = \frac{8.333}{\pi L \sin\alpha}\left(\frac{Q}{H_T}\right)\cdot \ln\left(\frac{L}{r}\right)\cdot 10^{-4} \quad \text{m/s} \qquad \text{(HOEK \& BRAY)}$$

$$lugeon = \frac{Q}{L\sin\alpha}\cdot\frac{100}{H_T} \quad \text{l/m/min} \qquad \text{(HOULSBY)}$$

Stage	Total Head (m)	Flow (l/min)	Calculated Lugeon values: Test Pressure	Q (L/m/min)	Lugeons (L/m/min)	Chosen Lugeon (L/m/min)
1	76.10	0.42	746.57	0.06	0.08	
2	98.53	0.49	966.57	0.08	0.08	
3	124.01	0.59	1216.57	0.09	0.07	0.071
4	98.53	0.44	966.57	0.07	0.07	
5	76.10	0.26	746.57	0.04	0.05	

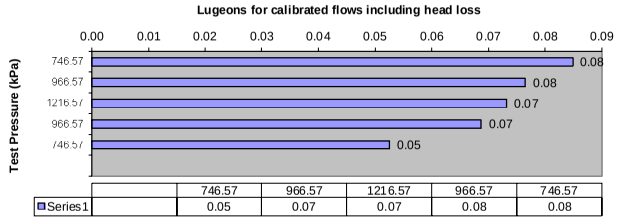

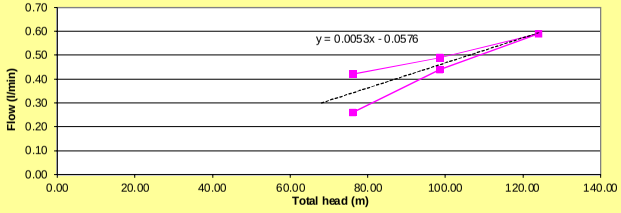

Conductivity Calculations:

MEAN Q/H$_T$	CANMET	HOEK & BRAY	MEAN LUGEONS 0.07	
0.005	1.3E-08	9.4E-09	9.3E-09	m/s

Mean Conductivity K = 1.1E-08 m/s

Job No: TAH4125

Location: Tahmoor Site No: TBF040 Borehole: TBF040 Depth Range: 220.9 -227.4 m

PACKER TEST RESULTS: K = 1.6E-07 m/s

PROJECT: TAH4125 **Site No:** TBF040 **BORE NAME:** TBF040 **HOLE DIP:** 90 **DIP Direction:** **DATE:** 08-Jan-14

Depth To Bottm Packer Test interval:	227.40	m	HEIGHT OF PRESSURE GAUGE:	1	m (above ground level)
Depth To Top Packer Test interval:	220.90	m	STATIC GROUNDWATER LEVEL:	40.7	m (below ground level)
LENGTH OF STAGE TEST:	6.50	m	SURFACE R.L.		m
BORE DIAMETER:	96	mm			

Recorded flow readings at indicated applied pressure heads.

Stage 1

Gauge Pressure	230	(kPa)
Gauge Pressure	23.45	(m)
Static Pressure	53.0	(m)
Head without loss correction	76.40	(m)
Head loss	0.03	(m)
High flow pressure calibration	0.00	(m)
Total Head	76.38	(m)

Minutes of test	Flowmet read (L)	Flow (L/min)
0	307.5	
1	313	5.5
2	318.6	5.6
3	324.4	5.8
4	330.2	5.8
5	336	5.8
6	341.6	5.6
7	347.4	5.8
8	352.8	5.4
9	358.4	5.6
10	363.7	5.3

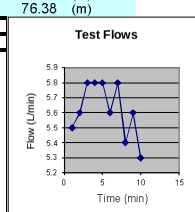

Arithmatic average = 5.62 (L/min)
Adopted average = 5.62 (L/min)

Stage 2

Gauge Pressure	450	(kPa)
Gauge Pressure	45.87	(m)
Static Pressure	53.0	(m)
Head without loss correction	98.83	(m)
Head loss	0.05	(m)
High flow pressure calibration	0.00	(m)
Total Head	98.78	(m)

Minutes of test	Flowmet read (L)	Flow (L/min)
0	372.8	
1	380.8	8
2	388.4	7.6
3	395.8	7.4
4	403.7	7.9
5	411	7.3
6	418	7
7	425	7
8	432	7
9	438.7	6.7
10	445.4	6.7

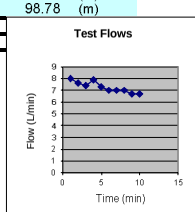

Arithmatic average = 7.26 (L/min)
Adopted average = 7.26 (L/min)

Stage 3

Gauge Pressure	700	(kPa)
Gauge Pressure	71.36	(m)
Static Pressure	53.0	(m)
Head without loss correction	124.31	(m)
Head loss	0.08	(m)
High flow pressure calibratior	0.00	(m)
Total Head	124.23	(m)

Minutes of test	Flowmet read (L)	Flow (L/min)
0	468	
1	478.5	10.5
2	489	10.5
3	499.2	10.2
4	509.6	10.4
5	520	10.4
6	529.4	9.4
7	539	9.6
8	547.7	8.7
9	556.5	8.8
10	566	9.5

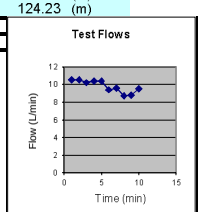

Arithmatic average = 9.8 (L/min)
Adopted average = 9.8 (L/min)

Stage 4

Gauge Pressure	450	(kPa)
Gauge Pressure	45.87	(m)
Static Pressure	53.0	(m)
Head without loss correction	98.83	(m)
Head loss	0.03	(m)
High flow pressure calibration	0.00	(m)
Total Head	98.80	(m)

Minutes of test	Flowmet read (L)	Flow (L/min)
0	570.2	
1	576.2	6
2	582.2	6
3	588.5	6.3
4	594.8	6.3
5	601	6.2
6	607.3	6.3
7	613.4	6.1
8	619.5	6.1
9	625.7	6.2
10	631.7	6

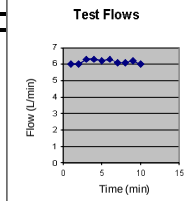

Arithmatic average = 6.15 (L/min)
Adopted average = 6.15 (L/min)

Stage 5

Gauge Pressure	230	(kPa)
Gauge Pressure	23.45	(m)
Static Pressure	53.0	(m)
Head without loss correction	76.40	(m)
Head loss	0.01	(m)
High flow pressure calibration	0.00	(m)
Total Head	76.39	(m)

Minutes of test	Flowmet read (L)	Flow (L/min)
0	633.5	
1	637	3.5
2	640.5	3.5
3	644.4	3.9
4	648.4	4
5	652.4	4
6	656.4	4
7	660.4	4
8	664.4	4
9	668.3	3.9
10	672.3	4

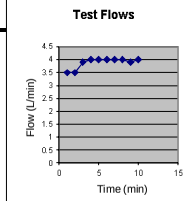

Arithmatic average = 3.88 (L/min)
Adopted average = 3.88 (L/min)

Stage 6

Gauge Pressure	0	(kPa)
Gauge Pressure	0.00	(m)
Static Pressure	53.0	(m)
Head without loss correction	52.96	(m)
Head loss	0.00	(m)
High flow pressure calibratior	0.00	(m)
Total Head	52.96	(m)

Minutes of test	Flowmet read (L)	Flow (L/min)
0	0	
1	0	0
2	0	0
3	0	0
4	0	0
5	0	0
6	0	0
7	0	0
8	0	0
9	0	0
10	0	0

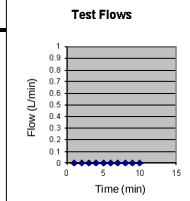

Arithmatic average = 0 (L/min)
Adopted average = 0 (L/min)

Comments:

Calculations used:

$$k = \frac{5.833}{\pi L \sin\alpha}\left(\frac{Q}{H_T}\right)\cdot 10^{-5} \text{ m/s} \quad \text{(CANMET)}$$

$$k = \frac{8.333}{\pi L \sin\alpha}\left(\frac{Q}{H_T}\right)\cdot \ln\left(\frac{L}{r}\right)\cdot 10^{-4} \text{ m/s} \quad \text{(HOEK \& BRAY)}$$

$$lugeon = \frac{Q}{L\sin\alpha}\cdot\frac{100}{H_T} \text{ l/m/min} \quad \text{(HOULSBY)}$$

Stage	Total Head (m)	Flow (l/min)	Calculated Lugeon values: Test Pressure	Q (L/m/min)	Lugeons (L/m/min)	Chosen Lugeon (L/m/min)
1	76.38	5.62	749.24	0.86	1.13	
2	98.78	7.26	969.06	1.12	1.13	
3	124.23	9.80	1218.68	1.51	1.21	1.043
4	98.80	6.15	969.19	0.95	0.96	
5	76.39	3.88	749.38	0.60	0.78	

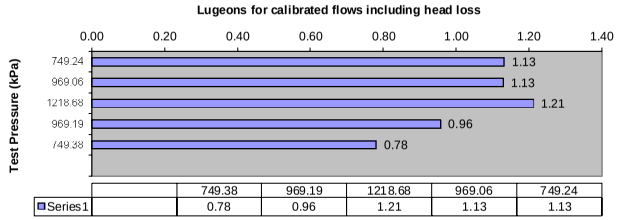

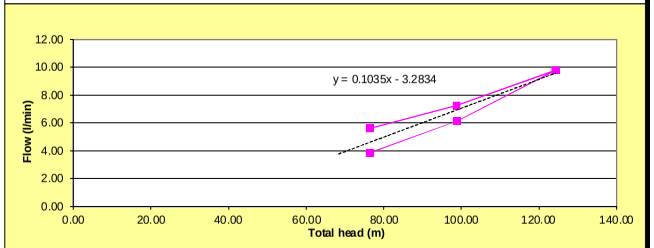

Conductivity Calculations:

MEAN Q/H$_T$	CANMET	HOEK & BRAY	MEAN LUGEONS	
			1.04	
0.070	2.0E-07	1.4E-07	1.4E-07	m/s
Mean Conductivity		K =	1.6E-07	m/s

Job No: TAH4125

Location: Tahmoor Site No: TBF040 Borehole: TBF040 Depth Range: 226.9 -233.4 m

PACKER TEST RESULTS: K = 1.9E-07 m/s

PROJECT: TAH4125 **Site No:** TBF040 **BORE NAME:** TBF040 **HOLE DIP:** 90 **DIP Direction:** **DATE:** 09-Jan-14

Depth To Bottm Packer Test interval:	233.40	m	HEIGHT OF PRESSURE GAUGE:	1	m (above ground level)
Depth To Top Packer Test interval:	226.90	m	STATIC GROUNDWATER LEVEL:	40.7	m (below ground level)
LENGTH OF STAGE TEST:	6.50	m	SURFACE R.L.		m
BORE DIAMETER:	96	mm			

Recorded flow readings at indicated applied pressure heads.

Stage 1

Gauge Pressure	230	(kPa)
Gauge Pressure	23.45	(m)
Static Pressure	53.3	(m)
Head without loss correction	76.70	(m)
Head loss	0.05	(m)
High flow pressure calibration	0.00	(m)
Total Head	76.65	(m)

Minutes of test		Flow (L/min)
0		
1		9
2		7.5
3		8
4		7.5
5		7.5
6		7
7		7.5
8		7
9		6.5
10		6.5

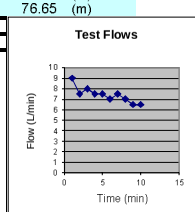

Arithmatic average = 7.4 (L/min)
Adopted average = 7.4 (L/min)

Stage 2

Gauge Pressure	450	(kPa)
Gauge Pressure	45.87	(m)
Static Pressure	53.3	(m)
Head without loss correction	99.13	(m)
Head loss	0.07	(m)
High flow pressure calibration	0.00	(m)
Total Head	99.05	(m)

Minutes of test	Flowmet read (L)	Flow (L/min)
0	118	
1	128	10
2	138	10
3	148	10
4	157	9
5	166	9
6	175	9
7	184	9
8	192.5	8.5
9	201	8.5
10	210	9

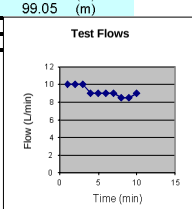

Arithmatic average = 9.2 (L/min)
Adopted average = 9.2 (L/min)

Stage 3

Gauge Pressure	700	(kPa)
Gauge Pressure	71.36	(m)
Static Pressure	53.3	(m)
Head without loss correction	124.61	(m)
Head loss	0.13	(m)
High flow pressure calibratior	0.00	(m)
Total Head	124.49	(m)

Minutes of test	Flowmet read (L)	Flow (L/min)
0	224	
1	236.5	12.5
2	249	12.5
3	261.5	12.5
4	273.5	12
5	285	11.5
6	296	11
7	308	12
8	320	12
9	332	12
10	343	11

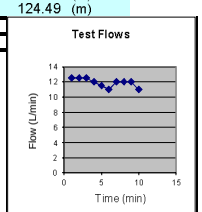

Arithmatic average = 11.9 (L/min)
Adopted average = 11.9 (L/min)

Stage 4

Gauge Pressure	450	(kPa)
Gauge Pressure	45.87	(m)
Static Pressure	53.3	(m)
Head without loss correction	99.13	(m)
Head loss	0.05	(m)
High flow pressure calibration	0.00	(m)
Total Head	99.08	(m)

Minutes of test		Flow (L/min)
0		
1		6
2		7
3		7.5
4		7.5
5		7.5
6		7
7		7.5
8		7.5
9		7
10		7.5

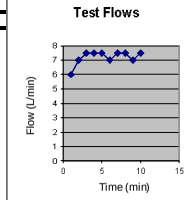

Arithmatic average = 7.2 (L/min)
Adopted average = 7.2 (L/min)

Stage 5

Gauge Pressure	230	(kPa)
Gauge Pressure	23.45	(m)
Static Pressure	53.3	(m)
Head without loss correction	76.70	(m)
Head loss	0.02	(m)
High flow pressure calibration	0.00	(m)
Total Head	76.69	(m)

Minutes of test	Flowmet read (L)	Flow (L/min)
0	419	
1	421	2
2	424.5	4.5
3	428	3.5
4	432	4
5	437	5
6	441.5	4.5
7	446	4.5
8	450.5	4.5
9	455.5	5
10	460	4.5

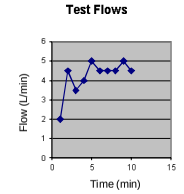

Arithmatic average = 4.2 (L/min)
Adopted average = 4.2 (L/min)

Stage 6

Gauge Pressure	0	(kPa)
Gauge Pressure	0.00	(m)
Static Pressure	53.3	(m)
Head without loss correction	53.26	(m)
Head loss	0.00	(m)
High flow pressure calibratior	0.00	(m)
Total Head	53.26	(m)

Minutes of test	Flowmet read (L)	Flow (L/min)
0	0	
1	465	465
2	0	-465
3	0	0
4	0	0
5	0	0
6	0	0
7	0	0
8	0	0
9	0	0
10	0	0

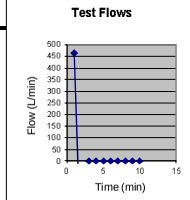

Arithmatic average = 0 (L/min)
Adopted average = 0 (L/min)

Comments:

Calculations used:

$$k = \frac{5.833}{\pi L \sin\alpha}\left(\frac{Q}{H_T}\right)\cdot 10^{-5} \text{ m/s} \quad \text{(CANMET)}$$

$$k = \frac{8.333}{\pi L \sin\alpha}\left(\frac{Q}{H_T}\right)\cdot \ln\left(\frac{L}{r}\right)\cdot 10^{-4} \text{ m/s} \quad \text{(HOEK \& BRAY)}$$

$$lugeon = \frac{Q}{L \sin\alpha}\cdot\frac{100}{H_T} \text{ l/m/min} \quad \text{(HOULSBY)}$$

Stage	Total Head (m)	Flow (l/min)	Calculated Lugeon values: Test Pressure	Q (L/m/min)	Lugeons (L/m/min)	Chosen Lugeon (L/m/min)
1	76.65	7.40	751.98	1.14	1.49	
2	99.05	9.20	971.72	1.42	1.43	
3	124.49	11.90	1221.23	1.83	1.47	1.269
4	99.08	7.20	972.01	1.11	1.12	
5	76.69	4.2	752.30	0.65	0.84	

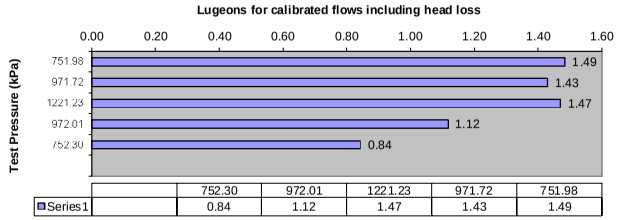

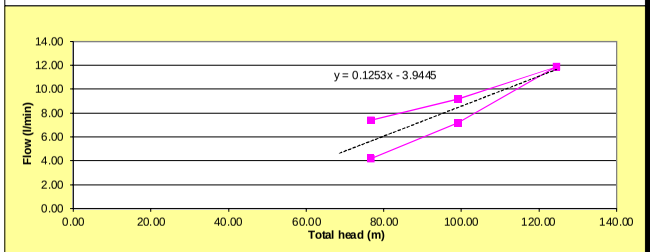

Conductivity Calculations:

MEAN Q/H$_T$	CANMET	HOEK & BRAY	MEAN LUGEONS	
			1.27	
0.085	2.4E-07	1.7E-07	1.6E-07	m/s
Mean Conductivity		K =	1.9E-07	m/s

Job No: TAH4125

Location: Tahmoor Site No: TBF040 Borehole: TBF040 Depth Range: 232.9 -239.4 m

PACKER TEST RESULTS: K = 9.5E-09 m/s

PROJECT: TAH4125 Site No: TBF040 BORE NAME: TBF040 HOLE DIP: 90 DIP Direction: DATE: 09-Jan-14

Depth To Bottm Packer Test interval:	239.40	m	HEIGHT OF PRESSURE GAUGE:	1	m (above ground level)
Depth To Top Packer Test interval:	232.90	m	STATIC GROUNDWATER LEVEL:	40.7	m (below ground level)
LENGTH OF STAGE TEST:	6.50	m	SURFACE R.L.		m
BORE DIAMETER:	96	mm			

Recorded flow readings at indicated applied pressure heads.

Stage 1

Gauge Pressure	230	(kPa)
Gauge Pressure	23.45	(m)
Static Pressure	53.6	(m)
Head without loss correction	77.00	(m)
Head loss	0.00	(m)
High flow pressure calibration	0.00	(m)
Total Head	77.00	(m)

Minutes of test	Flowmet read (L)	Flow (L/min)
0	692.5	
1	693.1	0.6
2	693.5	0.4
3	693.9	0.4
4	694.2	0.3
5	694.6	0.4
6	695	0.4
7	695.5	0.5
8	696	0.5
9	696.3	0.3
10	696.6	0.3

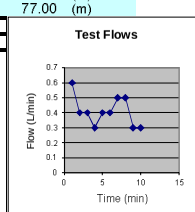

Arithmatic average = 0.41 (L/min)
Adopted average = 0.41 (L/min)

Stage 2

Gauge Pressure	450	(kPa)
Gauge Pressure	45.87	(m)
Static Pressure	53.6	(m)
Head without loss correction	99.43	(m)
Head loss	0.00	(m)
High flow pressure calibration	0.00	(m)
Total Head	99.43	(m)

Minutes of test	Flowmet read (L)	Flow (L/min)
0	697.7	
1	698.1	0.4
2	698.5	0.4
3	698.9	0.4
4	699.3	0.4
5	699.7	0.4
6	700	0.3
7	700.3	0.3
8	700.7	0.4
9	701	0.3
10	701.4	0.4

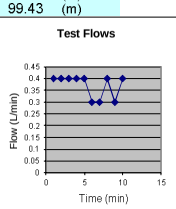

Arithmatic average = 0.37 (L/min)
Adopted average = 0.37 (L/min)

Stage 3

Gauge Pressure	700	(kPa)
Gauge Pressure	71.36	(m)
Static Pressure	53.6	(m)
Head without loss correction	124.91	(m)
Head loss	0.00	(m)
High flow pressure calibratior	0.00	(m)
Total Head	124.91	(m)

Minutes of test	Flowmet read (L)	Flow (L/min)
0	702.5	
1	703.3	0.8
2	703.9	0.6
3	704.4	0.5
4	705	0.6
5	705.4	0.4
6	705.9	0.5
7	706.4	0.5
8	707	0.6
9	707.4	0.4
10	708.1	0.7

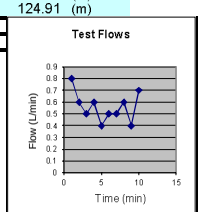

Arithmatic average = 0.56 (L/min)
Adopted average = 0.56 (L/min)

Stage 4

Gauge Pressure	450	(kPa)
Gauge Pressure	45.87	(m)
Static Pressure	53.6	(m)
Head without loss correction	99.43	(m)
Head loss	0.00	(m)
High flow pressure calibration	0.00	(m)
Total Head	99.43	(m)

Minutes of test	Flowmet read (L)	Flow (L/min)
0	708.2	
1	708.7	0.5
2	709.1	0.4
3	709.4	0.3
4	709.8	0.4
5	710.2	0.4
6	710.5	0.3
7	711	0.5
8	711.4	0.4
9	711.7	0.3
10	712.1	0.4

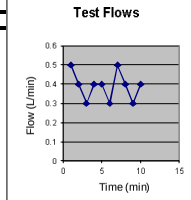

Arithmatic average = 0.39 (L/min)
Adopted average = 0.39 (L/min)

Stage 5

Gauge Pressure	230	(kPa)
Gauge Pressure	23.45	(m)
Static Pressure	53.6	(m)
Head without loss correction	77.00	(m)
Head loss	0.00	(m)
High flow pressure calibration	0.00	(m)
Total Head	77.00	(m)

Minutes of test	Flowmet read (L)	Flow (L/min)
0	712	
1	712.4	0.4
2	712.7	0.3
3	713	0.3
4	713.2	0.2
5	713.4	0.2
6	713.6	0.2
7	713.8	0.2
8	714	0.2
9	714.3	0.3
10	714.5	0.2

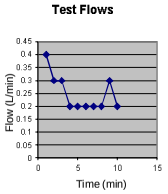

Arithmatic average = 0.25 (L/min)
Adopted average = 0.25 (L/min)

Stage 6

Gauge Pressure	0	(kPa)
Gauge Pressure	0.00	(m)
Static Pressure	53.6	(m)
Head without loss correction	53.56	(m)
Head loss	0.00	(m)
High flow pressure calibratior	0.00	(m)
Total Head	53.56	(m)

Minutes of test	Flowmet read (L)	Flow (L/min)
0	0	
1	0	0
2	0	0
3	0	0
4	0	0
5	0	0
6	0	0
7	0	0
8	0	0
9	0	0
10	0	0

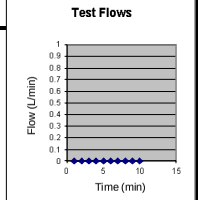

Arithmatic average = 0 (L/min)
Adopted average = 0 (L/min)

Comments:

Calculations used:

$$k = \frac{5.833}{\pi L \sin\alpha}\left(\frac{Q}{H_T}\right)\cdot 10^{-5} \quad \text{m/s} \qquad \text{(CANMET)}$$

$$k = \frac{8.333}{\pi L \sin\alpha}\left(\frac{Q}{H_T}\right)\cdot \ln\left(\frac{L}{r}\right)\cdot 10^{-4} \quad \text{m/s} \qquad \text{(HOEK \& BRAY)}$$

$$lugeon = \frac{Q}{L\sin\alpha}\cdot\frac{100}{H_T} \quad \text{l/m/min} \qquad \text{(HOULSBY)}$$

Stage	Total Head (m)	Flow (l/min)	Calculated Lugeon values: Test Pressure	Q (L/m/min)	Lugeons (L/m/min)	Chosen Lugeon (L/m/min)
1	77.00	0.41	755.40	0.06	0.08	
2	99.43	0.37	975.40	0.06	0.06	
3	124.91	0.56	1225.40	0.09	0.07	0.064
4	99.43	0.39	975.40	0.06	0.06	
5	77.00	0.25	755.40	0.04	0.05	

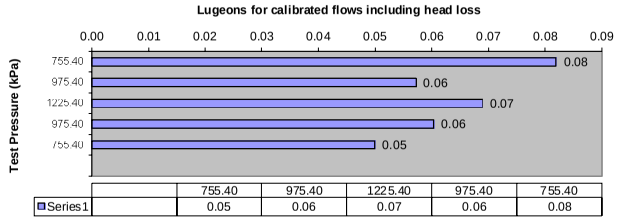

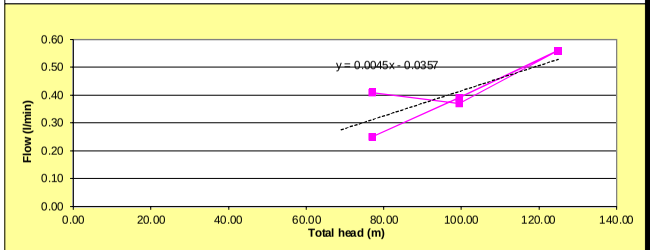

Conductivity Calculations:

MEAN Q/H$_T$	CANMET	HOEK & BRAY	MEAN LUGEONS 0.06	
0.004	1.2E-08	8.3E-09	8.3E-09	m/s
Mean Conductivity		K =	9.5E-09	m/s

APPENDIX 6 – BOREHOLE PHOTOS

Appendix 6.1: 74.8m - Core loss zone, Large cavity present in the Hawkesbury Sandstone.

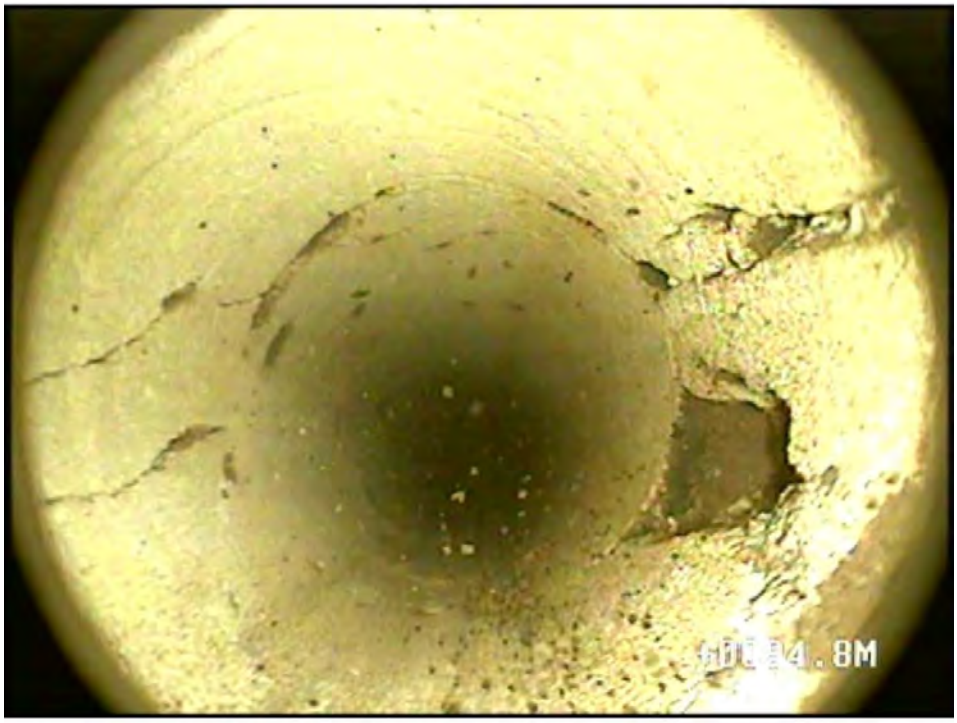

Appendix 6.2: 95.4m - Core loss zone, water loss zone, horizontal to vertical orientated joint zone, including a small cavity.

Appendix 6: Borehole camera investigation.

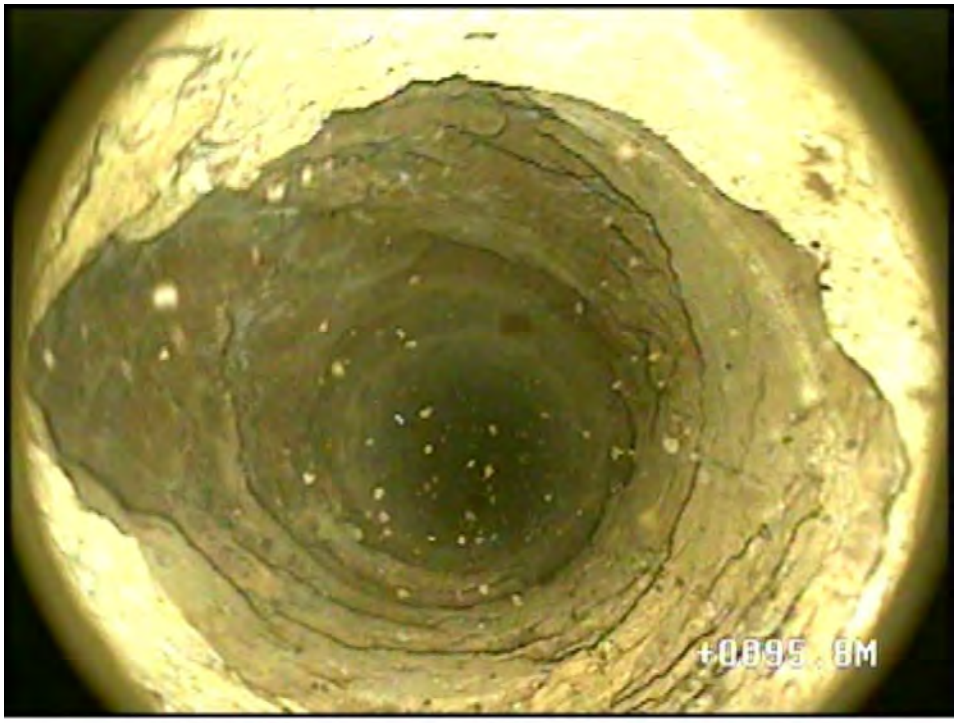

Appendix 6.3: 96.4m Core loss zone, Cavity present within the Hawkesbury Sandstone.

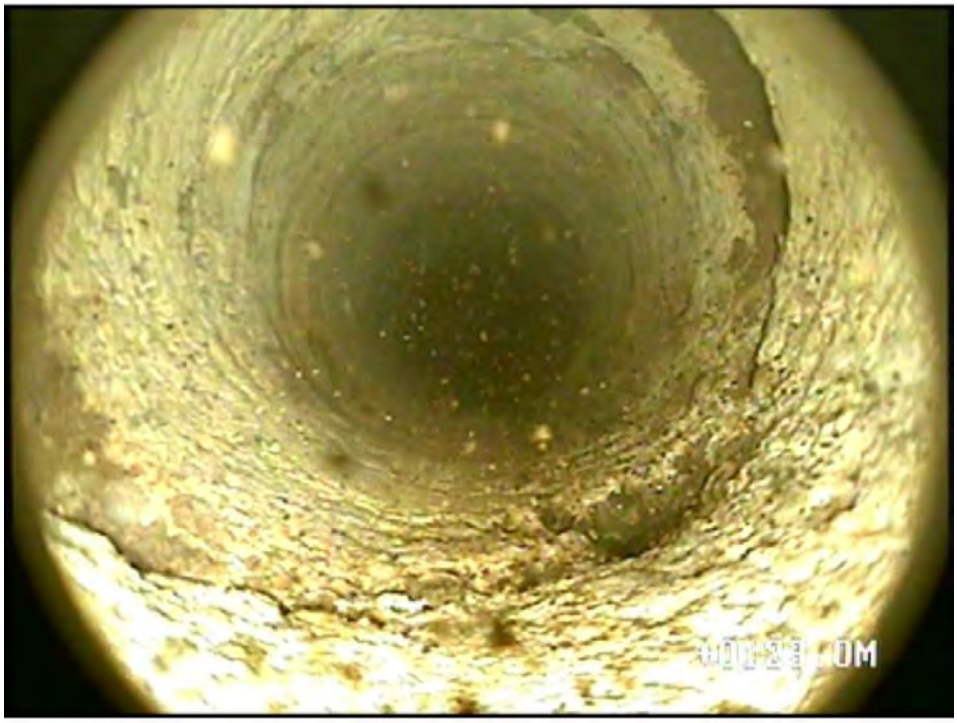

Appendix 6.4: 123.6m - Water loss zone, joint zone, mid angle fracture & small cavity.

Appendix 6: Borehole camera investigation.

Appendix 6.5: 136.8m - Core loss zone, water loss zone, horizontal joint zone & small cavity.

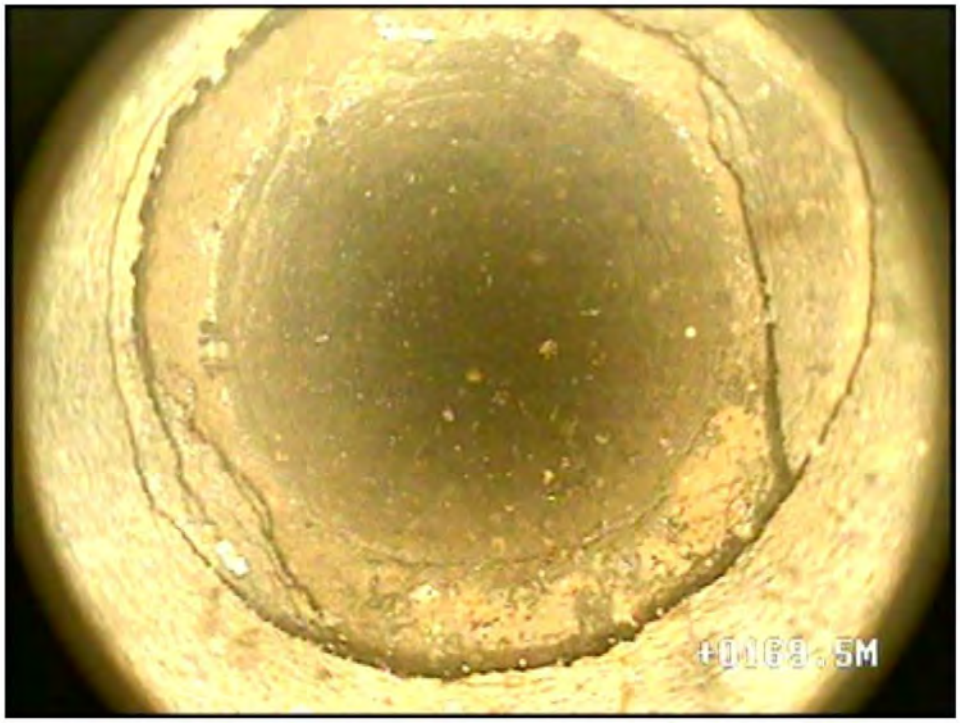

Appendix 6.6: 169.3m - Water loss zone, near horizontally orientated joint zone.

Appendix 6: Borehole camera investigation.

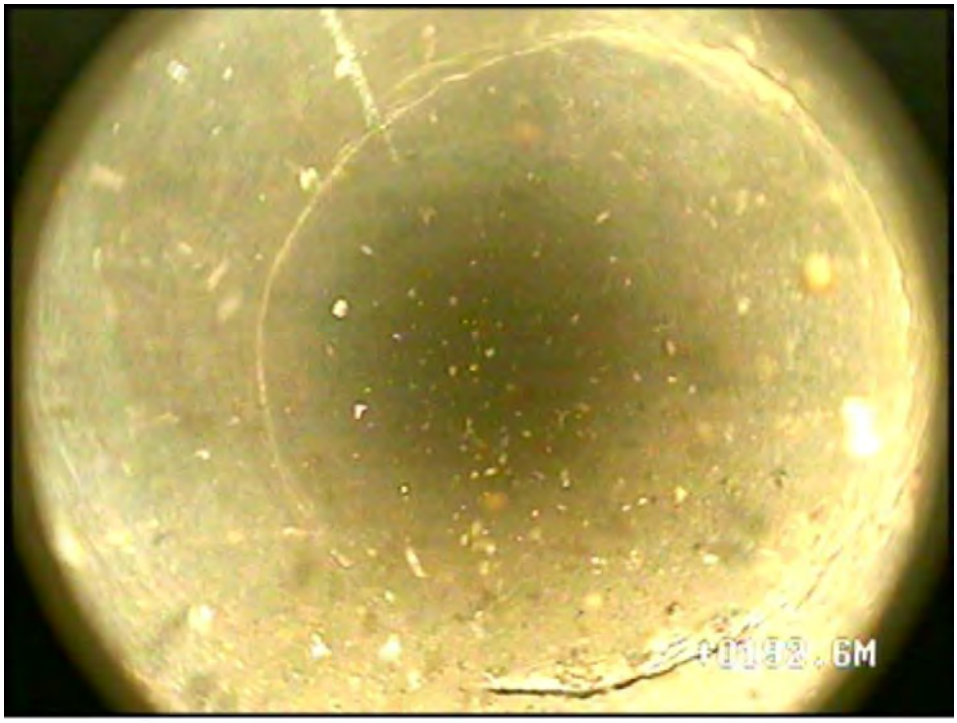

Appendix 6.7: 193.4m - Medium angled joints, abundant throughout the Bald Hill Claystone.

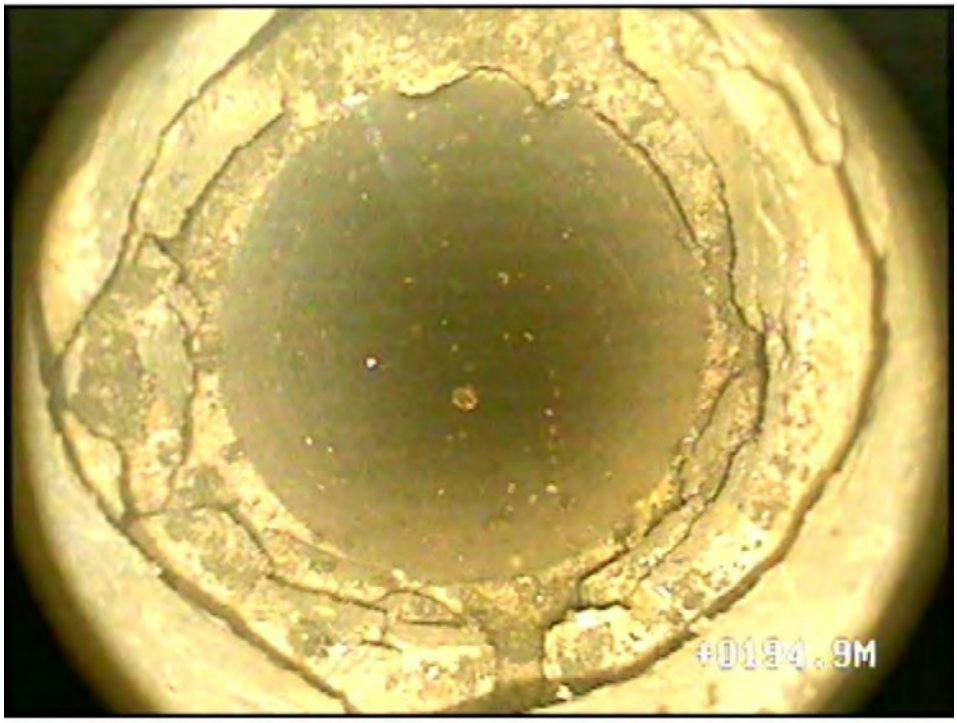

Appendix 6.8: 195.8m - Water Loss Zone within at the base of the Bald Hill, medium angled joint zone.

Appendix 6: Borehole camera investigation.

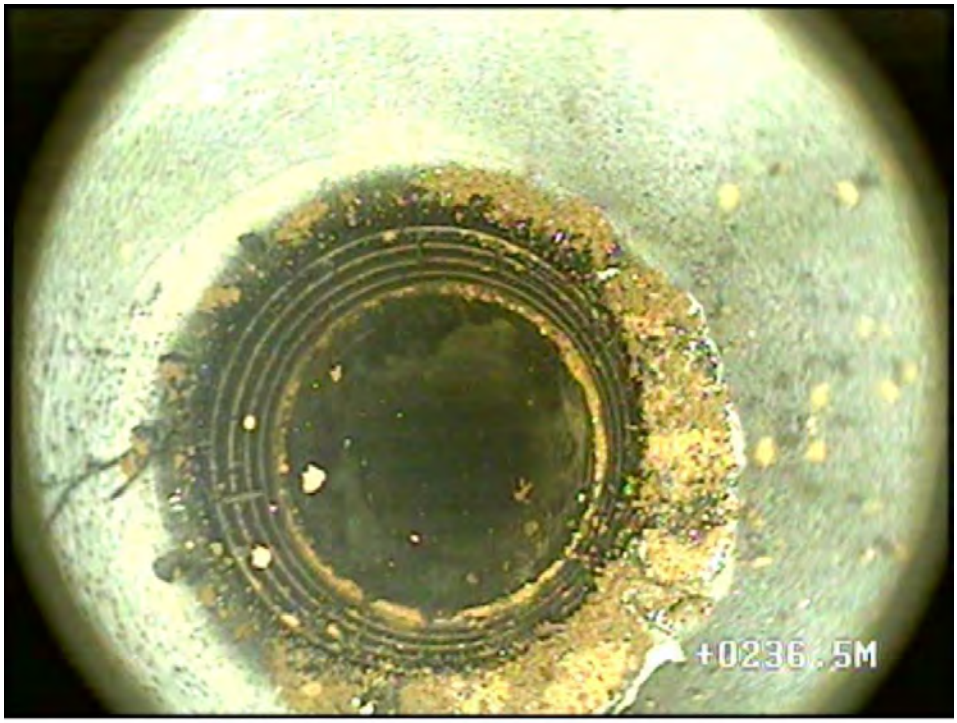

Appendix 6.9: 236.5m - Core barrel stuck at the base of the borehole.

Appendix 6: Borehole camera investigation.

APPENDIX 7 – ACOUSTIC SCANNER LOG
(PDF Only)

Acoustic Scanner Log

1:20

Weatherford®

COMPANY:	**XSTRATA COAL**
WELL:	**TBF040**
FIELD:	**TAHMOOR**
STATE:	**NEW SOUTH WALES**
COUNTRY:	**AUSTRALIA**
LOCATION:	**TBF040**
Latitude:	
Longitude:	
UTM Zone:	
UTM Easting:	
UTM Northing:	

REMARKS:
All orientation data (including images) are orientated to Magnetic North.

OTHER SERVICES:
DD6 NN2 MS2 VO4

Permanent Datum: G.L. Elevation: 0.00 metres
Log Measured From: G.L. metres above Permanent Datum
Drilling Measured From: G.L.

Elevations:
KB: NA metres
DF: NA metres
GL: NA metres

Date:	14-JAN-2014			
Run Number	5			
Depth Driller	243.90	metres		
Depth Logger	236.50	metres		
First Reading	236.63	metres		
Last Reading	68.63	metres		
Casing Driller	74.00	metres		
Casing Logger	74.00	metres		
Bit Size	96.00	millimetres		
Hole Fluid Type				
Density / Viscosity	g/c3	sec/qt		
PH / Fluid Loss		mL/30min		
Sample Source				
Rm @ Measured Temp	ohm-m @	deg C		
Rmf @ Measured Temp	ohm-m @	deg C		
Rmc @ Measured Temp	ohm-m @	deg C		
Source Rmf / Rmc				
Rm @ Max Temp	ohm-m @	deg C		
Time Since Circulation				
Max Recorded Temp		deg C		
Unit # / Base		N'CLE		
Equipment Name	ALT-ABI40-052301			
Recorded By	ALM			
Witnessed By	KT			

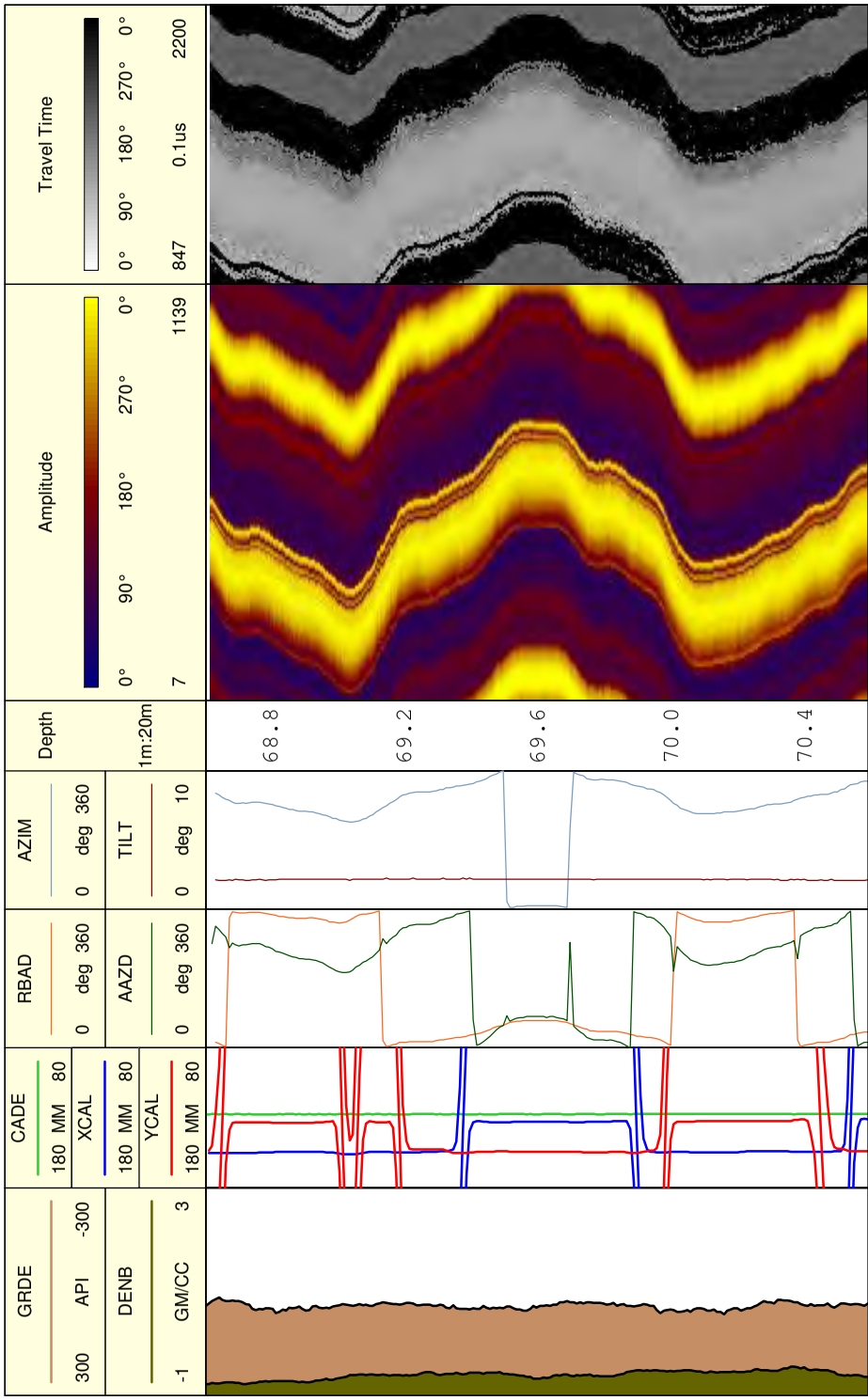

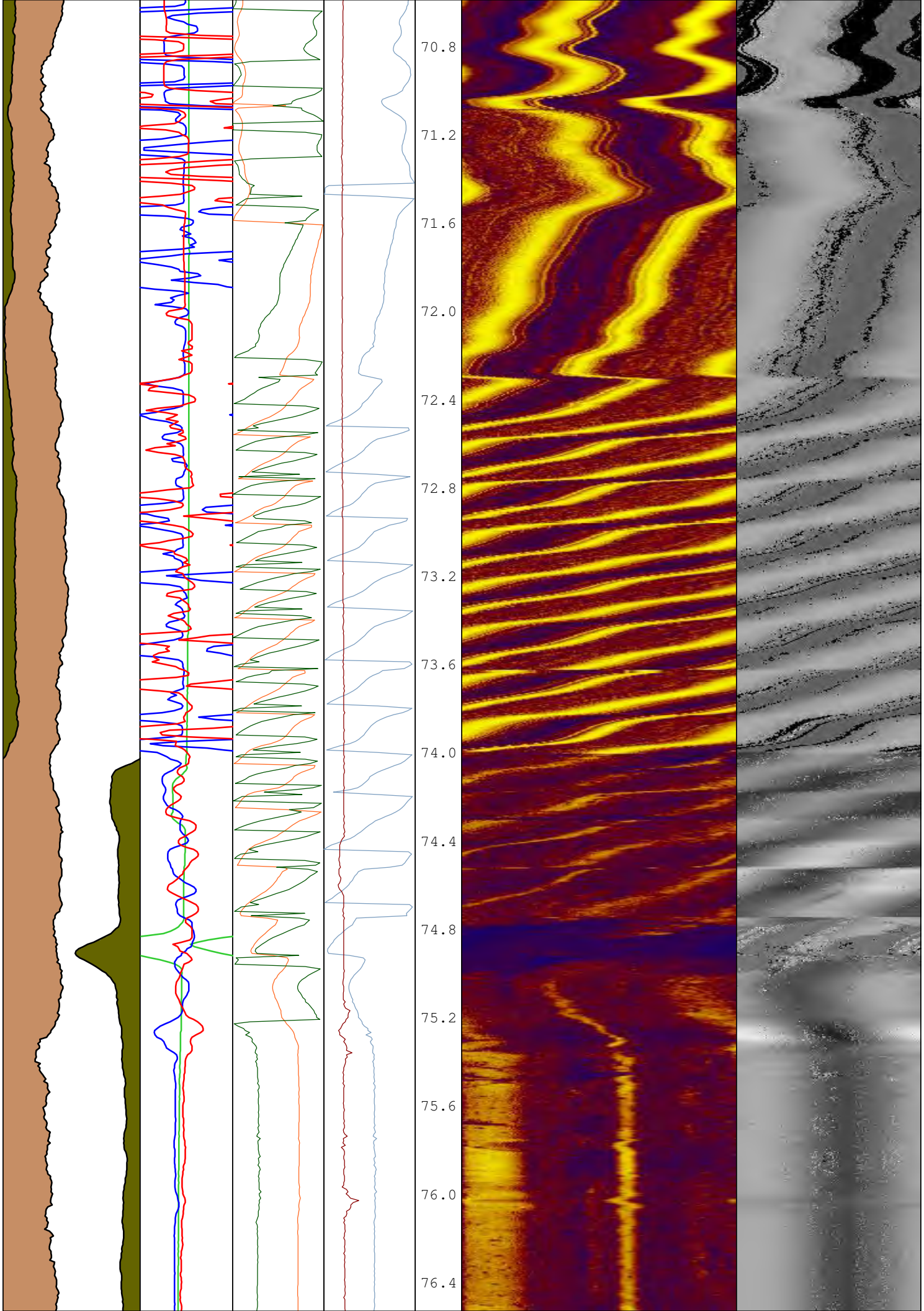
70.8
71.2
71.6
72.0
72.4
72.8
73.2
73.6
74.0
74.4
74.8
75.2
75.6
76.0
76.4

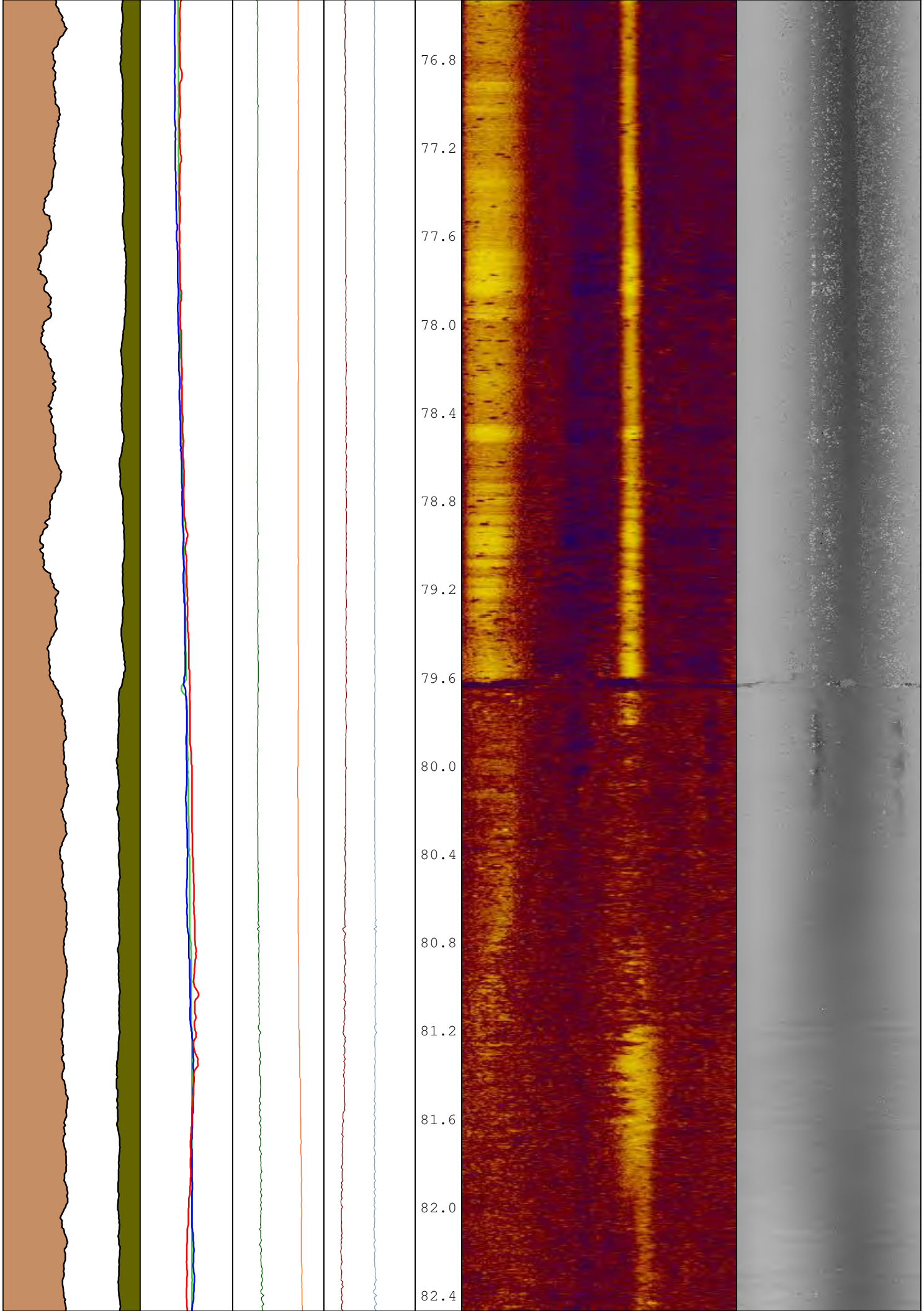
76.8
77.2
77.6
78.0
78.4
78.8
79.2
79.6
80.0
80.4
80.8
81.2
81.6
82.0
82.4

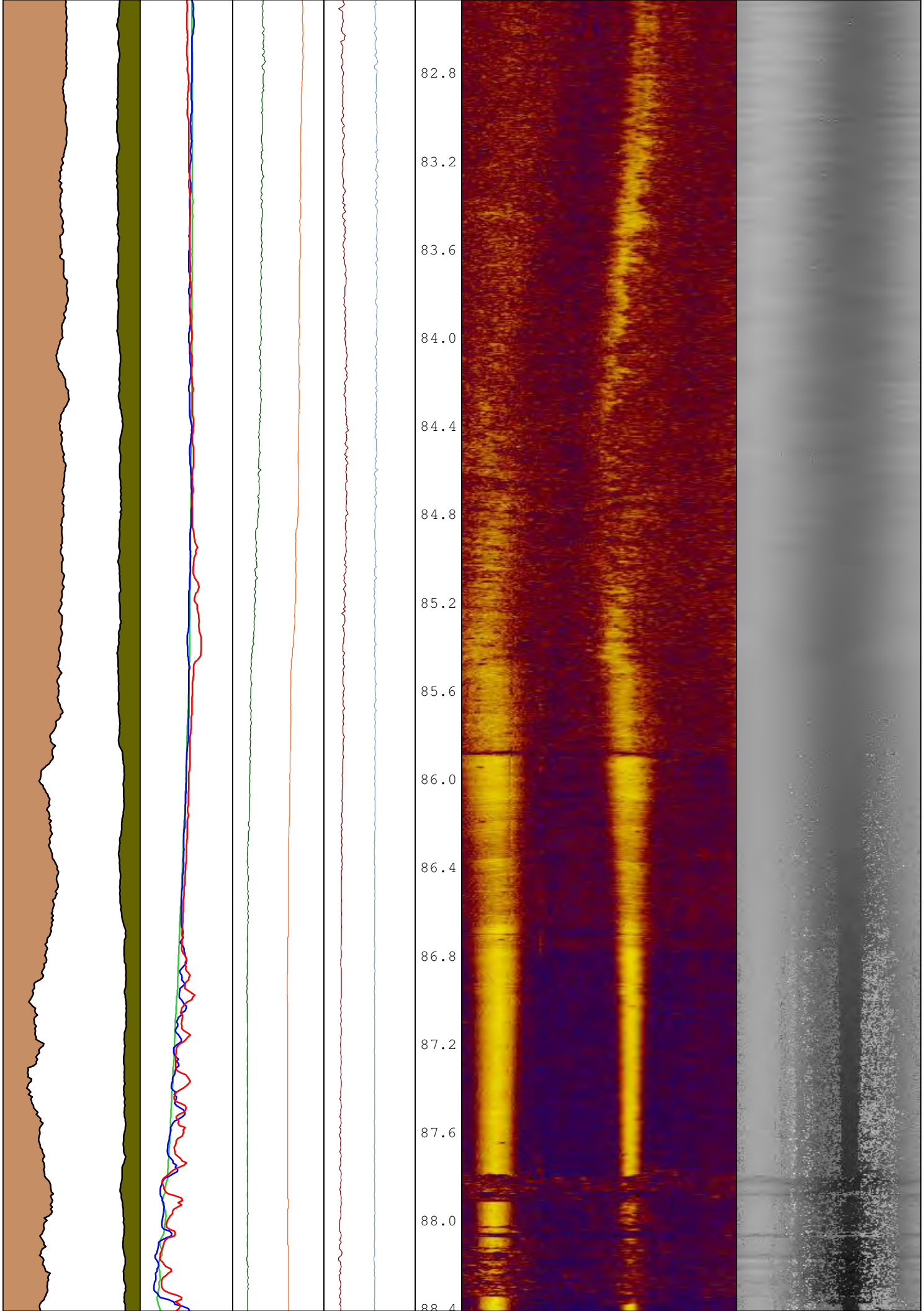
82.8
83.2
83.6
84.0
84.4
84.8
85.2
85.6
86.0
86.4
86.8
87.2
87.6
88.0

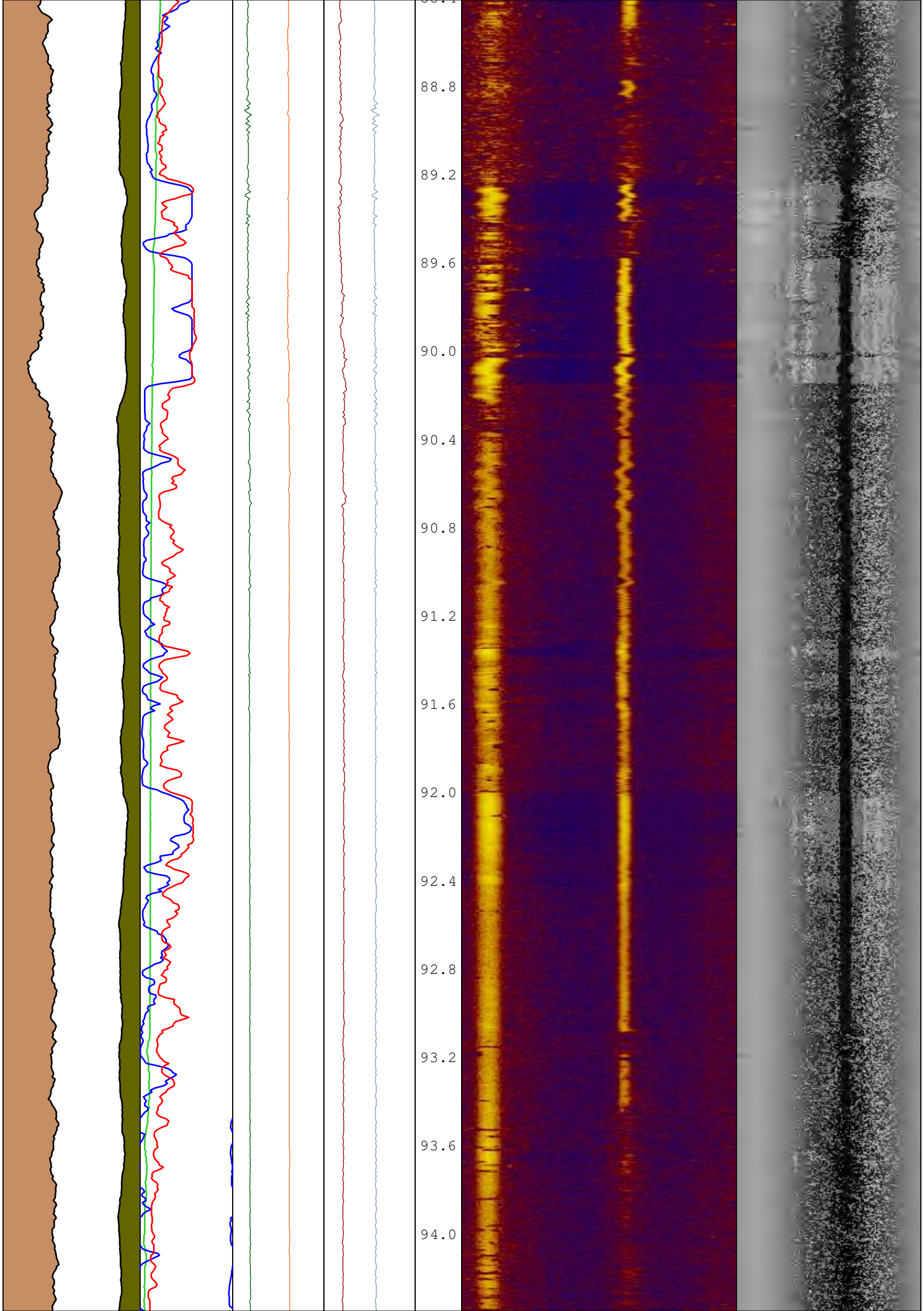
88.8
89.2
89.6
90.0
90.4
90.8
91.2
91.6
92.0
92.4
92.8
93.2
93.6
94.0

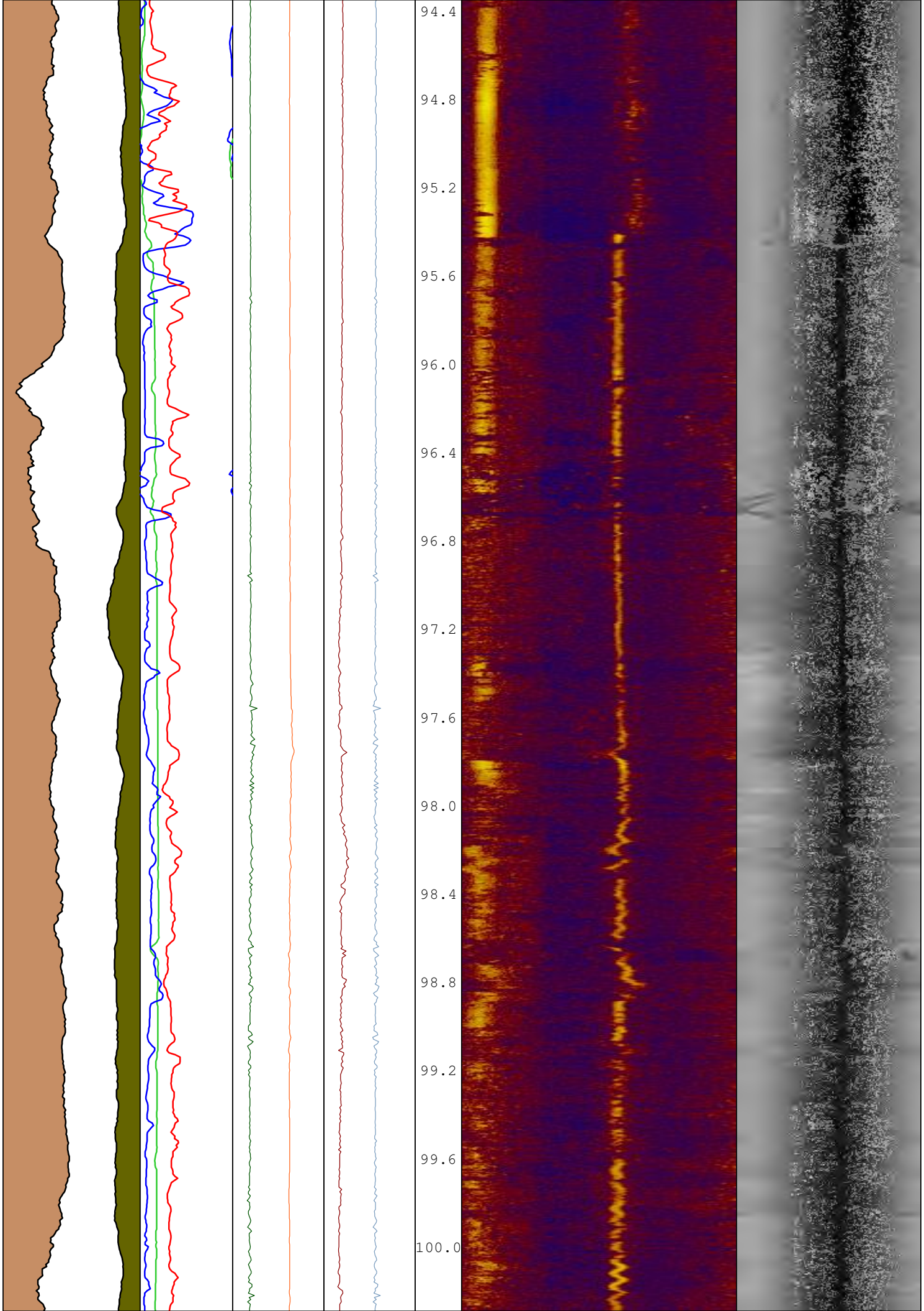
94.4
94.8
95.2
95.6
96.0
96.4
96.8
97.2
97.6
98.0
98.4
98.8
99.2
99.6
100.0

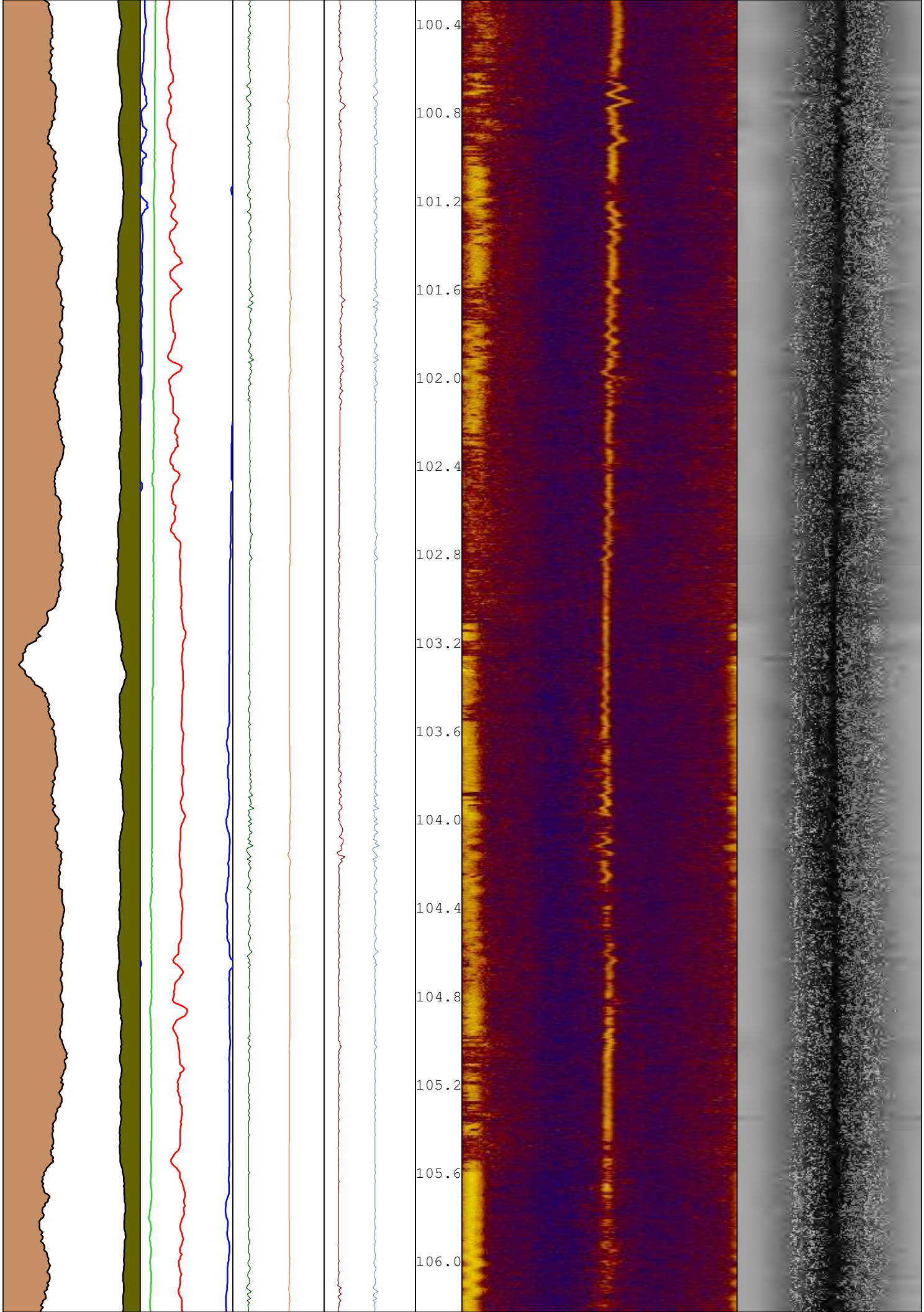
100.4
100.8
101.2
101.6
102.0
102.4
102.8
103.2
103.6
104.0
104.4
104.8
105.2
105.6
106.0

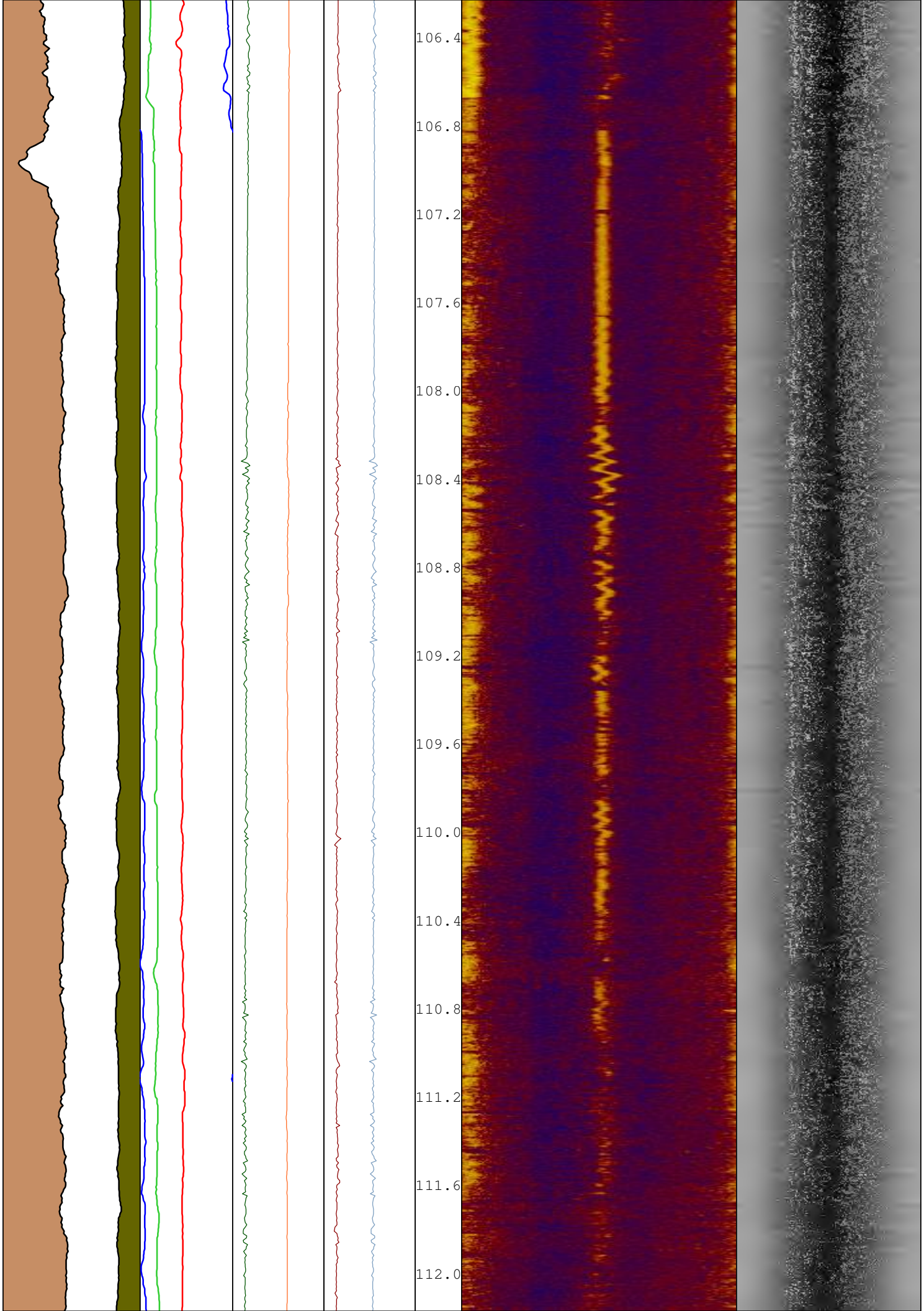
106.4
106.8
107.2
107.6
108.0
108.4
108.8
109.2
109.6
110.0
110.4
110.8
111.2
111.6
112.0

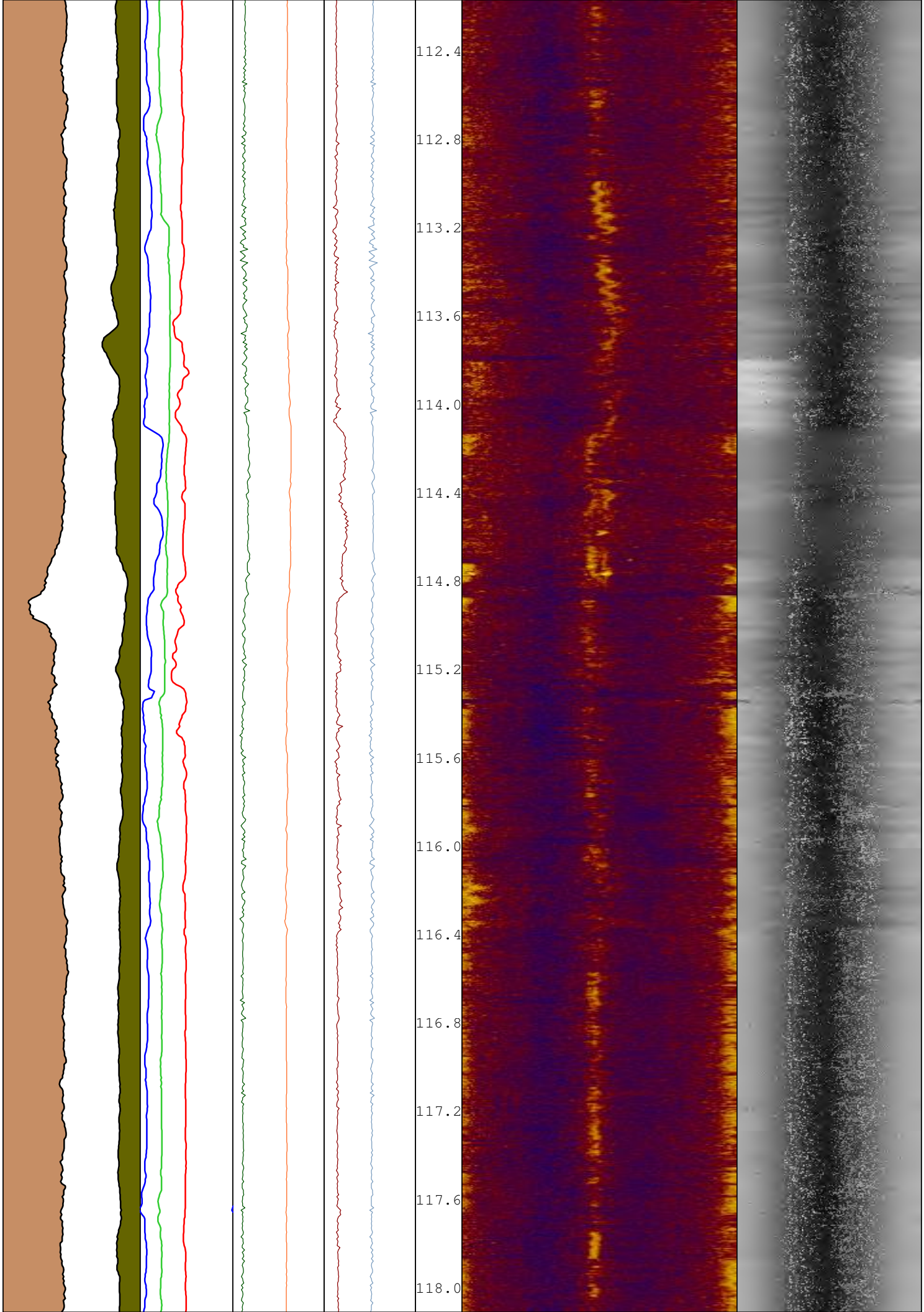
112.4
112.8
113.2
113.6
114.0
114.4
114.8
115.2
115.6
116.0
116.4
116.8
117.2
117.6
118.0

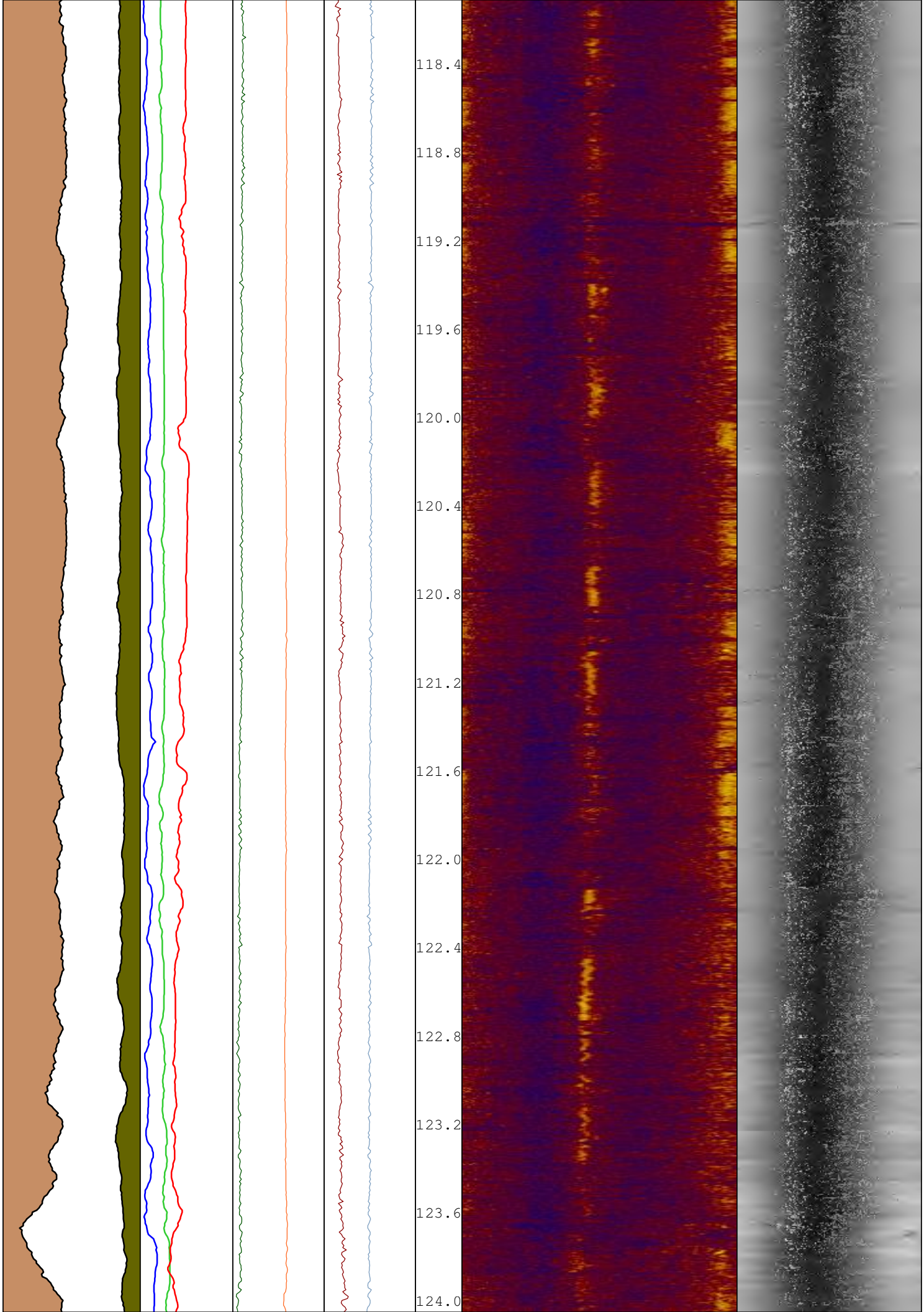
118.4
118.8
119.2
119.6
120.0
120.4
120.8
121.2
121.6
122.0
122.4
122.8
123.2
123.6
124.0

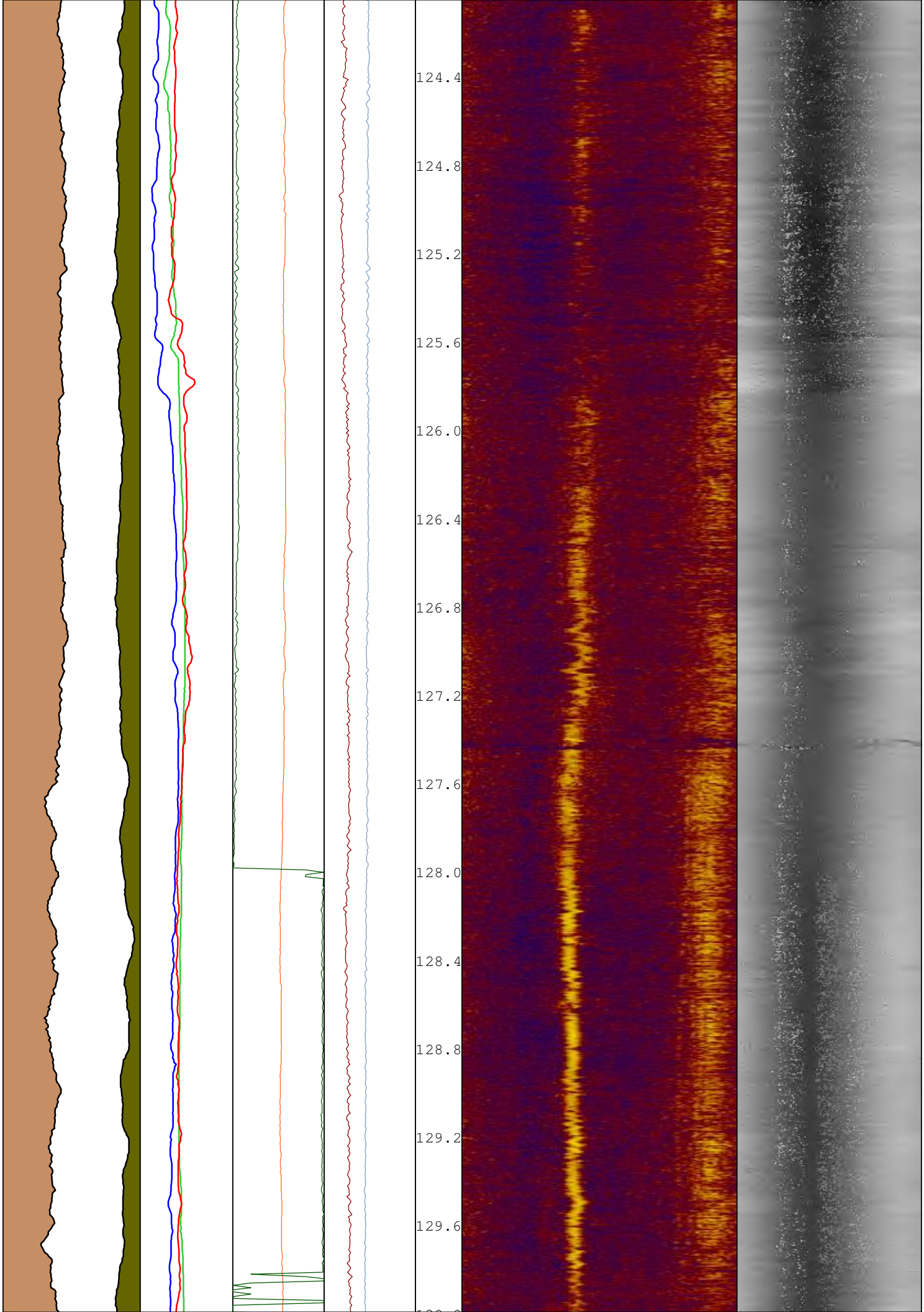
124.4
124.8
125.2
125.6
126.0
126.4
126.8
127.2
127.6
128.0
128.4
128.8
129.2
129.6

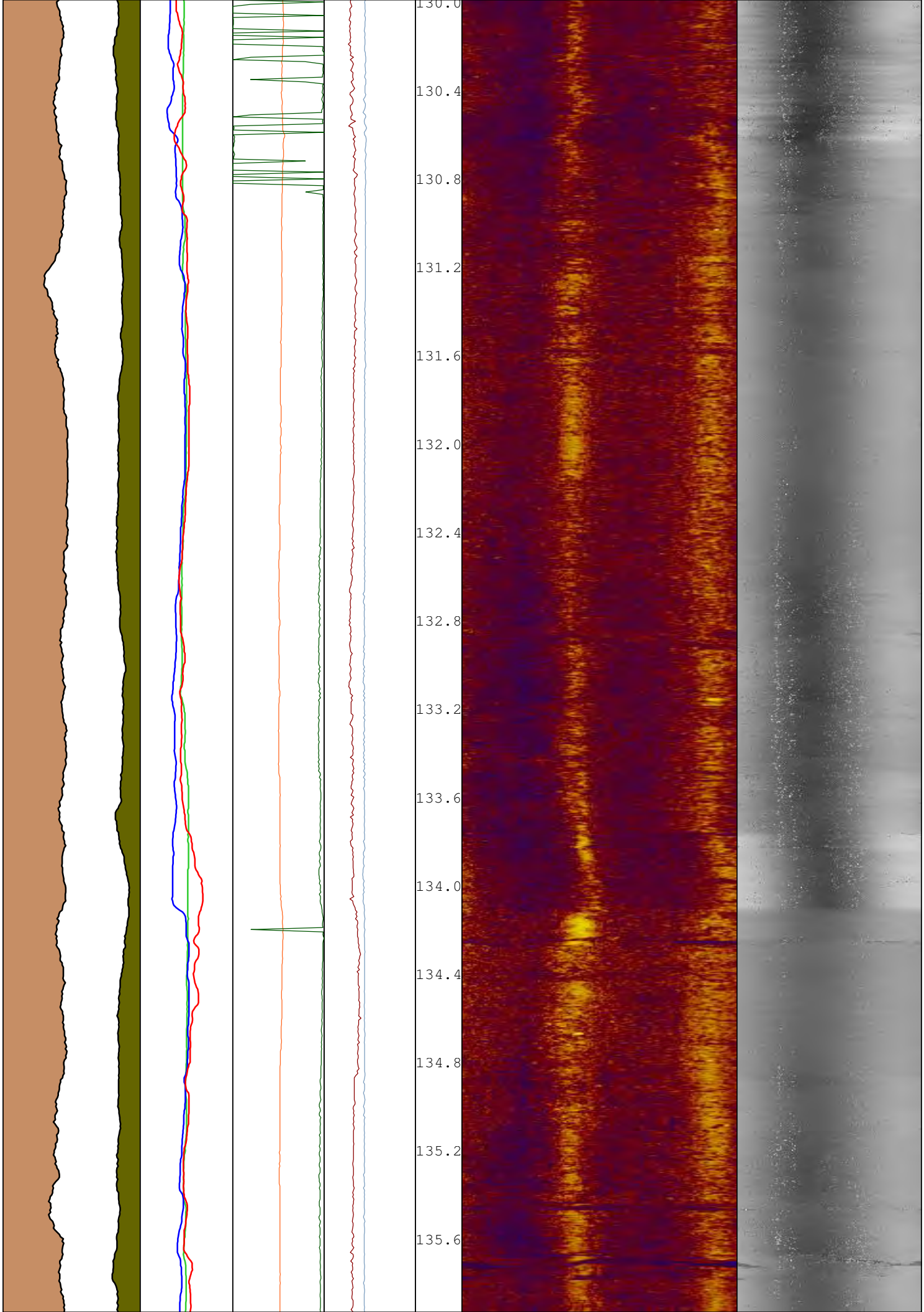
130.0
130.4
130.8
131.2
131.6
132.0
132.4
132.8
133.2
133.6
134.0
134.4
134.8
135.2
135.6

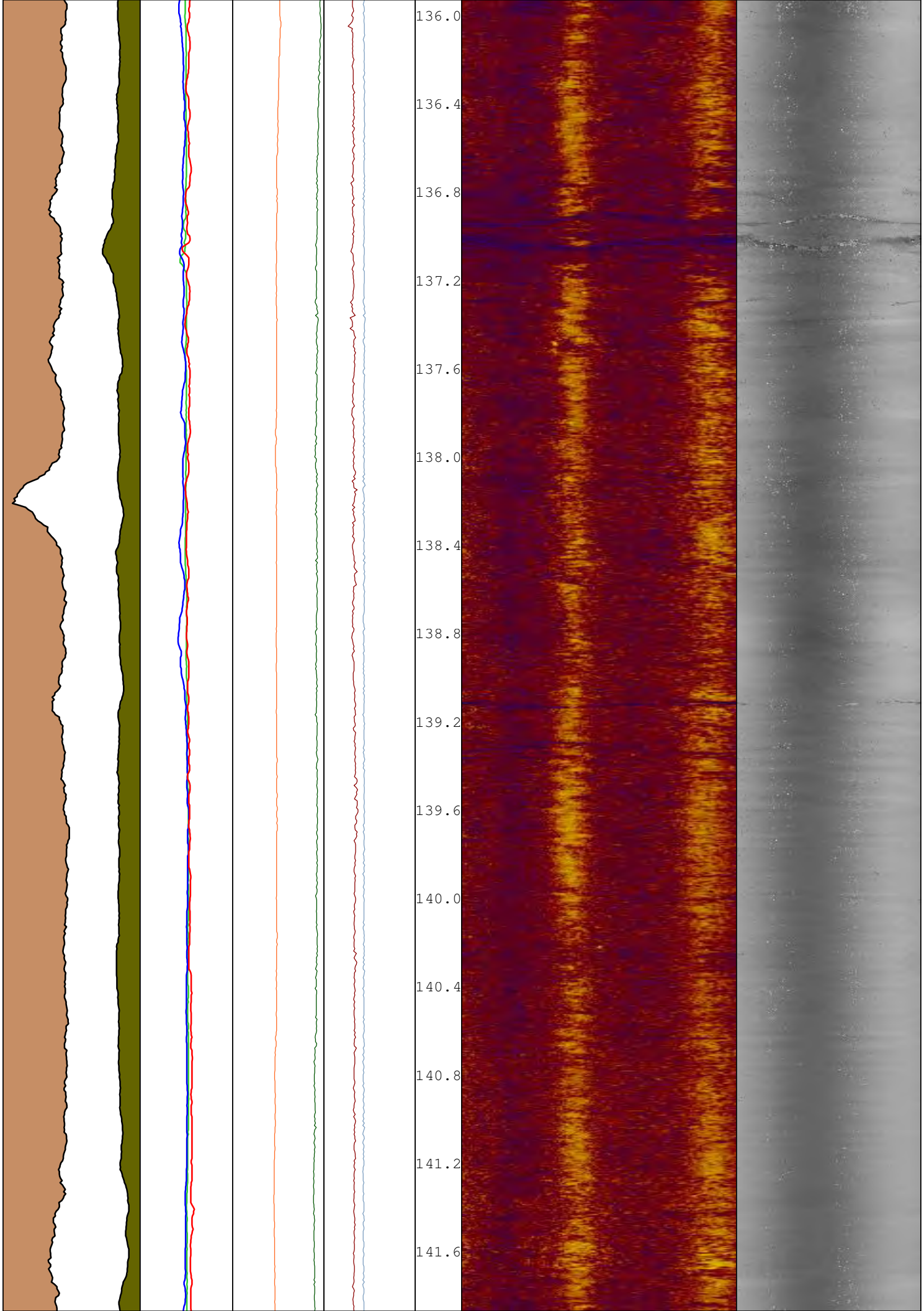
136.0
136.4
136.8
137.2
137.6
138.0
138.4
138.8
139.2
139.6
140.0
140.4
140.8
141.2
141.6

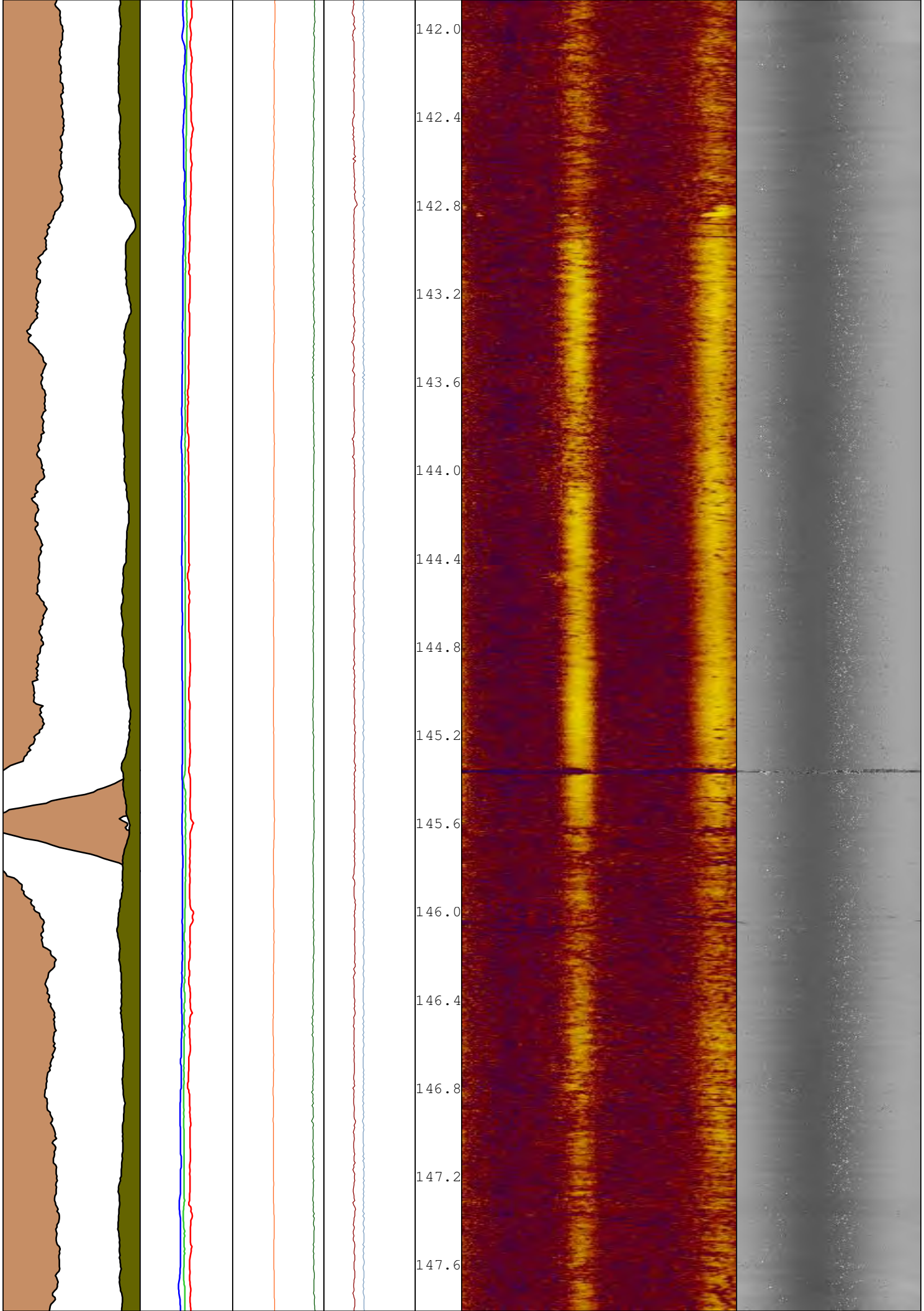
142.0
142.4
142.8
143.2
143.6
144.0
144.4
144.8
145.2
145.6
146.0
146.4
146.8
147.2
147.6

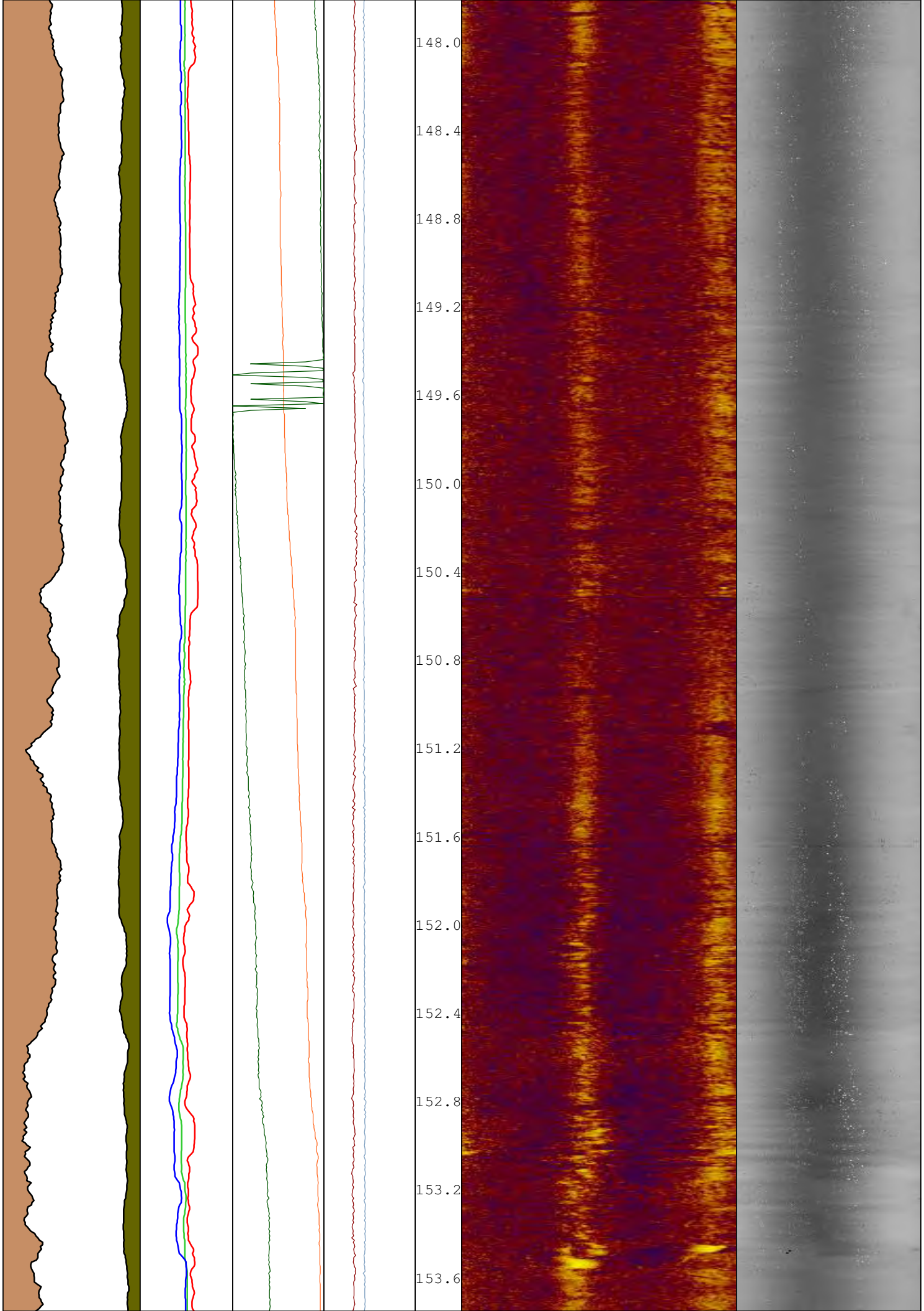
148.0
148.4
148.8
149.2
149.6
150.0
150.4
150.8
151.2
151.6
152.0
152.4
152.8
153.2
153.6

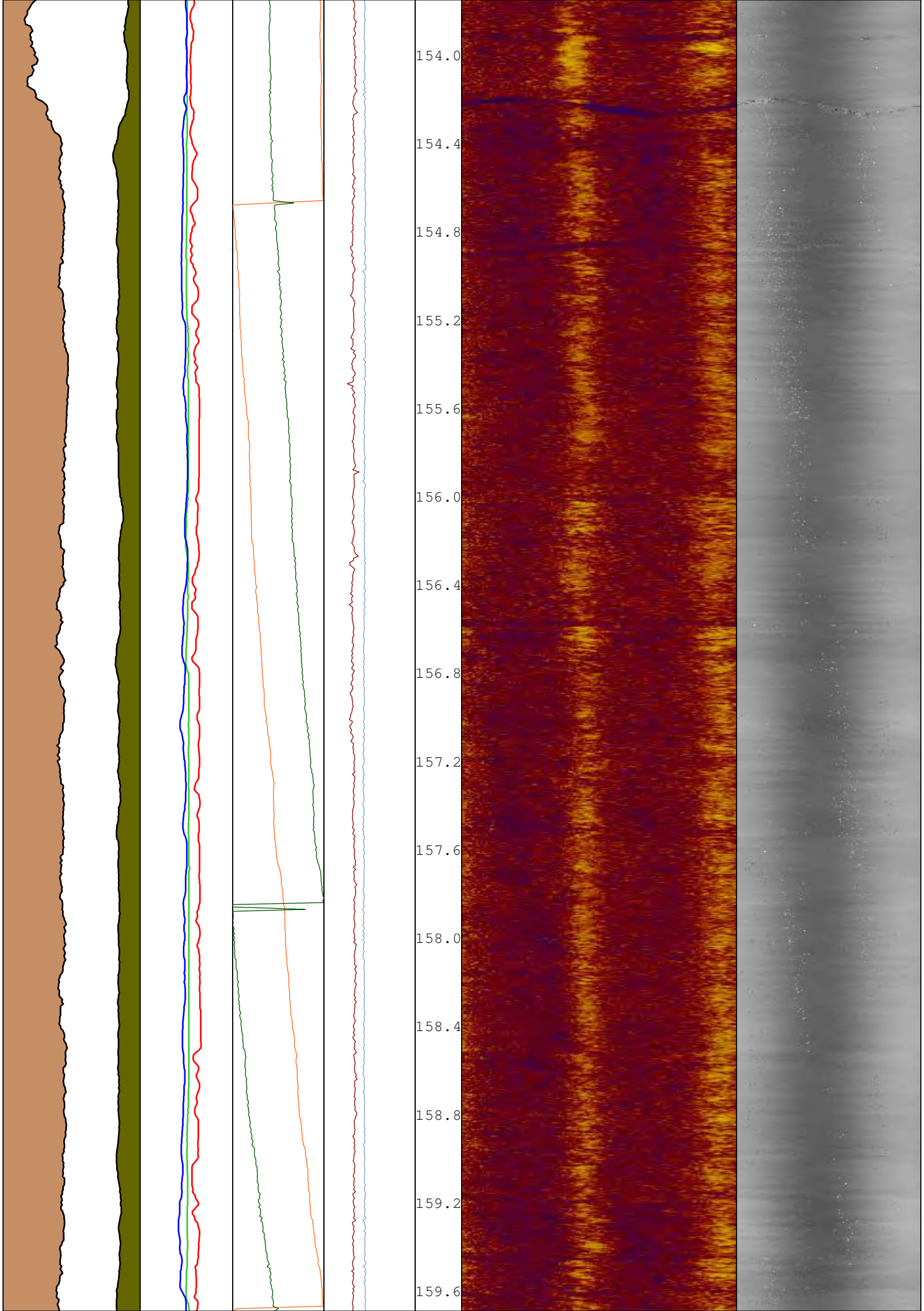
154.0
154.4
154.8
155.2
155.6
156.0
156.4
156.8
157.2
157.6
158.0
158.4
158.8
159.2
159.6

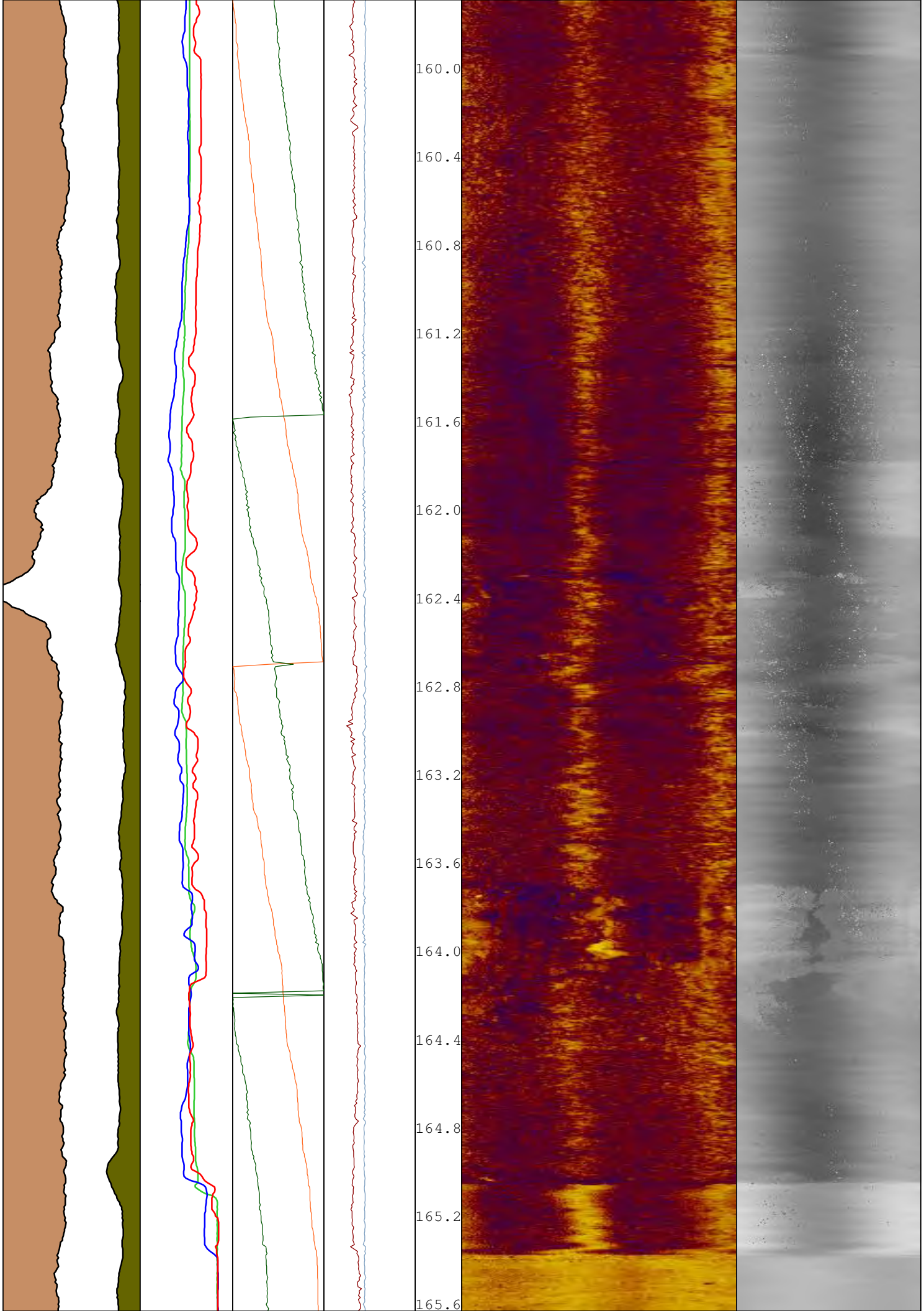
160.0
160.4
160.8
161.2
161.6
162.0
162.4
162.8
163.2
163.6
164.0
164.4
164.8
165.2
165.6

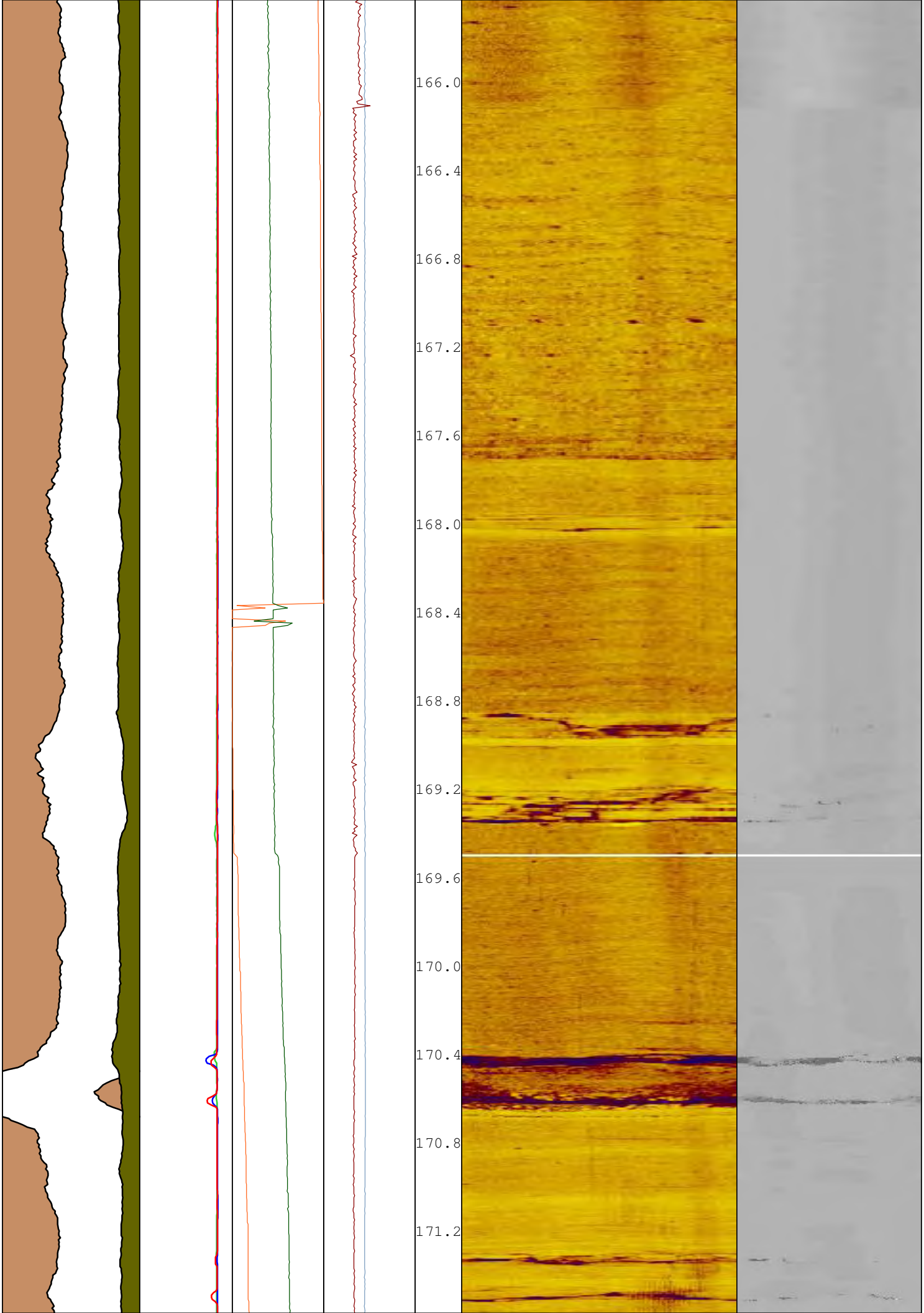
166.0
166.4
166.8
167.2
167.6
168.0
168.4
168.8
169.2
169.6
170.0
170.4
170.8
171.2

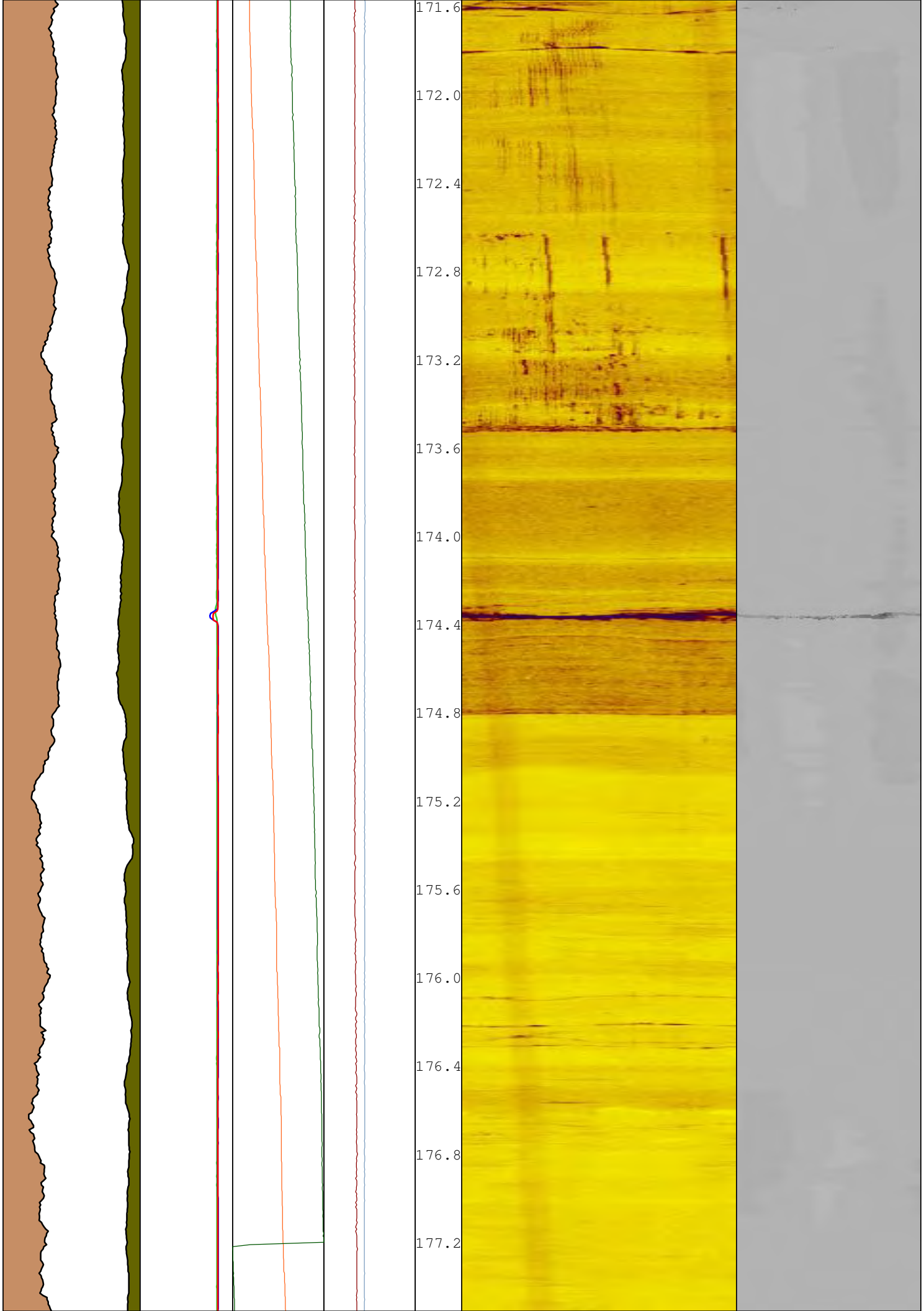
171.6
172.0
172.4
172.8
173.2
173.6
174.0
174.4
174.8
175.2
175.6
176.0
176.4
176.8
177.2

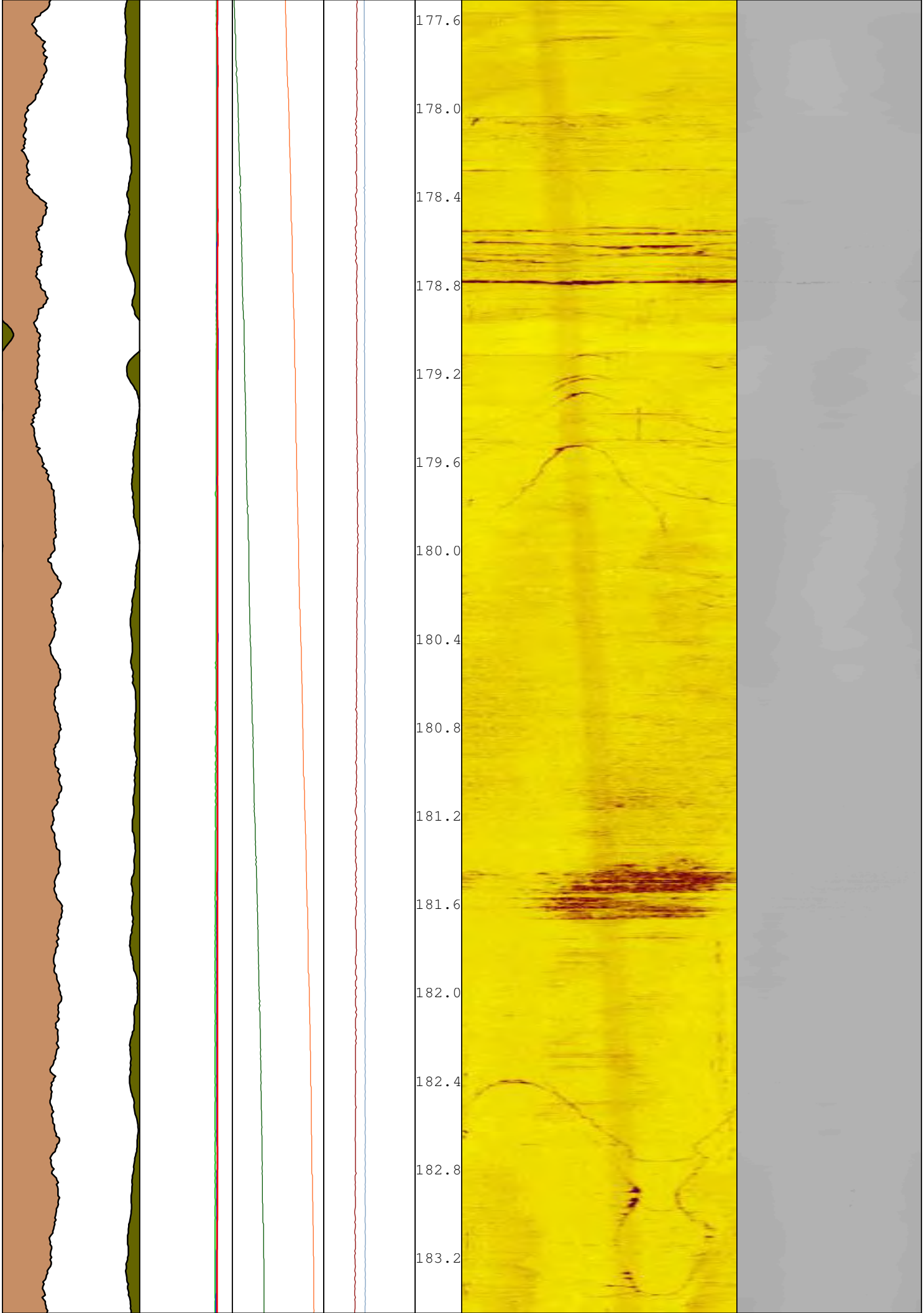
177.6
178.0
178.4
178.8
179.2
179.6
180.0
180.4
180.8
181.2
181.6
182.0
182.4
182.8
183.2

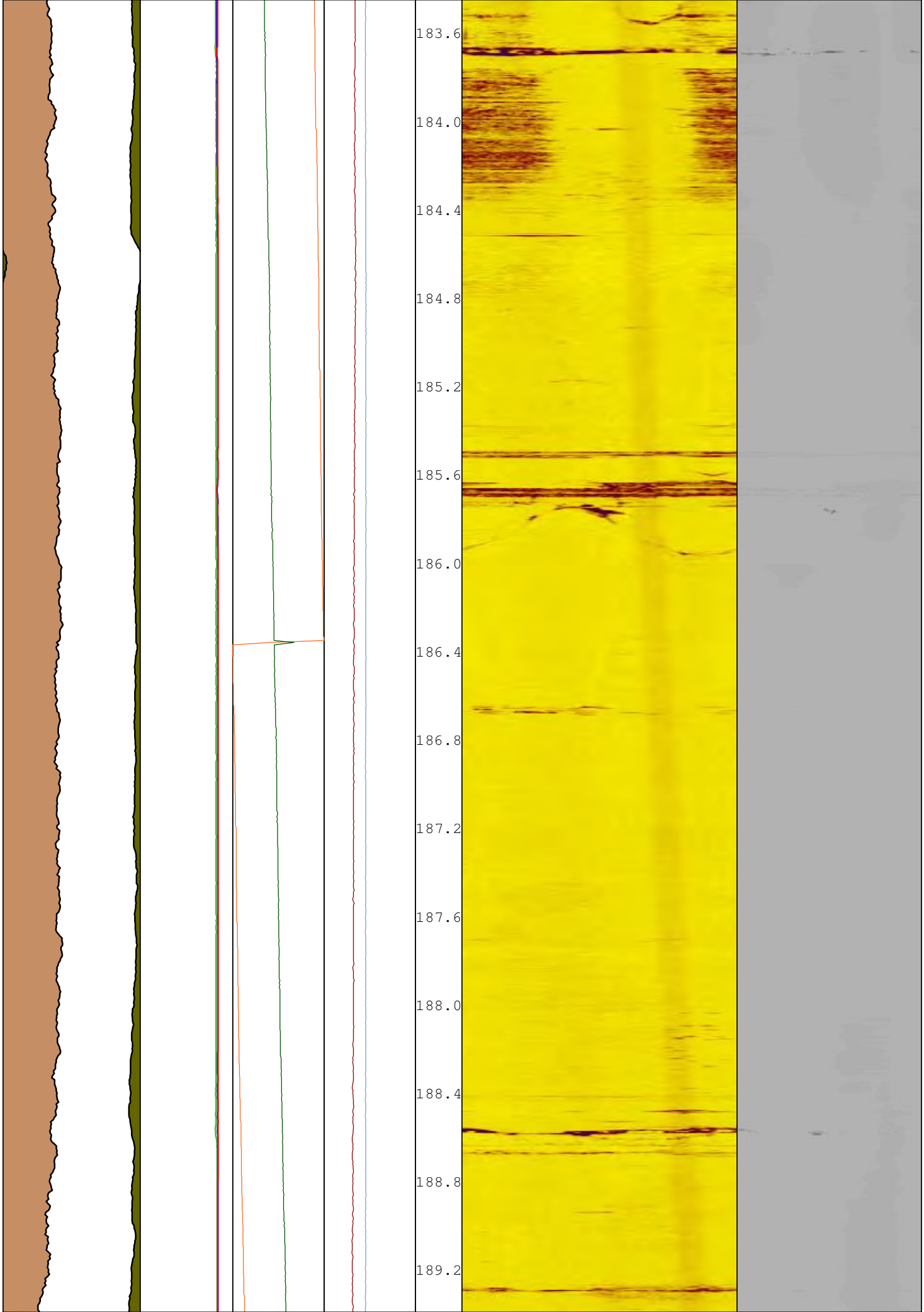
183.6
184.0
184.4
184.8
185.2
185.6
186.0
186.4
186.8
187.2
187.6
188.0
188.4
188.8
189.2

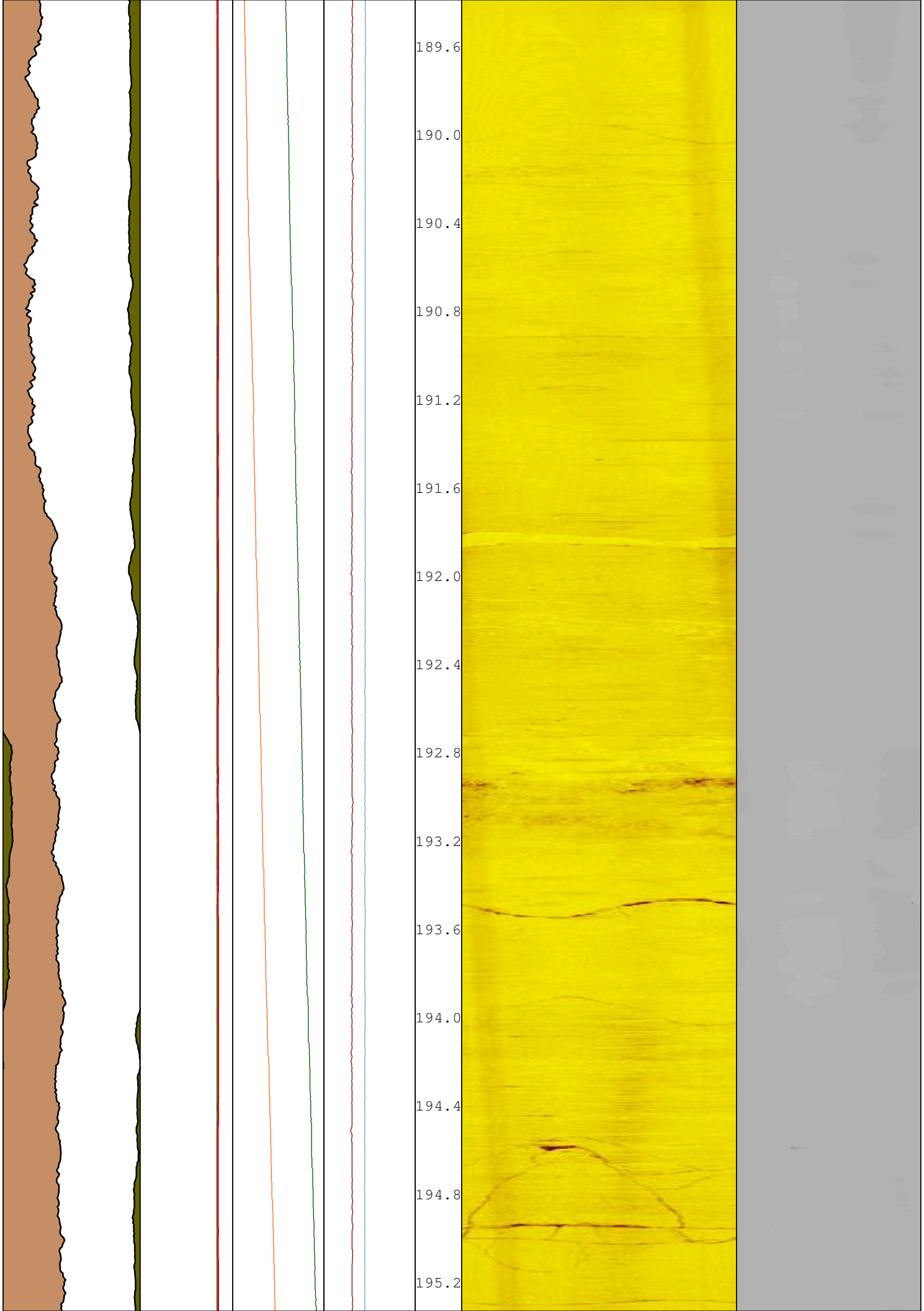
189.6
190.0
190.4
190.8
191.2
191.6
192.0
192.4
192.8
193.2
193.6
194.0
194.4
194.8
195.2

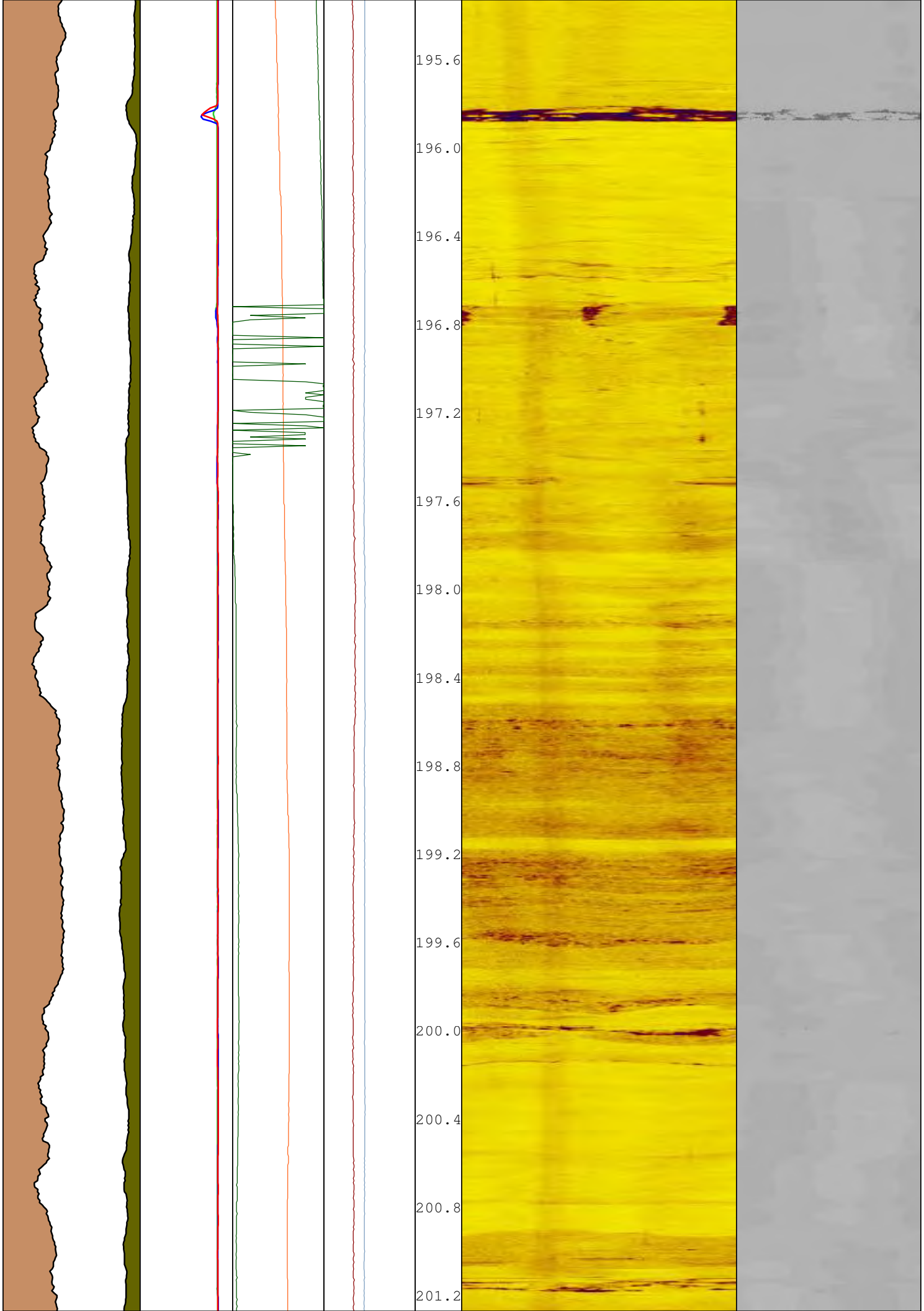
195.6
196.0
196.4
196.8
197.2
197.6
198.0
198.4
198.8
199.2
199.6
200.0
200.4
200.8
201.2

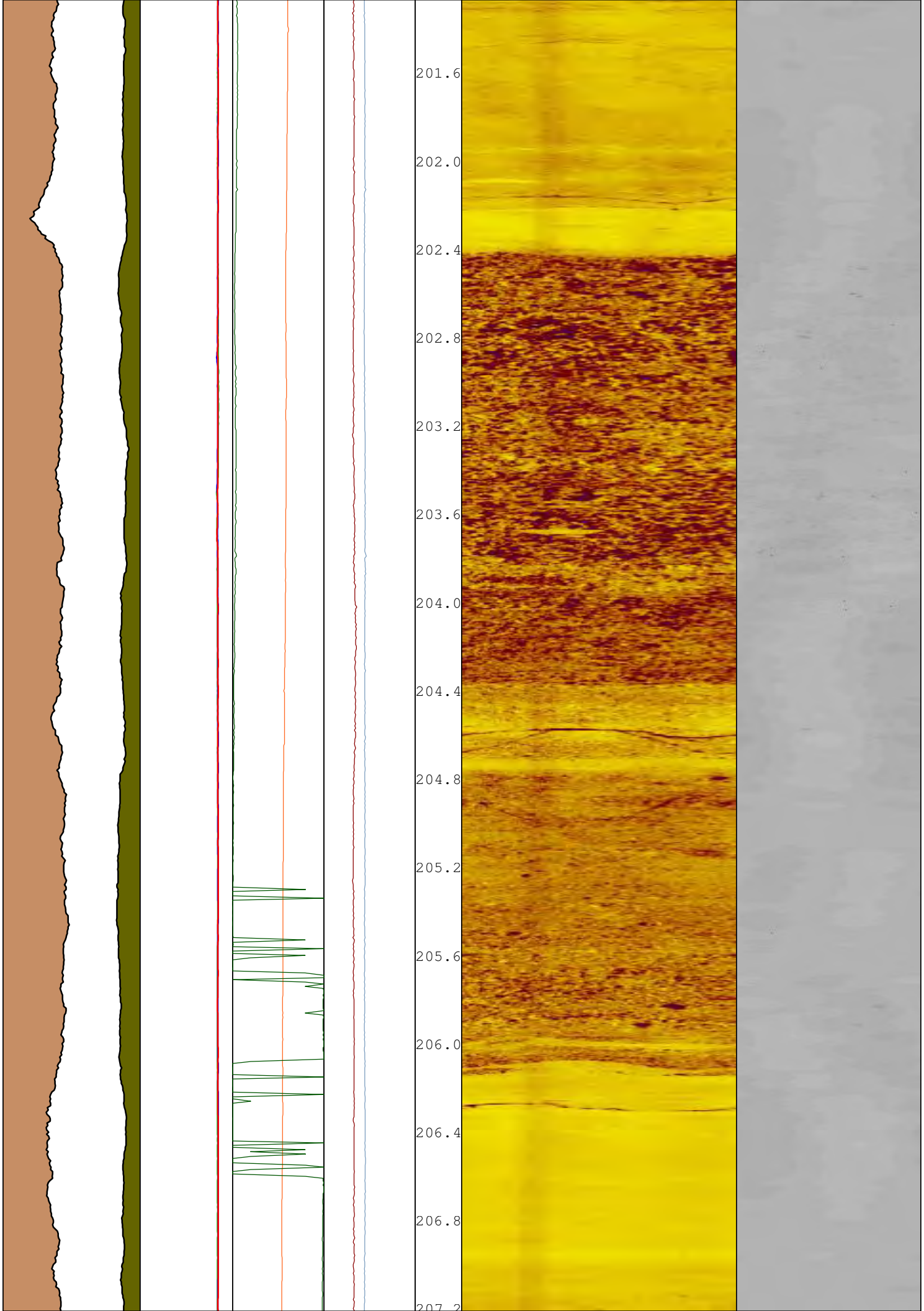
201.6
202.0
202.4
202.8
203.2
203.6
204.0
204.4
204.8
205.2
205.6
206.0
206.4
206.8
207.2

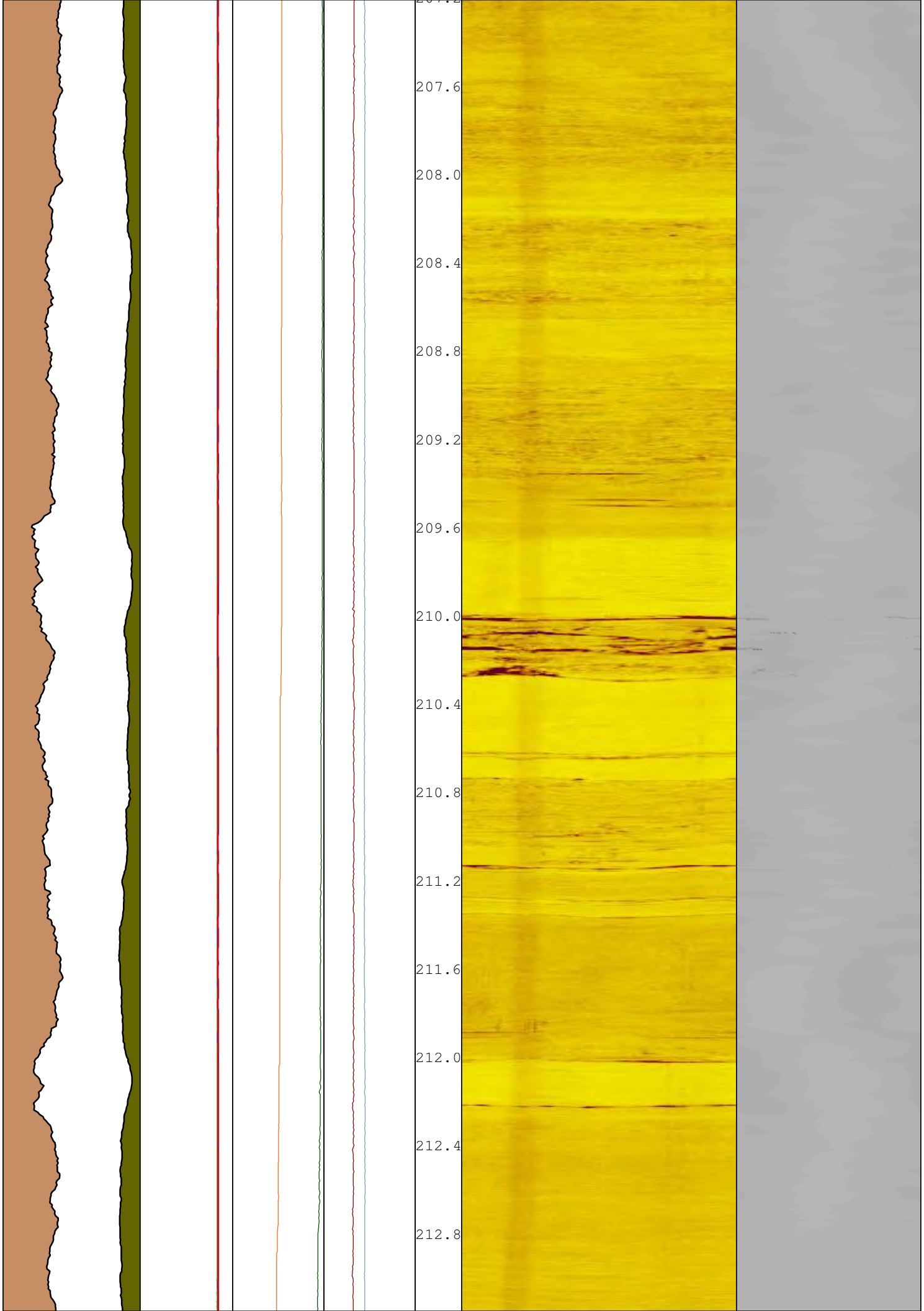
207.6
208.0
208.4
208.8
209.2
209.6
210.0
210.4
210.8
211.2
211.6
212.0
212.4
212.8


213.2
213.6
214.0
214.4
214.8
215.2
215.6
216.0
216.4
216.8
217.2
217.6
218.0
218.4
218.8

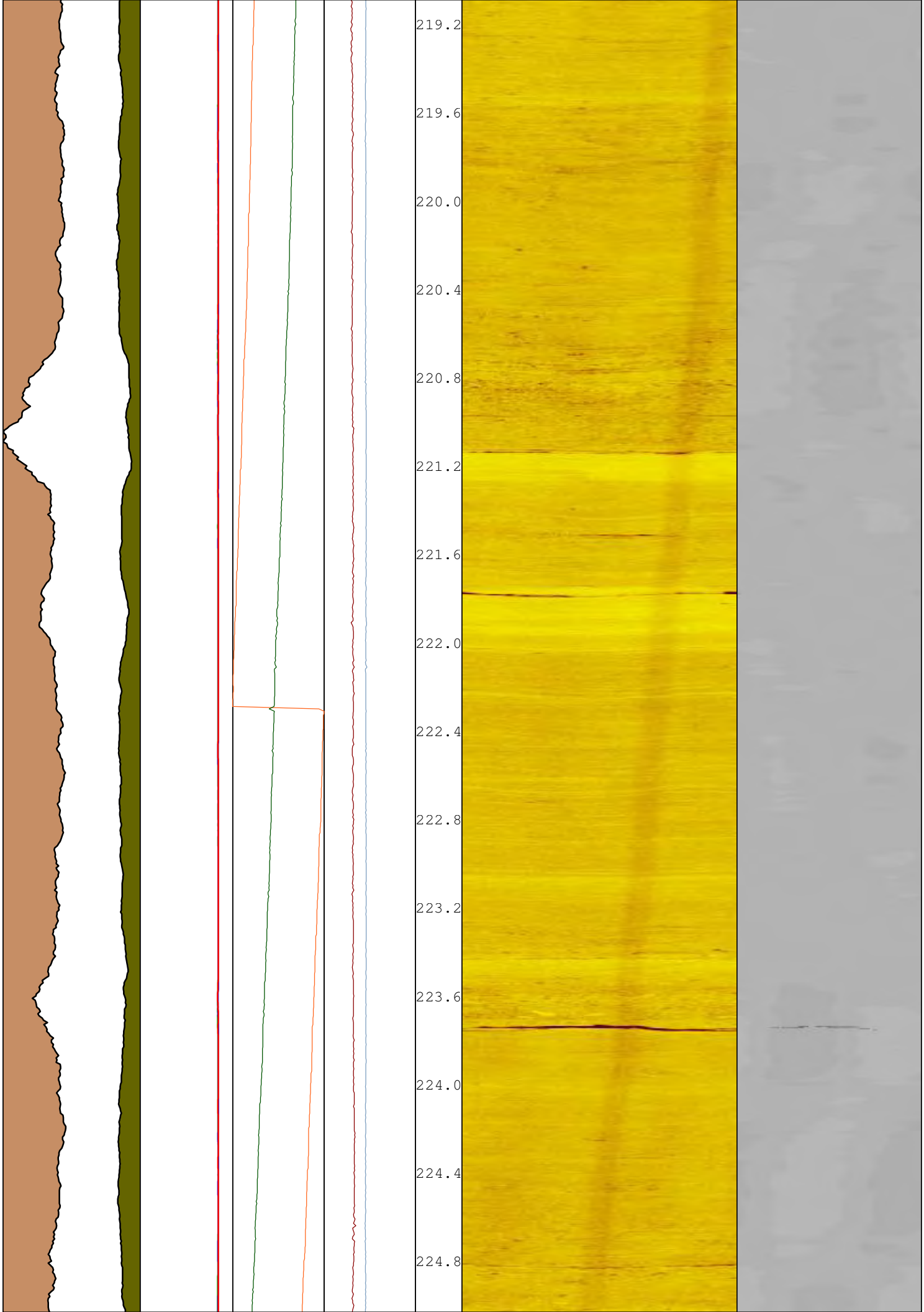
219.2
219.6
220.0
220.4
220.8
221.2
221.6
222.0
222.4
222.8
223.2
223.6
224.0
224.4
224.8

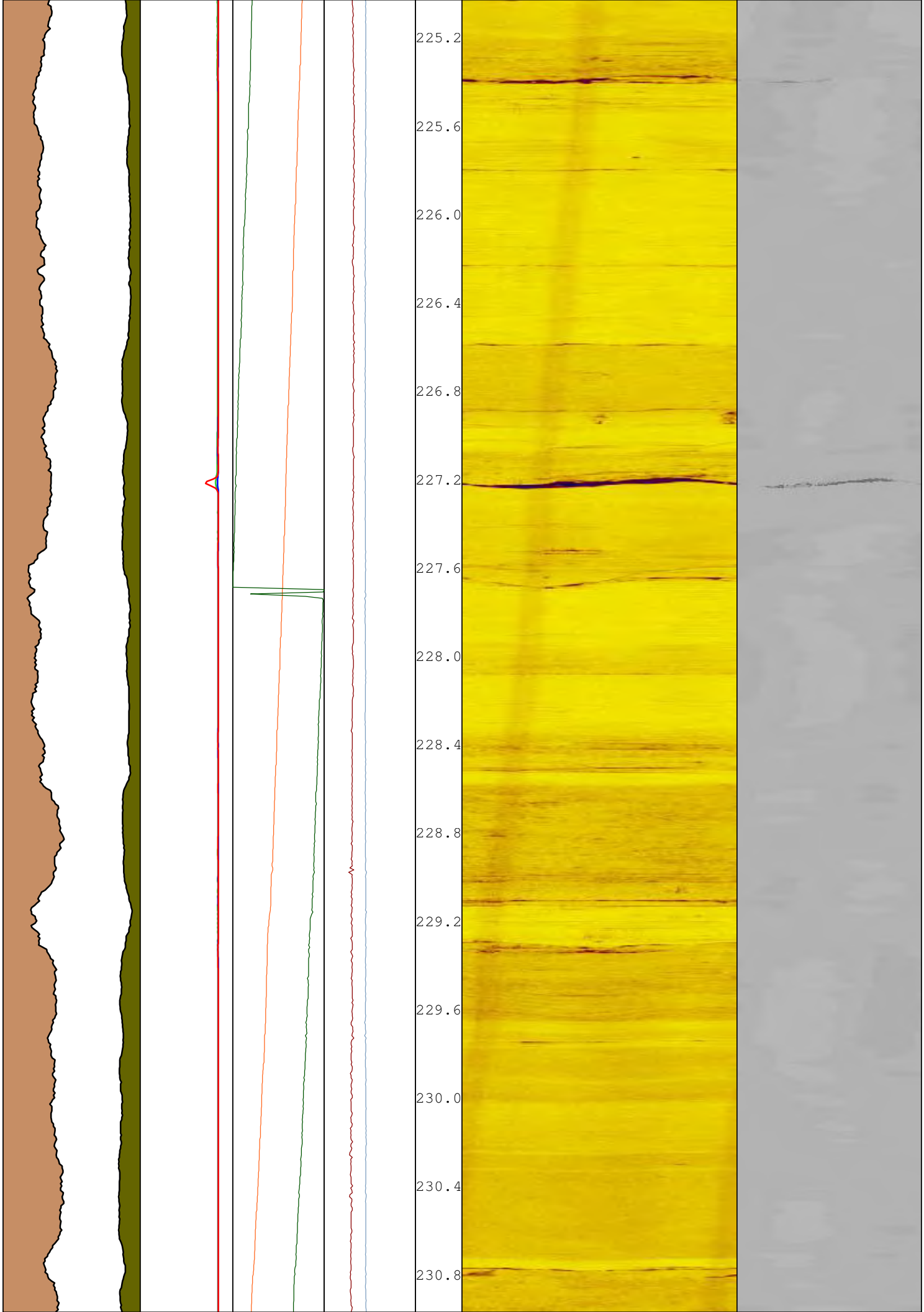
225.2
225.6
226.0
226.4
226.8
227.2
227.6
228.0
228.4
228.8
229.2
229.6
230.0
230.4
230.8

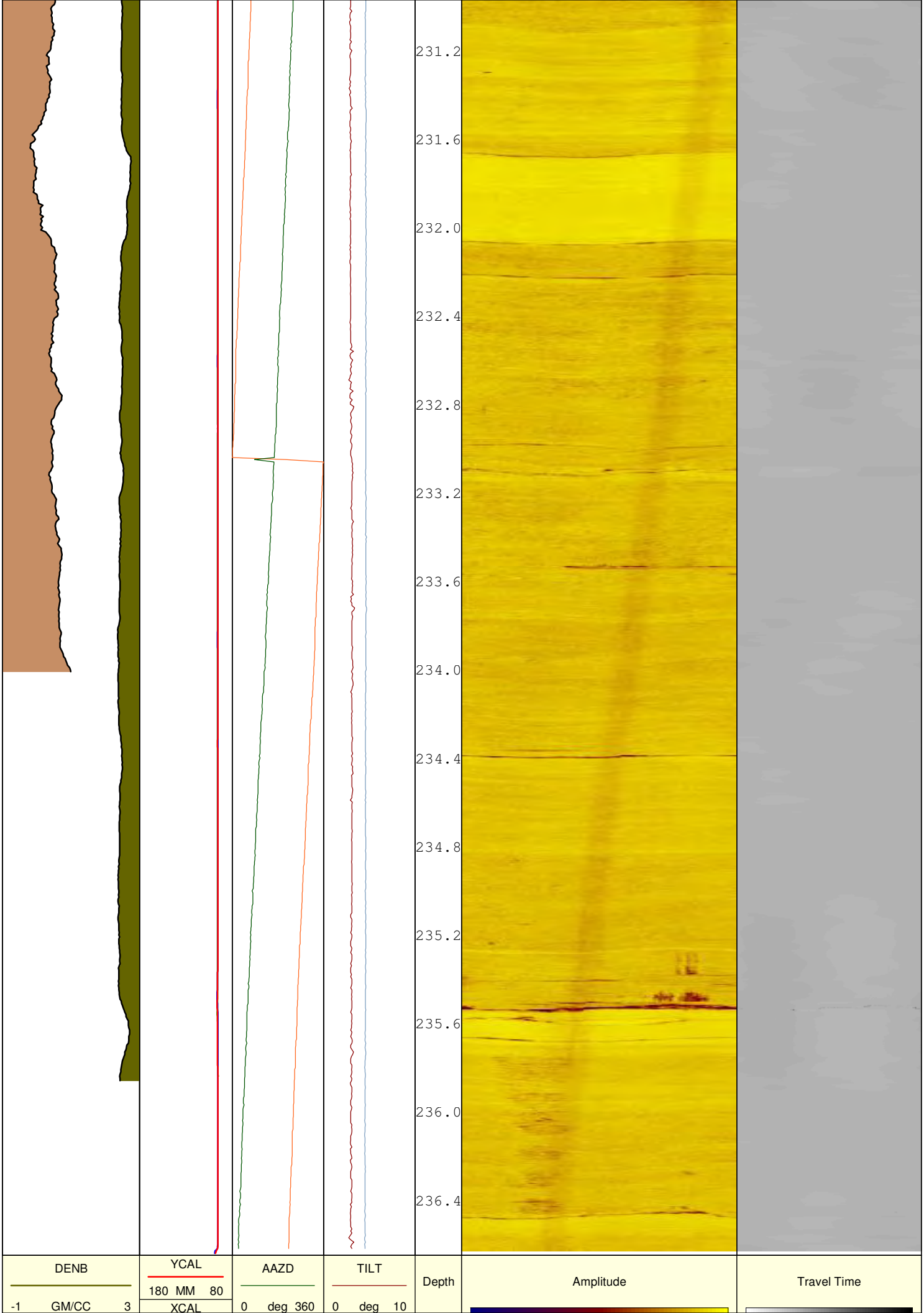
231.2
231.6
232.0
232.4
232.8
233.2
233.6
234.0
234.4
234.8
235.2
235.6
236.0
236.4
DENB
-1 GM/CC 3
YCAL
180 MM 80
XCAL
AAZD
0 deg 360
TILT
0 deg 10
Depth
Amplitude
Travel Time

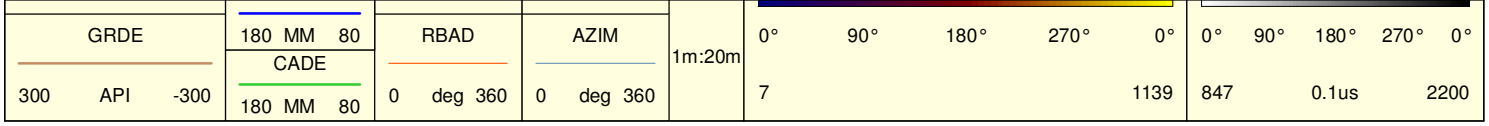
GRDE
300 API -300
180 MM 80
CADE
180 MM 80
RBAD
0 deg 360
AZIM
0 deg 360
1m:20m
0° 90° 180° 270° 0°
7 1139
0° 90° 180° 270° 0°
847 0.1us 2200

Strata Control Technology

REPORT TO:

TAHMOOR MINE

Subsidence Impact Assessment for Selected Archaeological Heritage Sites at Tahmoor South Project

TAH4090

Mining Research and Consulting Group
SCT Operations Pty Ltd PO Box 824 Wollongong NSW 2520 Australia
sctnsw@sct.gs

REPORT TO Ron Bush
Approvals Manager
Tahmoor South Project
Tahmoor Coal
PO Box 100
TAHMOOR NSW 2573

SUBJECT Subsidence Impact Assessment for Selected Archaeological Heritage Sites at Tahmoor South Project

REPORT NO TAH4090

PREPARED BY Ken Mills

DATE 20 December 2013

Ken Mills
Principal Geotechnical Engineer

SUMMARY

The Tahmoor South Project (TSP) is a proposed extension of current longwall mining operations at Tahmoor Mine located near Tahmoor approximately 75km southwest of Sydney in NSW, Australia. During investigations for the TSP Environmental Impact Statement, Niche Environment and Heritage (NEH) has identified a number of archaeological sites located under sandstone cliff formations within the project area. SCT Operations Pty Ltd (SCT) was commissioned by the TSP to provide a geotechnical assessment of the potential for these sandstone cliff formations to be impacted by mining subsidence and the likely nature of any impacts that might occur. This report presents our assessment of the likely impacts from proposed mining at each of these various sites.

The sites specifically assessed in this report are 52-2-1520 to 52-2-1529, 52-2-1533 and 52-2-1534, 52-2-1538 to 52-2-1540, 52-2-3960, and 52-2-3971, all of which are located adjacent to Dog Trap Creek and two of its tributaries. Our assessment should be read in conjunction with the Aboriginal Cultural Heritage Assessment prepared independently by NEH for the TSP that identifies, characterises, and assesses the significance of all the archaeological sites within the TSP. Three of these sites 52-2-1523, 52-2-1525, and 52-2-1528 are assessed by NEH as being of high significance; two additional sites 52-2-1524 and 52-2-1527 are assessed as being of moderate significance; and the remaining sites as having low significance.

Our assessment recognises three categories of impacts to these archaeological sites: rock falls, surface cracking, and shear movements on bedding planes. The following table outlines the potential for each of these categories of impact at each of the sites. It should be noted that the potential for impacts directly to art work sites is one or two orders of magnitudes less than the probability of impact to the site as a whole because of the limited extent of individual artworks.

Site ID	Significance indicated by NEH	Rock Falls (greater than background)	Surface Cracking (greater than background)	Shear Movements
52-2-1520	Low	Unlikely (<5%)	Possible (<20%)	Possible (<10%)
52-2-1521	Low	No Increase	No Increase	Unlikely (<2%)
52-2-1522	Low	No Increase	No Increase	No Potential
52-2-1523	High	No Increase	No Increase	Unlikely (<2%)
52-2-1524	Moderate	No Increase	No Increase	No Potential
52-2-1525	High	No Increase	No Increase	No Potential
52-2-1526	Low	No Increase	No Increase	Unlikely (<2%)
52-2-1527	Moderate	No Increase	No Increase	Unlikely (<2%)
52-2-1528	High	No Increase	No Increase	Unlikely (<2%)
52-2-1529	Low	No Increase	No Increase	No Potential
52-2-1533	Low	Unlikely (<5%)	Possible (<20%)	Possible (<10%)
52-2-1534	Low	Unlikely (<5%)	Possible (<20%)	Possible (<10%)
52-2-1538	Low	Unlikely (<5%)	Possible (<20%)	Possible (<10%)
52-2-1539	Low	Unlikely (<5%)	Possible (<20%)	Possible (<10%)
52-2-1540	Low	No increase	Unlikely (<5%)	Unlikely (<5%)
52-2-3960	Low	No Increase	No Increase	Unlikely (<2%)
52-2-3971	Low	No Increase	No Increase	No Potential

Our assessment is based on experience of observing impacts of mining on rock formations in the Western and Southern Coalfields of NSW and on observations of impacts to two major cliff lines inspected alongside the Bargo River downstream of Picton Weir where Longwalls 14-19 at Tahmoor Mine mined directly under them some 10-15 years ago causing subsidence of up to 0.8m.

General experience of mining below sandstone cliff formations in the Western and Southern Coalfields of NSW indicates that mining induced rock falls are almost entirely limited to within the footprint of mining. Perceptible surface cracking may occur to a distance of up to 0.4 times overburden depth (approximately 160m) from the centre of the start line of the longwall panel with the distance reducing towards the edges of the panel. Shear movements may occur up to 400m from the edge of the longwall panels, but are most likely to occur in areas where mining occurs in a downslope direction and not at the start of a panel.

The high and moderate significance sites are all located outside the longwall panels and sufficiently far that there is considered to be no potential for increased risk of cracking above natural background levels. There is however a small potential for shear movements on low strength bedding planes to be perceptible in the back of overhanging cliff formations on the same side of the creek as mining.

There is some potential for adjacent watercourses, in particular Dog Trap Creek and its tributaries to be impacted by mining subsidence with bedrock cracking, surface flow diversion, and iron staining considered possible in some sections of the creeks.

Notwithstanding the expected impacts from mining subsidence, it is noted that relatively high levels of natural ground movement and impacts from high intensity rainfall events early in 2013 were observed during the site visits, especially in the vicinity of Dog Trap Creek. These impacts included natural rock falls, block movements opening up cracks in the ground, tree root invasion, and sediment rich water flowing out from the back of overhanging rock formations depositing sediment and causing discolouration and of the back walls. These natural changes have potential to degrade the archaeological sites irrespective of any mining activity.

TABLE OF CONTENTS

PAGE NO

1. INTRODUCTION

The Tahmoor South Project (TSP) is a proposed extension of current longwall mining operations at Tahmoor Mine located near Tahmoor approximately 75km southwest of Sydney in NSW, Australia. During investigations for the TSP Environmental Impact Statement, Niche Environment and Heritage (NEH) has identified a number of archaeological sites located under sandstone cliff formations within the project area. SCT Operations Pty Ltd (SCT) was commissioned by the TSP to provide a geotechnical assessment of the potential for these sandstone cliff formations to be impacted by mining subsidence and the likely nature of any such impacts. This report presents our assessment of the likely impacts from proposed mining at each of these various sites.

Our assessment should be read in conjunction with the Aboriginal Cultural Heritage Assessment report prepared independently by NEH for the TSP that identifies, characterises, and assesses the significance of all the archaeological sites within the TSP.

The report is structured to provide an overview of the sites relative to the proposed longwall panels, a review of previous experience of mining under cliff formations at Tahmoor Mine, a discussion of natural erosion processes that may impact the sites, a description of each of the sites, and an assessment of the impacts that are expected.

2. SITE DESCRIPTION

Figure 1 shows a plan of the proposed longwall panels superimposed onto a 1:25,000 topographic series map of the area and the locations of the archaeological sites in the area reported by NEH. The sites specifically assessed in this report are 52-2-1520 to 52-2-1529, 52-2-1533 and 52-2-1534, 52-2-1538 to 52-2-1540, 52-2-3960, and 52-2-3971, all of which are located adjacent to Dog Trap Creek and two of its tributaries. Three of these sites 52-2-1523, 52-2-1525, and 52-2-1528 are assessed by NEH as being of high significance; two additional sites 52-2-1524 and 52-2-1527 are assessed as being of moderate significance; and the remaining sites as having low significance.

Table 1 provides a summary of the sites, their specific locations, and significance assessed by NEH.

Photographs of each of these sites are presented in Appendix 1 together with a summary of the key characteristics of each site such as length, height, and size of overhang.

Overburden depth to the Bulli Seam is approximately 380m in the bottom of Dog Trap Creek and its tributaries and approximately 400m on the plateau away from the creek. The Bulli Seam ranges in thickness from 2.6m to about 2.8m in this area. Longwall panels are nominally 300m wide measured roadway centre to roadway centre and therefore create a void that is nominally 305m wide.

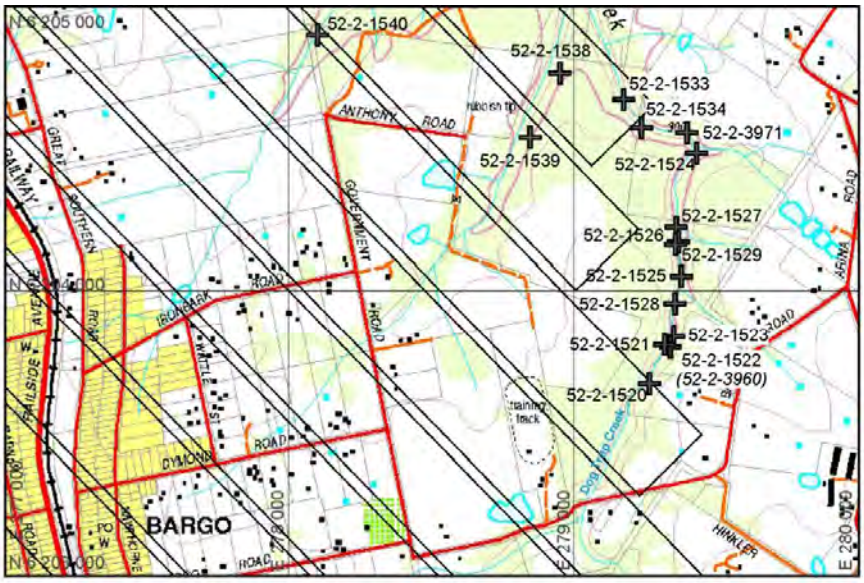

Figure 1: Site plan showing location or archaeological heritage sites relative to longwalls on a 1:25,000 topographic series map.

Table 1: Archaeological Heritage Site Locations Assessed

Site_ID	MGAE	MGAN	Significance
52-2-1520	279264	6203676	Low
52-2-1521	279240[1]	6203656[1]	Low
52-2-1522	279336[1]	6203805[1]	Low
52-2-1523	279349	6203841	High
52-2-1524	279430	6204485	Moderate
52-2-1525	279376	6204052	High
52-2-1526	279356	6204163	Low
52-2-1527	279358	6204225	Moderate
52-2-1528	279354	6203958	High
52-2-1529	279366	6204172	Low
52-2-1533	279174	6204672	Low
52-2-1534	279236	6204574	Low
52-2-1538	N/A	N/A	Low
52-2-1539	278844	6204539	Low
52-2-1540	278098	6204900	Low
52-2-3960	279337[1]	6203804[1]	Low
52-2-3971	279396	6204556	Low

[1]Approximate only - exact coordinates to be confirmed

MSEC (2013) predicts maximum subsidence of up to about 1.8m in the centre of each of the longwall panels. Goaf edge subsidence is expected to be less than 100mm at the corner of each longwall panel and approximately 200mm along the start line and the edge of each panel. Valley closure across Dog Trap Creek is predicted to range up to 300-400mm in areas directly mined under and up to 100-200mm in the vicinity of most of the archaeological sites located alongside Dog Trap Creek.

3. BASIS OF ASSESSMENT AND BACKGROUND EXPERIENCE

In this section, the basis of the assessment and general observations of mining subsidence impacts on cliff formations are discussed.

This assessment is based on:

- Site visits on 6/3/13, 22/4/13, and 29/4/13 to inspect archaeological heritage sites adjacent to Dog Trap Creek with Jamie Reeves and Renee Regal from NEH.

- A site visit on 30 October 2013 with Ron Bush to inspect a section of the Bargo River downstream of Picton Weir where significant cliffs either side of the river were directly mined under by Longwalls 14 to 19.
- Experience of observing and monitoring subsidence and subsidence impacts on cliff formations in the Western and Southern Coalfields of N.S.W.

Each of the sites (with the exception of 52-2-3971 which is small and located in an area not expected to have any potential to be impacted by mining subsidence) has been inspected to provide a context for assessment. These inspections also provided an indication of the rate of natural erosion mechanisms including cliff instability and lateral sliding.

Cliff formations are recognised to occur naturally as part of ongoing erosion processes. At any given point in time, individual cliff formations are somewhere along the pathway toward natural instability as part of these natural erosion processes. The mechanisms that cause instability of cliff formations typically involve a combination of factors:

1. Undercutting along the base of the cliff through a variety of processes including, water erosion, wind erosion, and slabbing from the roof.

2. Lateral sliding toward the valley along a basal shear plane typically driven by ingress of rainfall runoff and commonly accelerated by tree root invasion and natural jointing.

3. The final stages of failure usually involve toppling failure of part or all of the overhanging cliff formation.

Determining the current state of any or all of the factors is difficult without a high degree of invasive geotechnical measurement and monitoring. The level of investigation required is typically more intrusive than any potential mining induced impacts and so an approach based on inspection and informed judgement is preferred. This approach has been used in this assessment. The assessment is based on the author's experience of observing impacts of mining on sandstone cliff formations in the Southern and Western Coalfields of N.S.W. over approximately 25 years.

The interaction of mining subsidence with cliff formations is recognised to be a function of multiple factors that cannot easily be determined. The mining subsidence processes that interact with the rock structures in which cliffs and waterfalls have developed are becoming better understood as more detailed subsidence and ground deformation measurements become available. However, the fundamental challenge for assessing subsidence impacts from mining at any given site remains that these features occur in areas where natural erosion processes are ongoing and the rate of associated instability is relatively high. It is difficult to determine with confidence how far along the path to natural instability any given feature may be and what level of additional movement is necessary to precipitate instability.

3.1 Types of Mining Induced Subsidence Impacts

Several types of mining induced impact on sandstone cliff formations are recognised:

- Compression fracturing at points where horizontal compression causes the rock strata to become overloaded, typically in the base of river channels and in rock gullies, but also along cliff formations subject to horizontal compression.

- Rock falls as a consequence of horizontal compression movements that cause complete detachment of rock material from the formation.

- Tensile cracking of intact rock strata, with opening across the cracks usually revealing fresh sandstone strata within the crack.

- Shear movements on bedding planes, typically along the back of overhanging rock structures.

Each of these types of impact tends to occur at specific locations around a longwall panels. Each has potential to be significant, but compression fracturing and associated rock falls tend to cause impacts that are most apparent.

Horizontal compression movements tend to occur within the boundaries of longwall mining activity except in a few unusual circumstances. Compression fracturing or evidence thereof in the bed of a river channels has been observed at up to 400m from the nearest longwall panel goaf edge in a very

steep gorge (Kay et al 2006) but compression movements are more common directly over and immediately adjacent to longwall mining areas.

As a consequence, mining induced rock falls which are caused by horizontal compression movements also tend to occur within the boundary of longwall mining activity. All the mining induced rock falls that are known to have occurred within the Western and Southern Coalfields have occurred within or immediately adjacent to the boundary of longwall panels.

Rock falls tend to occur where horizontal compression movements are concentrated and where the compressive strength of the sandstone strata is reduced. Thus, the potential for rock falls tends to be elevated wherever:

- Horizontal compression movements are parallel to the face of a cliff line.
- The cliff line is long enough for horizontal compression movements to be transferred into the sandstone rock strata.
- Re-entrant (cut back) gullies concentrate horizontal compression movements.
- Overhanging formations reduce the strength of the rock strata in horizontal compression through the complex interaction of rock stresses around overhangs.

Compression fracturing also occurs in topographic low points, but except at waterfalls this compression movement does not typically lead to rock falls. In creek lines where sandstone rock strata is exposed in the base of the creek, compression fracturing is likely along most of the length that is mined under and may be perceptible for up to about 400m outside the mining area depending on topography (Kay et al 2006). Flow diversion and other surface expressions of this compression fracturing may occur depending on circumstances.

Tensile fracturing and shear on bedding planes also affect rock formations, but in general these types of fracture tend to be less apparent and do not usually cause rock falls. Tensile fracturing tends to be concentrated at topographic highs and along the edges of longwall panels and may be perceptible to a distance outside the mining area of up to about 0.4 times the depth to the mining horizon in the central part of the start area and to lesser distances elsewhere. The mechanics of the processes that cause tensile fracturing are such that tensile fracturing is unlikely to be evident on the far (non-mining) side of valleys.

Shear on bedding planes can occur both inside and outside the mining area but tends to be limited outside of mining areas by topographic low points such as creek lines. Shear movements tend to be most evident at horizons where there is a contrast in lithology and existing low strength bedding planes or

finer grained material. These fine grained horizons often erode more quickly than the surrounding sandstone strata and are frequently apparent in the deepest part of rock overhangs.

3.2 Observations of Natural Cliff Instability

During other site inspections conducted in the general vicinity of the TSP, two naturally occurring rock falls, evidence of high volume groundwater inflows from the back of numerous overhanging cliff formations, and lateral movement of large blocks of sandstone were observed in areas where there had been no mining activity. One of the rock falls occurred adjacent to Dog Trap Creek near 52-2-1533 during the January/February 2013 high intensity rainfall events and the other one occurred on sandstone cliffs adjacent to Dry Creek near its confluence with the Nepean River and although recent and probably during the same event, the timing is not known. These natural rock falls are shown in Figure 2.

Large cracks were also observed at another site alongside Dog Trap Creek on the western side of the creek opposite 52-2-1524 in an area where there has been no mining. An example of these cracks, shown in Figure 3, is likely to have occurred during the January/February 2013 high intensity rainfall event as a result of mass translation of large sandstone blocks. Figure 3 also shows an older example of mass movements. There are similar features all along both sides of Dog Trap Creek.

Sediment rich water flows were evident from the back of many of the overhanging rock formations alongside Dog Track Creek including at several of the archaeological sites. Figure 4 shows an example of this type of flow at 52-2-1527. These flows had ceased at the time of the site inspection in April 2013, but the presence of sediment on the sandstone indicates that they most likely occurred during high intensity rainfall events down through cracks in the rock on the slope behind the formations.

3.3 Mining Induced Instability

A site inspection conducted along approximately 1500m of cliff line in the Bargo River Valley downstream of Picton Weir indicated that the sandstone cliff formations were relatively unaffected by the mining subsidence that occurred in this area. Sandstone cliff formations up to 40m high, 60m long, and with overhangs up to 8m were directly mined under by Longwalls 14-19 at Tahmoor Mine causing between 0.6m and 0.8m of vertical subsidence. Figure 5 shows some examples of the cliff formations in this area. There were only two minor rock falls evident and only one of these was clearly associated with mining. There were also several areas of relatively minor fracturing similar to the example shown in Figure 5. It is estimated that over the total length of cliff lines inspected there was 100-150m (<10%) where cracking was perceptible.

Figure 2: Examples of natural rock falls observed in 2013 adjacent to Dry Creek and Dog Trap Creek.

Figure 3: Examples of natural rock slides observed in 2013 adjacent to Dog Track Creek (one from February 2013 rain event and another older one).

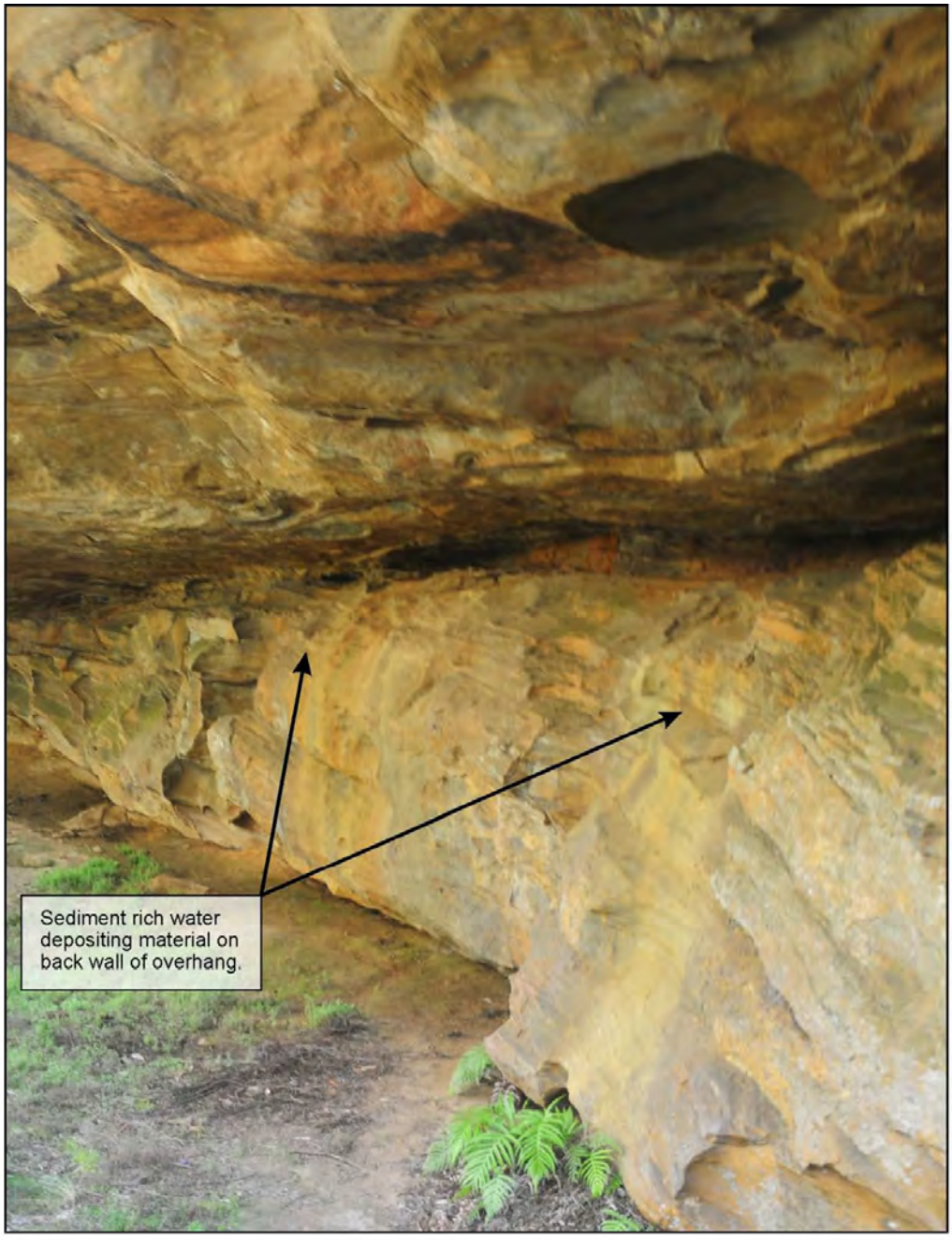

Figure 4 : Example of sediment deposits on back wall of overhang indicating ingress of water in heavy rain events as a possible precursor to natural instability.

Figure 5: Examples of sandstone cliff formations mined under by Longwalls 14-19. Right hand photographs show minor rock fall and cracking observed.

These observations indicate that for the sandstone cliff formations in the vicinity of Tahmoor Mine there is a relatively high level of natural instability and retreat of sandstone cliff formations compared to a relatively low level of impact from mining subsidence.

The relatively high level of natural instability may be a consequence of the creek systems being in the early stages of down cutting into the plateau. The low level of mining induced instability observed along the cliffs above Longwalls 14-19 is at the low end of the spectrum of general experience in the Southern Coalfield which indicates rock falls are typically evident on up to about 3-5% of the length of sandstone cliffs directly mined under.

Although the subsidence observed over Longwalls 14-19 was only 0.6-0.8m and the subsidence expected adjacent to Native Dog Creek is 1.6-1.8m, the observations at Bargo River provide context for the impacts that are likely to be observed in the vicinity of Dog Trap Creek where the cliff formations are directly mined under. In most of the areas of interest to this assessment, longwall panels do not mine directly under the creek, so the Bargo River observations are considered to be an upper bound on the impacts that can be expected adjacent to Dog Trap Creek.

4. ASSESSMENT OF SELECTED ARCHAEOLOGICAL SITES

In this section, and assessment is presented for each of the selected archaeological sites based on each sites position relative to the longwall panels and to the topography.

A summary of the assessment for each site are presented in Table 2 and in Appendix 1 with photographs.

Sites are assessed as having no increased potential for rock falls if they are located outside the area of mining on the basis that mining induced rock falls have not been observed to occur outside the boundaries of longwall mining. Sites within the footprint of mining are assessed as having a less than 5% probability of rock falls based on experience elsewhere in the Southern Coalfield of N.S.W. Observations of cliffs adjacent to the Bargo River downstream of Picton Weir that were mined under indicate that 5% may be an upper limit, but a conservative approach has been adopted given the higher levels of subsidence (1.8m) expected above the TSP longwall panels compared to the 0.8m subsidence observed above Longwalls 14-19 alongside the Bargo River. Although there is considered to be no potential for mining induced rock falls to occur outside the boundaries of longwall mining, there is still recognised to be a relatively high level of natural instability in the rock formations adjacent to Dog Trap Creek.

Sites are assessed as having no potential for mining induced surface cracking greater than the levels of cracking associated with natural instability beyond a distance of 0.4 times overburden depth (approximately 160m) from the straight side of a longwall panel and 0.1 times depth (about 40m) from the

corner of a panel. Sites directly above the panel are assessed as having potential for surface cracking along less than 20% of their length based on observations of a less than 10% length of perceptible cracking on cliff formations adjacent to the Bargo River.

Sites are assessed as having potential to experience shear movements when they are located on the same side of a creek as the adjacent longwall panels. Sites on the opposite bank are not expected to be impacted because the shear movements are constrained by topography. Sites located directly above the longwall panels are considered to have potential to experience greater subsidence than those over solid coal.

Table 2: Assessment of Impacts of Mining for Archaeological Heritage Sites

Site ID	Significance indicated by NEH	Rock Falls (greater than background)	Surface Cracking (greater than background)	Shear Movements
52-2-1520	Low	Unlikely (<5%)	Possible (<20%)	Possible (<10%)
52-2-1521	Low	No Increase	No Increase	Unlikely (<2%)
52-2-1522	Low	No Increase	No Increase	No Potential
52-2-1523	High	No Increase	No Increase	Unlikely (<2%)
52-2-1524	Moderate	No Increase	No Increase	No Potential
52-2-1525	High	No Increase	No Increase	No Potential
52-2-1526	Low	No Increase	No Increase	Unlikely (<2%)
52-2-1527	Moderate	No Increase	No Increase	Unlikely (<2%)
52-2-1528	High	No Increase	No Increase	Unlikely (<2%)
52-2-1529	Low	No Increase	No Increase	No Potential
52-2-1533	Low	Unlikely (<5%)	Possible (<20%)	Possible (<10%)
52-2-1534	Low	Unlikely (<5%)	Possible (<20%)	Possible (<10%)
52-2-1538	Low	Unlikely (<5%)	Possible (<20%)	Possible (<10%)
52-2-1539	Low	Unlikely (<5%)	Possible (<20%)	Possible (<10%)
52-2-1540	Low	No increase	Unlikely (<5%)	Unlikely (<5%)
52-2-3960	Low	No Increase	No Increase	Unlikely (<2%)
52-2-3971	Low	No Increase	No Increase	No Potential

APPENDIX 1 – ARCHAEOLOGICAL SITES ASSESSED IN THIS REPORT

25m long

6-7m overhang

Impact Potential:

Rock Fall <5%

Perceptible Cracks <20%

Shear movements <10%

Significance: Low

Appendix 1.1: Archaeological heritage site: 52-2-1520 Dog Trap Creek.

35m long

6-7m high

2.6m overhang

Significance: Low

Impact Potential:

Rock Fall 0% (no increase above natural)

Perceptible Cracks 0%

Shear movements <2%

Appendix 1.2: Archaeological heritage site: 52-2-1521 Dog Trap Creek.

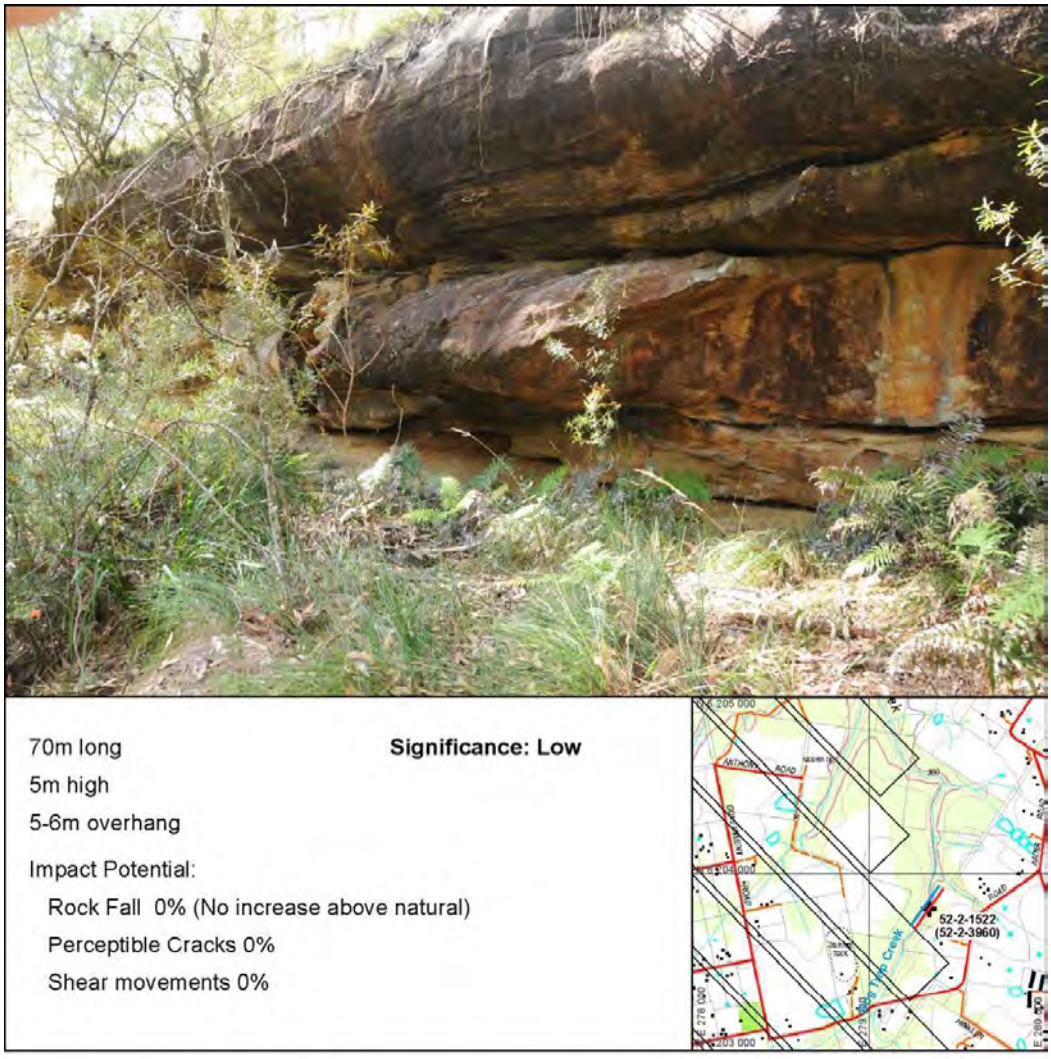

Appendix 1.3: Archaeological heritage site: 52-2-1522 and 52-2-3960 Dog Trap Creek.

40+m long

6-7m overhang

Significance: Low

Impact Potential:

Rock Fall 0% (No increase above natural)

Perceptible Cracks 0%

Shear movements 0%

Compression movements in creek possible

Appendix 1.4: Archaeological heritage site: 52-2-1523 Dog Trap Creek.

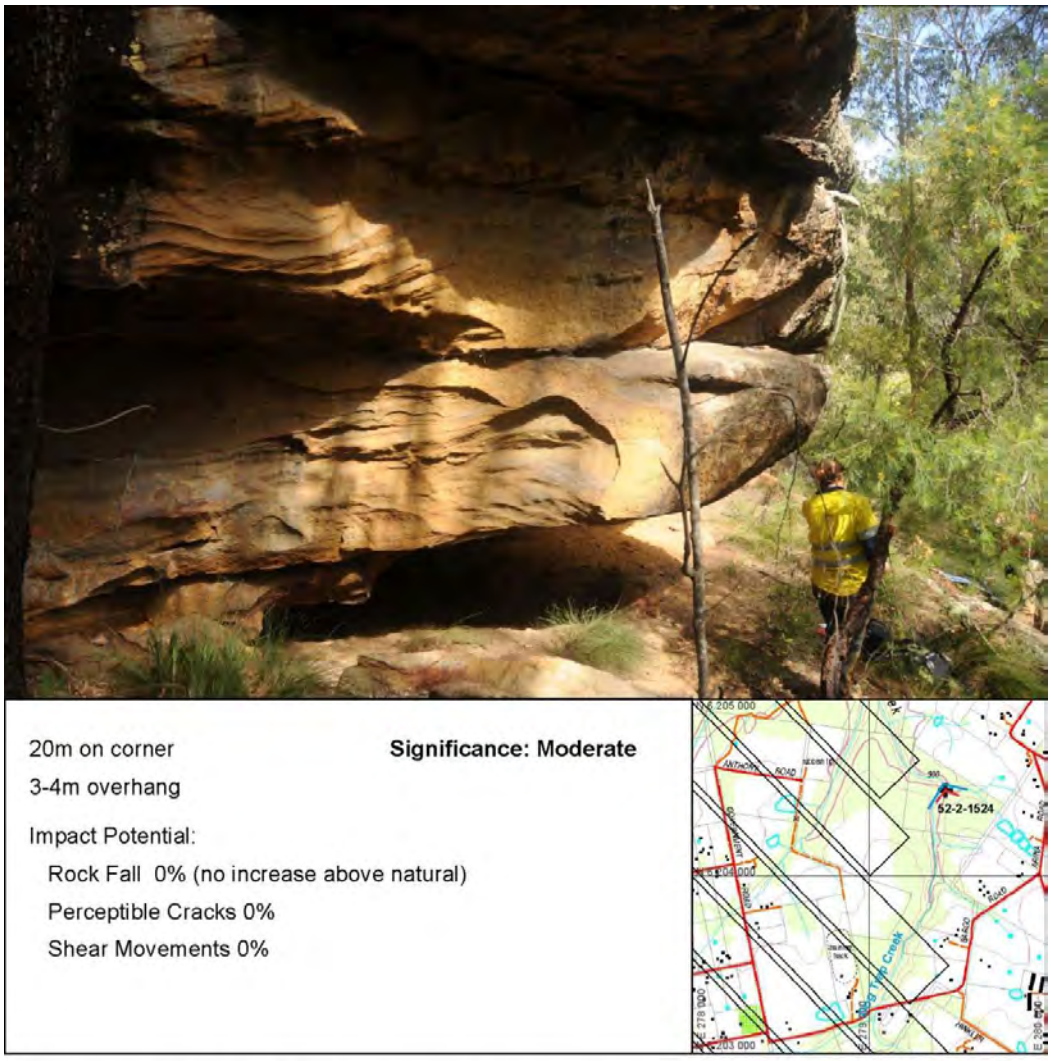

Appendix 1.5: Archaeological heritage site: 52-2-1524 Dog Trap Creek.

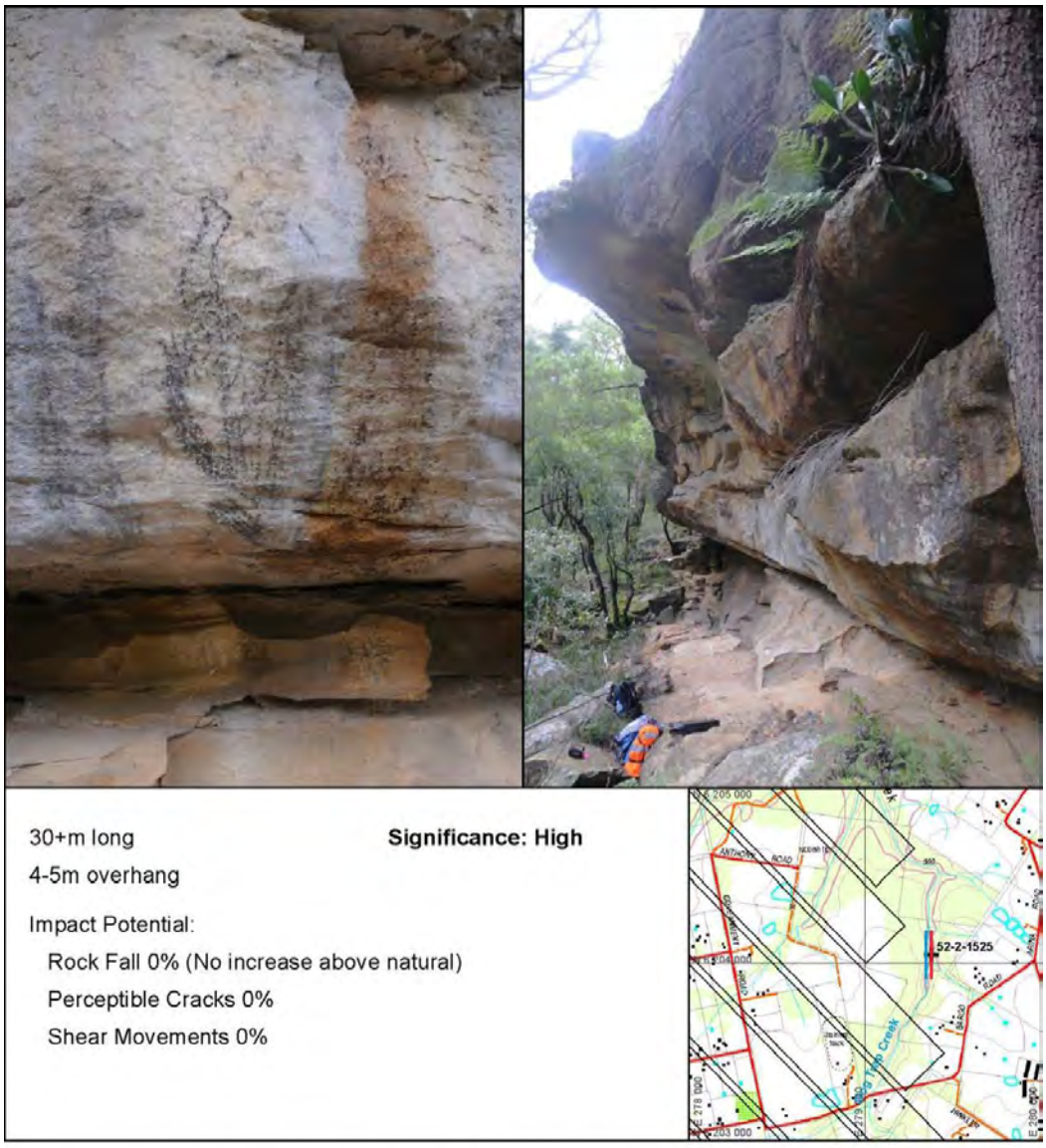

Appendix 1.6: Archaeological heritage site: 52-2-1525 Dog Trap Creek Upside down man.

20m long on corner **Significance: Low**

3-4m overhang

Impact Potential:

Rock Fall 0% (No increase above natural)

Perceptible Cracks 0%

Shear Movements <2%

Appendix 1.7: Archaeological heritage site: 52-2-1526 Dog Trap Creek.

65m long

6-7m overhang

Significance: Moderate

Impact Potential:

Rock Fall 0% (no increase above natural)

Perceptible Cracks 0%

Shear Movements <2%

Appendix 1.8: Archaeological heritage site: 52-2-1527 Dog Trap Creek.

60+m long

Significance: High

7-8m overhang

Rock Fall 0% (No increase above natural)

Perceptible Cracks 0%

Shear Movements <2%

Appendix 1.9: Archaeological heritage site: 52-2-1528 Dog Trap Creek.

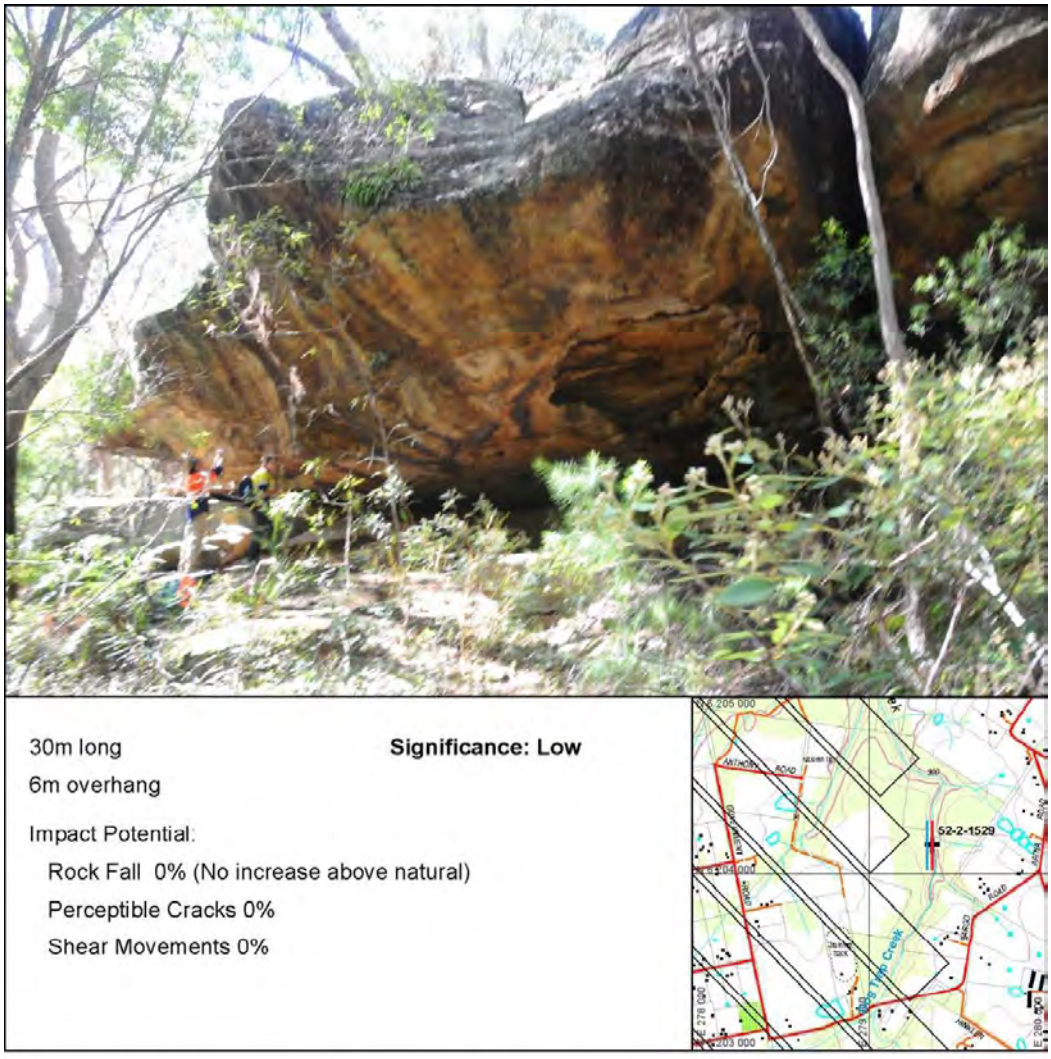

Appendix 1.10: Archaeological heritage site: 52-2-1529 Dog Trap Creek Grinding Grooves.

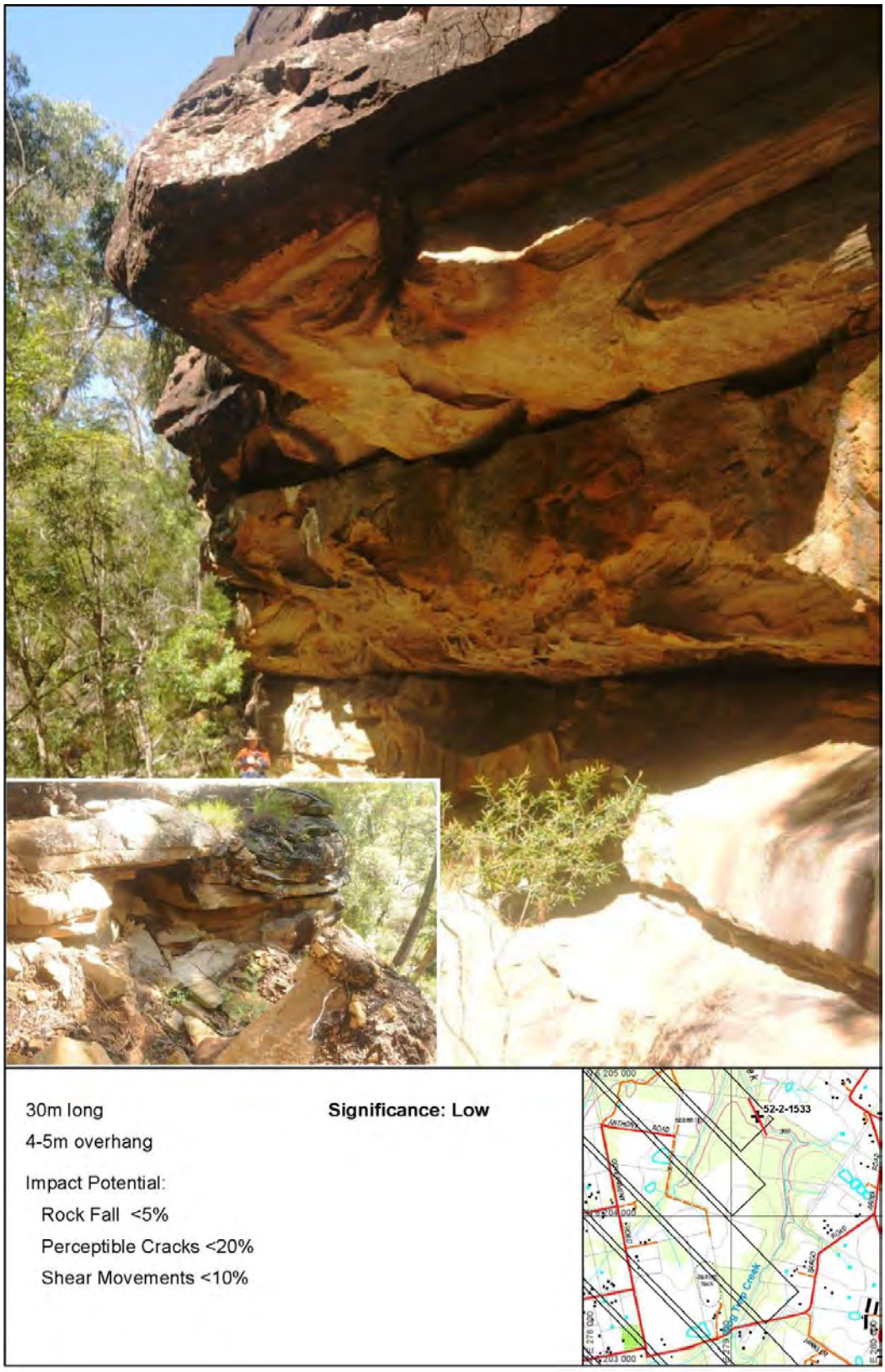

Appendix 1.11: Archaeological heritage site: 52-2-1533 Dog Trap Creek.

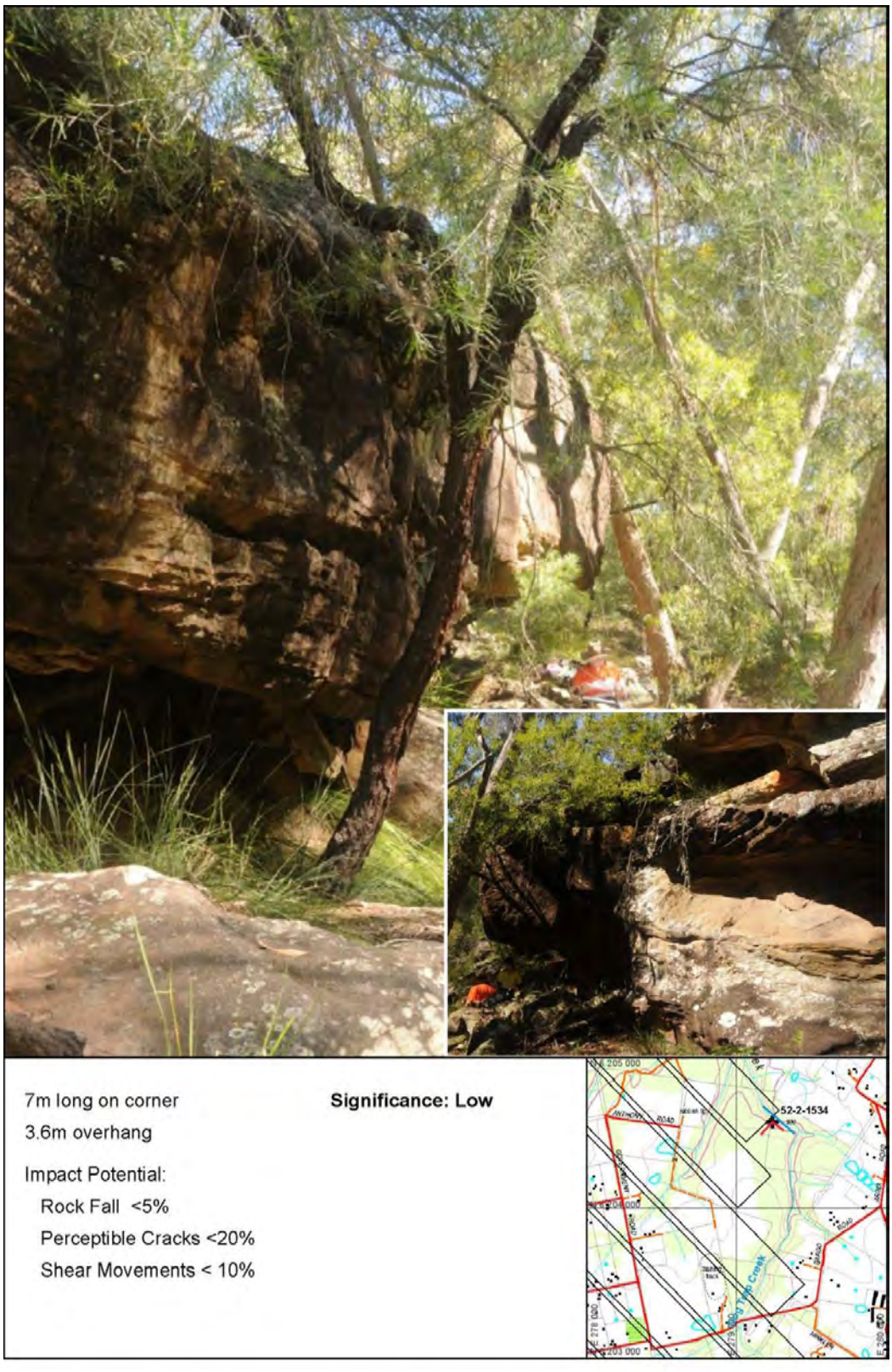

Appendix 1.12: Archaeological heritage site: 52-2-1534 Dog Trap Creek.

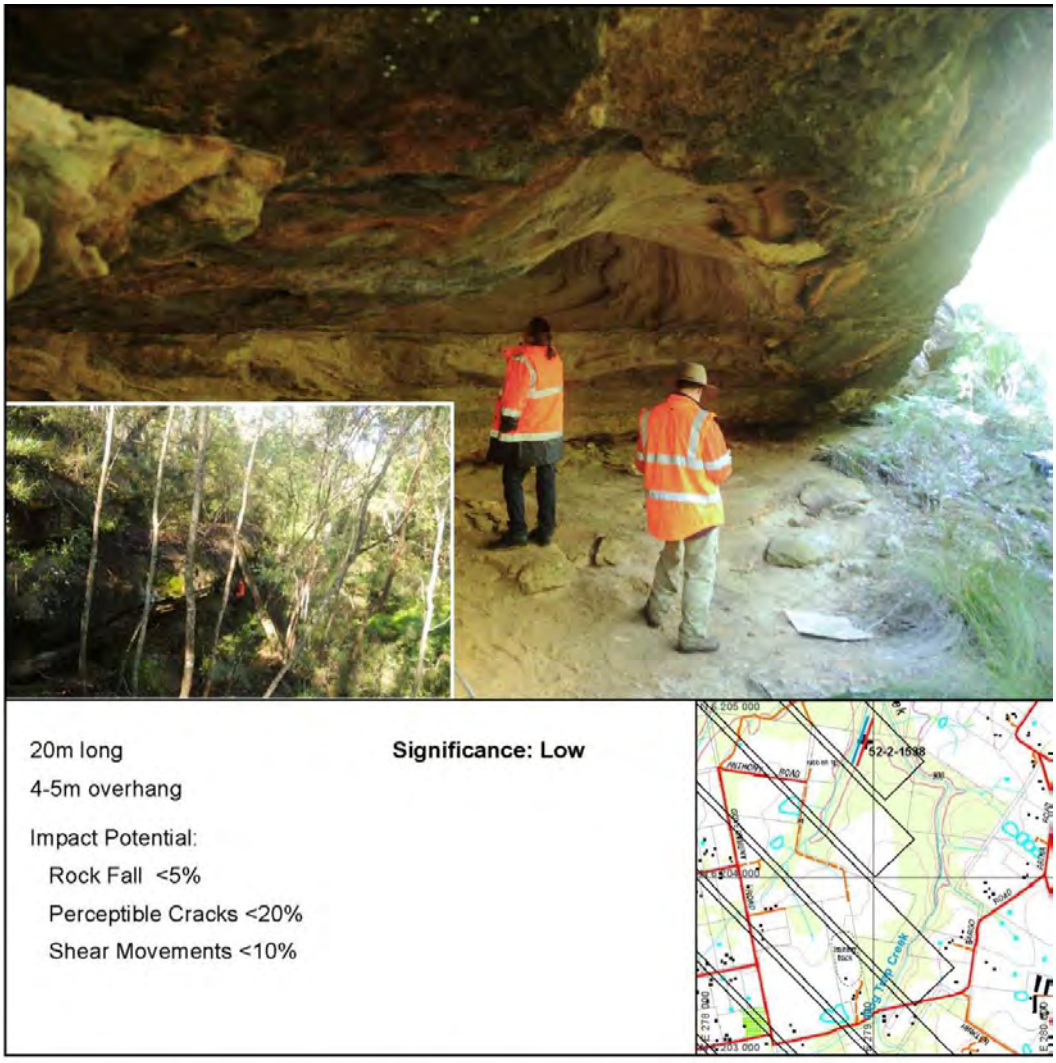

Appendix 1.13: Archaeological heritage site: 52-2-1538 North end of tip Dog Trap Creek Tributary.

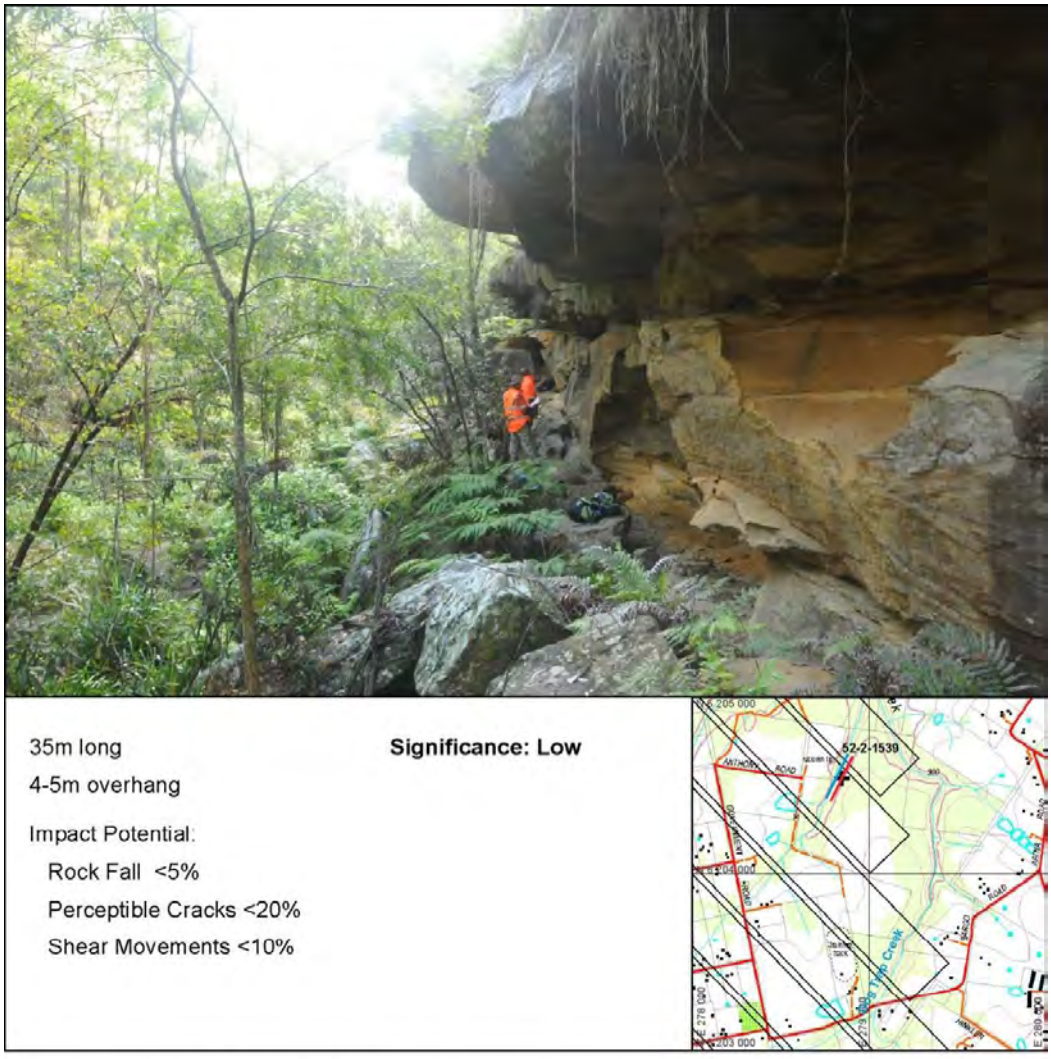

Appendix 1.14: Archaeological heritage site: 52-2-1539 South end of tip Dog Trap Creek Tributary.

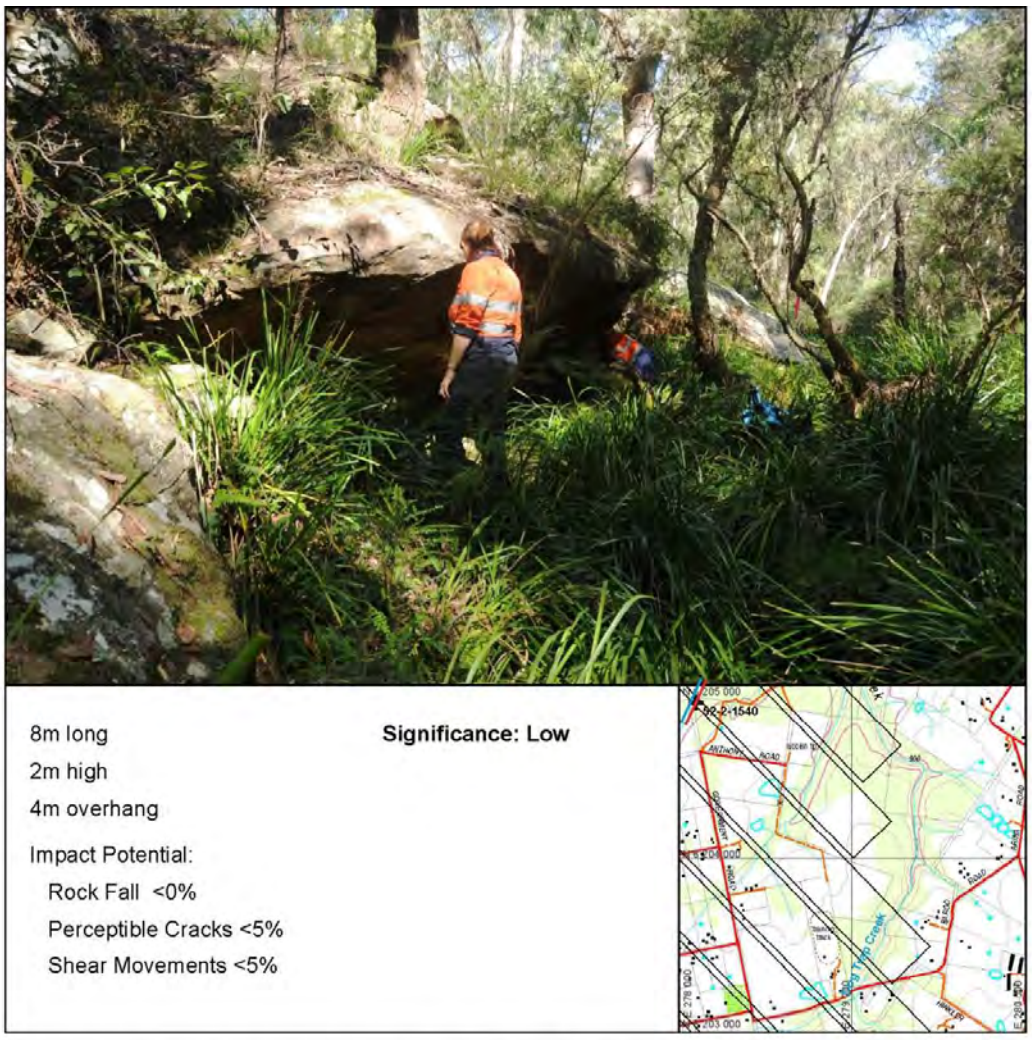

8m long

2m high

4m overhang

Impact Potential:

Rock Fall <0%

Perceptible Cracks <5%

Shear Movements <5%

Significance: Low

Appendix 1.15: Archaeological heritage site: 52-2-1540 Dog Trap Creek Tributary 2.

This page has been left blank intentionally.